COLLOIDAL POLYMERS

SYNTHESIS AND CHARACTERIZATION

edited by
Abdelhamid Elaissari
CNRS-bioMérieux
Lyon, France

Library of Congress Cataloging-in-Publication Data
A catalog record for this book is available from the Library of Congress.

ISBN: 0-8247-4304-0

This book is printed on acid-free paper.

Headquarters
Marcel Dekker, Inc., 270 Madison Avenue, New York, NY 10016, U.S.A.
tel: 212-696-9000; fax: 212-685-4540

Distribution and Customer Service
Marcel Dekker, Inc., Cimarron Road, Monticello, New York 12701, U.S.A.
tel: 800-228-1160; fax: 845-796-1772

Eastern Hemisphere Distribution
Marcel Dekker AG, Hutgasse 4, Postfach 812, CH-4001 Basel, Switzerland
tel: 41-61-260-6300; fax: 41-61-260-6333

World Wide Web
http://www.dekker.com

The publisher offers discounts on this book when ordered in bulk quantities. For more information, write to Special Sales/Professional Marketing at the headquarters address above.

Current printing (last digit):

10 9 8 7 6 5 4 3 2 1

PRINTED IN THE UNITED STATES OF AMERICA

SURFACTANT SCIENCE SERIES

1. Nonionic Surfactants, *edited by Martin J. Schick* (see also Volumes 19, 23, and 60)
2. Solvent Properties of Surfactant Solutions, *edited by Kozo Shinoda* (see Volume 55)
3. Surfactant Biodegradation, *R. D. Swisher* (see Volume 18)
4. Cationic Surfactants, *edited by Eric Jungermann* (see also Volumes 34, 37, and 53)
5. Detergency: Theory and Test Methods (in three parts), *edited by W. G. Cutler and R. C. Davis* (see also Volume 20)
6. Emulsions and Emulsion Technology (in three parts), *edited by Kenneth J. Lissant*
7. Anionic Surfactants (in two parts), *edited by Warner M. Linfield* (see Volume 56)
8. Anionic Surfactants: Chemical Analysis, *edited by John Cross*
9. Stabilization of Colloidal Dispersions by Polymer Adsorption, *Tatsuo Sato and Richard Ruch*
10. Anionic Surfactants: Biochemistry, Toxicology, Dermatology, *edited by Christian Gloxhuber* (see Volume 43)
11. Anionic Surfactants: Physical Chemistry of Surfactant Action, *edited by E. H. Lucassen-Reynders*
12. Amphoteric Surfactants, *edited by B. R. Bluestein and Clifford L. Hilton* (see Volume 59)
13. Demulsification: Industrial Applications, *Kenneth J. Lissant*
14. Surfactants in Textile Processing, *Arved Datyner*
15. Electrical Phenomena at Interfaces: Fundamentals, Measurements, and Applications, *edited by Ayao Kitahara and Akira Watanabe*
16. Surfactants in Cosmetics, *edited by Martin M. Rieger* (see Volume 68)
17. Interfacial Phenomena: Equilibrium and Dynamic Effects, *Clarence A. Miller and P. Neogi*
18. Surfactant Biodegradation: Second Edition, Revised and Expanded, *R. D. Swisher*
19. Nonionic Surfactants: Chemical Analysis, *edited by John Cross*
20. Detergency: Theory and Technology, *edited by W. Gale Cutler and Erik Kissa*
21. Interfacial Phenomena in Apolar Media, *edited by Hans-Friedrich Eicke and Geoffrey D. Parfitt*
22. Surfactant Solutions: New Methods of Investigation, *edited by Raoul Zana*
23. Nonionic Surfactants: Physical Chemistry, *edited by Martin J. Schick*
24. Microemulsion Systems, *edited by Henri L. Rosano and Marc Clausse*
25. Biosurfactants and Biotechnology, *edited by Naim Kosaric, W. L. Cairns, and Neil C. C. Gray*
26. Surfactants in Emerging Technologies, *edited by Milton J. Rosen*
27. Reagents in Mineral Technology, *edited by P. Somasundaran and Brij M. Moudgil*
28. Surfactants in Chemical/Process Engineering, *edited by Darsh T. Wasan, Martin E. Ginn, and Dinesh O. Shah*
29. Thin Liquid Films, *edited by I. B. Ivanov*
30. Microemulsions and Related Systems: Formulation, Solvency, and Physical Properties, *edited by Maurice Bourrel and Robert S. Schechter*
31. Crystallization and Polymorphism of Fats and Fatty Acids, *edited by Nissim Garti and Kiyotaka Sato*

32. Interfacial Phenomena in Coal Technology, *edited by Gregory D. Botsaris and Yuli M. Glazman*
33. Surfactant-Based Separation Processes, *edited by John F. Scamehorn and Jeffrey H. Harwell*
34. Cationic Surfactants: Organic Chemistry, *edited by James M. Richmond*
35. Alkylene Oxides and Their Polymers, *F. E. Bailey, Jr., and Joseph V. Koleske*
36. Interfacial Phenomena in Petroleum Recovery, *edited by Norman R. Morrow*
37. Cationic Surfactants: Physical Chemistry, *edited by Donn N. Rubingh and Paul M. Holland*
38. Kinetics and Catalysis in Microheterogeneous Systems, *edited by M. Grätzel and K. Kalyanasundaram*
39. Interfacial Phenomena in Biological Systems, *edited by Max Bender*
40. Analysis of Surfactants, *Thomas M. Schmitt* (see Volume 96)
41. Light Scattering by Liquid Surfaces and Complementary Techniques, *edited by Dominique Langevin*
42. Polymeric Surfactants, *Irja Piirma*
43. Anionic Surfactants: Biochemistry, Toxicology, Dermatology. Second Edition, Revised and Expanded, *edited by Christian Gloxhuber and Klaus Künstler*
44. Organized Solutions: Surfactants in Science and Technology, *edited by Stig E. Friberg and Björn Lindman*
45. Defoaming: Theory and Industrial Applications, *edited by P. R. Garrett*
46. Mixed Surfactant Systems, *edited by Keizo Ogino and Masahiko Abe*
47. Coagulation and Flocculation: Theory and Applications, *edited by Bohuslav Dobiáš*
48. Biosurfactants: Production • Properties • Applications, *edited by Naim Kosaric*
49. Wettability, *edited by John C. Berg*
50. Fluorinated Surfactants: Synthesis • Properties • Applications, *Erik Kissa*
51. Surface and Colloid Chemistry in Advanced Ceramics Processing, *edited by Robert J. Pugh and Lennart Bergström*
52. Technological Applications of Dispersions, *edited by Robert B. McKay*
53. Cationic Surfactants: Analytical and Biological Evaluation, *edited by John Cross and Edward J. Singer*
54. Surfactants in Agrochemicals, *Tharwat F. Tadros*
55. Solubilization in Surfactant Aggregates, *edited by Sherril D. Christian and John F. Scamehorn*
56. Anionic Surfactants: Organic Chemistry, *edited by Helmut W. Stache*
57. Foams: Theory, Measurements, and Applications, *edited by Robert K. Prud'homme and Saad A. Khan*
58. The Preparation of Dispersions in Liquids, *H. N. Stein*
59. Amphoteric Surfactants: Second Edition, *edited by Eric G. Lomax*
60. Nonionic Surfactants: Polyoxyalkylene Block Copolymers, *edited by Vaughn M. Nace*
61. Emulsions and Emulsion Stability, *edited by Johan Sjöblom*
62. Vesicles, *edited by Morton Rosoff*
63. Applied Surface Thermodynamics, *edited by A. W. Neumann and Jan K. Spelt*
64. Surfactants in Solution, *edited by Arun K. Chattopadhyay and K. L. Mittal*
65. Detergents in the Environment, *edited by Milan Johann Schwuger*

66. Industrial Applications of Microemulsions, *edited by Conxita Solans and Hironobu Kunieda*
67. Liquid Detergents, *edited by Kuo-Yann Lai*
68. Surfactants in Cosmetics: Second Edition, Revised and Expanded, *edited by Martin M. Rieger and Linda D. Rhein*
69. Enzymes in Detergency, *edited by Jan H. van Ee, Onno Misset, and Erik J. Baas*
70. Structure–Performance Relationships in Surfactants, *edited by Kunio Esumi and Minoru Ueno*
71. Powdered Detergents, *edited by Michael S. Showell*
72. Nonionic Surfactants: Organic Chemistry, *edited by Nico M. van Os*
73. Anionic Surfactants: Analytical Chemistry, Second Edition, Revised and Expanded, *edited by John Cross*
74. Novel Surfactants: Preparation, Applications, and Biodegradability, *edited by Krister Holmberg*
75. Biopolymers at Interfaces, *edited by Martin Malmsten*
76. Electrical Phenomena at Interfaces: Fundamentals, Measurements, and Applications, Second Edition, Revised and Expanded, *edited by Hiroyuki Ohshima and Kunio Furusawa*
77. Polymer-Surfactant Systems, *edited by Jan C. T. Kwak*
78. Surfaces of Nanoparticles and Porous Materials, *edited by James A. Schwarz and Cristian I. Contescu*
79. Surface Chemistry and Electrochemistry of Membranes, *edited by Torben Smith Sørensen*
80. Interfacial Phenomena in Chromatography, *edited by Emile Pefferkorn*
81. Solid–Liquid Dispersions, *Bohuslav Dobiáš, Xueping Qiu, and Wolfgang von Rybinski*
82. Handbook of Detergents, *editor in chief: Uri Zoller*
    Part A: Properties, *edited by Guy Broze*
83. Modern Characterization Methods of Surfactant Systems, *edited by Bernard P. Binks*
84. Dispersions: Characterization, Testing, and Measurement, *Erik Kissa*
85. Interfacial Forces and Fields: Theory and Applications, *edited by Jyh-Ping Hsu*
86. Silicone Surfactants, *edited by Randal M. Hill*
87. Surface Characterization Methods: Principles, Techniques, and Applications, *edited by Andrew J. Milling*
88. Interfacial Dynamics, *edited by Nikola Kallay*
89. Computational Methods in Surface and Colloid Science, *edited by Małgorzata Borówko*
90. Adsorption on Silica Surfaces, *edited by Eugène Papirer*
91. Nonionic Surfactants: Alkyl Polyglucosides, *edited by Dieter Balzer and Harald Lüders*
92. Fine Particles: Synthesis, Characterization, and Mechanisms of Growth, *edited by Tadao Sugimoto*
93. Thermal Behavior of Dispersed Systems, *edited by Nissim Garti*
94. Surface Characteristics of Fibers and Textiles, *edited by Christopher M. Pastore and Paul Kiekens*
95. Liquid Interfaces in Chemical, Biological, and Pharmaceutical Applications, *edited by Alexander G. Volkov*

96. Analysis of Surfactants: Second Edition, Revised and Expanded, *Thomas M. Schmitt*
97. Fluorinated Surfactants and Repellents: Second Edition, Revised and Expanded, *Erik Kissa*
98. Detergency of Specialty Surfactants, *edited by Floyd E. Friedli*
99. Physical Chemistry of Polyelectrolytes, *edited by Tsetska Radeva*
100. Reactions and Synthesis in Surfactant Systems, *edited by John Texter*
101. Protein-Based Surfactants: Synthesis, Physicochemical Properties, and Applications, *edited by Ifendu A. Nnanna and Jiding Xia*
102. Chemical Properties of Material Surfaces, *Marek Kosmulski*
103. Oxide Surfaces, *edited by James A. Wingrave*
104. Polymers in Particulate Systems: Properties and Applications, *edited by Vincent A. Hackley, P. Somasundaran, and Jennifer A. Lewis*
105. Colloid and Surface Properties of Clays and Related Minerals, *Rossman F. Giese and Carel J. van Oss*
106. Interfacial Electrokinetics and Electrophoresis, *edited by Ángel V. Delgado*
107. Adsorption: Theory, Modeling, and Analysis, *edited by József Tóth*
108. Interfacial Applications in Environmental Engineering, *edited by Mark A. Keane*
109. Adsorption and Aggregation of Surfactants in Solution, *edited by K. L. Mittal and Dinesh O. Shah*
110. Biopolymers at Interfaces: Second Edition, Revised and Expanded, *edited by Martin Malmsten*
111. Biomolecular Films: Design, Function, and Applications, *edited by James F. Rusling*
112. Structure–Performance Relationships in Surfactants: Second Edition, Revised and Expanded, *edited by Kunio Esumi and Minoru Ueno*
113. Liquid Interfacial Systems: Oscillations and Instability, *Rudolph V. Birikh, Vladimir A. Briskman, Manuel G. Velarde, and Jean-Claude Legros*
114. Novel Surfactants: Preparation, Applications, and Biodegradability: Second Edition, Revised and Expanded, *edited by Krister Holmberg*
115. Colloidal Polymers: Synthesis and Characterization, *edited by Abdelhamid Elaissari*
116. Colloidal Biomolecules, Biomaterials, and Biomedical Applications, *edited by Abdelhamid Elaissari*

ADDITIONAL VOLUMES IN PREPARATION

Gemini Surfactant Synthesis: Interfacial and Solution-Phase Behavior and Applications, *edited by Raoul Zana and Jiding Xia*

Colloidal Science of Flotation, *Anh V. Nguyen and Hans Joachim Schulze*

Surface and Interfacial Tension: Measurement, Theory, and Applications, *edited by Stanley Hartland*

Dedication

This book is dedicated to Doctor Christian Pichot for his great scientific contribution in the polymer colloids domain and in honor of his retirement in October 2002.

Christian Pichot completed chemistry studies at Université Pierre et Marie Curie in Paris, France, and then started his research career as a contract laboratory technician at the Faculté des Sciences d'Orsay in a Chemistry-Physics Laboratory directed by Professor M. Magat, one of the founders of Polymer Science in France. After a national service teaching in Ivory Coast, he was welcomed by A. Guyot, Director of Research, under a research contract allowing him to join the CNRS (National Center for Scientific Research) catalysis research institute and to be involved in various topics (physico-chemical characterization of polyphenylsiloxane, degradation studies of PVC models). In October 1972, he got a permanent position at the CNRS and he prepared a doctorate thesis on kinetic anomalies in radical-initiated copolymerization and their explanations, a work that he defended in 1976.

He completed a one-year postdoctoral fellowship (from the National Science Foundation) at the Emulsion Polymers Institute (Lehigh University, Bethlehem, Pennsylvania), under the guidance of Professors J. Vanderhoff and M. S. El-Aasser, giving him the opportunity to be trained in the field of latex synthesis and characterization. When he went back to the Laboratory of Organic Materials, first in Villeurbanne then in Vernaison in 1980, together with J. Guillot he played a significant role in setting up and developing a research team devoted to kinetics, characterization, and properties of radical copolymers produced in dispersed media (mostly in emulsion). He was responsible for training young research scientists who all went on to successful careers in industry. He dealt with a wide range of problems, both applied and fundamental, leading him to publish over 50 high-quality papers. The thesis students and scientists working under his direction particularly appreciated his availability and devotion, along with his friendly manner under all circumstances. He investigated three main topics: first, he tried to establish synthesis–structure–properties relationships in various emulsion (co)-polymers; second, he made a significant contribution to

the knowledge of inverse emulsion polymerization mechanisms, a subject that had been covered only by a restricted number of analyses; finally, he took particular interest in the original behavior of zwitterionic surfactants in emulsion polymerization, especially to produce monodisperse nanosized particles.

In 1988, his scientific reputation helped him to take part in the creation of a joint research unit between the CNRS and bioMérieux, a worldwide company partly located in the Lyon area and dealing with the manufacture of automatic diagnostic analyzers and reagents. This joint project soon resulted in patent registrations, but, above all, Christian Pichot initiated various research subjects related to the preparation of functionalized polymer supports with appropriated properties to interact with biological fluids. For that purpose, he particularly

contributed to the design and elaboration either of reactive "linear" copolymers or of functionalized, stimuli-responsive, and magnetic latex particles. He developed a passionate interest in the complexity of these problems, resulting in the establishment of a laboratory considered an exemplary success. He chaired the Chemistry Group of the joint research unit from its creation until 2002, helping this team, now comprising a good balance of researchers with various expertises and coming from the CNRS and bioMérieux, to acquire an internationally acknowledged reputation.

Since 1980, he has been a member of the International Colloid Polymer Group, where he represents all those from the Lyon area working in this field. He is regurlarly invited as a lecturer in various meetings organized by the scientific community, and he has contributed to the creation of a large number of contacts and developed many collaborative research projects. From 1984, he was co-organizer in Lyon of four international symposia dealing mainly with polymers in dispersed media on both academic and applied aspects. He welcomed and trained in the lab many students who have gone on to careers as researchers in France and throughout the world.

Preface

Polymerization in dispersed media is arousing an increasing interest from both practical and fundamental points of view. Since the birth of the polymer-based colloids elaboration process fifty years ago, the need for well-defined dispersion has led to the production of diverse types of particles. Latexes or hybrid colloids are used in very different areas, such as adhesives, thermoplastics, textiles, paints, paper, and biomedical applications. Polymers colloids have received increasing interest in numerous applications, including in the biomedical and biotechnological fields. This is due to the versatility of the many heterophase polymerization processes (emulsion, dispersion, and precipitation) available for making well-defined microspheres of various particle sizes and surface reactive groups. The specialty chemicals industry is particularly interested in a large number of uses involving the elaboration of latexes with specific characteristics, such as narrow size distribution, and often surface functionalization. The main objective of this book is to report on the preparation of polymer colloids by presenting original processes and innovative materials leading to original properties. Further, a selection of extended reviews and detailed papers are included in order to give an overview of related fields. In addition, some special topics are presented. This book examines the following points:

Synthesis of reactive polymer colloids. The preparation of classical polymers as well as the preparation of new reactive latex particles is stressed. To make the study comprehensive, various conventional and nonconventional polymerization processes were explored (emulsion, mini-emulsion, macro-emulsion, dispersion, and precipitation polymerization). Moreover, the effect of each reagent on the polymerization process was studied to identify the critical parameters governing the polymerization properties such as the polymerization rate, the conversion, and the final particles properties.

Physico-chemical and colloidal characterization of prepared latexes Once the colloidal dispersion has been prepared, a number of features need to be determined before any special use. These include particle size and particle size distribution, surface polarity, charge density or surface reactive groups, loca-

tion of reactive groups, presence of residual monomer in the elaborated dispersions, morphology of the particles (soft, core-shell, hemisphere, etc.), the chemical composition of the particles, the thickness of the steric stabilizing layer, the nature of the interactions between the particles, the nature of the particle surface (rough or smooth), and finally the colloidal stability of the particles. The characterization study is a step that is of paramount importance for understanding not only the polymerization mechanism but also the interactions between latex particles and biomolecules or active agents.

Biomolecules–polymer colloids interactions. The interaction studies between biomolecules (or drugs) and colloidal particles are of paramount importance in the biomedical field. Then, to target any specific immobilization or interaction monitoring the fixation processes of proteins, nucleic acids, or viruses, systematic studies as a function of physico-chemical parameters are incontestably of great interest in both academic research and biomedical applications.

The goal of this book is to present recent results and information on polymer colloids beginning with their preparation and biomolecules interactions and going further into a study of some of their finer biomedical applications. A combination of various extended reviews and some special papers are also presented.

Abdelhamid Elaissari

Contents

Contributors

Ammar Azioune Interfaces, Traitements, Organisation et Dynamique de Systèmes (ITODYS) de l'Université Paris, Paris, France

Elodie Bourgeat-Lami CNRS-LCPP, Villeurbanne, France

Smain Bousalem Interfaces, Traitements, Organisation et Dynamique de Systèmes (ITODYS) de l'Université Paris, Paris, France

Carine Burguière Université Pierre et Marie Curie, Paris, France

Jean-Paul Chapel Claude Bernard–Lyon I University, ISTIL, Villeurbanne, France

Bernadette Charleux Université Pierre et Marie Curie, Paris, France

Mohamed M. Chehimi Interfaces, Traitements, Organisation et Dynamique de Systèmes (ITODYS) de l'Université Paris, Paris, France

Jerôme Claverie CNRS-LCPP CPE Lyon, Villeurbanne, France

Jean-Claude Daniel The French Group for Polymers Development and Applications (GFP), Fontenay-sous-Bois, France

Abdelhamid Elaissari CNRS-bioMérieux, Lyon, France

Céline Farcet Université Pierre et Marie Curie, Paris, France

Shoukuan Fu Fudan University, Shanghai, China

Alain Guyot CNRS-LCPP CPE Lyon, Villeurbanne, France

Katharina Landfester Max Planck Institute of Colloids and Interfaces, Potsdam, Germany

M. Lansalot CNRS-bioMérieux, Lyon, France

Chantal Larpent Université de Versailles Saint-Quentin-en-Yvelines, Versailles, France

Françoise Meunier CNRS-bioMérieux, Lyon, France

O. Mondain-Monval Centre de Recherche Paul Pascal, CNRS, Pessac, France

Franck Montagne CNRS-bioMérieux, Lyon, France

Peihong Ni Soochow University, Suzhou, China

Christian Pichot CNRS-bioMérieux, Lyon, France

Brian R. Saunders University of Manchester and UMIST, Manchester, United Kingdom

Florence Sauzedde CNRS-bioMérieux, Lyon, France

Serap Şenel Hacettepe University, Ankara, Turkey

Amel Ben Slimane Interfaces, Traitements, Organisation et Dynamique de Systèmes (ITODYS) de l'Université Paris, Paris, France

Remi Soula CNRS-LCPP CPE Lyon, Villeurbanne, France

Robert Spitz CNRS-LCPP CPE Lyon, Villeurbanne, France

Tatsuo Taniguchi Yamagata University, Yamagata, Japan

Ali Tuncel Hacettepe University, Ankara, Turkey

Ender Ünsal Hacettepe University, Ankara, Turkey

Changchun Wang Fudan University, Shanghai, China

Wuli Yang Fudan University, Shanghai, China

Abderrahim Yassar Interfaces, Traitements, Organisation et Dynamique de Systèmes (ITODYS) de l'Université Paris, Paris, France

1

A Long History with Many Challenges to Meet in the Future

Free-Radical Emulsion Polymerization and Aqueous Polymer Dispersions

JEAN-CLAUDE DANIEL The French Group for Polymers Development and Applications (GFP), Fontenay-sous-Bois, France

Free-radical polymerization is a widely utilized technology to prepare synthetic polymers in aqueous colloidal dispersion form. It is by far the most commonly used process in industry; manufacturers find that it has a large number of technical advantages (conventional reaction vessels, easy-to-run operations, high molar mass polymers, and wide variety of potential products) and economic advantages (good productivity, inexpensive reagents, relatively low investments).
The "synthetic latexes," which are obtained from polymerization reaction vessels (Fig. 1), can be processed on the production site to separate the polymer, dry it, and then market it in various dry forms (powders, granules, chips, etc.). Large quantities of inexpensive commodity polymers are manufactured in this way: they may be thermoplastics, such as certain polyvinyl chloride (PVC) grades, or elastomers, such as styrene-butadiene rubbers (SBRs) or polychloroprene rubbers. Other products, more complex in terms of molecular structure, are also produced via free-radical emulsion polymerization and offered on specialty markets in dry powder or granule form. Graft copolymers, such as Acrylonitrile Butadiene Styrene (ABS) or Methyl Methacrylate Butadiene Styrene resins (MBS), used in the composition of high mechanical performance polymeric materials, intended for the automobile or packaging industries, are illustrative examples of this product class.

However, for many applications it is preferable to use latex as is, with the polymer kept in dispersed form; in this way, a little over 4 million metric tons of aqueous synthetic polymer dispersions, essentially produced by free-radical emulsion polymerization processes, was marketed in the European Union in

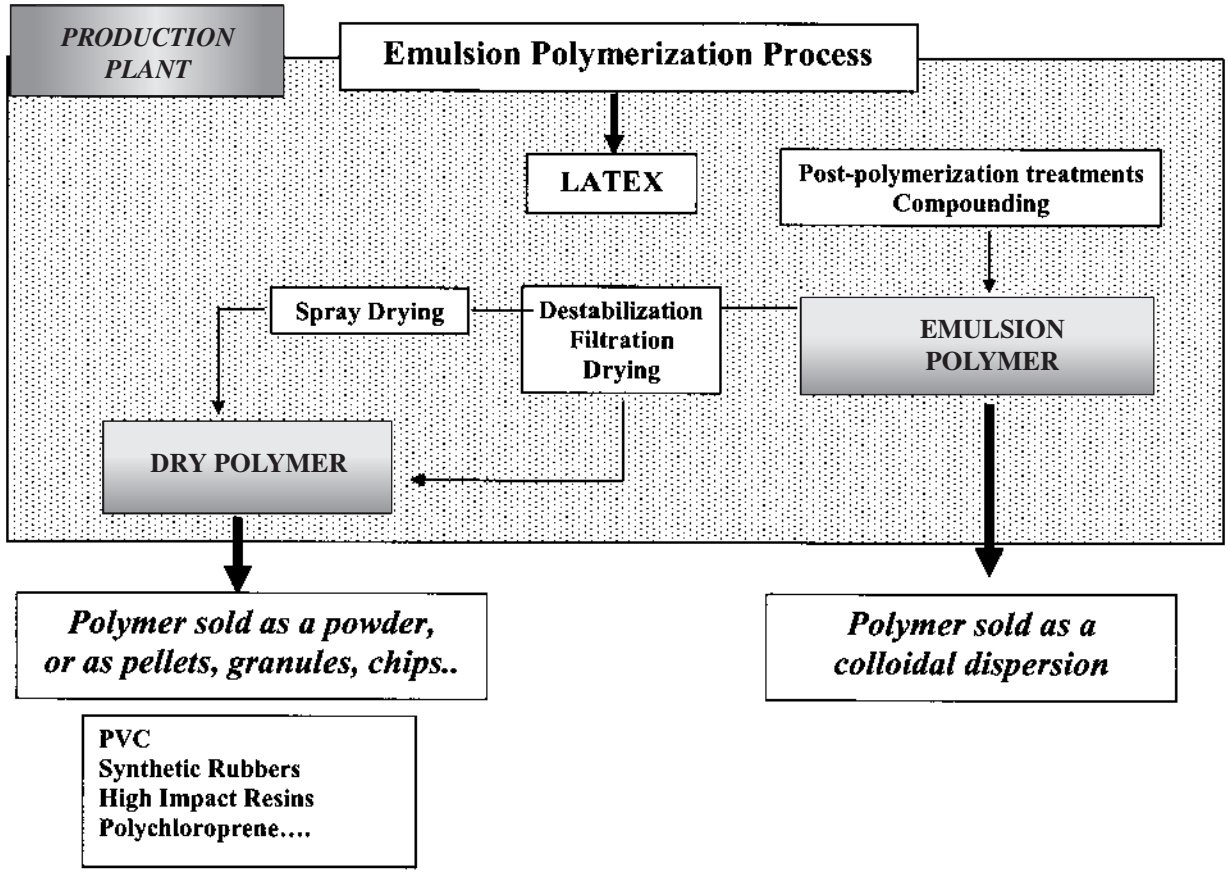

FIG. 1 Emulsion polymerization process: synopsis of a production plant.

2000. This represents approximately 2 million metric tons of dry polymer and probably triple this figure for global production.

Many specific properties are associated with the presentation of the polymer in colloidal form and extremely varied areas of activity make use of them. All industries involved in surface protection or modification are interested in such products. As a matter of fact, they are very widely used as binders in industrial formulations for paints, adhesives, textiles, paper coatings, etc. In all these applications, the polymer particles are soft and must be capable of coalescing at least partially when the latex is dried at a temperature close to ambient temperature and then adhering strongly on the surface of mineral pigments, textile fibers, or various other substrates. In this way, it is possible, using a mixture of latex particles and inorganic pigments (kaolin, calcium carbonate, titanium dioxide, etc.), to obtain pigmented coatings to protect and decorate a substrate (case of paints) or enhance its surface properties (case of paper coatings). Similarly, aqueous polymer dispersions are used to increase the mechanical performances and abrasion resistances of textile items (nonwoven fabrics, floor coverings, etc.).

Besides these large-scale industrial applications, the colloidal presentation of the polymer is of value in other areas. The biomedical field is a remarkable example that will be extensively illustrated in this book. Film formation due to coalescence is no longer the key point in this case; on the contrary, the aim is to preserve the integrity of the particles that are used to carry and separate molecules or to amplify and detect reactions taking place on their surface (as in medical diagnostics). However, other specific properties of latexes will be largely used beneficially. These include:

Very large specific surface area
Great versatility in terms of particle sizes and surface properties
Ability to attach biological molecules
    by adsorption, or
    by covalent binding, via surface functional groups
Sensitivity of metastable colloidal systems to the presence of particular ionic or molecular species, used as a detection tool in certain immunodiagnostic tests.

I. DEVELOPMENT OF FREE-RADICAL EMULSION POLYMERIZATION: A HISTORIC OVERVIEW

It is difficult to separate the contributions of academic research and industrial research in the development of the resulting processes and products. Their complementarity has been remarkable and certainly a rare example of close fruitful cooperation, for over 70 years, in the United States and Europe.

A. D. Dunn [1] presented pioneering research at the end of the 1920s and 1930s in Germany, the United States, and USSR on emulsion polymerization, essentially oriented to synthetic rubber production. The first patents held by Goodyear Tyre and Rubber Company and IG Farben date back to 1927 and 1928, respectively. However, it was only in the mid-1930s that the first commercial products based on butadiene (Bunas S and N) and vinyl acetate were launched in Germany. In 1937, the annual German production of Buna S was 5000 metric tons.

The startup of mass productions dates back to World War II with the decision by the U.S. government to create a genuine synthetic rubber industry to counter the consequences of the Japanese invasion of Southeast Asia, particularly that of Malaysia, on natural rubber supplies. The vast research and development program set up, associating industry and academics, resulted in a copolymer of butadiene and styrene (GR-S) for which production rose from 2000 metric tons in 1942 to over 650,000 metric tons in 1944.

The immediate postwar period saw the development of other polymer families, based on vinyl chloride, vinyl acetate, chloroprene, and acrylic monomers, along with significant diversification of the markets to plastics and coating applications: architectural paints, adhesives, textiles, and so forth. This success was in fact the result of improved knowledge on polymerization mechanisms. The micellar model proposed by W. D. Harkins in 1947 [2], reworked and completed by W. V. Smith and R. H. Ewart in 1948 [3], accounted reasonably well for the experimental results obtained on styrene and butadiene–styrene mixtures under the conditions of the time; it served as a reference for development studies for this generation of products, until the 1970s. However, the limitations of this model appeared when the polymerization recipe progressed, involving monomers that were more hydrophilic than styrene or using much lower surfactant contents. Other mechanistic models were then developed to complete Harkins' representation; they are based on work by R. M. Fitch and C. H. Tsai (1971) [4], followed by J. Ugelstad and M. S. El-Aasser (1973–1979) [5–7]. These authors demonstrated that polymer particles could also be generated by precipitation of radicals growing in aqueous phase or by the entry of radicals into monomer droplets, if these droplets are sufficiently small. They also identified limited flocculation phenomena liable to occur during the particle growing step and affect their final size. These models are now well accepted, the most significant addition being made since then by R. G. Gilbert with the coagulative nucleation theory in 1987 [8]. They have been used to develop quantitative approaches describing polymerization kinetics as well as the particulate and molecular characteristics of the homopolymers and copolymers formed. In this context, refer to the publications by Gardon [9], Hansen and Ugelstad [10,11], Hamielec [12,13], Nomura [14], Guillot [15,16], and, more recently, those by

Gilbert [17], Charmot [18], and Asua [19–22], which provide models of interest to process relatively complex systems, similar to those found in industry.

On the basis of this data and concomitant progress in colloidal physics and surface chemistry (DLVO theory in 1948 [23], the works by W. Heller [24], D. Napper [25], P. G. de Gennes [26] and J. Israelachvili [27] on the behavior and the effects of polymers on interfaces, manufacturers were able to identify, in a more detailed manner, the parameters controlling processes and product characteristics. This gave rise to latexes with better defined particle sizes, less rich in surfactants, but with much higher stability to shear stress, ionic strength, or freeze–thaw. Their end-use value improved considerably and, in the early 1970s, it is possible to speak of the birth of a second generation of latexes accompanied by significant growth in the quantities produced, for paint and paper applications in particular.

It was also at this time that latexes for biomedical applications were introduced onto the market by Dow Chemical in the USA and Pechiney-Saint-Gobain in Europe. Perfectly calibrated latex particles, known since 1947 [28] but considered as curiosities, could be reliably prepared in a very wide range of particle sizes. It was then possible to meet the needs of biologists who had been seeking for some years artificial substrates to replace red blood cells in diagnostic kits to detect rheumatoid factor [29], pregnancy hormone (human chorionic gonadotropin, HCG) [30], and subsequently multiple substances associated with infectious disease. Particles labeled with various dyes, fluorescent pigments, or even radioactive isotopes were available on the market at the end of the 1970s.

This progression in the quality of commercial products was also a consequence of the mutations taking place in processes and process operating modes. At the end of the 1960s, the move from batch polymerization to semicontinuous polymerization resulted in reaction vessel productivity gains and better control of the composition and microstructure of the copolymers. The introduction of seeded polymerization techniques in the 1960s, associated with more advanced monomers feeding programs, made it possible not only to improve control of the particle size characteristics but also toact interestingly on the morphology and internal structure of particles. These seeded techniques paved the way for new innovation applied in industry from 1965 to 1970 so as to create rubber-toughened plastics, thanks to graft copolymers such as ABS, MBS, or various modifiers for PVC which, in France, enabled the significant development of plastic bottles for mineral water.

Initially, academic research only dealt with these processes in a very theoretical way through the controversy generated by the research by D. J. Williams, M. R. Grancio, and P. Keusch (1970–1973) [1,31] which suggested that, during polymerization, polymer generation is not carried out homogeneously within the

particles but takes place in the peripheral zone. This situation changed considerably after 1975, when J. W. Vanderhoff, on the strength of his industrial experience at Dow Chemical, set up the Lehigh University research group with M. S. El Aasser; "structured particle" latexes, i.e., those in which several polymer phases coexist in the same particle, then became a major academic research theme. The teams headed by T. Matsumoto and M. Okubo in Japan [31,32–34] and J. Guillot and C. Pichot in France [35–38] also played important roles, contributing to improved knowledge of the physicochemical phenomena governing the morphology of particles prepared with monomers of different reactivities and polarities.

A review of the publications and patents shows that structured particle latexes still represent an active area of research today, the objective being to improve the performances of latexes for coatings and also prepare additives to reinforce varied polymer matrices (acrylics, polycarbonates, polyamides, epoxies, etc.). Despite all the efforts on the part of academic partners, solid predictive models of the final structures are not available to date, kinetic aspects being often more significant than thermodynamics. However, papers from the teams headed by V. Dimonie [39], A. Rudin [40,41], D. C. Sundberg [42–44], and J. M. Asua [45,46], which account for interfacial tensions between the phases present along with parameters related to the diffusion of the species present gives basic information and reliable guidelines to describe certain problems encountered in the industry.

Hollow latex particles, i.e., void-containing particles, represent a peculiar category of structured particle latexes. They were successfully introduced by Rohm and Haas [47], in the mid-1980s, as original opacifying pigments offering specific advantages with respect to conventional pigments (lower density, better UV resistance) appreciated by paper and paint manufacturers. In fact, they consist of "core shell" particles in which the core is an alkali-swellable hydrophilic polymer capable, during drying, of releasing the water stored and retracting to leave an empty microvolume limited by the particle shell. This success stimulated research, and many other solutions have since been proposed to prepare hollow latex particles. In this context, refer to the seeded dispersion polymerization process using a "dynamic swelling" method, developed by M. Okubo [48–50], and to the technique described by S. Omi; it consists in emulsifying via a microporous membrane and then polymerizing a mixture of hydrophobic solvent, hydrophilic monomer, and cross-linking agent [51].

Attempts made by academic and industrial researchers to extend the range of particle sizes associated with conventional free-radical polymerization also represent a significant event of the last 20 years.

The race for large particles started in the early 1980s with the zero-gravity polymerization experiments conducted in the Columbia and Challenger space shuttles [52]. Record sizes of 50 and even 100 μm were produced laboriously

and at costs relatively incompatible with industrial applications and then equaled and exceeded by J. Ugelstad's Norwegian team in a less exotic environment. The Norwegians' success was the result of detailed physicochemical analysis of mechanisms involved in the swelling of polymer particles in the presence of monomer and, as a result, it was demonstrated that a relatively minor modification of the process was sufficient to increase the ability of the particles considerably to swell with monomers [53].

Another process, possibly more attractive for manufacturers, to prepare latexes of sizes greater than 1 μm, is dispersion polymerization, which has emerged from the transposition to an aqueous environment of the concepts presented by K. E. J. Barett for organic media in a work published in 1975 [54]. This approach, introduced by Y. Almog of the Weizman Institute in 1980 [55], was developed by the research teams at Xéros in Canada and those at ICI in the United Kingdom [56–60]. An interesting variant of the technique is the dynamic swelling method, mentioned above, developed by S. Okubo and used to prepare large particles of very various shapes and structures.

For small-diameter particles (less than 80 nm), academics have had successful results in France with research conducted in Lyon by C. Pichot and A. Guyot, in 1988–1990, on polymerization in the presence of zwitterionic sulfobetaine-type surfactants [61], by C. Larpent in Rennes on polymerization in direct microemulsions [64,65] and by F. Candau on polymerization in inverse microemulsions [62,63]. Most of the other studies published on this subject involved extremely high surfactant concentrations, sometimes higher than the monomer concentration, rendering these systems difficult to operate.

With respect to commercial developments, the research strategy oriented to large particles proved to be relatively disappointing. It did not lead to large-scale markets. The range of latexes for paints based on polymerization in dispersion technology, marketed by ICI Paints in the late 1980s, remains in a conventional grain size range [56]. However, in highly technical niches, accepting high-added-value products, it has been possible to introduce monosized particles in excess of 1 μm with some success. In this way, it has been possible to process to manufacture chromatographic substrates, electrophotographic toners, diagnostic reagents, or spacers for liquid crystal display (LCD) panels.

Very fine particle latexes have also been used in diagnostic reagents but have also given rise to large-scale industrial developments. New flocculants, intended for water treatment, have been developed on the basis of the inverse microemulsion polymerization process, which makes it possible to obtain very high molar mass hydrosoluble polymers—a decisive advantage over conventional inverse emulsion processes. New binders for paints with particle sizes ranging from 30 to 60 nm are now available [66]. These products, intermediate between dispersions and solutions, offer considerable advantages due to their optical properties, their easy penetration in porous substrates, and a remarkably low film for-

mation temperature in comparison with the T_g of the polymer. In this way, they make it possible to obtain, at room temperature, high-hardness and low-porosity films.

Of the significant events of recent years, it is important to mention the interest focused on composite particle dispersions. They consist of polymer particles in which an inorganic phase is included. Many articles and patents have been published, particularly since 1990, on the synthesis of such particles, with various inorganic phases: titanium oxide, silica, calcium carbonate [67–71]; however, to date, none appears to have led to major developments.

On the other hand, "magnetizable latexes," in which the polymer particles contain metal oxides with magnetic properties, have seen great success in biomedical applications and are now marketed by several companies. These particles are in fact superparamagnetic, meaning that they respond to a magnetic field but lose their magnetization when the field is canceled. In this way, they can be separated from the aqueous phase by a magnet, be washed if required, and then be redispersed in another aqueous phase. There is now a high demand for such products in the field of biotechnologies since they are perfectly suited to robotized equipment. A large number of examples are given in [127–131]. These products form attractive solid substrates for diagnostic reagents (immunotests and DNA-probe tests), for cell separation or to isolate molecules of biological interest; they also represent markers of interest for medical imaging.

The first patent claiming the preparation of magnetic latexes by means of radical polymerization was filed in 1977 [72]; it was restricted to hydrophilic acrylic polymer particles usable for cell separation. In 1980, our team at Rhône-Poulenc filed a second patent disclosing a miniemulsion-type process wherein styrene was polymerized in droplets containing a mixture of styrene and organic ferrofluid [73]. In spite of the broad particle size distribution of this latex, it was marketed from 1981 and used in radioimmunoassay (RIA)–type diagnostic reagents, very popular at that time. Many improvements have since been made to the process [74,75], and a wide range of more defined products in terms of particle size, richer in magnetic pigment levels and comprising various functional groups, are now commercially available.

A second route was followed successfully in Norway by J. Ugelstad [76,77] using porous polymer particles containing oxidative groups. These particles are then impregnated with an aqueous Fe(II) solution and treated so as to precipitate the Fe(III) oxides within the polymer matrix. This very versatile process also led to a wide variety of products now widely used by biologists.

Although the majority of magnetic latexes present on the present market stem from either of these processes, research on synthesis in this area is still active and many other new approaches are being studied, as demonstrated below by Elaissari and many other approaches are being studied (see Chapter 11).

II. CHALLENGES AND FUTURE DIRECTIONS IN EMULSION POLYMER TECHNOLOGIES: WHAT PRODUCTS FOR TOMORROW?

Although emulsion polymers have been known as products for over half a century, it is surprising to note that growth in the volumes used by industry worldwide has continued to rise and is still estimated at 6% a year up to 2005. Current growth is particularly the result of concerns relating to the protection of human health and the environment all over the world; therefore, market demand is very high to replace solvent-borne polymer systems by water-borne polymers of equivalent or superior performances in applications as paints or adhesives. In addition, developments in technologies used by downstream product consumer industries are accelerating and impose increasingly strict requirements that can only be met with new product generations.

Like all other industrial manufacturers, latex producers are under pressure from consumer associations as well as by new legislations and standards requiring them to incorporate not only all environmental aspects linked with production (such as effluents), but also consumer protection and quality of life.

New problems emerge every day but this situation is also highly stimulating, offering opportunities for innovation that must be taken up to improve the manufacturer's position with respect to the competition. To illustrate these ideas, we will mention a number of issues of concern to many manufacturers below:

A. How to Get Rid of Small Molecules?

The problem of volatile organic compounds (VOCs) is now crucial. These compounds are found in latexes at the end of polymerization; many of them are considered as toxic or liable to toxicity, and regulations are increasingly severe in order to reduce emissions on production sites or further downstream in processing industries. In addition, due to possible migrations, the presence of such products poses problems of even greater importance in some applications, such as foodstuff packaging.

Residual monomers account for a large proportion of the composition of VOCs, but they also contain other organic compounds such as nonpolymerizable impurities of monomers and particularly by-products generated by side reactions taking place in the reaction vessel at the same time as polymerization. Under the effect of radicals, temperature, and pH, reactions between monomer molecules (e.g., Diels-Alder addition reactions, if a dienic monomer is present) are possible, as are chemical modifications of the monomers, transfer agents, surfactants, or other ingredients present in the reaction vessel, by oxidation or hydrolysis.

Major efforts have been devoted by producers to the detection and quanti-

tative analysis of these impurities, but their total elimination still poses considerable problems. This requires increasingly costly effluent extraction and processing operations on industrial sites, the efficacy of which is not always satisfactory. There is thus high receptiveness to any new technology that would enable decisive progress in eliminating these low molar mass impurities under economically acceptable conditions.

Another strategy consists of preventing the formation of these products as much as possible. This highlights the importance of the kinetics at the end of polymerization, which are always very slow; it is therefore necessary to activate them to reduce the residual level of monomers and therefore also the periods at high temperatures in the reaction vessels which favor side reactions. Increased awareness on the part of university researchers of this type of problem would be desirable in terms of progress toward effective solutions.

Polymerization in supercritical CO_2 introduced by J. M. DeSimone in 1994 [78] gave hope for a spectacular reduction in effluent volumes on production sites, but this process, which involves heavy investment, can only function with emulsifiers and initiators suited to these media, which are not readily available and are relatively expensive. In addition, since the vast majority of monomers are highly soluble in supercritical CO_2, its application is restricted to dispersion polymerization or polymerization in inverse emulsion of monomers such as acrylamide [79]. Therefore, it does not appear to be very likely that this type of process will be generalized and adopted for large-tonnage productions of polymer dispersions. On the other hand, the use of supercritical CO_2 as an extraction solvent to remove the last traces of VOCs could be an appropriate solution for processing polymer emulsions for which a high purity is required.

Surfactants, which are also small molecules, pose problems due to their negative effect on the properties of films in wet conditions; their relative incompatibility with polymers induces their migration and segregation at the interfaces, during coalescence and film formation. Therefore, the trend is to reduce their concentration to a maximum in polymerization recipes or to bind chemically to the polymer molecules during polymerization. The new range of polymerizable surfactants (surfmers) now available gives hope for progress [80,81].

B. How to Improve Products' Technical Performances?

In most applications using latexes due to their binding properties, developments are often obstructed by technical difficulties associated with the latex film quality. Three issues are considered to be particularly critical:

Surface hardness,
Solvent sensitivity, and
in particular, mechanical properties under wet conditions

For each of these issues, latex films show deficiencies when compared to the performances of films obtained from organic solutions.

Adding a coalescing aid to formulations is a conventional method to lower the Minimum Film-Forming Temperature (MFT) of high-T_g polymer emulsions and thus obtain a relatively hard surface when the film is formed. This approach is now condemned by a market that is increasingly reluctant to accept the presence of solvent, even at very low levels, in an aqueous formulation.

In addition to the very fine particle size latexes mentioned above, structured latexes represent a possible way to overcome the usual compromises between surface hardness and film formation properties, without requiring the addition of solvent. Some of these products are now marketed, but this approach, which was considered as very promising for a long time, does not appear to have brought about the expected performance levels.

Research is now focusing on the development of hydrodispersed systems in which the physicochemical properties of the polymer are modified markedly during or after coalescence. It is thus hoped to dissociate the factors governing stability in the vessel, coalescence, and mechanical film properties so that they can act separately at the most favorable time.

The development of "cross-linkable latexes" stems from its approach. Some room temperature cross-linkable or photo-cross-linkable products have been developed for specific applications and are now on the market [82,83]. Recent articles [84] propose attractive solutions, particularly using functionalized latexes with acetal functions that only react under dry conditions. However, to our knowledge, there is not yet an entirely satisfactory general solution, and it can be said that research to find a "one-pack system" that is reactive at ambient temperature but stable in storage, and does not pose problems in terms of VOCs, toxicity, film blistering, or formation of colored material, is still underway.

C. How to Increase the Solid Content of Dispersions?

Most industrial processes produce latexes with polymer contents between 40% and 55%. A marked increase in the polymer content offers many potential technical and economic advantages arising from productivity gains for reaction vessels and a reduction of storage and transport costs. The decrease in production costs is particularly significant if the latex is spray-dried to allow recovery of the polymer and its marketing it as a dry powder. In terms of applications, a high solid content reduces film drying times and limits problems due to film shrinkage during drying.

It has been known for some time that it is possible to expect particle volume fractions in excess of 70%, while retaining an acceptable viscosity by adjusting the grain size distribution of the particles. There are a number of recipes to

produce synthetic rubber latexes showing very broad particle size distributions and solid contents above 60%, which are used for foam production. However, these recipes are the result of semiempirical approaches that cannot easily be generalized to other systems.

It is reasonable to assume that this situation may change with increased understanding of polymerization mechanisms and particularly the new sensors that are emerging to indicate in real time what is happening in a reaction vessel [85–89]. Recent studies by T. McKenna [90–92] demonstrate that by selecting the appropriate initiator system and programming seed introductions, it is possible to reliably obtain multimodal latexes with solid contents in excess of 70%.

D. How to Meet Demand from "High Technology" Markets?

The versatility and diversity of emulsion polymerization processes make it possible to propose an astounding variety of particles. Nevertheless, the demand is insatiable for ever more complex products. In the face of fantastic developments in biotechnologies and the overactive imagination of biologists, latex producers, startups, or major chemical groups are continuously required to broaden their product range further. This is a delicate situation given that the volumes required are often low and technologies frequently become rapidly obsolete in these areas.

Since quality is a crucial issue, research chemists in close cooperation with their biologist partners must bear in mind that they must supply well-defined and perfectly reproducible products.

In terms of products, it appears clear that diagnostic or biotechnology applications will amplify their demand for particle families that are already utilized but in which they would like to see modifications. Significant interest will be aimed at more recent products currently in the R&D stage.

Magnetic latexes belong to the first category. "Smart particles," introduced into the biomedical field by the research conducted by Kawaguchi in Japan and C. Pichot and H. Elaissari in France, and which will be presented in another chapter of this book, are certainly an example of the second category. These particles show remarkable surface properties that can be controlled by temperature, ionic strength, or pH; positively or negatively charged and even magnetizable, they represent a very attractive product class that should be used advantageously in cell sorting and analytical affinity chromatography or preparative chromatography.

To date, polymer particles were essentially considered by biologists as substrates enabling improved management of reactions between antagonistic molecular species and the isolation of certain products. Very recent research is attracting attention to the possibilities of labeling biological molecules with suitable

latex particles, as performed conventionally with an enzyme, a fluorescent marker, or a radioactive isotope. In this way, Y. Chemla [93] envisages the emergence of a new class of diagnostic tests based on the detection by ultrasensitive tools of magnetic signals that appear when molecules labeled with very fine magnetic particles react with a target. They represent highly sensitive, direct-reading homogeneous medium tests, involving no separation stages.

Another interesting example is that of polymer particles containing "quantum dots" of cadmium selenide [94]. Each particle of this composite can transmit a very pure fluorescence signal contingent on the size and number of crystals it contains. By associating particles of this type with molecules, it becomes possible to create an identification system using an optical "spectral code," similar to a "bar code," and thus distinguish between each of its neighbors. This system implies significant potential applications in high-throughput screening tests associated with the developing combinatorial strategies for the selection of new active molecules.

Nanotechnologies certainly represent another area in which "smart" polymer-based particles have a future. They can be used advantageously in microfluidics and more particularly to produce "lab-on-a-chip" systems, in which the mixing, separation/washing, and analysis operations are carried out in sequence. Magnetic particles, capable of swelling or retracting, in which the surface area may vary under the effect of various stimuli, are potentially of great interest as vehicles to carry molecules and release them in the desired areas, or to produce microvalves and routing systems for fluid management. Another benefit of magnetic particles is that they can be used to produce self-assembling micronetworks under the effect of a magnetic field. Initial applications of this sophisticated technique are proposed by J. L. Viovy and J. Bibette for the separation of biological objects of micronic size such as large DNA molecules or cells [95,96].

Several works [97,98], (Chapter 13 in this volume) have demonstrated that it is possible to envisage selective deposition of colloidal particles of very uniform diameter on plane surfaces and thus obtain patterned surfaces. Therefore, it is possible to access microelectronic devices and chemo- or biosensors the already rapid development of which can only be expected to grow in coming years.

E. What Will the Processes and Products of Tomorrow Be?

It is somewhat surprising to note that the miniemulsion polymerization process, introduced by El Aasser and Ugelstad over 25 years ago, and which has been the subject of a large number of academic research projects, has not seen genuine success in industry. The need to produce large volumes of very fine and very stable monomer emulsions to feed the reaction vessels poses some technical and

economic problems, and this probably explains this reluctance. This situation seems to be changing due to progress in emulsification technology and dispersion equipment, as well as due to increased awareness of the potential offered by many aspects of this technology. For example, polymerization in droplets is an asset for the development of continuous polymerization processes; polyaddition and ring-opening polymerizations can be carried out in dispersed media using this technique [99,100]; it is also an easy method to access structured particles, particularly composite particles which are under growing demand for high added value applications [101,102].

New prospects are also emerging from the association of this process with the latest progress in macromolecular synthesis. For example, the use of miniemulsions enabled J. Claverie to make significant progress in the polymerization of ethylene and other olefins in aqueous media with new chelated Ni catalysts [103]. New, highly hydrophobic emulsion polymers with a high chemical resistance should result from this pioneering work. The miniemulsion process also seems to be the most promising to adapt controlled radical polymerization technology to dispersed media [104,105]. The repercussions of controlled radical polymerization on the development of polymers in dispersion are still difficult to assess. It will be seen in Chapter 2 in this volume that many teams are currently working actively on this very attractive subject, with various reversible radical deactivation or degenerative transfer reaction processes. The long-term objective is the synthesis of polymer particles and particularly molecular architecture copolymers, but the literature is not very explicit concerning the real advantages that can be expected in terms of applications. It is more realistic to consider that initially these techniques will be more useful for carrying out molecular engineering on the surface of particles and obtaining higher colloidal stabilities and new properties. The synthesis of new thickeners or new polymer surfactants of particular interest for polymerization also appears to be relatively easy to access using approaches, and research could lead to commercial products of this type in the near future [106,107].

Although radical polymerization in emulsion is now the most frequently used technology to prepare aqueous polymer dispersions used in the composition of paints or other coatings, it is possible to ask whether this situation will continue when the progress achieved in recent years by alkyd resin, polyester, polyurethane, and silicone producers is evaluated. These various polymers are now available in the form of high-quality aqueous dispersions, practically free of VOCs, which are very well positioned with respect to vinyl or acrylic dispersions to substitute solvent systems. The association of various families of dispersions, with different film formation mechanisms, also merits consideration to try to combine the advantages of each system and weaken their drawbacks. This may be envisaged by mixing dispersions [108] or with hybrid particles containing two types of polymers.

For applications in biotechnologies, biodegradable polymer particles are in considerable demand for drug encapsulation and delivery. Such particles are prepared using processes other than free-radical emulsion polymerization. Ionic emulsion polymerizations have thus been used to obtain particles or nanocapsules of polyalkylcyanoacrylates. Another strategy consists of emusifying a biodegradable polymer that can be of natural or synthetic origin, using an organic solvent that is subsequently eliminated; many examples with cellulose derivatives, polyhydroxyalkanoates, or poly(lactide-co-glycosides) are reported in the literature [109–111]. There are also methods to prepare nanoparticles or nanocapsules of polymers by precipitating the polymer in a controlled manner using an aqueous or organic solution or by self-assembly of amphiphilic polymers in an aqueous phase; in this way, micro- and nanoparticles or capsules based on alginate [112,113], chitosan [114], polyanhydrides [115], or polyaminoacids [116] have been described.

C. Vauthier, who recently conducted an exhaustive review of these techniques [117], and S. Slomkowski, both present in chapters of this book (chapters 28 and 29, respectively) examples of alkylcyanoacrylate-based nanocapsule and nanoparticle synthesis and applications. This will give a clearer idea of the benefits involved if it is taken into account that an increasing fraction of the new generations of drugs and vaccines is composed of active substances that are slightly soluble in water or of high molar masses (peptides, proteins, DNA, etc.). For this reason, their bioavailability is low when they are administered in a conventional manner. The use of biodegradable polymer nanoparticles as a vehicle is considered with great interest to solve this problem; it is hoped that such materials will improve the transport of active substances, protect them from degradation, bring them more specifically to the vicinity of their target, and prolong their action.

III. CONCLUDING REMARKS

A brief overview of the long history of polymer emulsions may give the impression that these products have reached a mature phase and not much can be expected in this area in terms of innovation. We have tried to show that this is not the case. Academic research is still very active and industry is showing clear strategies to develop new products capable of substituting the still-in-use solvent systems advantageously or to broaden the scope of technologies available in this area.

Appropriate solutions are now expected to meet universal demand for products with higher performances that protect the environment, are easier to use, and/or contribute to the exceptional expansion currently seen in bio- and nanotechnologies.

In the face of all these challenges, we have seen that polymer chemists still have many promising ideas to meet them. However, polymer chemists are not

the only ones who can offer solutions. It is necessary to consider the remarkable progress achieved in inorganic synthesis chemistry, which is now capable of preparing large quantities of inorganic dispersions using very simple procedures and very mild operating conditions. These colloidal systems are often also perfectly defined in terms of shape and size, and range from a few nanometers to a few hundred nanometers in particle diameter. Nanoparticles of noble metals, metal oxides, or semiconductor materials, such as CdS, CdSe, TiO_2, etc., may, for example, be generated through perfect control of the growth of nuclei from small precursor molecules by means of thermal decomposition, hydrolysis, reduction, or any other chemical reaction in solution [118–124]. The optical, electronic, magnetic, or catalytic properties of these nanoparticles are often astounding; they depend on the size and immediate environment, and are different from those of bulk products of the same composition. Their use is starting to become more widespread in diagnostics (as in gold nanoparticles), but there are other promising prospects in the area of coatings [125] or perfectly organized nanostructured materials [126]. This situation indicates that future generations of products will probably be devised from a very broad vision of colloidal physicochemicals and as a result of selecting or associating appropriate technologies by all those on offer by polymer chemists and experts in inorganic synthesis.

REFERENCES

1. Dunn, A.S. Harkins, Smith-Ewart and related theories. In *Emulsion Polymerization and Emulsion Polymers*, Lovell, P.A., El-Aasser, M.S., Eds.; John Wiley & Sons Ltd: Chichester, 1997; 125–163.
2. Harkins, W.D. J. Am. Chem. Soc. **1947**, *69*, 1428.
3. Smith, W.V.; Ewart, R.H. J. Chem. Phys. **1948**, *16* (6), 592.
4. Fitch, R.M.; Tsai, C.H. In *Polymer Colloids*; Fitch, R.M., Ed.; Plenum Publishers: New York, 1971; 73–101.
5. Ugelstad, J.; El Aasser, M.S.; Vanderhoff, J.W.. Polym. Lett. **1973**, *111*, 503.
6. Ugelstad, J.; Hansen, F.K.; Lange, S. Makromol. Chem. **1974**, *175*, 507.
7. Hansen, F.K.; Ugelstad, J. J. Polym. Sci., Polym. Chem. Ed. **1979** *17*, 3069.
8. Napper, D.H.; Gilbert, R.G. Makromol. Chem., Macromol. Symp. **1987**, *10/11*, 503.
9. Gardon, J.L. In *Polymerization Processes*, 2nd Ed.; Schildknecht, C.E., Skeist, I., Eds.; Interscience: New York, 1977; 143.
10. Hansen, F.K.; Ugelstad, J. In *Emulsion Polymerization*; Piirma, I., Ed.; Academic Press: New York, 1982; 51.
11. Hansen, F.K. In *Polymer Latexes*: *Preparation*, *Characterization and Application*. Daniels, E.S., Sudol, E.D., El-Aasser, M.S., Eds.; ACS Symp. Series 492: Washington, DC, 1992; 12–27.
12. Hamielec, A.E.; MacGregor, J.F. Modelling copolymerizations: Control of chain microstructure, long chain branching, crosslinking and molecular weight distribu-

tion. In *Proceedings of International Berlin Workshop on Polymer Reaction Engineering*, Berlin, 1983.
13. Broadhead, T.O.; Hamielec, A.E.; MacGregor, J.F. Dynamic modelling of the batch, semi-batch and continuous production of styrene/butadiene copolymers by emulsion polymerization. Makromol. Chem. **1985,** (Suppl 10/11), 105–128.
14. Nomura, M.; Horie, I.; Kubo, M.; Fujita, K. J. Appl. Polym. Sci. **1989**, *37*, 1029.
15. Guillot, J. In *Polymer Reaction Engineering*. Reichert, R., Geiseler, W., Eds.; Huthig and Wepf: Berlin, 1986; 147.
16. Guillot, J. Thermodynamic aspects in emulsion copolymerization. Makromol. Chem. **1985** (Suppl 10/11), 235–264.
17. Gilbert, R.G. Modelling rates, particle size distributions and molar mass distributions. In *Emulsion Polymerization and Emulsion Polymers*; Lovell, P.A., El-Aasser, M.S., Eds.; John Wiley and Sons Ltd: Chichester, 1997; 165–203.
18. Charmot, D. Network formation in free-radical emulsion polymerization. In *Polymeric Dispersions*: *Principles and Applications*; Asua, J.M., Ed.; NATO ASI Series E: Applied Sciences, 335, Kluwer Academic: Dordrecht, 1997; 79–96.
19. Plessis, C.; Arzzamendi, G.; Leiza, J.R.; Schoonbrood, H.A.S.; Charmot, D.; Asua, J.M. Kinetics and polymer microstructure of the seeded semibatch emulsion copolymerization of n-butyl acrylate and styrene. Macromolecules **2001**, *34* (15), 5147–5157.
20. Sayer, C.; Araujo, P.H.H.; Arzamendi, G.; Asua, J.M.; Lima, E.L.; Pinto, J.C. Modeling molecular weight distribution in polymerization reactions with transfer to polymer. J. Polym. Sci. A-Polym. Chem. **2001**, *39* (20), 3513–3528.
21. Asua, J.M. Control of emulsion polymerization reactors using a hierarchical fuzzy logic/model based controller. Polym. React. Eng. **2001**, *9* (1), 37–67.
22. Vicente, M.; Sayer, C.; Leiza, J.R.; et al. Dynamic optimization of non-linear emulsion copolymerization systems: Open loop control of composition and molecular weight distribution. Chem. Eng. J. **2002**, *85*, 339–349.
23. Verwey, E.J.W.; Overbeck, J.T.G. *Theory of the Stability of Lyophobic Colloids*; Elsevier: Amsterdam, 1948.
24. Heller, W.; Pugh, T.L. J. Chem. Phys. **1954**, *22*, 1778.
25. Napper, D.H. *Polymeric Stabilization of Colloidal Dispersion*. Academic Press: London, 1983.
26. de Gennes, PG. Polymers at an interface: A simplified view. Adv. Colloid Interface Sci. **1987**, *27*, 189–209.
27. Israelachvili, J.; Wennerstrom, H. Role of hydration and water structure in biological and colloidal interactions. Nature **1996**, *379*, 219–225.
28. Bangs, L.B. Uniform latex particles. Am. Clin. Prod. Rev. **1988**, Jan.
29. Singer, J.M.; Plotz, C.M. The latex fixation test. Am. J. Med. **1956**, *21*, 888–892.
30. Hager, H. U.S.Patent 3,857,931, 1974.
31. Daniel, J.C. Latex de particules structurées. Makromol. Chem., **1985**, (Suppl 10/11), 359–390.
32. Okubo, M.; Kanaida, K.; Matsumoto, T. J. Appl. Polym. Sci. **1987**, *33*, 1511.
33. Okubo, M.; Kanaida, K.; Matsumoto, T. Colloid Polym. Sci. **1987**, *265*, 876.

34. Okubo, M. Makromo. Chem., Macromol. Symp. **1990**, *35*, 307.
35. Guyot, A.; Guillot, J.; Pichot, C.; Rios-Guerros, L. In *New Design for Producing Constant Composition Copolymers in Emulsion Polymerization*; Bassett, D.R., Hamielec, A.H., Eds.; ACS Symp. Series 165: Washington, DC, 1981; 415.
36. Rios, C.; Hidalgo, M.; Cavaillé, J.Y.; Guillot, J.; Guyot, A.; Pichot, C. Polystyrene(1) polybutylacrylate-methacrylic acid(2) core-shell emulsion polymers. Part I, Synthesis and colloidal characterization. Colloid Polym. Sci. **1991**, *269*, 812.
37. Kong, X.Z.; Pichot, C.; Guillot, J.; Cavaillé, J.Y.. Studies on particle morphology in vinyl acetate-butyl acrylate emulsion copolymers. In *Polymer Latexes*: *Preparation*, *Characterization and Application*; Daniels, E.S., Sudol, E.D., El-Aasser, M.S., Eds.; ACS Symp. Series 492; Washington DC, 1992; 163.
38. Durant, Y.G.J.; Guillot, J. Colloid Polym. Sci. **1993**, *271*, 607.
39. Dimonie, V.L.; Daniels, E.S.; Shaffer, O.L.; El-Aasser, M.S. Control of particle morphology. In *Emulsion Polymerization and Emulsion Polymers*; Lovell, P.A., El-Aasser, M.S., Eds.; John Wiley and Sons Ltd: Chichester, 1997; 293–326.
40. Lee, S.; Rudin, A. In *Polymer Latexes*: *Preparation*, *Characterization and Application*. Daniels, E.S., Sudol, E.D., El-Aasser, M.S., Eds.; ACS Symp Ser 492; Washington, DC, 1992; 234.
41. Lee, S.; Rudin, A. J. Polym. Sci. A. Polym. Chem. **1992**, *30*, 865–871.
42. Sundberg, D.C.; Casassa, A.P.; Pantazopoulos, J.; Muscato, M.R. J. Appl. Polym. Sci. **1990**, *41*, 1425.
43. Ivarsson, L.E.; Karlson, O.J.; Sundberg, D.C. Influence of glass transition temperature on latex particle morphology. In *Polymers in Dispersed Media*; Claverie, J., Charreyre, M.-T., Pichot, C., Eds.; Macromol. Symp. 150–151; Wiley VCH: Weinheim, 2000; 407–412.
45. Gonzales-Ortiz, L.J.; Asua, J.M. Development of particle morphology in emulsion polymerization. I. Cluster dynamics. Macromolecules **1995**, *28*, 3135–3145.
46. Gonzales-Ortiz, L.J.; Asua, J.M. Development of particle morphology in emulsion polymerization. 2. Cluster dynamics in reacting systems. Macromolecules **1996**, *29*, 383–389.
47. Kowalski, A.; Vogel, M.; Blankenship, M. Eur. Patent 22,633. US Patent 4,427,836.
48. Okubo, M.; Shiozaki, M.; Tsujihiro, M.; Tsukuda, Y. Preparation of micron-size polymer particles utilizing the dynamic monomer swelling method. Colloid Polym. Sci. **1991**, *269*, 222–226.
49. Okubo, M.; Minami, H. Colloid Polym. Sci. **1997**, *275*, 992.
50. Okubo, M.; Minami, H. Production of microsized monodispersed anomalous polymer particles having red blood corpuscle shape. In *Polymers in Dispersed Media*; Claverie, J., Charreyre, M.-T., Pichot, C., Eds.; Macromol. Symp. 150–151; Wiley VCH: Weinheim, 2000; 201–210.
51. Omi, S.; Ma, G.-H.; Nagai, M. Membrane emulsification—a versatile tool for the synthesis of polymeric microspheres. In *Polymers in Dispersed Media*; Claverie, J., Charreyre, M.-T., Pichot, C., Eds.; Macromol. Symp. 150–151; Wiley VCH: Weinheim, 2000; 319–330.
52. Vanderhoff, J.W.; El-Aasser, M.S.; Kornfeld, D.M.; Micale, Y.; Sudol, E.D.; Tseng, C.M.; Shen, H.R. *Mater. Res. Soc. Symp. Proc.* 87, 1987, 213–223.

53. Ugelstad, J.; Mork, P.C.; Nordhuus, I.; Mfutakamba, H.; Soleimany, E. Thermodynamics of swelling. Preparation and application of some composite, monosized polymer particles. Makromol. Chem. **1985,**(Suppl 10/11) 215–234.
54. Barrett, K.E.J., Ed. *Dispersion Polymerization in Organic Media*; Wiley-Interscience: New York, 1975.
55. Almog, Y.; Levy, M. J. Polym. Sci., Chem. Ed. **1980**, *18*, 1.
56. Bromley, C.W.; Davies, S.P. Novel waterborne latices. In Proceedings of the 11th Waterborne and High Solids Coatings Symposium, New Orleans, 1986; 133–145.
57. Croucher, M.D.; Winnick, M.A. In *Future Directions in Polymer Colloids*; El-Aasser, M.S., Fitch, R.M., Eds.; NATO ASI Applied Sciences; Martinus Nijhoff: Boston, 1987; 209–227.
58. Paine, A.J. Dispersion polymerization of styrene in polar solvents. I- Grafting mechanism of stabilization by hydroxypropyl cellulose. J. Colloid Interface Sci. **1990**, *138* (1), 157–169.
59. Paine, A.J.; Deslandes, Y.; Gerroir, P.; Henrissat, B. Dispersion polymerization of styrene in polar solvents. II. Visualization of surface layers of steric stabilizers on dispersion-olymerized and precipitated polystyrene latex particles by transmission electron microscopy. J. Colloid Interface Sci. **1990**, *138* (1), 170–181.
60. Paine, A.J. Dispersion polymerization of styrene in polar solvents. IV. Solvency control of particle size from hydroxypropyl cellulose stabilized polymerizations. J. Polym. Sci. A Polym. Chem. **1990**, *28*, 2485–2500.
61. Graillat, C.; Pichot, C.; Guyot, A. Preparation and characterization of low size polystyrene latex particles with various strong acid surface charges. Colloids Surf. **1991**, *56*, 189.
62. Larpent, C.; Bernard, E.; Richard, J.; et al. Macromolecules **1997**, *30*, 354–362.
63. Larpent, C.; Bernard, E.; Richard, J.; et al. React. Funct. Polym. **1997**, *33*, 49–59.
64. Candau, F. Inverse emulsion and microemulsion polymerization. In *Emulsion Polymerization and Emulsion Polymer*; Lovell, P.A., El-Aasser, M.S., Eds.; John Wiley and Sons Ltd: Chichester, 1997; 723–741.
65. Candau, F. Microemulsion polymerization. In *Polymeric Dispersions*: *Principles and Applications*; Asua, J.M., Ed.; NATO ASI Series E: Applied Sciences, 335; Kluwer Academic: Dordrecht, 1997; 127–140.
66. Rhodia,. *Coatings and Construction Materials*. *The Ultrafine Technology*; Technical brochure, 2000.
67. Espiard, P.; Revillon, A.; Guyot, A.; Mark, J.E. Nucleation of emulsion polymerization in the presence of small silica particles. In *Polymer Latexes*: *Preparation*, *Characterization and Application*; Daniels, E.S., Sudol, E.D., El-Aasser, M.S., Eds.; ACS Symp. Series 492, Washington, DC, 1992; 387.
68. Bourgeat-Lami, E.; Lang, J. Silica-polystyrene composite particles. In *Polymers in Dispersed Media*; Claverie, J., Charreyre, M.-T., Pichot, C., Eds.; Macromol. Symp. 150–151, Wiley VCH: Weinheim, 2000; 377–385.
70. Caris, C.H.M.; Kuijpers, R.P.M.; van Herk, A.M.; German, A.L. Makromol. Chem., Makromol. Symp.; **1990**, *35/36*, 535–548.

71. van Herk, A.M. Encapsulation of inorganic particles. In *Polymeric Dispersions*: *Principles and Applications*; Asua, J.M., Ed.; NATO ASI Series E: Applied Sciences, 335; Kluwer Academic: Dordrecht, 1997; 435–450.
72. Yen, S.P.S.; Rembaum, A.; Molday, R.S. US Patent 4,157,323, 1977.
73. Daniel, J.C.; Schuppiser, J.L.; Tricot, M. Magnetic polymer latex and preparation process. Fr. Pat. Appl. 80 08696, 1980, Apr. 18. US Patent 4,358,388.
74. Charmot, D.; Vidil, C. Fr. Pat. Appl. 8904231. Eur. Patent Appl. 0 390 634 B1.
75. Richard, J.; Vaslin, S. Fr. Patent Appl. 95 07486. Eur. Pat. 0 777 691 B1.
76. Ugelstad, J.; Ellingsen, T.; Berge, A.; Helgee, B. PCT Patent Appl. W0 837/03920.
77. Ugelstad, J.; Mork, P.C.; Kaggerud, K.H.; Ellingsen, T.; Berge, A. Swelling of oligomer particles. New methods of preparation of emulsions and polymer dispersions. Adv. Colloid Interface Sci. **1990**, *13*, 101–140.
78. DeSimone, J.M.; Maury, E.E.; Menceloglu, Y.Z.; et al. Science **1994**, *265*, 356.
79. Kendall, J.L.; Canelas, D.; Young, J.; DeSimone, J.M. Polymerization in supercritical carbon dioxide. Chem. Rev **1999**, *99*, 543–563.
80. Yang, H.S.; Adam, H.; Kiplinger, J.; et al. New polymerizable surfactants for emulsion polymerization. In Int. Waterborne, High-Solids and Powder Coatings Symposium, New Orleans, Feb. 21–23, 2001.
81. Mestach, D. New high performance materials for waterborne acrylic surface coatings. Eurocoat 2001, 1: 35–49.
82. Mestach, D. Polym. Paint Col. J. **2000**, *190* (4431), 28.
83. Akzo Nobel Resins. Setalux self-crosslinking dispersions for industrial wood coatings. Technical brochure, Sept. 2001.
84. Soares, C.; Charleux, B.; Vairon, J.P.; Vergé, C.; Loyen, K. New acetal functionalized latex films capable of crosslinking at ambiant temperature. In *Film Formation in Coatings*: *Mechanisms*, *Properties and Morphology*; Provder, T., Urban, M.W., Eds.; ACS Symp. Series 790, 9: Washington, DC, 2001; 157.
85. Hergeth, W.D. On-line characterization methods. In *Polymeric Dispersions*: *Principles and Applications*; Asua, J.M., Ed.; NATO ASI Series E: Applied Sciences, 335; Kluwer Academic: Dordrecht, 1997; 267–288.
86. van den Brink, M.; Pepers, M.; van den Herk, A.M.; et al. Emulsion (co)polymerization of styrene and butyl acrylate monitored by on-line Raman Spectroscopy. In *Polymers in Dispersed Media*; Claverie, J., Charreyre, M.-T., Pichot, C., Eds.; Macromol. Symp. 150–151, Wiley-VCH: Weinheim, 2000; 121–126.
87. Agnely, M.; Amram, B.; Charmot, D.; et al. On-line monitoring of styrene/butadiene emulsion polymerization by Raman spectroscopy. In Proceedings of the 4th International Symposium on Polymers in Dispersed Media, Lyon, 1999; 53.
88. Siali, A.; Sorti, G.; Morbidelli, M. Proceure for calibrating an ultrasonic sensor for monitoring of conversion in latex reactors. J. Appl. Sci. **1999**, *72*, 1451.
89. Veira, R.A.M.; Sayer, C.; Lima, E.L.; Pinto, J.C. In-line and in situ monitoring of semi-batch emulsion copolymerizations using near-infrared spectroscopy. J. Appl. Polym. Sci. **2002**, *84* (14), 2670–2682.
90. McKenna, T.F. Production de latex à hauts taux de solides: Mise au point et caractérisation rhéologique. 20ème Réunion du Club Emulsion, Lyon, Oct 29–30, 2001.
91. Schneider, M.; Graillat, C.; Guyot, A.; McKenna, T.F. High solids content emul-

sions. Part III: Synthesis of concentrated latexes via classic emulsion polymerization. J. Appl. Polym. Sci. **2002**, *84* (10), 1916–1934.
92. Schneider, M.; Graillat, C.; Guyot, A.; Betrémieux, I.; McKenna, T.F. High solids content emulsions. Part IV: Improved strategies for producing concentrated latexes. J. Appl. Polym. Sci. **2002**, *84* (10), 1935–1948.
93. Chemla, Y.; Grossman, H.L.; Poon, Y.; McDermott, R.; Stevens, R.; Alper, M.D.; Clarke, J. Ultrasensitive magnetic biosensor for homogeneous immunoassay. Proc. Natl. Acad. Sci. USA **2000**, *97* (26), 14268–14272.
94. Han, M.; Gao, X.; Su, J.Z.; Nie, S. Quantum-dot-tagged microbeads for multiplexed optical coding of biomolecules. Nature Biotechnol. **2001**, *19* 631–635.
95. Bibette, J.; Michel, J.; Mayer, P.; Viovy, J.L. Eu. Patent 0 941 142.
96. Doyle, P.; Bibette, J.; Bancaud, A.; Viovy, J.L. Self-assembled magnetic matrices for DNA separation chips. Science **2002**, *295*, 2237.
97. Slomkowski, S. Polyacrolein containing microspheres: Synthesis, properties and possible medical applications. Prog. Polym. Sci. **1998**. *23*, 815–874.
98. Zheng, H.; Lee, H.; Rubner, M.R.; Hammond, P.T. Two-dimensional patterning of colloidal arrays on polymer templates for photonic applications. Polym. Prepr. **2002**, *43* (1), 17–18.
99. Landfester, K.; Tiarks, F.; Hentze, H.-P.; et al. Polyaddition in miniemulsions: A new route to polymer dispersions. Macromol. Chem. Phys. **2000**, *2001*, 1.
100. Barrere, M.; Maitre, C.; Dourges, M.A.; Hemery, P. Anionic polymerization of 1,3,5-tris(trifluoropropylmethyl)cyclotrisiloxane in miniemulsion. Macromolecules **2001**, *34* (21), 7276–7280.
101. Tiarks, F.; Landfester, K.; Antonietti, M. Encapsulation of carbon black by miniemulsion polymerization. Macromol. Chem. Phys. **2001**, *202* (1), 51–60.
102. Tiarks, F.; Landfester, K.; Antonietti, M. Silica nanoparticles as surfactants and fillers for latexes made by miniemulsion polymerization. Langmuir **2001**, *17*, 5775.
103. Soula, R.; Saillard, B.; Spitz, R.; Claverie, J. Catalytic copolymerization of ethylene and polar and non polar alpha-olefins in emulsion. Macromolecules **2002**, *35* (5), 1513–1523.
104. Pan, G.; Sudol, E.D.; Dimonie, V.L.; El Aasser, M.S. Nitroxide-mediated living free radical miniemulsion polymerization. Macromolecules **2001**, *34*, 481–488.
105. Qiu, J.;Charleux, B.; Matyjaszewski, K. Controlled/living radical polymerization in aqueous media: Homogeneous and heterogeneous systems. Progr. Polym. Sci. **2001**, *26* (10), 2083–2134.
106. Davis, K.A.; Charleux, B.; Matyjaszewski, K. Preparation of block copolymers of poly(styrene) and poly(t-butylacrylate) of various molecular weights and architectures by atom transfer radical polymerization. J. Polym. Sci., Polym. Chem. **2000**, *38*, 2274.
107. Bruguiere, C.; Pascual, S.; Bui, C.; et al. Block copolymers of poly(styrene) and poly(acrylic acid) of various molecular weights and topologies applied as stabilizers in styrene emulsion polymerization. Macromolecules **2001**, *34*, 4439.
108. Dekker, G.H. Water, the "solvent" of the near future. Eurocoat 2001, 1, 19–32.
109. Rice, T.R.; Gilley, R.M. Preparation of injectable controlled-release microcapsules by a solvent-evaporation process. J. Contr. Rel. **1985**, *2*, 343–452.
110. Rhône-Poulenc. Fr. Patent Appl. 90 04471, 91 08041, 91 08042.

111. Gref, R.; Minamitake, Y.; Peracchia, M.T.; Trubetskoy, V.; Torchilin, V.; Langer, R. Science **1994**, *18*, 1600.
112. Rajaonarivony, M.; Vauthier, C.; Couarraze, G.; et al. Developments of a new drug carrier made from alginate. J. Pharm. Sci. **1993**, *82*, 912–917.
113. Rastello-de Boisseson, M. Microparticules d'alginates associatifs: Elaboration, caractérisation et encapsulation de molécules actives. PhD dissertation, Institut National Polytechnique de Lorraine, Nancy, France, 2002.
114. Calvo, P.; Remunan-Lopez, C.; Vila-Jato, J.L.; Alonso, M.J. J. Appl. Polym. Sci. **1997**, *63*, 125–132.
115. Mathiowitz, E.; Jacob, J.S.; Jong, Y.S.; et al. Biologically erodable microspheres as potential oral drug delivery systems. Nature **1997**, *386*, 410–414.
116. Flamel Technologies. Fr. Pat. Appl. 95 03978. US Patent 5904936.
117. Fattal, E.; Vauthier, C. Nanoparticles as drug delivery systems. In *Encyclopedia of Pharmaceutical Technology*; Swarbrick, J., Boylan, J.C., Eds.; Marcel Dekker: New York, 2002; 1874–1892.
118. Privman, V.; Goia, D.V.; Park, J.; Matijevic, E. Mechanism of formation of monodispersed colloids by aggregation of nanosize precursors. J. Colloid. Interface Sci. **1999**, *213*, 36–45.
119. Goia, D.; Matijevic, E. Tailoring the particle size of monosizes colloidal gold. Colloids Surf A. Physicochem. Eng. Asp. **1999**, *146*, 139–152.
120. Feltin, N.; Pileni, M.P. Langmuir **1997**, *13*, 3927.
121. Peng, X.; Manna, L.; Yang, W.; Wickham, J.; Scher, E.; Kadavanick, A.; Alivasitos, P. Shape control of CdSe nanocrystals. Nature **2000**, *404* (March 12), 59–61.
122. Puntes, V.; Krishnan, K.; Alivasitos, P. Colloidal nanocrystals: Shape and size control—The case of cobalt. Science **2001**, *291* (March 16), 2115–2117.
123. Hyeon, T.; Lee, S.S.; Park, J.; Chung, Y.; Bin Na, H.. Synthesis of highly crystalline and monodispersed maghemite nanocrystallites without a size-selection process. J. Am. Chem. Soc. **2001**, *123* (51), 12798–12801.
124. Limanovitch, O.E.; Bogdanov, A.G.; Papisov, I.M. Polym. Sci. Series B **2001**, *43* (1), 26.
125. Coy, D.C. (Nanophase Technology Co). The industrial manufacture and applications of nanoparticles. AIChE Fall Meeting, Nov 2001.
126. Niemeyer, C.M. Nanoparticles, proteins, and nucleic acids: Biotechnology meets materials science. Angew. Chem. Int. Ed. **2001**, *40*, 4128–4158.
127. Liu, M.; Ragheb, A.; Zelisko, P.; Brook, M.A. In *Colloidal Polymers*: *Preparation and Biomedical Applications*; Elaissari, A., Ed. Marcel Dekker: New York, 2002; 309–327.
128. Delair, T. Colloidal particles. In *Colloidal Polymers*: *Preparation and Biomedical Applications*; Elaissari, A., Ed. Marcel Dekker: New York, 2002; 309–327.
129. Vouthier, C.; Couvreur, P.; Dubernet, C. In *Colloidal Polymers*: *Preparation and Biomedical Applications*; Elaissari, A., Ed. Marcel Dekker: New York, 2002; 349–370.
130. Slomkowski, S. In *Colloidal Polymers*: *Preparation and Biomedical Applications*; Elaissari, A., Ed. Marcel Dekker: New York, 2002; 371–427.
131. Richard, J.; Deschamps, F.S. Applications in the therapeutic area. In *Colloidal Polymers*: *Preparatin and Biomedical Applications*; Elaissari, A., Ed. Marcel Dekker: New York, 2002; 429–475.

2

Controlled Free-Radical Polymerization

A Way to Design Polymer Architecture and Surface Properties of Latex Particles

CÉLINE FARCET, CARINE BURGUIÈRE, and BERNADETTE CHARLEUX Université Pierre et Marie Curie, Paris, France

I. INTRODUCTION

Free-radical polymerization offers the invaluable advantage of being tolerant to water, allowing the reaction to be carried out in aqueous solution or aqueous dispersed systems. With the various types of radical polymerization in aqueous dispersions, such as suspension, emulsion, miniemulsion, microemulsion, and so forth, combined with multistep processes, it is possible to fine-tune the size, morphology, and chemical functionality of the polymer particles [1–3].

However, because of the features of radical chemistry, the polymer composing those particles is generally ill defined. With the emergence of controlled radical polymerization (CRP), the possibility of controlling the polymer molecular characteristics was brought about [4–8]. Whereas CRP has been initially applied to bulk or solution polymerizations, the transfer to aqueous dispersed systems is more recent, and was shown to be possible but not straightforward [9]. Therefore, the synthesis of latexes with well-defined homopolymers or copolymers with complex architecture can be anticipated. From this new chemistry, novel types of polymer particles will arise with still unknown properties.

Controlled free-radical polymerization offers the additional possibility to synthesize amphiphilic block copolymers, with controlled structure, predetermined molar mass, and narrow molar mass distribution. Such amphiphilic block copolymers can be used as stabilizers in emulsion polymerization to control both the number of particles and their surface properties [10]. Hairy particles can thus be obtained with a tailored hydrophilic shell. The same goal can be achieved by

grafting water-soluble polymer chains from the particle surface, owing to the advantage that CRP offers to design well-defined initiators that remain stable in conventional free-radical polymerization and can be activated under selected conditions.

This chapter aims at presenting the results obtained in the Laboratoire de Chimie Macromoléculaire of University Pierre and Marie Curie (Paris) and concerning controlled free-radical polymerization in conjunction with various aspects of emulsion polymerization. In a first part, nitroxide-mediated controlled free-radical polymerization performed in emulsion and miniemulsion systems is exposed. In a second part, the use of amphiphilic block copolymers as stabilizers in emulsion polymerization is described. Finally, aqueous polymerization initiated from the surface of latex particles is reported.

II. NITROXIDE-MEDIATED CONTROLLED FREE-RADICAL POLYMERIZATION IN AQUEOUS DISPERSED SYSTEMS

A. A Brief Description of Controlled Free-Radical Polymerization

The different methods that lead to "living"/controlled free-radical polymerization can be divided into two groups according to their mechanism [4,5]. They are based either on a *reversible termination* reaction or on a *reversible chain transfer reaction*. In both cases, macromolecular chains undergo successive activation/deactivation cycles. A very small fraction of chains are instantaneously active. During the deactivation period they are end-functionalized by a specific group and are called dormant. In conventional free-radical polymerization, chains grow usually for less than a few seconds and terminate. In CRP, macromolecular chains are built up and grow simultaneously during several minutes or hours, allowing many synthetic manipulations on a conventional time scale. The main feature of CRP is that the number average degree of polymerization (DP_n) increases linearly with monomer conversion and can be predicted at any conversion by the very simple relationship:

$$DP_n = \frac{[M]_0}{[I]_0} \times \text{conversion} \tag{1}$$

where $[M]_0$ = initial monomer concentration and $[I]_0$ = initial initiator concentration. Molar mass distribution is narrow, provided that a fast exchange occurs between active and dormant chains. Typically polydispersity is low, $M_w/M_n < 1.5$ (M_w, weight–average molar mass; M_n, number average molar mass) and such a value cannot be reached with a conventional free-radical polymerization process. The second important feature is that the macromolecular chains are

end-functionalized and can be further extended with either the same or another monomer. This opens the way to the synthesis of block copolymers and other more complex architectures.

B. Nitroxide-Mediated Controlled Free-Radical Polymerization

Nitroxides are stable radicals that are able to trap carbon-centered radicals at a nearly diffusion-controlled rate. At low temperatures, the formed alkoxyamine is stable and therefore the trapping reaction corresponds to an irreversible termination step. However, at elevated temperature, the C-O bond may undergo homolytic cleavage, leading back to the propagating radical and to the nitroxide. This equilibrium between propagating radical and inactive alkoxyamine is the key step in nitroxide-mediated CRP. Moreover, owing to the stability of their alkoxyamine end group, the dormant macromolecules can be isolated and further used as macroinitiators for the polymerization of the same or a different monomer.

Initially, TEMPO (2,2,6,6-tetramethylpiperidinyl-1-oxy) (Fig. 1) was the most widely used and studied nitroxide for CRP. The system is illustrated in Fig. 2 with the rate constants of activation and deactivation for the polymerization of styrene at 130°C [11]. TEMPO-mediated CRP was successfully performed for styrene and derivatives, leading to the synthesis of well-defined block copolymers and star-shaped structures [6]. The application of this method to other monomers appeared to be less straightforward. The poor results that were initially obtained for the CRP of acrylic ester monomers could be overcome providing a good control of the concentration of free nitroxide in the system [12]. In the case of methacrylic esters, however, until now no controlled polymerization could be obtained owing to the preferred TEMPO-induced β-hydrogen

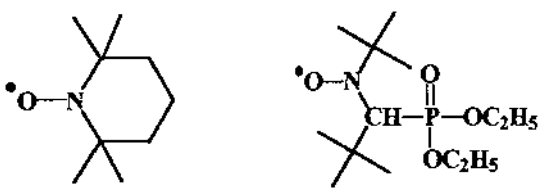

TEMPO SG1

FIG. 1 Structure of TEMPO (2,2,6,6-tetramethylpiperidinyl-1-oxy) and SG1 [*N-tert*-butyl-*N*-(1-diethylphosphono-2,2-dimethylpropyl)nitroxide].

Polystyrene/TEMPO at 130 °C (from Reference 11)

$k_d = 2.5\times10^{-3}\ s^{-1}$

$k_c = 1.2\times10^{8}\ L.mol^{-1}.s^{-1}$

$K = 2\times10^{-11}\ mol.L^{-1}$

Polystyrene/SG1 at 120 °C (from Reference 15)

$k_d = 3.4\times10^{-3}\ s^{-1}$

$k_c = 5.7\times10^{5}\ L.mol^{-1}.s^{-1}$

$K = 6.0\times10^{-9}\ mol.L^{-1}$

Poly(n-butylacrylate)/SG1 at 120 °C (from Reference 15)

$k_d = 7.1\times10^{-3}\ s^{-1}$

$k_c = 4.2\times10^{7}\ L.mol^{-1}.s^{-1}$

$K = 1.7\times10^{-10}\ mol.L^{-1}$

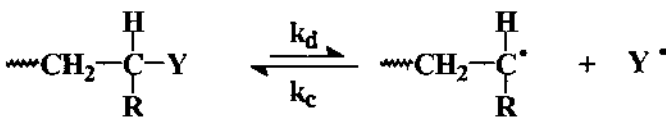

FIG. 2 Activation-deactivation equilibrium in nitroxide-mediated controlled free-radical polymerization (R = Ph, $COOC_4H_9$; $Y^{\bullet}$ = TEMPO, SG1). k_d = rate constant of homolytic cleavage of the C-O alkoxyamine bond (activation step); k_c = rate constant of coupling of propagating radical and free nitroxide (deactivation step). $K = k_d/k_c$ = equilibrium constant.

elimination from the propagating radicals leading to the formation of ω-unsaturated dead chains [13].

A new class of acyclic nitroxides was more recently used [14–16]. One of them is the *N*-*tert*-butyl-*N*-(1-diethylphosphono-2,2-dimethylpropyl)nitroxide (also called SG1) (Fig. 1) [14,15]. Faster kinetics than with TEMPO were observed for styrene polymerization and, additionally, this nitroxide was shown to be particularly well suited for the controlled polymerization of acrylic esters such as *n*-butyl acrylate [14,15,17]. This feature opened the way to the synthesis of complex copolymer architectures using nitroxide-mediated polymerization [6], as was already the case with the other CRP techniques, i.e., atom transfer radical polymerization (ATRP) [7,8] and reversible addition–fragmentation transfer (RAFT) [18–20].

The early published results on nitroxide-mediated polymerization in aqueous dispersed systems concerned the use of TEMPO as a mediator in suspension, seeded emulsion, batch emulsion, and miniemulsion polymerizations. Styrene was the most studied monomer [9], but more recently, the polymerization of *n*-butyl acrylate was also controlled, using TEMPO in a miniemulsion system [21]. Nevertheless, TEMPO presents many drawbacks that contraindicate its use in aqueous dispersed systems; more recent progress have been made with SG1 as a mediator, as illustrated below.

C. Polystyrene Homopolymer

The very first SG1-mediated polymerizations of styrene in aqueous dispersed systems were carried out at a temperature of 90°C [22,23]. Both batch miniemulsion and emulsion polymerization processes were applied with 10 wt % of monomer with respect to water. Stable latexes with particle diameters in the range 100–300 nm were obtained with the classical sodium dodecyl sulfate anionic surfactant. In order to keep the experimental conditions close to the usual ones, a bicomponent initiating system was chosen, i.e., a conventional radical initiator (the redox system $K_2S_2O_8/Na_2S_2O_5$) together with added free nitroxide. The optimal nitroxide/persulfate initial molar ratio was 1.2 as it corresponded to the best compromise between fast polymerization and good control over the molar mass and molar mass distribution [22]. The batch miniemulsion process [24]—in which the very complex nucleation step existing in a classical emulsion polymerization is eliminated—was further selected for insightful investigation. A complete kinetic study was performed to illuminate the polymerization mechanism [23]. The parameters that affect both the kinetics of polymerization and the control of molar mass and molar mass distribution have been examined, such as pH of the water phase, initiator concentration, monomer/water ratio, and process for chain extension.

A typical logarithmic conversion (x) vs. time plot is shown in Fig. 3. After an induction period of less than 1 h, the conversion progressed quite rapidly to reach more than 90% within 8 h. With the use of a water-soluble radical initiator, polymerization starts in the aqueous phase. There, it was assumed that water-soluble alkoxyamines were initially formed during the induction period, by addition of a primary radical to one monomer unit, followed by rapid coupling of the formed carbon-centered radical by SG1. After complete consumption of the nitroxide in excess, propagation could start, leading to oil-soluble oligomers that were progressively absorbed by the monomer droplets to continue propagation. At this stage, polymerization was restricted to the dispersed organic phase of the system and kinetics was regulated by the activation–deactivation equilibrium given in Fig. 2.

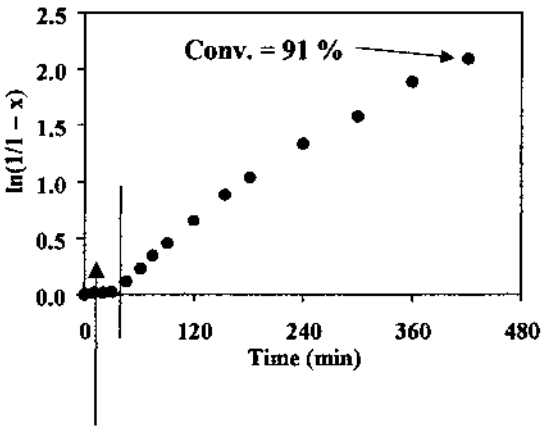

Formation of the water-soluble alkoxyamine (with X = $SO_4^{\cdot}$ or HSO_3):

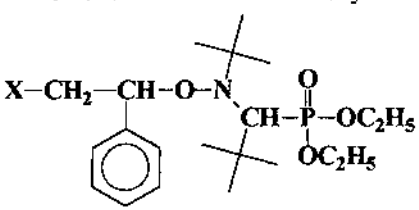

FIG. 3 Typical logarithmic conversion (x) vs. time plot for SG1-mediated miniemulsion polymerization of styrene, using $K_2S_2O_8/Na_2S_2O_5$ as an initiator at 90°C. Experimental conditions: temperature = 90°C; styrene/water = 1 : 9 (wt/wt); Initiator: $K_2S_2O_8/Na_2S_2O_5$; $[K_2S_2O_8] = 0.037$ mol $L^{-1}_{org.}$; $[SG1]/[K_2S_2O_8] = 1.2$; $[NaHCO_3] = 0.009$ mol L^{-1}_{water}; [SDS] = 0.015 mol L^{-1}_{water}; final diameter = 180 nm.

Because of inevitable radical–radical termination, the persistent radical effect [25–27] also operated like in bulk and was responsible for the slow decay of the concentration of propagating radicals with time (Fig. 4). Polymerizations were usually faster than in bulk. This was assigned to partition of the nitroxide between the aqueous and the organic phases, leading to a concentration within the polymerization locus smaller than in bulk, and hence to a shift of the activation–deactivation equilibrium toward the formation of a larger concentration of active macroradicals. Actually, slow simultaneous degradation of SG1 also occurred, depending on the pH as will be shown below.

The typical M_n vs. conversion plot is represented in Fig. 5. As expected for controlled polymerization, M_n increased linearly with monomer conversion and eventually matched the theoretical value. The molar mass distributions, even at final conversion, were not as narrow as observed in bulk, owing to faster polymerization. However, the M_w/M_n values continuously decreased with conversion, indicating simultaneous growth of all polymer chains. In addition, "livingness" of the polymer chains was evidenced by in situ chain extension; a good reinitiation demonstrated that chains obtained in the first step were still bearing the alkoxyamine end group [23].

The effect of pH on polymerization rate was studied. When insufficiently buffered, the water phase became acidic during the initiation period (as a consequence of use of the persulfate/metabisulfite redox couple). The decrease in pH was accompanied by an increased polymerization rate along with a low "initiator efficiency" (larger M_n than theoretically predicted). These features were assigned to side reactions between SG1 and the two components of the initiating

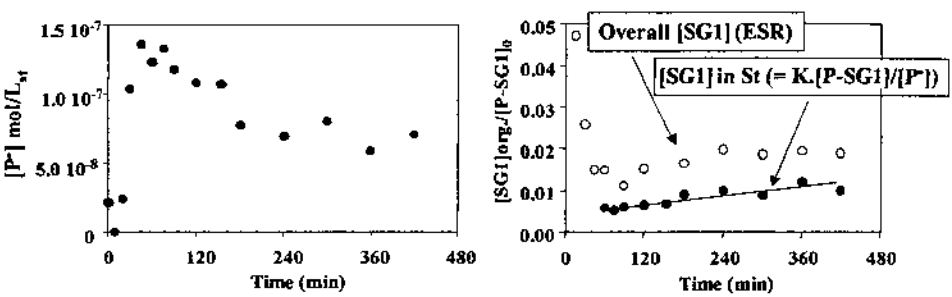

FIG. 4 Respective concentrations of propagating radical (P•) and free SG1 during the course of a miniemulsion polymerization (see Fig. 3 for experimental conditions). [$P^\bullet$] was determined by the slope of $\ln(1/1-x)$ vs. time in Fig. 3; $[SG1]_{org.}/[P\text{-}SG1]_0$ (with $[P\text{-}SG1]_0$, the concentration of "living" chains in the system) was determined from the activation–deactivation equilibrium (concentration in the monomer phase) and from ESR measurements (overall concentration).

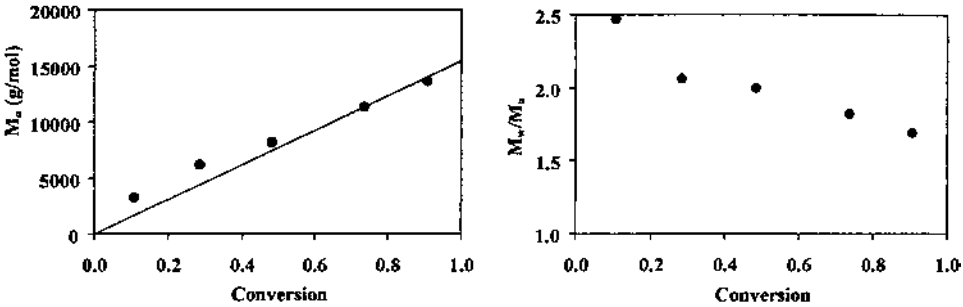

FIG. 5 Molar mass and molar mass distribution for polystyrene obtained via SG1-mediated miniemulsion polymerization using $K_2S_2O_8/Na_2S_2O_5$ as an initiator at 90°C (see Fig. 3 for experimental conditions).

system, leading to a decrease in the concentration of alkoxyamines produced *in situ*. At neutral pH, these side reactions were unimportant, which ensured a better control over the polymer characteristics. The persulfate/metabisulfite initiator concentration was also varied to target different molar masses, but the pH had to be adjusted simultaneously to reach the goal and avoid the above-mentioned features [23].

Increasing the monomer/water ratio in the miniemulsion from 10 wt % to 30 wt % did not affect the latex stability but had a strong impact on the molar mass distribution, which became significantly narrower. Indeed, an M_w/M_n as low as 1.22 could be reached with $M_n = 17500$ g mol^{-1}. This improvement was assigned to favored partitioning of free nitroxide in the oil phase (i.e., the polymerization locus), ensuring a better control over the polymer characteristics [23].

In contrast to miniemulsion polymerizations with classical radical mechanism, the colloidal characteristics of the latexes were far from perfect: particle diameter was somewhat larger but, more importantly, the particle size distribution was significantly broader as illustrated in Fig. 6. This result might be assigned to longer polymerization times leading to extended collision/fusion between the particles, which remain soft for a longer time.

As a conclusion, the use of a bicomponent initiating system with a conventional radical initiator and free nitroxide is a very simple way to achieve CRP in a miniemulsion system. From a practical viewpoint, very few parameters have to be changed with respect to a classical polymerization. Nevertheless, the fact that kinetics and control of molar mass are very sensitive to small changes in nitroxide concentration makes the control of large molar masses fairly difficult to achieve since the concentrations of each component have to be very carefully adjusted.

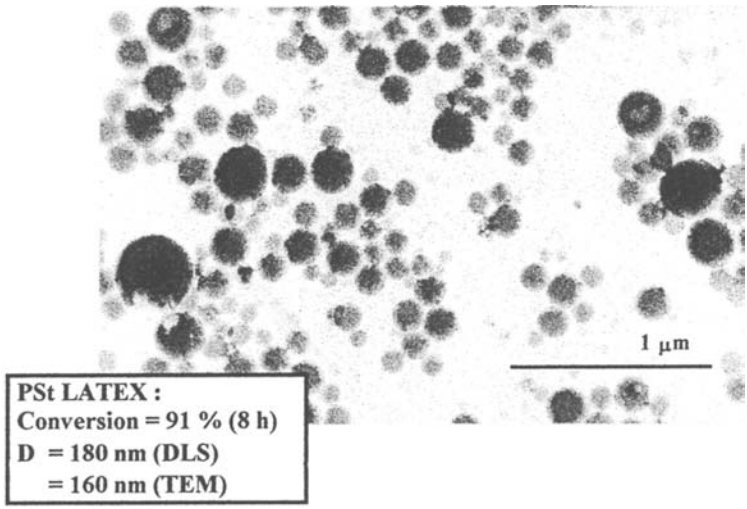

FIG. 6 Typical transmission electron micrograph (TEM) of a polystyrene latex prepared via SG1-mediated miniemulsion polymerization at 90°C, using $K_2S_2O_8/Na_2S_2O_5$ as the initiator. (DLS: dynamic light scattering).

For this reason, the bicomponent initiating system was changed for a monocomponent one, i.e., an oil-soluble preformed SG1-based alkoxyamine (named Monams, Fig. 7). This type of well-defined initiator, which mimics the chain-end structure, allows a good control over the initiation step, the concentration of "living" chains, and the concentration of free nitroxide. In other words, both molar mass and kinetics can be perfectly adjusted. In this case, as illustrated in Fig. 8, molar masses larger than previously observed were obtained with narrower distribution [28]. This particularly interesting system was then used as an initiator in the homopolymerization of *n*-butyl acrylate and in the synthesis of block and gradient copolymers.

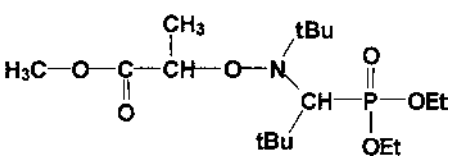

FIG. 7 Structure of the Monams alkoxyamine.

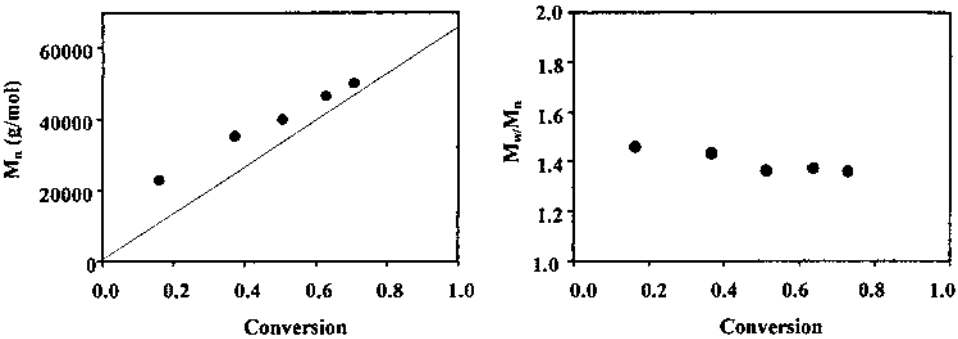

FIG. 8 Molar mass and molar mass distribution for polystyrene obtained via SG1-mediated miniemulsion polymerization using the Monams alkoxyamine as an initiator at 120°C. Experimental conditions: temperature = 120°C; batch conditions; styrene/water = 2:8 (wt/wt); [Monams] = 0.014 mol $L^{-1}_{org.}$; [added free SG1]/[Monams] = 0.025; [$NaHCO_3$] = 0.013 mol L^{-1}_{water}; [anionic surfactant] = 2 wt % with respect to monomer; final diameter = 400 nm.

D. Poly(*n*-butyl acrylate) Homopolymer

For the poly(*n*-butyl acrylate)/SG1 system, the activation–deactivation equilibrium constant is smaller than that for polystyrene/SG1: $K = 1.7 \times 10^{-10}$ mol L^{-1} at 120°C instead of $K = 6.0 \times 10^{-9}$ for polystyrene (Fig. 2). Therefore, polymerization of *n*-butyl acrylate is better controlled at higher temperature, typically in the 110–120°C range. Controlled free-radical homopolymerization of *n*-butyl acrylate was successfully performed in batch aqueous miniemulsion at 112°C under 3 bars pressure, using the Monams alkoxyamine initiator (Fig. 7) and the SG1 nitroxide as a mediator [29]. The performed "living" miniemulsion polymerizations led to stable latexes with 20–45 wt % solids and were obtained neither with coagulation during synthesis nor with destabilization over time. For some experiments, the alkoxyamine was used alone, whereas in other cases, a small fraction of free SG1 was added simultaneously (not more than 2.5 mol % with respect to the initial alkoxyamine) to regulate the polymerization rate, decrease the extent of macroradicals' self-termination, and reduce the polydispersity. Kinetics of these miniemulsion polymerizations were studied (1) as a function of the initial $r = [SG1]_0/[alkoxyamine]_0$ molar ratio for a given alkoxyamine concentration; (2) as a function of the alkoxyamine initial concentration for a given *r* value; and (3) as a function of the initial monomer/water ratio. In addition, the colloidal characteristics of the particles have been studied as a function of the type of surfactant.

In contrast to what is usually observed in classical radical polymerization, rates of homopolymerization of *n*-butyl acrylate carried out in miniemulsion were not larger than those previously observed in bulk, with the same initiator [15,17]. Indeed, the compartmentalization effect that enhances the rate in classical emulsion and miniemulsion systems with respect to bulk or solution polymerizations does not operate in nitroxide-mediated polymerization when particle diameter is sufficiently large, as is the case here [30]. The polymerization rate inside the particles is essentially governed by the activation–deactivation equilibrium. When polymerizations were performed with a given alkoxyamine initial concentration and various $r = [SG1]_0/[\text{alkoxyamine}]_0$ molar ratios, the M_n values were not affected, whereas the polydispersity indexes and the rates of polymerization depended on r. The larger r was, the slower the polymerization (Fig. 9) and the narrower the molar mass distribution (Fig. 10).

In contrast, the polymerization rates were the same for reactions where the initiator concentration was varied while the ratio r was kept constant (equal to 0.025). In these experiments, different molar masses were targeted. In all cases, M_n increased linearly with monomer conversion, matched the predicted value, and the molar mass distribution was narrow. For instance, M_n up to 50,000 g

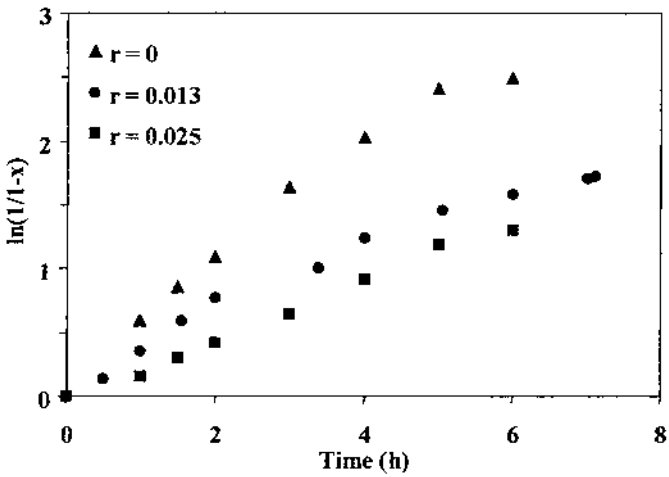

FIG. 9 Logarithmic conversion (x) vs. time for miniemulsion polymerizations of *n*-butyl acrylate carried out with the same Monams initial concentration and various SG1 concentrations ($r = [SG1]_0/[\text{Monams}]_0$). Experimental conditions: Temperature = 112°C; batch conditions; BA/water = 2:8 (wt/wt); [Monams] = 0.028 mol $L^{-1}_{org.}$; [$NaHCO_3$] = 0.012 mol L^{-1}_{water}; [anionic surfactant] = 2 wt % with respect to monomer; final diameter > 500 nm.

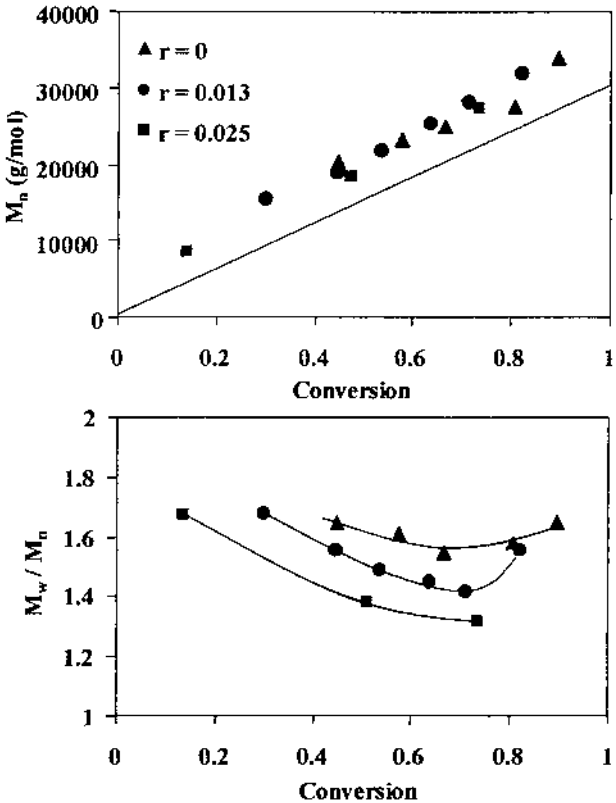

FIG. 10 Molar mass and molar mass distribution for miniemulsion polymerizations of *n*-butyl acrylate carried out with the same Monams initial concentration and various SG1 concentrations ($r = [SG1]_0/[Monams]_0$) (see Fig. 9 for experimental conditions).

mol^{-1} could be obtained with polydispersity indexes ranging between 1.2 and 1.4. As a consequence, polymerization rate and molar mass can be adjusted independently with two parameters, namely, r and the initiator concentration.

As shown above, the important parameter to control the kinetics was not directly the initiator concentration but the initial $r = [SG1]_0/[alkoxyamine]_0$ molar ratio. Indeed, the rate of propagation for the homopolymerization of a given monomer M can be expressed as:

$$\frac{-d[M]}{dt} = k_p[P\cdot][M] = k_p K([P\text{-}SG1]_0/[SG1])[M] \quad (2)$$

with k_p, [$P^\bullet$], K, and [P-SG1]$_0$ the rate constant of propagation, the concentration of propagating macroradicals in the organic phase, the activation–deactivation equilibrium constant (Fig. 2), and the alkoxyamine initial concentration, respectively. The variation of propagation rate with conversion depends not only on the initial nitroxide/alkoxyamine molar ratio but also on the buildup of nitroxide concentration owing to the persistent radical effect [25–27]. However, it was demonstrated that for *n*-butyl acrylate the contribution of radical–radical termination was quite small with respect to the initial alkoxyamine concentration. As a consequence, a very small fraction of dead chains is formed during polymerization, and kinetics is mainly governed by the initial concentration of free nitroxide and, more specifically, by the initial nitroxide/alkoxyamine molar ratio [31,32].

As in the previous examples of styrene miniemulsion polymerizations, the average particle diameters of the final latexes were rather large, and the particle size distribution was broad and very often multimodal. Nevertheless, a narrow particle size distribution was obtained when an amphiphilic block copolymer of polystyrene and neutralized poly(acrylic acid) was used as a stabilizer instead of a classical anionic surfactant.

E. Poly(styrene-*co*-*n*-butyl acrylate) Random Copolymers

Random copolymerization of styrene and *n*-butyl acrylate was performed in miniemulsion using the same experimental conditions as for *n*-butyl acrylate homopolymerizations [31]. The copolymerization rates were not strongly affected by the molar ratio of styrene and were similar to those of *n*-butyl acrylate homopolymerizations, carried out with the same $r = [SG1]_0/[Monams]_0$ ratio and the same initiator concentration. In all of the miniemulsion copolymerizations carried out with added free nitroxide, the polymers were well controlled, as molar masses increased linearly with monomer conversion and followed the predicted values, with narrow distributions. In addition to the good control over molar mass and molar mass distribution, controlled radical copolymerization offers advantages concerning the structure of the random copolymers. Indeed, since the chain concentration remains constant throughout the reaction (as demonstrated by the proportionality between M_n and conversion), the composition drift due to difference in reactivity of the comonomers affects the distribution of the monomer units in every chain but not the composition distribution in the system, in contrast to conventional radical polymerization. As a consequence, a narrow composition distribution is expected and chains should exhibit a gradient composition. This feature was demonstrated by liquid adsorption chromatography, which is an analytical technique that gives information on the copolymer composition distribution (conditions to achieve separation according to the com-

position independently of the molar mass were established). Results confirmed that composition distribution of the final living copolymers was much narrower than exhibited by analogous noncontrolled copolymers.

As a conclusion, SG1-mediated copolymerization of styrene and *n*-butyl acrylate allowed synthesis of latex particles containing living gradient copolymers with both a narrow molar mass distribution and a narrow composition distribution.

F. Poly(*n*-butyl acrylate)-*b*-polystyrene Block Copolymers

Diblock copolymers were also synthesized in miniemulsion polymerization, using a sequential addition of the monomers, *n*-butyl acrylate first, then styrene [29]. The linear increase in M_n after styrene addition, the complete shift of the size exclusion chromatography traces (both refractive index and UV traces), and the decrease in M_w/M_n clearly indicated that chain extension from the first poly(*n*-butyl acrylate) living segment was effective. Furthermore, liquid adsorption chromatography did not show any detectable poly(*n*-butyl acrylate) homopolymer signifying efficient reinitiation by the first block.

In conclusion, nitroxide-mediated controlled radical polymerization in miniemulsion is not restricted to the synthesis of homopolymers but can be extended to the direct preparation of block copolymers, entirely performed in an aqueous dispersed system.

III. USE OF AMPHIPHILIC BLOCK COPOLYMERS AS LATEX PARTICLE STABILIZERS

Controlled free-radical polymerization is a very convenient tool to get copolymer architectures with a variety of possible properties [6]. In this work, amphiphilic systems were synthesized and employed as stabilizers in emulsion polymerization. Nitroxide-mediated polymerization was not the only approach used for this purpose; atom transfer radical polymerization was also employed, as is briefly described below.

A. Atom Transfer Radical Polymerization

Atom transfer radical polymerization (ATRP) is based on the reversible transfer of a halogen atom between a dormant alkyl halide (P-X) and a transition metal catalyst (M_t^n/L) by redox chemistry [7,8]. The alkyl halide is reduced to a growing radical and the transition metal is oxidized via an inner sphere electron transfer process. In the first reaction, the role of the activator is often played by a copper(I) species complexed by two bipyridine ligands and the role of the deactivator by the corresponding copper(II) species (Fig. 11).

FIG. 11 Activation–deactivation equilibrium in ATRP.

ATRP can be used for a large range of monomers, including methacrylates, and it is generally faster than nitroxide-mediated polymerization. The rate of ATRP can be adjusted conveniently not only by the concentration of deactivator but also by the concentration of activator. Another advantage of ATRP is a multitude of available initiators.

B. Synthesis of Amphiphilic Block Copolymers Using Nitroxide-Mediated CRP or ATRP

With the emergence of CRP, a wide range of monomers can now be polymerized in a controlled manner. Amphiphilic structures can be obtained by a proper design of the macromolecular architecture and the nature of the incorporated monomers. Such macromolecules can be used as efficient stabilizers in emulsion polymerization to replace the more regular low molar mass surfactants, which have many drawbacks. They are expected to possess some advantages due to their better compatibility with the polymer particles and to a lower migration rate. They should provide steric stabilization owing to the formation of a hydrophilic shell surrounding the particles. They should also provide electrostatic stabilization when the hydrophilic segment is a polyelectrolyte. Combination of both effects is known as electrosteric stabilization. Until now, well-defined amphiphilic block copolymers were usually synthesized using anionic or cationic living polymerizations [33]. However, those techniques require very drastic experimental conditions, and a new trend is to replace them by controlled radical polymerization.

First, nitroxide-mediated CRP was applied to the synthesis of amphiphilic diblock copolymers such as poly(styrenesulfonate)-*b*-polystyrene [34] (Fig. 12) and poly(vinylbenzyltriethylammonium chloride)-*b*-polystyrene (Fig. 12) [35]. As expected, they behaved as good stabilizers in the emulsion polymerization of styrene, leading to smaller particles and larger rates of polymerization than the conventional surfactants used in the same proportion.

Synthesis of amphiphilic block copolymers using ATRP was further considered [36]. Copper-mediated ATRP was used to prepare polystyrene-*b*-poly(*tert*-butyl acrylate) block copolymers with different block lengths and different architectures. Subsequent hydrolysis of the ester groups afforded the amphiphilic counterpart with poly(acrylic acid) blocks. For example, diblock (Fig. 12), triblock, and three-

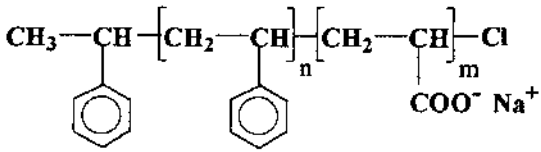

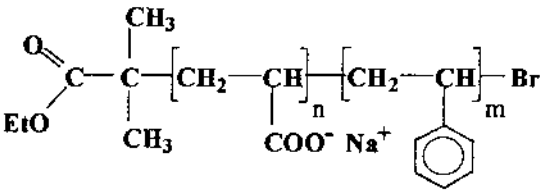

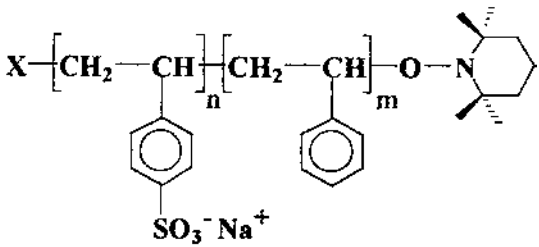

X = -SO_3^- or -OSO_3^-

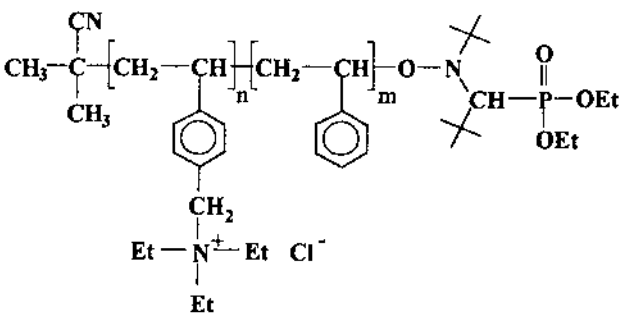

FIG. 12 Examples of amphiphilic diblock copolymers prepared via controlled free-radical polymerization and used as stabilizers in emulsion polymerization.

arm star block copolymers (Fig. 13) were prepared with the precisely controlled proportions of polystyrene in the range 10 to 50 mol %, with molar masses ranging from M_n = 3000 to 30,000 g mol^{-1} and low polydispersities, M_w/M_n = 1.1–1.3. The block lengths were varied from 10 to 30 units for the polystyrene block and from 13 to 266 units for the poly(acrylic acid) block.

C. Use of Amphiphilic Block Copolymers as Stabilizers in Emulsion Polymerization

The aforementioned series of amphiphilic diblock, triblock, and star block copolymers composed of polystyrene and poly(acrylic acid) were used as stabilizers in emulsion polymerization, under alkaline conditions. The copolymers in the acidic form did not dissolve directly in water. They had to be ionized in the presence of potassium carbonate, for example, and heated to 70°C to obtain clear solutions. At that stage, all of the acrylic acid units were in the potassium salt form and the copolymers with more than 60 mol % of acrylic acid perfectly dissolved.

Efficiency of the block copolymers as stabilizers in emulsion polymerization was correlated with their structural characteristics. For this purpose, a model recipe of styrene emulsion polymerization was selected and systematically ap-

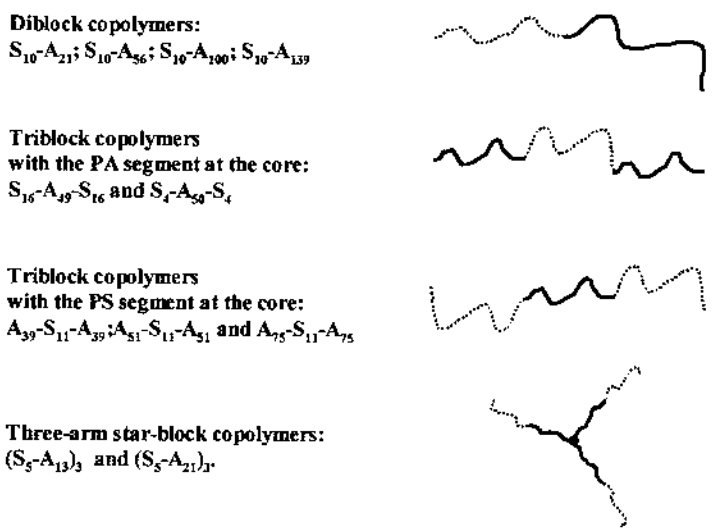

FIG. 13 Examples of structure and composition of block copolymers prepared via ATRP and used as stabilizers in emulsion polymerization. ____, polystyrene hydrophobic segment; . . . . . ., poly(acrylic acid) hydrophilic segment.

plied. It was batch polymerization, with monomer content of 10 wt %, initiated by potassium persulfate at 70°C. The final particle density, $N_p(L^{-1})$, obtained at 100% conversion was used as a criterion to compare the stabilizers efficiency: the larger N_p was, the larger the stabilized surface area for a given solids content and therefore the better the stabilizing efficiency.

The diblock copolymers, the triblocks with polystyrene segment in the middle, and the star block copolymers (Fig. 13) led to stable polystyrene latexes. Even very low weight fractions of stabilizer with respect to monomer led to stable latexes with small diameters and a large number of particles (Table 1). Nevertheless, it was shown that triblock and star block copolymers did not behave better than diblock copolymers of similar composition. The latter should then be preferred as their structure combines efficient stabilization with easier preparation.

These amphiphilic block copolymers have structures that enable them to properly adsorb or anchor onto the particle surface, while the charged hydrophilic segments are well extended in the water phase and ensure electrosteric stabilization. This was confirmed by measurement of the hydrodynamic diameter of the particles (D) by dynamic light scattering as a function of pH: D increased very significantly when the pH was increased (i.e., when the degree of ionization was increased). The smallest measurable value was obtained at pH 3. For a pH lower than 3, aggregation of the particles was observed. The value of D measured at pH 3 was considered to be the closest estimation of the particle diameter (including the hydrophobic core and the collapsed hydrophilic shell).

The effect of the poly(acrylic acid) block length was studied for a series of diblock copolymers with the same polystyrene block (10 styrene units) and increasing poly(acrylic acid) block lengths (from 21 to 139 acid units). As seen in Fig. 14, in the range of studied concentrations, the highest number of particles was obtained for the diblock copolymer with 56 acid units. In the series of triblock copolymers with 11 styrene units in the middle and increasing hydrophilic blocks on both sides, the best efficiency was observed for the copolymer containing 51 acid units in each poly(acrylic acid) block. It was thus clearly demonstrated that, for a given hydrophobic block, the length of the hydrophilic one(s) is of importance as far as N_p is regarded. A value of approximately 50–56 acid units seemed to be optimal when the hydrophobic block contained approximately 10 styrene units. In other words, for a given initial molar concentration of these amphiphilic copolymers, the final stabilized area per macromolecule (which increases when N_p increases) did not continuously increase with the size of the hydrophilic block(s) but went through a maximum for approximately 50–56 acid units; additional acid units did not contribute to efficiency enhancement of the stabilizer.

The evolution of the number of latex particles with the concentration of diblock copolymer was also studied, and N_p was shown to be proportional to

TABLE 1 Emulsion Polymerizations of styrene 70°C Using Amphiphilic Polystyrene-*b*-poly(acrylic acid) (S_x-A_y) Diblock Copolymers as Stabilizers: Structure of the Copolymers and Final Characteristics of the Latexes

Copolymer structure	$M_n(M_w/M_n)$	Composition (mol % of acrylic acid units)	Concentration wt % vs. styrene	Concentration Diameter 10^{-4} (mol L^{-1})	(at pH 3) (nm)	N_p 10^{17} L^{-1}
S_{10}-A_{21}	2540 (1.20)	0.66	0.78	3.11	70	4.3
			1.12	4.04	62	6.0
			1.63	6.53	54	9.1
			2.23	8.97	52	11.0
			2.45	8.82	46	13.5
S_{10}-A_{56}	5070 (1.14)	0.84	0.25	0.50	102	1.6
			0.56	1.11	79	3.3
			1.96	3.94	62	6.9
			2.41	4.87	57	8.9
			3.80	7.80	48	15
S_{10}-A_{100}	8230 (1.44)	0.91	0.50	0.61	95	1.6
			0.82	1.00	93	2.0
			1.06	1.30	79	2.0
			1.62	2.00	85	2.5
			2.38	2.96	61	4.3
			2.41	3.00	64	4.1
			2.43	3.03	60	4.1
			3.00	3.76	63	4.2
			3.86	4.88	62	5.4
S_{10}-A_{139}	11090 (1.28)	0.93	0.53	0.48	97	1.5
			0.73	0.67	89	1.8
			0.99	0.90	80	2.6
			1.47	1.35	69	2.8
			2.19	2.02	74	3.3
			2.90	2.70	65	4.1

$[K_2S_2O_8] = 0.005$ mol L^{-1}; $[K_2CO_3] = 0.020$ mol L^{-1}.

[copolymer]$^{\alpha}$ over a wide concentration range. The value of the exponent α was a function of the block copolymer composition irrespective of the individual block lengths: it was 1 for block copolymers with a poly(acrylic acid) content lower than 75 mol % and decreased to 0.4 when the hydrophilic content was increased. A low value of α means that several copolymer micelles are needed to stabilize a given latex particle; in other words, nonnucleated micelles play the role of stabilizer reservoir, which is usually the case with low molar mass

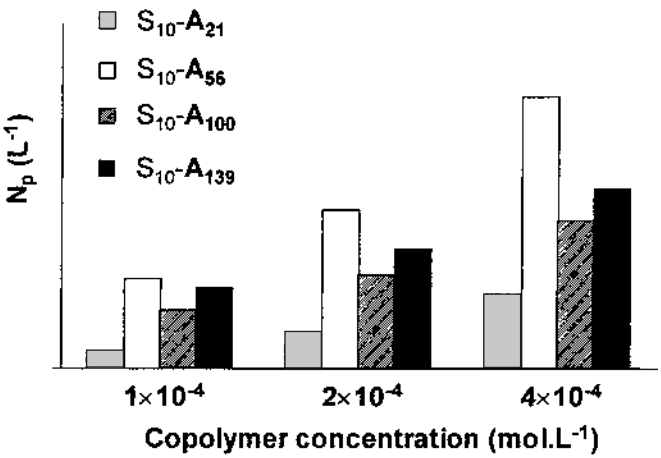

FIG. 14 Effect on N_p of the poly(acrylic acid) block length for amphiphilic diblock copolymers used as stabilizers in styrene emulsion polymerization.

surfactants. In contrast when $\alpha = 1$, every latex particle originates from a single micelle. This trend can be correlated with the exchange dynamics of the stabilizer. The results obtained with various initiator concentrations, temperatures, and ionic strengths corroborated this observation and let us conclude that the important point to explain the evolution of α with the copolymer composition was the competition between direct nucleation of the micelles and exchange of the block copolymers between the micelles and the continuously created polymer–water interfaces in the system. The time scale of this exchange (which is very fast for small-molecule surfactants) was on the same order of magnitude as the initiation step for emulsion polymerizations carried out in the presence of block copolymers. The more hydrophilic block copolymers behaved quite similarly to low molar mass classical surfactants, with a fast exchange. In contrast, the more hydrophobic ones led to micelles that were sufficiently stable to be directly nucleated. In the latter case, the final number of particles matched the initial number of micelles. Thus, a good prediction of N_p can be anticipated, and this possibility was successfully applied for emulsion copolymerizations of methyl methacrylate and *n*-butyl acrylate at 45 wt % solids [37].

D. Formation of a Hydrophilic Shell by ATRP at the Surface of Latex Particles

Atom transfer radical polymerization was applied to the homopolymerization of water-soluble monomers (namely, 2-hydroxyethyl acrylate and 2-(methacryloyl-

oxy)ethyltrimethylammonium chloride) at the surface of a cross-linked polystyrene latex functionalized with alkyl bromide groups [38]. Polymerization was carried out in water and was initiated by the surface groups of the dialyzed latex. This technique led to controlled polymerization resulting in particles with a well-defined hydrophilic shell and possible chain end functionalization. Precise design of the aqueous ATRP system was the key factor in obtaining controlled architectures at the surface of latex particles.

IV. CONCLUSION

Nitroxide-mediated controlled free-radical polymerization is not restricted to bulk or solution polymerizations but can be applied to aqueous dispersed systems. To date, miniemulsion was the most successful method to get a latex of living polymers. New latexes containing well-defined homopolymers, gradient and block copolymers are now accessible. Their properties are still under investigation and can open the door to new applications. With the possible synthesis of a variety of amphiphilic structures, CRP can also be particularly useful in classical emulsion polymerization. Very efficient stabilizers can be obtained, leading to a precise control of the particle number. In addition, new particle morphology can be achieved like the presented hydrophobic–hydrophilic particles with a controlled polyelectrolyte shell.

ACKNOWLEDGMENTS

The authors thank Atofina for financial support of the doctoral research of C. Farcet (Atofina grant) and C. Burguière (CNRS-Atofina grant), and for providing SG1 nitroxide and Monams alkoxyamine. The contributions of R. Pirri, O. Guerret and J. L. Couturier from Atofina are particularly appreciated. The authors thank P. Tordo and M. Culcasi from the SREP laboratory (University of Aix-Marseille) for their helpful advice and ESR analyses. Melissa Manuszak's participation in part of this work is gratefully acknowledged. The authors (particularly BC) also thank Christian Pichot for his constant support and very kind counsel.

REFERENCES

1. Lovell, P.A.; El-Aasser, M.S., Eds.; *Emulsion Polymerization and Emulsion Polymers*. John Wiley and Sons: New York, 1997.
2. Gilbert, R.G. *Emulsion Polymerization: A Mechanistic Approach*. Academic Press: San Diego, 1995.
3. Pichot, C.; Charleux, B.; Charreyre, M.T.; Revilla, X. Macromol. Symp. **1994**, *88*, 71–87.

4. Matyjazszewski, K. *Controlled Radical Polymerization*. ACS Symp. Series 685. American Chemical Society: Washington, DC, 1998.
5. Matyjazszewski, K. *Controlled/Living Radical Polymerization*: *Progress in ATRP*, *NMP*, *and RAFT*. ACS Symp. Series 768. American Chemical Society: Washington, DC, 2000.
6. Hawker, C.J.; Bosman, A.W.; Harth, E. Chem. Rev. **2001**, *101*, 3661–3688, and references therein.
7. Matyjaszewski, K.; Xia, J. Chem. Rev. **2001**, *101*, 2921–2990, and references therein.
8. Kamigaito, M.; Ando, T.; Sawamoto, M. Chem. Rev. **2001**, *101*, 3689–3745, and references therein.
9. Qiu, J.; Charleux, B.; Matyjaszewski, K. Prog. Polym. Sci. **2001**, *26*, 2083–2134, and references therein.
10. Burguière, C.; Pascual, S.; Bui, C.; Vairon, J.P.; Charleux, B.; Davis, K.; Matyjaszewski, K.; Bétremieux, I. Macromolecules **2001**, *34*, 4439–4450.
11. Goto, A.; Terauchi, T.; Fukuda, T.; Miyamoto, T. Macromol. Rapid Commun. **1997**, *18*, 673–681.
12. Keoshkerian, B.; Georges, M.; Quinlan, M.; Veregin, R.; Goodbrand, B. Macromolecules **1998**, *31*, 7559–7561.
13. Burguière, C.; Dourges, M.A.; Charleux, B.; Vairon, J.P. Macromolecules **1999**, *32*, 3883–3891.
14. Grimaldi, S.; Finet, J.P.; Le Moigne, F.; Zeghdaoui, A.; Tordo, P.; Benoit, D.; Fontanille, M.; Gnanou, Y. Macromolecules **2000**, *33*, 1141–1147.
15. Benoit, D.; Grimaldi, S.; Robin, S.; Finet, J.P.; Tordo, P.; Gnanou, Y. J. Am. Chem. Soc. **2000**, *122*, 5929–5940.
16. Benoit, D.; Chaplinski, V.; Braslau, R.; Hawker, C. J. Am. Chem. Soc. **1999**, *121*, 3904–3920.
17. Lacroix-Desmazes, P.; Lutz, J.F.; Chauvin, F.; Severac, R.; Boutevin, B. Macromolecules **2001**, *34*, 8866–8871.
18. Chiefari, J.; Chong, Y.K.; Ercole, F.; Krstina, J.; Jeffery, J.; Le, T.P.T.; Mayadunna, R.T.A.; Meijs, G.F.; Moad, C.L.; Moad, G.; Rizzardo, E.; Thang, S.H. Macromolecules **1998**, *31*, 5559–5562.
19. Chong, Y.K.; Le, T.P.T.; Moad, G.; Rizzardo, E.; Thang, S.H. Macromolecules **1999**, *32* 2071–2074.
20. Mayadunne, R.T.A.; Rizzardo, E.; Chiefari, J.; Krstina, J.; Moad, G.; Postma, A.; Thang, S.H. Macromolecules **2000**, *33*, 243–245.
21. Keoshkerian, B.; Szkurhan, A.R.; Georges, M.K. Macromolecules **2001**, *34*, 6531–6532.
22. Lansalot, M.; Farcet, C.; Charleux, B.; Vairon, J.P.; Pirri, R.; Tordo, P. *Controlled/Living Radical Polymerization*: *Progress in ATRP*, *NMP*, *and RAFT*; Matyjaszewski, K., Ed.; ACS Symp Series 768; 2000; 138–151.
23. Farcet, C.; Lansalot, M.; Charleux, B.; Pirri, R.; Vairon, J.P. Macromolecules **2000**, *33*, 8559–8570.
24. Landfester, K. Macromol. Rapid Commun. **2001**, *22*, 896–936.
25. Fischer, H. J. Polym. Sci. A Polym. Chem. **1999**, *37*, 1885–1901.

26. Souaille, M.; Fischer, H. Macromolecules **2000**, *33*, 7378–7394.
27. Fischer, H. Chem. Rev. **2001**, *101*, 3581–3610.
28. Farcet, C. "Polymérisation radicalaire contrôlée par les nitroxydes en miniémulsion aqueuse." PhD dissertation. Paris 6 University, 2002.
29. Farcet, C.; Charleux, B.; Pirri, R. Macromolecules **2001**, *34*, 3823–3826.
30. Charleux, B. Macromolecules **2000**, *33*, 5358–5365.
31. Farcet, C.; Charleux, B.; Pirri, R. Macromol. Symp., **2002**, *182*, 249–250.
32. Farcet, C.; Nicholas, J.; Charleux, B. Polym. Sci. Polym. Chem. **2002**, *40*, 4410–4420.
33. Perrin, P.; Millet, F.; Charleux, B. *Physical Chemistry of Polyelectrolytes*; Radeva, T., Ed.; Surfactant Science Series; Marcel Dekker: New York, 2001; 363–445, and references therein.
34. Bouix, M.; Gouzi, J.; Charleux, B.; Vairon, J.P.; Guinot, P. Macromol. Rapid Commun. **1998**, *19*, 209–213.
35. Burguière, C.; Pascual, S.; Coutin, B.; Polton, A.; Tardi, M.; Charleux, B.; Matyjaszewski, K.; Vairon, J.P. Macromol. Symp. **2000**, *150*, 39–46.
36. Davis, K.A.; Charleux, B.; Matyjaszewski, K. J. Polym. Sci. A Polym. Chem. **2000** *38*, 2274–2283.
37. Burguière, C. "Synthèse de copolymères à blocs amphiphiles par polymérisation radicalaire contrôlée: application à la stabilisation en polymérisation en émulsion." PhD dissertation. Paris 6 University, 2001.
38. Manuszak-Guerrini, M.; Charleux, B.; Vairon, J.P. Macromol. Rapid Commun. **2000**, *21*, 669–674.

3

Preparation of Microlatexes Using Polymeric Surfactants or Mixed Surfactants

PEIHONG NI Soochow University, Suzhou, China

SHOUKUAN FU Fudan University, Shanghai, China

I. INTRODUCTION

Emulsion polymerization is in widespread use for preparation of stable aqueous suspensions of polymeric particles of submicrometer size and offers many advantages for colloid polymer in biological, medical, and pharmaceutical applications [1,2]. Among the components used in a classical emulsion polymerization recipe, the surfactant or stabilizer has two key roles. One role of the surfactant is its participation in the nucleation step and contribution to the creation of stable particles. The final number of latex particles is directly related to the initial concentration of the surfactant. Another role of the surfactant is to impart good stability to the latex particles during polymerization as well as storage [3]. Ionic surfactants ensure the particles' stability by electrostatic repulsion, whereas nonionic stabilizers, e.g., poly(ethylene oxide), possess a steric effect and are particularly efficient against electrolyte, high-shear, and/or freeze–thaw–induced destabilizations [4,5].

Besides the classical ionic and nonionic surfactants, a unique class of stabilizers can be used in emulsion polymerization, namely, the amphiphilic copolymers or polymeric emulsifiers [3,5]. They can provide many significant benefits to the latex industry, including low foamability, good chemical and mechanical stability, rheology modification, and improved coating quality [6–8].

Many investigations have developed water-soluble macromonomers, block or graft amphiphatic polymeric emulsifiers, and polyelectrolytes [9–15]. Among the various polymeric surfactants, amphiphilic block copolymers, especially those containing poly[2-(dimethylamino)ethyl methacrylate] (PDMAEMA), have at-

tracted increasing research interest because of their potential application as stabilizers, emulsifiers, or dispersants in industrial and pharmaceutical preparations [16–23]. They are also useful in colloid chemistry and self-assembly chemistry.

In general, amphiphilic block copolymers composed of hydrophilic and hydrophobic segments can form a micellar structure [24–27]. These micelles have a hydrophobic compact inner core and a hydrophilic swollen outer shell in aqueous medium. In contrast to micelles formed from low molecular weight surfactants, block copolymeric micelles show a better structural stability, slower dissociation into free polymeric chains, and lower critical micelle concentration (CMC) [17,18,28–31].

Traditionally, well-defined block copolymers have been synthesized by living anionic polymerization via the sequential addition of monomers [32–34], group transfer polymerization techniques [17,20,25,31], living radical polymerization [21], and atom transfer radical polymerization (ATRP) [35,36]. Living polymerization is an excellent and well-established method for controlling copolymer architecture and obtaining narrow molecular weight distributions. However, these methods are invalid for the preparation of block copolymer containing both a polyether segment and a polyacrylate moiety by direct addition of polyether oligomer. Furthermore, anionic polymerization is performed under rigorous conditions such as in high-vacuum, highly purified monomers and quite low reaction temperature.

Oxyanion-initiated polymerization is an attractive polymerization technique from which well-defined block copolymers or macromonomers with narrow molecular weight distribution can be prepared [37–40]. In 1997, Nagasaki and coworkers [41,42] reported that 2-(diethylamino)ethyl methacrylate (DEAEMA) could polymerize using potassium 4-vinylbenzyl alcoholate as a functional initiator at or above ambient temperature. Subsequently, Armes and coworkers [37–40] extended the synthetic method to preparations of block copolymer and macromonomers with different chemical structures including 2-(dimethylamino)ethyl methacrylate (DMAEMA). One of the advantages of oxyanion-initiated polymerization is that it does not require such strict experimental conditions as in anionic polymerization. Therefore, this living process provides a new approach for the synthesis of block copolymers or macromonomers [43] with controlled molecular weight and molecular weight distribution. Another advantage of the technique is that it facilitates the incorporation of polyether blocks with poly(tertiary amine methacrylates) to give diblock, triblock, or hyperbranched copolymers [37,38,44,45].

Several research groups have investigated the possibility of using water-soluble diblock copolymers in place of conventional small-molecule surfactants for latex syntheses via emulsion polymerization [3,12,40,46–48]. Surprisingly, however, very few papers have described the applications of narrow-distribution, well-defined block copolymers containing cationic polyelectrolyte (e.g., DMAEMA

polymer) as surfactants in emulsion polymerization, especially in the preparation of surface functional particles.

The properties of polymeric microlatex, including surface properties, particle size, size distribution, and colloid stability, are remarkably important in biomedical applications [49,50]. The surface of polymeric microlatex particles should be changed easily for incorporation of proper biological ligands. Tuncel et al. [51] achieved the synthesis of monosized polystyrene latexes carrying functional groups on their surfaces. The polystyrene (PS) latexes prepared using poly(acrylic acid) (PA) as a steric stabilizer were used as the seed latex, and styrene/acrylate monomers, e.g., DMAEMA, were copolymerized onto the PS latex particles. Clinically, the PS latex carrying DMAEMA (labeled with ^{99m}Tc) has been used as a radionuclide for imaging of human gastrointestinal system by gamma scintigraphy [52,53]. Therefore, the research has a potential importance for latexes bearing poly(DMAEMA) on their surface.

More recently, a series of novel amphiphilic polymers with narrow molecular weight distribution have been designed and synthesized in the authors' laboratory [43,44]. The authors have successfully obtained an ABA triblock amphiphilic copolymer, poly[2-(dimethylamino)ethyl methacrylate]-*b*-poly(propylene oxide)-*b*-poly[2-(dimethylamino)ethyl methacrylate] (PDMAEMA-PPO-PDMAEMA), via oxyanion-initiated polymerization [44]. The hydrophilic blocks were poly(DMAEMA), whereas the hydrophobic segment was poly(propylene oxide) above ambient temperature. A novel Y-type poly(DMAEMA)-based macromonomer and benzyl-capped poly(DMAEMA) were also prepared through the same method [43]. All of these amphiphilic polymers are highly surface active in aqueous media. They were employed alone as polymeric surfactants in the classical batch emulsion polymerization of styrene, respectively. As the results of transmission electron microscopy (TEM) measurement and dynamic light scattering (DLS) analysis, the yielded microlatex particles had the obvious "hairy" fringe [54].

In addition to block or graft polymeric surfactants, comblike amphiphilic copolymers are also useful in polymer colloids [55–57]. In general, it is considered that random copolymer can be easily prepared via conventional free-radical polymerization, but their structure is usually ill defined due to their heterogeneity in composition. More recently, the authors used methacrylate monomers connecting hydrophilic or hydrophobic pendant groups to prepare comblike amphiphilic copolymers containing poly(ethylene glycol) (PEG) or epoxy group using special comonomer via free-radical copolymerization. This method is efficient for production of commercial polymer latex [58].

To obtain the stable microlatex particles, emulsion polymerization can be performed using this kind of polymeric emulsifier alone, or using mixed surfactants composed of anionic amphiphililes and polymeric surfactants [59–63]. The latex particles stabilized only by nonionic emulsifier are less stable and show a tendency to flocculate with one another during polymerization in comparison

with the recipe containing both anionic and nonionic emulsifiers. The electrostatic stabilization provided by anionic emulsifier improves latex stability at high temperature, whereas the steric stabilization provided by nonionic emulsifier enhances the chemical and freeze–thaw stability of latex products [61].

This chapter will mostly cover the syntheses and characterization of polymeric surfactant and their applications in preparations of microlatex in the author's laboratory. We will discuss (1) the effect of ABA triblock copolymer containing poly(DMAEMA) segments on the control of the emulsion polymerization process of styrene; (2) applications of a novel Y-type poly(DMAEMA)-based macromonomer in the preparation of monodispersed particles; and (3) comblike amphiphilic copolymer as surfactant.

II. MICROLATEX SYNTHESES USING ABA TRIBLOCK COPOLYMER AS SURFACTANT

A. Synthesis and Characterization of (PDMAEMA-PPO-PDMAEMA) [15]

It is well known that Pluronic block copolymers are commercially available symmetrical triblock copolymers with poly(ethylene oxide) (PEO) as the nonionic hydrophilic end block and poly(propylene oxide) (PPO) as the hydrophobic middle block [64–68]. Aqueous solution of PPO, with a degree of polymerization (DP) of 40, exhibits temperature dependence. Below approximately 15°C, water is a good solvent for PPO, whereas PPO aggregates at higher temperatures. In a likewise symmetrical structure, when PEO blocks are changed into cationic hydrophilic segments (such as DMAEMA), the new ABA triblock copolymer exhibits the very interesting properties.

In our laboratory, a series of novel near-monodispersed, well-defined ABA triblock copolymers, poly[2-(dimethylamino)ethyl methacrylate]-*b*-poly(propylene oxide)-*b*-poly[2-(dimethylamino)ethyl methacrylate] (PDMAEMA-PPO-PDMAEMA), were synthesized via oxyanion-initiated polymerization. Table 1 summarizes the compositions, molecular weights, and molecular weight distributions of the series of PDMAEMA-PPO-PDMAEMA triblock copolymers. The initiator was telechelic-type potassium alcoholate prepared from poly(propylene glycol) and KH in dry tetrahydrofuran (THF) at ambient temperature. The facile processes of polymerization of the triblock copolymer are depicted in Fig. 1. Fourier transform infrared (FTIR) and ^{1}H nuclear magnetic resonance (^{1}H NMR) measurements confirmed the well-defined triblock copolymers. The molecular weight of copolymers mainly depended on the molar ratio of DMAEMA monomer to initiator of potassium alcoholate. The M_w/M_n values of the copolymers measured by gel permeation chromatography (GPC) were 1.09–1.11, very close to that of the original PPO ($M_n = 2.0 \times 10^3$, $M_w/M_n = 1.09$ measured by GPC).

TABLE 1 Summary of the Compositions, Molecular Weights, and Molecular Weight Distributions of a Series of PDMAEMA-PPO-PDMAEMA Triblock Copolymers Prepared via Oxyanion-Initiated Polymerization

Run no.	[DMAEMA]/[PPO] (molar ratio)	Alcoholate T^a (°C)	Polym T (°C)	Time[b] (h)	M_n Theoretical	M_n NMR[c]	GPC M_w/M_n
DP20-1	25:1	30	50	2	6125	7600	1.11
DP06-3	25:1	30	30	2	6125	6750	1.09
DP07-2	25:1	30	30	2	6125	6660	1.10
DP12-1	24:1	0	30	1	5968	5770	1.11
DP07-4	26:1	0	30	2	6236	6040	1.14

[a]Reaction temperature in the process of forming potassium alcoholate.
[b]Reaction time of polymerization for DMAEMA.
[c]Experimental values were determined by ^{1}H NMR spectroscopy.

Figure 2 shows a typical ^{1}H NMR spectrum of the ABA triblock copolymer. Signals assigned to PDMAEMA moiety (at $\delta = 2.3$–2.4 ppm, $\delta = 2.6$–2.7 ppm, and $\delta = 4.1$–4.2 ppm) and the PPO moiety (at $\delta = 3.4$–3.5 ppm and $\delta = 3.7$–3.8 ppm) are clearly visible.

All the triblock copolymers obtained were readily soluble in dilute and aqueous hydrochloric acid. The aqueous solution was carefully adjusted to the de-

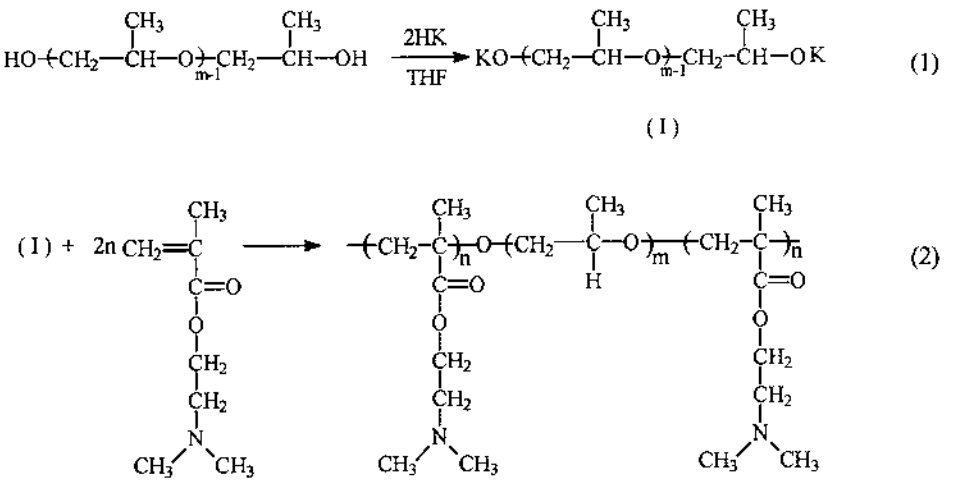

(1)

(2)

FIG. 1 Reaction scheme for the synthesis of a PDMAEMA-PPO-PDMAEMA triblock copolymer.

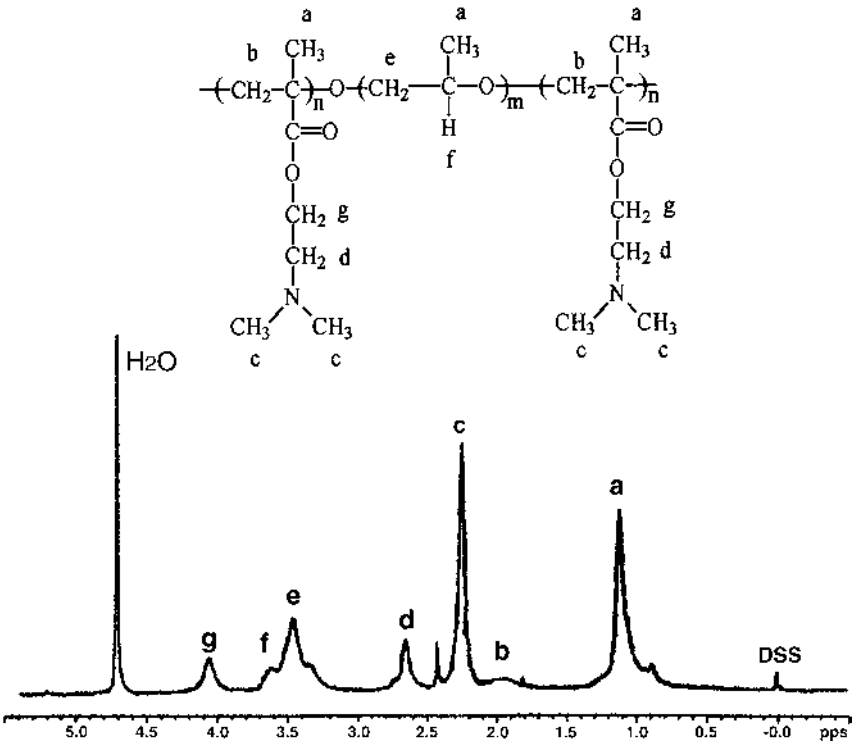

FIG. 2 Typical ^{1}H NMR spectrum for a PDMAEMA-PPO-PDMAEMA triblock copolymer at 20°C in D_2O.

sired pH. The surface activity of the copolymer DP07–2 ($PDMAEMA_{15}$-PPO_{36}-$PDMAEMA_{15}$) at the air–water interface was evaluated by determining surface tension under the conditions of pH 3.0 and 6.2, respectively. The CMC can be obtained by distinct change in the curve of surface tension vs. concentration of copolymer at 20°C. Figure 3 depicts the relationship between surface tension and the concentration of the ABA triblock copolymer. It indicates that the surface tension decreased rapidly with increasing copolymer concentration up to 0.1 g/L at pH 3.0 and 0.12 g/L at pH 6.2, respectively. Above these concentrations, a significantly higher limiting surface tension is approximately 40 mN m^{-1} for $PDMAEMA_{15}$-PPO_{36}-$PDMAEMA_{15}$ triblock copolymer. This datum is in reasonable agreement with the observation by Báñez and coworkers [38]. They presented the limiting surface tension of the DMAEMA homopolymer (DP = 66) as 43 mN m^{-1} at pH 9.5 and 52 mN m^{-1} at pH 6.0. The surface-active property of the ABA triblock copolymer suggests that such triblock copolymer

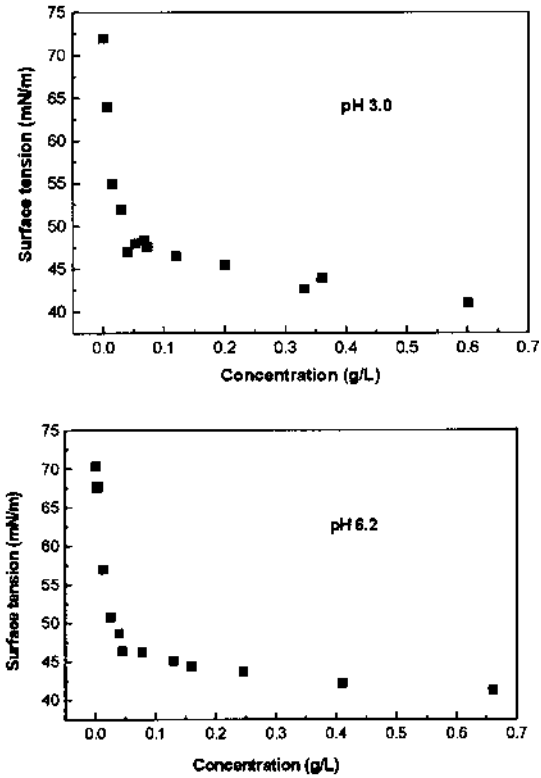

FIG. 3 Variation of the surface tension with the $PDMAEMA_{15}$-PPO_{36}-$PDMAEMA_{15}$ triblock copolymer concentration in an aqueous solution at pH 3.0 and pH 6.2.

may have interesting applications as surfactant or emulsifier in preparation of surface-clean and functional latex.

Above ambient temperature, the copolymer shows amphiphilic properties. PDMAEMA blocks were used as the cationic polyelectrolyte segments displaying pH-dependent ionization in acidic or neutral media, whereas PPO moiety used as the hydrophobic middle block above 15°C.

B. ABA Triblock Copolymer in Emulsion Polymerization of Styrene [54]

The batch emulsion polymerization of styrene in the presence of the PDMAEMA-PPO-PDMAEMA triblock copolymer as emulsifier was studied and compared with an emulsifier-free emulsion polymerization. All emulsion polymerizations

TABLE 2 Recipe for Emulsion Polymerization Using ABA Triblock Copolymer as Emulsifier

Ingredients	Quantities (g)
Styrene	1.0
$PDMAEMA_{15}$-PPO_{36}-$PDMAEMA_{15}$	0.005–0.100
V50	0.02
H_2O	50.0

were carried out at different pH aqueous solutions marked series A (pH 3.4), series B (pH 5.0), and series C (pH 7.0), respectively. A typical recipe for the emulsion polymerization is shown in Table 2.

The prerequisite for ABA triblock copolymer as surfactant is that the A blocks are swollen by the diluent and extend away from the particle surface, whereas the B blocks are entangled with each other to form micelles in aqueous solution. The efficient fixation of the polymeric emulsifier onto the particle surface mainly depends on the molecular structure and its amphiphilic property, as well as the concentration in solution. In our present study, the ABA triblock copolymer acted well both as a polycationic polymeric surfactant to form block copolymeric micelles for emulsion polymerization and as a stabilizer to be anchored in the polystyrene microlatex or adsorbed onto its surface (Fig. 4). The cationic polyelectrolyte layer with A blocks provided a protective barrier against flocculation.

The ABA triblock copolymer plays a critical role in the polymerization mechanism during the nucleation period and consequently on the final particle properties. Figure 5 describes the conversion vs. reaction time curves for the emulsion polymerization both in the presence of the polycationic triblock copolymer surfactant (2.0 g/L) at pH 3.4 and in the absence of any emulsifier.

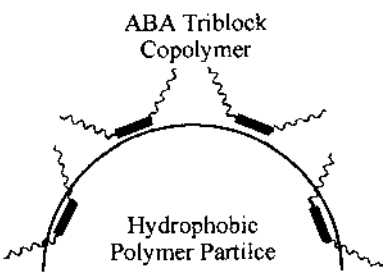

FIG. 4 Schematic representation of a polystyrene microlatex stabilized by adsorption or anchor of PDMAEMA-PPO-PDMAEMA triblock copolymer onto the surface.

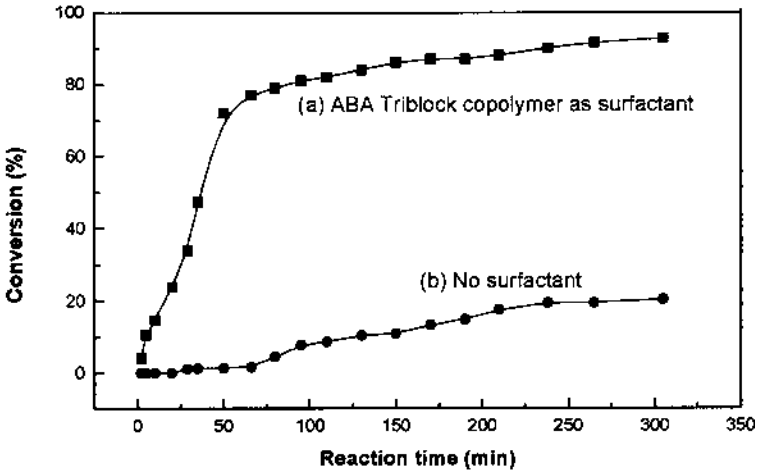

FIG. 5 Conversion vs. reaction time curves for (a) the emulsion polymerization of styrene in the presence of $PDMAEMA_{15}$-PPO_{36}-$PDMAEMA_{15}$ triblock copolymer as surfactant (2.0 g/L) at pH 3.4, and (b) the emulsifier-free polymerization of styrene at pH 3.4.

2′,2-Azobis(2-amidinopropane) dihydrochloride (V50) was used as a cationic initiator. The monomer conversions were determined by the gravimetric method. The significant differences in polymerization behavior can be observed. Curve (a) shows a very rapid polymerization of styrene in the presence of $PDMAEMA_{15}$-PPO_{36}-$PDMAEMA_{15}$ as emulsifier. The polymerization of styrene reached a high conversion value in the initial 60 min. After 5 h, the conversion of styrene is practically above 93%. In contrast, curve (b) of the conversion vs. reaction time without any emulsifier exhibits a slow slope during the polymerization process and a low conversion value within the same experiment range.

A consistent explanation of these behaviors can be given when we take into account the nucleation mechanisms for particle formation in emulsion polymerization, i.e., micellar and homogeneous nucleation. In the ABA triblock copolymer system (above the CMC), the particle nucleation takes place with a combination of micellar and homogeneous nucleation mechanisms, whereas in the case of surfactant-free emulsion polymerization, the values are the primary nucleation mechanism should be homogeneous nucleation since styrene is relatively low water solubility [1], and little micellization results in a very low polymerization rate.

The influence of triblock copolymer concentration on the particle size of microlatexes has been investigated by the analyses of TEM and DLS. In all cases, the particle size decreased when the amount of the copolymer stabilizer

increased. For a series A system, typical values are given in Table 3 for microlatexes prepared in the presence of the ABA triblock copolymer, suggesting that particles of low polydispersity can be obtained when the concentration of copolymer is over CMC.

Figure 6 a–c shows transmission electron micrographs of the particles of emulsion polymerization, corresponding to the PDMA-PPO-PDMA triblock copolymer concentrations at 0, 0.1, and 2.0 g/L, respectively. Due to the domination of homogeneous nucleation in emulsifier-free emulsion polymerization, the resulting particle diameter (D_n) was about 130 nm as shown in Fig. 6a, larger than that in all cases of $PDMAEMA_{15}$-PPO_{36}-$PDMAEMA_{15}$ triblock copolymer. For the ABA triblock copolymer system with the concentration of 2.0 g/L, the particle diameter (D_n) was about 35 nm, as shown in Fig. 6c. However, lower emulsifier concentration resulted in a larger size of the particle and wider particle size distribution. Fig. 6b shows the microlatexes, in which the concentration of the ABA triblock copolymer was 0.l g/L, just reaching the lowest limit of CMC. It can be observed that the particle size is not uniform. This result also can be attributed to the presence of two major mechanisms, i.e., micellar nucleation and homogeneous nucleation.

The particle sizes (D_n) obtained by TEM are systematically smaller than those of (D_z) from DLS measurement. This is the evidence of the presence of the PDMAEMA fringe on the particle surface, as DLS leads to the hydrodynamic radius of the microlatex including the surface layer of poly(DMAEMA), whereas in TEM experiments this fringe is collapsed and the particles are in dry state. For example, the hydrodynamic diameter (z average) as measured by DLS was 76 nm for sample No. 0724 in Table 3 (2.0 g/L of triblock copolymer). For

TABLE 3 Summary of the PDMAEMA-PPO-PDMAEMA Concentration, Particle Size of Microlatexes, and Particle Size Distribution in Series A

Exp. No.	W_{ABA} (g)	[ABA] (g/L)	Particle size[a] (nm)	Polydisperisty[b]	pH (before reaction)	pH (after reaction)
0725	0	0	351	0.20	3.40	3.65
0721	0.005	0.1	171	0.34	3.42	3.62
0723	0.025	0.5	91	0.11	3.38	3.74
0720	0.050	1.0	84	0.13	3.40	3.64
0724	0.100	2.0	76	0.06	3.42	3.61

[a]Particle diameters (z average) were measured by dynamic light scattering instrument (Malvern Autosizer 4700).

[b]Particle size distribution was expressed as polydispersity that is a model-independent estimate of the width of the size distribution.

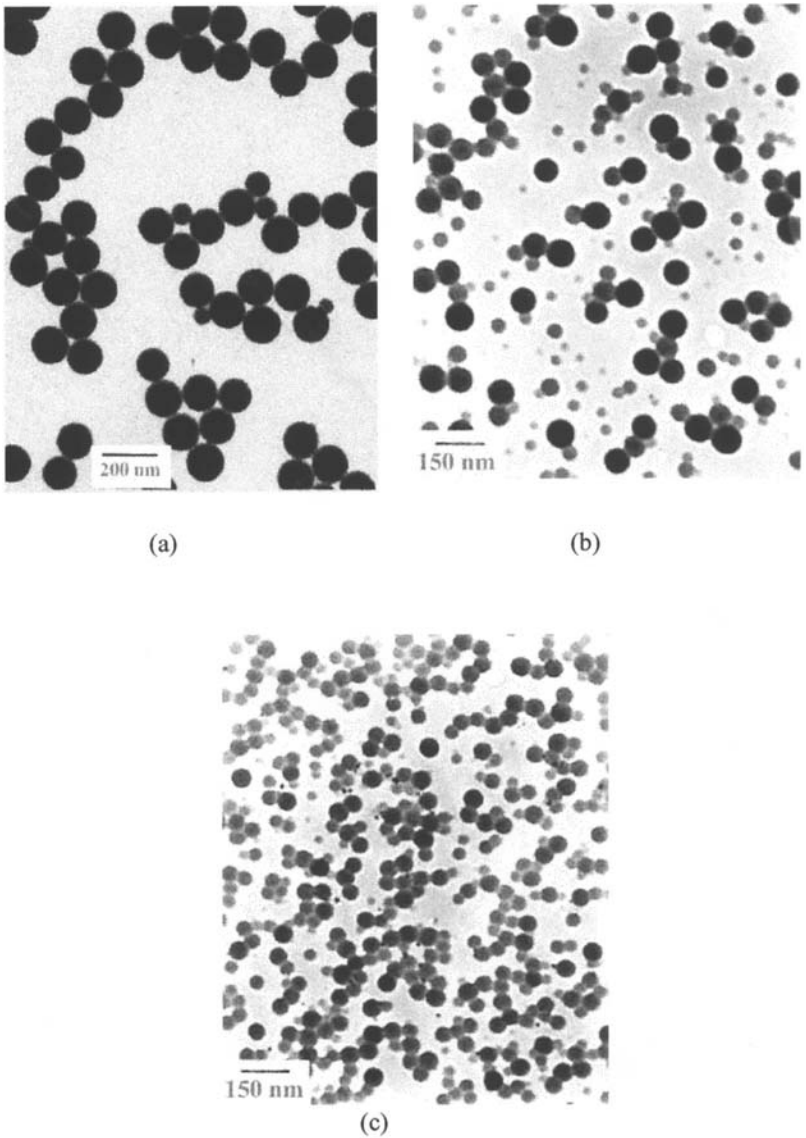

FIG. 6 Transmission electron micrographs of polystyrene latex synthesized by (a) emulsifier-free emulsion polymerization, (b) emulsion polymerization using 0.1 g/L of PDMAEMA-PPO-PDMAEMA triblock copolymer, and (c) emulsion polymerization using 2.0 g/L of the triblock copolymer. These polymerization processes were carried out at pH 3.4. [From Ref. 54.]

the same sample, compared with the average hard-core diameter as measured from the TEM micrograph about 35 nm in size, the adsorbed poly(DMAEMA) layer thickness was approximately 20 nm. The observation was in good agreement with the results obtained by other researchers [12,46]. This fact has been mentioned in the literature [69] as an effect of the adsorbed surfactants and the electrical double layers, which may become significant for small particle sizes because of the shrinkage of the dried particles in the electron beam. It is obvious that the highly effective, steric barriers can be generated by these adsorbed hydrophilic blocks.

Baines et al. [25] demonstrated that poly[2-(dimethylamino)ethyl methacrylate-*b*-alkyl methacrylate] copolymers are effective steric stabilizers for the dispersion polymerization of styrene. They found that variation of DMAEMA content in the copolymers produced relatively little change in latex particle size. As the concentration of block copolymer stabilizer was increased, the latex particle size decreased slightly. Riess [12] reported the use of PS-PEO di- and triblock copolymers for the preparation of microlatexes or microgels. The block copolymer offers the possibility of preparing hairy latexes, e.g., latex particles having a fringe of PEO on their surface.

To get a better understanding of the stabilization of PDMAEMA-PPO-PDMAEMA for emulsion polymerization in definite pH scope, three series of pH values were chosen. At the same solid content, all polymerization processes were carried out at 70°C in aqueous solution with definite pH value. Fig. 7 a–c presents the plots of particle diameter (z average)–concentration and polydipersity–concentration of the block copolymer at different pH media. In all cases, microlatex particle diameters decreased with the increase of $PDMAEMA_{15}$-PPO_{36}-$PDMAEMA_{15}$ concentration in the pH range 3.4–7.0. With the same concentration of copolymeric surfactant, the decreasing tendencies of particle diameter were interestingly similar to each other in the scope of pH 5.0–7.0 as shown in Fig. 7 b and c, indicating that microlatex particles were not largely influenced by pH media alone. Furthermore, the particle size distribution as expressed with polydispersity is getting narrower with the increase of the concentration of the ABA triblock copolymer.

Further increase in the amount of ABA triblock copolymer (4.0 g/L) led to much smaller microlatex particles, as shown in Fig. 8 a and b. The former microlatexes were prepared at pH 3.4, and the latter at pH 7.0. Even though the emulsion polymerization processed at pH 7.0, smaller microlatexes with better dispersity were still obtained. It was attributed to the swelling of the hydrophilic segments of poly(DMAEMA) in acidic condition and to their shrinking at neutral aqueous solution, which led to the larger microlatex in size at acidic condition than that of particles at neutral media.

Since these kinds of hydrophilic microlatex particles bearing cationic groups on their surface are likely to be utilized in biological applications involving high

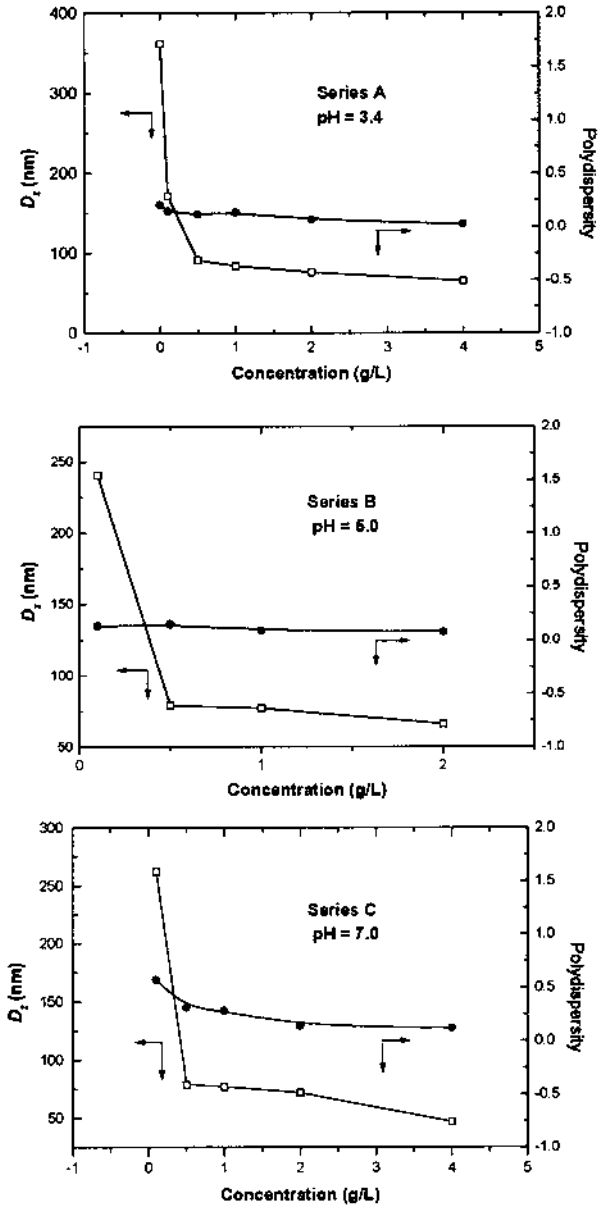

FIG. 7 Effect of concentration of triblock copolymer $PDMAEMA_{15}$-PPO_{36}-$PDMAEMA_{15}$ on the particle size and size distribution of PS microlatex prepared at different pH media. These data were measured by a dynamic light scattering instrument (Malvern Autosizer 4700). [From Ref. 54.]

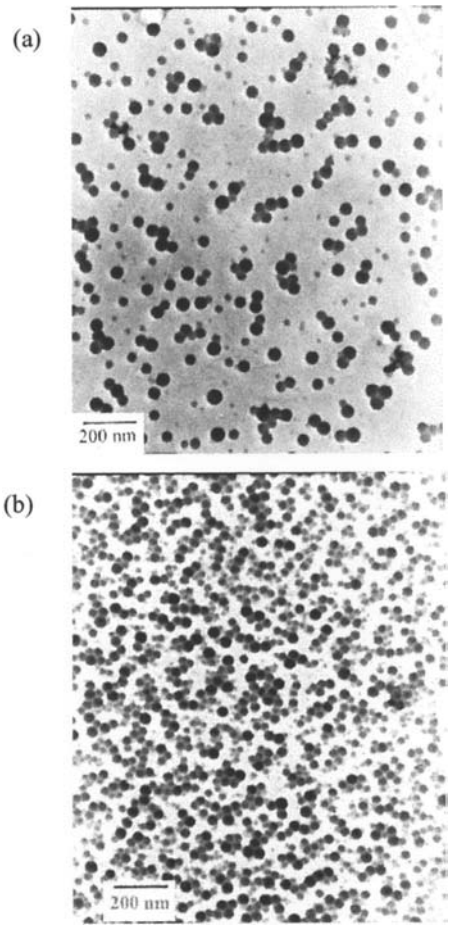

FIG. 8 Transmission electron micrographs of polystyrene microlatexes synthesized by emulsion polymerization using 4.0 g/L of $PDMAEMA_{15}$-PPO_{36}-$PDMAEMA_{15}$ triblock copolymer at (a) pH 3.4 and (b) pH 7.0. [From Ref. 54.]

ionic strength, it is also valuable to evaluate their stability behavior against electrolyte, e.g., KCl and NaCl aqueous solution [70]. This measurement was conducted through a turbidimetric method or observation of the microlatex particles from TEM. These results exhibited that all PS paticles using the ABA triblock copolymer as emulsifier were stable against KCl or NaCl solutions up to the concentration of salts at 2.5 mol/L. This evidence implied that these

microlatexes stabilized by the polymeric surfactant gave remarkable resistance against flocculation.

Figure 9 shows the microlatex particles prepared at pH 3.4 and 2.0 g/L of ABA triblock copolymer. The sample had been kept at ambient temperature for 8 months before it was run by TEM. It is clear that no coagulation appeared in this system, indicating that the PS particles carried cationic hairy groups have excellent colloid stability.

III. PREPARATION OF MONODISPERSITY MICROLATEX BEARING CATIONIC GROUPS

A. Y-type Poly(DMAEMA)-Based Macromonomers

A novel well-defined Y-type macromonomer based on DMAEMA methacrylate was synthesized via oxyanion-initial polymerization [43]. In this process, the dipotassium alcoholate of trimethylolpropane allyl ether (TMPAE) initiated the polymerization of DMAEMA in THF at ambient temperature. The reactive C=C double bonds located in the center of the macromonomer are shown in Fig. 10. Table 4 shows the synthesis and characterization of macromonomers. ^{1}H NMR spectroscopy is a useful method for the accurate determination for absolute molecular weights by end-group analysis [40,41]. Figure 11 shows a ^{1}H NMR spectrum of a typical macromonomer with $M_n = 12{,}800$ and $M_w/M_n =$

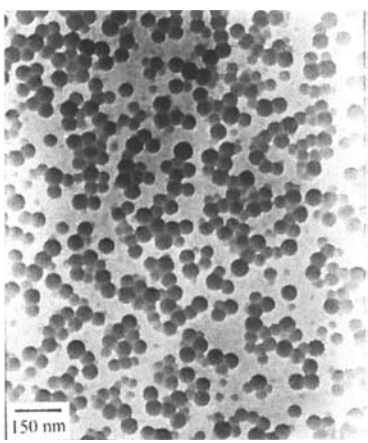

FIG 9. Transmission electron micrograph of polystyrene microlatex stabilized by triblock copolymer $PDMAEMA_{15}$-PPO_{36}-$PDMAEMA_{15}$ with concentration of 2.0 g/L at pH 3.4 after the sample was kept at ambient temperature for 8 months.

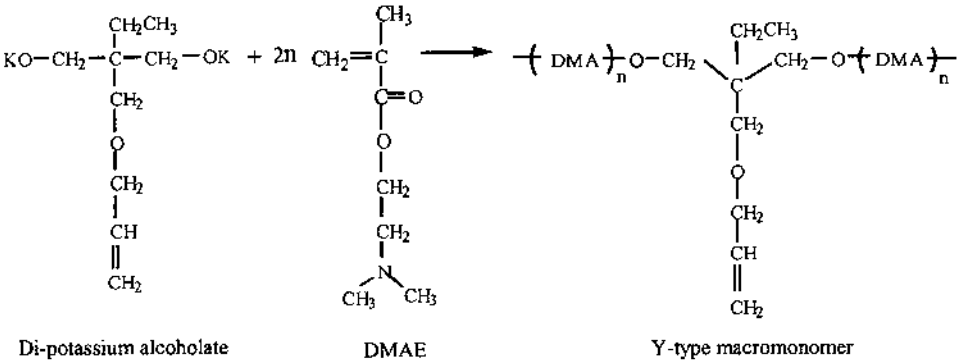

FIG. 10 Reaction scheme for the synthesis of the poly(DMAEMA)-based macromonomer via oxyanion-initiated polymerization with functional initiator.

1.27. Signals due to the allyl protons of the TMPAE are clearly visible at δ 5.0–6.0 ppm. A comparison of the peak integrals with those associated with the poly(DMAEMA) residues (at about 2.2–2.3 ppm, due to the six dimethylamino protons) allowed calculation of M_n. As derived by ^{1}H NMR, the molecular weights of macromonomers were basically in agreement with those expected from the corresponding monomer/initiator ratios.

GPC measurement also confirmed the molecular weight distribution of the Y-type macromonomer as very narrow (Fig. 12). Neither TMPAE trace nor other linear polymer residue was detected in the lower molecular weight region, suggesting that all of the TMPAE had reacted with DMAEMA monomer and gave the desired product.

TABLE 4 Synthesis of Macromonomers: Molar Ratio of the Monomer to Initiator in the Feed, and Characteristics of ^{1}H NMR and GPC

Exp. no.	Molar ratio of [DMAEMA] to [TMPAE]	t(°C)	Theor. M_n of macromers	M_n of macromers by ^{1}H NMR	M_w/M_n[a]
YM-01	33 / 1	30	5400	5700	1.07
YM-06	36 / 1	30	5800	6100	1.14
YM-11	38 / 1	25	6100	6800	1.35
YM-13	44 / 1	25	7100	6400	1.10
YM-23	74 / 1	25	11800	12300	1.30
YM-28	76 / 1	25	12100	12800	1.27

[a]As measured by GPC.

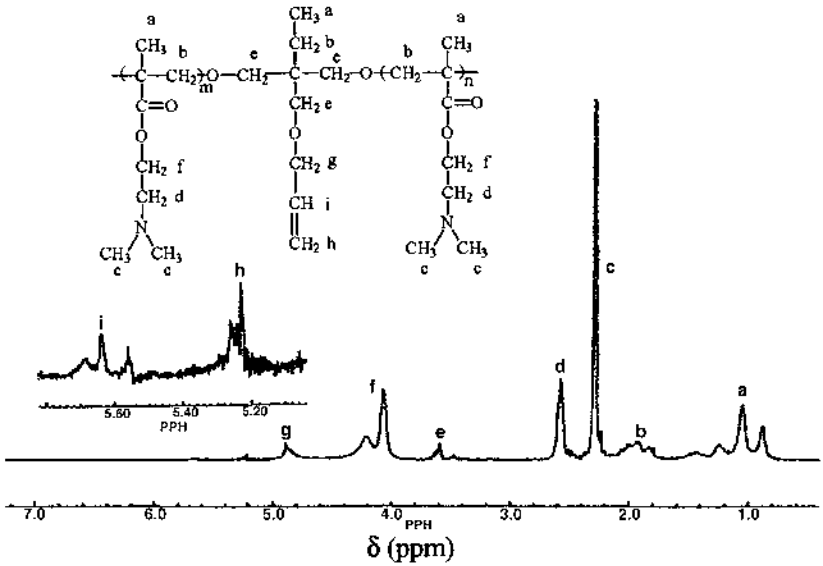

FIG. 11 Assigned ^{1}H NMR spectrum for a typical poly(DMAEMA)-based macromonomer prepared by oxyanion-initiated polymerization using the dipotassium alcoholate of trimethylolpropane allyl ether as initiator. [From Ref. 43.]

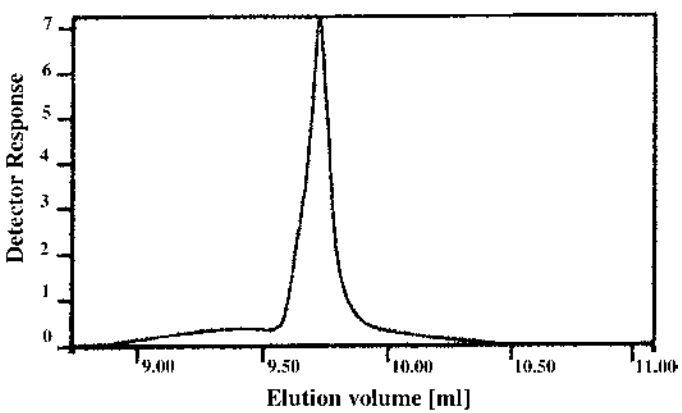

FIG. 12 A typical gel permeation chromatograph of the poly(DMAEMA)based macromonomer, which was determined with a GPC (HP-1100 instrument) calibrated by polystyrene standards.

Figure 13 exhibits the evolution of the surface tension with the macromonomer concentration for a representative macromonomer. The CMC value was determined with a JYW-200A automatic surface tensiometer equipped with an electrical torsion balance and a platinum ring (Chengde Experimental Instrument Co., Chengde China). The CMC appeared in the range 0.1–0.3 g/L. The lowest surface tension achieved was 46 mN m^{-1} at 20°C.

B. Benzyl-Capped Poly(DMAEMA)

Potassium 4-vinylbenzyl alcoholate was used as a functional initiator to prepare poly[2(diethylamino)ethyl methacrylate] macromonomer [41] or poly(DMAEMA) macromonomer [40]. Commercially, 4-vinylbenzyl alcoholate is, however, much more costly than benzyl alcohol. More recently, the authors tried to utilize potassium benzyl alcoholate as an initiator to perform the oxyanion-initiated polymerization of DMAEMA and successfully obtained well-defined benzyl-capped poly(DMAEMA) (Bz-PDMA) as shown in Table 5. FTIR, GPC, and ^{1}H NMR measurements indicated that the products were the desired polymer.

The results of surface tension measurement proved that the benzyl-capped poly(DMAEMA) had as good surface properties as other polymeric surfactants that the authors have synthesized. For Bz-$PDMA_{20}$, the lowest surface tension was about 39 mN m^{-1} at the concentration of 10 g/L.

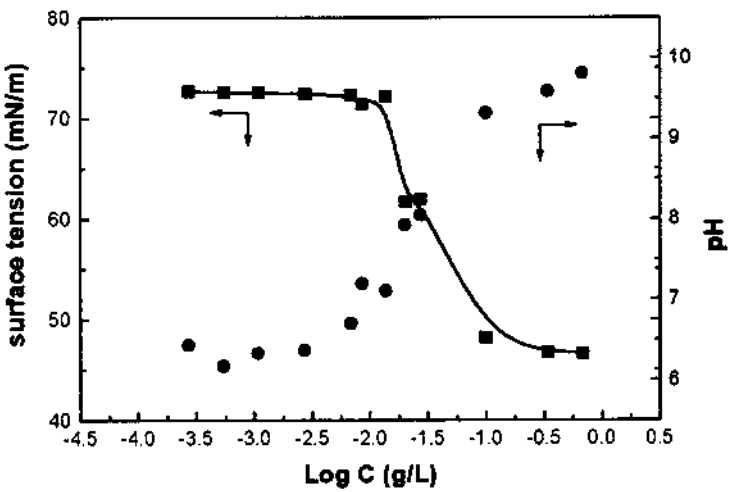

FIG. 13 Surface tension and pH value curves as a function of concentration of the poly(DMAEMA)-based macromonomer ($M_n = 12800$, $M_w/M_n = 1.21$) in aqueous solution. [From Ref. 43.]

TABLE 5 Synthesis of Benzyl-Capped Poly(DMAEMA): Molar Ratio of the Monomer to Initiator in the Feed, and Characteristics of ^{1}H NMR and GPC

Exp. no.	Molar ratio of [BzOH] to [DMAEMA]	Theor M_n of macromers	M_n of macromers by ^{1}H NMR	M_w/M_n[a]
Bz-PDMA$_{10}$	1:10	1680	1730	1.14
Bz-PDMA$_{20}$	1:20	3250	4550	1.21
Bz-PDMA$_{30}$	1:30	4820	5990	1.20

[a]As measured by GPC.

C. Polystyrene Microlatexes Bearing Cationic Groups on the Surface

To evaluate if the obtained Y-type macromonomer can be copolymerized with other common monomers, the copolymerization with styrene was carried out using 2,2′-azobisisobutyronitrile (AIBN) as initiator. The macromonomer was employed as both comonomer and emulsifier in the emulsion polymerization of styrene. Since the Y-type macromonomer contained a reactive double bond, it could incorporate into polystyrene particles [36], whereas its two hydrophilic "tails," i.e., poly(DMAEMA) segments, were left in aqueous phase. They worked more efficiently as steric barriers than those containing only one hydrophilic chain. Figure 14 presents a typical TEM image of the Y-type macromonomer-stabilized polystyrene microlatexes synthesized by aqueous emulsion polymerization at pH 5 and 70°C using 20% stabilizer (based on the amount of

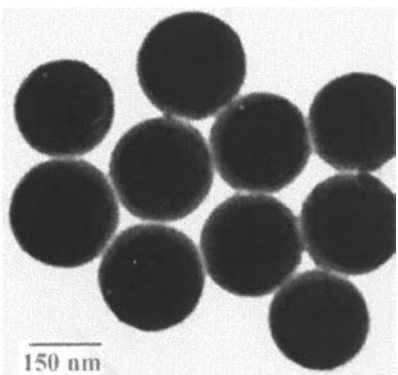

FIG. 14 A TEM image of a polystryrene core-poly(DMAEMA) corona microsphere stabilized by 20 wt % Y-type poly(DMAEMA)-based macromonomer at pH 5 and 70°C.

styrene monomer). The number average particle size was 210 nm. For the same sample, the particle size (D_z) and polydipersity measured by DLS were 246 nm and 0.01, respectively. It has been obvious that the poly(DMAEMA) layer thickness was approximately 18 nm because of the shrinkage of the dried particles in the electron beam. This observation was in reasonable agreement with the results obtained by Riess [12].

The DMAEMA-based macromonomer proved to be particularly efficient, with a minimum stabilizer concentration of only 1.0 g/L required for successful colloid formation. However, DMAEMA homopolymer proved to be completely ineffective, with only precipitate being obtained even at higher stabilizer concentrations up to 10 g/L.

Very interestingly, benzyl-capped poly(DMAEMA) contributed its efficient surface activity as a stabilizer in emulsion polymerization of styrene. For example, in a range of the low concentration of Bz-DMA_{20}, from about 0.05 g/L to 0.2 g/L, nearly monodispersed particles were obtained, while a broad particle size distribution appeared out of the limited concentrations. Figure 15a shows a TEM image of polystyrene microlatexes stabilized by Bz-DMA_{20} with the concentration of 7.4×10^{-2} g/L, and Fig. 15b with the concentration of 5.0×10^{-3} g/L, without any other surfactant in the system.

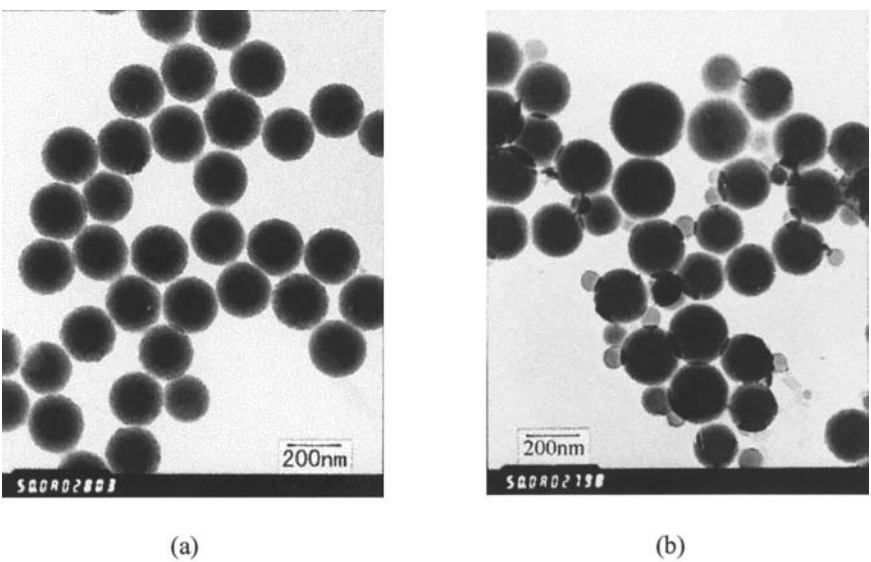

FIG. 15 Transmission electron micrographs of polystyrene microlatexes stabilized by Bz-DMA_{20} with the concentration of (a) 7.4×10^{-2} g/L and (b) 5.0×10^{-3} g/L. The emulsion polymerization of styrene was carried out at pH 5 and 70°C.

D. Mixed Surfactants of Comblike Copolymer and Anionic Surfactant in Emulsion Polymerization

1. Comblike Copolymer Surfactant Containing PEG

Free-radical polymerization is the referred process for polymer manufacturing because it possesses a relating economical process that can tolerate trace impurities and be carried out under mild reaction conditions. This method is efficient for production of commercial polymer latex.

Amphiphilic copolymers containing PEG have attracted much attention for their preparation strategies and physicochemical properties. In addition due to PEG's unique hydrophilic properties, there has been growing interest in their applications in the design of drug delivery systems and for the modification of biomedical polymer surfaces [55–57].

In formulating products such as paints, inks, cosmetics, and pharmaceuticals, it is often necessary to emulsify liquid components and to stabilize dispersions of solid particles in a single aqueous formulation [71]. As complex formulations, however, one component may interact with increasing levels of emulsifier or stabilizer, depriving other components and thus causing instability. Haak [72] and Creutz et al. [73] suggested use of a polymeric emulsifier with multiple functionalities. We primarily investigated the synthesis of a comblike copolymer of PEGMA-*co*-SMA-*co*-MAA-*co*-AA via conventional free-radical copolymerization [58]. In this study, the comonomers included (1) PEG methacrylate (PEGMA; a nonionic hydrophilic monomer), (2) stearyl methacrylate (SMA; a hydrophobic monomer), and (3) several anionic hydrophilic monomers in basic aqueous solution, such as acrylic acid (AA) and methacrylic acid (MAA), with the initial feed molar ratio of PEGMA:SMA:AA:MA equal to 50:20:25:5. In order to obtain different molecular weight of the copolymer, transfer agent was adopted. The idealized structure is shown in Fig. 16. ^{1}H NMR and FTIR analyses (not shown) confirmed that the copolymer was the expected product.

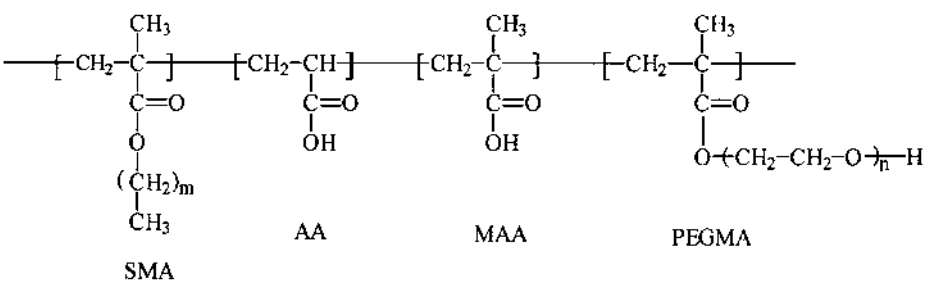

FIG. 16 Idealized structure of PEGMA-*co*-SMA-*co*-MAA-*co*-AA comblike copolymers synthesized. [From Ref. 68.]

The surface-active properties of a representative copolymer ($M_n = 1.4 \times 10^4$) at an air–water interface was determined by surface tension measurement. Figure 17 depicts the surface tension vs. concentration curve. As expected, the random copolymer exhibited significant surface-active behavior, as indicated by the substantial decrease in surface tension with increasing copolymer concentration in water. The lowest surface tension achieved was 38 mN m^{-1} at 25°C—a decrease of at least 30 mN m^{-1} compared with pure water.

2. Comblike Copolymer Surfactant Containing Epoxy Group

Amphiphilic copolymer containing epoxy groups, which has potential applications in advanced biotechnology, such as DNA separations, target medicines, enzyme immobilizations, and immunology determinations by the easy conversion of epoxy groups into a series of functional groups (e.g., −OH, $-NH_2$, and −COOH), has not been the subject of much attention [74]. Consequently, the authors prepared comblike amphiphilic copolymer using PEGMA, SMA, and glycidyl methacrylate (GMA) via conventional free radical copolymerization. ^{1}H NMR and FTIR analyses (not shown) confirmed that PEGMA-*co*-SMA-*co*-GMA copolymer was the desired product. The results of titration for epoxy group showed that the epoxy content in the copolymer corresponded to the initial feed proportion.

Figure 18 shows a typical TEM image of micelles prepared by first dissolving a PEGMA-*co*-SMA-*co*-GMA copolymer in deionized water and then diluting with deionized water to a final copolymer concentration of 10 g/L at 20°C.

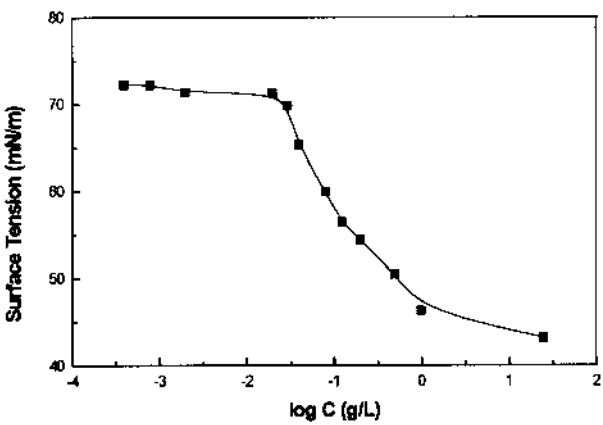

FIG. 17 Plot of surface tension vs. logarithm of the concentration of aqueous surfactant solution for the PEGMA-*co*-SMA-*co*-MAA-*co*-AA comblike copolymer.

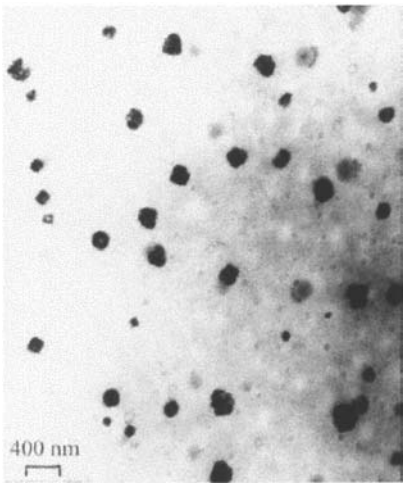

FIG. 18 TEM image of micelles produced by poly(SMA-*co*-GMA-*co*-PEGMA) comblike copolymer ($M_n = 1.3 \times 10^4$, $M_w/M_n = 1.95$) with a concentration of 10 g/L.

This image exhibits the existence of spherical micelles with diameters in the 100- to 300-nm range.

3. Preparation of MMA/BA Microlatex Particles

Comblike polymers with stearyl side chains, PEG pendant, and a statistical distribution of carboxylate groups synthesized by free-radical polymerization were chosen to investigate whether such copolymers really are effective as surfactant in emulsion polymerization. The solution of this problem will constitute an important contribution to industrial applications.

The emulsion copolymerization of MMA/BA was performed using the poly(PEGMA-*co*-SMA-*co*-AA-*co*-MAA) [58] alone as emulsifier at pH 8 and 70°C. It was shown that this kind of amphiphilic copolymer acted as an efficient stabilizer. The hydrophobic stearyl side chains anchored into the MMA/BA core; the main backbone was adsorbed onto the particle surface; while the hydrophilic PEG chains extended to the water phase and formed PEG corona. Carboxylate groups in the copolymer impart electrostatic repulsion. From the TEM image in Fig. 19, one can observe the rough surface of the particles.

The synergic effect of anionic surfactant and polymer surfactant was considered in the study because anionic surfactant reduced largely the interface tension of oily monomer–water [71,75]. As a steric stabilizer, polymeric surfactant is more compact on the particle surface than that of the case that only anionic surfactant used [73,76]. Figure 20 shows a TEM image of MMA/BA copolymer

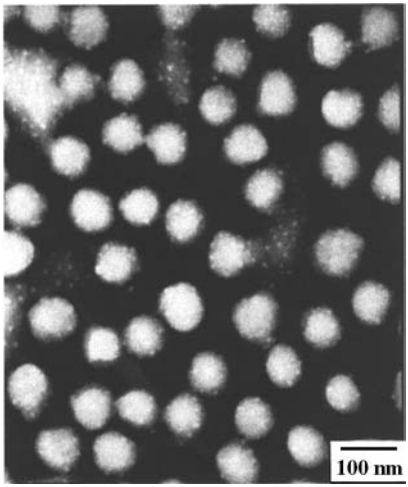

FIG. 19 Transmission electron micrograph of latex of poly(MMA/BA) stabilized by comblike polymeric surfactant of poly(PEGMA-*co*-SMA-*co*-AA-*co*-MAA) with concentration of 0.25 g/L at pH 7.5, without anionic surfactant SDS.

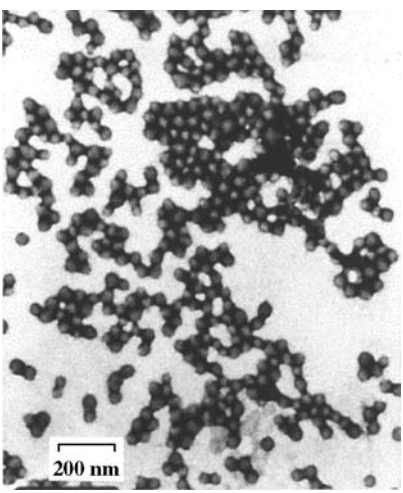

FIG. 20 Transmission electron micrograph of representative latexes of poly(MMA/BA) stabilized by the mixed surfactants of comblike copolymeric surfactant and SDS with concentrations of 0.17 g/L and 0.01(SDS) g/L, respectively. The emulsion polymerization was carried out at pH 8.

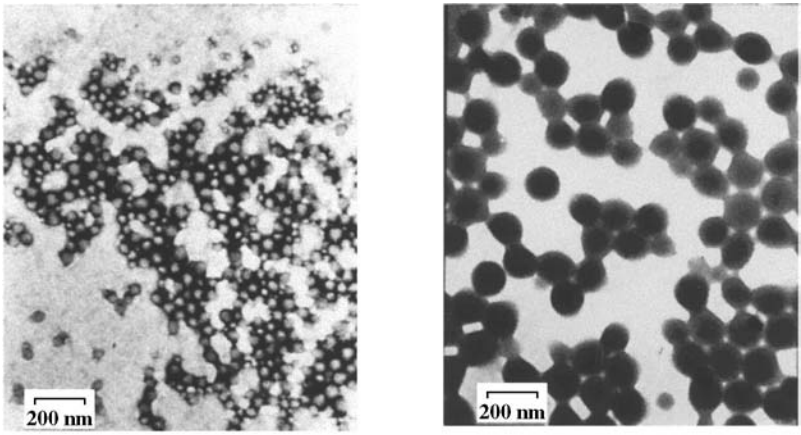

FIG. 21 Transmission electron micrographs of MMA/BA copolymer latexes using poly (SMA-*co*-GMA-*co*-PEGMA) and SDS as mixed surfactants for (a) 0.1 g SDS and (b) 0.01 g SDS. The emulsion polymerization processes were carried out at pH 8.

particles stabilized by the mixed surfactant of sodium dodecyl sulfate (SDS) and poly(PEGMA-SMA-AA-MA). The particle size is much smaller than that of the system without any SDS in Fig. 19.

Using the mixture of SDS and the polymeric surfactant poly(PEGMA-SMA-GMA) instead of poly(PEGMA-SMA-AA-MA), we were able to obtain fine and stable microlatex particles containing epoxy groups on their surface as shown in Fig. 21. At the same concentration of polymeric surfactant, the particle size decreased with the increase of the concentration of SDS, indicating that anionic surfactant was more efficient than polymeric emulsifier in reducing interface tension.

REFERENCES

1. Lovell, P.A.; El-Aasser, M.S. *Emulsion Polymerization and Emulsion Polymers*; John Wiley and Sons: New York, 1997; 37–117.
2. Pichot, C.; Delair, T.; Elaïssari, A. Polymer colloids for biomedical and pharmaceutical applications. In *Polymeric Dispersions*: *Principles and Applications*; Asua, J.M., Ed.; Kluwer Academic Publisher: Dordrecht, The Netherlands, 1997; 515–539.
3. Burguière, C.; Pascual, S.; Bui, C.; Vairon, J.P.; Charleux, B.; Davis, K.A.; Matyjaszewski, K.; Bétremieux, I. Block copolymers of poly(styrene) and poly(acrylic acid) of various molar masses, topologies and compositions prepared via con-

trolled/living radical polymerization. Application as stabilizers in emulsion polymerization. Macromolecules **2001**, *34*, 4439–4450.
4. Piirma, I. *Polymeric Surfactants*; Surfactant Science Series Vol 24; Marcel Dekker: New York, 1992.
5. McCartney, T.L.; Piirma, I. Preparation of a water-soluble polyester surfactant and its use in the emulsion polymerization of styrene. Polym. Bull. **1990**, *23*, 367–371.
6. El-Nokaly, M.A. Preparation of microlatex with functionalized polyesters as surfactants; In *Polymer Association Structures Microemulsions and Liquid Crystals*, Cuirassier, F., Baradji, C.H., Riess G., Eds.; ACS Symposium Series 384; American Chemical Society: Washington, DC, **1989**; 100–115.
7. Alexandridis, P.; Athanassiou, V.; Fukuda, S.; Hatton, T.A. Surface activity of poly(ethylene oxide)–*block*-poly(propylene oxide)–*block*-poly(ethylene oxide) copolymers. Langmuir **1994**, *10*, 2604–2612.
8. Charmeau, J.Y.; Kientz, E.; Holl, Y. Adhesion of latex films; influence of surfactants. Prog. Org. Coat. **1996**, *27*, 87–93.
9. Riess, G.; Bahadur, P.; Hurtrez, G. *Encyclopedia of Polymer Sciences and Engineering*, 2nd Ed., Vol. 2; John Wiley and Sons, New York, 1985; 324.
10. Cochin, D.; Laschewsky, A.; Nallet, F. Emulsion polymerization of styrene using conventional, polymerizable, and polymeric surfactants. A comparative study. Macromolecules **1997**, *30*, 2278–2287.
11. Müller, H.; Leube, W.; Tauer, K.; Förster, S.; Antonietti, M. Polyelectrolyte block copolymers as effective stabilizers in emulsion polymerization. Macromolecules **1997**, *30*, 2288–2293.
12. Riess, G. Block copolymers as polymeric surfactants in latex and microlatex technology. Colloids & Surf. A: Physiochem. Eng. Asp. **1999**, *153*, 99–110.
13. Akashi, M.; Chao, D.; Yashima, D.; Miyauchi, N.J. Graft copolymers having hydrophobic backbone and hydrophilic branches. 5. Microspheres obtained by the copolymerization of poly(ethylene glycol) macromonomer with methyl methacrylate. J. Appl. Polym. Sci. **1990**, *39*, 2027–2030.
14. Chen, M.Q.; Kishida, A.; Serizawa, T.; Akashi, M. Graft copolymers having hydrophobic backbone and hydrophilic branches. 27. Nanosphere formation in copolymerization of methyl methacrylate with poly(ethylene glycol) macromonomers. J. Polym. Sci. Polym. Chem. Ed. **2000**, *38*, 1811–1817.
15. Ishizu, K.; Yamashita, M.; Ichimura, A. Microsphere synthesis by emulsion copolymerization of methyl methacrylate with poly(acrylic acid) macromonomers. Polymer **1997** *38*, 5471–5474.
16. Wen, S.; Yin, X.N.; Stevenson. W.T.K. Preparation and characterization of polyelectrolyte copolymers containing methyl methacrylate, and 2-hydroxyethyl methacrylate. II. Polymers based on dimethylaminoethyl methacrylate. J. Appl. Polym. Sci. **1991**,*43*, 205–212.
17. Baines, F.L.; Armes, S.P.; Billingham, N.C.; Tuzar, A.Z. Micellization of poly(2-(dimethylamino)ethyl methacrylate-block-methyl methacrylate) copolymers in aqueous solution. Macromolecules **1996**, *29*, 8151–8159.
18. Antoun, S.; Gohy, J.F.; Jérôme, R. Micellization of quaternized poly(2-(dimethylamino)ethyl methacrylate)–*block*–poly(methyl methacrylate) copolymers in water. Polymer **2001**, *42*, 3641–3648.

19. Baines, F.L.; Billingham, N.C.; Armes, S.P. Synthesis and solution properties of water-soluble hydrophilic–hydrophobic block copolymers. Macromolecules **1996**, *29*, 3416–3420.
20. Lowe, A.B.; Billingham, N.C.; Armes, S.P. Synthesis and characterization of zwitterionic block copolymers. Macromolecules **1998**, *31*, 5991–5998.
21. Zhang, Z.R.; Liu, G.J.; Bell, S. Synthesis of poly(solketal methacrylate)–*block*–poly(2-(dimethylamino)ethyl methacrylate) and preparation of nanospheres with cross-linked shells. Macromolecules **2000**, *33*, 7877–7883.
22. Bütün, V.; Billingham, N.C.; Armes, S.P. Synthesis and aqueous solution properties of novel hydrophilic–hydrophilic block copolymers based on tertiary amine methacrylates. Chem. Commun. **1997**, 671–672.
23. Bütün, V.; Billingham, N.C.; Armes, S.P. Synthesis of shell cross-linked micelles with tunable hydrophilic/hydrophobic cores. J. Am. Chem. Soc. **1998**, *120*, 12135–12136.
24. Bütün, V.; Billingham, N.C.; Armes, S.P. Unusual aggregation behavior of a novel tertiary amine methacrylate-based diblock copolymer: formation of micelles and reverse micelles in aqueous solution. J. Am. Chem. Soc. **1998**, *120*, 11818–11819.
25. Baines, F.L.; Dionisio, S.; Billingham, N.C.; Armes, S.P. Use of block copolymer stabilizers for the dispersion polymerization of styrene in alcoholic media. Macromolecules **1996**, *29*, 3096–3102.
26. Dowling, K.C.; Thomas, J.K. A novel micellar synthesis and photophysical characterization of water-soluble acrylamide styrene block copolymers. Macromolecules **1990**, *23*,1059–1064.
27. Astafieva, I.; Zhong, X.F.; Eisenberg, A. Critical micellization phenomena in block polyelectrolyte solutions. Macromolecules **1993**, *26*, 7339–7352.
28. Gao, Z.S.; Eisenberg, A. A model of micellization for block copolymers in solutions. Macromolecules **1993**, *26*, 7353–7360.
29. Wilhelm, M.; Zhao, C.L.; Wang, Y.C.; Xu, R.L.; Winnik, M.A. Polymer micelle formation. 3. Poly(styrene-ethylene oxide) block copolymer micelle formation in water—a fluorescence probe study. Macromolecules **1991**, *24*, 1033–1040.
30. Quintana, J.R.; Villacampa, M.; Katime, I.A. Micellization of a polystyrene-*b*-poly(ethylene/propylene) block copolymer in n-dodecane/1,4-dioxane mixtures. 2. Structure and dimensions of micelles. Macromolecules **1993**, *26*, 606–611.
31. An, S.W.; Su, T.J.; Thomas, R.K.; Baines, F.L.; Billingham, N.C.; Armes, S.P.; Penfold, J. Neutron reflectivity of an adsorbed water-soluble block copolymer: a surface transition to micelle-like aggregates at the air/water interface. J. Phys. Chem. Part B **1998**, *102*, 387–393.
32. Creutz, S.; Teyssié, P.; Jérôme, R. Living anionic homopolymerization and block copolymerization of (dimethylamino)ethyl methacrylate. Macromolecules **1997**, *30*, 6–9.
33. Antoun, S.; Wang, J.S.; Jérôme, R.; Teyssié, P. Anionic polymerization of various methacrylates initiated with LiCl-complexed s-BuLi. Polymer **1996**, *37*, 5755–5759.
34. Antoun, S.; Teyssié, P.; Jérôme, R. Lithium diisopropylamide as initiator for the anionic polymerization of methacrylates. Macromolecules **1997**, *30*, 1556–1561.

35. Zhang, X.; Matyjaszewski, K. Synthesis of well-defined amphiphilic block copolymers with 2-(dimethylamino)ethyl methacrylate by controlled radical polymerization. Macromolecules **1999**, *32*, 1763–1766.
36. Zeng, F.Q.; Shen, Y.Q.; Zhu, S.P.; Pelton, R. Synthesis and characterization of comb-branched polyelectrolytes. 1. Preparation of cationic macromonomer of 2-(dimethylamino)ethyl methacrylate by atom transfer radical polymerization. Macromolecules **2000**, *33*, 1628–1635.
37. Vamvakaki, M.; Billingham, N.C.; Armes, S.P. Synthesis of controlled structure water-soluble diblock copolymers via oxyanionic polymerization. Macromolecules **1999**, *32*, 2088–2090.
38. Báñez, M.V.P.; Robinson, K.L.; Armes, S.P. Synthesis and solution properties of dimethylsiloxane-2-(dimethylamino)ethyl methacrylate block copolymers. Macromolecules **2000**, *33*, 451–456.
39. Báñez, M.V.P.; Robinson, K.L.; Bütün, V.; Armes, S.P. Use of oxyanion-initiated polymerization for the synthesis of amine methacrylate-based homopolymers and block copolymers. Polymer **2001**, *42*, 29–37.
40. Lascelles, S.F.; Malet, F.; Mayada, R.; Billingham, N.C.; Armes, S.P. Latex syntheses using novel tertiary amine metharylate-based macromonomers prepared by oxyanionic polymerization. Macromolecules **1999**, *32*, 2462–2471.
41. Nagasaki, Y.; Sato, Y.; Kato, M. A novel synthesis of semitelechelic functional poly(methacrylate)s through an alcoholate initiated polymerization. Synthesis of poly[2-(*N*,*N*-diethylaminoethyl)methacrylate] macromonomer. Macromol. Rapid Commun. **1997**, *18*, 827–835.
42. Iijima, M.; Nagasaki, Y.; Kato, M.; Kataoka, K. A potassium alcoholate-initiated polymerization of 2-(trialkylsiloxyethyl) methacrylate. Polymer **1997**, *38*, 1197–1202.
43. Ni, P.H.; Pan, Q.S.; Fu, S.K. Synthesis of Y-type macromonomer based on 2-(*N*,*N*-dimethylamino)-ethyl methacrylate via oxyanoin-initiated polymerization. Chem. J. Chinese Univ. (in Chinese) **2002**, *23*, 748–750.
44. Ni, P.H.; Pan, Q.S.; Zha, L.S.; Wang, C.C.; Elaïssari, A.; Fu, S.K. Syntheses and characterizations of poly[2-(dimethylamino)ethyl methacrylate]–poly(propylene oxide)–poly[2-(dimethylamino)ethyl methacrylate] ABA triblock copolymers. J. Polym. Sci. A Polym. Chem. **2002**, *40*, 624–631.
45. Ni, P.H.; Cao, X.P.; Yan, D.Y.; Hou, J.; Fu, S.K. Synthsis of novel temperature/pH responsive polymer via oxyanionic polymerization. Chinese Sci. Bull. **2002**, *47*, 280–283.
46. Leemans, L.; Fayt, R.; Teyssié, P.; Jaeger, N.C.D. Poly(alkyl methacrylate-b-sulfonated glycidyl methacrylate). A new amphiphilic polymeric surfactant for the preparation and stabilization of polymer acrylic latices in aqueous medium. Macromolecules **1991**, *24*, 5922–5925.
47. Leemans, L.; Jérôme, R.; Teyssié, P. Diffusive radical entry as the rate-determining step in amphiphilic block polyelectrolyte mediated emulsion polymerization. Macromolecules **1998**, *31*, 5565–5571.
48. Winzor, C.L.; Mrazek, Z.; Winnik, M.A.; Croucher, M.D.; Riess, G. Stabilization of dispersion polymerization by poly(styrene-*b*-ethylene oxide) copolymers. Eur. Polym. J. **1994**, *30*, 121–128.

49. Lee, J.H.; Kopeckova, P.; Kopecek, J.; Andrade, J.D. Surface properties of copolymers of alkyl methacrylates with methoxy(polyethylene oxide) methacrylates and their application as protein-resistant coatings. Biomaterials **1990**, *11*, 455–464.
50. Chiu, H.C.; Chern, C.S.; Lee, C.L.; Chang, H.F. Synthesis and characterization of amphiphilic poly(ethylene glycol) graft copolymers and their potential application as drug carriers. Polymer **1998**, *39*, 1609–1616.
51. Tuncel, A.; Kahraman, R.; Piskin, R. Monosize polystyrene latices carrying functional groups on their surfaces. J. Appl. Polym. Sci. **1994**, *51*, 1485–1498.
52. Ercan, M.T.; Tuncel, S.A.; Caner, B.E.; Mutlu, M.; Piskin, E. Evaluation of Tc-99m-labeled monodisperse polystyrene polyacrylate latex particles for the study of colon transit and morphology. Nucl. Med. Biol. **1991**, *l18*, 253–258.
53. Ercan, M.T.; Tuncel, S.A.; Caner, B.E.; Piskin, E. Tc-99m-labeled monodisperse latex particles coated with amino or carboxyl groups for studies of GI function. J. Microencap. **1993**, *10*, 67–76.
54. Ni, P.H.; Zhang, M.Z.; Zhuge, L.J.; Fu, S.K. Amphiphilic ABA triblock copolymer as surfactant in syntheses of microlatexes bearing cationic groups. J. Polym. Sci. A Polym. Chem. **2002**, *40*, 3734–3742.
55. Bo, G.; Wesslén, B.; Wesslén, K.B. Amphiphilic comb-shaped polymers from poly(ethylene glycol) macromonomers. J. Polym. Sci. A Polym. Chem. **1992**, *30*, 1799–1808.
56. Kawaguchi, S.; Ito, K. Aqueous solution behavior of amphiphilic poly(ethylene oxide) comblike polymers. Colloids Surf. A Physicochem. Eng. Asp. **1999**, *153*, 173–178.
57. Wesslén, B.; Wesslén, K.B. Preparation and properties of some water-soluble, comb-shaped, amphiphilic polymer. J. Polym. Sci. A Polym. Chem. **1989**, *27*, 3915–3926.
58. Ni, P.H.; Jones, F.N.; Fu, S.K. Synthesis of amphiphilic copolymers based on acrylates by free-radical polymerization and their application in alkyd emulsions. J. Macromol. Sci. A Pure Appl. Chem. **2000**, *37*, 1391–1406.
59. Khan, A.; Marques, E.F. Synergism and polymorphism in mixed surfactant systems. Curr. Opin. Colloid Interface Sci. **2000**, *4*, 402–410.
60. Staples, E.; Tucker, I.; Penfold, J.; Warren, N.; Thomas, R.K. The structure and composition of surfactant-polymer mixtures of sodium dodecyl sulfate, hexaethylene glycol monododecyl ether and poly(dimethyldialyl ammonium chloride) adsorbed at the air-water interface. J. Phys. Condens. Mater. **2000**, *12*, 6023–6038.
61. Lin, S.Y.; Capek, I.; Hsu, T.J.; Chern, C.S. Nonconventional emulsion polymerization of styrene with mixed anionic and nonionic emulsifiers. Polym. J. **2000**, *32*, 932–940.
62. Pons, R.; Taylor, P.; Tadros, T.F. Investigation of the interactions in emulsions stabilized by a polymeric surfactant and its mixtures with an anionic surfactant. Colloid Polym. Sci. **1997**, *275*, 769–776.
63. Chern, C.S.; Sheu, J.C. Effects of carboxylic monomers on the styrene miniemulsion polymerizations stabilized by SDS/alkyl methacrylates. Polymer **2001**, *42*, 2349–2357.
64. Mortensen, K.; Pedersen, J.S. Structural study on the micelle formation of poly(ethylene oxide)–poly(propylene oxide)–poly(ethylene oxide) triblock copolymer in aqueous solution. Macromolecules **1993**, *26*, 805–812.

65. Mortensen, K.; Brown, W.; Norden, B. Inverse melting transition and evidence of 3-dimensional cubatic structure in a block-copolymer micellar system. Phys. Rev. Lett. **1992**, *68*, 2340–2343.
66. Brown, W.; Schillen, K.; Hvidt, S. Triblock copolymers in aqueous solution studied by static and dynamic light-scattering and oscillatory shear measurements:influence of relative block sizes. J. Phys. Chem. **1992**, *96*, 6038–6044.
67. Mortensen, K.; Brown, W. Poly(ethylene oxide)–poly(propylene oxide)–poly(ethylene oxide) triblock copolymers in aqueous solution: the influence of relative block size. Macromolecules **1993**, *26*, 4128–4135.
68. Nagarajan, R. Solubilization of hydrocarbons and resulting aggregate shape transitions in aqueous solutions of Pluronic (PEO-PPO-PEO) block copolymers. Colloids Surf. B Biointerfaces **1999**, *16*, 55–72.
69. Reb, P.; Margarit-Puri, K.; Klapper, M.; Müllen, K. Polymerizable and nonpolymerizable isophthalic acid derivatives as surfactants in emulsion polymerization. Macromolecules **2000**, *33*, 7718–7723.
70. Duracher, D.; Sauzedde, F.; Elaïssari, A.; Pichot, C.; Nabzar, L. Cationic amino-containing N-isopropylacrylamide-styrene copolymer particles: 2-surface and colloidal characteristics. Colloid Polym. Sci. **1998**, *276*, 920–929.
71. Hofland, A. Making paint from alkyd emulsion. In *Technology for Waterborne Coatings*; Glass, J.E., Ed.; ACS Symp. Series 663; American Chemical Society: Washington, DC, 1997; 184–195.
72. Haak, H.J.W. Design of pigment dispersants: methodology for selection of anchoring groups. J. Coat. Technol. **1997**, *69*(873), 137–142.
73. Creutz, S.; Jerome, R.; Kaptijn, G.M.P.; Werf, A.W.; Akkerman, J.M. Design of polymeric dispersants for waterborne coatings. J. Coat. Technol. **1998**, *70*(883), 41–46.
74. Chen, Z.M.; Bao, H.L.; Liu, J.Z. Synthesis of a well-defined epoxy copolymer by atom transfer radical polymerization. J. Polym. Sci. A Polym. Chem. **2001**, *39*, 3726–3732.
75. Osberg, G.; Hulden, M.; Bergenstahl, B.; Holmberg, K. Alkyd emulsions. Prog. Org. Coat. **1994**, *24*, 281–297.
76. Makarewicz, E. Studies on the stability of aqueous emulsions containing linseed oil and alkyd resin modified by linseed oil. Prog. Org. Coat. **1996**, *28*, 125–132.

4

Catalytic Polymerization of Olefins in Emulsion

A Breakthrough in Polymer Colloids

REMI SOULA, JERÔME CLAVERIE, ROBERT SPITZ, and ALAIN GUYOT CNRS-LCPP CPE Lyon, Villeurbanne, France

I. INTRODUCTION

In order to obtain cheap paint binder, industrial production of ethylene copolymers in emulsion (chiefly ethylene-vinyl acetate) has been carried out for a long time. The process involves rather moderate conditions and low pressure (100 bars and 70–80°C) as compared with the conditions needed for the radical polymerization of ethylene alone (1500–3000 bars and more than 200°C). These homopolymerization conditions obviously exclude the use of emulsion polymerization procedures with water as continuous phase. Only one trial is mentioned in the literature for the production of low-density polyethylene (LDPE) [1].

On the other hand, currently the major processes for ethylene and olefin polymerization involve the use of coordination catalysts such as the Phillips chromium or Ziegler-Natta titanium-aluminum system. In both of these systems, as well as with the more recent metallocene catalysts, it is not possible to conceive the introduction of water or even of protic compounds. Water is indeed a strong poison for the catalyst (Phillips), and reacts explosively with the organometallic aluminum derivatives of the Ziegler-Natta system as well as with the aluminoxanes in the metallocene catalysts.

The catalytic polymerization of ethylene in water is very recent, the first paper having been published only at the beginning of the twentieth century; however, a few studies can be considered as preliminary works, presented here as earlier works. Before presenting the recent studies of the catalytic emulsion polymerization of ethylene and other olefins, it is important to recall some early studies dealing with nickel and palladium catalysts capable of being active without being associated with other organometallic componds as for the classical Ziegler-Natta catalysts.

There are not yet any biomedical applications for ethylene polymer and copolymers in emulsion polymerizations because the first successful polymerizations were discovered only in the 2 last years; furthermore, the possibility of functionalizing the surface of the particles was disclosed even later, at the beginning of 2002. However, the use of latex compounds in diagnostic materials is now well known and well developed. There is no reason that polyethylene-supported latexes might not find use in the same field. Furthermore, polyethylene is a very inert polymer. Compared with polystyrene, which remains the basic support of many diagnostic products, its metabolism is probably safer for living systems.

II. EARLIER WORKS

Catalytic polymerization of butadiene using rhodium chloride as catalyst and producing *trans*-1,4-polybutadiene in aqueous systems was known a long time ago, but the mechanism has not been clarified [2–6]. The yields are low and can be somewhat increased upon activation with 1-4 cyclohexadiene or formic acid. These two compounds, in conjunction with the rhodium species, are supposed to produce a catalyst hydride–initiating moiety. Owing to these low yields, and because the polymer is 1-4 trans, which does not have industrial applications, the topic was not studied further. Using the same rhodium catalyst, Natta et al. were able to polymerize the double bond of norbornene without opening the ring [7]. Later on the team of Lattes succeeded in polymerizing norbornene as well as some functionnal derivatives in the presence of water, but with a water-soluble palladium catalyst with sulfonated triphenylphosphine ligand [8].

More recently, metathetic catalysts working with functional derivatives of norbornene have been disclosed. These have been shown to work in the presence of water [9,10]. Another report indicates that a dimethoxy derivative of norbornene can be polymerized in emulsion using $RuCl_3$ as catalyst and a triblock copolymer of oxiranes as stabilizer [11]. The particle size was dependent on the amount of stabilizer in the range 40–60 nm, but the yield of these polymerizations was low.

A more successful study of metathetic emulsion polymerization is in progress in our laboratory. The monomer is norbornene, the catalyst is ruthenium based, and the surfactant is SDS [12]. The ring-opening metathetic polymerization of norbornene and its derivatives in aqueous medium has been recently reviewed, together with other related topics, such as alkynes polymerization (also in aqueous media), as well as a few other catalytic polymerizations [13].

The most important challenge in nonradical polymerization systems is certainly the possibility of polymerizing olefins with Ziegler catalytic system in emulsion. Very little work has been carried out on that topic. Polymerization of butadiene to produce the 1,2 polymer has been done in the United States by

researchers of Goodyear in a series of patents that mainly appeared in the early 1990s [14–17]. The catalyst is cobalt-based compounds associated with alkylaluminum derivatives. It is assumed that low molecular weight oligomers act as sterically hindered hydrophobic ligand, able to protect the transition metal and its coordination bond with the monomer from the aqueous environment. The catalytic system is initially dispersed in an emulsion of butadiene and hexane, with SDS as stabilizer.

III. STUDIES OF DERIVATIVES OF THE LATE-TRANSITION METALS IN POLAR MEDIA

In the years 1987–1991, Klabunde of DuPont has developed a family of chelated nickel catalysts, capable of working in the presence of protic compounds, and even in water [18]. These catalysts are derived from the family of nickel complexes with bidentate ligands (carboxylic phosphine, or enolate phosphine introduced by Keim [19]) and developed industrially for the SHOP process of olefin oligomerization [20]. This class of catalysts has been extended to olefin polymerization from the use of phosphine sponges and electron-rich ligands [18,21]. As was already stated, these monometallic catalysts are tolerant to polar media. For instance, the SHOP process is carried out in 1,4-butanediol, which simplifies separation of the products. Klabunde showed that it is possible to copolymerize ethylene with monomers containing polar groups [22], but the polar group has to be separated from the double bond by at least one methylene group. The effect of water on these kinds of catalysts was studied by Beach and Harrison [23]. The authors did not find any drastic reduction of the catalytic activity when the water content was kept under 20%.

More recently, at the American Chemical Society meeting in Dallas (April 1998), K. Brown presented suspension polymerization of butene in an ethyl acetate environment using a palladium-based catalyst belonging to a class recently described by Broockart et al. and patented by DuPont [24]. A branched polymer was produced as bead 10–100 μm in diameter, with a rather broad particle size distribution. Additional details about this work and related olefin polymerizations are described in a series of patents by Brown et al. [25–29]. It might be suggested here that a miniemulsion be used instead of a suspension, and that ethyl acetate be replaced with vinyl acetate. As a result, the polymerization would take place in two steps, the first one catalytic, and the second through a radical mechanism with oligo radicals coming from the water phase.

IV. POLYETHYLENE LATEXES

Polyethylene latexes are produced industrially for such applications as floor polish or inks. Rather low molecular weight polyethylene from radical polymeri-

zation are first dissolved in a light solvent and then emulsified in water in the presence of surfactants. Finally the solvent has to be evaporated. This is a somewhat costly procedure, and the production is rather limited. The first attempt to use catalytic polymerization in water medium was reported in 1993 [30] using a tridentate rhodium complex with a 1,4,7-trimethyl-1,4,7-triazacyclononane ligand at room temperature and 60 bars ethylene. A low molecular weight compound ($M_n = 5100$) was produced after 90 days. This extremely low activity (turnover of 1 per day) cannot be increased upon heating at higher temperature due to hydrolysis of the Rh-alkyl bond.

The discovery of catalytic systems for ethylene polymerization able to work in emulsion, and then to prepare polyethylene latexes is very recent, and, up to now, only two teams have been working successfully in that domain. One is in our laboratory, and the second one is from the Macromolecular Institute in Freiburg in Germany.

A. Studies Published by the Team of Freiburg

Following the work of Brookhart, in which Mecking participated [31], the first paper of the Mecking team [32] dealt with palladium diimine cationic complex with SbF_6 as counterion (Scheme 1), known to polymerize ethylene to form a very special branched polymer in organic solvents. As observed by Mecking et al., polymerization took place at room temperature, giving a high molecular weight, branched and rubbery polymer. A few selected data are reported in Table 1. The activity in water is lower than in methylene chloride where the ethylene solubility is high. In spite of the low monomer solubility in water at room temperature, the molecular weights are much higher, whereas the polydis-

Diimine Palladium complex

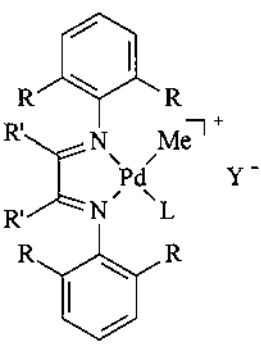

6a:
R = R' = Me; L = NCMe;
$Y^- = SbF_6^-$

SCHEME 1 Diimine–palladium complex.

TABLE 1 Results of Ethylene Polymerization Using a Palladium Diimine Complex Catalyst (Scheme 1)

Medium	Pressure (b)	Hours	Yield (g)	M_w(x 10^4)	M_w/M_n	Br./1000 C
CH_2Cl_2	2	16	29.2	3.8	2.3	106
Water	2	16	3.5	48	3.5	71
Water	20	15	23	41	3.9	68
Water	40	3	2.3	18	2.8	64

Mw = average molecular weight. Mn = average molecular weight.

persity is just a little bit higher and the branching a bit lower. In addition, polymerization in organic solvents leads to a viscous oil instead of a rubbery material. A special feature observed is that the polymerization activity goes through a maximum with the ethylene pressure. The explanation for this phenomenon was given in a more complete paper [33]. The effect is believed to translate the predominant role of the branching mechanism through the migratory insertion step, as observed in a previous study [31]. A kinetic study of the polymerization was carried out as described in an extended paper [33], showing stable activity throughout the process. Mass transfer of ethylene was also studied; it was concluded that it is important but not critical. Gas phase polymerization upon isolation of catalyst showed that the polymerization can be continued and it does not require solubilization of ethylene in the water phase. Addition of a water-soluble sulfonated phosphine fully deactivates the catalyst before polymerization but does not affect a polymerization already started. Thus, it can be concluded that during the polymerization the catalytic sites are protected against water through encapsulation by the growing polymer. The catalyst is stable in water, but addition of more than 5% water in the catalyst dissolved in acetone totally deactivates the catalyst, with the activity reappearing following addition of 80% water. Finally, it is assumed that the polymerization mechanism involves an intermediate hydrid. A ^{13}C NMR study of the structure of the branches reveals a broad distribution of short and long branches independent of the nature of the solvent (water or methylene chloride). The polymers are mainly amorphous with T_g near $-45°C$ in water and $-70°C$ in methylene chloride. The rubbery materials produced in water display elastic recovery in Dynamic Mechanical Analyzer (DMA) analysis [34].

In the first paper [32] another catalyst was shown to polymerize ethylene in water medium. It was a sulfonated bidentate P_O Ni(II) complex in the presence of Rh(CH_2=CH_2)(acac) as phosphine scavenger with Rh/Ni=2 (Scheme 2). The polymerizations were carried out at 70°C under 50 bar ethylene pressure. Selected data are reported in Table 2. Then linear polymers are produced with much lower molecular weight than with the palladium catalyst. Pure organic

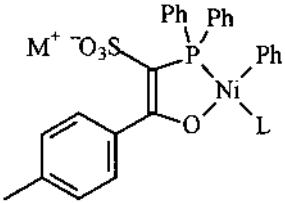

L = PPh_3 or pyridine

7a: $M^+ = Na^+$ (hydrophilic)

7b: $M^+ = H_{33}C_{16}NMe_3^+$ (lipophilic)

SCHEME 2

solvents lead to higher yields and higher molecular weight, but with very broad distribution. While this kind of catalyst has been reported as inactive in pure water, it can be seen that a small percentage of organic solvent facilitates significant activity in water medium, even if the sodium counterion of the sulfonate group makes the complex soluble in water. The activity does not decrease drastically upon extending the duration of the polymerization, so that the stability of the catalyst vs. water can be considered as good. However, the use of a lipophilic counterion, long-chain alkyl quaternary ammonium, gives a higher polymer yield. There is no drastic deactivation of the active site by the water, but the decrease in rate can be explained by the fact that water may act as a ligand competing with the monomer, which has a limited solubility in the water–

TABLE 2 Ethylene polymerization Using Bidentate Ni(II) Complex (Scheme 2), Ethylene Pressure 50 bar, 70°C, phosphine Scavenger $Rh(CH_2 = CH_2)(acac)$,Rh/Ni = 2

C ion	N (μmol)	S/water	Hours	Yield(g)	M_n	M_w/M_n
Na	130	A-50 : 50	1.5	2.5	nd	
Na	121	A-50 : 50	3	3.2	nd	
Na	108	A-5 : 95	2	2.2	970	2.3
Na	89	T-5 : 95	2	5.9	960	3.1
Na	12	T-100 : 0	2	9	13900	42
Na	26	A-100 : 0	2	22.2	3700	25
$C_{16}Nme_3$	116	T-5 : 95	1.5	1	nd	
$C_{16}Nme_3$	104	T-5 : 95	3	1.6	nd	
$C_{16}Nme_3$	9	T-100 : 0	1.75	5.2	5440	5.3

Salicylaldimine Nickel (II) complex

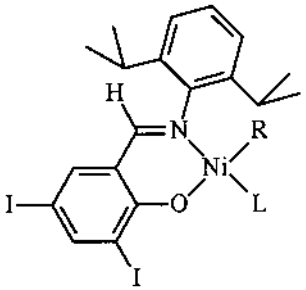

10a: R = Ph and L = PPh_3

10b: R = Me and L = pyridine

(activation of the PPh_3 complex for polymerization by $[Rh(CH_2{=}CH_2)_2(acac)]$ as a phosphine scavenger)

SCHEME 3 Silicylaldimine–nickel(II) complex.

solvent mixture (e.g., 6 bar pressure in acetone corresponds to 50 bar in acetone-water 50:50).

It was noted in this first paper [32] that upon the introduction of surfactants, such as sodium dodecyl sulfate, or of the nonionic Triton one obtains stable emulsions of polyethylene with particle sizes ranging between 80 and 300 nm [32].

These data were reviewed in a third paper [35], which reports on a third class of N_O bidentate Ni(II) neutral catalyst (Scheme 3). Like the previous catalyst, this one is used together with the same phosphine scavenger and needs to be introduced with a small amount of solvent, which can be pentane, acetone, or toluene. Selected data are reported in Table 3. Again catalytic activities are

TABLE 3 Results of Ethylene Polymerization Using Bidentate N_O Ni(II) Catalyst (10a, Scheme 3) Ethylene Pressure 50 bar, 50°C, 2 h

N cat.(μmol)	Medium	Yield(g)	M_n	M_w/M_n
41 (*T*°C = 25)	Water	10.6	nd	
36 (*T*°C = 70)	Water	0.7	57000	6.1
56	50 : 50 water/acet.	2.2 (1 h)	12000	1.5
71	50 : 50 water/acet.	3	14000	1.6
21	Acetone	3 (1 h)	nd	
35	Toluene	0.7 (8 b)	19000	2.3
80 (Ni Met)	Water	2.9 (1 h)	120000	2.6
19 (*T*°C = 70)	Water	1.9	100000	4.1
37 (*T*°C = 70)	Pentane	10.7	110000	3.7

TABLE 4 Miniemulsion Polymerization of Ethylene Using Bidentate N_O Ni(II) Complex (scheme 3) 30°C, 45 bar, 2 h

N cat. (μmol)	T/H (vol %)	Surf (mmol/L)	MolE/m.cat	M_n	M_w/M_n	*D*(nm)
25	1 : 2	SDS 17	2515	140000	2.3	330
23	1 : 0.3	SDS 35	1206	120000	2.7	220
36	1 : 0.3	SDS 17	1135	85000	3.1	260
29	1 : 0.3	SDS 5	1230	100000	4.5	485 floc
36	1 : 0.3	Triton 11	959	89000	2.1	100

lower in water than in organic media. These catalysts lead to higher molecular weight than the previous Ni(II) complexes, so that semicrystalline polyethylene is produced. However, some branching (between 5 and 20 methyl branches/1000 C) occurs. Comparison of runs with only 1 h duration showed that a rather important deactivation takes place. These catalysts are also able to copolymerize ethylene with norbornene. Depending on the amount of norbornene in the copolymer (between 14 and 25 mol %), the glass transition temperature can be varied from – 4°C to 25°C. The norbornene units are incorporated mostly as isolated units as shown by NMR analysis.

These catalysts also lead to lattices upon addition of surfactants (SDS or Triton) without detrimental effect on the polymer yields, with particle sizes of 80 to several hundred nanometers in diameter.

The preparation of high-polymer latexes from ethylene miniemulsion polymerization has finally been reported by Freiburg et al. [36]. The catalyst used is the salicylaldimine–nickel complex shown in Scheme 3 dissolved in toluene with hexadecane, which acts as a hydrophobe in the miniemulsion; the organic solution is dispersed in a water solution of surfactant (SDS or Triton) and sheared in very fine droplets upon sonification (or sometimes using a high-pressure mixing device). A few data are reported in Table 4. High polymers with rather narrow molecular weight distributions are obtained. Polymerization takes place under constant ethylene pressure-fed continuously. A high ratio of hexadecane to toluene favors the solubilization of ethylene and then the polymerization yield, in agreement with experimental sizes. When the amount of SDS is too low, the latex is unstable and tends to flocculate, so giving large particles. Otherwise, the latexes are stable for weeks or longer. TEM analysis of the latex particles reveals nonspherical shapes probably caused by the crystalline structure of the polymer, which is around 40–50% crystalline with a melting range of 120–130°C, the polymer being moderately branched.

B. Studies Published by the Group of Lyon

The first work published by this group was presented in May 1999 in a symposium held in Lyon [37]. The authors used a special binuclear complex of bidentate P-O ylide nickel(II) compound (Scheme 4) similar to that previously described by Klabunde [18,21], except that the two nickel atoms are tethered by a norbornene cycle. These binuclear complexes have been shown by Tomov et al. [38] to be much more active than the simpler coumpounds of Klabunde, and then to be able to polymerize ethylene in water–methanol mixtures. These catalysts were engaged in ethylene polymerization in toluene solutions and in the presence of SDS as surfactant and of dicyclooctadienyl nickel as phosphine scavenger. Typical results are shown in Table 5. With this catalyst again, the polymer yield is much lower in water than in toluene, but it seems that SDS does not affect the productivity to any great extent. Part of the polymer is recovered as a latex, but the major portion precipitates out of the dispersion, unless one starts with a miniemulsion. In that case big particles of 600 nm are produced, and low molecular weight polyethylene is formed. The molecular weight is also lower in emulsion than in solution, probably because the ethylene concentration in the particles is limited. The polymer is linear and semicrystalline with a melting point of 135°C, and the chains are ended by a double bond. TEM analysis of the latex show polyhedral shapes of the particles.

Synthesis of the binuclear complex is a difficult task, and simpler synthetic methods are desirable. On the other hand, because the catalytic activity is always lower in the presence of water it is important to prepare catalysts with the highest potential activity. It has been theorized that the catalytic activity should be

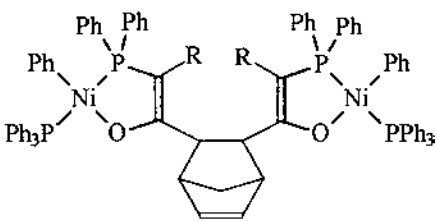

R = C(O)OMe; Ph

SCHEME 4 Bicycloylide–Ni(II) complex.

TABLE 5 Ethylene Polymerization with Bicycloylide Complex (Scheme 4) at 65°C

Cat. (μm/L)	Cat./scav	SDS(g/L)	*P*(bar)	Prod (kg/mNi)	M_w	*D*(nm)	% latex
28	6	0	4	4300	103700	—	0
62	14	0	26	1056	51000	—	0
20	9	1.5	24	766	22000	266	10
15	24	3	25	2500	68000	230	9
34	15	6	27	1100	18500	230	20
22	7	12	22	650	58000	265	12
115[a]	19	12	20	1100	8700	620	100

[a]Miniemulsion, hexadecane as costabilizer.

increased if electron-withdrawing substituents are introduced on the double bond of the ylide moiety. Fluorinated groups were chosen, e.g., CF_3 and C_6F_5. A series of bidentate ligands R−CO−C−R′)=PPh_3, with R=CF_3 or C_6F_5, and R′=COOEt or COOX, with X being another alkyl group, were prepared and reacted with dicyclooctadienyl Ni(0), i.e., $Ni(COD)_2$, to prepare the catalyst [39]. After some study of the reaction conditions it was decided that the catalyst should be prepared by *in situ* reaction of the ligand dissolved in toluene with two equivalent of $Ni(COD)_2$ at room temperature in the presence of an olefin. The excess of nickel complex acts as a phosphine scavenger and does not inhibit the catalytic activity up to four equivalents (Scheme 5).

A few of these catalysts have been involved in emulsion and miniemulsion polymerization of ethylene [40]. Table 6 presents data on miniemulsions. Some experiments have also been carried out to produce latexes via normal emulsion polymerization, but results have been disappointing because the latexes were not stable. One obtains a milky liquid, but most of the polyethylene is separated

In situ synthesis of the fluorated ylide Ni(II) catalyst

1a : R = CF_3, R' = CO_2Et
1b : R = C_3F_7, R' = CO_2Et
1c : R = C_6F_5, R' = CO_2Et
1d : R = C_6F_5, R' = $CO_2{}^tBut$
1e : R = C_6F_5, R' = CO_2Bn
1f : R = C_6H_5, R' = CO_2Et
1g : R = CH_3, R' = CO_2Et

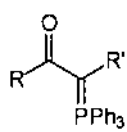

1

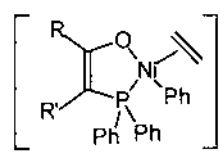

2

SCHEME 5 In situ synthesis of the fluorated Ni(II) catalyst.

TABLE 6 Ethylene Polymerization Using the Floronated Ylide Ni(II) Complex 1a (Scheme 5) Water 500 mL, except for the First Run

n (μmol)	Toluene (mL)	Hexa-decane (g/L)	*P* (bar)	*T*(°C)	Acti. (kg/gN/hour)	SDS (g/L)	*D* (nm)	Solid (%)	M_w	M_w/M_n
2	400	0	3	70	>2000	0	—	—	3500	2.7
23	32	0	25	65	23	20	—	2	4200	3.2
31	20	12	25	70	23	5	600	2.2	4100	3.5
31	10	8	25	70	40	5	240	3.7	4000	3.4
32	10	10	25	65	45	5	240	8.5	4100	3.2
31	20	10	25	65	83	5	210	10.2	3900	3.2
15	15	6	25	70	56	3	370	1.5	3800	3.3

as soon as the stirring is stopped, and floats on the surface of the emulsion, from which it can be easily filtered. A small amount of product (<1%) remains in the emulsion as a very broad dispersion of particles of 250–750 nm. Compared to solution polymerization, the catalytic activity in the presence of water decreases by about two orders of magnitude. This is true also in the case of miniemulsions although the use of hexadecane seems to minimize this effect. The surfactant seems not to strongly affect the process. Even if catalyst preparation is carried out at room temperature, polymerization starts only upon heating above 50°C. It also depends on the ethylene pressure and, less drastically, on the catalyst concentration inside the droplets of the miniemulsion. The miniemulsification was carried out following sonification of a catalyst solution in the mixture of toluene and hexadecane, which was transferred in a reactor. The reactor was then pressurized to 25 bar with ethylene and heated under constant pressure from a reservoir; measurement of the pressure drop in the reservoir allows determination of catalytic activity. The catalyst droplets show a very broad particle size distribution that is hardly affected by the ethylene pressure. The size of the particles depends on the power used in the sonifier, which must be high enough to obtain small particles. Upon polymerization the size generally decreases, showing a complex nucleation mechanism, and the distribution remains very broad, as shown by field flow fractionnation analysis. Solid contents up to 10% can be obtained, being dependent on both the amount of catalyst and of solvent used for dissolving the catalyst. The polymers are low molecular weight compounds not highly dependent on the conditions. The molecules are chiefly linear, with no methyl branches or unsaturated chain ends. The particles are separated as crystalline platelets with melting point around 130°C. It seems that during polymerization the polymer cannot remain inside the droplets, and this leads to a high number of particles from the same droplets.

The last step of that study was devoted to the use of reactive olefin as costabilizer. After a few attempts to use 1-octene, the decision was made to use hexadecene, which was more hydrophobic and closer to the common hexadecane. Some copolymerization data [41] are reported in Table 7. Of course, the use of hexadecene instead of hexadecane leads to production of a copolymer containing some costabilizer. However, the incorporation of hexadecene is limited due to the low reactivity of hexadecene compared to ethylene. Between one-third and two-thirds of the hexadecene remains unconverted. The maximal incorporation was observed to be 11.7%. It affects chiefly the melting point of the copolymer, which is depressed following incorporation of additional hexadecene. Otherwise, the polymer is essentially linear, with a few methyl branches (less than 2 per 1000 carbon atoms), and some long branches ($>C_4$) corresponding chiefly to hexadecene units. As in many olefin polymerizations, the macromolecules present a terminal double bond due to monomer transfer. There are also some internal double bonds (1–3%). The molecular weight of the polymer is rather low, around 2000, and the polydispersity is moderate (M_w/M_n 2–3).

The productivity depends on several factors. The best results are obtained at moderate temperatures at 55°C. Under 50°C, the catalyst is not yet activated, whereas at higher temperatures some deactivation takes place. However, that deactivation is not so drastic, so that the productivity increases with the duration of the polymerization. More surprisingly, the concentration of the catalyst com-

TABLE 7 Miniemulsion Polymerization of Ethylene with the Fluoronated P_O Ylide Catalyst1a (Scheme 5) SDS 20 g/L, Hexadecene 20 g/L as costabilizer, ethylene pressure 20 bars

n (μmol)	mL solv	*T*(°C)	Time (min)	Product (kg/g Ni)	Size (nm)	Solid (%)	N_p/N_d	M_n	M_p(°C)	%Hene
50	40	70	65	10.5	190 ± 70	12	0.75	2110	118.8	7.6
100	40	60	140	9.8	195 ± 80	15.4	0.76	1840	112.6	10.1
50	40	60	175	24.8	200 ± 85	18.8	0.94	2090	115.3	8.9
50	60	55	140	30.5	210 ± 85	23.7	0.83	2370	116.6	7.6
25	40	60	50	14.2	210 ± 75	14.3	0.77	2220	117.2	7.8
25	20	55	150	22.0	210 ± 75	12.3	1.03	2000	115.7	9.4
30	40	55	145	23.9	190 ± 75	14.9	0.70	2120	111.2	11.7
25	40	55	150	34.0	225 ± 80	17	0.97	2140	117.1	7.7
25	60	55	150	42.0	240 ± 90	19	0.86	2190	117.9	6.7
50	20	55	150	29.2	250 ± 85	20.5	3.85	2120	118.4	4.6
50	40	55	150	43.4	240 ± 90	30	2.97	2040	118.9	4.3
50	40	55	150	20.9	190 ± 70	23.8	0.96	1580	116.8	6.4

[a]60 g/L hexadecene.

plex in the solvent should be limited, and larger volumes of solvent should be introduced. Of course, the polymerization is probably dependent on the amount of ethylene in contact with the catalyst inside the miniemulsion droplets. This amount is obviously dependent on the volume of the organic phase (solvent + hexadecene).

The particle sizes are all of the same order of magnitude, around 200 nm, but the particle size distribution is rather broad. Solid contents up to 30% have been reached. It seems that the nucleation is chiefly droplet nucleation, which is expected because the catalyst is almost water insoluble. However, the number of polymer particles is somewhat different from the initial number of droplets, except in a few cases.

The final step of that research was to study the miniemulsion copolymerization of ethylene with a few functional comonomers in the presence of hexadecane as costabilizer. Some results are reported in Table 8. In the case of styrene, the productivity is much reduced due to the chelating effect of the benzene ring, which competes with the monomer to occupy the vacancy freed by the phosphine scavenger. However, a significant incorporation can be reached (15%) before the reaction stops before whole conversion. The copolymer is strongly modified compared to polyethylene as shown by the melting point of 101°C.

The C_{10} diene monomer (α-ω) has been used with the purpose of increasing the molecular weight, and it seems to work rather well. It has been observed that using a longer diene (C_{14}) it is possible to stabilize a miniemulsion without hexadecane. However, one must be careful to avoid cross-linking with these dienes. Differential scanning calorimetric experiments show two melting transitions, one of which might correspond to a cross-linked material.

Long-chain olefins ω-terminated by a functional group were finally tested. Although the acid function inhibits the catalytic activity, the experiments were successful in the case of an ester and also with an alcohol. Productivity and the

TABLE 8 Data with Functional Comonomers Catalyst. 1a of Scheme 5 (50 μmol), Ethylene Pressure 20 bars, Toluene 40 mL, Comonomer 6 g, Hexadecane 20 mL, water 300 mL, SDS 20 g/L

Comonomer	Product (kg/g Ni)	Size (nm)	Solid (%)	N_p/N_d	M_w	% comonomer	Residual comonomer %	M_P (°C)
Styrene	4.5	230 ± 90	12.6	1.4	1190	15	73	101.0
C_{10}-diene	16.7	230 ± 90	17.4	0.97	48000	nd	nd	113.0
C_{11}-ester	12.7	220 ± 90	15.6	0.73	4400	7.6	53	115.6
C11 acid	0.1							
C11 alcohol	11.2	190 ± 80	14.4	0.63	3800	6.2	66	114.5
No	17.7	220 ± 80	16.9	2	9100	0	0	119.8

molecular weight are only slightly reduced in comparison with the case where no comonomer is added.

V. CONCLUSION

It seems clear that ethylene emulsion polymerization catalyzed by late transition metals with chelating ligands is much more effective when miniemulsions are first prepared with solutions of catalysts. The studies of both the Freiburg group and the Lyon group are conclusive on that point. It is interesting, in that connection, to mention that recently researchers from BASF have used this technique to polymerize styrene in syndiotactic polymer with metallocene catalyst [42]. Up to now there have not been any applications of this new technology. In the thesis of Soula [43], it is demonstrated that such copolyethylene latex is very efficient against corrosion of metals by a mixture of nitric and chlorhydric acids.

The fact that ethylene can be copolymerized with some functional monomers will probably open new fields in many domains, so why not in biotechnology? The basic material, polyethylene, is fully inert in the living world, and this constitutes a significant advantage if the materials can be obtained in fine particles that can be injected in the body, e.g., in vectorization applications or drug delivery systems. When the functional group is somewhat hydrophilic, as in the C_{11} alcohol, one may expect that it will be located on the particle surface and thus might be useful to bind a bioactive compound. In that connection, it should be necessary to enlarge the number of useful comonomers. This is not a simple task due to the need to separate the polymerizable olefinic double bond from the functional group to be introduced.

Of course, this tehnology is still in its infancy, and the range of functional comonomers should be enlarged. The use of norbornene derivatives may be suggested in that connection, e.g., those already studied by Lattes et al. [8]. Another possibility should be to build core-shell copolymers with a polyethylene core and a bioactive shell. There is no doubt that such studies, as well as others, will be actively pursued in a near future.

REFERENCES

1. Stryker, H.K.; Mantell, G.J.; Helin, A.F. Polyethylene latexes in floor polishes. J. Polym. Sci. C, **1969**, *27*, 35.
2. Rinehart, R.E.; Smith, H.P.; Witt, H.S.; Romelyn, H. trans-1,4 polybutadiene by rhodium salt catalysis. J. Am. Chem. Soc. **1961**, *83*, 4145, 4684.
3. Canale, A.J.; Hewett, W.A.; Shryn, M.; Youngman, E.A. Polymerisation of butadiene in emulsion with rhodium salts. Chem. Ind. **1962**, 1054.
4. Teyssie, P. Mecanisme de la polymerisation du butadiene catalysée par le chlorure de rhodium. Compt. Rend. Acad. Sci. **1964**, *256*, 2846, and Polym. Lett. **1964**, *2*, 413.

5. Rinehart, R.E. Polymerization catalyzed by noble metal olefin complexes. J. Polym. Sci. C **1969**, *27*, 7.
6. Halpern, J.; Taylor, S.M. Disc. Ethylene polymerization of binuclear nickel ylide. Faraday Soc. **1960**, *29*, 174.
7. Natta, G.; Dall'asta, G.; Montroni, G. Coordination polymerisation of norbornene catalyzed by rhodium chloride. Polym. Lett. **1964**, *2*, 349.
8. Eychenne, P.; Perez, E.; Rico-Lattes, I.; Bon, M.; Lattes, A.; Moisand, A. First example of latexes synthesis via oligomerization of norbornene in aqueous emulsion catalyzed by palladium chloride. Colloid Polym. Sci. **1993**, *271*, 1049, and New. J. Chem. **1996**, *21*,1229.
9. Novak, B.M.; Grubbs, R.H. Catalytic organometallic chemistry: the aqueous ring opening metathesis polymerization of oxanorbornene derivatives, J. Am. Chem. Soc. **1988**, *110*, 7542.
10. Feast, W.J.; Harrison, D.H. Application of ring opening metathesis polymerisation for the synthesis of polymers in aqueous media, J. Mol. Catal. **1991**, *65*, 63.
11. Lu, S.Y.; Quayle, P.; Booth, C.; Yeates, S.G.; Padget, J.C. Aqueous ring opening metathesis polymerisation of oxanorbornene catalyzed by ruthenium chloride. Polym. Int. **1993**, *32*, 1.
12. Claverie, J.; Viala, S.; Maurel, V.; Novat, C. Metathesis polymerization in emulsion. Macromolecules **2001**, *34*, 382.
13. Mecking, S.; Held, A.; Bauers, F.M. Aqueous catalytic polymerization of olefins. Angew. Chem. Int. Ed., **2002**, *41*, 544–561.
14. Henderson, J.N.; Donbar, K.W.; Barbout, J.; Bell, A.J. Nickel catalysts for homo and copolymerization of ethylene. US Patent 4,429,085, 1984.
15. Burroway, G.L.; Magoun, G.F.; Gujarathi, R.N. US Patent 5,012,381, 1991.
16. Bell, A.J.; Ofstead, E.A. Eur. Patent Appl. 0475221A, 1990.
17. Bell, A.J.; Ofstead, E.A.US Patent 5,011,896, 1991.
18. Klabunde, U.; Mulhaupt, R.; Herskovitz, T.; Janowicz, A.; Calabrese, J.; Ittel, S. Ethylene homopolymerization with P,O chelated nickel catalysts. J. Polym. Sci. A Chem. **1987**, *25*, 1989.
19. Keim, W.; Kowalt, F.H.; Goddard, R.; Kruger, C. New coordination mode of (benzoylmethylene)triphosphorane nickel oligomerisation catalysts. Angew. Chem. Int. Ed. **1978**, *17*, 466.
20. Keim, W. Nickel: an element with many uses in homogeneous catalysis. Angew. Chem. **1990**, *102*, 251.
21. Klabunde, U.; Ittel, S. Nickel: an element for homo and copolymerization. J. Mol. Catal. **1987**, *41*, 123.
22. Klabunde, U. Nickel catalized polymerization of ehtylene. US Patents 4,716,205, 1987; 4,698,403, 1987.
23. Beach, D.L.; Harrison, J.J. Polymerization of higher olefin. US Patent 4,293,727, 10_1981.
24. Johnson, L.; Killian, C.M.; Feldman, J.; EcCord, E.; McLain, S.J.; Kreutzner, K.A.; Bennet, M.A.; Couglin, E.B.; Ittel, S.; Parthasarathy, A.; Tempel, D.; Brookhart, M.S. PCT WO 96/23010.
25. Brown, K.A.; Lammana, W.M.; Siedle, A.R.; Stewart, E.G.; Swanson, P.J. US Patent Appl. 97/17380, 1995.

26. Brown, K.A.; Kesti, M.R. WO Patent Appl. 97/48739, 1996.
27. Brown, K.A.; Kesti, M.R.; Stewart, G.; McGraph, J.M.; WO Patent Appl. 97/48740, 1996.
28. Brown, K.A.; Kesti, M.R. WO Patent Appl., 97/48739, 1996.
29. Brown, K.A.; Stewart, G.; Swanson, P.J.; Schristopher, S. WO Patent Appl., 97/48777, 1996.
30. Wang, L.; Lu, R.S.; Flood, T.C. Coordination polymerization of ethylene by single component rhodium catalyst in protic solvent. J. Am. Chem. Soc. **1993**, *115*, 6999.
31. Mecking, S.; Johnson, L.K.; Wang, L.; Brookhart, M. Mechanistic studies in the palladium catalyzed copolymerization of ethylene, α-olefins and methylacrylate. J. Am. Chem. Soc, **1998**, *120*, 888.
32. Held, A.; Bauers, M.; Mecking, S. Coordination polymerization of ethylene in water by Pd(II) and Ni(II) catalysts. Chem.Commun. **2000**, 301.
33. Held, A.; Mecking, S. Coordination polymerization in water affording amorphous polyethylenes. Chem. Eur. J. **2000**, *6*, 4623.
34. Held, A.; Weiss, F.; Mecking, S. Aqueous ethylene polymerization: stability of cationic Pd(II) complexes and polymer properties. Polym. Prepr. **2001**, *42*(1), 466.
35. Bauers, F.M.; Mecking, S. Aqueous homo and copolymerization of ethylene by neutral nickel(II) complexes. Macromolecules, **2001**, *34*, 1165.
36. Bauers, F.M.; Mecking, S. High molecular mass polyethylene aqueous latexes by catalytic polymerisation. Angew. Chem. Int. Ed. **2001**, *40*, 3020.
37. Tomov, A.; Broyer, J.P.; Spitz, R. Emulsion polymerisation of ethylene in water medium catalysed by organotransition metal complexes. Macromol. Symp. **2000**, *150*, 53.
38. Kurtev, K.; Tomov, A. J. Ethylene polymerization by binuclear nickel ylide. Mol. Cat., **1994**, *88*, 141 and **1995**, *103*, 95.
39. Soula, R.; Broyer, J.P.; Llauro, M.F.; Tomov, A.; Spitz, R.; Claverie, J.; Drujon, X.; Malinge, J.; Saudemont, T. Very active neutral P,O-chelated nickel catalysts for ethylene polymerisation. Macromolecules **2001**, *34*, 2438.
40. Soula, R.; Novat, C.; Tomov, A.; Spitz, R.; Claverie, J.; Drujon, X.; Malinge, J.; Saudemont, T. Catalytic polymerisation of ethylene in emulsion. Macromolecules **2001**, *34*, 2022.
41. Soula, R.; Saillard, B.; Spitz, R.; Claverie, J. Catalytic copolymerisation of ethylene and non-polar α-olefins in miniemulsion. Macromolecules **2002**, *35*, 1513.
42. Manders, B.;Sciandrone, L.; Hauck,G.; Christen, M.O. Polymerisation with metallocenes in water? A prejudice is refuted. Angew. Chem. Int. Ed. **2001**, *40*, 4006.
43. Soula, R. Polymerisation catalytique de l'ethylene en milieu aqueux. PhD dissertation, Lyon I University, Sept 18, 2001.

5

Functionalization of Colloidal Particles

CHANGCHUN WANG, WULI YANG, and SHOUKUAN FU
Fudan University, Shanghai, China

I. INTRODUCTION

Polymer colloids can be used either as models in academic research dealing with colloid phenomena or as dispersed materials in a wide variety of industrial applications. Heterogeneous polymerization, especially emulsion polymerization, occupies an important place in the production of polymer materials because it permits the production of colloidal dispersions of polymer or latex particles by free-radical reaction [1]. The nature of the process (very considerable subdivision of reaction sites) results in latex polymers with high solids content. Commonly used in industry to synthesize widely available polymers (synthetic elastomers, binders for paints, films for paper, textile finishing, adhesives, and so forth), this method is also used to produce increasingly technical materials (supports for biological compounds, colored and magnetic latexes, measurement scales, etc.). Thanks to the major advances in identifying the mechanisms of polymerization in heterogeneous media and in characterizing colloid properties, it is now possible to better adapt latex to predefined final uses.

A large number of processes have been developed during the last decade, permitting the synthesis of latexes with specific properties. There are the so-called structured latexes [in which a heterogeneous distribution of two (or more) polymers of different natures within the particles is developed], and there are the functional latexes (in which the incorporation of a low-content chemical function is concentrated either at the surface or, more rarely, inside the particles) [2–4]. For practical reasons, these latexes are very often copolymers; hence the possibility, on the basic level, of preparing a large number of types of latex for use in process correlation studies of colloidal and/or weight properties/structure/synthesis.

Although the general methods of synthesizing these latexes are now well known, the control of their structural and colloidal properties remains somewhat uncertain due to the action of various but poorly understood phenomena: emulsion copolymerization mechanisms (particle nucleation), especially in the presence of a water soluble monomer, distribution of the functional monomer in the different latex phases, organization of the polymer inside the particles, and so forth. The use of modern analysis methods permits improved knowledge of the internal and superficial morphology of these latex particles and better understanding of their colloidal behavior and the properties of the films derived from them.

Much research have been undertaken over the last 20 years, with claims regarding the capacity to formulate latex from structured particles and the benefits this provides in terms of film properties and biomedical applications. Recently, various studies in this area have been developed using not only the classical polymerization processes but also the new methodologies, such as living polymerization, normally adapted for bulk polymerizations.

At present, it is possible to obtain very varied functional particle morphologies, from the relatively simple smooth and core-shell structure, studied most, to much more complex structures (hollow, microgel, etc.) (Fig. 1), sometimes leading to irregular, unstable forms.

The aim of this chapter is to report on the various polymerization and functionalization methodologies leading to reactive polymer colloids. The following points are reported and described: (1) direct preparation of functionalized latexes using conventional polymerization; batch, shot-growth, and seed polymerization process; and (2) particle functionalization via surface modification from the basic chemistry (i.e., hydrolysis) to living polymerization processes [atom transfer radical polymerization (ATRP), reversible addition–fragmentation transfer (RAFT), etc.]. In this chapter, special attention is focused on elaboration of functional latexes via emulsion polymerization, which is the common polymerization process used in various domains.

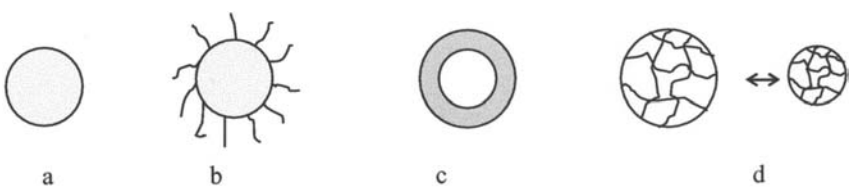

FIG. 1 Main morphology of functionalized particles: (a) smooth, (b) hairy particle, (c) core shell, (d) hydrogel.

II. FUNCTIONAL PARTICLES VIA EMULSION POLYMERIZATION PROCESSES

Functionalization of latex has become a common method for modifying its superficial and colloidal properties. In the first case, the advantage is chemical and mechanical stability. This permits increasing the interaction of the particles with different organic (cellulose and textile fibers), mineral (pigments), or metal substrates. In the second case, the desired improvement concerns the enhancement and control of the immobilization of biomolecules such as proteins, antibodies, and nucleic acids for biomedical purposes. This functionalization is implemented by incorporating reactive chemical groups contributed by the radical initiator (potassium persulfate, nitrosulfonated, carboxylated, cationic derivatives) or by an emulsifier (anionic, cationic, zwitterionic, nonionic) or, lastly, by a functional monomer. The latter method is that most used due to the availability and the variety of functional monomers (i.e., acrylic acid, methacrylic acid, aminoethyl methacrylate). Furthermore, it gives several advantages in comparison to surfactants: incorporation of the monomer by covalent linking, control of particle size and charge density, low foaming effect. Lastly, these monomers are used in low concentrations (generally from 0.1–5%). Table 1 highlights the functional groups and the main monomers used [4].

Although widespread, the use of these functional monomers raises certain problems, some of which are far from being solved or even well understood [15–17]. These are:

1. *The hydrophilic properties of these monomers* (except for specific cases), which favors their distribution in aqueous phase but which can also depend on the pH of the medium, especially for charged monomers such as (aminoethyl methacrylate, acrylic acid, etc.). This results in two possible polymerization sites—the aqueous phase and the polymer particles—with the consequences this causes to the polymerization mechanism (polymerization kinetics, number of particles, polymerization conversion, etc.). The production of more or less water-soluble polymer chains during reaction can lead to their precipitation (during nucleation), or to stabilizing the particles during growth or, on the contrary, favoring their flocculation. The predomination of any one of these phenomena depends on numerous parameters (quantity, composition, distribution of sequences, level of polymerization of these polymers, chain conformation, etc.).
2. *Localization of the functional monomer* at the end of polymerization. At the water–polymer interface or inside the particles or in the aqueous phase. The functional monomer distribution depends on several parameters among which are hydrophilic properties, the neutralization rate in the case of charged monomers (i.e., carboxylic, amine), reactivity in (co)polymeriza-

TABLE 1 Different Chemical Function Groups Used

Functional group	Monomer	Application	Ref.
$-COOH$	Acrylic acid	Covalent coupling of biomolecules	55 6
	Methacrylic acid	Covalent coupling of biomolecules	
	Itaconic acid	Coupling and chelation	
$-NH_2$	Aminoethyl methacrylate	Covalent coupling of biomolecules	7
$-CHO$	Acrolein	Covalent coupling of biomolecules	5
$-OH$	Hydroxyethyl methacrylate	Covalent coupling of trypsin	8
$-CH(O)CH_2$	Glycidyl methacrylate		9
$-CH_2Cl$	Chloromethylstyrene		10
$-SH$	Vinylbenzylisothiouronium chloride	Covalent coupling of antibody fragment	11
$-NCH_2OH$	*N*-Methylolacrylamide	Self-cross-linking in the film	12
$-N(CH_3)_3^+Cl$	*N*-Trimethyl-*N*-ethyl methacrylate ammonium	pH sensitive Change the hydrophilic properties of a latex	13
AMPHOTERIC (Carboxylic acid + amine)	Methacrylic acid + *p*-nitrophenyl acrylate	pH-sensitive microgel through postreaction	14

tion, pH of the aqueous phase, and method of adding the functional monomer in the reactive system.

3. *The optimization of functionalization processes* in terms of favoring the concentration of the functional monomer on the surface of the particles. This implies good control of the first two aspects.

According to the numerous functionalization processes, the chemical and physical properties of the chosen functional carrier (monomer, surfactant, and initiator) should be considered in order to target the desired localization of the functional compounds (particle surface or inside the polymer matrix). The parameters to consider are as follows:

The nature of the functional monomer is of great importance (partition coefficient, reactivity, pH effect, etc.)

The nature and concentration of the functional emulsifier (possible interactions with the ionic monomer and its polymers)
Functional initiator (transfer reaction, decomposition rate)

Following the choice of functional compound and the chemical carrier (monomer, initiator, or surfactant), the following main operating methods and distinctions can be made (here we consider the monomer only):

Batch polymerization, in which all of the reactants are introduced at the beginning in one step. This method, apart from certain exceptions, is of little interest because a large part of the functional monomer is consumed, providing substantial quantities of water-soluble polymers affecting nucleation process, the polymerization reaction, and the final properties of the particles (i.e., colloidal stabilization, surface charge density, size and size distribution, surface polarity, and in some cases morphology).
Semicontinuous addition, which is very useful for performing copolymerizations requiring well-controlled chain structure and particle composition. The functionalization efficiency is based on the reactivity of the functional monomer and its introduction in the polymerization medium at a suitable conversion, favoring their incorporation in the surface or its distribution in the vincinity of the interface. When the functional monomer is added at high conversion during the polymerization, the process is also called *shot polymerization*.
Multistage polymerization (seed polymerization), among which can be mentioned the deferred addition of an ionic comonomer (constituting the basic latex), favoring a highly efficient surface functionalization.

Generally, the batch process does not allow sufficient incorporation in the surface, since the penetration of the charged monomer (amine or carboxylic groups) predominates if the charged compound is not neutralized. On the contrary, polymerization in aqueous phase is privileged if it is completely neutralized (R-NH_2, or R-COOH) [18]. Then in batch process, most of the functional monomer is wasted (buried in the particles or as water-soluble polymers). The water-soluble polymer content depends on the water solubility of the monomer, and the percentage is found to be higher for acrylic acid, which is more water soluble than methacrylic acid. The more soluble in the particle the functional monomer is (e.g., methacrylic acid in comparison to acrylic acid), the more buried it will be. With the shot process, when the internal viscosity of the particles is high, functional monomer (i.e., methacrylic acid) favors better surface incorporation, and localization is optimized by adding a mixture of main monomer and functional comonomer.

To favor the immobilization of biomolecules on the particles, functional groups should be present at the surface of the particles. The monomer addition method (shot process) was successfully carried out with carboxylate butyl acry-

late–methyl methacrylate emulsion copolymers using either acrylic acid or methyacrylic acid [19]. When adding the carboxylic acid in the presence of the more hydrophobic comonomer (butyl acrylate), surface carboxyl group yield in the order of 70–80% was reached. The percentage and density of surface functional group increased when increasing the concentration of carboxylic acid by shot process [5].

Seed polymerization is the good process to obtain functional particles, and many functional spheres (such as carboxyl, hydroxyl, chloromethyl, amino, etc.) have been prepared [5,7,8,10].

In some applications (model colloids, biomedical field), it is necessary to eliminate the influence of the emulsifier; this requires the use of polymerization methods without surfactant which permit the production of monodispersed latexes. Surfactant-free emulsion polymerization is a good choice for the elaboration of surface-clean polymer colloid (Fig. 2). A study made by J. L. Guillaume concerned the functionalization of either carboxylated (using an azocarboxy initiator and carboxylic acid) or sulfonated (and sulfated) (with persulfate and a sulfonated monomer) butyl acrylate–styrene polymer colloids [18,20]. Although the introduction of a functional monomer permits varying the particle size in a wider range and produces more concentrated polymers (40% instead of 20% in their absence), the formation of water-soluble polymers is nonetheless substantial and surface localization remains low (from 15% to 30% as a function of the functional monomer).

Micrometer-sized functional monodispersed polymer particles have some special applications in biomedical and clinical diagnosis. Dispersion polymerization is a very attractive method to prepare such particles due to the inherent simplicity of its single-step process. It is especially suitable to prepare the beads with diameters in the range of 0.8–15 μm (Fig. 3). Polystyrene spheres containing a small amount of functional groups, such as hydroxyl, amines, epoxy, and

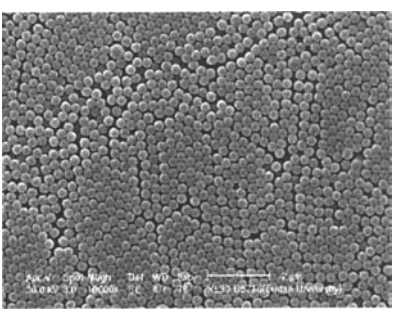

FIG. 2 Polystyrene particles containing hydroxyl obtained by surfactant-free emulsion polymerization.

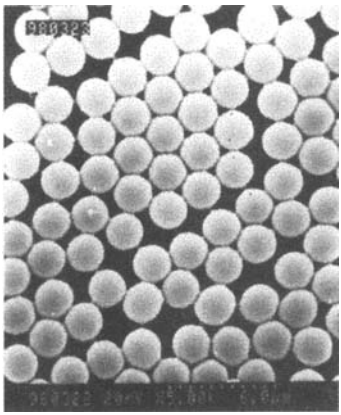

FIG. 3 Monodisperse poly(styrene-glycidyl methacrylate) copolymer particles prepared by dispersion copolymerization [9].

carboxyl, have been obtained by batch dispersion copolymerization of styrene and functional comonomers in polar media [9,21,22].

III. SURFACE MODIFICATION OF LATEX PARTICLES

A. Preparation of Functional Core Shell Particles by Conventional Method

Core-shell particle is a very important type of functional particle. A number of polymerization-based methods have been employed to produce particles that consist of solid cores coated with a shell of polymeric materials [23]. These include monomer adsorption onto particles followed by subsequent polymerization [24–30], heterocoagulation polymerization [31], and emulsion polymerization [23,32–34].

Sometimes two kinds of core materials were applied, i.e., inorganic and organic materials. For the inorganic core particles, a widely used strategy for the creation of core-shell particles is that of emulsion polymerization [23]. This approach has been used to encapsulate submicrometer- and micrometer-sized inorganic particles with polymer layers [32,33]. A major limitation of this method has been that it often leads to aggregated particles embedded in a polymer matrix. However, a recent study by Quaroni and Chumanov [34] has demonstrated the encapsulation of individual silver nanoparticles by a polymer shell comprising polystyrene and methacrylate via emulsion polymerization. Polymerization of styrene and/or methacrylic acid in emulsions of oleic acid afforded a uniform polymer layer around the metal core, the thickness of which could be

easily controlled in the range 2–10 nm by altering the concentration of monomers. This coating process appears to be most applicable to the formation of thin coatings as they follow the shape of the metal core, whereas thicker ones (>10 nm) take on a globular geometry and form irregular coatings.

It was also found that, unlike the uncoated particles, the polymer-encapsulated cores could be routinely centrifuged and redispersed, exhibited a strong resistance toward etching, and could be functionalized via protein attachment. This investigation is a prime example of the marked influence that a thin coating can have on the properties of a colloidal particle, thus making the previously single-component particles useful for other studies and even applications.

Another frequently employed method to obtain polymer shell on solid particles is the polymerization reaction, which can be catalyzed either by an initiator to promote the process or by the colloidal particles themselves. Matijevic et al. reported the coating of aluminum hydrous oxide–modified silica particles with poly(divinylbenzene) (PDVB) layers by pretreatment of the inorganic cores with coupling agents such as 4-vinylpyridine or 1-vinyl-2-pyrrolidone, followed by subsequent admixing of DVB and a radical initiator [24]. Other polymer layers were also synthesized around inorganic particles using a similar approach [25,26].

Multilayer core-shell particles were also produced by simply replacing the first monomer with a second and allowing polymerization to proceed. Using this technique, fine control over the shell thickness and coating may be difficult depending on the particle packing in the membrane.

For the organic core, two-stage seeded emulsion polymerization is the first general method developed to prepare latex particles having core-shell structure. The first stage, or core latex preparation, is carried out either separately or in situ, and the mode of polymerization for the second stage is usually a seeded swelling batch or a semibatch process.

Monodispersed latex core-shell particles are usually prepared by dispersion polymerization. Rudin's [35] group was prepared monodispersed latex core-shell particles with diameters of 3 μm by this method. There are also a few reports on core-shell particles prepared by dispersion polymerization: Laus et al. [36,37] formed monodispersed polystyrene particles of 2–10 μm in the presence of a polycarboxylic acid or polyepichlorohydrine steric stabilizer which itself then constitutes the shell. Okubo et al. [10] conducted dispersion copolymerizations of chloromethylstyrene and styrene on polystyrene seeds which adsorbed the monomer mixture and yielded micrometer-sized monodispersed polymer microspheres having chloromethyl groups in the shell. Li [38] reported monodispersed cross-linked poly(DVB-55) microspheres having diameters of 2–8 μm prepared by precipitation polymerization in acetonitrile. Use of functional comonomers including chloromethylstyrene [39], maleic anhydride [40], and methyacrylates [41] led to the corresponding monodispersed copolymer mi-

crospheres, whereas the presence of a good cosolvent such as toluene led to the formation of porous microspheres [42].

Several groups [43–45] have reported the formation of core-shell particles by stepwise heterocoagulation of smaller cationic polymer particles onto larger anionic polymer particles, followed by heat treatment at a temperature above the glass transition temperature (T_g) of the shell particles. For example [31], cationic particles of poly(butyl methacrylate) (PBMA) (167 nm in diameter) were heterocoagulated onto negatively charged polystyrene microspheres (600 nm in diameter). The PBMA particles had a nonionic polymer layer grafted onto their surface and this stabilized the resulting cluster. Subsequent heating of the sample to approximately 45°C above the T_g of PBMA caused it to spread while the nonionic polymer migrated to the outer surface and acted as a steric stabilizing layer. The resulting particles composed a polystyrene core coated with a relatively uniform shell of PBMA (Fig. 4). While this is an interesting method, difficulties exist in obtaining the desired coating of smaller particles that will in turn form a continuous film on the larger colloids. Colloidal stability may also be compromised when irregular coatings are obtained.

This method was said to give better control over certain types of composite particle morphology, as compared with the two-stage emulsion polymerizations.

B. Preparation of Functional Particles via Layer-by-Layer Process

Layer-by-layer (LbL) process is another important method to modify the particle surface. LbL is a new procedure that allows control over the shell composition, structure, and thickness at the nanometer level, and the method employs the stepwise adsorption of oppositely charged polymer (or nanoparticle) on colloidal templates (Fig. 5). The electrostatic interaction is the basis of LbL method, and

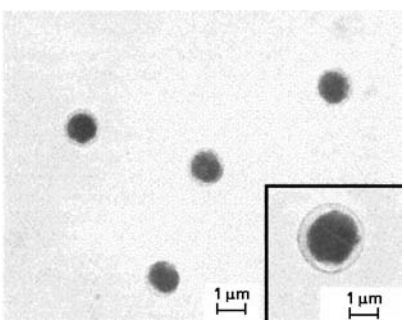

FIG. 4 TEM images of polystyrene core particles coated with a shell of PBMA. (From Ref. 31. Copyright 1997 Springer-Verlag.)

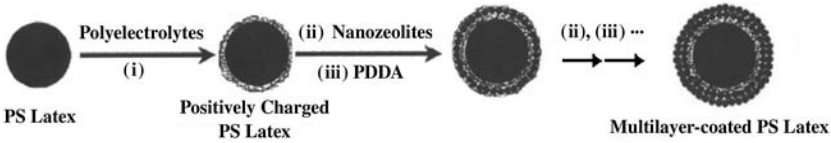

FIG. 5 Procedure for preparing zeolite-coated spheres.

the ionic strength and pH of adsorbed polymer (or nanoparticle) dispersion have important effects on the procedure [46].

Recent advances in particle coating strategies have made it possible to coat colloids with uniform single layer and multilayers of polyelectrolytes. Latex particles have been coated with a variety of polyelectrolytes by electrostatic self-assembly [47–51]. In this approach [51], a polymer solution in excess concentration of that required for saturation adsorption was added to a colloidal dispersion. The polymer selected had an opposite charge to that on the latex particles, thus predominantly adsorbing through electrostatic interactions. The coated particles were subsequently centrifuged and washed. Evidence showed that the polymer adsorbed was obtained by electrophoresis, which indicates a reversal in surface charge for the polymer-coated particles.

A novel and intriguing result arose from the subsequent addition of a second solution of oppositely charged polyelectrolyte to the polymer-coated particles; adsorption of a second layers on the particle surface occurred through electrostatic self-assembly in the same way that multilayered polymer films have been assembled on planar substrates [52,53]. Again, a reversal in surface charge was observed. Repetition of this process resulted in the formation of multiple bilayers on the particle surface in a controlled fashion. This was verified by single particle light scattering (SPLS) experiments [54]. The average thickness of adsorbed polyelectrolyte layers on polystyrene cores ($\phi = 640$ nm) was approximately 1.5 nm per layer [49]. These data demonstrate the remarkable nanoscale control that can be exerted over the shell thickness; the calculated average layer thickness increases with the number of polyelectrolyte layers deposited. Both SPLS and transmission electron microscopy (TEM) provided evidence that no significant aggregation of the coated polystyrene particles occurred.

LbL technique has several advantages: (1) the thickness of the polymer (nanoparticle) coatings can be finely tailored by changing the number of layers deposited and the solution conditions; (2) multicomposite films can be obtained through choice of a large variety of charges matter; (3) particles of different size, shape, and composition can be employed as template [53]. Using the LbL approach, polyelectrolytes, inorganic (such as SiO_2, Fe_3O_4, TiO_2, zeolite) nanoparticles, and protein multilayer films have been successfully constructed on spherical particle templates [46,55,56].

C. Preparation of Functional Particles via Grafting Process

In order to take advantage of these properties on the macroscopic scale, the particles should be incorporated into a host material possessing desirable properties, such as good processing characteristics, charge carrier mobility, transparency, and so on. The host materials should be linear polymer with one end anchored onto the particle's surface. Here we call this type of particle as "rambutan particle."

There are two ways to prepare rambutam particles from an existing particle cores. One is by binding linear polymer molecules onto the core particles from the polymer end group reacting with the corresponding functional group on the core particle surface—called "grafting-on." Usually, the linear polymers are hardly bound with high density and apt to be bound at any part of the surface. Another method corresponds to graft polymerization from the particle surface, i.e., "grafting-from." In this method, we can use conventional free-radical polymerization and "living" free-radical polymerization.

Generally, the rambutan particles were prepared with the grafting-from method. If the classical free-radical polymerization was used, the average chain is kept constant but the density of the grafting chain increases with increasing conversion.

In recent years, a number of papers have been published on the surface modification using either the stable free radical polymerization (SFRP) mediated by 2,2′,6,6-tetramethyl-1-piperidyloxy, reversible addition-fragmentation transfer polymerization or the atom transfer radical polymerization (ATRP) route for living/controlled radical polymerization [57–60]. Because the process can be well controlled, this method is an alternative to classical free-radical graft polymerization.

1. "Rambutan Particles" Prepared by Free-Radical Polymerization

In order to tailor the surface properties of organic or inorganic materials, ultrathin films have been prepared from a large variety of polymers [61–63]. Most systems described up to now are based on the physics adsorption of either homopolymers or block copolymers with a short block interacting with the surface. However, the interaction between the polymer and the surface is usually not so strong as in most cases it is caused by van der Waals forces or is due to hydrogen bonding.

A much stronger adhesion between the polymer chains and the substrate can be achieved when the macromolecules are covalently bound to the surface. In order to establish a chemical bond between the polymer chain end and the solid surfaces, suitable end-functionalized polymers were synthesized. However, only very small amounts of the polymer (typically less than 5 mg/m^2) can be immobi-

lized to the substrates [63–67]. This is due to the strong kinetic hindrance for the attachment of additional polymer chains to the surface and impedes further film growth. Therefore, the formation of surface-bound polymer monolayers by such a grafting-to technique is intrinsically limited to low graft densities and low film thicknesses.

In order to avoid these problems, Prucker and Ruhe [68–70] developed a system in which the complete initiator is attached to the substrate's surface in one reaction step. A schematic description of this system is given in Fig. 6. It consists of three basic components: an anchoring group (A) linking the imitator to the surface, the initiator itself (I-I), and a cleavable group (C) that allows for the degrafting of the macromolecules after polymerization for analytical purposes. In a first reaction step the initiator is self-assembled on the surface of the substrate.

In a subsequent reaction, the initiator is activated and polymer is formed *in situ* at the surface of the substrate.

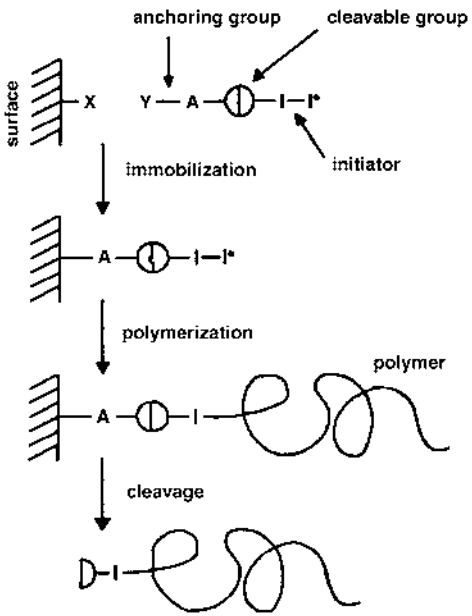

FIG. 6 Schematic description of the concept for the preparation of terminally attached polymer monolayers using covalently bonded initiators for free-radical polymerization ("grafting-from").

By now, we haven't found any papers to be published for preparing the rambutan particles using this method. We believe this is a nice method to prepare this kind of particle.

2. "Rambutan Particles" Prepared by Stable Free-Radical Polymerization

Controlled stable free radical polymerization (SFRP) has recently been an area of increasing interest [71,72]. This type of polymerization can be realized through reversible deactivation of growing radicals by stable radicals, such as 2,2,6,6-tetramethyl-1-piperidinyloxy (TEMPO) (Fig. 7).

For the synthesis of controlled polymer monolayers by polymerization started from surface-attached initiator molecules, one of the basic requirements is control of the chemical composition and graft density of the initiators. As reactions in surface-attached monolayers are not easily quantified, it is desirable to achieve the immobilization of the initiator in a one-step procedure. To obtain a high graft density, it is desirable that the reactivity of the initiator molecule be high under the given reaction conditions.

In order to full of the above consideration, an experimental procedure is designed as Fig. 8. It consists of an azo group that is structurally similar to AIBN and a monofunctional chlorosilane head group, which connects the initiator to the surface of the substrate. The ester group connecting the initiating group and the anchor can act as a "break-seal" group. Hence, this ester can be cleaved after completion of the layer formation, and the polymer can be removed from the surface and analyzed. Due to the existence of TEMPO, the molecular weight and polydispersity of the grafting chain can be well controlled.

3. "Rambutan Particles" Prepared by Atom Transfer Radical Polymerization

For the grafting process, a controlled/living polymerization technique would be optimal because such methods afford control over the molecular weight, molec-

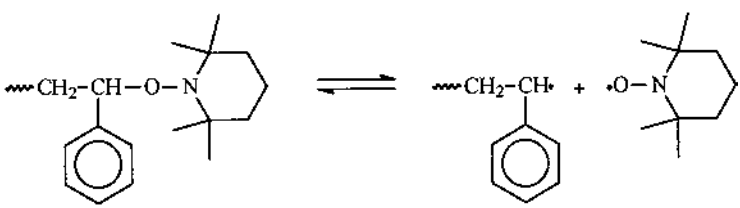

FIG. 7 Reversible termination of growing free-radical chains by using a stable free radical.

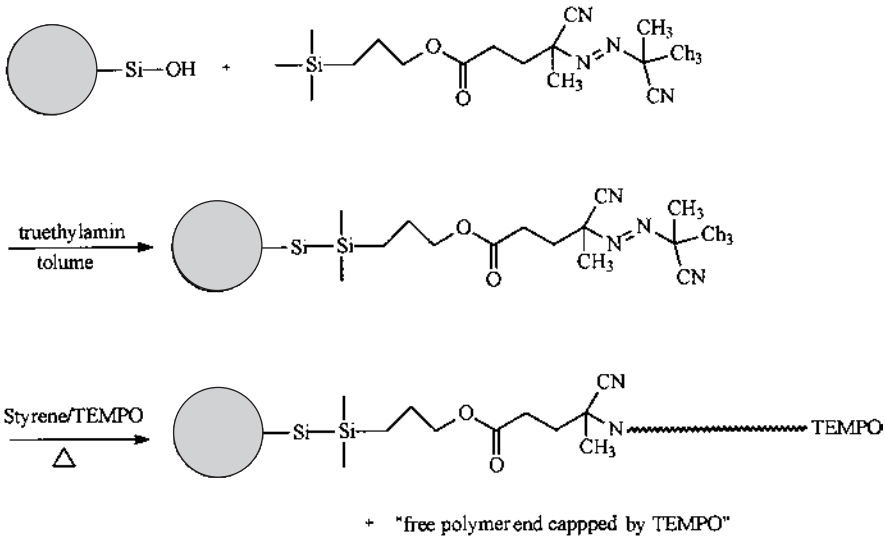

FIG. 8 Stable free-radical graft polymerization onto core particles.

ular weight distribution, and structure of the resulting polymer, and this method can cover many types of monomers [73].

Patten and his coworker [74] prepared such structured polymer hybrid particles by modifying the surface of silica nanoparticles with initiators for ATRP. To study the grafting of polymer chains from inorganic nanoparticles, they broke the problem down into two steps (Fig. 9). The first step is depositing a monolayer of polymerization initiators on a nanoparticle surface, then conducting polymerizations using the nanoparticle as a macroinitiator and examining the effect of varying synthetic parameters, such as monomer type and nanoparticle

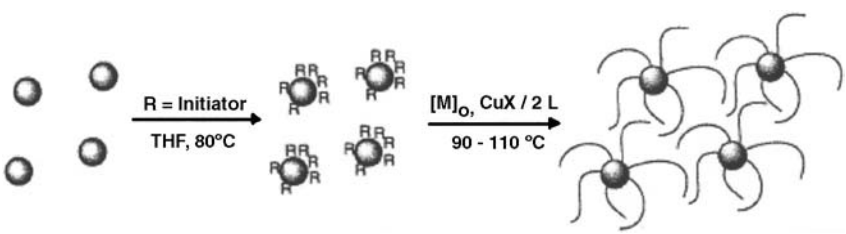

FIG. 9 Synthetic steps for forming hybrid polymer–inorganic nanoparticles.

diameter, on the polymerization reaction. Polymerizations of styrene and methyl methacrylate (MMA) using the nanoparticle initiators displayed the diagnostic criteria for a controlled/living radical polymerization under specific reaction conditions. Well-defined polymer chains were grown from the nanoparticle surfaces to yield individual particles composed of a silica core and a well-defined, densely grafted outer polystyrene or poly(methyl methacrylate) layer.

Polymerizations of styrene from smaller (75 nm diameter) silica nanoparticles exhibited good molecular weight control, whereas polymerizations of MMA from the same nanoparticles exhibited good molecular weight control only when a small amount of free initiator was added to the polymerization solution. The polymerizations of both styrene and MMA from larger (300 nm diameter) silica nanoparticles did not exhibit molecular weight control. Molecular weight control was induced by the addition of a small amount of free initiator to the polymerization but was not induced when 5–15 mol % of deactivator [Cu(II) complex] was added. These findings provide guidance for future efforts in using ATRP for the controlled grafting of polymers from high surface area substrates (i.e., small-diameter cylinders and spheres, highly porous materials) and low surface area substrates (i.e., flat surfaces, large-diameter cylinders and spheres, low-porosity materials).

Recently, a full organic "rambutan particle" (the composite particle made of two different polymers, one theoretically forming the core and the other the shell) was prepared in water phase by Guerrini et al. [75]. They prepared hydrophobic core-hydrophilic shell particles using hydrophobic functionalized latexes as substrates for ATRP of water-soluble monomers. In this system, surfactants must be chosen carefully so as not to influence the stability of the latex system.

In line with this study, Wang [76] prepared a new type of core-shell particle using ATRP in organic phase. Nonsurfactant was used in this system, and more functional groups can be introduced in the shell.

Using atom ATRP of MMA and MA to synthesize a well-controlled shell on cross-linked polystyrene seed particles (Fig. 10). The cross-linked seed particles were first prepared using classical emulsifier-free polymerization. Also, ATRP was performed on the modified seed polystyrene particles. To highlight the effectiveness of ATRP, the latexes were characterized before and after shell synthesis.

In this study, graft polymerization was conducted successfully on the surface of modified cross-linked polystyrene particles, and the shell thickness of the particles was controlled using the ATRP process. Using the chloromethylation method, the chloromethane group was directly introduced onto the polystyrene particle surface, which was prepared by emulsifier-free emulsion polymerization. The ATRP of MMA and MA was initiated by the chlorine atom on the surface of polystyrene particles. Under different reaction conditions, shell layer

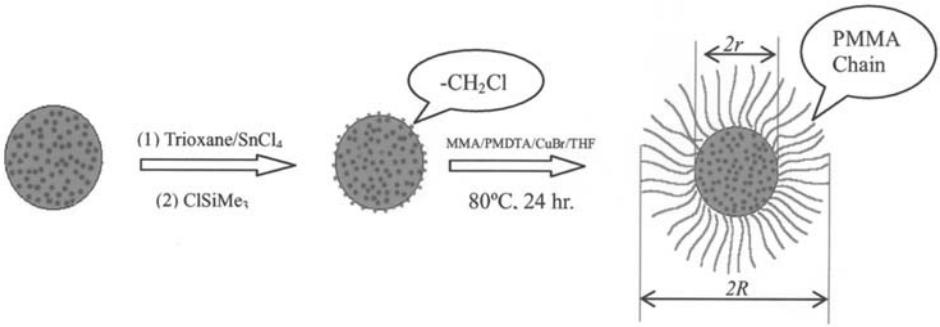

FIG. 10 Atom transfer radical graft polymerization onto core particles.

particles of different thicknesses were obtained. The shell layer thickness of the core-shell particles is between 7 nm and 22 nm, and the PMMA or PMA weight fraction in the core shell particles is between 11% and 33%.

For the above core-shell particles, the shell is linear MMA chain, the ester group can be easily hydrolyzed forming hydrophilic shell particles, these type particles can be dispersed in water quickly, and the dispersion is very stable.

4. "Rambutan Particles" Prepared by Reversible Addition–Fragmentation Transfer Polymerization

A much more effective and versatile version of the exchanging radical polymerization was described by Chefari et al. [77,78], who patented the RAFT process based on reversible addition–fragmentation chain transfer. Thermally, or otherwise, generated free radicals start to grow. When they encounter a dithiomolecule, which acts as a chain transfer agent, they add to it in a reversible fashion. They are subsequently replaced by longer polymeric residues and grow, after release, until the next encounter with a chain transfer agent.

Kawaguchi and coworkers [79] prepared the rambutan particles using the RAFT method. They prepared first the core particles using styrene and vinylbenzylchloride, then the core particles bearing a methyl chloride group. Using these particles, they can introduced the iniferter from the reaction shown in Fig. 11, and the result was confirmed by X-ray photoemission spectroscopy. Using these particles, they initiated the grafting polymerization of *N*-isopropylacrylamide (Fig. 12). They found that the conversion and hydrodynamic diameter both increased until the conversion reached 70% and the hydrodynamic diameter increased from 400 nm to 900 nm.

In this paper, they also studied the thermosensitive property of the grafting polymer chain and found that particle size exhibited a sharp transition in a very

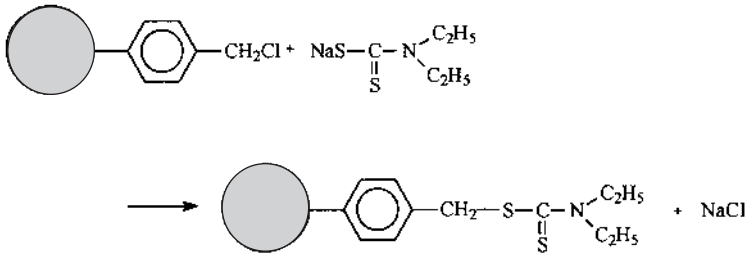

FIG. 11 Immobilization of sodium *N,N*-diethyldithiocarbamate to core particles.

narrow temperature range around 32°C. Using the same method, random and block grafting copolymer chain of *N*-isopropylacrylamide and acrylic acid was prepared. They found that the temperature- and pH-sensitive hydrodynamic size and transition temperature of NIPAN-AA copolymer hair particles were controlled by the content and distribution of AA in the PNIAM chain.

Although only a few papers have been published in this field, more attention may be paid in the future.

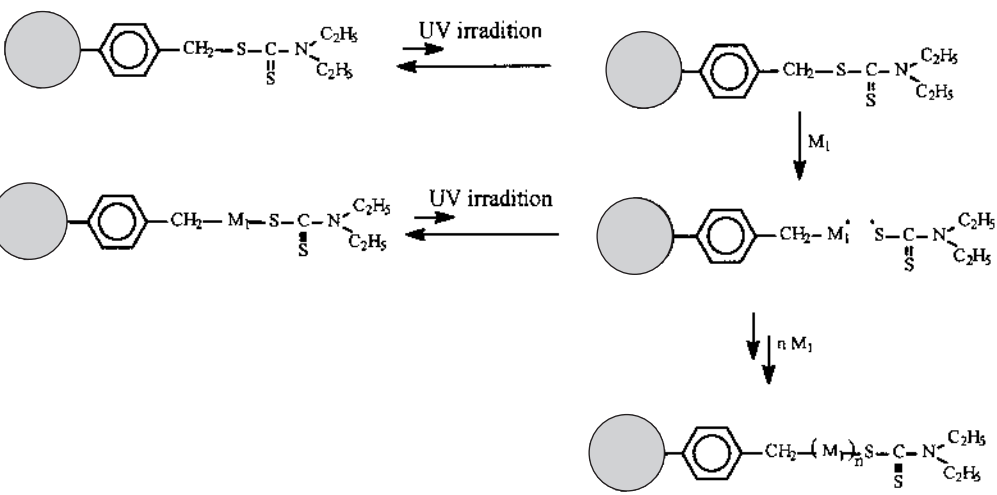

FIG. 12 Reversible addition–fragmentation chain transfer graft polymerization onto core particles.

5. "Rambutan Particles" Prepared by Oxyanion-Initiated Polymerization

In 1997, Nagasaki and coworkers [80] reported the homopolymerization of 2-(diethylamino)ethyl methacrylate (DEA) using potassium ethoxide in THF at or above ambient temperature. Such oxyanionic initiators do not normally polymerize methacrylate monomers, they attributed their unexpected success to complexation of the potassium counterion with the nitrogen heteroatom of the DEA. However, this explanation remains speculative; the precise mechanism for this polymerization has not yet been established. It was also shown that a potassium 4-vinylbenzyl alcoholate initiator led to formation of well-defined, styrene-capped DEA macromonomers $M_w/M_n < 1.30$. Recently, Armes extended [81] these macromonomer syntheses to include other tertiary amine methacrylates, via 2-(dimethylamino)ethyl methacrylate (DMA), 2-(*N*-morpholino)ethyl methacrylate (MEMA), and 2-(di*iso*propylamino)ethyl methacrylate (DPA). It was shown that these macromonomers can act as reactive polymeric stabilizers for polystyrene latex syntheses under both aqueous emulsion and alcoholic dispersion polymerization conditions. In a separate study, a poly(ethylene oxide)-based macroinitiator (PEO) was used to polymerize either DMA or DEA and hence obtain novel water-soluble poly(ethylene oxide-*block*-tertiary amine methacrylates) [82].

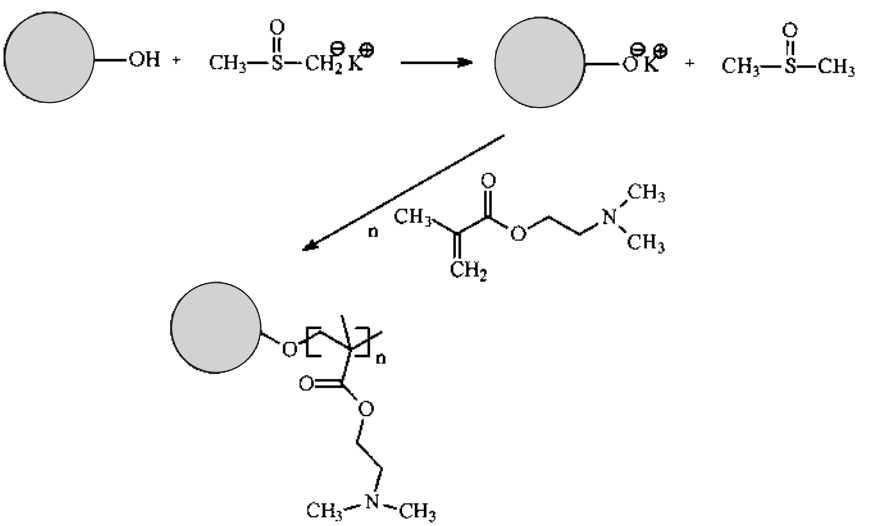

FIG. 13 Oxyanion-initiated graft polymerization onto core particles.

Because the special properties of oxyanion-initiated polymerization, it is very powerful to introduce this method to the surface modification of particles. Our group has done some work in this area. The experimental procedure is shown in Fig. 13. The final particles contain a hydrophilic shell and can disperse in water very easily, and can be used in the clinical diagnosis.

IV. CONCLUSION AND PERSPECTIVE

Research and application effects over the last 20 years have led to preparation technique of structured particles development quickly. At present, it is possible to obtain very varied particle morphologies, from the relatively simple and most frequently studied core-shell structure to much more complex structures (multilayer, with spherical and cellular inclusions, etc.), sometimes leading to irregular, unstable forms, and evolving into spherical forms. Under the conventional procedure, i.e., a classical polymerization process, it is hard to monitor both the core size and the thickness of the shell. In recent years, the method for living free-radical polymerization has been introduced into the preparation of core-shell particles with this method. With living free-radical polymerizations it is easier to tailor or control the shell thickness and surface properties, and more power is available to cater to our aim. In the future, with the development of synthesis technology, well-designed functional particles will be prepared to meet the different needs.

REFERENCES

1. Daniels, E.S.; Sudol, E.D.; El Aasser, M.S. *Polymer Latexes*: *Preparation*, *Characterization and Applications*; ACS Symp. Series 492. American Chemical Society: Washington, DC, 1992.
2. Upson, D.A. Reactive functional latex polymers. J. Polym. Sci. Polym. Symp. **1985**, *72*, 45–54.
3. Pichot, C.; Charleux, B.; Charreyre, M.T.; Revilla, J. Recent developments in the design of functionalized polymeric microspheres. Macromol. Symp. **1994**, *88*, 71–87.
4. Pichot, C.; Delair, T.; Elaissari, A. Polymer colloids for biomedical and pharmaceutical applications. In *Polymeric Dispersions*: *Principles and Applications*; Asua, J.M., Ed.; NATO ASI Series, Vol. 335; Kluwer Academic: Dordrecht, 1997; 515–539.
5. Yan, C. Study of ternary emulsifier-free emulsion copolymerization and its latex particles as support of protein. PhD dissertation, Zhejiang University, Hangzhou, China, 1998.
6. Rembaum, A.; Yen, S.P.S.; Cheong, E.; Molday, R.S.; Gordon, J.L.; Dryer, W.J. Functional polymeric microspheres based on 2-hydroxyethyl methacrylate for immunological studies. Macromolecules **1976**, *9*, 328–336.

7. Delair, T.; Meunier, F.; Elaissari, A.; Charles, M.; Pichot, C. Amino-containing cationic latex-oligodeoxyribonucleotide conjugates: application to diagnostic test sensitivity enhancement. Colloid Surf. A **1999**, *153*, 341–353.
8. Okubo, M.; Kamei, S.; Tosaki, Y.; Fukunaga, K.; Matsumoto, T. Covalent immobilization of trypsin onto poly(2-hydroxyethyl methacrylate)/polystyrene composite microspheres by cyanogen bromide method and its enzymatic activity. Colloid Polym. Sci. **1987**, *265*, 957–964.
9. Yang, W.L. Dispersion copolymerization of styrene and the application of microspheres. PhD dissertation, Fudan University, Shanghai, China, 1998.
10. Okubo, M.; Ikegami, K.; Yamamoto, Y. Preparation of micron-size monodisperse polymer microspheres having chloromethyl group. Colloid Polym. Sci. **1989**, *267*, 193–200.
11. Delair, T.; Pichot, C.; Mandrand, B. Synthesis and characterization of cationic latex particles bearing sulhydryl group and their use in the immobilization of Fab antibody fragments. Colloid Polym. Sci. **1994**, *272*, 962–970.
12. Li, J.; Cheng, S.; Xu, Z. Study on copolymer emulsion with N-methylolacrylamide. Polym. Mater. Sci. Eng. **1992**, (2):27–31.
13. Brouwer, W.M.; Van Der Vergt, M.; Van Haaren, P. Particle surface characteristics of permanently charged poly(styrene-cationic monomer) latices. Europ. Polym. J. **1990**, *26*, 35–39.
14. Kashiwabara, M.; Fujimoto, K.; Kawaguchi, H. Preparation of monodisperse, reactive hydrogel microspheres and their amphoterization. Colloid Polym. Sci. **1995**, *273*, 339–345.
15. Blackley, D.C. Preparation of carboxylated latices by emulsion polymerization. In *Science and Technology of Polymer Colloids*; Poehlein, G.W., Goodwill, R.H., Goodwin, J.W., Eds.; NATO ASI Series Vol. 68, Nijhoff: The Hague, 1983; 203–219.
16. Pichot, C. Recent developments in the functionalization of latex particles. Macromol. Symp. **1990**, *35/36*, 327–347.
17. Pichot, C. Position paper: functional polymer latexes. Polym. Adv. Tech. **1995**, *6*, 427–434.
18. Guillaume, J.L.; Pichot, C.; Guillot, J. Emulsifier-free emulsion copolymerization of styrene and butyl acrylate. III. Kinetic studies in the presence of a surface active comonomer, the sodium acrylamido undecanoate. J. Polym. Sci. A Polym. Chem. **1990**, *28*, 137–152.
19. Emelie, B.; Pichot, C.; Guillot, J. Characterization of the surface morphology in carboxylated methyl methacrylate-butyl acrylate emulsion copolymers. Macromol. Chem. Macromol. Chem. Phys. **1988**, *189*, 1879–1891.
20. Guillaume, J.L.; Pichot, C.; Guillot, J. Emulsifier-free emulsion copolymerization of styrene and butyl acrylate. II. Kinetic studies in the presence of ionogenic comonomers. J. Polym. Sci. A Polym. Chem. **1988**, *26*, 1937–1959.
21. Ober, C.K.; Lok, K.P. Formation of large monodisperse copolymer particles by dispersion polymerization. Macromolecules **1987**, *20*, 268–273.
22. Horak, D.; Svec, F.; Frechet, J.M.J. Preparation of control of surface properties of monodisperse micrometer size beads by dispersion copolymerization of styrene and butyl methacrylate in polar media. J. Polym. Sci. Polym. Chem. **1995**, *33*, 2329–2338.

23. Hofman-Caris, C.H.M. Polymers at the surface of oxide nanoparticles. New J. Chem. **1994**, *18*, 1087–1096.
24. Oyama, H.T.; Sprycha, R.; Xie, Y.; Partch, R.E.; Matijevic, E. Coating of uniform inorganic particles with polymers. 1. J. Colloid Interface Sci. **1993**, *160*, 298–303.
25. Sprycha, R.; Oyama, H.T.; Zelenev, A.; Matijevic, E. Characterization of polymer-coated silica particles by microelectrophoresis. Colloid Polym. Sci. **1995**, *273*, 693–700.
26. Partch, R.; Gangolli, S.G.; Matijevic, E.; Cai, W.; Arajs, S. Conducting polymer composites. I. Surface-induced polymerization of pyrrole on iron(iii) and cerium(iv) oxide particles. J. Colloid Interface Sci. **1991**, *144*, 27–35.
27. Huang, C.L.; Matijevic, E. Coating of uniform inorganic particles with polymers. 3. Polypyrrole on different metal oxides. J. Mater. Res. **1995**, *10*, 1327–1336.
28. Marinakos, S.M.; Brousseau, L.C.; Jones, A.; Feldheim, D.L. Template synthesis of one-dimensional Au, Au-poly(pyrrole), and poly(pyrrole) nanoparticle arrays. Chem. Mater. **1998**, *10*, 1214–1219.
29. Marinakos, S.M.; Shultz, D.A.; Feldheim, D.L. Gold nanoparticles as templates for the synthesis of hollow nanometer-sized conductive polymer capsules. Adv. Mater. **1999**, *11*, 34–37.
30. Marinakos, S.M.; Novak, J.P.; Brousseau, L.C.; House, A.B.; Edeki, E.M.; Feldhaus, J.C.; Feldheim, D.L. Gold particles as templates for the synthesis of hollow polymer capsules. Control of capsule dimensions and guest encapsulation. J. Am. Chem. Soc. **1999**, *121*, 8518–8522.
31. Ottewill, R.H.; Schofield, A.B.; Waters, J.A.; Williams, N.S.J. Preparation of core-shell polymer colloid particles by encapsulation. Colloid Polym. Sci. **1997**, *275*, 274–283.
32. Hergeth, W.D.; Steinau, U.J.; Bittrich, H.J.; Schmutzler, K.; Wartewig, S. Prog. Colloid Polym. Sci. **1991**, *85*, 82.
33. van Herk, A.M. Encapsulation of inorganic particles. In *Polymeric Dispersions*: *Principles and Applications*; Asua, J.M., Ed.; NATO ASI series, Vol. 335; Kluwer Academic: Dordrecht, 1997; 435–450.
34. Quaroni, L.; Chumanov, G. Preparation of polymer-coated functionalized silver nanoparticles. J. Am. Chem. Soc. **1999**, *121*, 10642–10643.
35. O'Callaghan, K.J.; Paine, A.J.; Rudin, A. Emulsion polymerization of supermicron, monodisperse acrylic copolymer particles with core-shell structures. J. Polym. Sci. A Polym. Chem. **1995**, *33*, 1849–1857.
36. Laus, M.; Dinnella, C.; Lanarini, G.; Casagrande, A. Core-shell functional microspheres by dispersion polymerization. 2. Synthesis and characterization. Polymer **1996**, *37*, 343–347.
37. Laus, M.; Lelli, M.; Casagrande, A. Polyepichlorohydrine stabilized core shell microspheres by dispersion polymerization. J. Polym. Sci. A Polym. Chem. **1997**, *35*, 681–688.
38. Li, K.; Stover, H.D.H. Synthesis of monodisperse poly(divinylbenzene) microspheres. J. Polym. Sci. Polym. Chem. **1993**, *31*, 3257–3263.
39. Li, W.H.; Li, K.; Stover, H.D.H. Monodisperse poly(chloromethylstyrene-co-divinyl benzene) microspheres by precipitation polymerization. J. Polym. Sci. Polym. Chem. **1999**, *37*, 2295–2303.

40. Frank, R.S.; Downey, J.S.; Stover, H.D.H. Synthesis of divinylbenzene-maleic anhydride microspheres using precipitation polymerization. J. Polym. Sci. Polym. Chem. **1998**, *36*, 2223–2227.
41. Li, W.H.; Stover, H.D.H. Mono- or narrow disperse poly(methacrylate-co-divinylbenzene) microspheres by precipitation polymerization. J. Polym. Sci. Polym. Chem. **1999**, *37*, 2899–2907.
42. Li, W.H.; Stover, H.D.H. Porous monodisperse poly(divinylbenzene) microspheres by precipitation polymerization. Polym. Sci. Polym. Chem. **1998**, *36*, 1543–1551.
43. Okubo, M.; Ichikawa, K.; Tsujihiro, M.; He, Y. Production of anomalous polymer microspheres having uneven surfaces by stepwise heterocoagulation technique. Colloid Polym. Sci. **1990**, *268*, 791–796.
44. Okubo, M.; Lu, Y. Production of core-shell composite polymer particles utilizing the stepwise heterocoagulation method. Colloid Surf. A **1996**, *109*, 49–53.
45. Ottewill, R.H.; Schofield, A.B.; Waters, J.A.; Williams, N.S.J. Preparation of core-shell polymer colloid particles by encapsulation. Colloid Polym. Sci. **1997**, *275*, 274–283.
46. Wang, X.D.; Yang, W.L.; Tang, Y.; Wang, Y.J.; Fu, S.K.; Gao, Z. Fabrication of hollow zeolites spheres. Chem. Commun. **2000**, (21): 2161–2162.
47. Caruso, F.; Donath, E.; Mohwald, H. Influence of polyelectrolyte multilayer coatings on Forster resonance energy transfer between 6-carboxyfluorescein and rhodamine B-labeled particles in aqueous solution. J. Phys. Chem. B **1998**, *102*, 2011–2016.
48. Sukhorukov, G.B.;. Donath, E.; Lichtenfeld, H.; Knippel, E.; Knippel, M.; Mohwald, H. Layer-by-layer self assembly of polyectrolytes on colloidal particles. Colloids Surf. A Physicochem. Eng. Asp. **1998**, *137*, 253.
49. Caruso, F.; Lichtenfeld, H.; Donath, E.; Mohwald, H. Investigation of electrostatic interactions in polyelectrolyte multilayer films: binding of anionic fluorescent probes to layers assembled onto colloids. Macromolecules **1999**, *32*, 2317–2328.
50. Caruso, F.; Schuler, C.; Kurth, D.G. Core-shell particles and hollow shells containing metallo-supramolecular components. Chem. Mater. **1999**, *11*, 3394–3399.
51. Caruso, F. Hollow capsule processing through colloidal templating and self-assembly. Chem. Eur. J. **2000**, *6*, 413–419.
52. Decher, G.; Hong, J.D. Buildup of ultrathin multilayer films by a self-assembly process. 2. Consecutive adsorption of anionic and cationic bipolar amphiphiles and polyelectrolytes on charged surfaces. Ber. Bunsenges Phys. Chem. **1991**, *95*,1430–1434.
53. Decher, G. Fuzzy nanoassemblies: toward layered polymeric multicomposites. Science **1991**, *277*, 1232–1237.
54. Lichtenfeld, H.; Knapschinsky, L.; Sonntag, H.; Shilov, V. Fast coagulation of nearly spherical ferric-oxide (hematite) particles. 1. Formation and decomposition of aggregates—experimental estimation of velocity constants. Colloids Surf. A **1995**, *104*, 313–320.
55. Caruso, F. Nanoengineering of particles surfaces. Adv. Mater. **2001**, *13*, 11–22.
56. Caruso, F.; Caruso, R.A.; Mohwald, H. Nanoengineering of inorganic and hybrid hollow spheres by colloidal templating. Science **1998**, *282*, 1111–1114.
57. Hawker, C.J.; Hedrick, J.L.; Malmstrom, E.E.; Benoit, D.; Dao, J. Synthesis and

application of functionalized specialty polymers using "living" free radical procedures. ACS Polym. Prepr. **1998**, *39*, 626–627.
58. Huang, X.; Doneski, L.J.; Wirth, M.J. Surface-confined living radical polymerization for coatings in capillary electrophoresis. Anal. Chem. **1998**, *70*, 4023–4029.
59. Ejaz, M.; Yamamoto, S.; Ohno, K.; Tsujii, Y.; Fukada, T. Controlled graft polymerization of methyl methacrylate on silicon substrate by the combined use of the Langmuir-Blodgett and atom transfer radical polymerization techniques. Macromolecules **1998**, *31*, 5934–5936.
60. Husseman, M.; Malmstrom, E.E.; McNamara, M.; Mate, M.; Mecerreyes, D.; Benoit, D.G.; Hedrick, J.L.; Mansky, P.; Huang, E.; Russel, T.P.; Hawker, C.J. Controlled synthesis of polymer brushes by "living" free radical polymerization techniques. Macromolecules **1999**, *32*, 1424–1431.
61. Halperin, A.; Tirrell, M.; Lodge, T.P. Tethered chains in polymer microstructures. Adv. Polym. Sci. **1992**, *100*, 31–71.
62. Ulmann, A. *An Introduction to Ultrathin Organic Films*; Academic Press: New York, 1991.
63. Fleer, G.J.; Cohen-Stuart, M.A.; Scheutjens, J.M.H.M.; Cosgrove, T.; Vincent, B. *Polymers at Interfaces*; Chapman and Hall: London, 1993.
64. Krenkler, K.P.; Laible, R.; Hamann, K. Polyreactions on pigment surfaces. 7. Reactions of polymers with chlorosilane end groups on silicon dioxide surfaces. Angew. Makromol. Chem. **1978**, *53*,101–123.
65. Tsubokawa, N.; Hosoya, M.; Yanadori, K.; Sone, Y. Grafting onto carbon-black reaction of functional-groups on carbon-black with acyl chloride-capped polymers. J. Macromol. Sci. Chem. **1990**, *A27*, 445–457.
66. Bridger, K.; Vincent, B. The terminal grafting of poly(ethylene oxide) chains to silica surfaces. Eur. Polym. J. **1980**, *16*, 1017–1021.
67. Benouada, H.; Hommel, H.; Legrand, A.P.; Balard, H.; Papirer, E. Organization of the layers of polyethylene oxide grafted with different densities on silica. J. Colloid. Interface Sci. **1988**, *122*, 441–449.
68. Ruhe, J. Customized surfaces. Nachr. Chem. Tech. Lab. **1994**, *42*, 1237.
69. Ruhe, J. Habilitationsschrift (Habilitation thesis), University of Bayreuth, Bayreuth, Germany, 1995.
70. Prucker, O.; Ruhe, J. Synthesis of poly(styrene) monolayers attached to high surface area silica gels through self-assembled monolayers of azo initiators. Macromolecules **1998**, *31*, 592–601.
71. Georges, M.K.; Veregin, R.P.N.; Kazmaier, P.M.; Hamer, G.K. Narrow molecular-weight resins by a free-radical polymerization process. Macromolecules **1993**, *26*, 2987–2988.
72. Solomon, D.H.; Rizzardo, E.; Cacioli, P. US Patent 4,581,429, 1985.
73. Webster, OW. Living polymerization methods. Science **1991**, *251*, 887–893.
74. von Werne, T.; Patten, T.E. Atom transfer radical polymerization from nanoparticles: a tool for the preparation of well-defined hybrid nanostructures and for understanding the chemistry of controlled/"living" radical polymerizations from surfaces. J. Am. Chem. Soc. **2001**, *123*, 7497–7505.
75. Guerrini, M.M.; Charleux, B.; Vairon, J.P. Functionalized latexes as substrates for atom transfer radical polymerization. Macromol. Rapid Commun. **2000**, *21*, 669–674.

76. Min, K.; Hu, J.H.; Wang, C.C.; Elaissari, A. Surface modification of polystyrene latex particles via atom transfer radical polymerization. J.Polym. Sci. Polym. Chem. **2002**, *40*, 892–900.
77. Huang, X.; Wirth, M.J. Surface initiation of living radical polymerization for growth of tethered chains of low polydispersity. Macromolecules **1999**, *32*, 1694–1696.
78. Ejaz, M.; Yamamoto, S.; Ohno, K.; Tsujii, Y.; Fukuda, T. Controlled graft polymerization of methyl methacrylate on silicon substrate by the combined use of the Langmuir-Blodgett and atom transfer radical polymerization techniques. Macromolecules **1998**, *31*, 5934–5936.
79. Kawaguchi, H.; Isono, Y.; Tsuji, S. Hairy particles prepared by living radical graft-polymerization. Macromol. Symp. **2002**, *179*, 75–87.
80. Nagasaki, Y.; Sato, Y.; Kato, M. A novel synthesis of semitelechelic functional poly(methacrylate)s through an alcoholate initiated polymerization. Synthesis of poly[2-(*N*,*N*-diethylaminoethyl) methacrylate] macromonomer. Macromol. Rapid Commun. **1997**, *18*, 827–835.
81. Lascelles, S.F.; Malet, F.; Mayada, R.; Billingham, N.C.; Armes, S.P. Latex syntheses using novel tertiary amine methacrylate-based macromonomers prepared by oxyanionic polymerization. Macromolecules **1999**, *32*, 2462–2471.
82. Vamvakaki, M.; Billingham, N.C.; Armes, S.P. Synthesis of controlled structure water-soluble diblock copolymers via oxyanionic polymerization. Macromolecules **1999**, *32*, 2088–2090.

6

Poly(*N*-isopropylacrylamide)-Based Particles

Preparation and Colloidal Characterization

FRANÇOISE MEUNIER and ABDELHAMID ELAISSARI
CNRS-bioMérieux, Lyon, France

I. INTRODUCTION

Within the last decades, precipitation polymerization leading to the preparation of thermally sensitive materials (i.e., polymers, gels, and microgel latex particles) has been reported and discussed as evidenced by the numerous reported papers. The first polymerization leading to linear thermally sensitive polymers has been investigated by Heskins et al. [1] using *N*-isopropylacrylamide (NIPAM). The obtained linear homopolymer exhibits a low critical solution temperature (LCST) at 32°C corresponding to dramatic change in the solubility parameters of the corresponding polymer. In fact, below the LCST the polymer is totally soluble in the aqueous medium, whereas above the LCST the solution exhibits phase separation induced by the polymer precipitation. The LCST of poly(NIPAM)-based polymers has been largely studied using different physical methods and approaches, such as fluorescence, turbidity, dynamic light scattering, viscosity, and calorimetric measurements.

Concerning hydrogel latex particles, the first paper has been reported by Pelton et al. [2] who investigated precipitation polymerization of NIPAM, with methylenebisacrylamide (MBA) as a cross-linker and potassium persulfate (KPS) as initiator. Since that time, various thermally sensitive colloidal systems have been utilized in investigations of such diverse parameters as initiator nature and the use of acrylamide derivatives as the main monomer. In addition, the effect of surfactant on the elaboration of such microgel particles has been studied by McPhee et al. [3] and Wu et al. [4].

The colloidal and physicochemical properties of such thermally sensitive microgel particles have been reported by several authors, as can be evidenced by

the high number of reported papers. To same extent, internal structure, hydrodynamic particle size, electrokinetic study (i.e., electrophoretic mobility and ζ potential), hydrophilic–hydrophobic balance of the particle surface, and colloidal stability have been investigated as a function of temperature, pH, and ionic strength of the medium [5]. All the reported results exhibit principally the drastic effect of temperature on the colloidal properties. For a better understanding of the mechanistic approach of precipitation polymerization involved in the preparation of such stimuli-responsive particles and the colloidal properties of obtained latexes, a systematic polymerization study was of good interest. In fact, the thermally sensitive property of such latex particles has been used for several biomedical applications. Based on the hydrophilic property of such particles below the LCST of the corresponding linear polymer, the latex particles have been used as a support of various biomolecules (proteins, enzymes, nucleic acids, peptides, viruses, and antibodies). Recently, several reported works have been dedicated to the preparation of thermally sensitive magnetic latex particles [6] and their application in the biomedical field [7,8].

The aim of the presented chapter is to report on the preparation and colloidal preparation of thermally sensitive NIPAM-based particles. In addition, the investigation of various parameters as a systematic study will be presented and discussed in order to point out the role of each reactant on the polymerization process. In other words, we aimed at reporting the driving parameters controlling the precipitation polymerization of such *N*-alkylacrylamide monomer derivatives in order to target appropriate colloidal support applicable in the biomedical field. In addition, their colloidal properties will be presented and discussed on the basis of pertinent physicochemical parameters.

II. SYNTHESIS OF *N*-ISOPROPYLACRYLAMIDE-BASED MICROGEL PARTICLES

The first thermally sensitive acrylamide derivative polymers have been reported by Heskins et al. [1] by the elaboration of poly(NIPAM) polymer via radical polymerization method. Since that time, an increasing interest has been focused on both syntheses of new temperature-sensitive polymers bearing reactive compounds and the physical properties of such materials. In fact, various papers have been dedicated to the studies concerning the comprehension of the coil to globule transition temperature of the considered polymer induced by the solvent nature (Fig. 1).

The preparation methodologies of thermally sensitive materials (linear polymers, gels, and particles) are summarized in Fig. 2 in which the relationships between the reactant composition, the polymerization condition, and the physical state of the final material are depicted.

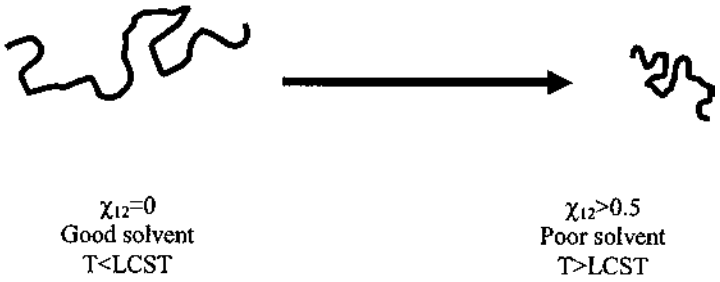

FIG. 1 Illustration of thermally sensitive polymer as a function of temperature.

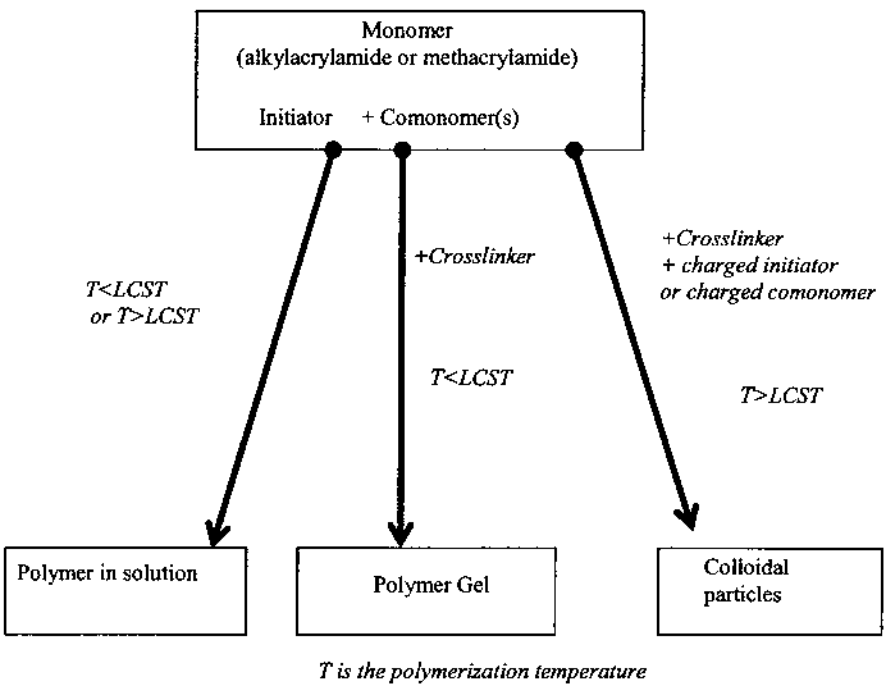

FIG. 2 Different polymerization processes leading to thermally sensitive bulk polymers, gels, and colloidal particles.

The first synthesis of NIPAM-based particles was described by Pelton et al. [2]. It was carried out with NIPAM as main monomer, KPS as initiator, and MBA as cross-linking agent. Since this pioneering work, a variety of research on the elaboration of diverse microgel particles has been carried out as will be clearly presented below.

A. Influence of Each Reactant on the Nipam Polymerization Reaction

The chemical composition or the reactants generally used to elaborate thermally sensitive particles of submicrometer size are basically NIPAM as the main monomer, water-soluble cross-linker agent (i.e., MBA), and charged initiator (Fig. 3). The polymerization temperature should be high enough to induce at less initiator decomposition. In addition, the solid content should be lower than 5% (w/v) in order to avoid particle aggregation.

1. Effect of Temperature

To induce a polymerization reaction, the medium temperature should be high so as to stimulate initiator decomposition as for emulsion and classical radical polymerization process. In addition, the polymerization temperature should en-

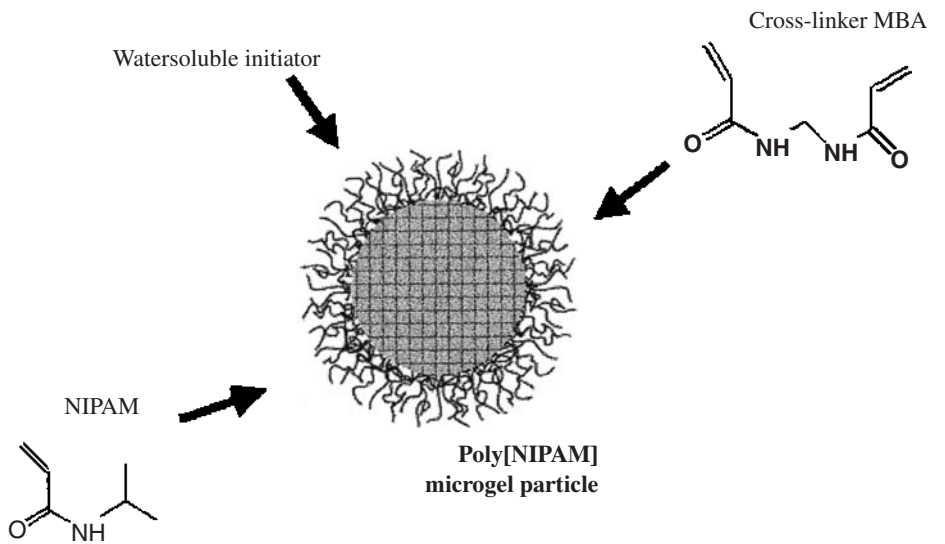

FIG. 3 Illustration of necessary reactants to obtain thermally sensitive poly(NIPAM) microgel particles (NIPAM/MBA/KPS (or any charged initiator). Polymerization temperature > 60°C.

hance the precipitation process of the polymer chains (i.e., oligomers) so as to induce nucleation (particle formation). In fact, the effect of polymerization temperature on both particles and water-soluble formation has been reported and found to be the key parameter that controls the particle yield. It has been observed that below 65°C a high percentage of aggregated polymer particles (more then 40 wt %) and water-soluble polymer were formed [9], whereas above 65°C the colloidal dispersions obtained were found to be colloidally stable with low water-soluble polymer formation. As well known, high temperature leads to increase the decomposition rate of the initiator and consequently the polymerization rate as illustrated in Fig. 4. The increase in temperature has a slight effect on the hydrodynamic particle size by reducing the particle size as expected and reported in Fig. 5. This behavior can be explained as follows: the increase in the polymerization temperature enhances the oligoradical concentration (i.e., the polymerization loci), resulting in a high number of particles with small hydrodynamic size.

2. Effect of Initiator Concentration

As mentioned above, the initiator is needed for two major raisons: (1) to initiate the polymerization reaction and (2) to maintain and ensure the colloidal stability of the particles via electrostatic stabilization. The first elaborated poly(NIPAM) microgel particles have been prepared using the classical KPS [2]. Later, cat-

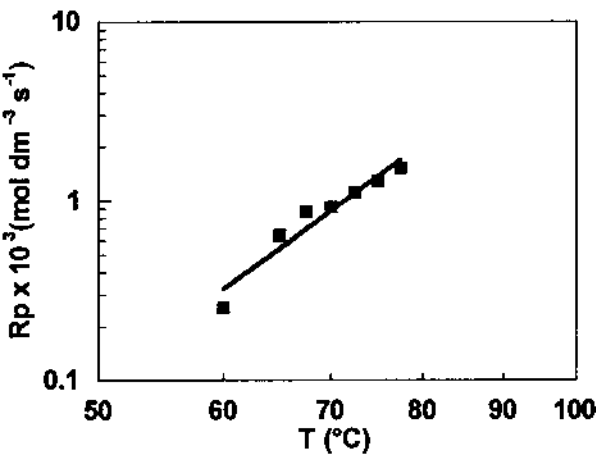

FIG. 4 Polymerization rate vs. polymerization temperature in semilog scale. 48.51 mmoles NIPAM, 0.3 mmol V50 and 3 mmol MBA. The polymerization was carried in 250 mL water.

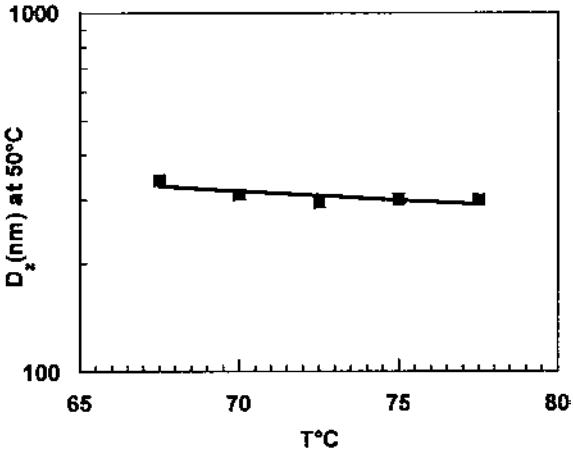

FIG. 5 Effect of polymerization temperature on final hydrodynamic particle size (measured at 50°C) in semilog scale. 48.51 mmol NIPAM, 0.3 mmol V50, 3 mmol MBA. The polymerization was carried in 250 mL water.

ionic poly(NIPAM) particles were prepared by using 2,2′-amidinopropane dihydrochloride (V50) as a cationic initiator [10].

The effect of the initiator concentration on the polymerization rate and particle formation has been studied [9,10]. It was observed that the polymerization rate was increased with an increase in the initiator concentration as illustrated by Fig. 6 in which the NIPAM conversion is plotted as a function of time for two V50 concentrations. The maximal polymerization conversion was reached only after 10 min polymerization time. As expected, the polymerization rate increases as the initiator concentration increases (Fig. 7), revealing the power low between R_p and initiator concentration ($R_p \approx [I]^{0.18}$).

The measured hydrodynamic particle size (at 50°C) of the final particles was found to be slightly affected by the initiator concentration in the investigated range (Fig. 8), whereas the particles size measured at 20°C was dramatically affected by the initiator concentration and increased with increasing initiator concentration. This result was also qualitatively confirmed using transmission electron microscopy (TEM) [9,10].

3. Effect of Cross-linking Agent

The cross-linking agent is needed in the elaboration of thermally sensitive microgel particles. In fact, during synthesis the utilization of a cross-linking agent prevents polymer chain redispersion when the sample is cooled below the LCST

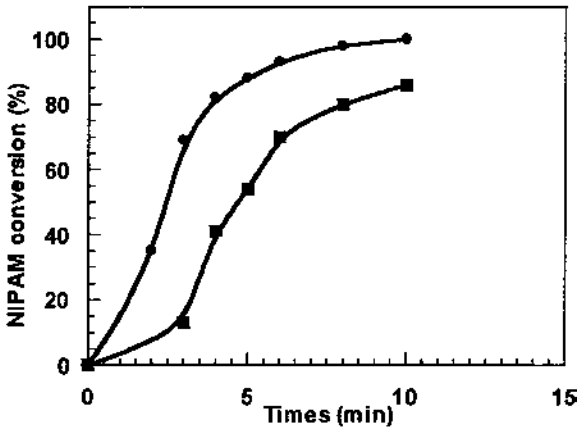

FIG. 6 NIPAM conversion vs. polymerization time for two initiator concentrations. Temperature = 70°C, 48.51 mmol NIPAM and 3 mmol MBA. The polymerizations were performed in 250 mL water. (■) 0.15 mmol and (●) 1.1 mmol

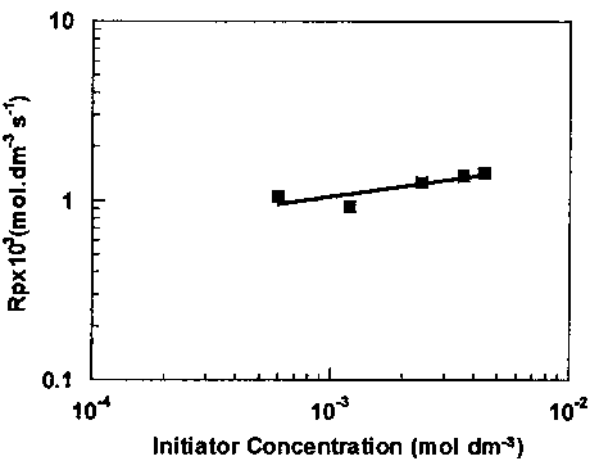

FIG. 7 Dependence of polymerization rate on the initiator concentration in log-log scale. Temperature = 70°C, 48.51 mmol NIPAM and 3 mmol MBA. Total volume = 250 mL ($R_p \approx [I]^{0.18}$).

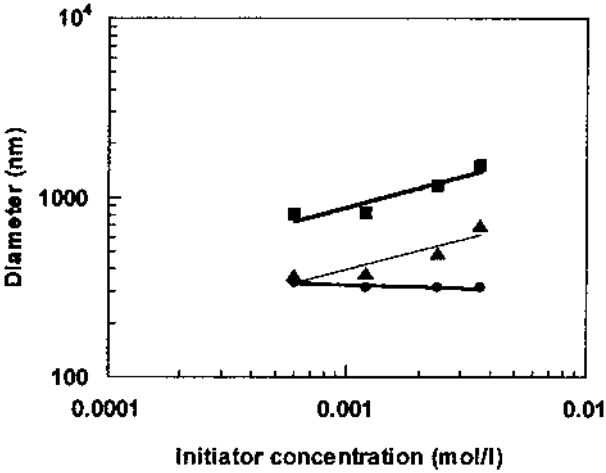

FIG. 8 Log-log plot of hydrodynamic particle diameter vs. initiator concentration used in the polymerization. Temperature = 70°C, 48.51 mmol NIPAM and 3 mmol MBA. Total volume = 250 mL. (■) QELS at 20°C, (●) QELS at 50°C, (▲) TEM.

of the poly(NIPAM) and maintains particle cohesion. In all of the reported studies, MBA was used as the water-soluble cross-linker. The effect of MBA on the poly(NIPAM) microgel latex particle preparation was investigated. The initial rate of the polymerization reaction was found to be constant irrespective of MBA concentration, as reported in Fig. 9. The observed behavior may be attributed to the high reactivity of MBA and to the low concentration used compared to the principal monomer (NIPAM).

The hydrodynamic diameters (at 20°C) of the final particles were comparable, whereas the swelling ability decreased when the amount of MBA in the initial polymerization recipe increased. The cross-linking agent concentration was found to drastically affect the water-soluble polymer formation. In fact, the amount of water-soluble polymer decreased with an increase in the cross-linking agent concentration. This behavior can be attributed to the high MBA polymerization rate compared to the NIPAM. Consequently, MBA is rapidly consumed during the nucleation period and the first step of the growing process. The residual NIPAM leads to water-soluble polymer formation as reported in Fig. 10 in which the amount of water-soluble polymer is reported as a function of MBA concentration.

4. Effect of Ionic Strength

The salt concentration of the polymerization medium is a very important parameter to control during the polymerization. In fact, ionic strength dramatically

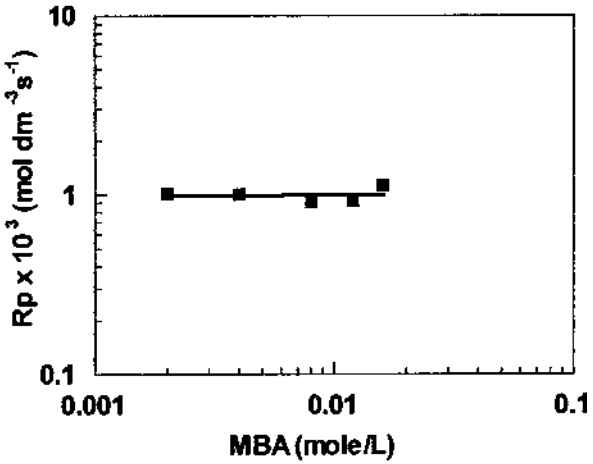

FIG. 9 Polymerization rate vs. MBA concentration in log-log scale. Temperature = 70°C, 48.51 mmol NIPAM, 0.3 mmol V50, and 250 mL water.

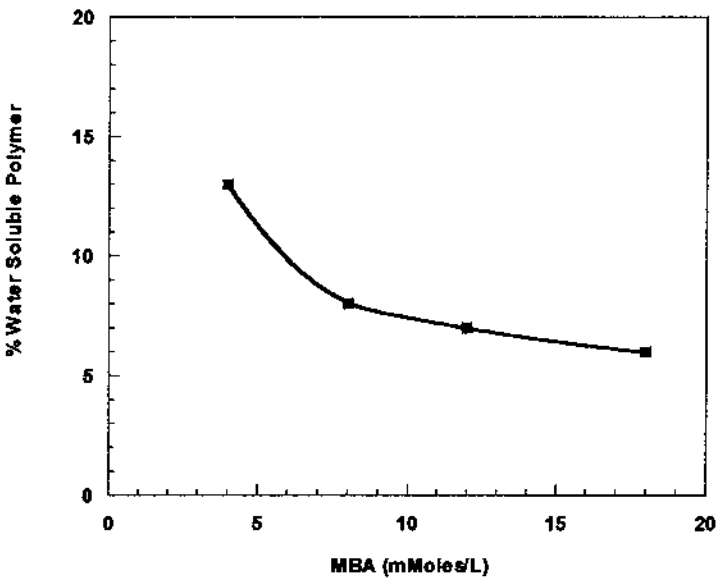

FIG. 10 Effect of MBA on water-soluble polymer formation. Temperature = 70°C, 48.51 mmol NIPAM, 0.3 mmol V50, and 250 mL water.

affects the colloidal stability of the particles as is well known via the DLVO theory [11,12]. Indeed, the increase of ionic strength reduces the repulsive electrostatic stabilization of colloidal dispersion, which induces the aggregation phenomenon. Based on DLVO theory, the effect of salinity on the emulsion polymerization has been investigated. The obtained results can be summarized as follows: the increase in the ionic strength of the polymerization medium affects the colloidal stability of primary particles, which induces aggregation of the small particles leading to the large particle size. If the ionic strength is too high, the colloidal stability of the final particles generally ensured by repulsive electrostatic stabilization, can be totally reduced leading to the final aggregated particles and polydispersed latex. On the whole, similar observations were evidenced in the investigated precipitation polymerization using monovalent salt (NaCl). In addition, the salinity also affects the solubility of oligomers and water-soluble polymer, and consequently the final particle size.

5. Effect of Surfactant Concentration

As for emulsion polymerization, the effect of the classical surfactant sodium dodecyl sulfate (SDS) on such precipitation has been investigated as reported by Wu et al. [4]. The principal result obtained was that the higher the concentration of SDS, the smaller the final particles. This phenomenon is observed as long as the concentration of SDS is lower than the critical micelle concentration (CMC) [3]. In fact, SDS dramatically affects the LCST of poly(NIPAM) chains and, consequently, the nucleation period and particle number formation.

6. Effect of Comonomer Nature and Concentration

The purpose of introducing a comonomer is to modify the final properties of a poly(NIPAM) particles. The comonomer acts on polymerization kinetics, water-soluble polymer formation, colloidal stability, and composition of the final particles. Several monomers have been polymerized in the presence of NIPAM: acrylamide was the first comonomer used in order to increase the volume phase transition of the poly(NIPAM) microgel particles as reported by Pelton et al. [2]. In this case, the volume phase transition temperature was dramatically shifted.

Styrene monomer was copolymerized with NIPAM and the particles obtained exhibit core-shell structure with polystyrene core and poly(NIPAM) shell [13, 14]. Such a system has been studied in terms of polymerization mechanism, individual conversion, and shell composition.

The copolymerization of charged comonomer was found to affect drastically the polymerization process and the properties of the final particles as recently reported by Duracher et al. [15] who investigated the polymerization of *N*-isopropylmethacrylamide (NIPMAM), *N*-(vinylbenzylimino)diacetic acid (IDA), MBA, and KPS.

Additional systematic studies have been performed using various kinds of functional monomers such as itaconic acid [7], 2-aminoethyl methacrylate hy-

drochloride (AEMH) [10], vinylbenzylisothiouronium chloride (VBIC) [16], and acrylonitrile [17].

III. FUNCTIONALIZED POLY(NIPAM) MICROGEL LATEX PARTICLES

The utilization of functional monomer in the copolymerization with NIPAM has three objectives: (1) to increase the surface charge density of the colloidal particles so as to improve colloidal stability; (2) to introduce charged compounds on the particles surface to confer new properties to the colloidal dispersion; and (3) to achieve functionalization by introducing reactive groups (aldehyde, carboxylic, amine, thiol, etc.) on the surface of the particles. The last point is of interest in the biomedical field in which the colloids are used as support of biomolecules.

Anyway, the major objective in poly(NIPAM) particle functionalization is to create new polymer supports for biomolecules' immobilization principally via covalent coupling chemistry or via specific fixation processes. Whatever the immobilization approach, the two entities (particle and biomolecule) must have reactive groups capable of reacting together and forming a covalent link either directly or after having undergone prior activation.

The functionalization of poly(NIPAM) by introduction of a functional comonomer has been well described for linear polymers [18–23]. In these cases, syntheses have been performed via the conventional radical copolymerization. Concerning NIPAM-based particles, only a few examples have been reported in the literature as first reported by Kitano et al. [24] by the achievement of poly(NIPAM-*g*-allylamine) particles and then by Kondo et al. [13,14] by reporting core-shell particles bearing poly(NIPAM-*co*-methacrylic acid) or poly(NIPAM-glycidyl acrylate) in the shell. The object of the next part is to present pertinent results related to the preparation of functionalized poly(NIPAM)-based particles.

A. Amino-Containing *N*-Isopropylacrylamide Microgel Particles

The first amino-containing poly(NIPAM) microgel particles have been reported by Meunier et al. [9,10]. In this study, 2-aminoethyl methacrylate hydrochloride (AEMH) was used as a functional monomer. The increase of AEMH concentration in the NIPAM/MBA/V50 system reduces the final hydrodynamic particle size, as reported in Fig. 11. As for emulsion polymerization, the utilization of charged comonomer dramatically affects the particle size, the polymerization rate, and finally the water-soluble polymer formation. The charge density (i.e., amine concentration on the microgel particles) was chemically determined. The transfer effect of such functional "protected" monomer was clearly evidenced by the water-soluble polymer molecular weight analysis.

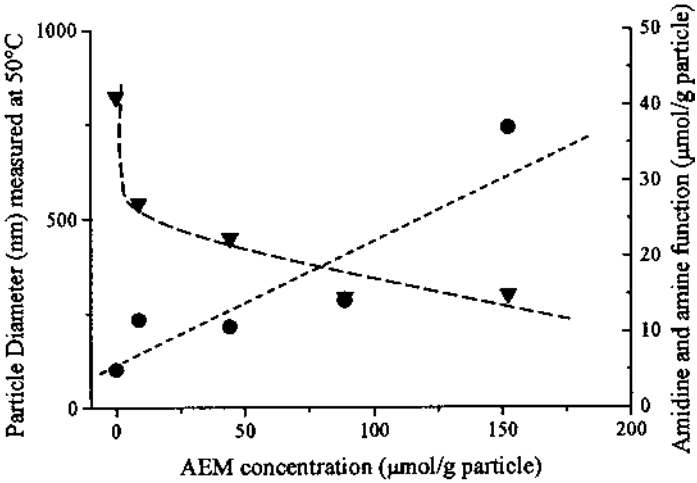

FIG. 11 Hydrodynamic particle diameter at 50°C (▼) and particle charge density (amidine and amine in μmol/g particle) (●) as a function of AEMH in the polymerization (μmol/g particle at 100% conversion). Polymerizations were realized with 48.51 mmol NIPAM, 0.3 mmol V50, 3 mmol MBA, 0–0.73 mmol AEM, and 250 mL water. The polymerization temperature was about 70°C.

B. Thiol-Containing *N*-Isopropylacrylamide Microgel Particles

The preparation of poly(NIPAM) microgel particles bearing thiol reactive groups has been investigated using vinylbenzylisothiouronium chloride (VBIC) as a functional comonomer. Such a charged and water-soluble comonomer has an important role in the polymerization process of *N*-isopropylacrylamide. Indeed, for high VBIC monomer concentrations, the particle yield was dramatically decreased (Fig. 12). This behavior can be attributed to the high water solubility of the cationic monomer, which causes an increase in the precursor concentration and higher water-soluble polymer (Fig. 13). The molecular weight (M_w) of the formed water-soluble oligomers and polymers was dramatically reduced when the amount of VBIC was increased. However, the behavior of charged comonomer can increase the stability of the primary particles, thus inducing small-particle formation (Fig. 14). The thiol density in and on the particles was found to be low and nil in same cases. The behavior observed has been attributed to the transfer character of such monomer as schematically illustrated in Fig. 15 [16].

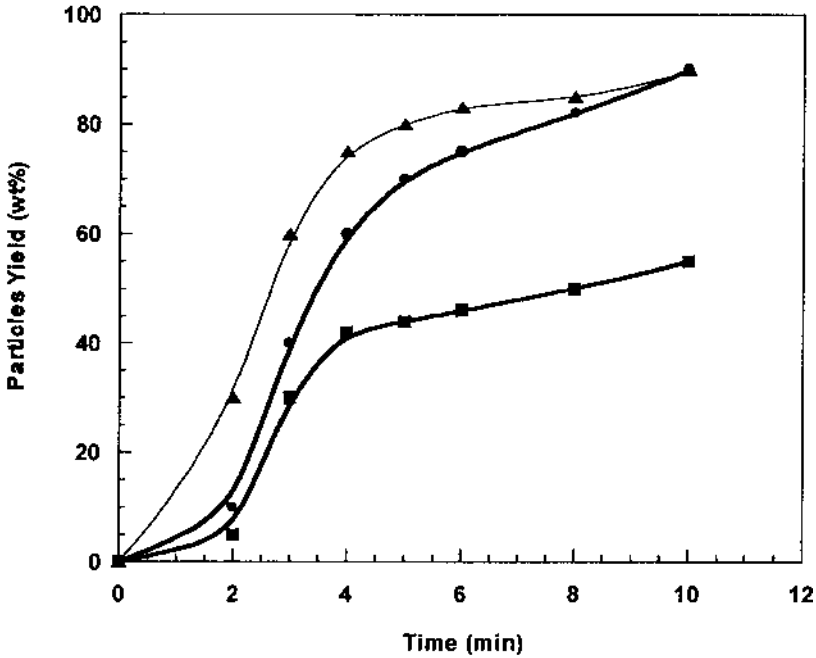

FIG. 12 Particles yield vs. polymerization time for three VBIC concentrations; (▲) 0, (●) 0.096, and (■) 0.48 mmol/L; 48.51 mmol NIPAM, 0.3 mmol V50, 3 mmol MBA, and 250 mL water. The polymerization temperature was fixed at 70°C and total volume = 250 mL.

C. Cyano-Containing *N*-Isopropylacrylamide Microgel Particles

The functionalization of *N*-isopropylacrylamide based microgel particles using noncharged comonomer has been recently reported by Zhou et al. [17]. In his study, acrylonitrile (AN) was chosen in order to prepare particles bearing cyano groups. The polymerization was performed via batch and shot-grow process using NIPAM/MBA/KPS. The amount of incorporated functional monomer can be adjusted. It appeared that the amount of cyano group was higher in shot-grown functionalized latexes than those obtained by batch polymerization. Moreover, the particle morphology of functionalized particles was quite uneven compared to that of pure poly(NIPAM) latexes. The observed behavior was probably due to the formation of small polyacrylonitrile-rich nodules onto the seed particles.

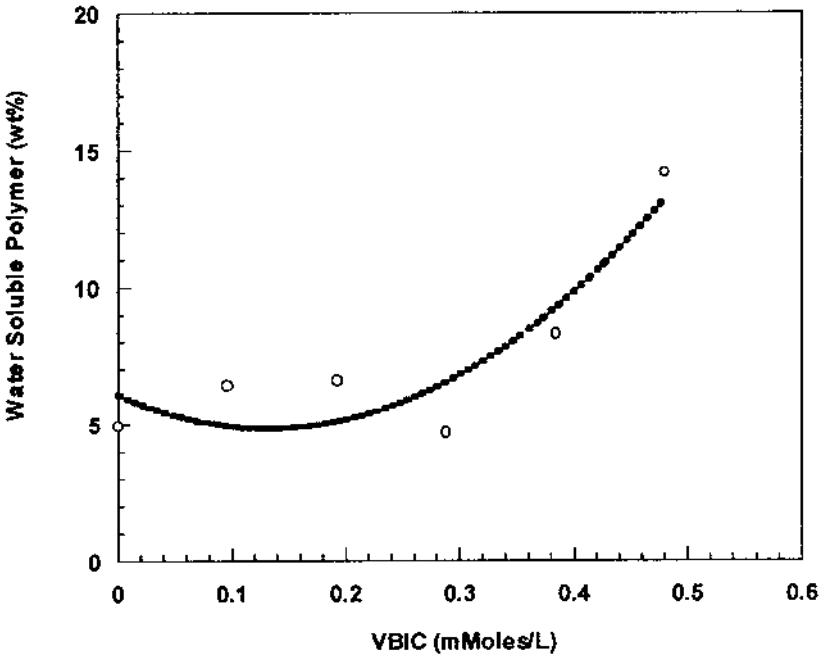

FIG. 13 Water-soluble polymer formation as a function of VBIC monomer concentration. 48.51 mmol NIPAM, 0.3 mmol V50, 3 mmol MBA, and 250 mL water. The polymerization temperature was fixed at 70°C.

IV. POLYMERIZATION REACTION MECHANISM

The preparation methods can be classified into four types: suspension polymerization [25,26], dispersion polymerization [27,28], precipitation polymerization [27,29], and emulsion polymerization [30]. These polymerizations can be distinguished by the solubility, the reactivity of the initial reactants, and the specific properties of the final products. Concerning the precipitation process, polymerization mechanism of *N*-alkylacrylamide derivatives, water soluble cross-linkers, and water-soluble initiator systems, only a few works have been dedicated to the question by discussing the effect of cross-linker agent [4]. From the investigated systematic studies, a more detailed mechanism has been suggested as reported by Meunier et al. [9].

A. Polymerization in Water Phase

Initially, all the reagents are water soluble leading to homogeneous solution. The initiator was first thermally decomposed, which induces oligomer forma-

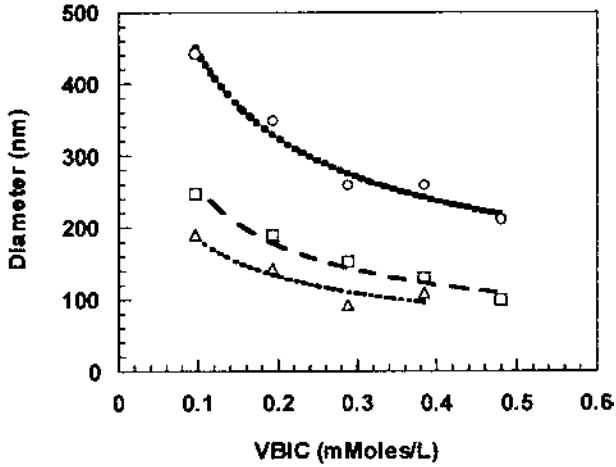

FIG. 14 Particle size vs. VBIC concentration; (●) QELS at 20°C, (□) QELS at 50°C, and (△) TEM; 48.51 mmol NIPAM, 0.3 mmol V50, 3 mmol MBA, and 250 mL water. The polymerization temperature was fixed at 70°C.

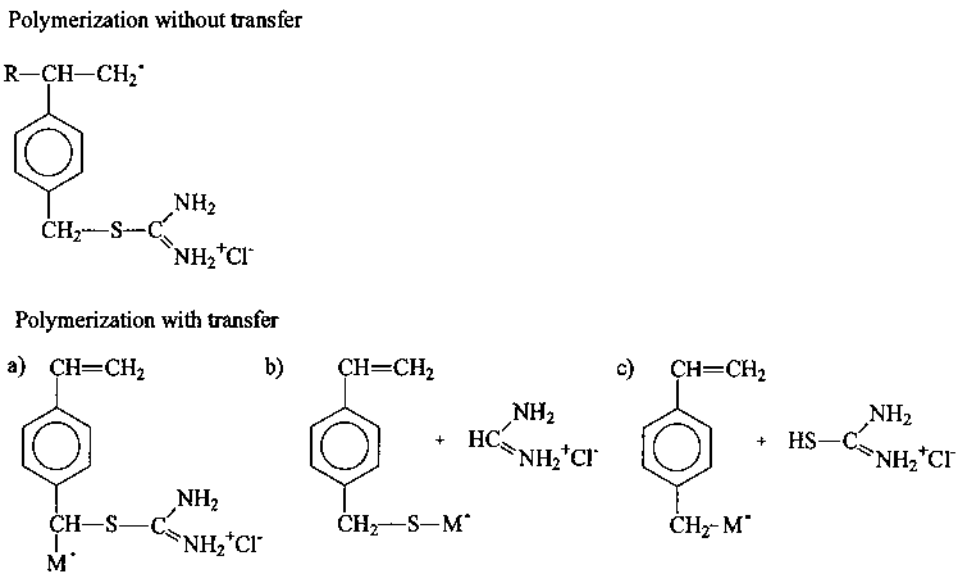

FIG. 15 Transfer reactions induced by vinylbenzylisothiouronium chloride during polymerization ($M^{\bullet}$ radical).

tion. The induction period (1–2 min) generally observed was attributed to the presence of oxygen trace, which has been described as an inhibiting agent. The oligomer concentration increases with increased polymerization temperature or amount of initiator.

B. Nucleation Step

During the polymerization, the NIPAM chains reach a critical length above which such oligomers are water insoluble at the polymerization temperature. The precipitation of oligomers leads to formation of unstable primary particles (precursors). Consequently, colloidally stable particles are formed by coagulation process of the precursors leading to more stable particles. This transition from precursors to stable particles is questionable. In fact, the nucleation period of such a system is too short to confirm the coagulation process. The rapid nucleation step and narrowly size distribution of the formed particles suggest the constancy of the particles number during the polymerization. On the other hand, to elucidate the relationship between the polymerization temperature, the solvent's nature, and the oligomers' critical chain length is of paramount importance. In fact, the LCST of poly(NIPAM) is related to various parameters, such as ionic strength and solvent nature. In addition, since MBA is assumed to be more reactive than NIPAM monomer [4], the oligomer composition during the nucleation step should be considered. Thus, it is realistic to assume that the first oligomers have an important percentage of MBA and the oligomers formed later have a lower ratio of the cross-linker agent. It's interesting to note that an important concentration of MBA in the polymerization recipe leads to formation of aggregated dispersion during the first minutes of polymerization. This behavior may be attributed to low charge density of precursors leading to instable primary particles. The transition period leading to precursor formation is about 2–3 min. After this period, primary stable particles were formed and the maximal particle was reached. The colloidal stability was ensured by the charges from initiator or functional monomer, and the NIPAM conversion was at less 50%. As a short conclusion of this part, the nucleation is fast, occurring in less than 4 min.

C. Growing Process of the Formed Particles

After 4 min (i.e., nucleation period), the polymerization takes place both in aqueous phase and in (or at) the particles. In fact, the monomer may have a partition coefficient between the two possible phases: continuous aqueous phase and poly(NIPAM) particles. Thus, the growing state of the formed particles results from three actions: (1) monomer diffusion from the medium to the particle which constitutes new polymerization site; (2) capture of formed oligomers via adsorption or cross-linking processes; (3) aggregation of primary particles or adsorption of small primary particles onto lightly mature ones. The residual cross-linker agent is of paramount importance at this stage. In fact, it contributes

to enhancing the physical growing of the particles by physical entanglement and cross-linking of poly(NIPAM) chains. This growing period reaches a plateau (growing limit) less than 10 min, above which the residual MBA amount reaches zero concentration.

D. End of Polymerization

After the total consumption of the cross-linker agent (here MBA), the residual monomer leads principally to water-soluble polymers. The water-soluble polymer would be essentially desorbed from the particles or originated from produced small polymer chains. In fact, after cooling the dispersion, the adsorption of precipitated chains on the particles surface was easily desorbed. The amount of water-soluble polymer and particle yield is thermogravimetrically determined after phase separation via centrifugation process.

The schematic illustration of such polymerization of a water-soluble system (i.e., NIPAM/MBA/charged initiator) is reported in Fig. 16. The suggested mechanism is principally main monomer and water-soluble cross-linker reactivities dependent. In fact, the high reactivity of cross-linker compared to the principal monomer also leads to water soluble formation, whereas low reactivity of cross-linker increases the nucleation period and consequently leads to low particle yield. On the other hand, the comparable reactivities may lead to homogeneous distribution of cross-linker in the particles and low water soluble formation.

V. PROPERTIES OF POLY(NIPAM) MICROGEL LATEX PARTICLES

Smart or intelligent polymers are defined as material sensitive to one or various physicochemical parameters (stimuli) such as ionic strength, pH, solvent nature, temperature, UV light, electrical field, magnetic field, mechanical stress, and so on. In the biomedical field, the understanding and control of the colloidal properties of such stimulus-responsive particles is of paramount importance. In fact, the control of biomolecules' adsorption and desorption will present an incontestable interest for biological molecule extraction, concentration, and purification as needed in analytical biochemistry and biomedical diagnostics, whereas control of drug release after encapsulation in the microgel particles or immobilization on the particle surface has been targeted whatever the biodegradability of the materials.

A. Volume Phase Transition Temperature of Poly(NIPAM) Microgel Particles

The LCST of linear poly(NIPAM) homopolymer has been largely investigated as a function of various parameters such as salt concentration, solvent composition, and surfactant nature. The effect of temperature is related to transition

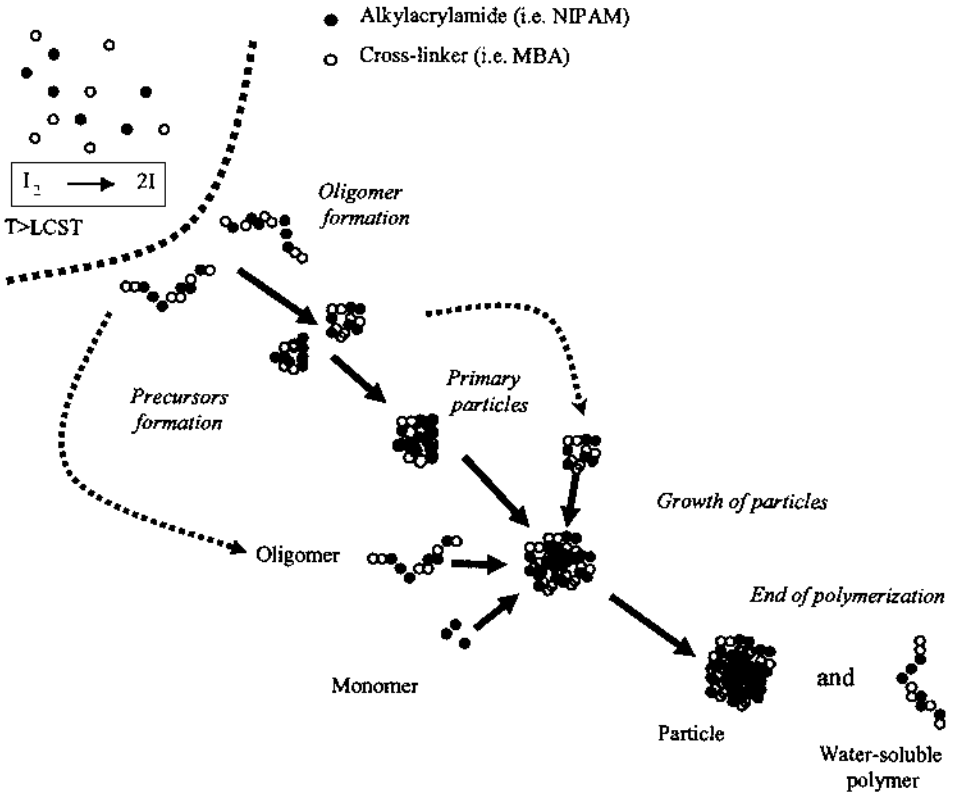

FIG. 16 Schematic illustration of precipitation polymerization mechanism of water-soluble *N*-alkyacrylamide and *N*-alkymethacrylamide monomer derivatives.

which occurs by breaking of hydrogen bonds between water molecules and acrylamide groups [31]. This phenomenon can be reversed [32] and controlled, which is most interesting for applications where the swelling rate requires adjustment. It depends neither on the polymer's molecular weight nor its concentration [33,34]. The reversibility of the effect of temperature has been also discussed in various papers. Concerning poly(NIPAM) derivatives, the hydration–dehydration process of the polymer chains can vary as a function of different factors such as chemical composition and microstructure (i.e., ionic or hydrophobic comonomer) of the chains in addition to the salt concentration [35], solvent composition (i.e., water–methanol mixture) [36,37], and pH. Before dealing with volume phase transition temperature of microgel particles, a short

discussion on parameters affecting the LCST of *N*-alkylacrylamide-based polymers is first presented.

The first study on the effect of surfactant on the thermal properties of poly (NIPAM)-based materials was performed by Eliassaf et al. [38]. They showed that with 1 wt % of SDS the viscosity of poly(NIPAM) polymer solution increased as a function of temperature without any polymer precipitation; thus, LCST is no longer observable. This effect was confirmed by various authors [39–41] who observed a dependency of LCST on the SDS concentration. These observations are specific to SDS, which induces chain expansion by enhancing the solubility of isopropyl domains. In this direction, Cho et al. [42] pointed out the relationship between the poly(NIPAM) transition (LCST) and the hydrophobic character of the considered surfactant.

LCST of thermally sensitive linear polymers can be controlled by incorporating hydrophobic or hydrophilic comonomers [43–46]. In fact, the introduction of hydrophobic compounds leads to lower the transition temperature by reducing the polymer solvency in the considered aqueous phase [47], whereas the incorporation of charged or noncharged hydrophilic compounds (such as acrylamide or acrylic acid) increases the LCST of the corresponding copolymers by enhancement of the polymer's solubility in water. In the case of polyelectrolyte thermally sensitive like copolymers, the pH and the salinity should also be considered. The LCST can also be controlled by adapting suitable *N*-alkylacrylamide derivatives as reported in Table 1.

TABLE 1 Chart of chemical structure-transition temperature (cloud point of 1% aqueous solution)

Polymer	Transition temperature/°C
Poly(N-ethylacrylamide)	72
Poly(N-cyclopropymethacrylamide)	59
Poly(N-methyl-N-ethylacrylamide)	56
Poly(N-acryloylpyrrolidine)	56
Poly(N-ethylmethacrylamide)	50
Poly(N-cyclopropylacrylamide)	45.5
Poly(N-isopropylmethacrylamide)	44
Poly(N,N-diethylacrylamide)	32
Poly(N-isopropylacrylamide)	30.9
Poly(N-n-propylmethacrylamide)	28
Poly(N-methyl-N-isopropylacrylamide)	22.3
Poly(N-n-propylacrylamide)	21.5
Poly(N-methyl-N-n-propylacrylamide)	19.8
Poly(N-acryloylpiperidine)	5.5
Poly(acrylic acid)	50

All parameters affecting the LCST of thermally sensitive *N*-alkylacrylamide polymers are to be considered in the case of gels, microgel particles, and core-shell microspheres. In fact, all results reported in the literature for both linear polymers and colloidal particles reflect such general behavior. The T_{VPT} of microgel particles are easily determined using turbidity measurement as a function of temperature of highly diluted dispersion. The transition temperature is generally reported to be in a broad temperature domain compared to the corresponding linear polymer as shown in Fig. 17 comparing turbidity with temperature for poly(NIPAM)-based polymer and colloidal particles. The volume phase transition temperature domain can also be investigated using various techniques such as hydrodynamic particle size [9], fluorescence analysis [48], electrokinetic study [49], and viscosity [50] measurements.

1. Effect of Temperature on Hydrodynamic Particle Size

The influence of temperature on hydrodynamic particle size has been found to be one of the methods for investigating the volume phase transition and the swelling ability of the microgel dispersions. According to the temperature sensitivity of poly(NIPAM) chains, the temperature was found to dramatically affect the hydrodynamic particles size. In fact, the particle size decreases with increasing the incubation temperature, which induces the shrinkage of the poly(NIPAM) chains and domains. The effect of temperature was generally more marked for slightly cross-linked microgel particles than for core-shell systems such as polystyrene-core/poly(NIPAM)-shell. In any case, the hydrodynamic

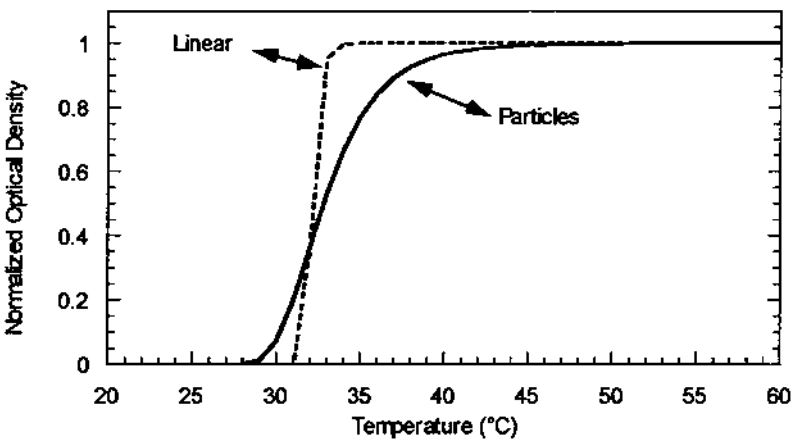

FIG. 17 Normalized turbidity vs. temperature for poly(NIPAM)-based polymer and colloidal particles.

particle size above the volume phase transition is larger than the particle measured by TEM. This observed behavior is attributed to the residual water amount in the particles. In fact, more than 20% (water/polymer) amount was retained in the particles [3]. In any case, the amount of water in the particles or poly(NIPAM) gel is gravimetrically analyzed [3,51]. The results revealed that the water percent in the polymer matrix was above 80% (wt/wt) at 20°C and less than 25% below the volume phase transition. The volume phase transition temperature can't be exactly determined from TEM but the transition range can be defined irrespective of temperature-sensitive particles morphology (microgel, core-shell, hairy-like particles).

2. Effect of Temperature on Electrokinetic Properties

The electrophoretic mobility of the NIPAM-based particles has been investigated as a function of three major parameters (pH, ionic strength, and temperature). The effect of pH at a constant salinity and temperature reveals principally the surface charge from positive to negative charge density, or vise versa, as well as the isoelectric point.

Concerning the effect of temperature, the general result exhibits low electrophoretic mobility values at 20°C (i.e., below the T_{VPT}) than at 40°C (i.e., above the T_{VPT}). This difference is mainly attributed to the reduction of particles leading to an increase in surface charge density [52] (Fig. 18). Various studies have been dedicated to advancing the understanding of such phenomena by development of new theories [53] or new models related to charge distribution [49]. According to the particle structure complexity, various parameters should be considered before any hazardous interpretation (e.g., charge distribution in the particles, cross-linking density, residual water-soluble polymer when crude samples are used, presence of surfactant traces) is presented. For the reader, a very interesting review was recently reported by Saunders [54].

B. Colloidal Stability

According to the effect of temperature and ionic strength on the LCST of thermally sensitive *N*-alkylacrylamide-based polymer, the colloidal stability of the corresponding particles is also affected by the behavior parameters for instance. The increase in salt concentration induces a dramatic decrease in the LCST. Consequently, the colloidal stability should be discussed on the basis of the following considerations: (1) below the T_{VPT}, the particles are extended and highly hydrated ensuring good colloidal stability via hydration forces and electrosteric stabilization, and (2) above the T_{VPT}, the particles are under shrunken state (suppression of steric stabilization) leading to low colloidal stabilization via electrostatic process. Thus, the colloidal stability of such system can be schematically presented as a function of temperature as reported in Fig. 19. The presented

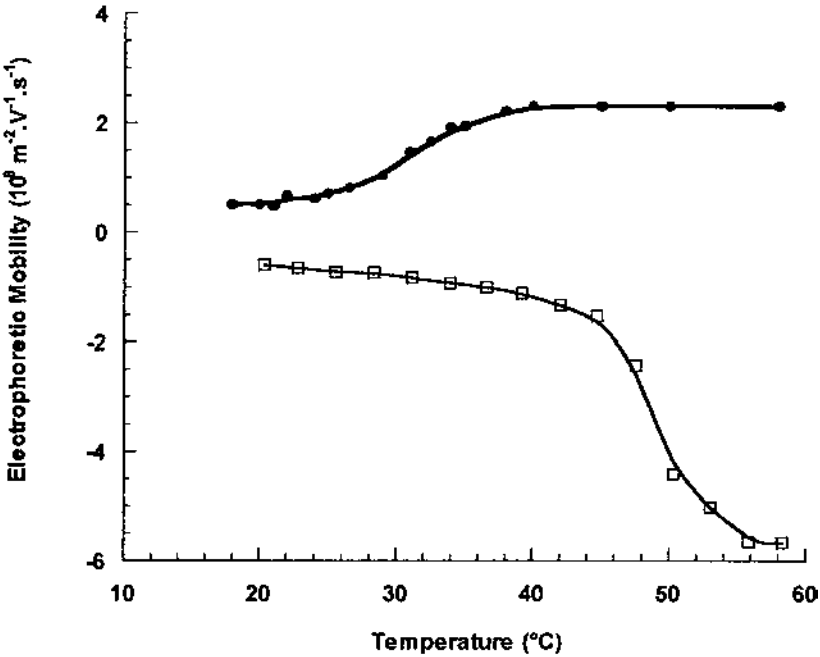

FIG. 18 Electrophoretic mobility of thermally sensitive particles as a function of temperature. (●) cationic poly(NIPAM) particles and (□) anionic poly(NIPAM) particles.

domains are totally reversible by reducing the incubation temperature or by diluting the salinity of the medium. The behavior observed is directly related to hydration property and swelling ability of such smart colloidal particles.

VI. SOME FINE APPLICATIONS OF POLY(NIPAM)-BASED PARTICLES IN BIOMEDICAL DIAGNOSTIC

Applications of colloidal particles in the biomedical field have been widely reported in the literature [55,56]. The main objective of the results reported has been focused on the thermal dependence properties of such stimuli-responsive particles. The firsts reported works have focused on the relation between proteins adsorption onto poly(NIPAM) particles and the incubation temperature. For more information, the reader can consult Kwaguchi et al. chapter in this book. Concerning the real applications of thermally sensitive submicrometer particles in biomedical field, the first work has been reported by Rodrigue et al.

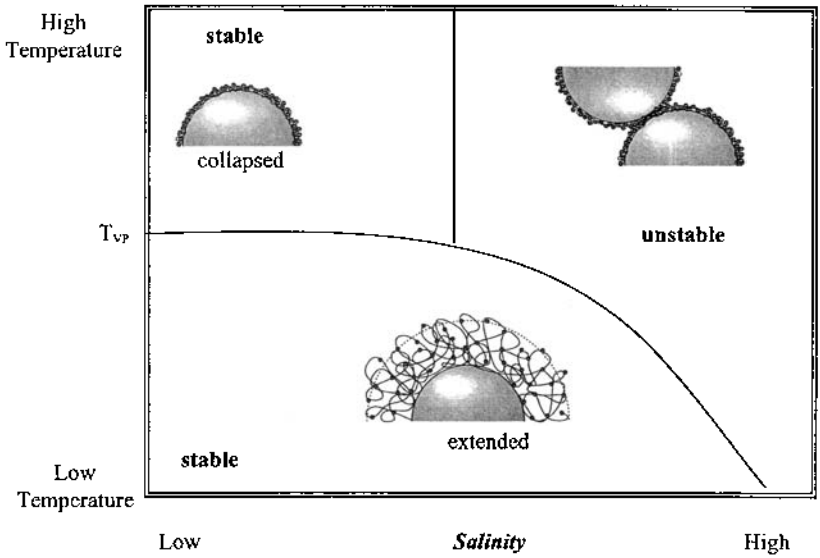

FIG. 19 Illustration of the colloidal stability of temperature-sensitive colloidal particles as a function of salt concentration and temperature.

in this book by investigating DNA and RNA extraction and concentration using thermally sensitive magnetic latexes.

VII. CONCLUSION

Sixteen years had passed since the first synthesis of particles composed with *N*-isopropylacrylamide. Numerous publications and reviews have been published concerning their synthesis, their properties, and their applications in various domains. Few works were dedicated to the kinetics of such precipitation polymerization. The systematic variation of each reactant reveals the important role of the initiator, cross-linker, polymerization temperature, and the chemical nature and concentration of the comonomer. Thus, careful control of the polymerization recipe and conditions lead to desired colloidal particles bearing expected properties. It is interesting to note that water-soluble polymer formation during the particles elaboration was totally marginalized in the literature. The presence of water-soluble polymer in the latex particles dramatically affects the colloidal property of colloidal dispersion. The colloidal properties of NIPAM-based colloidal particles have been studied as evidenced by the exhaustive reported publication. The first papers have been principally dedicated to the effect of solvent

nature on the LCST of poly(NIPAM)-based materials. Two points are fascinating the researchers: (1) the geological property of thermally sensitive colloidal dispersion as a function of external stimulus and (2) the electrokinetic properties of such dispersion as a function of ionic strength and temperature.

NIPAM-based particles were found to be of good interest in biomedical field. In fact, the hydrophilic character of such thermally sensitive colloids was found to be well adapted in nucleic acids amplification and proteins immobilization. Such colloidal particles have been used for proteins and nucleic acids concentration by monitoring the pH, the salinity of the medium, and the incubation temperature.

REFERENCES

1. Heskins, M.; Guillet, J.E. Solution properties of poly(N-isopropylacrylamide). J. Macromol. Sci. **1968**, *2* (8):1441–1455.
2. Pelton, R.H.; Chibante, P. Preparation of aqueous latices with N-isopropylacrylamide. Colloids Surf. **1986**, *20*, 247–256.
3. McPhee, W.; Tam, K.C.; Pelton, R. Poly(N-isopropylacrylamide) latexes prepared with sodium dodecyl sulfate. J. Colloid Interface Sci. **1993**, *156* (1), 24–30.
4. Wu, Y.; Pelton, R.H.; Hamielec, A.E.; Woods, D.R.; McPhee, W. The kinetics of poly(N-isopropylacrylamide) microgel latex formation. Colloid and Polym. Sci. **1994**, *272*, 467–477.
5. Pelton, R.H. Polystyrene and polystyrene-butadiene latexes stabilized by poly (N-isopropylacrylamide). J. Polym. Sci. A Polym. Chem. **1988**, *26* (1). 9–18.
6. Ding, X.B.; Sun, Z.H.; Wan, G.X.; Jiang, Y.Y. Preparation of thermosensitive magnetic particles by dispersion polymerization. React. Funct. Polym. **1998**, *38* (1), 11–15.
7. Sauzedde, F.; Elaissari, A.; Pichot, C. Thermosensitive magnetic particles as solid phase support in an immunoassay. Macromol. Symp. 151 (Polymers in Dispersed Media) **2000**, 617–623.
8. Elaissari, A.; Bourrel, V. Thermosensitive magnetic latex particles for controlling protein adsorption and desorption. J. Magnet. Magnet. Mater. **2001**, *225* (1–2), 151–155.
9. Meunier, F. Poly(N-isopropylacrylamide) hydrogel particles preparation. PhD dissertation, Lyon University, 1996.
10. Meunier, F.; Elaissari, A.; Pichot, C. Preparation and characterization of cationic poly(N-isopropylacrylamide) copolymer latexes. Polym. Adv. Technol. **1995**, *6* (7), 489–496.
11. Deryagin, B.; Landau, L. Theory of the stability of strongly charged lyophobic sols and of the adhesion of strongly charged particles in solutions of electrolytes. Acta Physicochim. USSR **1941**, *14*, 633–662.
12. Verwey, E.J.W.; Overbeek, J.T.G. Theory of the stability of lyophobic colloids. J. Colloid Sci. **1955**, *10*, 224–225.
13. Kondo, A.; Kamura, H.; Higashitani, K. Development and application of thermo-

sensitive magnetic immunomicrospheres for antibody purification. Appl. Microbiol. Biotechnol. **1994**, *41* (1):99–105.
14. Kondo, A.; Kaneko, T.; Higashitani, K. Development and application of thermosensitive immunomicrospheres for antibody purification. Biotechnol. Bioeng. **1994**, *44* (1), 1–6.
15. Duracher, D.; Elaissari, A.; Mallet, F.; Pichot, C. Preparation of thermosensitive latexes by copolymerization of N-isopropylmethacrylamide with a chelating monomer. Macromol. Symp. 150 (Polymers in Dispersed Media) **2000**, 297–303.
16. Meunier, F.; Elaissari, A.; Pichot, C. Synthesis of cationic poly[N-isopropylacrylamide] microgel latexes using a thiol-containing monomer, vinylbenzylisothiouronium chloride. Macromol. Symp. 150 (Polymers in Dispersed Media) **2000**, 283–290.
17. Zhou, G.; Elaissari, A.; Delair, T.; Pichot, C. Synthesis and characterization of surface-cyano-functionalized poly(N-isopropylacrylamide) latexes. Colloid Polym. Sci. **1998**, *276* (12), 1131–1139.
18. Luong, J.H.; Nguyen, A.L. Affinity partitioning of bioproducts. Biotechnology **1990**, *8* (4), 306–307.
19. Chen, J.P.; Hoffman, A.S. Polymer–protein conjugates. II. Affinity precipitation separation of human immunogammaglobulin by a poly(N-isopropylacrylamide)–protein A conjugate. Biomaterials **1990**, *11* (9), 631–634.
20. Yang, H.J.; Cole, C.A.; Monji, N.; Hoffman, A.S. Preparation of a thermally phase-separating copolymer, poly(N-isopropylacrylamide-co-N-acryloxysuccinimide), with a controlled number of active esters per polymer chain. J. Polym. Sci. A Polym. Chem. **1990**, *28* (1), 219–226.
21. Nguyen, A.L.; Luong, J.H.T. The development and application of a new affinity partitioning system for enzyme isolation and purification. Enzyme Microb. Technol. **1990**, *12* (9):663–668.
22. Yoshida, R.; Sakai, K.; Okano, T.; Sakurai, Y. Drug release profiles in the shrinking process of thermoresponsive poly(N-isopropylacrylamide-co-alkyl methacrylate) gels. Ind. Eng. Chem. Res. **1992**, *31* (10), 2339–2345.
23. Chen, G.; Hoffman, A.S. Preparation and properties of thermoreversible, phase-separating enzyme-oligo(N-isopropylacrylamide) conjugates. Bioconj. Chem. **1993**, *4* (6), 509–514.
24. Kitano, H.; Yan, C.; Nakamura, K. Microspheres prepared from temperature-sensitive graft polymers. Makromol. Chem. **1991**, *192* (12), 2915–2923.
25. Guyot, A. Synthesis of spherical polymer particles with controlled size. J. Chim. Phys. Phys.-Chim. Biol. **1987**, *84* (9), 1085–1093.
26. Hunkeler, D.; Candau, F.; Pichot, C.; Hemielec, A.E.; Xie, T.Y.; Barton, J.; Vaskova, V.; Guillot, J.; Dimonie, M.V.; Reichert, K.H. Heterophase polymerizations: a physical and kinetic comparison and categorization. Adv. Polym. Sci. 112 (Theories and Mechanism of Phase Transitions, Heterophase Polymerizations, Homopolymerization, Addition Polymerization) **1994**, 115–133.
27. Barrett, K.E.J.; Thomas, H.R. Kinetics and mechanism of dispersion polymerization. Dispers. Polym. Org. Media **1975**, 115–200.
28. Tseng, C.M.; Lu, Y.Y.; El-Aasser, M.S.; Vanderhoff, J.W. Uniform polymer parti-

cles by dispersion polymerization in alcohol. J. Polym. Sci. A Polym. Chem. **1986**, *24* (11), 2995–3007.
29. Arshady, R. Suspension, emulsion, and dispersion polymerization: a methodological survey. Colloid Polym. Sci. **1992**, *270* (8), 717–732.
30. Blackey, D.C. *Emulsion Polymerization*; Applied Science Publishers: Londres, 1975.
31. Fujishige, S. Intrinsic viscosity–molecular weight relationships for poly(N-isopropylacrylamide) solutions. Polym. J. (Tokyo) **1987**, *19* (3), 297–300.
32. Yu, H.; Grainger, D.W. Thermo-sensitive swelling behavior in crosslinked N-isopropylacrylamide networks: cationic, anionic and ampholytic hydrogels. ACS Polym. Prepr. **1993**, *34* (1), 829–830.
33. Kubota, K.; Fujishige, S.; Ando, I. Solution properties of poly(N-isopropylacrylamide) in water. Polym. J. (Tokyo) **1990**, *22* (1), 15–20.
34. Kubota, K.; Fujishige, S.; Ando, I. Single-chain transition of poly(N-isopropylacrylamide) in water. J. Phys. Chem. **1990**, *94* (12), 5154–5158.
35. Snowden, M.J.; Vincent, B. Flocculation of poly(N-isopropylacrylamide) latexes in the presence of nonadsorbing polymer. ACS Symp Series 532 (Colloid-Polymer Interactions) **1993**, 153–160.
36. Winnik, F.M.; Ringsdorf, H.; Venzmer, J. Methanol-water as a co-nonsolvent system for poly(N-isopropylacrylamide). Macromolecules **1990**, *23* (8), 2415–16.
37. Asano, M.; Winnik, F.M.; Yamashita, T.; Horie, K. Fluorescence studies of dansyl-labeled poly(N-isopropylacrylamide) gels and polymers in mixed water/methanol solutions. Macromolecules **1995**, *28* (17), 5861–5866.
38. Eliassaf, J. Aqueous solutions of poly(N-isopropylacrylamide). J. Appl. Polym. Sci. **1978**, *22* (3), 873–874.
39. Inomata, H.; Goto, S.; Saito, S. Effect of sodium dodecyl sulfate on the volume phase transition of N-isopropylacrylamide gel. Langmuir **1992**, *8* (3), 1030–1031.
40. Mumick, P.S.; McCormick, C.L. Water-soluble copolymers. 54. N-Isopropylacrylamide-co-acrylamide copolymers in drag reduction: synthesis, characterization, and dilute solution behavior. Polym. Eng. Sci. **1994**, *34* (18), 1419–1428.
41. Ricka, J.; Meewes, M.; Nuffenegger, R.; Bimkert, T. Intermolecular and intramolecular solubilization: collapse and expansion of a polymer chain in surfactant solutions. Phys. Rev. Lett. **1990**, *65* (5), 657–660.
42. Cho, C.S.; Jung, J.H.; Sung, Y.K.; Lee, M.Y. Effect of polymeric surfactants on the cloud point of poly(N-isopropylacrylamide). Macromol. Rapid Commun. **1994**, *15* (9), 727–732.
43. Hoffman, A.S.; Afrassiabi, A.; Dong, L.C. Thermally reversible hydrogels. II. Delivery and selective removal of substances from aqueous solutions. J. Contr. Rel. **1986**, *4* (3), 213–222.
44. Takezawa, T.; Mori, Y.; Yoshizato, K. Cell culture on a thermo-responsive polymer surface. Biotechnology **1990**, *8* (9), 854–856.
45. Yu, H.; Grainger, D.W. Amphiphilic thermosensitive N-isopropylacrylamide terpolymer hydrogels prepared by micellar polymerization in aqueous media. Macromolecules **1994**, *27* (16), 4554–4560.
46. Deng, Y.; Pelton, R. Synthesis and solution properties of poly(N-isopropylacryl-

amide-co-diallyldimethylammonium chloride). Macromolecules **1995**, *28* (13), 4617–4621.
47. Taylor, L.D.; Cerankowski, L.D. Preparation of films exhibiting a balanced temperature dependence to permeation by aqueous solution. Lower consolute behavior. J. Polym. Sci. Polym. Chem. Ed. **1975**, *13* (11), 2551–2570.
48. Castanheira, E.M.S.; Martinho, J.M.G.; Duracher, D.; Charreyre, M.T.; Elaissari, A.; Pichot, C. Study of cationic N-isopropylacrylamide-styrene copolymer latex particles using fluorescent probes. Langmuir **1999**, *15* (20), 6712–6717.
49. Nabzar, L.; Duracher, D.; Elaissari, A.; Chauveteau, G.; Pichot, C. Electrokinetic properties and colloidal stability of cationic amino-containing N-isopropylacrylamide-styrene copolymer particles bearing different shell structures. Langmuir **1998**, *14* (18), 5062–5069.
50. Tam, K.C.; Wu, X.Y.; Pelton, R.H. Viscometry—a useful tool for studying conformational changes of poly(N-isopropylacrylamide) in solutions. Polymer **1992**, *33* (2), 436–438.
51. Dong, L.C.; Hoffman, A.S. Thermally reversible hydrogels. III. Immobilization of enzymes for feedback reaction control. J. Contr. Rel. **1986**, *4* (3), 223–227.
52. Makino, K.; Yamamoto, S.; Fujimoto, K.; Kawaguchi, H.; Ohshima, H. Surface structure of latex particles covered with temperature-sensitive hydrogel layers. J. Colloid Interface Sci. **1994**, *166* (1), 251–258.
53. Oshima, H. Electrophoretic mobility of soft particles. J. Colloid Interface Sci. **1994**, *163* (2), 474–483.
54. Saunders, B.R.; Vincent, B. Microgel particles as model colloids: theory, properties and applications. Adv. Colloid Interface Sci. **1999**, *80* (1), 1–25.
55. Charles, M.H.; Charreyre, M.T.; Delair, T.; Elaissari, A.; Pichot, C. Oligonucleotide-polymer nanoparticle conjugates: diagnostic applications. STP Pharma Sciences **2001**, *11* (4), 251–263.
56. Arshady, R. Microspheres, Microcapsules and Liposomes. 1. Preparation and Chemical Applications. 11–45, 1999.

7

Microemulsion Polymerization

A Way to Synthesize Well-Defined Highly Functionalized Nanoparticles

CHANTAL LARPENT Université de Versailles Saint-Quentin-en-Yvelines, Versailles, France

I. INTRODUCTION

Latexes, i.e., dispersions of polymer particles in the 0.05- to 1-μm range, commonly prepared via emulsion polymerization, are widely used for a variety of purposes. In industrial products, they find applications in paints, adhesives, coatings, textiles, and flocculants. In fundamental research, latexes are used as models for studying interparticle interactions as well as size calibration standards. In life science [1–10], the immobilization of biologically active molecules like proteins, enzymes, and antibodies [5–8] on latex particles is useful for enabling detection, quantification, or targeted delivery. Most of the latter applications involve polymer particles bearing functional groups that permit the covalent binding of biomolecules. Polymer microparticles have also been widely used as catalyst and reactant supports since they provide high surface area and can be prepared in a variety of sizes and compositions [11,12]. The activity of latex-supported catalyst depends on the accessibility of the active sites and the reaction rates are usually limited by diffusion.

Although much progress has been documented in recent years, the development of new selective materials with improved functionality and reagent accessibility as well as a good colloidal stability and suitable solubility properties is a challenging endeavor. In this context, the technique of polymerization in microemulsion offers new opportunities because it allows one to produce stable suspensions of ultrafine particles in the nanosize range (i.e., with diameter smaller than 30 nm), so-called microlatexes or nanolatexes, which exhibit a very large specific area and high surface functionality. As can be seen in Table 1, very large surfaces of up to 400–500 m^2/g are attainable for nanoparticles in the 10- to 15-nm range. Moreover, owing to the huge surface per volume ratio in

TABLE 1 Specific Area (S), Surface per Volume Ratio (S/V), Maximal Percentage of Functional Moieties at the Surface for Various Particle Sizes Containing 1mmol Functional Residue per g Polymer

Diameter (nm)	15	30	50	100	200	500
$S(m^2/g)$	400	200	120	60	30	12
$S/V(nm^{-1})$	0.4	0.2	0.12	0.06	0.03	0.01
% surface max[a]	100%	66%	40%	20%	10%	4%

[a]Calculated assuming a complete coverage of the particle and a surface of 0.5 nm^2 per functional group and a polymer density of 1.

nanoparticles, surface becomes prominent over volume so that, when functionalized particles are considered, most of the functional residues can be located at the surface, thus ensuring a very high accessibility. The colloidal stability is another outstanding feature of nanolatexes since, under appropriate conditions, microemulsion polymerization leads to very stable and transparent suspensions that show no settling and no change of the particle size over years.

The concept of polymerization in microemulsions appeared in the early 1980s. Since then the field has developed rapidly and the number of related papers is increasing every year. Most of the early work has been reviewed by Candau with an emphasis on inverse systems [13,14]. More recently, three reviews by Capek reported the main mechanistic and kinetic features of radical polymerization of polar acrylic or methacrylic monomers as well as styrene in direct microemulsions [15–17]. Nevertheless, except for a feature article by Antonietti and the related papers of his group [18–22], as well as our own studies [23–28], the synthesis of functionalized nanoparticles via microemulsion polymerization is much less documented.

In this chapter, we report the main results obtained so far in the synthesis of functionalized nanoparticles by using microemulsion polymerization. We will focus on the results obtained in our laboratory on the development of general and versatile methods for producing aqueous suspensions of nanoparticles bearing various functionalities, so-called functionalized nanolatexes, from oil-in-water microemulsions. First, we briefly summarize the most outstanding features of microemulsion polymerization. Then the synthesis of functionalized nanoparticles (1) via copolymerization with functional comonomers, polymerizable cosurfactants, or surfactants and (2) via postfunctionalization will be described. This will be followed by specific examples, such as the development of metal-complexing nanoparticles and the use of nanoparticles as carriers or supports for biomolecules.

II. GENERAL FEATURES OF POLYMERIZATION IN MICROEMULSIONS

A. Structure and Formulation of Microemulsions

Microemulsions are thermodynamically stable, isotropic, and optically transparent dispersions of two immiscible liquids, oil and water, obtained in the presence of a surfactant system consisting either of a single surfactant, a mixture of surfactants, or a mixture of a surfactant and a cosurfactant [29–31]. In the water- or oil-rich regions, globular oil-in-water (o/w) or water-in-oil (w/o) microemulsions consist of small microdroplets ($d < 10$ nm) surrounded by a surfactant monolayer (Fig. 1). The small size of the droplets accounts for the transparency, which is commonly used as a criterion for the preparation of microemulsions. The thermodynamic stability of the microemulsions arises from the very low interfacial tension and the entropic gain resulting from the reduced droplet size. Consequently, the formation of a microemulsion is a spontaneous process that does not need any input of energy in contrast with the formation of classical emulsions. On the other hand, in microemulsions a large amount of surfactant (about 10–15 wt %) is needed for achieving their thermodynamic stability

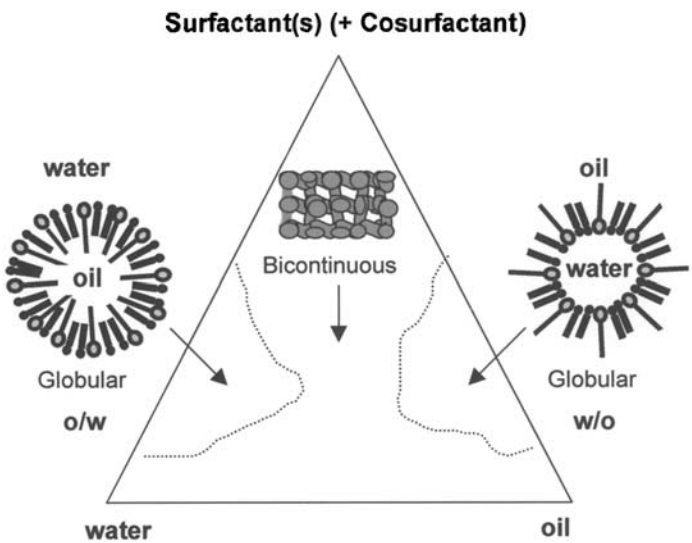

FIG. 1 Isotropic microemulsion domains in the phase diagram of multicompartment systems.

whereas the weight fraction of dispersed liquid does not exceed 10–15% in globular microemulsions.

As a consequence of the very low interfacial tension, which requires a close packing of the surfactant monolayer, there are few examples of microemulsions formed with a single surfactant (so-called three-component or ternary microemulsions): w/o microemulsions from Aerosol OT and o/w microemulsions from dodecyltrimethylammonium bromide (DTAB) are classical examples. In these cases, the average size of the microdroplets depends on the dispersed phase-to-surfactant molar ratio and can be predicted by simple geometrical models [32]. Microemulsions are more commonly prepared by using a mixture of a classical ionic surfactant plus a so-called cosurfactant, a small amphiphilic molecule such as a short-chain alcohol (butanol to hexanol); sodium dodecylsulfate (SDS) plus pentanol and cetyltrimethylammonium bromide (CTAB) plus butanol are classical examples [29–31]. The cosurfactant molecules are located within the interfacial monolayer between the surfactant molecules. Penetration of the alcohol in the surfactant layer increases the flexibility of the interfacial film so that the spontaneous curvature can be modified by changing the cosurfactant/surfactant molar ratio or the oil/water volume ratio. Phase inversion from w/o to o/w globular microemulsion and vice versa occurs upon changing the proportion of components through an isotropic bicontinuous domain containing equivalent amounts of water and oil (Fig. 1).

Microemulsions have been successfully used in a variety of chemical reactions owing to the following qualities: (1) thermodynamic stability, (2) optical transparency, (3) very large interfacial area and very low interfacial tension, (4) solubilization of substrates, and (5) compartmentalization effect and selective orientation [33–35]. A variety of polymeric materials have been obtained by polymerizing either the dispersed phase or the continuous phase of globular and bicontinuous microemulsions [13,14].

B. Polymerization in Microemulsions

1. Polymerization in Globular Oil-in-Water Microemulsions

Numerous studies have been devoted to free-radical polymerizations in globular o/w or w/o microemulsions: lipophilic monomers like styrene, methyl methacrylate, or other (meth)acrylic derivatives have been polymerized within the oil core of o/w microemulsions [13–28,36–50], and water-soluble monomers like acrylamide have been polymerized within the core of aqueous microdroplets of w/o microemulsions [13,14]. Polymerizations have been performed under various experimental conditions using oil-soluble or water-soluble free-radical initiators or under γ radiolysis. Thermally or photochemically initiated poly-

merizations with AIBN (Azobisisobutyronitrile) and thermally initiated polymerizations with persulfate have been mainly used. The polymerizations are very rapid and are usually achieved within 15 min to a few hours.

Under appropriate conditions, the polymerization of o/w microemulsions gives stable transparent bluish nanolatexes containing 5–10 wt % polymer. The mean diameters of particles are in the 20- to 60-nm-diameter range. The particle size distribution is commonly narrow. The molecular weights of the polymers are usually high, above 10^6, and the number of chains per particle is generally very small ($N_p \leq 3$). The comparison between the particle size and the dimension of the linear polymers indicates that the chains are highly compressed within the particles.

The most widely studied o/w microemulsions were (1) ternary microemulsions prepared with a cationic surfactant, i.e., DTAB [27–28,44–48] or CTACl [18–20,22,49], and (2) microemulsions prepared using a mixture of a surfactant plus a cosurfactant, i.e., SDS plus pentanol [23–25,36–43]. The monomer content that can be incorporated is low (a few percent for styrene), and usually lower than the amount of surfactant.

2. Size Control of Nanolatexes Produced in Oil-in-Water Globular Microemulsions

The size of the particles resulting from o/w microemulsion polymerization has been found to depend on the following parameters:

1. *The monomer content and the surfactant-to-monomer ratio*. The higher the surfactant/monomer weight ratio, the smaller the particle size. A simple geometrical model has been proposed to describe the relation between the droplet size and the weight ratio of monomer to surfactant for the polymerization of styrene in ternary microemulsions using cationic surfactants [18, 49]. Nevertheless, the model fails for polar monomers like methyl methacrylate partitioned between the oil droplets, the interface, and the water phase.
2. *The presence of comonomers*. Both the phase diagram of the starting microemulsion and the particle size are dependent on the introduction of polar comonomers. This will be discussed in following sections.
3. *The polymerization rate*. The higher the polymerization rate, the smaller the particle size. The increase of the initiator concentration usually gives smaller particles.
4. *The presence of a cross-linking agent*. The positive influence of cross-linking on the particle size has been reported, although the size still depends both on the rate of polymerization and on the composition of the microemulsion [18,43].

3. Improvement of the Formulation of Polymerizable Microemulsions

One of the main drawbacks of microemulsion polymerization is the low monomer content that can be incorporated in the starting microemulsion and the large amount of surfactant, which leads to low polymer content.

In the field of aqueous nanolatexes, efforts have been made to develop new surfactant systems that allow the formation of polymerizable o/w microemulsions at low surfactant load and high monomer load [51–54]: metallosurfactants [51], associations of ionic surfactants with appropriate organic counterions [52], gemini cationic surfactants [53,54], as well as mixtures of nonionic surfactants [24–26,50] have been used. Alternatively, the use of polymerizable surfactants and/or cosurfactants has also been proposed in order to increase the final polymer concentration (this will be detailed in Sections II.C and II.D).

4. Mechanism of Microemulsion Polymerization

From the numerous reported kinetic studies in both o/w and w/o microemulsions, a mechanism similar to emulsion polymerization with a large amount of surfactant is commonly proposed. A well-accepted scheme is a continuous particle nucleation mechanism which is supported (1) by the particle size, which is usually larger than the parental microdroplets, (2) by the small number of polymer chain per particle, and (3) by the increase of the number of particles with the conversion [13–14,18]. The Candau-Leong-Fitch model, first developed for inverse systems, describes most of the observations and is now well accepted for o/w microemulsion polymerization (Fig. 2) [13,14]. In the first step the polymerization is initiated by the entry of radicals into the droplets (water-soluble initiator) or by radicals generated within the oil droplets (oil-soluble initiator). In the second step, nucleated particles grow by diffusion of monomer from inactive droplets through the continuous phase or by collision-coalescence with neighboring droplets. Since the particles are usually larger than the starting droplets, new micelles are formed. At the end of the polymerization, particles are accompanied by empty small surfactant micelles.

II. PREPARATION OF FUNCTIONALIZED NANOPARTICLES BY MICROEMULSION COPOLYMERIZATION

A. Background

Although numerous studies have been devoted to polymerization and copolymerization in o/w microemulsions [13–17], the preparation of functionalized nanoparticles is still under development. Most of the studies have been devoted to the copolymerization of styrene and methyl methacrylate or other (meth)-

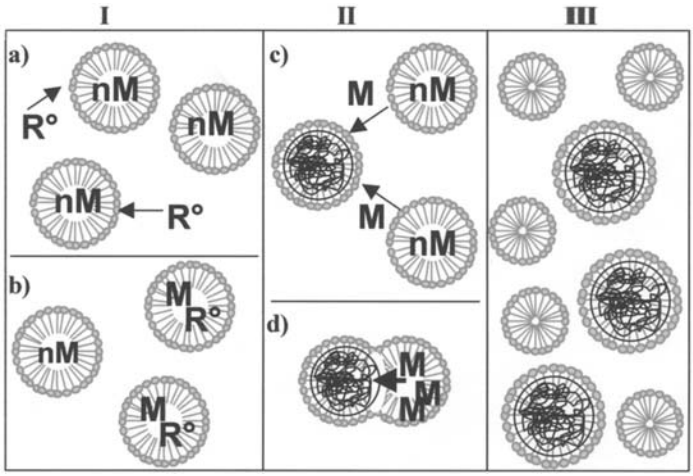

FIG. 2 Schematic polymerization mechanism in oil-in-water microemulsions. (I) Microdroplets are initiated by free radicals (a) with water-soluble initiator or (b) oil-soluble initiator. (II) Particle growth (c) by monomer diffusion through the continuous phase and (d) by collision between droplets (nonionic surfactants). (III) End of polymerization: polymer particles + empty micelles.

acrylic derivatives [13–15,18,26,50,55]. In most cases, the introduction of a second monomer was found to modify the microemulsion domains, the size of the resulting particles, as well as the stability of the final microlatexes. The partitioning of the comonomer between oil droplets, interface, and water as well as the chemical modification of the particle surface were proposed to account for the experimental results [15,26,55]. Kinetic studies have shown that the polymerization process, and subsequently the structure of the final particles, is affected by the relative concentrations of the reacting partners at the polymerization locus [13–15,23,55].

A limited number of contributions have dealt with the synthesis of functionalized nanoparticles. Antonietti et al. studied the copolymerization of styrene with some functional comonomers (10% molar ratio) in ternary CTACl microemulsions at 60°C using AIBN as initiator [19,20]. Polar and water-soluble comonomers like vinylpyridine (VP) or vinylbenzenesulfonate were found to destabilize the microemulsions and resulted in very large and polydispersed latex particles. On the other hand, nanolatexes in the 27- to 50-nm range have been obtained in the presence of hydroxyethyl, dimethylaminoethyl, or glycidylmethacrylate. Nevertheless, the composition of the resulting copolymers and the content of functional residues are not given. The same group also reported that the poly-

merization of styrene-in-water microemulsions using a mixture of a cationic surfactant CTACl plus a polystyrene-polyvinylpyridine block copolymer as a cosurfactant leads to pyridinium-functionalized nanoparticles by embedding of the block copolymer [19,20]. Ammonium-functionalized nanoparticles, in the 30- to 55-nm-diameter range, have been obtained by copolymerizing styrene with a cationic comonomer, methacrylamidopropyltrimethylammonium chloride, in the presence of a cross-linking agent in o/w cationic CTAB microemulsions [56]. Metal-complexing nanoparticles in the 25- to 40-nm-diameter range have been synthesized by copolymerization of styrene in o/w CTACl microemulsions using functional comonomers where a bipyridine is coupled to a methacrylic unit [22]. Tieke and coworkers have shown that styrene-in-water microemulsions can be prepared using polymerizable cationic surfactants: as discussed in Section II.D, under favorable conditions, subsequent polymerization gave small cationic polymer particles [57,58]. The use of surface-active initiators (Inisurf) to improve some properties of polymer latexes, previously described in emulsion polymerization, has also been extended to microemulsion processes [59,60]: cationic and nonionic surface active peresters have been used as photoinitiator for the polymerization of styrene-in-water microemulsions leading to microlatexes in the 20- to 40-nm range.

In our group, we have developed general and versatile methods to produce well-defined, highly functionalized nanoparticles with various functionalities that may find applications as polymer supports in chemical processes as well as carriers or sensors in life science.

We have developed two main synthetic approaches: microemulsion copolymerization with functional monomers and postfunctionalization of primary "reactive" nanoparticles [23–25,27,28]. The scope and limitations of both pathways have been examined and are discussed in the following sections.

B. Preparation of Functionalized Nanoparticles by Copolymerization with Functional and Reactive Comonomers in Oil-in-Water Microemulsions [23–25,27,28]

With the objective of producing nanoparticles with various surface characteristics and functionalities (acid, amine, alcohol, etc.) from a one step o/w microemulsion copolymerization process or a two-step process involving a postfunctionalization, the copolymerization of styrene has been investigated with various comonomers (Fig. 3):

Functional comonomers: methacrylic acid (MA), VP, as well as hydroxyalkyl-(meth)acrylic esters, which were found to act as cosurfactants and are the topic of Section II.C.

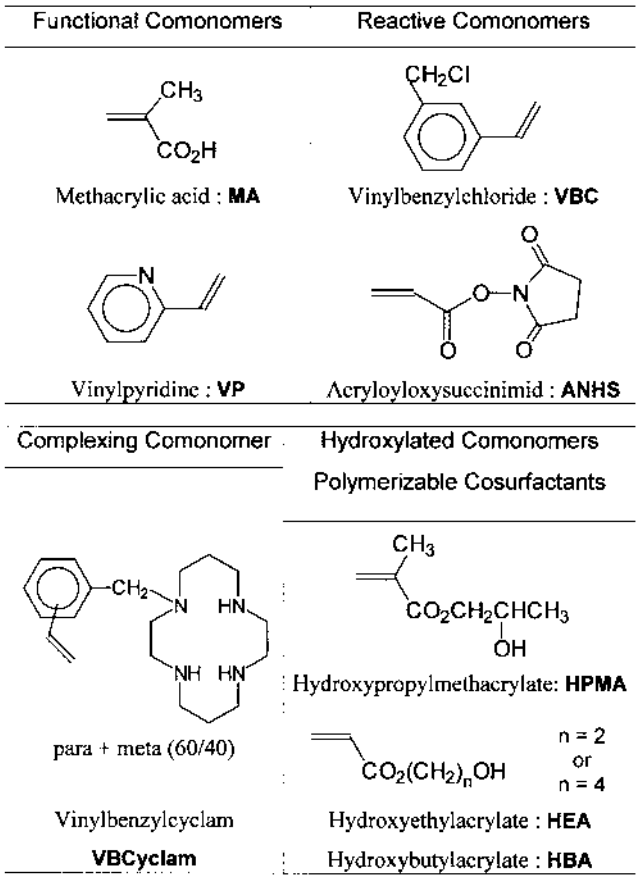

FIG. 3 Comonomers used in microemulsion polymerizations.

Reactive comonomers: vinylbenzyl chloride (VBC) and *N*-acryloyloxysuccinimide (ANHS), which permit the linkage of various residues, including biomolecules, in a second postfunctionalization step.

Complexing comonomer: vinylbenzylcyclam, a polymerizable derivative of cyclam (tetraazacyclotetradecane), a well-known selective metal-complexing macrocycle that can be used as a specific receptor and sensor.

In some cases, polymerizations were performed in the presence of a cross-linking agent, divinylbenzene (DVB).

1. General and Versatile Methods to Prepare Microemulsions Containing Mixtures of Monomers

One of the most important limitations for performing copolymerization in microemulsion is the preparation of the starting microemulsion; as already mentioned, the addition of a new component usually modifies the composition of the microemulsion domain. Most of the comonomers used in this study, except perhaps VBC, are polar molecules and are likely to interfere with the surfactant layer. Actually, microemulsions of mixture of monomers are easily prepared using titration processes. These very simple and versatile methods, depicted in Fig. 4, readily permit a fine adjustment of the composition of the microemulsion

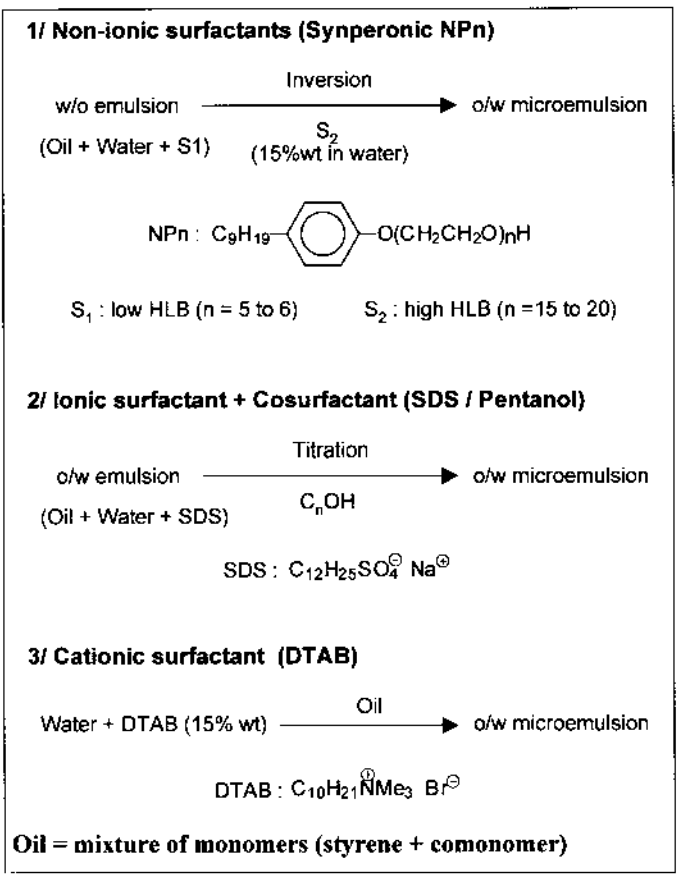

FIG. 4 Preparation of microemulsions using titration methods.

for a given mixture of monomers. Moreover, microemulsions can thus be obtained with different types of surfactants (nonionic, anionic, or cationic). The first method uses a mixture of two nonionic surfactants: this consists of forming a water-in-oil emulsion using a low hydrophilic–lipophilic balance (HLB) surfactant (typically synperonic NP5) and then titrating with an aqueous solution of a high HLB surfactant (typically synperonic NP15) until a clear transparent microemulsion is obtained. Average weight compositions are 6.5–8.5% oil and 14–15% surfactant [24–26].

The second type of formulation, widely studied with styrene, uses a mixture of an ionic surfactant and a cosurfactant (short alcohol) [36–43]. The preparation consists of titrating an o/w emulsion with the alcohol until a clear microemulsion is obtained. SDS in association with pentanol or with a polymerizable cosurfactant hydroxyalkyl(meth)acrylate has mainly been used [23–25]. Typical weight compositions are 5.5–9% oil, 8–9% surfactant, and 4–9% cosurfactant [23,24].

Ternary cationic microemulsions are obtained upon progressive addition of oil to an aqueous solution of DTAB [27,28,44]. The maximal oil volume fraction that can be incorporated is easily deduced at the cloud point. Average weight compositions are 3–6% oil, 14–15% surfactant [27,28].

All these titration methods have been found successful for preparing o/w microemulsions containing mixtures of styrene and functional or reactive comonomers (3–8 wt %) with molar ratios of styrene to comonomer ranging from 95:5 to 70:30. When SDS–cosurfactant systems are used, the amount of cosurfactant required for forming the microemulsions is lower in the presence of polar comonomers like VP, MA, or ANHS than with styrene alone or with mixtures of styrene and hydrophobic VBC [24]. These results indicate that polar comonomer molecules are preferentially partitioned at the interface and replace the cosurfactant molecules in the surfactant monolayer. Such behavior as already been observed for other polar comonomers [13–15,18–20,49,61]. The preferential location of these polar comonomers in the interfacial region plays a major role on the mechanism of polymerization as well as on the structural features of the resulting nanoparticles and especially on the accessibility of the functional groups.

2. Synthesis of Functionalized Nanoparticles by Copolymerization of Styrene with Functional and Reactive Comonomers

(*a*) *Experimental Conditions*. In order to avoid side reactions on functional groups, especially with reactive chloromethyl or activated hydroxysuccinimide ester, and to ensure that the microemulsions remain stable during the reaction, polymerizations have been performed under very mild conditions and in every case below 35°C. The following free-radical initiators have been used:

Water-soluble redox systems introduced in the microemulsions just before the polymerization: Hydrogen peroxide/ascorbic acid at 30–35°C [23–26,50] and ammonium persulfate/tetramethyldiaminomethane (TMDAM) at room temperature [23–25,62].

Oil-soluble initiator dissolved in the mixture of monomers before the preparation of the microemulsion in order to avoid any diffusion limitation: 2,2-dimethoxy-2-phenylacetophenone (DMPA) at room temperature, decomposed under light irradiation (UV or white light) [23–25,27–28]. DMPA has been preferred to the widely used AIBN because the rate of radical production is much higher at room temperature [63].

All these systems have been found successful for initiating the polymerization of styrene alone as well as copolymerization of styrene with functional comonomers [23–28]. The reactions are very rapid and complete conversion is achieved within a few minutes to a few hours: 2 h, 1 h, and 10–15 min for DMPA (UV)–, persulfate/diamine–, and hydrogen peroxide/ascorbic acid–initiated polymerizations, respectively [23–25,27–28]. In the latter case, the conversion rate has been significantly improved by optimizing the composition of the redox couple [23].

As can be seen in Tables 2 and 3, the copolymerization of styrene with functional or reactive comonomers gives access to stable translucent bluish suspensions of functionalized nanoparticles with diameter in the region 13–30 nm and a narrow size distribution. It turns out that the particle size does not significantly depend on the surfactant used (entries 4–6,9–10,11–12). Moreover, nuclear magnetic resonance (NMR) and infrared (IR) spectroscopic studies as well as elemental analysis of the resulting particles demonstrate that the comonomer is incorporated in the polymer with a molar ratio styrene/comonomer close to that expected on the basis of the composition of the monomer mixture used in its preparation [24,27,28]. The amounts of surface end groups range from 0.25 to 1.2 meq/g.

(*b*) *Functionalized Nanoparticles Resulting from Copolymerization with Reactive Comonomers [24].* Copolymerizations of styrene with acryloyloxysuccinimid ANHS (15–20 mol %) leads to 20-nm-range nanoparticles containing 0.8–1.2 meq/g of activated ester surface end groups (Table 2, entries 1–3) that corresponds, in the latter case, to an almost complete coverage of the surface. The amount of surface end groups dramatically depends on the initiating system: when water-soluble redox systems are used about 40–45% of the activated esters are located at the surface (entries 1 and 3), while this percentage reaches up to 70% when the oil-soluble initiator DMPA is used (entry 2). An initiator-dependent mechanism of polymerization, observed with polymerizable cosurfactants, may account for such an effect (Section II.C) [23]. These results indicate

TABLE 2 Nanoparticles Obtained from Microemulsion Copolymerization with Reactive Comonomers

Starting microemulsion[a]				Nanoparticles[b]		
Comonomer (mol %)	wt %	Surf.	Init.	*D* (nm)	Comp. (mol)	Surf. funct. (meq/g)
Acryloyloxysuccimide						
1 S-ANHS (20)	6.1	SDS	A	20	80/20	1.02
2 S-ANHS (15)	6.4	SDS	C	21	85/15	1.20
3 S-ANHS (15)	6.4	SDS	B	23	85/15	0.79
Vinylbenzyl chloride						
4 S-VBC (15)	6.5	NPn	A	27	87/13	0.80
5 S-VBC (15)	7.5	SDS	A	25	86/14	0.85
6 S-VBC (11)	3.9	DTAB	C	17	92/8	—
7 S-D-VBC (14)	3.9	DTAB	A	23	87/13	>0.23
8 S-D-VBC (14)	3.9	DTAB	C	16	91/9	>0.27

[a]S, styrene; S-D, styrene + DVB (50:50); wt %, weight fraction of monomers. Initiator—A: $(NH_4)_2S_2O_8$/TMDAM; B: H_2O_2/ascorbic acid; C: DMPA/UV or white light. Reaction time: 12 h; temperature, 20°C except for B: 30–35°C.

[b]Mean diameter determined by QELS and TEM; molar composition of the polymer; amount of surface end groups.

Source: Adapted from Ref. 24.

that the density of functional residues at the surface can thus be easily modulated by the proper choice of the initiating system.

In the same way, chloromethylated nanoparticles from 16 to 35 nm containing up to 1.2 meq of chlorine per gram of polymer are obtained by copolymerizing VBC (Table 2). The smallest particles are obtained from DMPA-initiated copolymerization with low monomer content. In this peculiar copolymerization, anionic or nonionic surfactant-based microemulsions should be preferred since, when the cationic surfactant DTAB is used, side reactions on the reactive groups (hydrolysis and replacement of chlorine per bromine) occur during the polymerization. High concentrations of bromine and hydroxide anions associated with the cationic surfactant monolayer may account for these side reactions.

These nanoparticles containing reactive chloromethyl or active ester surface end groups has been used for the covalent binding of functional molecules including biomolecules as described in Section III.

(*c*) *Functionalized Nanoparticles Resulting from Copolymerization with Functional Comonomers [24,27,28].* Copolymerization with polar functional comonomers like VP and MA also affords functionalized nanoparticles in the 17-

TABLE 3 Nanoparticles Obtained from Microemulsion Copolymerization with Functional Comonomers

Starting microemulsion[a]				Nanoparticles[b]		
Comonomer (mol %)	wt %	Surf.	Init.	*D* (nm)	Comp. (mol)	Surf. funct. (meq/g)
Vinylpyridine						
9 S-VP (10)	8	NPn	A	20	90/10	0.48
10 S-VP (20)	7.9	SDS	A	30	84/16	0.75
Methacrylic acid						
11 S-MA (25)	6.7	NPn	B	17	85/15	0.73
12 S-MA (15)	5.6	SDS	B	20	84/16	0.40
Vinylbenzylcyclam						
13 S-VBcyc. (10)	4	DTAB	C	15	91/9	0.30
14 S-VBcyc. (15)	2.9	DTAB	C	15	90/10	0.35
15 S-D-VBcyc. (11)	3.9	DTAB	C	13	91/9	0.48
16 S-D-VBcyc. (5)	4.1	DTAB	C	14	95/5	0.25
17 S-D-Vbcyc. (11)[c]	3.9	DTAB	C	20	89/11	0.30

[a]S, styrene; S-D, styrene + DVB (50:50), wt %, weight fraction of monomers. Initiator—A: $(NH_4)_2S_2O_8$/TMDAM; B: H_2O_2/ascorbic acid; C: DMPA/UV or white light. Reaction time: 12 h; temperature, 20°C except for B: 30–35°C.

[b]Mean diameter determined by QELS and TEM; molar composition of the polymer; amount of surface end groups.

[c]2 eq of NaOH per VBcyc was added.

Source: Adapted from Refs. 24 and 27.

to 30-nm-diameter range (Table 3, entries 9–12) [24]. When such polar ionizable comonomers are involved, the experimental conditions (initiator and comonomer content) should be properly chosen. For VP, slightly water soluble and probably partitioned between the oil droplets and the aqueous phase, nanoparticles are only obtained at low comonomer content (10–20 mol %). At higher VP contents, larger particles or gels are obtained. Polymerization in the water phase may account for these results as well as for the deficit of pyridine residues in the polymer for a 80:20 styrene/VP molar ratio (entry 10). Furthermore, large particles with a broad size distribution are obtained from hydrogen peroxide–initiated polymerization. For this basic comonomer, anionic or neutral radical initiators are preferred.

With MA, hydrogen peroxide or DMPA initiators should be preferred since large particles are obtained from persulfate-initiated copolymerization. Moreover, when the MA molar ratio exceeds 15%, polymerization partially takes place in the water phase as indicated by the deficit of MA residues in the resulting copolymer (entry 11).

Microemulsion copolymerization with the polymerizable macrocycle vinylbenzylcyclam has also been found successful for the preparation of ultrafine and highly functionalized metal-complexing nanoparticles containing up to 0.75 meq of macrocycle residues per gram of polymer (Table 3, entries 13–17) [27,28]. For this comonomer, cationic surfactant–based microemulsions and DMPA-initiated copolymerization should be preferred since copolymerizations performed in the presence of either an anionic surfactant (SDS) or an anionic initiator (persulfate) give larger particles or unstable suspensions. Owing to the pK_a values of the macrocyclic tetramine (about 2.3, 2.8, 10.4, and 11.4), the formation of ion pairs between the protonated macrocycle at neutral pH and the anionic surfactant or initiator may account for these results.

Whatever the composition of the starting mixture of monomers (molar ratio, presence or absence of a cross-linking agent), DMPA-initiated copolymerizations in cationic surfactant–based microemulsions afford stable aqueous suspensions of very small nanoparticles (13–15 nm) among the smallest ever described (Fig. 5, Table 3 entries 13–16). Slightly larger particles, with a mean diameter of 20 nm, are obtained in basic medium, i.e., when the macrocycle is not protonated (entry 17). The molar content of macrocycle in the nanoparticles reaches up to 11%. When higher comonomer concentrations are introduced in the starting

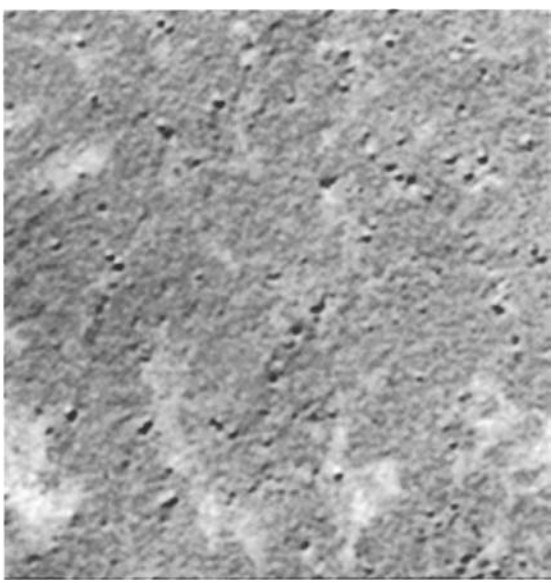

FIG. 5 Freeze fracture electron microscopy (×102,000) of ligand-functionalized nanolatex (Table 3, entry 15).

microemulsion (15% or more), the polymerizable cage is only partly incorporated in the particles (entry 14). In this case, the comonomer is probably partitioned between the aqueous phase and the interface, so that polymerization partly takes place in water giving rise to a water-soluble low molecular weight polymer, which is removed during the purification.

Moreover, the density of macrocycle residues at the surface of the particles, deduced from complexation studies (see Section IV.A), depends on the experimental conditions. For a given composition of the starting microemulsion, the amount of cyclam surface end groups is much higher on nanoparticles resulting from polymerization at neutral pH (entry 15, about 70% of the total amount of cyclam moieties in the particles) than on nanoparticles resulting from polymerization at basic pH (entry 17, about 40%). The decrease of the surface/volume ratio resulting from the increase of the size of the particles in the latter cases may account for these results. Furthermore, for same concentrations of polymerizable ligand and comparable sizes, the density of ligand at the surface is significantly increased by cross-linking (entries 13–15). Thus, the proper choice of the experimental conditions allows the synthesis of highly functionalized nanoparticles of 130- to 150-Å-diameter range containing more than 400 cyclam moieties per particle and up to about 350 ligand surface end groups. It is notable that by controlling the chain polymerization reaction in microemulsions, we reach the size and the functionalization range of large dendrimers prepared by multiple step-by-step procedures [64].

The binding capacity and the use of these ligand-functionalized nanoparticles as sensors are detailed in Section IV.A.

(*d*) *Discussion*. Microemulsion copolymerization is a useful and versatile technique for the synthesis of very small and well-defined nanoparticles containing high densities of a variety of functional surface end groups as diverse as chloromethyl, activated ester, amine, acid, or cage molecule. The titration method gives easy access to microemulsions containing mixtures of styrene and target comonomer. Under appropriate conditions, polymerization affords functional monodispersed nanolatexes. The main parameters that should be controlled are: (1) the location of the reactive species (comonomer and free radicals initiator) and (2) the nature of the surfactant that plays a major role in the colloidal stability of the nanolatex and might favor side reactions on reactive groups. As a general rule, when polar slightly water-soluble functional comonomers are considered, the copolymerization should be performed at low comonomer content. Under these conditions, the oil droplet (core and shell) is the main polymerization locus and the extent of polymerization in the aqueous phase is limited. Accordingly, the nature and the location of the free-radical initiator play a major role on the structure of the resulting nanoparticles: oil-soluble initiators solubilized within the oil droplet lead usually to the highest amount of polar surface end groups.

C. Preparation of Functionalized Nanoparticles by Copolymerization in Oil-in-Water Microemulsions Stabilized with Polymerizable Cosurfactants [23,25]

As was mentioned above, one of the main drawbacks of microemulsion polymerization is the low monomer content. The use of polymerizable surfactant systems (surfactant and/or cosurfactant) has thus been investigated as an alternative to increase the final polymer content of the resulting nanolatex [23,25, 57,58,65]. Interestingly, this approach allows a substantial molecular economy since a component of the surfactant system is incorporated in the final polymer.

For example, in o/w microemulsions prepared using a mixture of a surfactant and a cosurfactant, the oil content does not usually exceed 5–10% and is much lower than the overall amount of amphiphiles (about 12–15% including 4–9% of cosurfactant for typical SDS-pentanol microemulsions). Consequently, the substitution of the classical alcohol cosurfactant for a polymerizable cosurfactant that will be incorporated in the resulting polymer is an interesting way to increase the solid content of nanolatexes. Moreover, incorporation of the cosurfactant in the polymer may be a mean to overcome solvency problems previously encountered in cosurfactant-based microemulsions polymerizations of styrene [14,16]. It will also increase the hydrophilicity and polarity of the polymer particle surface, which may be of interest for biological applications.

We have investigated the use of short polymerizable alcohols, hydroxyalkylacrylic or hydroxyalkylmethacrylic esters like HEA (hydroxyethylacrylate), HBA (hydroxybutylacrylate), and hydroxypropyl methacrylate (HPMA), as cosurfactants and the polymerization of the resulting microemulsions (Fig. 3) [23,25].

1. Preparation of Oil-in-Water Microemulsions with Polymerizable Cosurfactants [23]

Styrene-in-water microemulsions have been obtained with SDS as the surfactant and HEA, HBA, or HPMA as the cosurfactant using the previously described titration method (Table 4). HPMA was found to be the most effective cosurfactant allowing the preparation of microemulsions containing about 7 wt % of styrene with an overall content of polymerizable materials (styrene plus cosurfactant) reaching 13% (Table 4, entry 5). Microemulsions containing an additional comonomer like MA or VBC can also be prepared using SDS-HPMA system (Table 4, entries 6–11). Hydroxyalkyl(meth)acrylate cosurfactants have also been found successful in the preparation of microemulsions in association with other ionic surfactants, such as CTAB or dodecylbenzenesulfonate.

The cosurfactant behavior of HEA, HBA, and HPMA has been studied by surface tension measurements. The reduction in the SDS critical micelle concentration (CMC) value demonstrates that comicellization does occur and that the polymerizable cosurfactant molecules are preferentially located at the interface

TABLE 4 Nanoparticles Obtained from Microemulsion Copolymerization with Polymerizable Cosurfactants

Starting microemulsion[a]					Nanoparticles Size and composition	
Monomer(s) and cosurfactant[b]		mol %	wt %	Init[c]	D(nm)	% mol
1 Styrene	HEA	85/15	4.1	A	27	92/8
2 Styrene	HBA	65/35	5.9	A	20	85/15
3 Styrene	HPMA	60/40	6.5	A	20	60/40
4 Styrene	HPMA	60/40	10.7	B	17	70/30
5 Styrene	HPMA	60/40	13.0	C	15	60/40
6 St + VBC	HPMA	(48 + 12)/40	6.5	B	15	(59 + 17)/24
7 St + VBC	HPMA	(48 + 12)/40	6.5	C	20	(50 + 12)/38
8 St + VBC	HPMA	(47 + 8)/45	7.3	A	18	(47 + 7)/46
9 St + MA	HPMA	(57 + 8)/35	9.9	A	22	(65 + 10)/25
10 St + MA	HPMA	(47 + 14)/39	5.9	B	12	(65 + 10)/25
11 St + MA	HPMA	(47 + 14)/39	6.5	C	20	(48 + 12)/40

[a]Microemulsions prepared using SDS + polymerizable cosurfactants; the compositions are given in Ref 23.
[b]% mol: Monomer(s)/polymerizable cosurfactant molar ratio and wt %: weight fraction of polymerizable materials (monomers + polymerizable surfactant).
[c]Initiator A: $(NH_4)_2S_2O_8$/TMDAM; B: H_2O_2/ascorbic acid; C: DMPA/UV; reaction time: 2 h; temperature, 20°C except for B: 30–35°C.
[d]Mean diameter determined by QELS and TEM; molar composition of the polymer.
Source: Adapted from Ref. 23.

between the surfactant molecules. Interestingly, such surface tension measurements could be used for screening the cosurfactant potentialities of other series of polymerizable polar molecules in association with different surfactants.

2. Preparation of Nanoparticles from Polymerizable Cosurfactant–Based Microemulsions [23]

The polymerization of these polymerizable cosurfactant–based microemulsions, performed under the mild conditions previously described, leads to highly functionalized, stable, transparent nanolatexes in the 12- to 30-nm range, with high polymer contents reaching up to 13 wt % (Table 4). The nanoparticles have a very narrow size distribution; as illustrated in Fig. 6, the autocorrelation function of the scattered light is a pure monoexponential in agreement with an unimodal population. Furthermore, these microlatexes are very stable, and no sedimentation or flocculation has been observed over long periods of time.

The incorporation of the cosurfactants in the resulting particles has been demonstrated by elemental analysis and spectroscopic characterization (IR, NMR)

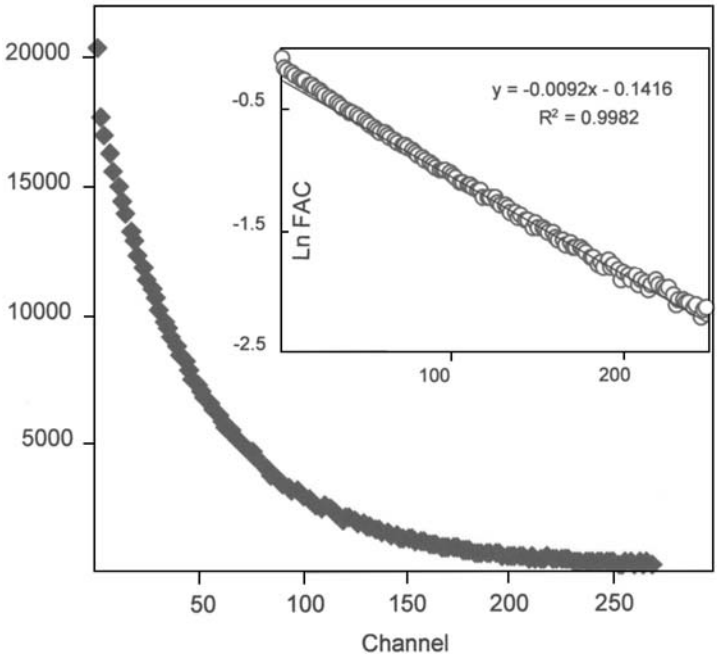

FIG. 6 QELS autocorrelation function of microlatexes obtained by polymerization of styrene and VBC in HPMA-based microemulsion (composition Table 4, entry 8).

of the isolated and purified polymers. Whatever the radical initiator, when HPMA is used the polymer composition is very close to that can be expected from the styrene/HPMA molar ratio in the starting microemulsion (Table 4, entries 3–11). DMPA-initiated polymerizations give rise to the best overall incorporation yields within the particles (entries 5, 7, 11). In the presence of HBA or HEA, the proportion of hydroxyester incorporated in the polymer is slightly lower probably owing to partial acrylate polymerization in the water phase (entries 1–2). It is noteworthy that, whatever the polymerizable cosurfactant HEA, HBA, or HPMA, copolymers containing very high amounts of hydroxy groups (8–45 mol %, *i.e.*, 0.7–3.7 meq/g) are obtained. Moreover, polyfunctional nanoparticles are produced in the presence of a third monomer: terpolymerization with VBC leads to nanoparticles containing high contents of both hydroxyester residues (2–3.6 meq/g) and chloromethyl reactive groups (0.6–1.5 meq/g). Further surface reactions indicate that the amount of accessible chloromethyl surface end groups is about 0.35 meq/g (Section III.A). Similarly, nanoparticles

containing both alcohol (2.2–3.4 meq/g) and carboxylic acid (1 meq/g) residues are obtained in the presence of MA.

Owing to the high content of cosurfactant incorporated in the particles and the high surface per volume ratio of the 12- to 20-nm nanoparticles, the major part of the surface is expected to be covered by polar hydroxyester moieties.

3. Purification of the Nanolatexes

The use of polymerizable cosurfactants not only affords a substantial molecular economy but also makes the purification easier. Thus, SDS is poorly soluble in pure water below a critical temperature of 16°C, the so-called Krafft point [31]. In nanolatexes prepared from microemulsions based on polymerizable cosurfactants, SDS readily precipitates upon cooling below the Krafft point (e.g., 10°C). Two cycles of cooling and filtration allow the removal and the recovery of about 85% of the surfactant introduced in the starting microemulsion. A last step of dialysis affords surfactant-free nanolatexes.

4. Kinetic Studies [23]

Further kinetic studies of the copolymerization of styrene with HPMA have clearly indicated that the location of the free-radical initiator is a critical parameter. In the presence of water-soluble initiators, the study of the conversion of styrene and HPMA vs. time shows that both monomers polymerize simultaneously with high conversion yields reaching 100% in a very short period of time (30 min to 1 h) and that the polymerization of styrene is greatly enhanced in the presence of the polymerizable cosurfactant. On the other hand, when an oil-soluble radical initiator like DMPA is used, the conversion vs. time curves show that a "two-step" polymerization process takes place: styrene polymerizes first and polymerization of HPMA begins when about 60–70% styrene has been converted. The polymerization rate and the conversion of styrene are not significantly modified in the presence of the polymerizable cosurfactant.

The polymerization mechanism is clearly dependent on the microenvironment and on the local monomer concentrations at the region where the free radicals are produced and where the initiation step takes place. The relative location (aqueous phase, interface, or droplet core) of the reactive species and the so-called compartmentalization effect play a major role. In o/w microemulsions, more than 60% of the cosurfactant partitions into the interface with most of the styrene (about 90%) residing in the oil phase [38,39]. Thus, when the free radicals are produced within the oil droplets (oil-soluble initiating system), the local concentration of styrene at the reaction site is much higher than that of HPMA: the polymerization thus proceeds first with styrene until the concentration of polymerizable cosurfactant at the reaction locus becomes sufficient (molar ratio HPMA/styrene: 1.5 for 60% conversion of styrene). In contrast, when a water-soluble initiator is used, the free radicals are produced in the

aqueous phase, the initiation takes place in the cosurfactant-rich interfacial region so that HPMA acts as a "phase transfer agent" for radicals. The very first oligomeric radicals produced from HPMA are more lipophilic than their monomer precursor and they probably partition between the oil droplet core and the interface. Therefore, a random polymerization is observed since the monomer proportions are not so different at the polymerization locus. The Candau-Leong-Fitch kinetic model, described in Section I, may account fairly well for these results.

Consequently, it may be proposed that the structure of nanoparticles resulting from copolymerization of styrene with polar comonomer preferentially located at the interface like cosurfactants depends on the location of the radical initiator; when a water-soluble initiator is used, the polar monomer moieties are randomly distributed within the whole particle volume. In this case the amount of accessible polar groups is controlled by the size of the particle (surface/volume ratio). In contrast, when an oil-soluble initiator is used the polar groups are preferentially located in the particle shell, resulting in higher densities of surface end groups. Obviously, this effect is expected to be broader when kinetic prevails over thermodynamic for example in the presence of a lipophilic cross-linking agent. It is worth noting that the polymerization scenario drawn here for polymerizable cosurfactants account fairly well for the results obtained with other polar monomers like ANHS and vinylbenzylcyclam (Section II.B) and offers a mean to control the accessibility of functional groups in well-defined nanoparticles.

D. Preparation of Functionalized Nanoparticles by Copolymerization in Oil-in-Water Microemulsions Stabilized with Polymerizable Surfactants [57,58,65]

Tieke and coworkers have shown that ternary microemulsions of styrene (1–5 wt %) in water can be prepared using the polymerizable cationic surfactants AUTMAB and MEDDAB (Fig. 7) [57,58]. Polymerizations of both monomers (styrene and polymerizable surfactant) have been performed at room temperature upon γ irradiation and led to copolymers with completely different morphologies. With the T-type surfactant AUTMAB, containing the polymerizable group at the hydrophobic tail, microlatexes in the 19- to 30-nm range with rather broad particle size distribution have been obtained. The surfactant is only partially incorporated in the nanoparticles (molar ratio styrene/AUTMAB = 3:2). A core-shell type of structure with blocks of polystyrene in the core and blocks of polyAUTMAB forming the shell has been proposed for these ammonium-functionalized nanoparticles. In contrast, transparent nanogels with high water contents are obtained in the presence of the H-type surfactant where the polymerizable group is at the hydrophilic head group.

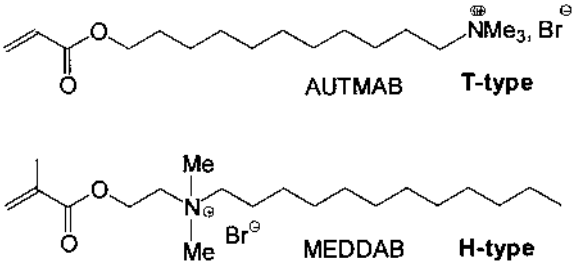

FIG. 7 Polymerizable surfactants used in the formulation of ternary styrene-in-water microemulsions [57,58].

On the basis of these results, and in good agreement with our previous observations and proposals, the following model has been proposed [57]. The T-type molecules are preferentially copolymerized with styrene because the reactive tails are located within the styrene droplets core where the polymerization proceeds thus leading to electrostatically stabilized particles. On the contrary, with the H-type surfactant the polymerizable groups are located at the surface of the microdroplets and are sterically more favored for bulk copolymerization with other surfactant molecules located in the aqueous phase rather than copolymerization with styrene.

Recently, Guyot and coworkers have studied the polymerization of styrene in microemulsions stabilized by both a polymerizable surfactant (dodecylmaleic hemiester) and a polymerizable cosurfactant (the previously described HPMA) [65]. Small particles ranging between 15 and 30 nm of diameter have been obtained in a limited range of composition. The cosurfactant is well copolymerized with styrene but the surfactant is shown to be only partially incorporated.

E. Conclusion

One can take advantage of the unique microenvironment provided by microemulsions to control copolymerization processes and the structural features of the resulting functionalized nanoparticles, e.g., particle size, polydispersity, capacity, and accessibility. The studies presented here give clear evidence that the location of the reactive species is the most critical parameter that should be considered. Polymerization in microemulsion based on polymerizable amphiphiles, either surfactants or cosurfactants, holds the most promise because it gives access to surfactant-free functionalized microlatexes with high polymer content.

III. PREPARATION OF FUNCTIONALIZED NANOPARTICLES BY POSTFUNCTIONALIZATION

The synthesis of well-defined highly functionalized nanoparticles can also be achieved by performing surface modifications of previously prepared nanolatexes. Postfunctionalization could be an efficient and versatile alternative to copolymerization for binding various functional residues, including expensive and sensitive reactants like biomolecules, giving access to nanoparticles with modulable functionalities and controlled size from a same microemulsion polymerization recipe.

Although postfunctionalization of classical latexes and polymer gels has been widely used and is now well documented [11], there are few examples of such chemical modifications on nanoparticles prepared by microemulsion polymerization [24,25,66]. Nevertheless, owing to the very high surface area and reagent accessibility, nanoparticles are expected to permit a high functionalization rate [67].

In this context, we have studied the binding ability of nanoparticles bearing reactive surface end groups like chloromethyl and activated ester (Fig. 8) [24]. Indeed, nucleophilic substitutions on polychloromethylstyrene microspheres or cross-linked resins have been found successful in introducing various chemical functions via reaction of nucleophilic anions or amines [68,70]. In the same way, the activating group of *N*-hydroxysuccinimide ester can be readily replaced by amines, providing a simple reaction pathway for the synthesis of functional polymers [71–74].

A. Surface Reactions on Nanoparticles Bearing Reactive Surface End Groups [24]

1. Nucleophilic Substitution on Chloromethylated Nanoparticles

The reactions of nucleophiles with chloromethylated nanoparticles were performed at room temperature directly in aqueous suspensions obtained by copolymerization in microemulsions formulated either with nonionic (NPn), anionic (SDS), or (occasionally) cationic (DTAB) surfactants, as described in Section II.B (Fig. 8, Tables 5a and 5b).

Substitution of the chloromethyl surface end groups occurs with various nucleophiles: anionic nucleophiles such as sulfite or thiocyanate and neutral nucleophiles such as primary or secondary amines and polyfunctional amino ligands (Tables 5a, b). The amount of functional groups linked to the resulting particles ranges from 0.1 to 0.8 meq/g, as deduced from elemental analysis of the polymer. Interestingly, acceptable yields are obtained with only a slight excess of reactant (2 eq).

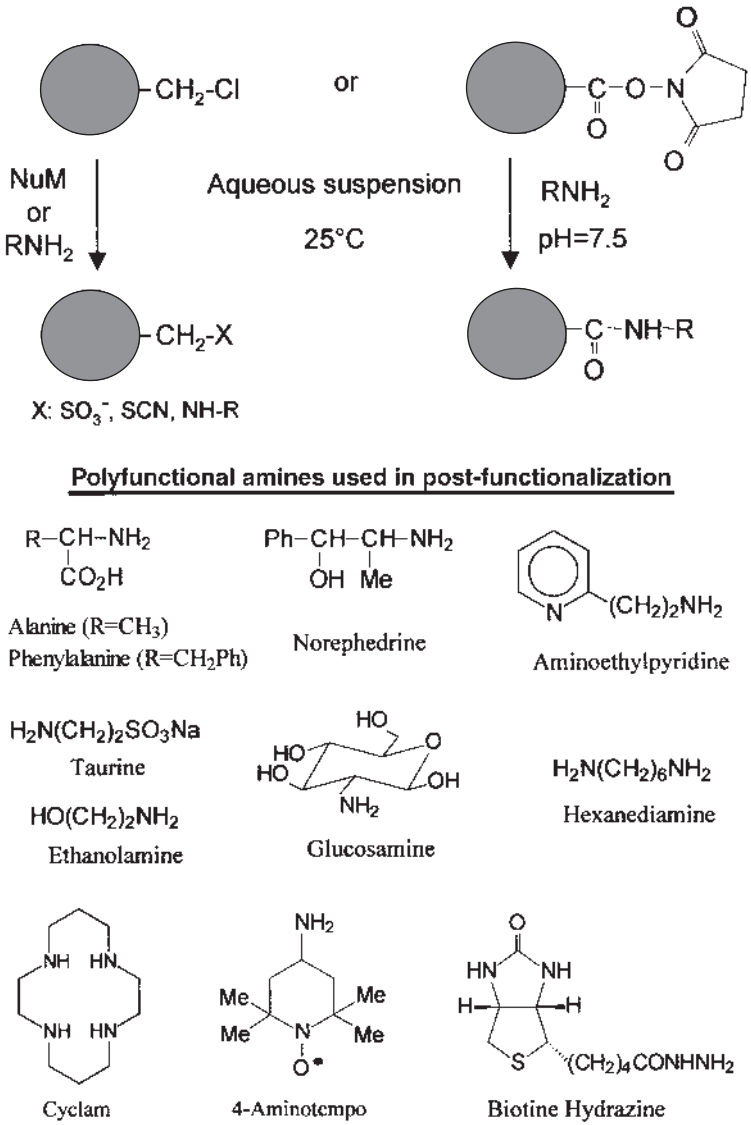

FIG. 8 Preparation of functionalized nanoparticles by postfunctionalization.

TABLE 5a Surface Reactions on Particles Bearing Chloromethyl Groups 1–9

Nucleophile and suspension[a]	Yield and bound reactant (meq/g)[b]	D(nm)[c]
KSCN[e]		
1 **P1** (NPn); 12 eq	71% (0.83 meq/g)	28
2 **P2** (SDS); 12 eq	40% (0.48 meq/g)	
3 **P1** dial.[d]; 12 eq	57% (0.66 meq/g)	
4 **P2** dial.[d]; 12 eq	5% (0.06 meq/g)	18
Na_2SO_3[e]		
5 **P1** (NPn); 12 eq	35% (0.40 meq/g)	
6 **P2** (SDS); 12 eq	13% (0.16 meq/g)	
$MeNH_2$[f]		
7 **P1** (NPn); 9 eq	36% (0.41 meq/g)	31
8 **P2** (SDS); 9 eq	68% (0.83 meq/g)	19
$EtNH_2$[f]		
9 **P3** (SDS-HPMA); 9 eq	58% (0.35 meq/g)	19

[a]Reaction time: 48 h; Starting nanolatexes: P1 (nonionic microemulsion, initiation: persulfate; 27 nm), P2 (SDS-pentanol microemulsion, initiation: persulfate; 18 nm), P3 (SDS-HPMA microemulsion, initiation: persulfate; 18 nm), P4 (DTAB microemulsion, initiator: DMPA, 16 nm); *n* equiv. nucleophile.
[b]Substitution yield calculated from the total amount of chlorine in the starting polymer and amount of reactant in the final polymer.
[c]Mean diameter; stable suspensions.
[d]Reaction performed after removal of surfactant by dialysis (about 90% for NPn and 98% for SDS).
[e]pH ~ 7.
[f]pH ~ 10–12.
Source: Adapted from Ref. 24.

The particle size distributions remains almost unchanged after surface modifications. In most cases, the surface reaction does not affect the colloidal stability of the nanolatexes, which remain transparent and stable for months. Thus, functionalized nanoparticles bearing various surface functionalities, such as sulfonate, amine, aminoalcohol, amino acid, pyridine, proteins, or cage molecules, are readily obtained by performing surface reactions on a same starting nanolatex.

The substitution yields, relative to the total amount of chlorine in the starting polymer, range from 10% to about 70% and depend both on the nucleophilic reactant and on the surfactant. From the highest substitution yields obtained with an excess of good nucleophiles like thiocyanate or primary amines (methyl-

TABLE 5b Surface Reactions on Particles Bearing Chloromethyl Groups 10–20

Nucleophile and suspension[a]	Yield and bound reactant (meq/g)[b]	D (nm)[c]
Aminoethylpyridine[f]		
10 **P2** (SDS); 12 eq	64% (0.78 meq/g)	
11 **P2** (SDS); 2 eq	57% (0.69 meq/g)	
12 **P2** dial.[d]; 2 eq	25% (0.30 meq/g)	18
Alanine[f]		
13 **P2** (SDS); 12 eq	70% (0.86 meq/g)	28
14 **P2** (SDS); 2 eq	40% (0.49 meq/g)	19
Ethanolamine[f]		
15 **P1** (NPn); 9 eq	30% (0.35 meq/g)	27
Norephedrine[f]		
16 **P2** (SDS); 2 eq	62% (0.76 meq/g)	19
Taurine[f]		
17 **P2** (SDS); 2 eq	38% (0.47 meq/g)	
Hexanediamine[f]		
18 **P2** (SDS); 2 eq	70% (0.37 meq/g)	17
Cyclam[e]		
19 **P4** (DTAB); 4 eq	34% (0.27 meq/g)	19
20 **P4** (DTAB); 1 eq	16% (0.14 meq/g)	19

See footnotes in Table 5a.
Source: Adapted from Ref. 24.

or ethylamine), one can assume that about 70% (0.8–0.85 meq/g) of the chloromethyl groups are accessible for nucleophilic substitution. It is worth noting that for nanoparticles resulting from polymerization with the polymerizable cosurfactant HPMA (Table 5a, entry 10), the amount of accessible chloromethyl groups is slightly lower (55–60%) in agreement with a high coverage of the surface by the hydroxyester groups: in this case, the nucleophilic substitution gives rise to bifunctional nanoparticles.

From the results reported in Tables 5a and 5b, it turns out that for a given reactant, the surfactant plays a major role in the nucleophilic substitution. With anionic nucleophiles, the substitution yields are higher in suspensions containing nonionic surfactants than in suspensions containing an anionic surfactant: respectively 70% and 40% for potassium thiocyanate, 35% and 13% for sodium sulfite (Table 5a, entries 1–2 and 5–6). Electrostatic repulsions between anionic surfactant molecules adsorbed on the particles and the anionic reactant, hindering the approach of the reactant, may account for the low yields in suspensions containing SDS. On the other hand, reactions with amines, performed in basic

medium, occur with higher yields in suspensions containing the anionic surfactant than in suspensions containing nonionic or cationic surfactants (Table 5a, entries 7–8). In the latter cases, hydrolysis of the chloromethyl groups becomes a competitive side reaction as demonstrated by the deficit of chlorine in the resulting polymer: up to 35% of the chloromethyl groups are hydrolyzed when methylamine is reacted in the presence of nonionic surfactants, whereas hydrolysis does not exceed 20% when the same reaction is performed in the presence of SDS. Accordingly, blank experiments in the absence of nucleophile demonstrate that hydrolysis of the chloromethyl groups by hydroxy anions readily occurs in basic medium (pH 12) with a higher extent in the presence of nonionic surfactants (50–55%) than in the presence of anionic SDS (40%). Owing to the above-mentioned electrostatic repulsions, anionic surfactant molecules adsorbed on the particles are expected to limit the hydrolysis side reaction, resulting in higher substitution yields with neutral amino nucleophiles. In contrast, ionic attractions between cationic surfactant molecules adsorbed on the surface and hydroxy anions dramatically favor the hydrolysis reaction, giving rise to poor substitution yields with primary or secondary amines.

Consequently, for a given nucleophile, the surfactant used for the preparation of the starting nanolatex should be properly chosen to ensure the highest substitution yield; when reactions with anionic nucleophiles are intended, it is highly preferable to start from a microemulsion stabilized with nonionic or cationic surfactants. On the contrary, when reactions with neutral aminonucleophiles are intended, an anionic surfactant is preferred.

Reactions performed in dialyzed suspensions show that, whatever the nucleophile, the substitution yields are always much higher in the presence of surfactant than after removal of the surfactant (Table 5a, entries 1–4, 10–11). The wetting of the particle surface and the reduction in the interfacial solid–liquid tension may account for this tremendous effect of the surfactant concentration on these reactions involving a water-soluble reactant and a fairly hydrophobic particle surface. The influence of the hydrophilicity of the reactive group's microenvironment has already been observed during reactions of water-soluble reactants on chloromethylated cross-linked polymers [69].

From a practical point of view, one can thus take advantages of these surfactant effects to get the highest substitution yields by the proper choice of the starting microemulsion. If surfactant-free functional nanolatexes are required, it is highly preferable to remove the surfactant after the chemical modification.

2. Reaction of Amino Reactants on Activated Esters Surface End Groups

Reactions of various primary amines with nanoparticles bearing N-hydroxysuccinimide (NHS)–reactive ester surface end groups have been performed at room

temperature directly in aqueous suspension at neutral pH (Table 6, Fig. 8). Taking advantage of the previously described surfactant effect on surface reactions, nanolatexes prepared in SDS microemulsions have been used to limit the expected hydrolysis of the reactive NHS esters. Accordingly, blank experiments demonstrate that hydrolysis does not compete significantly at pH 7.5 and never exceeds 5% of the ester surface end groups.

The "reactive" nanolatexes were obtained as described in Section II.B by copolymerization with ANHS initiated with hydrogen peroxide/ascorbic acid redox system (P5) or DMPA (P6). In both cases, the nanoparticles have a mean diameter of 20 nm but differ in the amount of reactive ester surface end groups. Surface reactions, monitored by UV absorption of NHS liberated *in situ* [71], readily take place at room temperature with fairly good yields (60–100%) whatever the amount of ester surface end groups (nanolatexes P5 and P6, Table 6). The chemical modifications were confirmed by elemental analysis and IR and NMR spectroscopy of the resulting polymers. The amount of accessible reactive

TABLE 6 Surface Reactions on Particles Bearing *N*-Hydroxysuccinimide Ester Groups

Reactants[a]	Yield (surface)[b]	Bound ligand (meq/g)	*D* (nm)[c]
$EtNH_2$			
1 **P5**; 1000 eq	42	1.00	
2 **P5**; 1.5 eq	42 (100)	1.00	23
3 **P6**; 1000 eq	70	1.20	
3 **P6**; 1.5 eq	70 (100)	1.20	20
Norephedrine			
4 **P5**; 1.5 eq	40 (95)	0.95	25
5 **P6**; 1.5 eq	64 (92)	1.10	
Phenylalanine			
8 **P5**; 1.5 eq	30 (70)	0.71	
Glucosamine			
7 **P5**; 1.5 eq	25 (60)	0.61	28
AminoTempo			
8 **P5**; 0.6 eq	30 (72)	0.72	23
Biotin Hydrazine			
9 **P6**; 0.1 eq	3.5 (40)[d]	0.06	

[a]Reactions performed in HEPES buffer (pH = 7.5) for 1–4 days. Starting nanolatexes: P5 (SDS-microemulsion, initiation: H_2O_2/ascorbic acid, 20 nm, 2.4 mmol ester/g), P6 (SDS-microemulsion, initiation: DMPA, 21 nm, 1.7 mmol ester/g); n. eq. nucleophile per eq. ANHS in the polymer.
[b]Substitution yield vs. total amount of ANHS in the polymer; in brackets. Substitution yield vs. active ester surface end groups.
[c]Mean diameter.
[d]In brackets: yield/nucleophile.
Source: Adapted from Ref. 24.

ester residues is readily deduced from the highest substitution yields obtained in the presence of a very large excess of a highly reactive primary amine (ethylamine, 1000 eq). As already mentioned in Section II.B, the percentage of accessible functional groups located at the surface is much higher in nanoparticles P6 resulting from DMPA-initiated polymerization (72%) than in nanoparticles P5 resulting from a water-soluble redox-initiated polymerization (42%) (Table 6, entries 1 and 3). It is worth noting that for nanoparticles with a mean diameter of 20 nm, and assuming a surface of about 40 $Å^2$ for an ester group, an amount of 1.2 meq/g of ester surface end groups corresponds to a complete coverage of the nanoparticles.

As can be seen in Table 6, the surface reactions readily take place with simple amines as well as with polyfunctional amino ligands and can be achieved with low molar excess or substoichiometric amounts of nucleophile. Furthermore, as was already observed for chloromethylated nanoparticles, the chemical modification does not modify the particle sizes or the colloidal stability. Further purification of the nanoparticles, e.g., removal of the excess of reactant and removal of the surfactant, can be achieved by dialysis. This postfunctionalization of active ester nanolatex thus affords a versatile method to produce nanoparticles of interest for biomedical or chemical applications bearing various surface end groups like chiral alcohols, acids, and sugars, 2,2,6,6-tetramethyl-1-piperidinyl oxy-radical, biotin, and proteins [25]. Interestingly, the linkage to the surface via an amide bond ensures non-pH-sensitive grafting as well as high chemical stability.

B. Oxidation of Polymethylstyrene Nanoparticles [66]

Li et al. described the preparation of nanoparticles (30–80 nm) with both aldehyde and carboxylic acid groups on the surface by oxidation of poly(methylstyrene) (PMS) nanolatex [66]. The copper-catalyzed oxidation of the PMS nanoparticles by *t*-butyl hydroperoxide has been performed at 60°C in aqueous suspensions. From the reported oxygen content in the resulting polymers, one can estimate that about 20–50% of the methyl groups have been oxidized. The particle size remains almost constant during oxidation, so that the amount of functional groups and the particle size could be controlled concurrently. The rate of oxidation was found to depend both on the size of the particles and on the amount of cationic surfactant.

C. Conclusion

Postfunctionalization gives access to highly functionalized ultrafine particles with a great variety of functions that hold most promise for biomedical or chemical applications. Postfunctionalization is a versatile and general method allowing the introduction of various functional groups from a same nanolatex without

changing the particle size so that the functionality and the size of the nanoparticles can be controlled concurrently. The results summarized here shed light on the positive role of the surfactant, which favors the surface reactions and, under appropriate conditions, inhibits side reactions. The suitable surfactant system can readily be chosen according to simple general rules: an anionic surfactant is preferred when nonionic reactants are involved, and an nonionic or cationic surfactant is preferred with anionic reactants.

IV. SPECIFIC NANOPARTICLES

The concept of immobilizing reagents or probes on polymer supports for use in chemistry and biology has received a great deal of attention. Since the activity of supported reagents depends on the accessibility of the active sites and is often limited by diffusion, considerable efforts have been made to develop new polymer supports with improved capacity, accessibility, and selectivity [11,12,75,76]. In this context, well-defined highly functionalized polymer nanoparticles offer new horizons in chemistry for the development of catalysts, reagents, or nanomaterials and in life science for the development of nanocarriers, nanosensors, and nanoprobes that are suitable for intracellular transport and measurements [77–81].

A. Selective Metal-Complexing Nanoparticles: Properties and Uses as Nanosensors

1. Introduction

Polymers as metal ion complexing agents have been proposed for an extensive variety of purposes as diverse as separation and recovery of metal ions, catalysis, chromatography, dioxygen transport, sensors [78, 82–88]. For such applications, the ability to control both the surface characteristic and the size of nanoparticles, offered by using the technique of polymerization in microemulsion, assumes paramount importance because of the high surface-to-volume ratio of the particles and the resulting ligand accessibilty. Pioneer studies have shown that metal complexing nanoparticles containing macrocyclic or bipyridine ligand can be prepared by a one-step microemulsion copolymerization process [22,27, 28]. Recently, fluorescent nanoparticles in the 20- to 200-nm range have been used as nanosensors for the detection of intracellular free zinc [78]. The sensor incorporates two fluorescent dyes: one is sensitive to zinc and the other acts as a reference. The dyes are entrapped within a polyacrylamide matrix by a microemulsion polymerization process previously described by Daubresse et al. (see following section) [89].

As previously described in Section II.B, we have prepared nanoparticles containing high densities of cyclam macrocycle via copolymerization of styrene

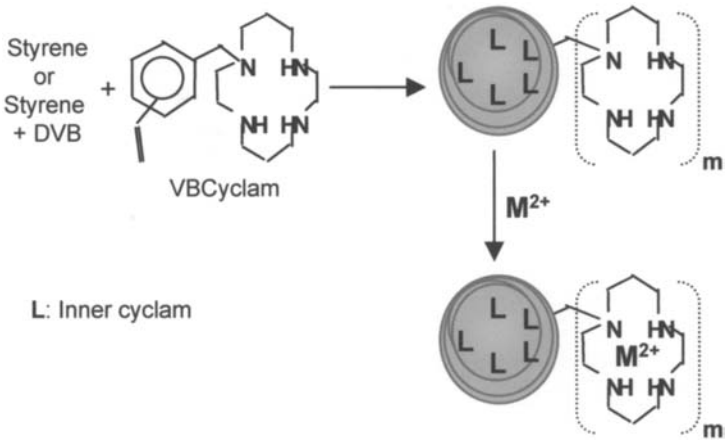

FIG. 9 Preparation of cyclam-functionalized nanoparticles.

with the polymerizable derivative, vinylbenzylcyclam, under mild conditions in ternary DTAB microemulsions with or without a cross-linking agent (Fig. 9, Table 7). Stable and ultrasmall transparent nanolatexes in the 13- to 20-nm-diameter range and narrow size distributions have been obtained from oil-soluble DMPA-initiated copolymerizations [27–28]. The molar contents of ligand

TABLE 7 Characteristics of Cyclam-Functionalized Nanoparticles Deduced from Cu(II) Binding Experiments and Spectroscopic Studies

Nanolatex[a]	P13	P15	P16	P17
Diameter (nm)[b]	15	13	13	20
Ligand content (meq/g)				
Total	0.71	0.65	0.35	0.73
Surface[c]	0.35	0.48	0.25	0.31
% Surface	50	74	72	41
n cyclam surf./particle[d]	370	330	140	780
Max Cu content (meq/g)[e]	0.58	0.62	0.32	0.61

[a]For experimental details, see Table 3 entries 13, 15–17.
[b]Mean diameter of the starting particles and after copper complexation determined by QELS and TEM.
[c]Accessible cyclam surface end groups from spectroscopic titration in dilute medium.
[d]Number of cyclam surface end groups assuming a density of 1.
[e]Under stoichiometric conditions, determined by elemental analysis.
Source: Adapted from Ref. 27.

in the particles range from 0.35 to 0.73 meq/g (5–11 mol %). Cyclam-functionalized nanoparticles can alternatively be obtained via postfunctionalization, but with a limited content of ligand that does not exceed 0.3 meq/g (Section III.A).

Cyclam is a well-known ligand, widely studied for selective complexation and extraction of metallic cations, that exhibits high affinities for transition metal cations that fit well in the macrocyclic cavity [83,84,90–92]. The thermodynamic stability constants, in solution as well as after anchoring to a polymer backbone or a resin [83,84], vary in the order Cu(II) > > Ni(II) > other cations so that cyclam specifically binds cupric ions, leading to a very stable deep violet copper–cyclam complex (stability constant $K = 10^{27}$) [90].

Taking advantages of both the transparency of the suspensions of nanoparticles and the specificity of the ligand, we have used these cyclam-functionalized nanoparticles as nanosensors for cupric ions as well as models to study the capacity, accessibility, and selectivity of ligand-functionalized nanoparticles.

2. Metal Binding Capacity of Cyclam-Functionalized Nanoparticles and Colloidal Stability of Metal-Loaded Nanolatexes [27,28]

Binding experiments performed under stoichiometric conditions clearly demonstrate the capacity and the ligand accessibility since, whatever the starting suspension, the complexation reaches 85–90% of the cyclam residues with copper contents reaching up to 0.6 meq/g (Table 7).

Remarkably, the particles size remains almost constant after complexation (Fig. 10). Furthermore, the nanolatexes are readily purified by dialysis without destabilization, affording very stable transparent violet surfactant-free suspensions of down to 13-nm functionalized nanoparticles containing up to 400 copper moieties, as previously illustrated by an electron microscopy study [27]. Electrostatic stabilization arising from ionic repulsions between the positively charged nanoparticles may account for the colloidal stability of the suspension of Cu-cyclam-functionalized nanoparticles.

It is worth noting that the cation binding capacity of these cyclam-functionalized nanoparticles, prepared by a straightforward one-step polymerization procedure, is comparable to those of the more sophisticated high-generation dendrimers like PAMAM [0.65 mmol Cu(II) per g for generation eight PAMAM] [27,85].

3. Spectrophotometric Study of the Complexation Process: Sensors for Cu(II) and Ligand Accessibility [27]

Taking advantage of the transparency of the suspensions, the amount of Cu(II)–cyclam complex in the nanoparticles is easily determined spectrophotometrically from its characteristic absorbance. Quantitative and reproducible measurements are obtained by using an integrating sphere to collect and integrate the scattered light. Upon progressive addition of a dilute 0.01 M solution of Cu(II), the sus-

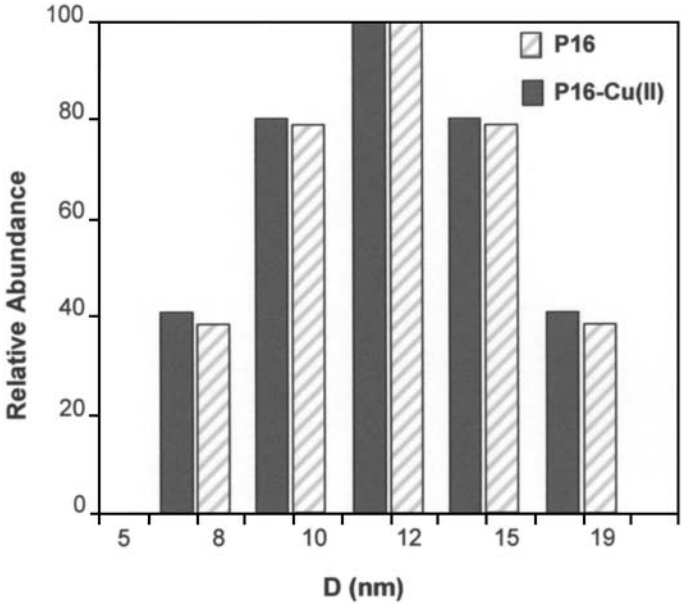

FIG. 10 Particle size distribution of nanolatex P16 before and after complexation of Cu(II).

pensions of cyclam-functionalized particles instantaneously turn violet, indicating that complexation readily takes place even at very low copper concentrations. The suspensions exhibit a maximal absorption wavelength at 536 nm (ε = 134 $Lmol^{-1}cm^{-1}$) very close to those of the monomeric Cu(II)/vinylbenzylcyclam complex. The Cu(II) detection limit is about 10^{-4} $molL^{-1}$.

As can be seen in Fig. 11, the absorbance of the copper complex increases linearly up to a maximal value that corresponds to the instantaneous complexation of all the accessible cyclam moieties in dilute medium. Thus, the amount of accessible ligand can be readily deduced from spectrophotometric titrations and compared for various suspensions (Table 7). Remarkably, for cross-linked nanoparticles in the 13- to 15-nm-diameter range, complexation of about 70–75% of the whole cyclam residue is reached in dilute medium at the minute time scale whatever the overall content of ligand, indicating a very high ligand accessibility on such ultrafine nanoparticles (Table 7, suspensions P15 and P16). On the other hand, for similar compositions, the amount of surface end groups is dramatically reduced when the particle size increases in agreement with the decrease of the surface-to-volume ratio (0.48 and 0.3 meq/g, respectively, for 13- and 20-nm particles, P15 and P17, Table 7).

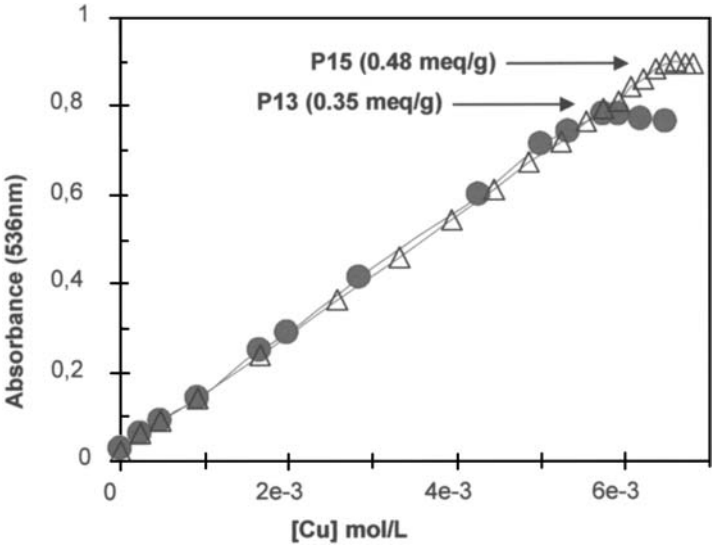

FIG. 11 Spectrophotometric titration of Cu-cyclam complex upon progressive addition of a dilute copper nitrate solution (0.01 M) to nanolatexes P13 and P15. Absorbance at 536 nm vs. copper concentration in suspensions P13 and P15.

When 20-nm particles, P17, containing the lowest amount of accessible cyclam moieties in dilute medium are considered, spectrophotometric studies clearly indicate that two complexation processes take place: a rapid "solution-like" complexation process involving the outer ligand residues located near the surface (so-called cyclam surface end groups), which occurs at the minute time scale in dilute medium, and a slow diffusion-limited complexation process involving the inner cyclam residues entrapped within the core of the particles. For these 20-nm nanoparticles, 40% of the cyclam moieties are accessible for complexation at the minute time scale in dilute medium. In agreement with a diffusion-limited process, the higher the copper concentration, the higher the extent of instantaneous complexation: the maximal complexation yield, 85%, is reached at the minute time scale in the presence of 2.5×10^{-2} mol Cu(II)/L.

Similar behaviors have been observed for 13- to 15-nm nanoparticles containing high densities of outer cyclam residues (suspensions P15, P16) with a very minor contribution of the diffusion-limited process: the overall maximal complexation yield is about 85–90% including 70–75% of outer cyclam residues involved in a rapid complexation process and only 10–15% of inner cyclam residues involved in a diffusion-limited complexation process.

These results shed light on the huge improvement of the ligand accessibility brought by decreasing the particle size with a clear relationship between the percentage of functional groups located at the surface and the surface-to-volume ratio of the particles.

4. Selectivity of Cyclam-Functionalized Nanoparticles [27,28]

The selectivity of the cyclam-functionalized nanoparticles for copper as well as their binding ability for other metals was studied by performing competition experiments with various metallic cations [Ni(II), Co(II), Zn(II)]. The cyclam-functionalized nanoparticles exhibit a very high selectivity for cupric ions since, whatever the competing cation, complete complexation of Cu(II) does take place even in the presence of a very large excess of competing ion (1000-fold excess). This remarkable selectivity makes them valuable specific nanosensors for cupric ions in complex mixtures such as biological media.

The nanoparticles also exhibit high binding abilities for Ni(II), Co(II), and Zn(II) with complexation yields reaching about 60–70% of the remaining free-cyclam moieties. The excess of competing ion in the aqueous phase is readily removed upon dialysis without destabilization, so that competition experiments give access to colloidal suspensions of ''bimetallic'' nanoparticles. Bimetallic nanoparticles with adjustable ratios of two cations, M^{2+} and Cu^{2+}, can alternatively be prepared by exchanging a given cation M^{2+} (Zn, Co, or Ni) for cupric ion. The cation exchange is then readily monitored by spectrophotometric titration of the copper–cyclam complex. Core-shell type nanoparticles with a Cu-rich shell and a Zn-rich core have thus been obtained in dilute medium.

5. Fluorescent Nanosensors Based on Cyclam-Functionalized Nanoparticles

Cyclam-functionalized nanoparticles may be used as selective sensors for cupric ions thanks to the characteristic absorption of the cyclam–copper complex (λ_{max} = 536 nm) that enables spectrophotometric detection. We have recently turned these sensors into fluorescent nanosensors by loading the nanoparticles with a fluorescent pyromethene dye ($\lambda_{em} = 541$ nm). The complexation of copper induces a decrease of the fluorescence of the dye entrapped in the polymer particle. This decrease is almost quantitative and more than 87% of the fluorescence is quenched. Due to the high sensitivity of fluorescence measurements and the high affinity of cyclam for cupric ions, latex concentrations as low as 4×10^{-5} g/mL have been used for the detection of cupric ions at a concentration of 10^{-6} mol/L. Moreover, these fluorescent nanosensors retain a remarkable selectivity for cupric ions since the complexation of other metallic cations, such as Zn or Ni, does not induce a fluorescence quenching.

6. Conclusion

As illustrated here in the case of metal-complexing nanoparticulate systems, microemulsion copolymerization is a very useful technique to synthesize well-defined nanoparticles with high densities of accessible specific ligands or recognition sites. The reported results shed light on the remarkable accessibility of such nanomaterials where the surface prevails over the volume. Moreover, the properties of selective ligands like macrocycles are not influenced by the binding to the particles, so that a real "solution-like" chemistry, very close to classical supramolecular chemistry, becomes accessible on colloidal polymer nanoparticles. As already stated, a comparably simple technique of microemulsion polymerization results in polymers with properties very similar to those of the more sophisticated dendrimers.

Our results show that metal-complexing nanoparticles can be used as specific UV-visible or fluorescent nanosensors. Considering their binding capacity, ligand accessibility, and selectivity, these nanoparticles are also very attractive supports for a variety of applications, such as catalysis, specific recovery, and chromatography, and may also find promising applications in materials science for the development of new polymer composites. Owing to the high density of charges, cationic metal-loaded nanoparticles may also serve as DNA carriers and sensors.

B. Nanoparticles as Supports or Carriers for Biological Applications

Polymer latexes are classically used for biological applications such as immobilization of proteins or antibodies as well as drug or gene delivery [1–10]. The critical parameters for these applications are the particles size, the possibility of covalent binding to the surface, as well as the stability of the colloidal suspension in biological media. Well-defined nanoparticles resulting from microemulsion polymerization are thus of great interest.

Immunoassay experiments or medical diagnostics use polymer particles that contain antibodies to detect diseases by specific interaction with antigens. The detection is based on the agglutination of particle-supported antibodies arising from antibody–antigen interactions and uses turbidity measurements or light scattering techniques [5–8]. The detection sensitivity is therefore substantially improved by using translucent aqueous nanolatexes: the smaller the particles, the higher the sensitivity. These applications require the presence of reactive surface end groups that permit the covalent binding of the antibody to the particle. The use of aqueous functionalized nanolatexes in the 15- to 30-nm range, prepared as described in Sections II and III, for medical diagnostics has been patented [25].

The immobilization of proteins in nanoparticles prepared from both w/o and o/w microemulsion polymerization processes has also been investigated. Daubresse et al. reported enzyme immobilization in nanoparticles produced by inverse microemulsion polymerization [89,93]. Typically, the nanoparticles were prepared by polymerization of acrylamide, a cross-linking agent (methylenebisacrylamide), and a functional comonomer [either *N*-acryloyl-1,6-diaminohexane (ADH, an amine promoter) or acrylic acid (a carboxylic acid promoter)] in w/o microemulsions. The enzyme to be entrapped, phosphatase alkaline, was dissolved in the aqueous phase prior to polymerization. The reported results demonstrate that polymerization in inverse microemulsion is a useful technique to immobilize an enzyme within cross-linked polyacrylamide nanoparticles in the 30- to 50-nm diameter range while keeping the catalytic activity essentially unmodified: 45% of the alkaline phosphatase remains immobilized for several weeks, whereas when using microparticles resulting from emulsion polymerization 90% of the enzyme is rapidly released.

In a similar way, Antonietti et al. reported the functionalization of nanoparticles of 23- to 35-nm-diameter range by incorporation of proteins (bovine serum albumin or lipase) in styrene-in-water microemulsions stabilized using a mixture of natural surfactants (lecithin and sodium cholate) [21]. Standard gel electrophoresis revealed that more than 90% of the proteins are fixed at the particle surface.

Surface reactions on nanoparticles bearing reactive groups like activated esters have also been found successful for the covalent binding of proteins onto nanoparticles in aqueous medium [25].

IV. CONCLUDING REMARKS

Polymerization in microemulsion provides a useful technique for the synthesis of very small functionalized nanoparticles with mean diameters from 12 to 30 nm that exhibit a very large specific area, i.e., up to 450 m^2/g. These nanolatexes are well defined with respect to size and chemical compositions. A variety of functional groups can be introduced in a one-step procedure by copolymerization with a functional monomer or in a two-step procedure involving a postfunctionalization. By combining both methods, functional nanolatexes with very high densities of functional groups as diverse as chloromethyl, activated ester, alcohol, amine, pyridine, acid, sulfonate, thiocyanate, chiral amino acid, chiral amino alcohol, macrocycle, sugar, organic radicals, or biomolecules become readily accessible.

Considering the preparation of functional nanolatex by copolymerization in microemulsion involving a functional comonomer, the reported results give clear evidence of the decisive role of the microenvironment and the compart-

mentalization effect provided by microemulsions. The critical parameters that should be controlled are the location of the reactive species (monomers and free radicals) and the nature of the surfactant. Both size control and high densities of functional surface end groups can be achieved when the comonomer is preferentially located at the interface and when the initiation step takes place within the droplet core. This is especially the case when polar monomers like polymerizable surfactants or cosurfactants are involved. In this field, the formulation of microemulsions with polymerizable amphiphiles, surfactants, and/or cosurfactants, and the subsequent polymerization, holds the most promise because it gives access to nanolatex with high polymer content and core-shell-type structures. With respect to the economical aspects, this affords a mean to overcome the main drawbacks of microemulsion polymerization process, which are the high surfactant concentration and the low monomer content.

It has also been shown that postfunctionalization of "reactive" nanolatexes permits covalent binding of a variety of reactants and allows one to control size and functionality concurrently. Emphasis must be placed on the decisive role of the surfactant in the polymerization process as well as in additional surface modifications. The choice of surfactant is a critical parameter for (1) the formulation of the microemulsion, which has to accept functional monomers; (2) the colloidal stability of the nanolatex, which depends on the adsorption of the surfactant onto the particle surface; and (3) the postfunctionalization since the approach of the reactant is greatly influenced by the nature of the particle surface (charge, wetting, interfacial solid–liquid tension). Interestingly, the postfunctionalization yield can be improved by an appropriate choice of the surfactant.

Functional latexes produced by microemulsion polymerization exhibit fascinating structural features very close to classical supramolecular assemblies, which makes them promising supports for reagents, catalysts, or biologically active agents as well as valuable precursors for the synthesis of new materials with specific properties.

REFERENCES

1. Guiot, P., Couvreur, P., Eds. *Polymeric Nanoparticles and Microspheres*; CRC Press: Boca Raton, FL, 1986.
2. Rembaum, A., Tökes, Z., Eds. *Microspheres*: *Medical and Biological Applications*. CRC Press: Boca Raton, FL, 1988.
3. Slomkowski, S.;Basinska, T. Detection and concentration measurements of proteins adsorbed onto polystyrene and poly(styrene-acrolein) latexes. In *Polymer Latexes*: *Preparation*, *Characterization and Applications*; Daniels, E.S., Sudol, E.D., El-Aasser, M.S., Eds.; ACS Symp. Series 492, American Chemical Society: Washington, DC, 1992; 329–346.
4. Ugelstad, J.; Berge, A.; Ellingsen, T.; Schmid, R.; Nilsen, T.N.; Mørk, P.C.; Sten-

stad, P.; Hornes, E.; Olsvik, Ø. Preparation and application of new monosized polymer particles. Prog. Polym. Sci. **1992**, *17*, 87–161.
5. Weetall, H.H.; Gaigalas, A.K. Studies on antigen-antibody reactions using light scattering from antigen coated colloidal particles. Anal. Lett. **1992**, *25*, 1039–1053.
6. Kitano, H.; Iwai, S.; Okubo, T.; Ise, N. Direct examination of chemical kinetics laws for visual imagery. 3. Association of latex particles modified with antigens and antibodies. J. Am. Chem. Soc. **1987**, *109*, 7608–7612.
7. Margel, S.; Dolitzky, Y.; Sivan, O. Immobilized polymeric microspheres: polyacrolein microspheres covalently bound in a monolayer structure onto glass surfaces. Colloids Surf. **1992**, *62*, 215–230.
8. Delair, T.; Pichot, C.; Mandrand, B. Synthesis and characterization of cationic latex particles bearing sulfhydryl groups and their use in the immobilization of Fab antibody fragments. Colloid Polym. Sci. **1994**, *272*, 72–81.
9. Elaissari, A.; Pichot, C.; Delair, T.; Cros, P.; Kurfurst, R. Adsorption and desorption studies of polyadenylic acid onto positively charged latex particles. Langmuir **1995**, *11*, 1261–1267.
10. Yan, C.; Zhang, X.; Sun, Z.; Hiromi, K.; Ise, N. Poly(styrene-co-acrolein) latex particles: copolymerization and characteristics. J. Appl. Polym. Sci . **1990**, *40*, 89–98.
11. Guyot, A.; Hodge, P.; Sherrington, D.C.; Widdecke, H. Recent studies aimed at the development of polymer-supported reactants with improved accessibility and capacity. Reactive Polym. **1991/1992**, *16*, 233–259.
12. Ford, W.T.; Badley, R.D.; Chandran, R.S.; Babu, S.H.; Hassanien, M.; Srinivasan, S.; Turk, H.; Yu, H.; Zhu, W. Polymer colloids as catalyst supports. In *Polymer Latexes*: *Preparation*, *Characterization and Applications*; Daniels, E.S., Sudol, E.D., El-Aasser, M.S., Eds.; ACS Symp. Series 492; American Chemical Society; Washington, DC, 1992; 423–431.
13. Candau, F. Polymerization in microemulsions. In *Handbook of Microemulsion Science and Technology*; Kumar, P., Mittal, K.L., Eds.; Marcel Dekker: New York, 1999; 679–712.
14. Candau, F. Polymerization in microemulsions. In *Polymerization in Organized Media*; Paleos, C.M., Ed.; Gordon and Breach: New York, 1992; 215–282.
15. Capek, I. Radical polymerization of polar unsaturated monomers in direct microemulsions. Adv. Colloid Interface Sci. **1999**, *80*, 85–149.
16. Capek, I. Microemulsion polymerization of styrene in the presence of anionic emulsifier. Adv. Colloid Interface Sci. 1999, *82*, 253–273.
17. Capek, I. Microemulsion polymerization of styrene in the presence of a cationic emulsifier. Adv. Colloid Interface Sci. **2001**, *92*, 195–233.
18. Antonietti, M.; Basten, B.; Lohmann, S. Polymerization in microemulsions—a new approach to ultrafine highly functionalized polymer dispersions. Macromol. Chem. Phys. **1995**, *196*, 441–466.
19. Antonietti, M.; Lohmann, S.; Van Niel, C. Polymerization in microemulsion. 2. Surface control and functionalization of microparticles. Macromolecules **1992**, *25*, 1139–1143.
20. Antonietti, M., Lohmann, S., Bremser, W. Polymerization in microemulsion-size and surface control of ultrafine latex particles. Prog. Colloid Polym. Sci. **1992**, *89*, 62–65.
21. Antonietti, M.; Basten, R.; Gröhn. Polymerization in microemulsion of natural sur-

factants and protein functionalization of the particles. Langmuir **1994**, *10*, 2498–2500.
22. Antonietti, M.; Lohmann, S.; Eisenbach, C.D.; Schubert, U.S. Synthesis of metal-complexing latices via polymerization in microemulsion. Macromol. Rapid Commun. **1995**, *16*, 283–289.
23. Larpent, C.; Bernard, E.; Richard, J.; Vaslin, S. Polymerization in microemulsions with polymerizable cosurfactants: a route to highly functionalized nanoparticles. Macromolecules **1997**, *30*, 354–362.
24. Larpent, C.; Bernard, E.; Richard, J.; Vaslin, S. Synthesis of functionalized nanoparticles via copolymerization in microemulsions and surface reactions. Reactive Funct. Polym. **1997**, *33*, 49–59.
25. Larpent, C.; Richard, J.; Vaslin-Reimann, S. Functionalized polymer nanoparticles, method of preparation and use thereof. PCT Int. Appl., 09 Dec 1993, WO 9324,534. CA 1994, 121, 206282u.
26. Larpent, C.; Tadros, T.F. Preparation of microlatex dispersions using oil-in-water microemulsions. Colloid Polym. Sci. **1991**, *269*, 1171–1183.
27. Amigoni-Gerbier, S.; Dessert, S.; Gulik-Kryswicki, T.; Larpent, C. Ultrafine selective metal-complexing nanoparticles: synthesis by microemulsion copolymerization, binding capacity and ligand accessibility. Macromolecules **2002**, *35*, 1644–1650.
28. Larpent, C.; Amigoni-Gerbier, S. Synthesis and properties of selective metal-complexing nanoparticles. Macromolecules **1999**, *33*, 9071–9073.
29. Robb, I.D., Ed. *Microemulsions*; Plenum Publishers: New York, 1982.
30. Prince, L.M., Ed. *Microemulsions*: *Theory and Practice*; Academic Press: New York, 1977.
31. Myers, D., Ed. *Surfactant Science and Technology*, 2nd Ed.; V.C.H. Publishers: New York, 1988.
32. Langevin, D. Structure of reversed micelles. In *Structure and Reactivity in Reversed Micelles*; Pileni, M.P., Ed.; Elsevier: New York, 1989; 13–43.
33. Fendler, J.H., Fendler, E.J., Eds. *Catalysis in Micellar and Macromolecular Systems*; Academic Press: New York, 1975.
34. Lattes, A.; Rico-Lattes, I. Communities of molecules and reactivity in organized molecular systems. C. R. Acad. Sci. Paris **1997**, *324* (Series IIb), 575–587.
35. Pileni, M.P., Ed. *Structure and Reactivity in Reversed Micelles*; Elsevier: New York, 1989.
36. Guo, J.S.; Sudol, E.D.;. Vanderhoff, J.W.; El-Aasser, M.S. Particle nucleation and monomer partitioning in styrene o/w microemulsion polymerization. J. Polym. Sci. A Polym. Chem. **1992**, *30*, 691–702.
37. Guo, J.S.; Sudol, E.D.; Vanderhoff, J.W.; El-Aasser, M.S. Modeling of the styrene microemulsion polymerization. J. Polym. Sci. A Polym. Chem. **1992**, *30*, 703–712.
38. Guo, J.S.; Sudol, E.D.; Vanderhoff, J.W.; Yue, H.J.; El-Aasser, M.S. Partitioning behavior and thermodynamic model for styrene o/w microemulsions. J. Colloid Interface Sci. **1992**, *149*, 184–196.
39. Guo, J.S.; El-Aasser, M.S.; Sudol, E.D.; Yue, H.J.; Vanderhoff, J.W. Phase compositions of styrene oil-in-water microemulsions. J. Colloid Interface Sci. **1990**, *140*, 175–184.
40. Kuo, P.L.; Turro, N.J.; Tseng, C.M.; El-Aasser, M.S.; Vanderhoff, J.W. Photoiniti-

ated polymerization of styrene in microemulsions. Macromolecules **1987**, *20*, 1216–1221.
41. Feng, L.; Ng, K.Y.S. Characterization of styrene polymerization in microemulsions by Raman spectroscopy. Colloid Surf. **1991**, *53*, 349–361.
42. Feng, L.; Ng, K.Y.S. In situ kinetic studies of microemulsion polymerizations of styrene and methyl methacrylate by Raman spectroscopy. Macromolecules **1990**, *23*, 1048–1053.
43. Schauber, C.; Riess, G. Preparation de microlatex acryliques par polymerisation photochimique de solutions micellaires et de microemulsions. Makromol. Chem. **1989**, *190*, 725–735.
44. Perez-Luna, V.H.; Puig, J.E.; Castano, V.M.; Rodriguez, B.E.; Murthy, A.K.; Kaler, E.W. Styrene polymerization in three-component cationic microemulsions. Langmuir **1990**, *6*, 1040–1044.
45. Lusvardi, K.M.; Schubert, K.V.; Kaler, E.W. Microemulsions: a medium for polymerization reactions. Ber. Bunsenges. Phys. Chem. **1996**, *100*, 373–379.
46. Morgan, J.D.; Lusvardi, K.M.; Kaler, E.W. Kinetics and mechanism of microemulsion polymerization of hexyl methacrylate. Macromolecules **1997**, *30*,1897–1905.
47. Morgan, J.D.; Kaler, E.W. Particle size and monomer partitioning in microemulsion polymerization. 1. Calculation of the particle size distribution. Macromolecules **1998**, *31*, 3197–3202.
48. Co, C.C.; Kaler, E.W. Particle size and monomer partitioning in microemulsion polymerization. 2. On line small angle neutron scattering studies. Macromolecules **1998**, *31*, 3203–3210.
49. Antonietti, M.; Bremser, W.; Müschenborn, D.; Rosenauer, C.; Schupp, B.; Schmidt, M. Synthesis and size control of polystyrene latices via polymerization in microemulsion. Macromolecules **1991**, *24*, 6636–6643.
50. Girard, N.; Tadros, T.F.; Bailey, A.I. Polymerization of oil (styrene and methylmethacrylate)-in-water microemulsions. Colloid Polym. Sci. **1998**, *276* , 999–1009.
51. Antonietti, M.; Nestl, T. Polymerization in microemulsions with metallosurfactants. Macromol. Rapid Commun. **1994**, *15*, 111–116.
52. Antonietti, M.; Hemtze, H.P. Microemulsion polymerization: new surfactants systems by counterion variation. Adv. Mater. **1996**, *8*, 840–844.
53. Dreja, M.; Tieke, B. Polymerization of styrene in ternary microemulsion using cationic gemini surfactants. Langmuir **1998**, *14*, 800–807.
54. Dreja, M.; Tieke, B. Polymerization of styrene in ternary microemulsion using gemini surfactants with hydrophilic and hydrophobic spacer groups. Ber. Bunsenges. Phys. Chem. **1998**, *102*, 1705–1709.
55. Xu, X.; Ge, X.; Zhang, Z.; Zhang, M. Copolymerization of styrene with acrylates in emulsion and microemulsion. Polymer **1998**, *39*,5321–5325.
56. Ono, H.; Deng, Y. Flocculation andretention of precipitated calcium carbonate by cationicpolymeric microparticle flocculants. J. Coll. Int. Sci.**1997**, *188*,183–192.
57. Dreja, M.; Pyckhout-Jintzen, W.;Tieke, B. Copolymerization behaviour and structure of styreneand polymerizable surfactants in three-component cationicmicroemulsion. Macromolecules **1998**, *31*,272–280.
58. Dreja, M.; Tieke, B. Microemulsions withpolymerizable surfactants. γ-Ray inducedcopolymerization of styrene and11-(acryloyloxy)undecyl(trimethyl)am-

moniumbromide in three-component cationic microemulsion.Macromol. Rapid Commun. **1996**, *17*, 825–833.
59. Wang, L.; Liu, X.; Li, Y. Microemulsion polymerization of styrene using surface-active peresters as photoinitiators. Langmuir **1998**, *14*, 6879–6885.
60. Wang, L.; Liu, X.; Li, Y. Synthesis and evaluation of a surface-active photoinitiator for microemulsion polymerization. Macromolecules **1998**, *31*, 3446–3453.
61. Capek, I.; Juranicova, V. On the free-radical microemulsion polymerization of alkyl methacrylates. Eur. Polym. J. **1998**, *34*, 783–788.
62. Roy, R.; Laferrière, C.A. Synthesis of antigenic copolymers of N-acetylneuraminic acid binding to wheat germ agglutinin and antibodies. Carbohyd. Res. **1988**, *177*, C1–4.
63. Ericsson, J.; Hult, A. Novel degradable methacrylate and p-vinylphenoxy–based oligomers.1. Synthesis and characterization. Makromol. Chem. **1991**, *192*, 1609–1619.
64. Slany, M.; Bardaji, M.; Caminade, A.M.; Chaudret, B.;. Majoral, J.P. Versatile complexation ability of large phosphino-terminated dendrimers. Inorg. Chem. **1997**, *36*, 1939–1945.
65. Favero, C.; Graillat, C.; Guyot, A. Reactive surfactants in styrene microemulsion polymerization. Macromol. Symp. **2000**, *150*,235–240.
66. Li, P.; Xu, J.; Wu, C. Surface functionalization of polymer latex particles. III. A convenient method of producing ultrafine poly(methylstyrene) latexes with aldehyde groups on the surface. J. Polym. Sci. A Polym. Chem. **1998**, *36*, 2103–2109.
67. Margel, S.; Nov, E.; Fisher, I. Polychloromethylstyrene microspheres: synthesis and characterization. J. Polym. Sci. A Polym. Chem. **1991**, *29*, 347–355.
68. Verrier-Charleux, B.; Graillat, C.; Chevalier, Y.; Pichot, C.; Revillon, A. Synthesis and characterization of emulsifier-free quaternarized vinylbenzylchloride latexes. Colloid Polym. Sci. **1991**, *269*, 398–405.
69. Itsuno, S.; Moue, I.; Ito, K. Oxyethylene networks. Nucleophilic substitution reactions of chloromethylated polystyrenes in aqueous media. J. Chem. Soc. Chem. Commun. **1992**, 1599–1601.
70. Camps, M.; Chatzopoulos, M.; Montheard, J.P. Chloromethylstyrene: synthesis, polymerization, transformations, applications. J. Macromol. Sci. Rev. Macromol. Chem. Phys. 1982–83, *C22*, 343–408.
71. Pollak, A.; Blumenfeld, H.; Wax, M.; Baughn, L.; Whitesides, G.M. Enzyme immobilization by condensation copolymerization into cross-linked polyacrylamide gels. J. Am. Chem. Soc. **1980**, *102*, 6324–6336.
72. Schnaar, R.L.; Lee, Y.C. Polyacrylamide gels copolymerized with active esters. A new medium for affinity systems. Biochemistry **1975**, *14*, 1535–1541.
73. Batz, H.G.; Franzmann, G.; Ringsdorf, H. Pharmakologisch aktive polymere, modellreaktionen zur umsetzung von pharmaka und enzymen mit monomeren und polymeren reaktiven estern. Makromol. Chem. **1973**, *172*, 27–47.
74. Arshady, R. Functional Monomers. J. Macromol. Sci. Rev. Macromol. Chem. Phys. 1992, *C32* (1), 101–132.
75. Sherrington, D.C. Polymer-supported reagents, catalysts and sorbents: evolution and exploitation a personalized view. J. Polym. Sci. A Polym. Chem. **2001**, *39*, 2364–2377.
76. Haag, R. Dendrimers and hyperbranched polymers as high-loading supports for organic synthesis. Chem. Eur. J. **2001**, *7*, 327–335.

77. Vo-Dinh, T.; Cullum, B.M.; Stokes, D.L. Nanosensors and biochips: frontiers in biomolecular diagnostics. Sens. Actuators B. **2001**, *74*, 2–11.
78. Sumner, J.P.; Aylott, J.W.; Monson, E.; Kopelman, R. A fluorescent PEBBLE nanosensor for intracellular free zinc. Analyst **2002**, *127*, 11–16.
79. Taylor, J.R.; Fang, M.M.; Nie, S. Probing specific sequences on single DNA molecules with bioconjugated fluorescent nanoparticles. Anal. Chem. **2000**, *72*, 1979–1986.
80. Davda, J.; Labhasetwar, V. Characterization of nanoparticle uptake by endothelial cells. Int. J. Pharm. **2002**, *233*, 51–59.
81. Maruyama, A.; Ishihara, T.; Kim, J.S.; Kim, S.W.; Akaike, T. Nanoparticle DNA carrier with poly(*L*-lysine) grafted polysaccharide copolymer and poly(D,L-lactic acid). Bioconj. Chem. **1997**, *8*, 735–742.
82. Beauvais, R.A.; Alexandratos, S.D. Polymer-supported reagents for the selective complexation of metal ions: an overview. React. Funct. Polym. **1998**, *36*, 113–123.
83. Puranik, D.B.; David, V.A.; Morris, R.E.; Chang, E.L. Energy Fuels **1997**, *11*, 1311–1312.
84. Altava, R.; Burguete, M.I.; Frias, J.C.; Garcia-Espana, E.; Luis, S.V.; Miravet, J.F. Preparation of polymer-supported polyazamacrocyles: the role of the polymeric matrix in the preparation of polymer-supported polyazamacrocycles. Ind. Eng. Chem. Res. **2000**, *39*, 3589–3595.
85. Diallo, M.S.; Balogh, L.; Shafagati, A.; Johnson, J.H.; Goddard, W.A.; Tomalia, D.A. Poly(amidoamine) dendrimers: a new class of high capacity chelating agents for Cu(II) ions. Environ. Sci. Technol. **1999**, *33*, 820–824.
86. Blacker, N.C.; Findlay, P.H.; Sherrington, D.C. Synthesis of Cu(II)-complexed polymers and use as catalysts in the hydrolytic decontamination of sarin nerve agent. Polym. Adv. Technol. **2001**, *12*, 183–196.
87. Cameron, J.H.; Graham, S.; Harvey, H.B.; Liggat, J.J.; McKee, A.; Soutar, I.; Scott, E.L. Copolymer-supported metal complexes capable of binding dioxygen. React. Funct. Polym. **1998**, 36:173–183.
88. Wang, B.; Wasielewski, M.R. Design and synthesis of metal ion-recognition-induced conjugated polymers: an approach to metal ion sensory materials. J. Am. Chem. Soc. **1997**, *119*, 12–21.
89. Daubresse, C.; Grandfils, C.; Jerome, R.; Teyssie, P. Enzyme immobilization in nanoparticles produced by inverse microemulsion polymerization. J. Colloid Interface Sci. **1994**, *168*, 222–229.
90. Thöm, V.J.; Hosken, G.D.; Hancock, R.D. Anomalous metal ion size selectivity of tetraaza macrocycles. Inorg. Chem. **1985**, *24*, 3378–3381.
91. Alexander, V. Design and synthesis of macrocyclic ligands and their complexes of lanthanides and actinides. Chem. Rev. **1995**, *95*, 273–275.
92. Christensen, J.J.; Eatough, D.J.; Izatt, R.M. The synthesis and ion binding of synthetic multidentate macrocyclic compounds. Chem. Rev. **1974**, *74*, 351–384.
93. Daubresse, C.; Grandfils, C.; Jerome, R.; Teyssie, P. Enzyme immobilization in reactive nanoparticle produced by inverse microemulsion polymerization. Colloid Polym. Sci. **1996**, *274*, 482–489.

8

Hollow Particles

Synthetic Pathways and Potential Applications

ELODIE BOURGEAT-LAMI CNRS–LCPP, Villeurbanne, France

I. INTRODUCTION

Hollow particles, also called nanocapsules or microcapsules (depending on their size), are organic, inorganic, or hybrid particles composed of an outer polymeric shell and an inner void space. The cavity inside the hollow spheres can be filled with air or with a liquid phase (water or oil), and in some applications may contain a dissolved encapsulated active ingredient. A multitude of such systems can be found in microencapsulation technologies. The earliest developments in this field principally concerned the elaboration of micrometric capsules in the typical range 1–1000 μm in diameter. They were specifically designed to encapsulate inks, pigments, and dyes for printing and photographic applications, for instance. Although historically the first microencapsulation techniques in the pharmaceutical industry date back to the late 1800s, the concept of microencapsulation really achieved significant recognition in 1954 with the development of carbonless copy paper based on microencapsulated dyes [1,2]. Microencapsulation techniques then found extensive developments in the coatings, food [3], agricultural [4], and pharmaceutical industries. Manufacturing methods of microcapsules have been extensively reviewed in the series *Microcapsules*, *Microspheres and Liposomes* edited by Reza Arshady [5]. Synthetic procedures principally involve coacervation techniques, direct polymerization methods, physicochemical (emulsification/solvent extraction) and mechanical processes (extrusion, spraying). If up to now most published works have concerned the elaboration of capsules of large dimensions, in very recent years microencapsulation technologies have expanded down to the nanometer range with the elaboration of nanometric capsules. Such nanocapsules offer numerous promising applications in various domains of advanced materials, especially in architectural coatings, optics, electronics, and biotechnologies. For example, hollow latex particles are used as synthetic pigments in paper coating [6] and paint mate-

rials [7]. By scattering light, the voids contribute to increase hiding and opacity, whereas microspheres with large voids (typically 10–100 μm) are inefficient in such processes.

We aim in this chapter to give an overview of the techniques recently developed for the elaboration of hollow particles with diameters in the range of several tens of nm up to a few micrometers. Contrary to most of the macrocapsule products mentioned above, based on preformed polymers (either natural or synthetic), the majority of nanometer-sized capsules are produced by direct chemical routes. Owing to the intense interest for this category of particles, most aspects associated to their elaboration have been reviewed in recent articles [8–12]. Since it will be almost impossible to avoid overlap with these previous reports, instead of extensive details, this chapter provides a general description of the different techniques and highlights the most significant advances. The chapter is divided into three parts. In a first part, chemical processes based on dispersion technologies, including emulsion, miniemulsion, dispersion, and suspension polymerizations, are described. Such strategies enable us to prepare hollow spheres in high yields using more or less sophisticated processes and multisequential procedures. In a second approach, hollow structures are produced from coated particles with core-shell morphologies. In this synthetic strategy, colloidal nanoparticles are used as sacrificial templates that are selectively removed in a subsequent step to generate the void space. In a last section, polymer and surfactant assemblies into vesicles, micelles, and other segregative morphologies are reported as a tool to elaborate hollow nanostructures with small dimensions and outstanding properties. Finally, potential applications of nanocapsules and hollow latexes are briefly described and illustrated by typical examples. Although voided particles are of great interest in a variety of domains, here the emphasis is placed on the potentialities of hollow particles in biotechnologies.

II. HOLLOW PARTICLES OBTAINED THROUGH DIRECT POLYMERIZATION TECHNIQUES

The possibility of synthesizing hollow particles by direct polymerization techniques, i.e., emulsion, miniemulsion, dispersion, suspension, and interfacial polymerizations, has constituted a major development in the field of polymer colloids in the last 20 years. Owing to the intense interest of industries for hollow spheres, it is not very surprising to see that most published works in this field are in the patent literature [13]. The earliest processes for making hollow latex particles have been developed in the research laboratories of Rohm & Haas [14]. Since their pioneering work, continuous efforts have been done to bring new developments and improve the existing technologies. This section describes the main synthetic strategies and briefly reports on recent advances in this area.

A. Emulsion and Miniemulsion Polymerizations

Fundamental and technical aspects associated to the elaboration of hollow latex particles through emulsion polymerization have been recently reviewed by McDonald and Devon [10]. Two synthetic approaches can be broadly distinguished. One prominent technique involves making a structured particle with a carboxylated core polymer and one or several outer shells. Ionization of the core material with bases under convenient experimental conditions expands the core by *osmotic swelling* (OS) and produces hollow spheres containing water and polyelectrolyte in the interior (Fig. 1).

The osmotic swelling technique largely dominates the literature. Based on the same general concept, a variety of alternative procedures describing the preparation of hollow latexes of all sizes and characteristics have been reported in successive patents. The principal structural variations concern the number of concentric shells surrounding the carboxylated core polymer and the experimental conditions required for ionization and expansion of the inner part of the structured particles. In a typical procedure, the core latex particles are composed of at least two monomers and contain around 10–30 wt % of an ionizable compound, which is principally an alkali-swellable carboxylic acid monomer. In order to overcome the problems encountered with ionic comonomers (e.g., instability induced by the formation of water-soluble oligomeric species that behave as flocculants), low molecular weight organic acids (e.g., benzoic acid or acid anhydrides) have also been reported. Next a hard polymeric shell, based on styrene or a mixture of styrene and methyl methacrylate, is formed onto the previously obtained carboxylated core latexes. Special care is taken at this stage to avoid forming a second crop of particles by renucleation. Indeed, the formation of an hydrophobic shell onto the hydrophilic carboxylic core is not the

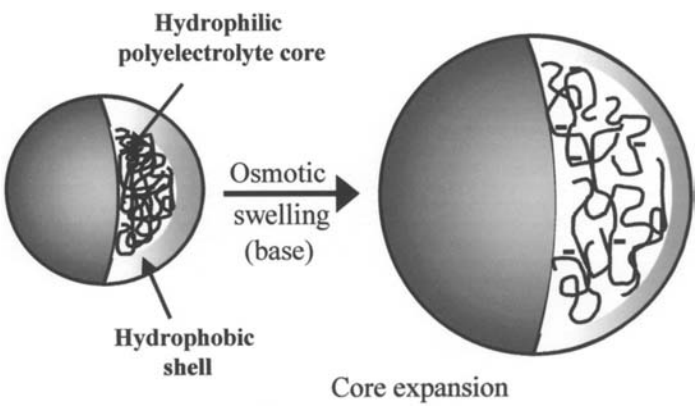

FIG. 1 Principle of formation of hollow latexes by the osmotic swelling process.

preferred morphology and full encapsulation of the core polymer is problematical. Alternative procedures, into which second-stage monomers are introduced in multistep sequences under starved feed conditions, are described in order to gradually decrease the polarity of the surface and promote the formation of a regular encapsulating polymer shell. This ensures a control over the hydrophilicity from the inner layer to the outer layer of the shell. The use of cross-linking monomers has also been described to minimize interdiffusion of polymer chains and help stabilize the morphology. In the final step of the process, the carboxyl groups of the core particles are ionized upon addition of a base that permeates the shell by osmotic swelling. Neutralization of the carboxyl groups expands the core and increases the particle volume, leaving behind a void when the water is removed. As described in most patents, the expansion temperature is a critical parameter. The particles must be heated above the softening point of the shell polymer to ensure efficient diffusion of the base from the water phase to the core polymer. In addition, the shell must have significant cohesion and thermoplastic flow properties so as to avoid collapse when the temperature is decreased back to ambient. Attainable void volume fractions by the osmotic swelling technique are in the range 30–50%. A typical illustration of the morphology of the resulting hollow spheres, commercially available under the name Ropaque, is shown on the transmission electron microscopy (TEM) image of Fig. 2.

Despite the industrial interest in voided particles, there are surprisingly very few academic reports on the fundamental aspects associated with the formation of hollow latexes by the osmotic swelling technique [15,16]. Indeed, most publications principally concern the properties and applications of the hollow spheres with no consideration of the synthetic procedure [7,17]. However, as shown before, elaboration processes often turn out to be much more sophisticated than previously described, and many aspects related to the preparation of the hollow latexes and control over the morphology remain unclear. Vanderhoff and coworkers, for instance, described the synthesis of complex multishell latexes and reported on the influence of the hydrophilicity of the core and shell monomers on the final morphology [15]. More recently, Pavlyuchenko et al. [16] systematically investigated the role of synthetic parameters on the formation of the hollow spheres, studying each of the synthesis steps separately to elucidate the effects of the various factors on the characteristics of the intermediate products and their influence on the final performance of the resulting hollow particles. They again underlined the determinant role of the processing conditions (i.e., starved feed addition of the monomers) on morphology, and indicated the necessity to heat the latex above the T_g value of the shell polymer for optimal swelling. The highest degrees of core expansion were obtained for equimolar carboxyl groups/base ratios. Among the academic reports, it is worth mentioning equally the articles by Okubo and coworkers on the synthesis of hollow [18] and multihollow [19] polymer spheres by the so-called stepwise alkali/acid method.

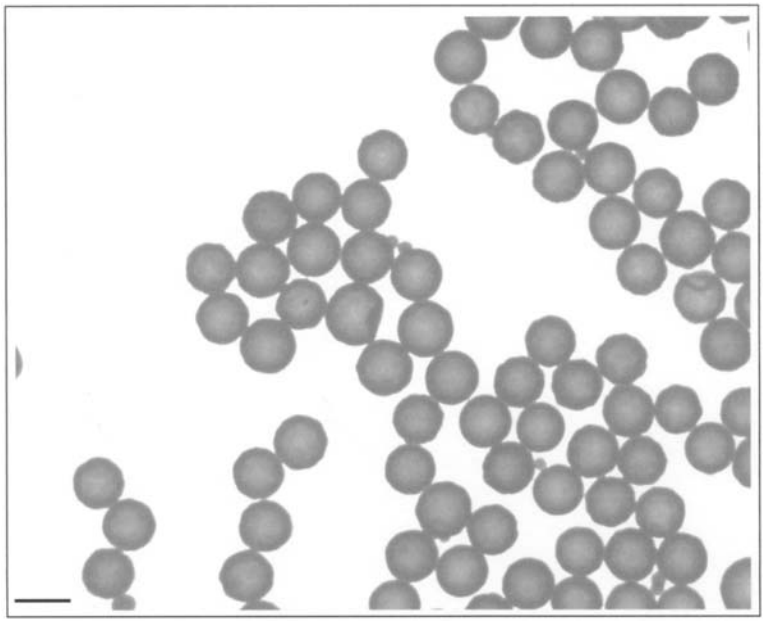

FIG. 2 TEM image of hollow polymer spheres produced by the osmotic swelling technique. Scale bar: 1 μm.

Although their technique presents some analogies to the osmotic swelling method, the main difference is that the hollows are generated in a single reaction, directly from uniform carboxylated polymer particles by consecutive addition of a base (KOH) and an acid (HCl). The particles swell under alkaline conditions and the ionic polymer moves toward the outside of the particle owing to its strong affinity with water. The swollen particles shrink during the acid treatment to give hollow particles of smaller size than the original beads. Contrary to the osmotic swelling technique, which produces particles containing one central hollow, the stepwise alkali/acid method principally gives multihollow particles. As an alternative procedure, the authors also demonstrated the possibility of producing multihollow structures from particles containing acid-swellable copolymers using the reverse method into which the particles are treated first by an acid and then by a base [20]. A similar alkali/acid treatment was performed by Yuan et al. on a series of core-shell particles [21]. As expected, only the carboxylated latexes gave rise to a hollow structure.

A second, much less developed approach involves using a dispersed ternary system composed of one or several monomers, oil, and water. The oil phase (preferentially a hydrocarbon) is a nonsolvent for the polymer being formed, and

phase separation takes place during the polymerization process. The technique, referred to as *hydrocarbon encapsulation*, was first patented by McDonald [13b], and further described in the open literature [22]. The thermodynamic and kinetic factors governing the morphology have been investigated in detail and modeled. A schematic representation of this approach is shown in Fig. 3.

The technique proceeds as follows: In the early stage of the process, a low molecular weight polymer (typically below 50,000 g/mol) is formed that promotes swelling and subsequently serves as the locus of polymerization. A chain transfer agent and a water-miscible alcohol are initially introduced to control molecular weight. As polymerization continues, the macromolecules become progressively incompatible with the oil phase and concentrate at the interface with water. The hollow morphology is further stabilized by addition of a second monomer charge containing a cross-linking agent. In a similar approach, Landfester and coworkers recently described the preparation of polymeric nanocapsules by miniemulsion polymerization [23]. As before, the process involves polymerizing a monomer in a dispersed hydrocarbon–monomer mixture. The morphology of the demixing polymer phase was controlled by the type and

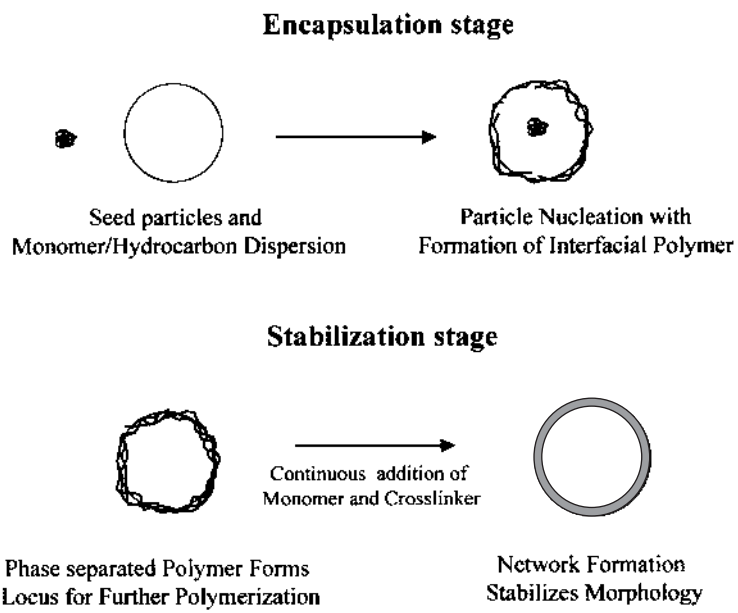

FIG. 3 Schematic representation of the hydrocarbon encapsulation technology. (From Ref. 22, with permission.)

amount of surfactant used to stabilize the particles, the polarity of the monomer, and the monomer-to-hydrophobe ratio. The differences in the hydrophilicity of the oil and the polymer turned out to be the driving force for the formation of the nanocapsules.

In alternative strategies, core latexes were synthesized in a preliminary step and swelled in good solvents for the polymer. A shell was subsequently formed onto the swollen seed particles. Phase separation and encapsulation took place when the core and shell polymers were of significantly different nature and polarity or when the shell was cross-linked [24]. For instance, hollow particles have been produced by seeded emulsion copolymerization of methyl methacrylate, methacrylic acid, and divinylbenzene (DVB) using polystyrene (PS) latexes as the seed [25,26]. Cross-linking at the surface of the monomer-swollen particles allowed phase separation to proceed at the corresponding polymer–water interface, thus producing a void space inside the hollow spheres.

B. Suspension and Dispersion Polymerizations

Experimental procedures similar to those reported above have been developed to generate macroporous cross-linked polymer particles for applications in separation processes [27]. Such particles are generally produced by suspension polymerization involving addition of a solvating and a nonsolvating diluent to the polymerizing mixture. After polymerization, the inert diluent is removed by solvent extraction or steam distillation, leaving a porous structure within the polymer particles. Following this procedure, the obtention of microcapsules having a single hollow in the inside have been reported by Okubo and coworkers [28,29]. The process involves polymerizing highly swollen DVB/toluene suspension droplets containing dissolved PS. Only the systems containing a sufficient amount of PS gave a hollow structure. However, the suspension process yields relatively broad size distributions and relatively large particles, which is disadvantageous with regard to packing efficiency and flow conditions in separation columns. In a series of subsequent works, improved procedures have been developed that consist of utilizing a novel swelling approach to seed polymer particles with a large amount of monomer called the *dynamic swelling method* [30]. Typically, DVB, benzoyl peroxide, poly(vinyl alcohol), and toluene were dissolved in an aqueous ethanolic suspensions containing micrometer-sized monodisperse PS seed particles, produced in dispersion polymerization. In a subsequent step, water was slowly added to the suspension to promote dynamic swelling of the particles. A seeded dispersion polymerization of the monodispersed (toluene/DVB)-swollen PS particles was then carried out to produce the hollow spheres. In an alternative procedure, a chemical oxidative seeded dispersion polymerization of 3,5-xylidine was performed onto PS seed particles to generate monodispersed, multihollow, PS/poly(3,5-xylidine) composite particles [31].

C. Interfacial Polymerizations

Submicrometer-sized capsules can also been produced by interfacial polymerization. Such polymeric capsules are potential carriers for delivery of pharmaceutically active compounds and have been widely studied in the past. Preparation of polyalkylcyanoacrylate nanocapsules, for instance, has been extensively described in the literature, and their potential values for a variety of pharmaceutical applications has been widely discussed. Since these aspects are reviewed in Chapter 28 of this volume [32,33], it is beyond the scope of this section to go into more details.

III. HOLLOW PARTICLES BY COLLOIDAL TEMPLATING

Aside from the direct polymerization techniques described above, templating approaches have been developed as means to mold the shape and control the size of the capsules. Various templates have been used for that purpose, including inorganic particles, polymer colloids, block copolymer micelles, and emulsion droplets. Contrary to the chemical route described previously, the obtention of hollow colloids by the templating approach involves three successive steps (Fig. 4).

1. Synthesis of the core material with the desired surface group and reactivity
2. Coating of the templating core material with an organic, inorganic, or hybrid shell, and
3. Removal of the templating core by chemical, physicochemical, or thermal treatment

The templating approach thus requires in a previous step the use of nanocoating technologies to elaborate core-shell materials with uniform shapes and surface characteristics. Such technologies have been extensively developed in

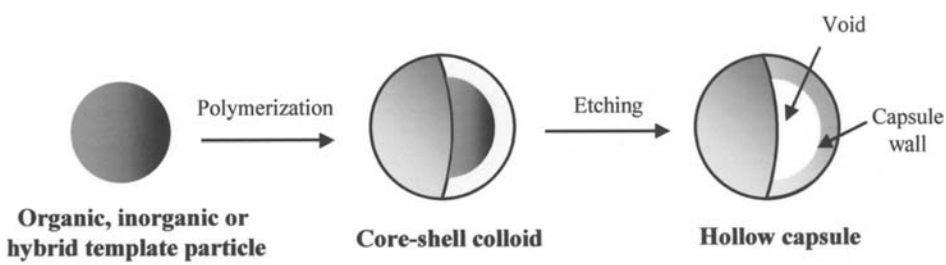

FIG. 4 Synthetic scheme for synthesis of hollow particles by colloidal templating.

recent years. The interest in the nanoengineering of particle surfaces mainly lies in the potentialities of this special class of materials in a variety of domains from the paint industry to biotechnologies. The coating is performed to protect the nanoparticles from chemical (oxidative, thermal, photochemical) and physical degradations, to improve their dispersion, or to impart specific properties to the colloid (magnetic, optical, catalytic, etc.). Readers interested to this topic should refer to recent reviews on the subject [34]. In addition to the above-mentioned interest, nanoengineering of particle surfaces also offers the possibility of controlling the shape of the resulting material by using templates of well-defined sizes and characteristics. Once the template is removed from the composite particles, replicas are formed that present interesting structural properties.

A. Inorganic Particles as Template

Inorganic colloids can be advantageously used as templates to generate organic, inorganic, and hybrid capsules. A range of hollow spheres have been prepared in this manner using silica materials as sacrificial templates. For example, monodispersed core-shell colloidal spheres of silica (SiO_2) and zinc sulfide (ZnS) have been elaborated by templating silica colloids [35]. Coating of SiO_2 with ZnS was performed in water–ethanol solutions by direct precipitation of ZnS onto the silica seed using thermally activated thioacetamide as a source of sulfide ions and acidic zinc nitrate aqueous solutions. Hollow ZnS spheres were obtained in a subsequent step by dissolving the SiO_2 core in hydrofluoric acid. Surprisingly, the ZnS shell dissolved slowly under these conditions and the particles retained their original shape. The reverse structure, composed of ZnS core coated with silica, was elaborated in a similar way by templating zinc sulfide colloids with tetraethoxysilane using a seeded growth technique adapted from the Stöber method. A mineral nitric acid, much less aggressive than HF, was used in this case to selectively dissolve the ZnS core from the structured particles. The resulting hollow spheres (either the silica shells or the high-dielectric ZnS capsules) were shown to display interesting optical properties with potential applications as colloidal crystals in photonic devices. The coating of silica with polymers has also been reported in several academic works [36]. Unfortunately, no mention was made in these articles of the possibility of producing organic capsules by chemical etching of the inorganic template although this could be theoretically envisaged. Another extensively described group of templating materials are gold colloids [37,38]. The coating of gold nanoparticles with silica has been reported by Mulvaney and coworkers. Coating serves first to stabilize particles against coagulation and also promotes ordering of the nanoparticles into two-dimensional arrays [37]. Their method involves three successive steps (Fig. 5). The gold surface was first rendered vitreophilic by addition of 3-aminopropyltrimethoxysilane, which strongly adsorbed on the metal. The anchored

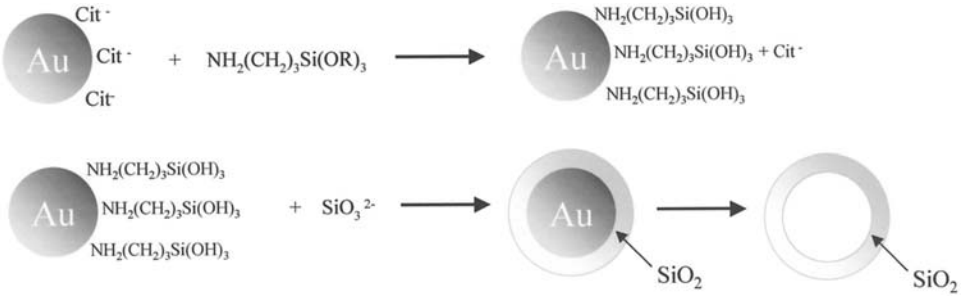

FIG. 5 Synthetic scheme involved in the coating of gold colloids with silica and the subsequent formation of hollow silica spheres.

silanol groups were then involved in the formation of a thin silica layer by direct precipitation of a native sodium silicate solution. In a final step, extensive growth was performed in ethanol–water mixtures using tetraethoxysilane (TEOS) as a precursor to afford silica-coated gold nanoparticles with shell thickness up to 80 nm. Again, the coated nanosized silica/gold colloids were shown to display very interesting optical properties [39]. Hollow silica capsules were obtained from the coated colloids by exposing the particles to cyanide ions [38]. The oxidized gold cores completely dissolved and diffused out of the silica shell. Several studies on silica particles grown using TEOS clearly attest for the presence of micropores ranging in size from 2 to 50 nm. The resulting microporous and hollow shell particles are potential carriers for slow release and drug delivery.

Inversely, gold particles have been reported to be useful templates for the growth polymerization of conductive polypyrrole and poly(*N*-methylpyrrole) on their surface [40]. The polymer–gold composite particles were converted in a subsequent step to hollow polymeric nanocapsules by chemical etching of the colloidal gold template. Not only were the gold particles useful templates but they also made it possible to entrap guest molecules in the capsule core: rhodamine B isothiocyanate (Structure 1). The loaded dye remained encapsulated in the hollow spheres after gold etching. This synthetic method obviously offers an interesting approach to guest encapsulation and could potentially be extended to the entrapment or enzymes and proteins.

Apart from the formation of dense coatings, self-assembly also provides an original and efficient way to modify particle surfaces [41]. The formation and structure of self-assembled monolayers (SAMs) and their use in surface engineering has been much described and recently reviewed [42]. On the other hand, the potentialities of polyelectrolyte self-assembly have been extensively explored over the last decade or so and will be reported below. For instance,

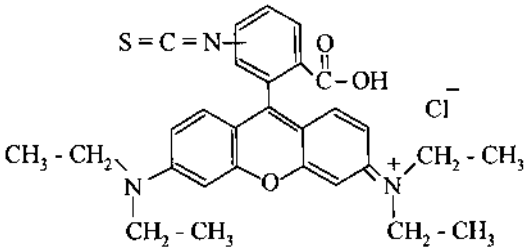

Structure 1

alkanethiol derivatives are known to self-assemble onto gold colloid surfaces in a monolayer fashion via a surface complexation reaction [43]. If convenient reactive groups are incorporated into the SAM, additional chemical reactions can be envisaged in order to elaborate core-shell particles and hollow capsules after degradation of the internal core (Fig. 6).

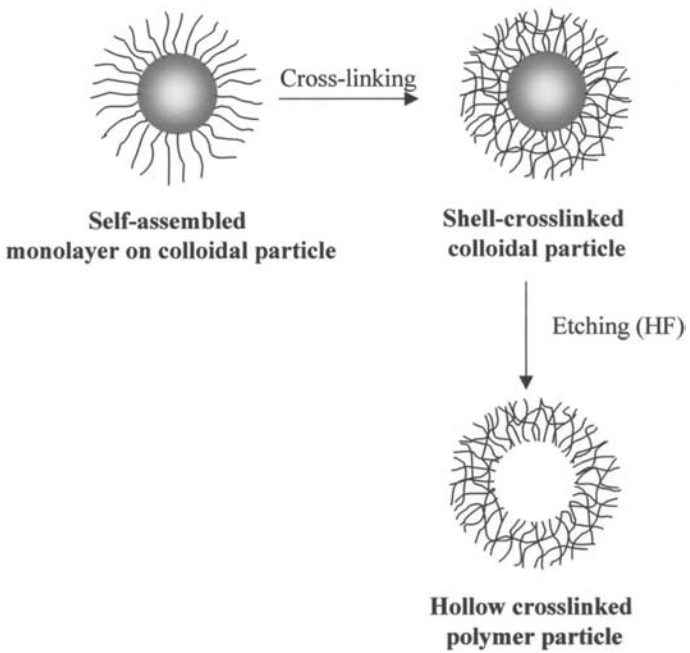

FIG. 6 Formation of shell-cross-linked capsules from self-assembled monolayers on colloidal surfaces.

Shell-cross-linked polymeric nanocapsules have been synthesized for instance by metathesis polymerization of alkene–functionalized alkylthiolate monolayers attached on gold surfaces [44]. The thiolated ligands were designed to maximize polymer cross-linking and contained three alkene groups. In a related work, Sun and coworkers reported on the preparation of monolayer-thick polymeric spheres by assembling thiolated-β-cyclodextrins (β-CD-SH) (Structure 2) around gold nanoparticles (Fig. 7) [45]. The core dissolved upon addition of iodine to the suspension while simultaneously disulfide bonds were formed on the surface to produce structurally rigid cross-linked nanocapsules.

Core-shell particles can also be elaborated by templating inorganic colloids with polymer brushes using living polymerization techniques. For example, hybrid nanoparticles with a block copolymer shell structure have been synthesized

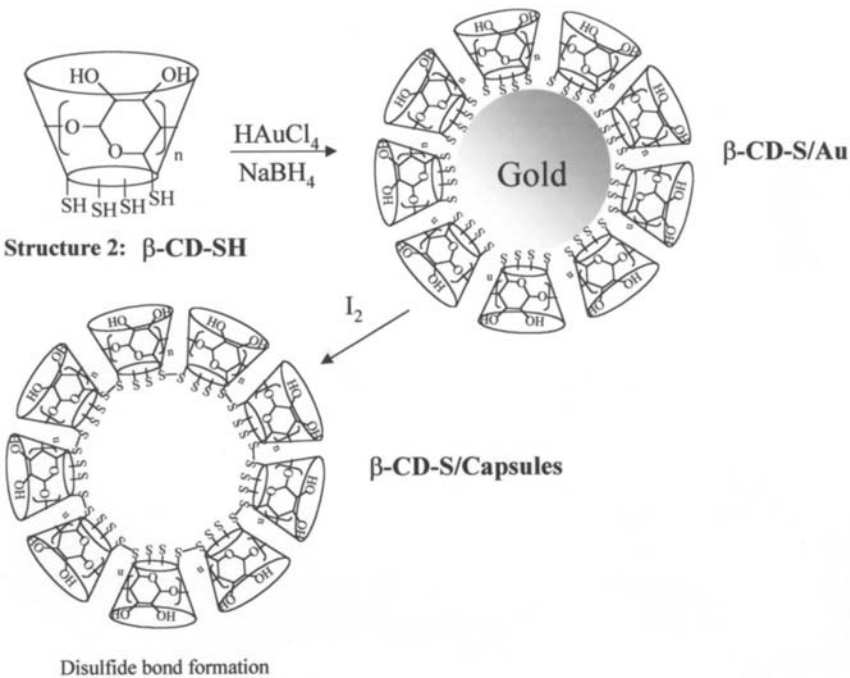

FIG. 7 Preparation of polycyclodextrin hollow spheres by templating β-CD-SH monolayers around gold nanoparticles. Disulfide bridges were formed upon reaction with iodine while simultaneously the core dissolved into metallic complexes to give shell-cross-linked hollow spheres.

by ring-opening polymerization of norbornenyl groups immobilized on gold colloids [46]. Shell-cross-linked polymeric capsules have been elaborated in a similar way by templating of colloidal silica with polymeric compounds and cross-linking of the polymer shell. The shell was produced by surface-confined living atom transfer radical polymerization (ATRP) initiated from the templates [47]. The silica core was subsequently dissolved by HF treatment, resulting in hollow capsules. More recently, Hawker and colleagues synthesized cross-linked, hollow polymeric spheres in a multistep procedure [48]. Micrometric silica beads were first modified by grafting on their surface polymer chains via a living free-radical polymerization procedure using a surface-attached alkoxylamine initiator. The polymer chains were designed so as to carry functional groups for further cross-linking reactions, such as maleic anhydride (Fig. 8). A diamine cross-linker was added in a second step to effect interchain coupling via the formation of a bisimide. The inorganic silica template was finally removed in a last step by chemical etching.

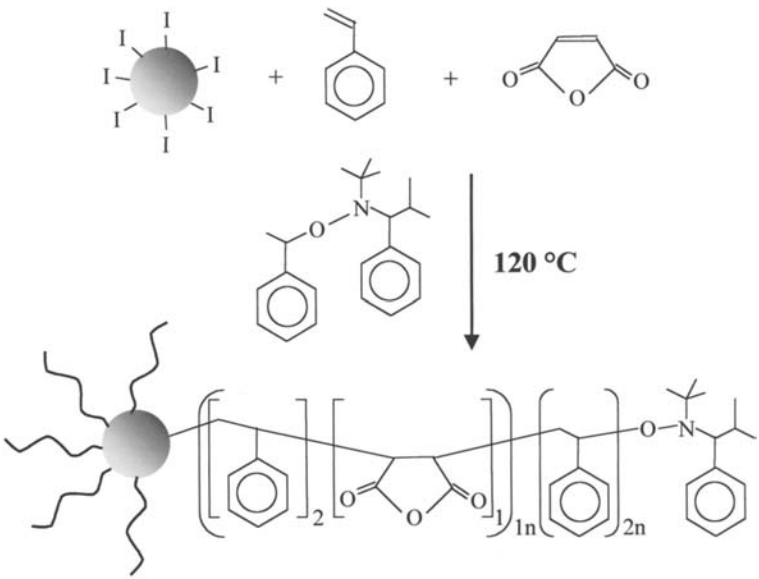

FIG. 8 Synthetic scheme for the preparation of maleic anhydride–functionalized silica beads. (From Ref. 48, with permission.)

B. Polymer Colloids as Template

Coating of polymer colloids with materials of different chemical compositions gives access to nanocomposite particles with tailored structures and morphologies. Contrary to inorganic templates that require relatively harsh conditions to decompose, organic colloids can be easily removed either chemically or thermally without damaging the shell materials. A large variety of such structures involving polymer latexes as sacrificial templates can be found in recent literature. For instance, submicrometer-sized hollow spheres of yttrium and zirconium compounds have been prepared by coating cationic polystyrene latex particles with basic yttrium carbonate [49] and basic zirconium sulfate [50], respectively, followed by calcination. Uniform coatings of copper [51] and iron [52] compounds have been formed in a similar way by aging at high-temperature aqueous solutions of the metal salt in the presence of urea, poly(*N*-vinylpyrrolidone) (PVP), and anionic polystyrene latexes. The coating was shown to proceed by *in situ* heterocoagulation of the precipitating metal colloids on the organic seed surface. Voids were produced in a subsequent step by complete thermal oxidative decomposition of the polymer core.

In related works, the coating of polystyrene latex particles with amorphous titanium dioxide has been achieved by the hydrolysis of titanium tetrabutoxide [53] and titanium tetraethoxide [54] in ethanolic suspensions. Due to the fast reactivity of the titanium alkoxide precursor in the sol-gel process, mixed suspensions with secondary titania particles were mostly produced. Optimal conditions were found to prevent the formation of separate particles and afford a regular coating. In order to overcome these difficulties, another approach, consisting of using cationic polystyrene particles as the seed, has been developed [55]. The positive charges on the surface ensured quick deposition of the titania precursors on the seed particles in the early beginning of the sol-gel reaction. Very thin (typically in the range of a few nanometers up to 50 nm), and smooth coatings were thus produced by a one-step method. Crystalline hollow spheres were further obtained by calcination of the TiO_2-coated particles at elevated temperatures. Increasing the temperature up to 600°C yielded hollow crystalline anatase titania particles whereas the rutile form of TiO_2 was obtained by calcining at 900–1000°C [56,57]. As an alternative solution, the latex core was dissolved by suspending the coated particles in toluene, a good solvent for the polymer.

Using a similar technique, Margel and coworkers described the coating of large polymer beads with silica and magnetic iron oxide [56]. The coating was performed by seeded polymerization of tetraethoxysilane and iron salts on micrometer-sized polystyrene seed particles. The polymer surface contained adsorbed PVP, which obviously played an active role in the coating procedure. However, separate inorganic nanoparticles were formed in this process that were

separated from the coated polymer beads by repeated centrifugations. Core removal was performed thermally and the hollow capsules were visualized by TEM from cross-sections of the particles. With the aim of improving chemical interaction between the core and shell materials, we have recently developed a coating strategy based on a two-step procedure (Fig. 9). Polymer latex particles carrying silanol groups on their surface were first synthesized in emulsion polymerization using 3-trimethoxysilylpropyl methacrylate (MPS) as a functional comonomer [57]. Then a silica shell was produced onto the functionalized PS seed particles by addition of tetraethoxysilane and ammonia to the colloidal suspension either in water [58] or in a mixture of ethanol and water [59]. No separate silica particles were formed in this work, indicating a strong affinity of the sol-gel precursor for the polymer colloid (Fig. 10). The SiOH-functionalized latexes have been extensively characterized using AUGER, solid-state nuclear magnetic resonance (NMR), and infrared spectroscopies [59]. The surface charge density was determined by chemical titration and was found to vary between

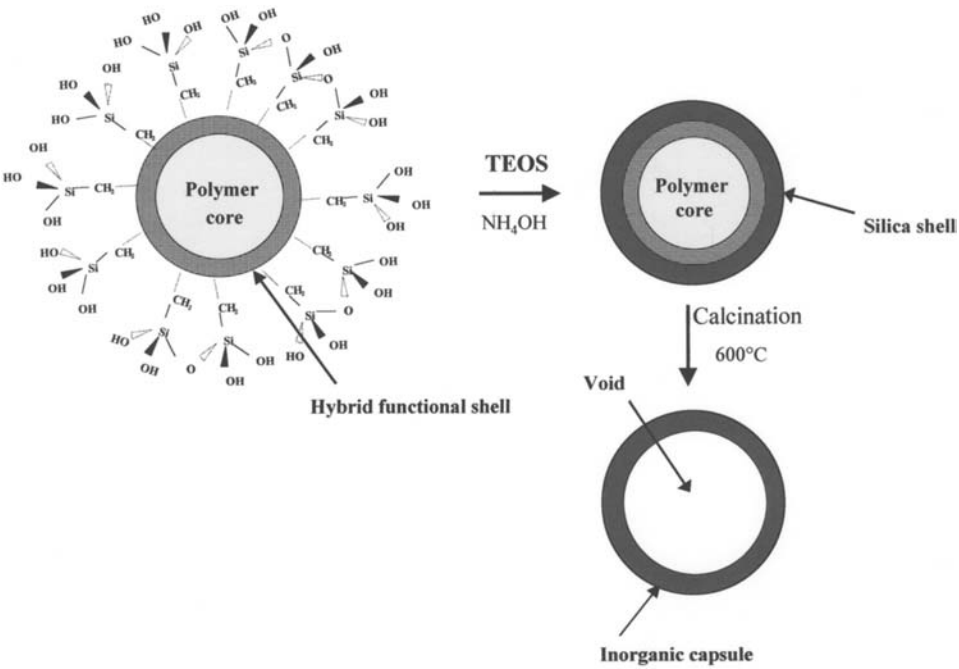

FIG. 9 Synthetic scheme for the formation of hollow silica nanoparticles from SiOH-functionalized latex particles.

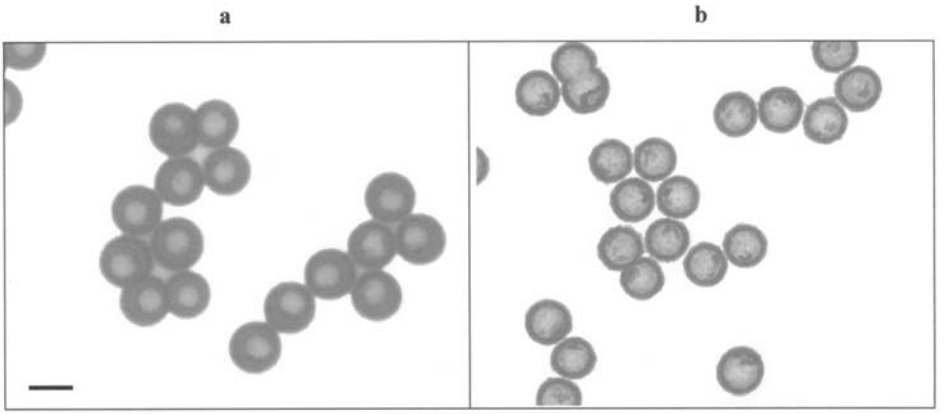

FIG. 10 TEM image of (a) hybrid latex particles and (b) hollow silica spheres. (From Ref. 58, with permission.)

1.15 and 3.7 $\mu C/cm^2$ depending on the MPS content in the monomer mixture. We demonstrated that the shell thickness and the void volume can be finely tuned by this technique.

Not only can inorganic precursors be used for coating, but preformed particles can also be homogeneously deposited onto sacrificial templates to generate core-shell structures. For instance, colloidal clay nanosheets have been adsorbed onto cationic polystyrene latexes as a thin and crystalline layer [60]. Tetramethoxysilane was used as inorganic precursor to consolidate the coating and increase shell stability. The polymer template was removed in a next step to generate hollow silicate capsules.

Pure carbonaceous organic capsules have also been produced from core-shell polystyrene/polyacrylonitrile colloids [61]. The polystyrene core was decomposed by pyrolysis of the particles in an argon atmosphere while simultaneously the polyacrylonitrile units were converted to carbon. The higher the polystyrene content in the particles, the thinner was the shell wall. Large pores were created by the release of the pyrolyzed products from the particles.

A convenient approach that combines colloidal templating and self-assembly strategies, first developed by Caruso and Möhwald's research group, has been extensively described in the last 5 years [12]. The general concept involves forming a sequential alternate layer-by-layer (LbL) deposition of polyelectrolytes [62], or polyelectrolyte and nanoparticles [63–67] through electrostatic self-assembly onto sacrificial polymeric colloidal templates. Removal of the or-

ganic core and the bridging polymer by chemical (dissolution, etching) or thermal treatments generates the hollow structure (Fig. 11).

By using this technique, determinant parameters such as size, composition, geometry, wall thickness, and uniformity can be precisely controlled. A huge variety of such hollow spheres has been successfully produced over a wide range of micrometer and submicrometer inner diameters, and the thickness and permeability of the walls has been varied by proven formulation variations. The investigated organic seeds are melamine-formaldehyde (MF) resins [62] and

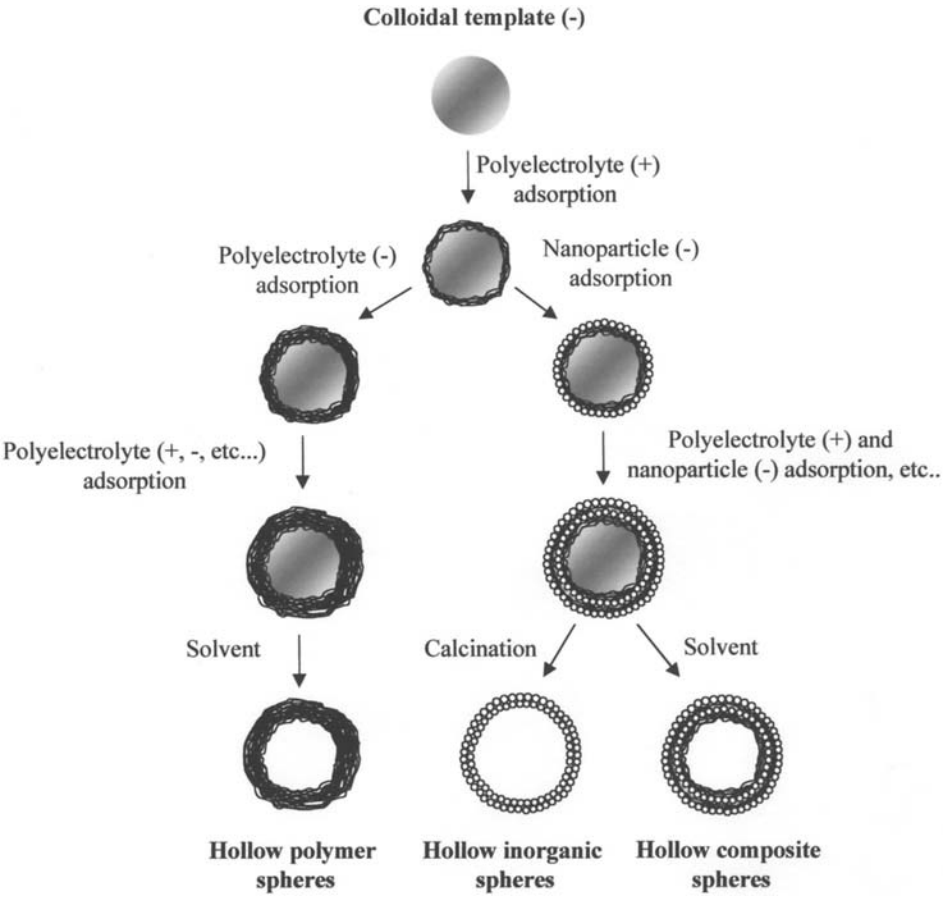

FIG. 11 Schematic representation of the steps involved in the synthesis of hollow particles using the LbL self-assembly technique. (From Ref. 12, with permission.)

polystyrene latex particles [63–67], although other templates (e.g., silica) have also been described. Poly(allylamine hydrochloride) (PAH), poly(sodium 4-styrenesulfonate) (PSS), and poly(diallyldimethylammonium chloride) (PDADMAC) have been used as the polyelectrolyte. Among the inorganic particles, silica [63–65], titanium dioxide [65], clays [65], zeolites [66], and iron oxide [67] have been successively reported. When MF colloids are used in place of PS, acid treatment is performed to chemically dissolve the core and generate the hollow spheres. For illustration, Fig. 12 shows a SEM image of MF particles coated with alternate layers of PSS and poly(allylamine) and the corresponding hollow spheres after core dissolution (Fig. 12b). Alternative procedures involve using inorganic precursors instead of preformed nanoparticles [68,69]. For example, water-soluble titanium(IV)bis(ammonium lactado) dihydroxide has been used to uniformly coat PS templates by a thin titania layer [68]. A regular and smooth coating was obtained by this approach.

The LbL nanoengineered capsules may potentially find applications as delivery systems and in biotechnology. For instance, magnetic hollow spheres are of particular interest in diagnostics and bioseparations where the particles can be selectively oriented and directed by application of an external magnetic field. The elaboration of magnetic colloidal supports and their utilization in the biomedical field are extensively described in Chapter 11 (Preparation of Magnetic Latices) in this volume. Potential applications of LbL engineered nanocapsules are reviewed below.

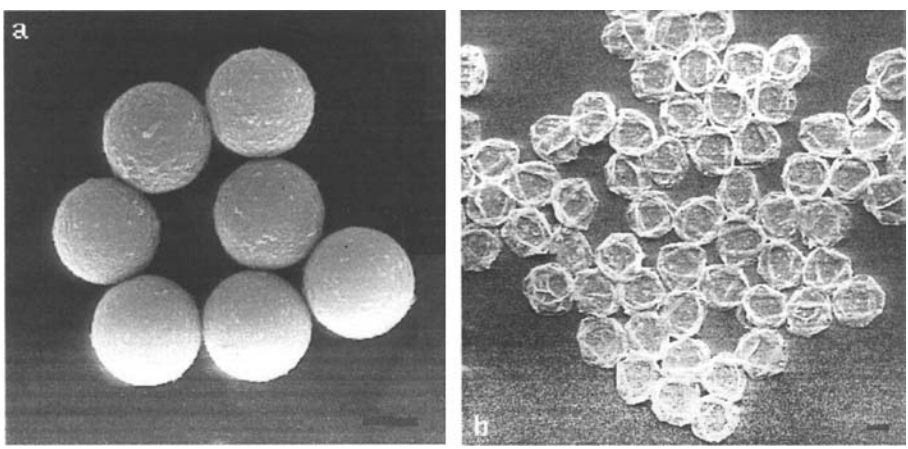

FIG. 12 (a) SEM micrographs of MF particles coated with nine layers of polyelectrolyte (PSA and PAH) and (b) the remaining hollow spheres after dissolution of the core at pH 1.3. (From Ref. 62b, with permission.)

C. Unconventional Templating Materials

A variety of organic and inorganic templates that do not fit into the aforementioned categories has been reported in the literature [70–73]. For example, poly(L-lysine) aggregates have been used as templates for the formation of hollow silica spheres [70]. Silica transcription was carried out by the addition of TEOS to aqueous solutions of poly(L-lysine) HBr in the presence of an organic amine, e.g., benzylamine. The amine was used as a basic catalyst for the sol-gel process and was shown to assist the transcription procedure by hydrogen-bonding to the silicate precursor. Biocolloids of human erythrocytes have been templated by nine alternating layers of PSS and PAH using the LbL technique [71]. After wall formation, the templating erythrocyte core was oxidatively decomposed in an aqueous solution of sodium hypochlorite. The products of decomposition were expelled through the multilayered shell wall and removed by extensive washing. An organic acidic dye 6-carboxyfluoroscein, was solubilized at high pH and loaded inside the nanocapsules. Lowering the pH to 6 enabled precipitation and physical entrapment of the dye within the hollow spheres. Similarly, microcrystalline and fluorescent compounds (e.g., pyrene and fluorescein diacetate, respectively) have been used as model uncharged organic templates in the LbL technique to investigate the potentiality of the polyelectrolyte assembly method in microencapsulation technology [73]. The encapsulated core molecules dissolved in an organic solvent, and their release behavior was monitored as a function of time using fluorescent spectroscopy.

In addition to the above-mentioned systems, a large variety of biological materials capable of generating original self-assembled structures can be found in the literature. Supramolecular assemblies of biomolecules into spherical, vesicular, and gel-like structures have found increased interest as templates for coating procedures by the sol-gel technique [37,74,75]. Hollow spheres and fibers can be produced by this approach. The formation of molecular and macromolecular aggregates and their use as template to direct the growth reaction of inorganic and organic polymers are described in the following section.

IV. VESICLES, LIPOSOMES, AND ASSEMBLIES

Hollow nanostructures can be elaborated from the assembly of preformed polymers into spherical aggregates. The ability of amphiphilic diblock copolymers, dissolved in a selective solvent, to self-assemble into colloidal size aggregates has been studied for several decades [76]. Core-shell architecture of micelles prepared from amphiphilic polymers permits the dissolution of large amounts of poorly water-soluble drugs, for instance, and affords protection against a potentially damaging environment. On the other hand, phospholipid molecules and synthetic amphiphiles with two long aliphatic chains attached to an ionic

head group are insoluble in water and are known to form highly ordered layers [77]. The bilayer structures separate an aqueous interior from an aqueous exterior and are versatile carriers in the area of drug delivery. The elaboration of vesicular, micellar, and related aggregate structures with hollow morphologies are briefly reviewed in this section. A fulfilled description of these systems can be found elsewhere [77,78].

A. Vesicles

Surfactant vesicles are an important class of bilayer aggregates that are extensively used as model membranes for artificial cells. They are nonequilibrium structures that are mostly kinetically stabilized. Vesicles are usually produced by shear-assisted means including sonication and extrusion. However, owing to the non-covalent interactions responsible for their formation, these nano-objects have only limited stability and inherently return to their native lamellar phase state. A variety of techniques has been employed in order to increase vesicle stability. One method involves using reactive polymerizable surfactants and polymerize the vesicle [79]. Another technique takes advantage of the bilayer morphology of the surfactant aggregates to solubilize organic substances such as monomers. Subsequent polymerization of the vesicles gives hollow spheres whose shape is a replica of the original bilayer structure (morphosynthesis). The shell is cross-linked so as to afford rigid and stable capsules after extraction of the templating surfactant matrix (Fig. 13). Pioneering work in this field has been done by Murtagh and Thomas [80]. Since that, polymerizations into vesicle bilayers have attracted much interest and have been reported by several groups [81–83]. Although it has been suggested by many authors that polymerized vesicles are indeed hollow, another morphology, into which the polymer forms separate domains giving rise to parachute-like architectures, has also been reported [82]. In addition to morphosynthesis, vesicles can also be used as templating materials for transcription into inorganic capsules as described by German and colleagues [84]. The transcriptive synthesis approach is identical to the colloidal templating strategy described in the previous section, and this aspect will not be discussed further here.

As an alternative to the above-mentioned systems, thermodynamically stable vesicles can be produced from mixtures of anionic and cationic surfactants under suitable conditions [85]. The resulting “catanionic” vesicles form spontaneously and the bilayers are the equilibrium state of aggregation. The nature and concentration of the surfactants dictate the size and thickness of the bilayer catanionic vesicles. As before, hollow and cross-linked polymer spheres can be produced by templating the vesicular aggregates [86,87]. In a typical example, equilibrium vesicles were formed by mixing cetyltrimethylammonium tosylate (CTAT, 0.7%) and sodium dodecylbenzenesulfonate (SDBS, 0.3%) in water

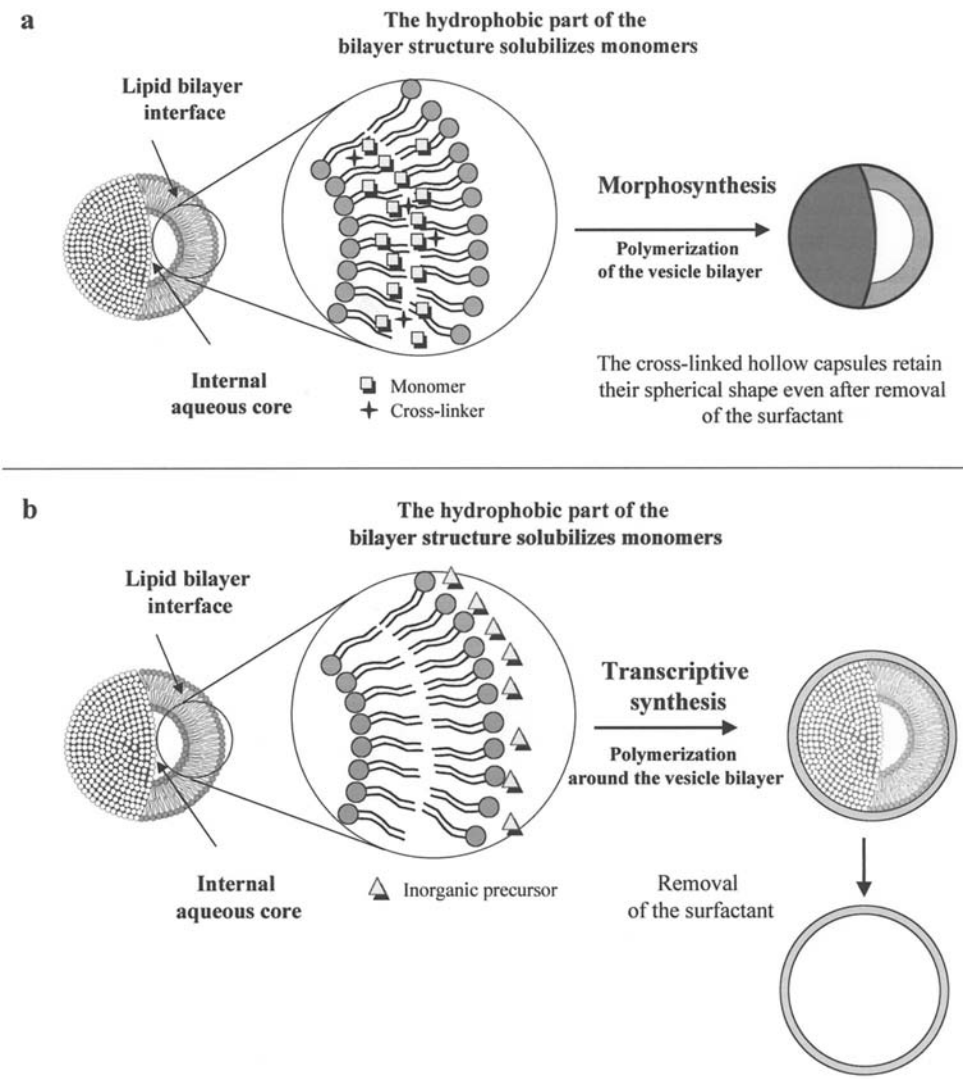

FIG. 13 Schematic representation of the vesicle templating strategies for synthesis of hollow polymeric organic and inorganic spheres. (a) Morphosynthesis and (b) transcriptive synthesis.

solutions (Structures 3a and 3b). The bilayer structures were swelled by styrene and divinylbenzene, and polymerized using a water-soluble cationic initiator.

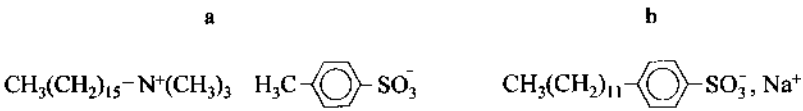

Structure 3

Block copolymers also arrange spontaneously into vesicular structures under suitable conditions. For instance, Jenekhe and Chen reported that block copolymers with rigid poly(phenylquinoline) (PPQ) rods and random coils of polystyrene (PPQ-*b*-PS, Structure 4) form vesicular bilayer aggregates into a selective solvent for PPQ. The vesicular capsules were contacted with a solution of fullerene molecules resulting in solubilization and encapsulation of a large amount of the guest compound into the spherical hollow spheres [88]. Hollow nanospheres have been produced in a similar way from polyisoprene-*b*-poly(2-cinnamoylethyl methacrylate) diblock copolymer vesicles (PI-*b*-PCEMA, Structure 5) [89]. Elaboration of the nanocapsules involved two steps: cross-linking of the insoluble PCEMA block forming the shell and subsequent hydroxylation of the inner PI block to produce the capsules. In another example, ABA triblock vesicles carrying polymerizable end groups have been elaborated by Meier et al. (see, e.g., Structure 6) [90]. The functionalized triblock vesicles formed spontaneously in dilute water solutions, and the vesicular structure was further stabilized by cross-linking polymerization of the reactive end groups through UV irradiation. Examples of block copolymer structures are listed in Table 1.

B. Liposomes

Liposomes are special class of vesicles made of phospholipid bilayers [91]. They have been widely studied in the last 20 years for their possible use as nanocapsules or carriers for drug delivery, gene transfer, and red cell substitutes. Because of the extensive literature in this field, an exhaustive presentation will not be attempted here.

Although liposomes are employed as delivery systems in the pharmaceutical and cosmetic industries, their limited stability and low permeability for polar molecules presents serious limitation for general use. In most applications, they have to be modified by specific additives, such as cholesterol. The additives improve membrane rigidity and hydrophobicity and reduce its permeability. The formation and stability of liposomic membranes are reviewed elsewhere [92,93].

TABLE 1 Examples of Diblock and Triblock Copolymer Structures Giving Rise to Formation of Vesicles into Selective Solvents for One of the Two Blocks

Structures	Ref
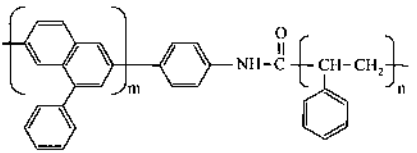	88
Structure 4: Poly(phenylquinoline)-*b*-polystyrene (PPQ-*b*-PS)	
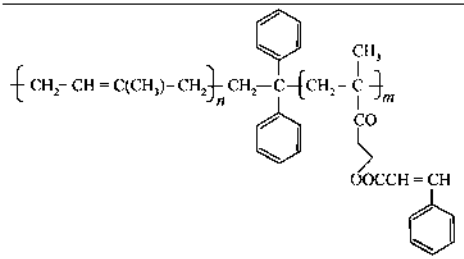	89
Structure 5: Polyisoprene-*block*-poly(2-cinnamoylethyl methacrylate) (PI-*b*-PCEMA)	
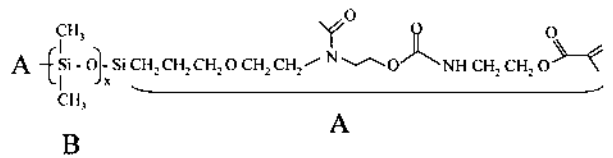	90
Structure 6: Poly(2-methyloxazoline)-*b*-poly(dimethylsiloxane)-*b*-poly(2-methyloxazoline) (PMOXA-*b*-PDMS-*b*-PMOXA)	
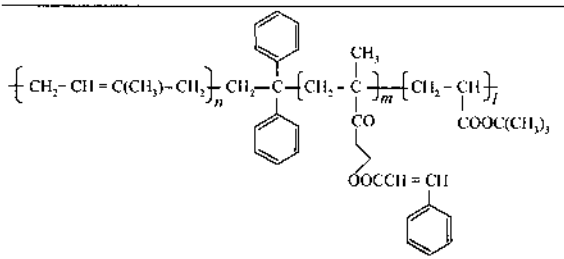	95
Structure 7: Polyisoprene-*b*-poly (2-cinnamoylethyl methacrylate)-*b*-poly(tert-butyl acrylate) (PI-*b*-PCEMA-*b*-PtBA)	

C. Block Copolymer Micelles

Block copolymers can adopt a variety of supramolecular structures in selective solvents. Gohy and coworkers described, for instance, the synthesis of pH-sensitive core-shell-corona (CSC) polystyrene-*b*-poly(2-vinylpyridine)-*b*-poly(ethylene oxide) triblock copolymer micelles [94]. Similarly, CSC polyisoprene-*b*-poly(2-cinnamoylethyl methacrylate)-*b*-poly(*tert*-butyl acrylate) micelles (PI-*b*-PCEMA-*b*-PtBA, Structure 7) have been produced by Stewart and Liu [95]. The micelles were further solidified by UV cross-linking of the PCEMA shell while the PI block was degraded by ozonolysis to generate nanospheres with a central cavity. The so-obtained nanocapsules were loaded with rhodamine B, a model molecule whose size is similar to that of drug compounds. Based on the same general concept, the synthesis of a variety of shell-cross-linked copolymer micelles has been reported in the literature [96,97]. Hollow particles are produced from the cross-linked micelles after degradation of the internal part of the micellar aggregates.

Non-covalently connected micelles can also be produced from the self-assembly of "complementary" homopolymers via intermolecular complexation reactions (e.g., hydrogen bonding or donnor–acceptor interactions) [98–100]. It was found, for example, that by mixing polystyrene oligomers carrying carboxyl end groups and poly(4-vinylpyridine) in a common solvent, "copolymer-like" aggregates were formed due to hydrogen bonding between the carboxyl and pyridine groups. In a similar way, hollow spherical aggregates of polyimide (a rod-like polymer) and poly(4-vinylpyridine) were obtained by simple immersion of the two polymers in a nonselective solvent such as chloroform.

V. APPLICATIONS

As shown above, hollow spheres can be constructed in a variety of ways from materials of diverse compositions including magnetic, semiconducting, ceramic, biomolecular, polymeric, and composite materials. Owing to their low density, large surface area, stability, and surface permeability, hollow spheres are of major technological and scientific interest. They are widely used in encapsulation and controlled release of various substances (dyes, drugs, cosmetics, and inks), and are particularly suited for biological applications such as drugs targeting, artificial cells, and diagnostics. In this section, the potentials of preformed hollow capsules in the pharmaceutical and biological fields are highlighted.

A. Biotechnological Applications

As mentioned previously, hollow spheres are potentially useful as microcapsules for the controlled release and targeting of drugs as well as for the protection of sensitive agents such as proteins or enzymes [71–73]. Not only can such capsules be used to dissolve or complex drug substances; they also display suitable

properties for transportation and subsequent release of the encapsulated molecules. However, despite their great potential in drug delivery, microcapsules often suffer from relatively poor stability in physiological solutions and thus need to be further optimized for clinical use. In this respect, liposomes appear to present some superiority but also have undesirable stability characteristics. Formulating lipid liposomes for therapeutic applications requires a set of conditions to be fulfilled. Liposomes must be able, for instance, to prolong the circulation time of drugs (drug encapsulation efficacy) and distribute more of them to sites of disease (site targeting). In addition, they must protect sensitive tissues from drug toxicity (site avoidance). Maintaining the stability of the liposome-encapsulated drug, reducing its toxicity, and improving its efficacy thus constitutes a major challenge for the pharmaceutical industry. Owing to the inherent limitations of conventional liposomes in biological environments, i.e., destabilization and rapid removal by macrophage uptake, stealth liposomes that avoid recognition by the immune system have been developed [101]. This special class of liposomes are stabilized with surface-grafted linear poly(ethylene glycol) (PEG) chains. The PEG coating is believed to create a physical steric barrier that inhibits the approach of other liposomes, cells, and proteins for instance. This ensures a long-term stability; the liposomes can circulate intact for many days and distribute more efficaciously in the body. The method of encapsulation (liposome formation) is also critical with respect to encapsulation efficiency and the ultimate drug-to-lipid ratio. If the drug is not quantitatively incorporated into the lipid capsule, the free drug must be removed prior to utilization. Although there exist a variety of manufacturing techniques, only the processes that can be done on a large scale will find potential industrial development. Formulations prepared in test tubes often appear difficult to scale up, and the elaboration of performant prototype formulations is not the only condition to commercial scale manufacturing.

Liposomes are also used in immunological studies for introducing a variety of molecules to the immune system [102]. Antigenic materials can be attached to the outer surface, encapsulated in the internal aqueous space, or dissolved in the liposome bilayers. They are employed in numerous immunization procedures and as vehicles for vaccine candidates. Phospholipid vesicles have also been reported to be useful carriers for red blood (hemoglobin) encapsulation [103]. They show a reversible oxygen binding and oxygen transport capability and are potentially suitable as red cell substitutes. Clinical applications of vesicles and liposomes is a very large field of research, and a fulfilled description of these systems encompasses the goal of the present chapter. Similarly, the very active domain of synthetic biodegradable polymeric capsules, familiar to researchers in pharmaceutics will not be covered here.

The LbL self-assembly technique also offers possibilities in encapsulation technologies with potential applications in drug delivery. The polyelectrolyte

walls are permeable to low molecular weight polymers and nonpermeable to high molecular weight compounds. Thus, loading of macromolecules inside the polyelectrolyte capsules can be envisaged. In addition, the permeability and diffusive properties of the shell can be controlled to a certain extent and adjusted to the intended application. Moreover, polyelectrolyte shells are extremely stable against chemical and physical influences, which is an important condition for clinical use. Hollow particles with stimuli-responsive shells are also particularly interesting for such applications. The elaboration of nanocapsules with cross-linkable, pH- or temperature-sensitive polymer walls have attracted much attention in recent years. For instance, water-soluble polyelectrolyte nanocapsules, able to undergo reversible swelling transitions upon changing the pH and/or salt concentrations have been patented by Meier et al. [83,104]. Poly(acrylic acid) (PAA) capsules were obtained by templating unilamellar dimethyldioctadecylammonium chloride vesicles with a mixture of *tert*-butyl acrylate and ethylene glycol dimethacrylate as the cross-linking agent. Selective saponification of the *tert*-butyl ester group yielded cross-linked PAA-responsive nanocapsules. In this application, the hollow particles were designed such as to encapsulate therapeutic and diagnostic agents. Typically, the particles are formed under conditions that result in nonpermeable polymeric capsules. Once the particles are exposed to an external stimuli, such as an increase of pH, the shell polyelectrolyte dissociates and the permeability of the swollen shell becomes increasingly important. The shell permeability promotes molecular exchange between the interior of the particles and the surrounding medium and enables the incorporation of active components. If the stimulus is removed, the active substance becomes encapsulated inside the nanocapsule. It is further delivered with increasing pH. If necessary, the particles surface can also be modified with specific ligands that allow the capsules to be directed to a specific target via molecular recognition.

B. Other Applications

Apart from the above biotechnological applications of hollow particles, it is also worth mentioning the intense interest in voided particles on the part of the coating industry. By scattering light, hollow particles contribute to increase hiding and better gloss retention [105]. In addition, it has been shown that hollow plastic microspheres can be used as fillers and toughening agents in epoxy resin composite materials [106]. Epoxies modified with the hollow latex particles showed a higher yield strength than epoxy resins modified with conventional rubber toughness [107].

The cavity inside the hollow spheres can also be used as a host space to precipitate organic and/or inorganic particles. Preformed hollow capsules are particularly well suited for such applications since they provide effective size limitations because of the compartmentalization of the precipitation chemistry

[71]. In a typical example, the spheres are first suspended in a solvent for the organic and/or inorganic solid to be precipitated. The solubilized reactive compound then permeates the sphere wall and enters the nanocapsules. A nonmiscible solvent is subsequently slowly introduced into the suspension to initiate precipitation of the principal compound contained inside the hollow spheres by osmotically shifting the original solvent. Precipitation can be alternatively induced by change in pH or by addition of a trigger. Different species can be incorporated into the hollow spheres, making them attractive for a wide range of applications from biotechnology to catalysis. For example, hollow polyelectrolyte shells have been used as microenvironments for the precipitation of inorganic salt and crystal deposition in the inner part of the capsules [108]. Nanoscale objects with controlled sizes and shapes have been successfully obtained by this technique. Polymerization reactions can also be conducted in the confined space of nanocapsules. As a typical example, an aqueous solution of hydrophilic monomers containing acrylamide has been entrapped inside the water pool of hollow spheres [109]. Subsequent polymerization produced cross-linked poly(acrylamide) gels filling the whole volume of the capsule. The imprinted latexes were found to adopt the dimensions and spherical shape of the mold.

VI. CONCLUSIONS

Hollow spheres can be elaborated in a variety of ways, e.g., emulsions, structured particles, and self-assembled polymers, using chemical or physicochemical routes. Depending on the synthetic strategy used for their elaboration, hollow spheres of various compositions and structural characteristics can be readily obtained by these techniques. Among the various synthetic schemes, emulsion polymerization offers great potentialities that have been largely exploited in the coating industry. The unique flexibility of emulsion processing makes it possible to produce robust hollow spheres with controlled size, composition, and shell thickness in large volumes. It can be anticipated that hollow latexes could also find interesting developments and applications in other fields such as controlled release. Colloidal templating also affords a versatile means for the elaboration of hollow capsules using organic, inorganic, biological, or hybrid colloids as sacrificial templates. The general nanocoating strategy obviously provides a new route to produce tailor-made, reproducible, and optimized systems for biotechnological applications. Among the advantages is the possibility of manipulating the size and permeability of the capsules. However, one major limitation is the biotoxicity and biocompatibility of the shell membrane. We also described the use of macromolecules and surfactant assemblies into vesicles and related aggregate structures to produce small and permeable capsules. Phospholipid vesicular membranes are potential carriers for drug, enzyme, protein, and hemoglobin encapsulation. However, liposomes have limited stability in biological environ-

ments, which drastically reduces the circulation time of the active species in the body. To this end, polymeric hollow spheres prepared from block copolymers appear particularly promising provided that the blocks are biocompatible and degradable. The copolymers can be additionally designed to carry recognition groups and affinity ligands to be directed to specific target sites.

Formulation of hollow particles thus requires a good knowledge of the final application in order to develop optimal performances. Not only can the size of the capsules be controlled for maximal hiding or loading efficacy; the composition of the wall material can also be selected to afford reversible and switchable permeation properties for encapsulation and subsequent release of active compounds.

REFERENCES

1. Thies, C. A short history of microencapsulation technology. In *Microspheres*, *Microcapsules and Liposomes*; Arshady, R., Ed.; Citus Book: London, 1999; Vol. 1, 47–54, and references therein.
2. Blythe, D.; Churchill, D.; Glanz, K.; Stutz, J. Microcapsules for carbonless copy paper, industrial and commercial aspects. In *Microspheres*, *Microcapsules and Liposomes*; Arshady, R., Ed.; Citus Book: London, 1999; Vol. 1, 419–439, and references therein.
3. Augustin, M.A.; Sanguansri, L.; Margetts, C.; Young, B. Microencapsulation of food ingredients. Food Australia **2001**, *53*, 220–223.
4. Tsuji, K. Microcapsules in agriculture. In *Microspheres*, *Microcapsules and Liposomes*; Arshady, R., Ed.; Citus Book: London, 1999; Vol. 1, 350–371, and references therein.
5. Arshady, R. Manufacturing methodology of microcapsules. In *Microspheres*, *Microcapsules and Liposomes*; Arshady, R., Ed.; Citus Book: London, 1999; Vol. 1, 279–326, and references therein.
6. Hemenway, C.P.; Latimer, J.J.; Young, J.E. Hollow-sphere polymer pigment in paper coating. Tappi J. **1985**, *68*, 102–105.
7. (a) Hislop, R.W.; McGinley, P.L. Microvoid coatings: pigmented, vesiculated beads in flat latex paints. J. Coatings Tech. **1978**, *50*, 69–77. (b) Fasano, D.M. Use of small polymeric microvoids in formulating high PVC paints. J. Coatings Tech. **1987**, *59*, 109.
8. Wilcox, D.L.; Berg, M. In *Hollow and Solid Spheres and Microspheres*: *Science and Technology Associated with Their Fabrication and Applications*; Wilcox, D.L., Berg, M., Bernat, T., Kellerman, D., Cochran, J.K., Eds.; MRS Proceedings: Pittsburgh, 1995; Vol. 372, 3–13, and references therein.
9. Cochran, J.K. Ceramic hollow spheres and their applications. Curr. Opin. Solid State Mater. Sci. **1998**, *3*, 474–479.
10. McDonald, C.J.; Devon, M.J. Hollow latex particles. In *Dendrimers*, *Assemblies and Nanocomposites*; Arshady, R., Guyot, A., Eds.; Citus Book: London, 2002; Vol. 5, and references therein.

11. Chang, T.M.S. Pharmaceutical and therapeutic applications of artificial cells including microencapsulation. Eur. J. Pharm. Biopharm. **1998**, *45*, 3–8, and references therein.
12. Caruso, F. Hollow capsule processing through colloidal templating and self-assembly. Chem. Eur. J. **2000**, *6*, 413–419, and references therein.
13. (a) Kowalski, A.; Vogel, M.; Blankenship, R.M. Titre. US Patent 4,427,836, 1984. (b) McDonald, C.; Chonde, Y.; Cohrs, W.; McWilliams, D. Titre. US Patent 4,973,670, 1990. (c) Nippon Zeon, K.K. Titre. Japanese Patent 052779409 A, 1993. (d) Kaino, M.; Takagishi, Y.; Toda, H. Titre. US Patent 5,360,827, 1994.
14. (a) Kowalski, A.; Blankenship, R.M. Titre. US Patent 4,468,498, 1984. (b) Kowalski, A.; Vogel, M. Titre. US Patent 4,469,825, 1984. (c) Blankenship, R.M.; Kowalski, A. Titre. US Patent 4,594,363, 1986. (d) Kowalski, A.; Vogel, M. Titre. US Patent 4,880,842, 1989. (e) Blankenship, R.M. Titre. US Patent, 5,494,971, 1996.
15. (a) Vanderhoff, J.W.; Park, J.M.; El-Aasser, M.S. Titre. *Polymeric Materials Science and Engineering*; Proceedings of the ACS Division of Polymeric Materials: Science and Engineering; American Chemical Society: Washington, DC, 1991, 64:345–346. (b) Vanderhoff, J.W.; El-Aasser, M.S. In *Polymer Latexes*: *Preparation*, *Characterization and Applications*; Daniels, E.S., Sudol, E.D., El-Aasser, M.S., Eds.; ACS Symp. Series 492; American Chemical Society: Washington, DC, 1992; 272–281.
16. Pavlyuchenko, V.N.; Sorochinskaya, O.V.; Ivanchev, S.S.; Klubin, V.V.; Kreichman, G.S.; Budtov, V.P.; Skrifvars, M.; Halme, E.; Koskinen, J. Hollow-particle latexes: preparation and properties. J. Polym. Sci. A Polym. Chem. **2001**. *39*, 1435–1449.
17. (a) Andrew, R.W.; Lestarquit, B. New additive helps cut the cost of hiding. Polym. Paint Colour J. **1984**, *174*, 442–446. (b) Rennel, C.; Rigdahl, M. Enhancement of the light scattering ability of coatings by using hollow pigments. Colloid Polym. Sci. **1994**, *272*, 1111–1117.
18. Okubo, M. Process for producing hollow polymer latex particles. US Patent 4,910,229, 1990.
19. (a) Okubo, M.; Ichikawa, K.; Fujimura, M. Production of submicron-size multihollow polymer microspheres by stepwise alkali/acid method. Polym. Mater. Sci. Eng. Prepr., American Chemical Society: Washington, DC 1991, *64*, 347–348. (b) Okubo, M.; Ichikawa, K.; Fujimura, M. Colloid Polym. Sci. **1991**, *269*, 1257–1262. (c) Okubo, M.; Ito, A.; Nakamura, M. Effect of molecular weight on the production of multihollow polymer particles by the alkali/cooling method. Colloid Polym. Sci. **1997**, *275*, 82–85. (d) Okubo, M.; Mori, H.; Ito, A. Effect of nonionic emulsifier on the production of multihollow polymer particles by the stepwise acid/alkali method. Colloid Polym. Sci. **2000**, *278*, 358–363.
20. Okubo, M.; Mori, H. Production of multihollow polymer particles by the stepwise acid/alkali method. Colloid Polym. Sci. **1997**, *275*, 634–639.
21. Kong, W.Z.; Kan, C.Y.; Li, H.H.; Yu, D.Q.; Yuan, Q. Synthesis and characterization of hollow polymer latex particles. Polym. Adv. Technol. **1996**, *8*, 627–630.
22. McDonald, C.J.; Bouck, K.J.; Bruce Chaput, A.; Stevens, C.J. Emulsion polymeri-

zation of voided particles by encapsulation of a nonsolvent. Macromolecules **2000**, *33*, 1593–1605.
23. Tiarks, F.; Landfester, K.; Antonietti, M. Preparation of polymeric nanocapsules by miniemulsion polymerization. Langmuir **2001**, *17*, 908–918.
24. (a) Vogel, M.; Kowalski, A.; Scott, J.D. Prepartion of core-shell particle dispersions for use as opacifying agents in coatings. Eur. Patent Appl. 267726, 1998. (b) Hattori, M.; Sakurai, N.; Takeuchi, H. Hollow Polymer Particles. US Patent 4,908,271, 1990.
25. Itou, N.; Masukawa, T.; Ozaki, I.; Hattori, M.; Kasai, K. Cross-linked hollow polymer particles by emulsion polymerization. Colloids Surf. A **1999**, *153*, 311–316.
26. Kasai, K.; Sakurai, F. Manufacture of crosslinked hollow polymer particles. Nippon gosei Gum Kaihatsu Cent., Kagaku Keizai. **1991**, *38*, 46–53.
27. Seidl, J.; Malinsky, J.; Dusek, K.; Heitz, W. Macroporous styrene-divinylbenzene copolymers and their application in chromatography and for the preparation of ion-exchange resins. Fortschritte der Hochpolymeren-Forschung **1967**, *5*, 113–213.
28. Okubo, M.; Konishi, Y.; Minami, H. Production of hollow polymer particles by suspension polymerization. Colloid Polym. Sci. **1998**, *276*, 638–642.
29. Okubo, M.; Konishi, Y.; Minami, H. Influence of the kind of end groups of polystyrene on the production of hollow particles by suspension polymerization for divinylbenzene/toluene droplets dissolving them. Colloid Polym. Sci. **2001**, *279*, 519–523.
30. (a) Okubo, M.; Minami, H. Control of hollow size of micron-sized monodispersed polymer particles having a hollow structure. Colloid Polym. Sci. Colloids and Surfaces, A: Physiochemical and Engineering Aspects **1996**, *274*, 433–438. (b) Okubo, M.; Minami, H. Formation mechanism of micron-sized monodispersed polymer particles having a hollow structure. Colloid Polym. Sci. **1997**, *275*, 992–997. (c) Okubo, M.; Minami, H.; Yamamoto, Y. Penetration/release behaviors of various solvents into/from micron-sized monodispersed hollow polymer particles. Colloids and Surfaces, A: Physicochemical and Engineering Aspects **1999**, *153*, 405–411.
31. Okubo, M.; Mukai, T.; Minami, H.; Fujii, S. Production of micron-sized monodispersed multihollow polystyrene/poly(3,5-xylidine) composite particles by oxidative seeded polymerization. Colloid Polym. Sci. **2000**, *278*, 275–279.
32. Wohlgemuth, M.; Mächtle, W.; Mayer, C. Improved preparation and physical studies of polybutylcyanoacrylate nanocapsules. J. Microencaps. **2000**, *17*, 437–448.
33. Tasset, C.; Barrete, N.; Thysman, S.; Ketelegers, J.M.; Lemoine, D.; Preat, V. Titre. J. Contr. Rel. **1995**, *33*, 23.
34. (a) Davies, R.; Schurr, G.A.; Meenan, P.; Nelson, R.D.; Bergna, H.E.; Brevett, C.A.S.; Goldbaum, R.H. Engineered particle surfaces. Adv. Mater. **1998**, *10*, 1264–1270, and references therein. (b) Caruso, F. Nanoengineering of particle surfaces. Adv. Mater. **2001**, *13*, 11–22, and references therein. (c) Caruso, R.A.; Antonietti, M. Sol-gel nanocoating: an approach to the preparation of structured materials. Chem. Mater. **2001**, *13*, 3272–3282, and references therein. (d) Bourgeat-Lami, E. Organic–inorganic nanostructured colloids. J. Nanosci. Nanotechnol. **2002**, *2*, 1–24, and references therein.
35. Velikov, K.P.; van Blaaderen, A. Synthesis and characterization of monodisperse

core-shell colloidal spheres of zinc sulfide and silica. Langmuir **2001**, *17*, 4779–4786.

36. (a) Janssen, E.A.W.G.; van Herk, A.M.; German, A.L. Encapsulation of inorganic filler particles by emulsion polymerization. ACS Div. Polym. Chem. Polym. Prep. **1993**, *34*, 532–533. (b) Sondi, I.; Fedynyshyn, T.H.; Sinta, R.; Matijevic, E. Encapsulation of nanosized silica by in-situ polymerization of *tert*-butyl acrylate monomer. Langmuir **2000**, *16*, 9031–9034. (c) Quaroni, L.; Chumanov, G. Preparation of polymer-coated functionalized silver nanoparticles. J. Am. Chem. Soc. **1999**, *121*, 10642–10643. (d) Bourgeat-Lami, E.; Lang, J. Encapsulation of inorganic particles by dispersion polymerization in polar media. 2. Effect of silica size and concentration on the morphology of silica-polystyrene composite particles. J. Colloid Interface Sci. **1999**, *210*, 281–289. (e) Corcos, F.; Bourgeat-Lami, E.; Novat, C.; Lang, J. Poly (styrene-b-ethylene oxide) copolymers as stabilizer for the synthesis of silica-polystyrene core-shell particles. Colloid Polym. Sci. **1999**, *277*, 1142–1151.
37. Liz-Marzan, L.M.; Giersig, M.; Mulvaney, P. Synthesis of nanosized gold-silica core-shell particles. Langmuir **1996**, *12*, 4329–4335.
38. Giersig, M.; Ung, T.; Liz-Marzan, L.M.; Mulvaney, P. Direct observation of chemical reactions in silica-coated gold and silver nanoparticles. Adv. Mater. **1997**, *9*, 570–575.
39. Mulvaney, P.; Liz-Marzan, L.M.; Giersig, M.; Ung, T. Silica encapsulation of quantum dots and metal clusters. J. Mater. Chem. **2000**, *10*, 1259–1270.
40. (a) Marikanos, S.M.; Novak, J.P.; Brousseau, III L.C.; House, A.B.; Edeki, E.M.; Feldhaus, J.C.; Feldheim, D.L. Gold particles as templates for the synthesis of hollow polymer capsules. Control of capsule dimensions and guest encapsulation. J. Am. Chem. Soc. **1999**, *121*, 8518–8522. (b) Marikanos, S.M.; Shultz, D.A.; Feldheim, D.L. Gold nanoparticles as templates for the synthesis of hollow nanometer-sized conductive polymer capsules. Adv. Mater. **1999**, *11*, 34–37.
41. Bergbreiter, D.E. Self-assembled, sub-micrometer diameter semipermeable capsules. Angew. Chem. Int. Ed. **1999**, *38*, 2870–2872.
42. Ulman, A. Formation and structure of self-assembled monolayers. Chem. Rev. **1996**, *96*, 1533:1554.
43. Templeton, A.C.; Wuelfing, W.P.; Murray, R.W. Monolayer-protected cluster molecules. Acc. Chem. Res. **2000**, *33*, 27–36.
44. Wu, M.; O'Neill, S.A.; Brousseau, L.C.; McConnell, W.P.; Shultz, D.A.; Linderman, R.J.; Feldheim, D.L. Synthesis of nanometer-sized hollow polymer capsules from alkanethiol-coated particles. Chem. Commun. **2000**, *9*, 775–776.
45. Sun, L.; Crooks, R.M.; Chechik, V. Preparation of polycyclodextrin hollow spheres by templating gold nanoparticles. Chem. Commun. **2001**, *4*, 359–360.
46. Warson, K.J.; Zhu, J.; Nguyen, S.T.; Mirkin, C.A. Hybrid nanoparticles with block copolymer shell structures. J. Am. Chem. Soc. **1999**, *121*, 462–463.
47. Mandal, T.K.; Fleming, M.S.; Walt, D.R. Production of hollow polymeric microspheres by surface-confined living radical polymerization on silica templates. Chem. Mater. **2000**, *12*, 3481–3487.
48. Blomberg, S.; Ostberg, S.; Harth, E.; Bosman, A.W.; van Horn, B.; Hawker, C.J.

Production of crosslinked, hollow nanoparticles by surface-initiated living free-radical polymerization. J. Polym. Sci. A **2002**, *40*, 1309–1320.
49. (a) Kawahashi, N.; Matijevic, E. Preparation and properties of uniform coated colloidal particles, V. Yttrium basic carbonate on polystyrene latex. J. Colloid Interface Sci. **1990**, *138*, 534–542. (b) Kawahashi, N.; Matijevic, E. Preparation of hollow spherical particles of yttrium compounds. J. Colloid Interface Sci. **1991**, *143*, 103–110.
50. Kawahashi, N.; Persson, C.; Matijevic, E. Titre. J. Mater. Chem. **1991**, *1*, 577.
51. Kawahashi, N.; Shiho, H. Copper and copper compounds as coatings on polystyrene particles and as hollow spheres. J. Mater. Chem. **2000**, *10*, 2294–2297.
52. Shiho, H.; Kawahashi, N. Iron compounds as coatings on polystyrene latex and as hollow spheres. J. Colloid Interface Sci. **2000**, *226*, 91–97.
53. Shiho, H.; Kawahashi, N. Titanium compounds as coatings on polystyrene latices and as hollow spheres. Colloid Polym. Sci. **2000**, *278*, 270–274.
54. Eiden, S.; Maret, G. Preparation and characterization of hollow spheres of rutile. J. Colloid Interface Sci. **2002**, *250*, 281–284.
55. Imhof, A. Preparation and characterization of titania-coated polystyrene spheres and hollow titania shells. Langmuir **2001**, *17*, 3579–3585.
56. Bamnolker, H.; Nitzan, B.; Gura, S.; Margel, S. Titre. J. Mater. Sci. Lett. **1997**, *16*, 1412.
57. Bourgeat-Lami, E.; Tissot, I.; Lefebvre, F. Synthesis and characterization of SiOH-functionalized latex particles using methacryloxy propyl trimethoxysilane in emulsion polymerization. Macromolecules, **2002**, *35*, 6185–6191.
58. Tissot, I.; Novat, C.; Lefebvre, F.; Bourgeat-Lami, E. Hybrid latex particles coated with silica. Macromolecules **2001**, *34*, 5737–5739.
59. Tissot, I.; Bourgeat-Lami, E. SiOH-functionalized polystyrene latexes. A step towards the synthesis of hollow silica nanoparticles. Chem. Mater. **2002**, *14*, 1325–1331.
60. zu Putlitz, B.; Landfester, K.; Fischer, H.; Antonietti, M. The generation of armored latexes and hollow inorganic shells made of clay sheets by templating cationic miniemulsions and latexes. Adv. Mater. **2001**, *13*, 500–503.
61. Tamai, H.; Sumi, T.; Yasuda, H. Preparation and characteristics of fine hollow carbon particles. J. Colloid Interface Sci. **1996**, *177*, 325–328.
62. (a) Donath, E.; Sukhorukov, G.B.; Caruso, F.; Davis, S.A.; Möhwald, H. Novel hollow polymer shells by colloid-templated assembly of polyelectrolytes. Angew. Chem. Int. Ed. **1998**, *37*, 2201–2205. (b) Sukhorukov, G.B.; Donath, E.; Davis, S.; Lichtenfeld, H.; Caruso, F.; Popov, V.I.; Möhwald, H. Stepwise polyelectrolyte assembly on particle surfaces: a novel approach to colloid design. Polym. Adv. Technol. **1998**, *9*, 759–767. (c) Gao, C.; Leporatti, S.; Moya, S.; Donath, E.; Möhwald, H. Stability and mechanical properties of polyelectrolyte capsules obtained by stepwise assembly of poly(styrenesulfonate sodium salt) and poly(diallyldimethyl ammonium) chloride onto melamine resin particles. Langmuir **2001**, *17*, 3491–3495.
63. Caruso, F.; Caruso, R.A.; Mohwald, H. Nanoengineering of inorganic and hybrid hollow spheres by colloidal templating. Science **1998**, *282*, 1111–1114.

64. Caruso, F.; Caruso, R.A.; Mohwald, H. Production of hollow microspheres from nanostructured composite particles. Chem. Mater. **1999**, *11*, 3309–3314.
65. Caruso, R.A.; Susha, A.; Caruso, F. Multilayered titania, silica, and laponite nanoparticle coatings on polystyrene colloidal templates and resulting inorganic hollow spheres. Chem. Mater. **2001**, *13*, 400–409.
66. (a) Wang, X.D.; Yang, W.L.; Tand, Y.; Wang, Y.J.; Fu, S.K.; Gao, Z. Fabrication of hollow zeolite spheres. Chem. Commun. **2000**, *21*, 2161–2162. (b) Rhodes, K.H.; Davis, S.A.; Caruso, F.; Zhang, B.; Mann, S. Hierarchical assembly of zeolite nanoparticles into ordered macroporous monoliths using core-shell building blocks. Chem. Mater. **2000**, *21*, 2832–2834.
67. Caruso, F.; Spasova, M.; Susha, A.; Giersig, M.; Caruso, R.A. Magnetic nanocomposite particles and hollow spheres constructed by a sequential layering approach. Chem. Mater. **2001**, *13*, 109–116.
68. Caruso, F.; Shi, X.; Caruso, R.A.; Susha, A. Hollow titania spheres from layered precursor deposition on sacrificial colloidal core particles. Adv. Mater. **2001**, *13*, 740–744.
69. Wang, D.; Caruso, F. Polyelectrolyte-coated colloid spheres as templates for sol-gel reactions. Chem. Mater. **2002**, *14*, 1909–1913.
70. van Bommel, K.J.C.; Jung, J.H.; Shinkai, S. Poly(L-lysine) aggregates as templates for the formation of hollow silica spheres. Adv. Mater. **2001**, *13*, 1472–1476.
71. Sukhorukov, G.; Dähne, L.; Hartmann, J.; Donath, E.; Möhwald, H. Controlled precipitation of dyes into hollow polyelectrolyte capsules based on colloids and biocolloids. Adv. Mater. **2000**, *12*, 112–115.
72. Caruso, F.; Trau, D.; Möhwald, H.; Renneberg, R. Enzyme encapsulation in layer-by-layer engineered polymer multilayer capsules. Langmuir **2000**, *16*, 1485–1488.
73. Caruso, F.; Yang, W.; Trau, D.; Renneberg, R. Microencapsulation of uncharged low molecular weight organic materials by polyelectrolyte multilayer self-assembly. Langmuir **2000**, *16*, 8932–8936.
74. Fendler, F.H. *Membrane-Mimetic Approach to Advanced Materials*; Springer: New York, 1994.
75. See, for example: (a) Jung, J.H.; Ono, Y.; Sakurai, K.; Sano, M.; Shinkai, S. Novel vesicular aggregates of crown-appended cholesterol derivatives which act as gelators of organic solvents and as templates for silica transcription. J. Am. Chem. Soc. **2000**, *122*, 8648–8653. (b) Gao, X.; Zhang, J.; Zhang, L. Hollow sphere selenium nanoparticles: their in-vitro anti hydroxyl radical effect. Adv. Mater. **2002**, *14*, 290–293.
76. (a) Price, C. In *Developments in Block Copolymers*; Goodman, I., Ed.; Applied Science: London, 1982; Vol. 1, 39. (b) Selb, J.; Gallot, Y. In *Developments in Block Copolymers;* Goodman, I., Ed.; Applied Science: London, 1985; Vol. 2, 27. (c) Riess, G.; Hurtrez, G.; Bahadur, P. *Encyclopedia of Polymer Science and Engineering*, 2nd ed.; John Wiley and Sons: New York, 1985; Vol. 2, 324.
77. Rosoff, M., Ed. *Vesicles*; Marcel Dekker: New York, 1996.
78. Zana, R. In *Surfactants in Solution;* Mitall, K.J., Botherel, P., Eds.; Plenum Publishers: New York, 1986; 115–113, and references therein.

79. For a review, see e.g., Hotz, J.; Meier, W. Vesicular polymerization. In *Reactions and Synthesis in Surfactant Systems*; Texter, J., Ed.; Surfactant Science Series; Marcel Dekker: New York, **2001;** Vol. 24, 501–514, and references therein.
80. Murtagh, J.; Thomas, J.K. Mobility and reactivity in colloidal aggregates with motion restricted by polymerization. Faraday Discuss. Chem. Soc. **1986**, *81*, 127–136.
81. Poulain, N.; Nakache, E.;. Pina, A.; Levesque, G. Nanoparticles from vesicle polymerization: characterization and kinetic study. J. Polym. Sci. A Polym. Chem. **1996**, *34*, 729–737.
82. (a) Jung, M.; Hubert, D.H.W.; Bomans, P.H.H.; Frederik, P.M.; Meuldijk, J.; van Herk, A.M.; Fischer, H.; German, A.L. New vesicle-polymer hybrids: the parachute architecture. Langmuir **1997**, *13*, 6877–6880. (b) Jung, M.; Hubert, D.H.W.; Bomans, P.H.H.; Frederik, P.; van Herk, A.M.; German, A.L. A topology map for novel vesicle-polymer hybrid architectures. Adv. Mater. **2000**, *12*, 210–213. (c) Jung, M.; Hubert, D.H.W.; van Herk, A.M.; German, A.L. The parachute morphology as equilibrium morphology of vesicle-polymer hybrids? Macromol. Symp. **2000**, *151*, 393–398.
83. (a) Hotz, J.; Meier, W. Vesicle-templated polymer hollow spheres. Langmuir **1998**, *14*, 1031–1036. (b) Hotz, J.; Meier, W. Polymer particles by templating of vesicles. Adv. Mater. 1998, *10*, 1387–1390. (c) Sauer, M.; Meier, W. Responsive nanocapsules. Chem. Commun. **2001**, *1*, 55–56.
84. Hubert, D.H.W.; Jung, M.; Frederik, P.M.; Bomans, P.H.H.; Meuldijk, J.; German, A.L. Vesicle-directed growth of silica. Adv. Mater. **2000**, *12*, 1286–1290.
85. Brasher, L.L.; Kaler, E.W. A small-angle neutron scattering (SANS) contrast variation investigation of aggregate composition in catanionic surfactant mixtures. Langmuir **1996**, *12*, 6270–6276.
86. Morgan, J.D.; Johnson, C.A.; Kaler, E.W. Polymerization of equilibrium vesicles. Langmuir **1997**, *13*, 6447–6451.
87. (a) McKelvey, C.A.; Kaler, E.W.; Coldren, B.; Jung, H.T.; Zasadzinski, J.A. Templating hollow polymeric spheres from catanionic equilibrium vesicles: synthesis and characterization. Langmuir **2000**, *16*, 8285–8290. (b) McKelvey, C.A.; Kaler, E.W. Characterization of nanostructured hollow polymer spheres with small-angle neutron scattering (SANS). J. Colloid Interface Sci. **2002**, *245*, 68–74.
88. (a) Jenekhe, S.A.; Chen, X.L. Self-assembly of ordered microporous from rod-coil block copolymers. Science **1999**, *283*, 372–375. (b) Jenekhe, S.A.; Chen, X.L. Self-assembled aggregates of rod-coil block copolymers and their solubilization and encapsulation of fullerenes. Sci. Rep. **1998**, *279*, 1903–1907.
89. Ding, J.; Liu, G. Water-soluble hollow nanospheres as potential drug carriers. J. Phys. Chem. **1998**, *102*, 6107–6113.
90. (a) Nardin, C.; Thoeni, S.; Widmer, J.; Winterhalter, M.; Meier, W. Nanoreactors based on (polymerized) ABA-triblock copolymer vesicles. Chem. Commun. **2000**, *15*, 1433–1434. (b) Nardin, C.; Hirt, T.; Leukel, J.; Meier, W. Polymerized ABA triblock copolymer vesicles. Langmuir **2000**, *16*, 1035–1041.
91. Lasic, D.D. *Liposomes. From Physics to Applications;* Elsevier: Amsterdam, 1993.
92. Betageri, G.V.; Kulkarni, S.B. Preparation of liposomes. In *Microspheres*, *Micro-*

capsules and Liposomes; Arshady, R., Ed.; Citus Book: London, 1999; Vol. 1, 489–521, and references therein.
93. Tsuchida, E.; Sakai, H. Phospholipid vesicles. Formation and stabilization. In: *Microspheres*, *Microcapsules and Liposomes*; Arshady, R., Ed.; Citus Book: London, 1999; Vol. 2, 464–502, and references therein.
94. Gohy, J.F.; Willet, N.; Varshney, S.; Zhang, J.X.; Jérôme, R. Core-shell corona micelles with a responsive shell. Angew. Chem. Int. Ed. **2001**, *40*, :3214–3216.
95. Stewart, S.; Liu, G. Hollow nanospheres from polyisoprene-*block*-poly(2-cinnamoylethyl methacrylate)-*block*-poly(*tert*-butyl acrylate). Chem. Mater. **1999**, *11*, 1048–1054.
96. Sanji, T.; Nakatsuka, Y.; Ohnishi, S.; Sakurai, H. Preparation of nanometer-sized hollow particles by photochemical degradation of polysilane shell cross-linked micelles and reversible encapsulation of guest molecules. Macromolecules **2000**, *33*, 8524–8526.
97. Huang, H.; Remsen, E.E.; Kowalewski, T.; Wooley, K.L. Nanocages derived from shell-crosslinked micelle templates. J. Am. Chem. Soc. **1999**, *120*, 3805–3806.
98. Ilhan, F.; Galow, T.H.; Gray, M.; Clavier, G.; Rotello, V.M. Giant vesicle formation through self-assembly of complementary random copolymers. J. Am. Chem. Soc. **2000**, *122*, 5895–5896.
99. Duan, H.; Chen, D.; Jiang, M.; Gan, W.; Li, S.; Wang, M.; Gong, J. Self-assembly of unlike homopolymers into hollow spheres in nonselective solvent. J. Am. Chem. Soc. **2001**, *123*, 12097–12098.
100. Wang, M.; Jiang, M.; Ning, F.; Chen, D.; Liu, S.; Duan, H. Block-copolymer-free strategy for preparing micelles and hollow spheres: self-assembly of poly(4-vinyl pyridine) and modified polystyrene. Macromolecules, **2002**, *35*, 5980–5989.
101. Martin, F.J. Stealth liposomes. In *Microspheres*, *Microcapsules and Liposomes*; Arshady, R., Ed.; Citus Book: London, 1999; Vol. 2, 436–461, and references therein.
102. Snippe, H.; Verheul, A.F.M. Liposomes in immunology. In *Microspheres*, *Microcapsules and Liposomes*; Arshady, R., Ed.; Citus Book: London, 1999; Vol. 2, 525–544, and references therein.
103. Tsuchida, E.; Sakai, H. Hemoglobin vesicles. In *Microspheres*, *Microcapsules and Liposomes*; Arshady, R., Ed.; Citus Book: London, 1999; Vol. 2, 503–523, and references therein.
104. Meier, W.; Sauer, M. Responsive polymeric hollow particles. Patent WO 01/37803 A2, 1999.
105. Strauss, J. Multilobed acrylic latices. Surf. Coat. Aust. **1988**, *25*, 6–12.
106. Bagheri, R.; Pearson, R.A. The use of microvoids to toughen polymers. Polymer **1995**, *36*, 4883–4885.
107. Kim, H.S.; Khamis, M.A. Fracture and impact behaviours of hollow micro-sphere/epoxy resin composites. Composites A **2001**, *32*, 1311–1317.
108. Sukhorukov, G.B.; Susha, A.S.; Davis, S.; Leporatti, S.; Donath, E.; Hartmann, J.; Möhwald, H. Precipitation of inorganic salt inside hollow micrometer-sized polyelectrolyte shells. J. Colloid Interface Sci. **2002**, *247*, 251–254.
109. Torchilin, V.P.; Klibanov, A.L.; Ivanov, N.N.; Ringsdorf, H.; Schlarb, B. Polymerization of liposome-encapsulated hydrophilic monomers. Makromol. Chem. Rapid Commun. **1987**, *8*, 457–460.

9

Preparation of Polymer and Hybrid Colloids by Miniemulsion for Biomedical Applications

KATHARINA LANDFESTER Max Planck Institute of Colloids and Interfaces, Potsdam, Germany

I. INTRODUCTION

The formulation and application of polymer particles and hybrid particles composed of polymeric and inorganic material is of high interest for biomedical applications. For such applications, it is necessary that the materials or especially the surface of the particles are biocompatible, nontoxic, and sometimes also biodegradable. Many different approaches are used for the generation of nanoparticles in order to obtain the needed properties. For the preparation of polymer particles, processes such as microemulsion [1] and emulsion polymerization [2] are used that are based on a kinetic control during the preparation; the particles are built from the center to the surface, and the particle structure is governed by kinetic factors. Due to the dictates of kinetics, serious disadvantages, such as lack of homogeneity and restrictions in the accessible composition, have to be accepted. Therefore, it is desirable to take advantage of a potential thermodynamic control for the design of nanoparticles and the concept of "nanoreactors" whereby the essential ingredients for the formation of the nanoparticles are present at the beginning [3]. It should be emphasized that particle formation in nanoreactors takes place in a highly parallel fashion, i.e., the synthesis is performed in 10^{18}–10^{20} nanocompartments per liter that are separated from each other by a continuous phase. However, previous systems show serious restrictions and failure mechanisms, as recently discussed [4].

The idea of polymerization in a nanoreactor is technically realized in high perfection in the suspension polymerization, where droplets in the micrometer range are created that can be polymerized without change of particle identity [5]. The suspension principle was transferred to obtain smaller droplet sizes by

Ugelstad [6] who scaled down the droplet size to several hundred nanometers by shearing the system.

The purpose of this chapter is to describe a recent development in which the availability of high-shear devices, such as those used for ultrasound and high-pressure homogenization, decreases the droplet or nanoreactor diameter to 30–100 nm using biocompatible surfactants. The integrity of each nanodroplet will be preserved in both reverse (aqueous solvent) and inverse (organic or hydrocarbon solvent) situations. It will be put forth that the developed concept permits functionalization of the polymer particle surface in order to bind antibodies onto it. The miniemulsion process permits formulation of hydrid particles for biomedical applications.

II. THE MINIEMULSION PROCESS

A system wherein small droplets with high stability in a continuous phase are created by using high shear [7–9] is classically called a "miniemulsion." One of the tricks to obtaining stability of the droplets is the addition of an agent that dissolves in the dispersed phase but is insoluble in the continuous phase. The small droplets can be hardened either by a subsequent polymerization or by decreasing the temperature (if the dispersed phase is a low-temperature melting material). For a typical oil-in-water miniemulsion, an oil, a hydrophobic agent (or several), an emulsifier, and water are homogenized by high shear (see Fig. 1) to obtain homogeneous and monodispersed droplets in the size range of 30–500 nm [3].

In a first step of the miniemulsion process, small stable droplets in a size range between 30 and 500 nm are formed by shearing a system containing the dispersed phase, the continuous phase, a surfactant, and an osmotic pressure agent. In a second step, these droplets are polymerized without changing their identity.

Based on the principle on miniemulsion, the preparation of new nanoparticles that could not be prepared in heterophase processes is now possible. The potential and the high impact of using miniemulsions for new developments in biomedical applications will be presented here. For creating a miniemulsion, the step of homogenization is of high importance since fairly monodispersed small droplets have to be achieved. The homogenization can be obtained by an ultrasonifier (for the miniemulsification of small quantities in a laboratory scale batch process) or a high-pressure homogenizer (for larger scales). At the beginning of homogenization the polydispersity of the droplets is still quite high, but by constant fusion and fission processes induced by the high shear, the size and polydispersity decreases until the miniemulsion reaches a steady state [10]. The process of homogenization was followed by different methods, e.g., by turbidity and by surface tension measurement. A constant value indicating the steady

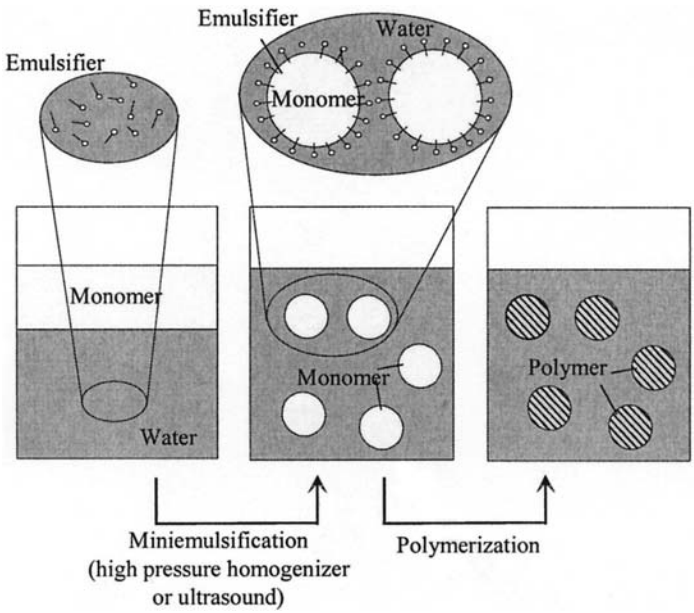

FIG. 1 The principle of miniemulsion polymerization.

state is reached in both experiments. The surface tension reaches high values, indicating that the coverage of the droplets by surfactant molecules is very low. Indeed, incomplete coverage of droplets by surfactant molecules is an important characteristic of miniemulsions and shows that the surfactant is very efficiently used. It was observed that the coverage of surfactant depends of the droplet size: The smaller the droplets are, the higher the coverage in order to obtain stable droplets. The exact size of the droplet can selectively be adjusted by the type and amount of surfactant used for the stabilization. Anionic and cationic surfactants allow the formation of monodispersed droplets between about 30 and 200 nm; nonionic oligomeric or polymeric surfactants are suitable for the formation of droplets between about 100 and 800 nm.

Such minidroplets were previously regarded as a somewhat unstable dispersion state of matter for two growth mechanisms for the droplets:

By Ostwald ripening (τ_1 mechanism)
By collisions (coalescence) (τ_2 mechanism)

Suppression of both processes is requested for the formulation of a stable miniemulsion. Coalescence can be controlled by the effective use of a surfactant. Ostwald ripening can efficiently be suppressed by the addition of a hydrophobic

agent to the dispersed phase. This agent cannot diffuse from one droplet to the other and is trapped in each droplet; this provides an osmotic pressure inside the droplets that counteracts the Laplace pressure. The effectiveness of the hydrophobe increases with decreasing water solubility in the continuous phase.

This mechanism was already used for the stabilization of fluoroalkane droplets by addition of the ultrahydrophobe perfluorodimorphinopropane, resulting in an effective and stable blood substitute [11]. A variety of molecules can be used as hydrophobes, and they can be selected to add a useful property to the final product, i.e., a dye, a plastisizer, or a cross-linker. For biomedical applications, this component could be also a fluorescent marker or a drug.

The addition of an ultrahydrophobe does not completely block droplet growth (due to a still finite solubility, the existence of droplet collisions, and surfactant-assisted transport) but, remarkably, slows it down. The final state to be expected is given by the balance of osmotic pressure and Laplace pressure. Since the Laplace pressure right after miniemulsification is usually larger than the osmotic pressure, the miniemulsion tend to grow on the time scale of days to weeks. Due to the time scale, this growth usually is not relevant for synthetic application, but it is also possible to handle it in a thermodynamic fashion. This can be done by increasing the amount of osmotic agent, increasing the particle size, or adding a second dose of surfactant after dispersion (to lower surface tension and the related Laplace pressure) [10].

The extremely high stability of those nanodroplets as well as the absent exchange of material between the droplets (in case of low solubility in the continuous phase) was graphically illustrated by classical color reaction such as the formation of Prussian blue or nickel murexid in inverse miniemulsion systems [12,13]. In the case of nickel murexid, one miniemulsion with droplets containing a murexid solution and another miniemulsion containing a Ni^{2+-} solution are mixed. The mixed miniemulsion (represented at 0 s) stays red and no nickel–murexid complex is formed. This indicates that droplets with murexid and droplets with Ni^{2+-} coexist and no fusion/fission process takes place. If one performs, as a comparison, the same experiment with two *micro*emulsions, an immediate reaction would take place because the low interfacial tension of close to zero leads to high dynamic processes in the system. The droplets in microemulsions do not hold their identity, whereas in miniemulsions they do. This is because in miniemulsions higher energy is required to perform this process, e.g., ultrasonication. In this case, fusion and fission processes are induced, and it can be seen that with increasing ultrasonication time the miniemulsion turns yellow. The overall droplet size does not change. Because of that, each miniemulsion droplet can be treated as a small nanoreactor, and stabilization of each of the nanoreactors can be obtained by using surfactants. This enables a whole set of new reactions that lead to nanoparticles as well as the synthesis of nanoparticles hybrids that were not accessible before. Some examples that are relevanct to

biomedical applications will be given in the following to show the wide applicability.

III. PREPARATION OF MINIEMULSIONS USING BIOCOMPATIBLE SURFACTANTS

The majority of the recipes described in the literature are based on the anionic sodium dodecyl sulfate (SDS) as a model system. The possibility of using cationic surfactants such as octadecylpyridinium bromide for the preparation of miniemulsions was first exploited in 1976. However, the emulsions were prepared by stirring and the resulting emulsions showed broadly distributed droplet sizes [14,15]. Recent work on steady-state miniemulsions showed that cationic and nonionic surfactants form well-defined miniemulsions for further miniemulsion polymerization processes, resulting in narrow-size distributed stable cationic and nonionic latex particles [16]. Nonionic miniemulsion can be made by using 3–5% of a poly(ethylene oxide) derivative as surfactant, resulting in larger but very well-defined latexes [16].

However, all of these surfactants show a low biocompatibility. Therefore, the use of other surfactants is required if latex particles should be used in biomedical applications. In the following, the formulation of miniemulsions with biocompatible and nontoxic surfactants is shown.

A. Lecithin

Lecithin is usually used as a synonym for phosphatidylcholine, which is the major component of a phosphatide fraction that is frequently isolated from either egg yolk or soya beans. Lecithin is a mixture of differently substituted *sn*-glycerol-3-phosphatidylcholine backbones. The structure of lecithin, which is given in Fig. 2, is variable and dependent on fatty acid substitution. In the sn-1 position saturated acyl groups and in the sn-2 position unsaturated species are more

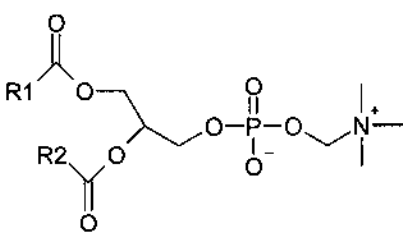

FIG. 2 Chemical structure of lecithin; RI, R2: typically linear aliphatic rests with 15 or 17 carbon atoms with up to four cis double bonds.

common [17]. Fatty acids of mainly 16–20 C in chain length dominate in egg lecithin. The sn-1 chain typically shows an average of 16 C, whereas the sn-2 chain shows an average of 18 C. Naturally occurring unsaturated fatty acids are almost entirely of all-cis conformation.

Only a limited number of emulsifiers are commonly regarded as safe to use for parenteral administration; one of these is lecithin. Compared with its synthetic alternatives, lecithin can be totally biodegraded and metabolized because it is an integral part of biological membranes, making it virtually nontoxic, whereas other emulsifiers can only be excreted via the kidneys. However, the natural origin of lecithin produces a rather complex composition, although in pharmacy in general well-defined singular excipients are favored. Lecithin is regarded as a well-tolerated and nontoxic compound, making it suitable for long-term and large-dose infusion. As an emulsifier of intravenously administered fat emulsions, its composition and behavior determine the structure and stability of the emulsion in a decisive way.

A high phosphatidylcholine content means that they represent a good source of choline. Choline is thought to be a vitamin-like substance which, according to recent research, may be essential under certain circumstances [18,19]. A lack of choline may lead to fat accumulation in the liver, necrosis of liver cells, and even liver cancer [20,21].

Lecithin can be used in an efficient way as a biocompatible surfactant for the preparation of miniemulsions. A surfactant concentration of only 0.3 wt % was sufficient to obtain stable styrene miniemulsions and after polymerization polymer dispersions with a particle size of 350 nm. By variation of the relative amount of the lecithin it was possible to decrease the particle size: At 3.3 wt % surfactant related to styrene, particles of 88 nm were obtained. Compared to latexes synthesized with the ionic surfactant sodium dodecyl sulfate (SDS) [10], the efficiency of the lecithin is lower and the whole size–concentration curve is shifted to larger sizes (Fig. 3). Compared to the nonionic Lutensol AT50, the lecithin is only more efficient at low surfactant concentration; at higher concentrations, the size of the lecithin-stabilized particles levels off whereas the size of the Lutensol AT50–stabilized particles still decreases with increasing surfactant amount.

As can be derived from the surface tension of the latexes and surfactant titrations, the particle surfaces are in all cases incompletely covered by lecithin molecules and the latexes show surface tensions well above the values of the saturated surfactant solution where saturated surfactant layers occur.

B. Cholic Acid

Cholic acid (3α,7α,12α-trihydroxy-5β-cholan-24 acid) is composed of a steroid unit with a carboxylic acid group and three hydroxyl groups, all located at one

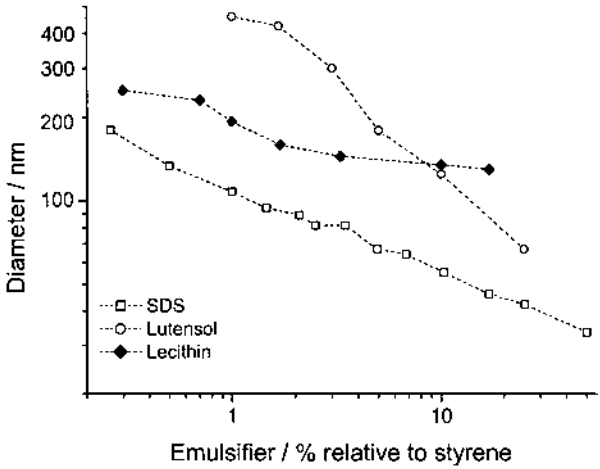

FIG. 3 Variation of the particle size by changing the amount of lecithin for the preparation of styrene miniemulsions. For comparison, the variations of the particle size using SDS and Lutensol AT50 are shown.

side of the steroid nucleus (Fig. 4). Cholic acid is one of the bile acids and its salt is found as a natural constituent of the bile. The nucleus of the bile acids is closely related to cholesterol, from which they are formed in the liver, and this conversion depends on their relative concentrations. Between 90% and 95% of bile acids are reabsorbed, mainly from the lower half of the small intestine, and undergo enterohepatic circulation [22]. Due to their amphiphilic character, bile salts affect the absorption of fats, fat-soluble vitamins, and various ions.

The salt of the cholic acid can be excellent for the formulation of miniemulsions. An amount of 0.6 wt % compared to the monomer styrene leads to stable styrene miniemulsions and, after polymerization of the styrene, to stable disper-

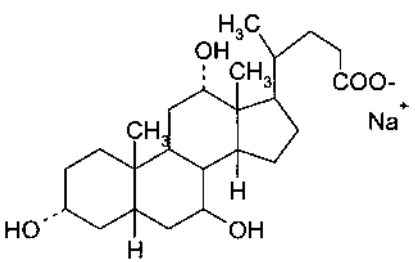

FIG. 4 Chemical structure of sodium salt of cholic acid.

sions with particles of 140 nm. The surface tension of the final latex, with a value of 68.5 mN m^{-1}, is close to the value of pure water (72 mN m^{-1}), indicating that the particles are not fully covered by the surfactant and the surfactant is therefore used in a very efficient way. Increasing the amount of the surfactant to 1.2 wt % leads to particles with a size of 104 nm; the surface tension of the dispersion is still high (68.3 mN m^{-1}). Using 3.3 wt % surfactant related to styrene, particles of 88 nm are obtained; the lower surface tension of 55.3 $mN \cdot m^{-1}$ indicates a higher but still incomplete coverage of the smaller particles with the surfactant—a behavior that was also observed for many other surfactants [10]. A further increase of the surfactant concentration did not result in smaller particles.

C. Tween 80

Tween 80 (polyethoxysorbitan monooleate) is a nonionic surfactant composed of a sorbitan ring and about 20 ethylene oxide units (Fig. 5). The surfactant is known as a nontoxic surfactant with excellent physiological properties and is widely used in biochemical applications, including emulsification and dispersion of substances for pharmaceutics, cosmetics, and food products.

The surfactant can be excellently used for the formulation of miniemulsions. Using 2.5 wt % Tween 80 related to styrene, stable miniemulsions were obtained. The polymerization of styrene miniemulsions leads to particles with a size of about 300 nm. Increasing amounts of Tween 80 up to 25 wt % permit a decrease in the particle size to 140 nm. The diameter depends linear on the concentration of the surfactant, which is quite unusual as can be seen in Fig. 6 where for comparison the variation of particle size by changing the amount of Lutensol AT50 Vf or the preparation of styrene miniemulsions is plotted.

D. Chitosan

Chitosan is a biodegradable, nontoxic, and naturally occurring polymer of β-(1-4)-2-amino-2-deoxy-D-glucopyranose, prepared by partial alkaline deacetylation of chitin, a main structural component of the cuticles of insects mollusks and

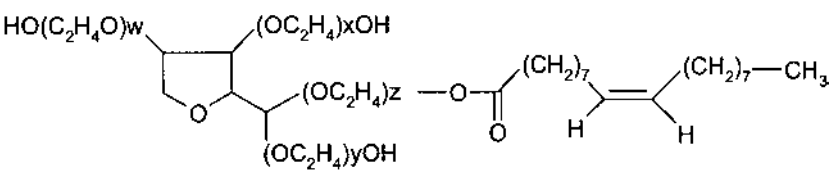

FIG. 5 Chemical structure of Tween 80, sum of $w,x,y,z = 20$.

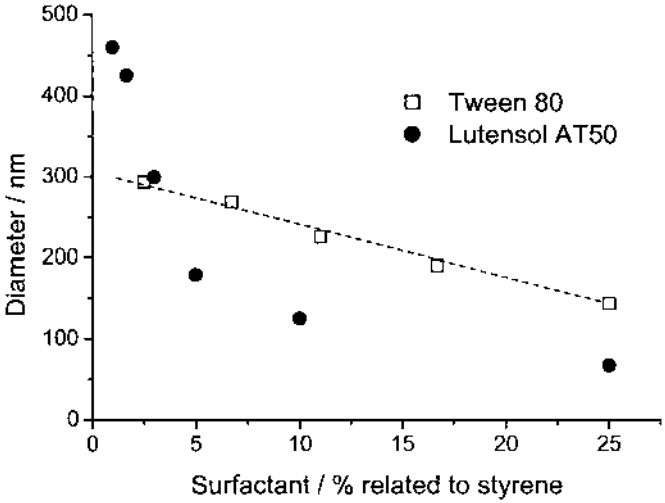

FIG. 6 Variation of the particle size by changing the amount of Tween 80 for the preparation of styrene miniemulsions. For comparison, the data of the particle size using Lutensol AT50 are shown.

crustaceans [23]. Its copolymer structure is depicted in Fig. 7. The amphiphilic biopolymer, which is insoluble in water at pH 7, becomes soluble and positively charged in acidic media and can therefore be used as a flocculating agent [24] or a biosurfactant [25]. This polyelectrolyte has been successfully used to stabilize polymer nanoparticles of poly(methyl methacrylate) [26] and of poly(butyl cyanoacrylate) [27]. In these cases, the chitosan is thought to be grafted onto the particles by a hydrogen abstraction mechanism. These positively charged nanoparticles can be used as ideal candidates for the purification of proteins from a crude biological mixture [26]. If its pH is kept above 7, the proteins carry a net

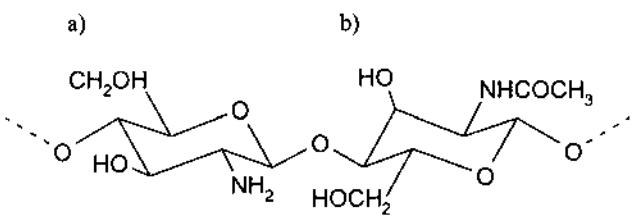

FIG. 7 Chemical structure of chitosan consisting of (a) deacetylated and (b) acetylated units.

negative charge and can therefore develop electrostatic interactions with the particles. These nanoparticles are also well suited as site-specific drug carriers [27].

Chitosan was also successfully used for the preparation of stable miniemulsions [28]. Use of either low or high molecular weight chitosan as a biocompatible surfactant produced stable styrene miniemulsions with as low as 0.5% chitosan compared to the monomer phase. However, during polymerization only a part of the polystyrene formed could be stabilized by the chitosan; the other part coagulated, resulting in a solid content that was lower than expected. By increasing the chitosan-to-styrene ratio, less coagulate was formed while keeping the particle size constant. Typical latex particles obtained are depicted by transmission electron microscopy (TEM) in Figure 8 [28]. The surface tension values of the final dispersions prepared by the low molecular weight chitosan were measured to be around 66 mN m^{-1}, indicating that in this case all the chitosan is mainly adsorbed on the particles. As chitosan bears amine functions, it can be grafted onto the particles via a hydrogen abstraction mechanism [26,27].

Chitosan alone as a stabilizer for nanometer-sized droplets is insufficient, and a large amount of coagulate is formed, possibly as a result of the fact that the chitosan cannot protect the final polymer particles against collision. Therefore, emulsification was supported by additional small amounts of other low molecular weight surfactants after the miniemulsification process or synthetic polymers were added to the oil phase.

An enhancement of stabilization was obtained by using the cationic surfactant cetyltrimethylammonium chloride (CTMA-Cl), which allows high solids content and synthesis of very small particles with diameters less than 100 nm.

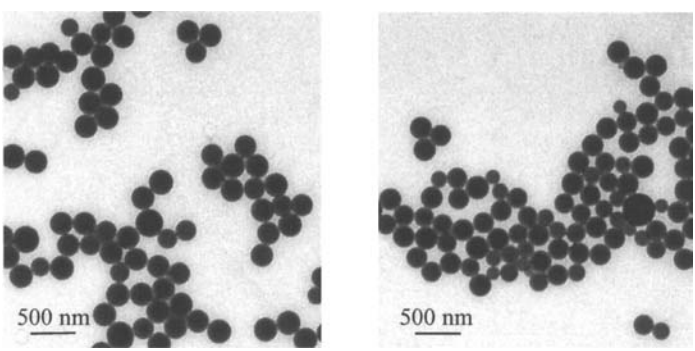

FIG. 8 TEM images of polystyrene latexes stabilized by chitosan. Left: low molecular weight chitosan. Right: High molecular weight chitosan.

However, the choice of CTMA-Cl hand was chosen as a cross-test to show the deficiencies of the system, since its use is prohibited by the demands of biocompatibility and biodegradability.

The synthetic biocompatible polymer, Jeffamine D2000, which was shown earlier to have interfacial properties [29], was added to the monomer phase to ensure cationic stabilization of the "weak spots" during the polymerization process. In this case, high solids contents were obtained at small amounts of Jeffamine (between 0.5 and 2.5 wt % with respect to the monomer phase), and very small and monodispersed latexes in the size range of about 100–200 nm without any coagulate could easily be synthesized. It is interesting to see that beyond 1% of Jeffamine, the particle size saturates at a similar value of 100 nm. It is expected that this is the primary particle size, which is now stabilized throughout the process.

IV. EPOXY HYBRID PARTICLES USING CHITOSAN AS REACTIVE SURFACTANT

It has recently been shown that the miniemulsion process is not restricted to radical polymerization but can also be applied to the polyaddition of different diepoxides with various diamines [29]. In these examinations, the standard surfactants SDS and Lutensol AT50 were used. For biocompatible applications, it is desirable to synthesize polyaddition latexes with chitosan/Jeffamine D2000 as the stabilizer/costabilizer system. Since both chitosan and Jeffamine bear amine functionalities, they can react with the diepoxides and can be considered as reactive stabilizers.

A monomer mixture containing the diepoxide Epikote E828 and the diamine Jeffamine was dispersed in the chitosan solution using the classical miniemulsion procedure. Stable and coagulate-free latexes were obtained with relatively broad size distributions [28]. Results suggest that the particle size decreases with the amount of low molecular weight chitosan, as is the case for the conventional surfactants [10], and also decreases with increasing ratio of dispersed to continuous phase. No clear tendency was obtained in the case of high molecular weight chitosan. Emulsions and after polymerization latexes with diameters as low as 100 nm and a cationic chitosan surface layer were generated. Using miniemulsion procedures with the addition of a low molecular weight surfactant or a more flexible polymer costabilizer significantly improve the surface layer structure and the coupled stabilization efficiency, and allow production of structures in the diameter range 100–300 nm. Using other diamines such as 1,12-diaminododecane and 4,4′-diaminodicyclohexylmethane chitosan alone was not sufficient to stabilize the polymerizing particles, underlining the importance of Jeffamine as a cosurfactant. With minor amounts of Jeffamine, it was possible to synthesize a great variety of epoxy resins.

V. FUNCTIONALIZATION OF NANOPARTICLES BY MINIEMULSION POLYMERIZATION FOR FURTHER BIOFUNCTIONALIZATION OF NANOPARTICLES

Acrylic acid can be copolymerized with styrene to obtain functionalized particles that can be used, e.g., to bind antibodies onto them. In order to avoid a polymerization of the acrylic acid in the aqueous phase, the oil-soluble initiator ADVN (2,2′-Azobis(2,4-dimethylvaleronitrile)) was used. Due to the hydrophilic character of the acrylic acid, its tendency to be on the particle surface is very high. For the synthesis, between 0 and 6 wt % acrylic acid was added to the styrene. The miniemulsification was carried out using 1.2 wt % SDS, which leads to particles with a size of about 90 nm independent of the amount of acrylic acid. As shown in Fig. 9, the charge density on the surface of a dialyzed sample increases with an increasing amount of acrylic acid. For a binding reaction of antibodies (e.g., streptavidin) onto the surface of the particles, a concentration of 3% acrylic acid proved optimal.

VI. FORMATION OF BIOCOMPATIBLE NANOCAPSULES

Chitosan as a biocompatible [30] and biodegradable cationic polyelectrolyte can also be used for the preparation of capsules, which are of great interest in pharmaceutical and biomedical fields [31,32]. The capsules can be prepared in different ways. One approach is the coacervation technique whereby a solution of chitosan is blown into a nonsolvent and the polymer precipitates at the surface

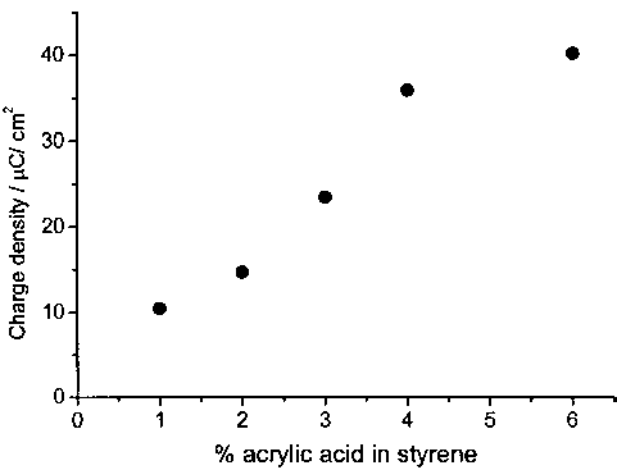

FIG. 9 Copolymerization of styrene with acrylic acid leads to charged particles.

of the droplets thereby forming capsules [32,33]. Another approach is the coating process [32,34] whereby the oil phase containing the product is blown in the chitosan solution, with the polymer precipitating at the surface of the droplets. The surface properties of chitosan were used to produce capsules by cross-linking the chitosan at the interface [35–37]. However, in most cases, the formed capsules are quite big (from 500 nm to several micrometers), and the size distribution is large.

Nanocapsules with diameters down to 100 nm and a cationic chitosan surface layer were successfully generated using miniemulsion procedures [28]. With the hybridization and stabilization chemistry, it was possible to cross-link chitosan and its cosurfactant Jeffamine D2000 with diepoxies to capsule structures. Here the amphiphilic hybrid copolymer is built up in situ around the material to be encapsulated, as long as it does not interfere with the polyaddition process in miniemulsion. Previously synthesized chitosan capsules were quite big and not very well defined, and the interfacial hybridization reaction in miniemulsions is expected to extend the accessible size range toward the nanocapsule region. A scheme of this interface reaction around the inert droplet is shown in Fig. 10 [28].

Toluene containing the diepoxide Epikote E828 and Jeffamine was dispersed in the chitosan solution. The starting oil phase products are miscible, and a stable miniemulsion can be formed. During the cross-linking reaction between the chitosan and the epoxide, phase separation between the toluene and the polymer product occurs, and in the case of appropriate speading coefficients, as reported earlier, capsules are formed [38].

Free toluene could not be detected after the reaction and could not be separated by centrifugation, indicating that it was indeed encapsulated. As expected, the capsules in the presence of Jeffamine were small (126 nm) and well defined, whereas those without Jeffamine were rather big. It was not possible to obtain TEM pictures of those samples as the material constituting the shell is a low-T_g polymer that degrades in the electron beam. Using diaminododecane as an amine component results in a polymer with higher T_g and higher stability against electron degradation. The shells of nanocapsules could be depicted by TEM as empty hulls (Fig. 11) since the toluene is evaporated in the vacuum.

A cross-linking/hybridization reaction was achieved by including another water-soluble, amphiphilic, biocompatible, and more easily biodegradable amine, namely, Gluadin APG, which is a partially hydrolyzed wheat gluten protein with a molecular weight of about 5000 g · mol^{-1}. Toluene containing Epikote and Jeffamine D2000 was thus dispersed in a solution of chitosan and Gluadin using the conventional miniemulsion process. It is emphasized that in this case, the costabilizer is water soluble and approaches the droplet surface from the water phase. After the reaction, again no free toluene was found in the latexes, indicating efficient encapsulation. From NMR experiments it was estimated that about

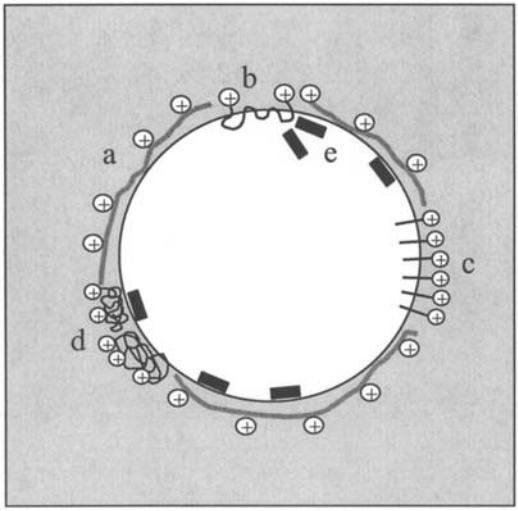

FIG. 10 Schematic view of the formation of nanocapsules by interfacial reaction. Chitosan acts as a reactive biocompatible stabilizer from the water phase forming patches on the interface (a); costabilizer like oligomeric diamines (b) (e.g., Jeffamine D2000) or low molecular cationic surfactants (c) (e.g., CTMA molecules) can improve the surface layer structure from the inside of the droplets and the coupled stabilization efficiency. A stabilization from the water phase can also be provided by a water-soluble but amphiphilic protein, e.g., Gluadin (d). A diepoxide (e) can additionally be used as stabilizing cross-linking agent.

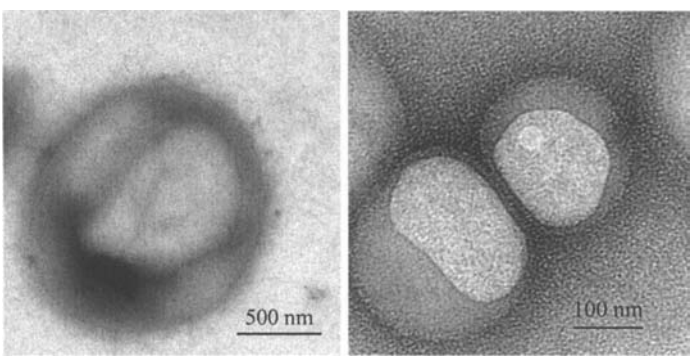

FIG. 11 TEM images of the capsule preparation.

90% of Gluadin has reacted. This means that a majority of the Gluadin can bind to the miniemulsion droplets, react with the oil-soluble diepoxy derivative, and bridge to the chitosan [28].

It is speculated that chitosan, due to its somewhat stiff polysaccharide backbone, shows rather flat adsorption and leaves out larger unstabilized "patches" which for packing reasons cannot be filled by the chitosan itself. This is why addition of a second, more flexible component, such as CTMA-Cl (ideally, but not biocompatible), Jeffamine D2000, or Gluadin has such a profitable influence. Similar effects are known from microemulsions and attributed to the "tree grass" principle [39]. The fact that the arrangement of Gluadin with chitosan at the droplet interface is still problematical is seen in the data set where both Jeffamine D2000 and Gluadin had to be added to the recipe in order to obtain a Gaussian distribution of the nanocapsules without the formation of larger ones. Here the particle size depends on the amount of Gluadin added, as should be expected for linear costabilizer efficiency [28].

Polyaddition of the chitosan stabilizer with two biocompatible costabilizers, Jeffamine D2000 and Gluadin, and a linking diepoxide in presence of an inert oil results, via an interface reaction, in thin but rather stable nanocapsules. Since both water- and oil-soluble aminic costabilizers can be used, these experiments show the way to a great variety of capsules with different chemical structure. These capsules are expected to be biocompatible and biodegradable and might find applications in drug delivery.

Another point is that in the presented scenario, polymer reactions on biopolymers take place at the relatively high internal surface areas of miniemulsions in a preoriented state (by the gradient of cohesion energy). Therefore, reaction in miniemulsions also allows both hydrophilic and hydrophobic modification of chitosan with high efficiency, up to the otherwise rather complicated coupling or grafting with a polypeptide, as delineated by the coupling with Gluadin [28].

VII. ENCAPSULATION OF INORGANIC MATERIALS FOR BIOMEDICAL APPLICATIONS USING MINIEMULSION PROCESSES

Biocompatible magnetic particles are important prerequisites for separation and purification processes [40–43], in immunoassays [44], as agents for the destruction of cells via magnetic fields [45], as contrast agents to enhance magnetic resonance imaging [46], and for targeted delivery of therapeutic agents [47]. Success in many applications requires particles of a specific size with a narrow size distribution. The encapsulation of small and uniformly sized superparamagnetic particles into hydrophobic polymer particles by the miniemulsion polymerization process is of high interest.

Recent investigations show that the miniemulsion process allows the encap-

sulation of hydrophobized calcium carbonate [48] and carbon black [49]. However, magnetite is hydrophilic and relies on an effective surface treatment before the encapsulation process. This is preferentially done by adsorption of a secondary surfactant on the magnetite surface that does not interfere with the primary surfactant system needed to stabilize the polymer particles.

Magnetite particles were encapsulated in a polystyrene matrix by a miniemulsion polymerization process [50]. In a first step, a stable dispersion of magnetite particles in styrene is required. For that purpose, an effective emulsifier system has to be used in order to make the particles hydrophobic and to prevent aggregation. Oleoyl sarcosine acid and more efficient oleic acid as a first surfactant system to handle the interface magnetite/styrene oleic acid, and magnetite particles down to 10 nm were effectively stabilized in styrene and related monomer mixtures. These lipophilic dispersions could be miniemulsified in water by using SDS as a second emulsifier system forming a stable emulsion. It is important to note that the simple magnetite particles remain well dispersed in the monomer droplets, as shown by electron microscopy. This means that the acid stays at the magnetite–styrene interface and is not redistributed toward the monomer–water interface, an important prerequisite to keeping such double dispersions stable.

Since hexadecane was added to the monomer phase as an ultrahydrophobe to prevent Ostwald ripening, the monomeric double miniemulsion was already kinetically stable. The polymerization was then started by raising the temperature. The final dispersion was free of coagulum and stable. The brown color did not change during the polymerization, which proves that the radical polymerization process did not significantly interfere with the oxidation state of the magnetite colloid. A simple test with a magnet showed that the dispersion is a ferrofluid, i.e., is magnetic. Thermogravimetric measurements revealed that the magnetite loading in the final particles was up to 20 wt %, indicating that no change of composition by a selective loss of inorganic material occurred throughout reaction.

In Figure 12, the TEM image of polystyrene particles with encapsulated magnetite is shown. Particles with diameters of about 100 nm are found.

VIII. CONCLUSION

The main aim of this chapter was to show the possibility of using the miniemulsion process for the formulation of nanoparticles which can be used for biomedical applications. The use of appropriate high-shear surfactants and the addition of a hydrophobe to suppress the influence of Ostwald ripening are key factors in the formation of the small, stable droplets in miniemulsions. It was shown that the strength of a miniemulsion is the formation of polymeric nanoparticles consisting of polymers or polymer structures, which are hardly accessible by other types of heterophase polymerization. The stabilization of such particles

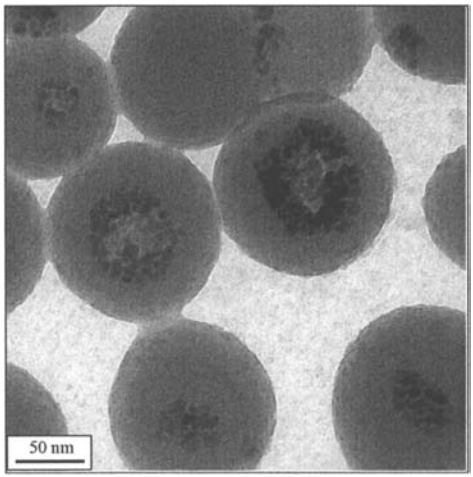

FIG. 12 Encapsulation of Fe_3O_4 in polystyrene particles.

can be easily obtained by the biocompatible, nontoxic, and sometimes biodegradable surfactants that make such particles interesting for biomedical applications. Functionalization of the particle surface allows the specific binding of antibodies. Nonradical polymerizations and the formation of hybrid materials by the encapsulation of inorganic materials are some examples, which show the wide applicability of the miniemulsions.

In my opinion, the potential for formulating miniemulsions for biomedical applications is still on its rise because numerous additional possibilities are available. One may envision single biomolecules trapped in each small droplet. Since miniemulsions allow a very convenient and effective separation of objects in compartments of 30–300 nm diameter, some general new perspectives for biochemistry are open as is the regular case in biochemical reactions since practically all reactions take place in different compartmentalized areas of the cell [51]. Physicochemical processes such as protein folding can be obtained which mainly take place as single molecular events in the nanocompartments [52]. Mimicking in biochemical processes would open the door to gain better control of the outcome of demanding complex processes for many biomedical applications.

REFERENCES

1. Candau, F. In *Polymerization in Organized Media*; Paleos, E.C., Ed.; Gordon and Breach: Philadelphia, 1992; 215–282.

2. Blackley, D.C. *Polymer Latices*, 2nd Ed.; Chapman and Hall: London, 1997.
3. Landfester, K. Macromol. Rapid Comm. **2001**, *22*, 896–936.
4. Antonietti, M.; Landfester, K. Chem. Phys. Chem. **2001**, *2*, 207–210.
5. Dawkins, J.V. Aqueous Suspension Polymerization in *Comprehensive Polymer Science;* Allen, Bevington, Eds.; Pergamon Press: Oxford, 1989; 231–241.
6. Ugelstad, J.; El-Aasser, M.S.; Vanderhoff, J.W. Polym. Lett. Ed. **1973**, *11*, 503.
7. Blythe, P.J.; Sudol, E.D.; El-Aasser, M.S. Macromol. Symp. **2000**, *150*, 179.
8. Schork, F.J.; Poehlein, G.W.; Wang, S.; Reimers, J.; Rodrigues, J.; Samer, C. Colloids Surf. A Physicochem. Eng. Asp. **1999**, *153*, 39.
9. Landfester, K. Macromol. Symp. **2000**, *150*, 171.
10. Landfester, K.; Bechthold, N.; Tiarks, F.; Antonietti, M. Macromolecules **1999**, *32*, 5222.
11. Lowe, K.C. Art. Cells Blood Subs. Immob. Biotech. **2000**, *28*, 25.
12. Landfester, K. Adv. Mater. **2001**, *10*, 765–768.
13. Antonietti, M.; Landfester, K. Prog. Polym. Sci. **2002**, *27*, 689–757.
14. Chou, Y.J.; El-Aasser, M.S.; Vanderhoff, J.W. J. Dispers. Sci. Technol. **1980**, *1*, 129–150.
15. Azad, A.R.M.; Ugelstad, J.; Fitch, R.M.; Hansen, F.K. In *Emulsion Polymerization*; Piirma, I., Gardon, J.L., Eds.; ACS: Washington, DC, 1976; Vol. 24, 1–23.
16. Landfester, K.; Bechthold, N.; Tiarks, F.; Antonietti, M. Macromolecules **1999**, *32*, 2679–2683.
17. Kuksis, A.; Myher, J.J.; Marai, L. J. Am. Oil Chem. Soc. **1985**, *62*, 762–767.
18. Zeisel, S.H. J. Nutr. Biochem. **1990**, *1*, 332.
19. Jacob, R.A.; Jenden, D.J.; Allman-Farinelli, M.A.; Swendseid, M.E. J. Nutr. **1999**, *129*, 712.
20. Ghoshal, A.K.; Farber, E. Lab. Invest. **1993**, *6*8, 255.
21. Buchman, A.L.; Dubin, M.D.; Moukarzel, A.A.; Jenden, D.J.; Roch, M.; Rice, K.M.; Gornbein, J.; Ament, M.E. Hepatology **1995**, *22*, 1399.
22. Stravitz, R.T.; Sanyal, A.J.; Pandak, W.M.; Vlahcevic, Z.R.; Beets, J.W.; Dawson, P.A. Gastroenterology **1997**, *113*, 1599–1608.
23. Roberts, G.A.F. *Chitin Chemistry*; Macmillan Press: London, 1992.
24. Ashmore, M.; Hearn, J.; Karpowicz, F. *Langmuir* **2001**, *17*, 1069–1073; M. Ashmore, J. Hearn, *Langmuir* **2000**, *16*, 4906–4911.
25. Blanco, L.F.D.; Rodriguez, M.S.; Schultz, P.C.; Agullo, E. Colloid Polym. Sci. **1999**, *277*, 1087–1092.
26. Chem, C.S.; Lee, C.K.; Ho, C.C. J. Polym. Sci. Polym. Chem. **1999**, *37*, 1489–1499.
27. Yang, S.C.; Ge, H.X.; Hu, Y.; Jiang, X.Q.; Yang, C.Z. Colloid Polym. Sci. **2000**, *278*, 285–292.
28. Marie, E.; Landfester, K.; Antonietti, M. Biomacromolecules **2002**, *3*, 475–481.
29. Landfester, K.; Tiarks, F.; Hentze, H.-P.; Antonietti, M. Macromol. Chem. Phys. **2000**, *201*, 1–5.
30. Weiner, M.L. *Advances in Chitin and Chitosan*; Elsevier Science: London, 1993.
31. Kumar, M.N.V.R.; Kumar, N. Drug Dev. Ind Pharm. **2001**, *27*, 1–30.
32. Yao, K.D. Peng, T. Yin, Y.J. Xu, M.X. J. M. S.-Rev. Macromol. Chem. Phys. **1995**, *C35*, 155–180.

33. Chen, R.H.; Tsaih, M.L. J. Appl. Polym. Sci. **1997**, *66*, 161–169.
34. Calvo, P.; Remunan-Lopez, C.; Vila-Jato, J.L.; Alonso, M.J. Colloid Polym. Sci. **1997**, *275*, 46–53.
35. Genta, I.; Perugini, P.; Conti, B.; Pavanetto, F.; Int. J. Pharm. **1997**, *152*, 237–246.
36. Yeom, C.K.; Oh, S.B.; Rhim, J.W.; Lee, J.M. J. Appl. Polym. Sci. **2000**, *78*, 1645–1655.
37. Saha, T.K.; Jono, K.; Ichikawa, H.; Fukumori, Y. Chem. Pharm. Bull. **1998**, *46*, 537–539.
38. Tiarks, F.; Landfester, K.; Antonietti, M. Langmuir **2001**, *17*, 908–917.
39. Antonietti, M.; Basten, R.; Lohmann, S. Macromol. Chem. Phys. **1995**, *196*, 441–466.
40. Ugelstad, J.; Berge, A.; Ellingsen, T.; Schmid, R.; Nilsen, T.-N.; Mork, P.C.; Stenstad, P.; Homes, E.; Olsvik, O. Prog. Polym. Sci. **1992**, *17*, 87–161.
41. Bangs, L.B. Pure Appl. Chem. **1996**, *68*, 1873–1879.
42. Kondo, A.; Kamura, H.; Hagashotani, K. Appl. Microbiol. Biotech. **1994**, *41*, 99–105.
43. Tyagi, R.; Gupta, M.N. Biocat. Biotransform. **1995,** *12*, 293–298.
44. Lim, P.-L. J. Immunol. Methods **1990**, *135*, 257–261.
45. Jordan, A.; Scholz, R.; Wust, P.; Schirra, H.; Schiestel, T.; Schmidt, H.; Felix, R. J. Magn. Magn. Mater. **1999**, *194*, 185–196.
46. Roger, J.; Pons, J.N.; Massart, R.; Halbreich, A.; Bacri, J.C. Eur. Phys. J. Appl. Phys. **1999**, *5*, 321–325.
47. Hassan, E.E.; Parish, R.C.; Gallo, J.M. Pharm. Res. **1992**, *9*, 390–397.
48. Bechthold, N.; Tiarks, F.; Willert, M.; Landfester, K.; Antonietti, M. Macromol. Symp. **2000**, *151*, 549–555.
49. Tiarks, F.; Landfester, K.; Antonietti, M. Macromol. Chem. Phys. **2001**, *202*, 51–60.
50. Hoffmann, D.; Landfester, K.; Antonietti, M. Magnetohydrodynamics **2001**, *37*, 217–221.
51. Stahler, K.; Selb, J.; Candau, F. Langmuir **1999**, *15*, 7565.
52. Hartl, F.U. Nature **1996**, *381*, 571.

10

Synthesis, Characterization, and Biomedical Applications of Conducting Polymer Particles

MOHAMED M. CHEHIMI, AMMAR AZIOUNE, SMAIN BOUSALEM, AMEL BEN SLIMANE, and ABDERRAHIM YASSAR Interfaces, Traitements, Organisation et Dynamique de Systèmes (ITODYS) de l'Université Paris, Paris, France

I. INTRODUCTION

Inherently conducting polymers (ICP*s*) have attracted a huge number of research groups worldwide for nearly three decades [1–4]. The main ICP*s* are polyaniline (PANI), polyaromatics (*e.g.*, polyparaphenylenes), and polyheterocyclic such as polypyrrole (PPy), polythiophene, and poly(ethylenedioxy)thiophene (PEDOT) of which chemical structures are shown in Fig. 1. ICPs can be synthesized electrochemically as thin films in the presence of a supporting electrolyte or chemically using $FeCl_3$ and ammonium persulfate $(NH_4)_2S_2O_8$ as oxidants. The chemical route has the advantage of yielding much larger scales of products. Counteranions from the oxidant salts or added salts are instantly incorporated during the ICP synthesis because the oxidation potential for polymerization is higher than for doping the ICP-chain [5]. Therefore, chemically polymerized ICP*s* are always formed in the conducting state. However, they can also be switched reversibly to a neutral insulating form. In the conducting form, ICP chains bear positive charges that are counterbalanced by anions (e.g., Cl^-, NO_3^-, SO_4^{2-}), called *dopants*. The ratio of dopant-to-repeat unit is the *doping level*. The nature of the counteranion is one of the determining factors controlling the properties of the ICP*s*, like the level and stability of the conductivity [6,7].

The classical syntheses of ICP*s* resulted in stiff and inflexible polymer chains, which seriously limits their processability and thus their applicability. However, recent work has shown that, under certain conditions, PANI [8,9], PPy [10–12], and polythiopehenes [13,14] can be obtained in soluble form in water or organic solvents.

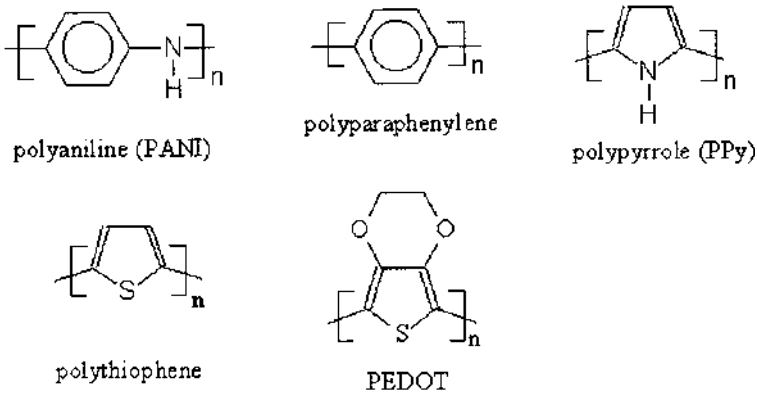

FIG. 1 Chemical structures of a selection of inherently conducting polymers.

ICPs have several potential applications including corrosion control of non-noble metals [15–17]; stationary phases in liquid chromatography [18–23]; electronic plastics such as organic light-emitting diodes [9,24,25], field effect transistors [26], and photovoltaic materials [27]; composite materials [5]; and biosensors [28,29]. As far as the latter application is concerned, polypyrrole is the most studied potential ICP. In addition, polypyrrole exhibits both redox and acid–base chemistry [30], ion-exchange properties [31], metallic-like conductivity (up to 300 S cm^{-1}) and electroactivity [28], relatively high surface free energy [32] and specific surface area [33–35] compared to conventional polymers. These attractive properties, together with the ease of chemical or electrochemical synthesis in aqueous media and its relative long-term stability, made polypyrrole a suitable candidate for the fabrication of biosensors [28], controlled drug release systems [36], and adsorbents for proteins [22,37,38] or DNA [39].

The latex particle synthesis route was a suitable alternative in the late 1980*s* and the 1990*s* to solve the processability problem associated with insoluble ICP*s*. However, other applications besides conducting polymer film formation and coatings were found using ICP particles. Tarcha and coworkers [40], for example, were very much interested in the deep black color of polypyrrole and took advantage of this property to develop immunodiagnostic assays. This was possible due to the chemical reactivity of the as-synthesized polypyrrole particles (see Section III.A.2). Reviews on colloidal dispersions [41,42] and nanocomposites [43] of conducting polymers have been published emphasizing several routes of preparation and potential applications in coatings, visual biological tests and bioadsorption, catalysis, energy storage, electrochromic activity, etc.

Of relevance to the present contribution and book, we shall review the prepa-

ration of ICP particles, especially those based on polypyrrole, in terms of mechanisms of bioadsorption of DNA and protein, on the one hand, and the possibility to develop immunodiagnostic assays, on the other hand. One of the important issues in characterizing the surface composition of the ICP particles is the determination of the surface composition in relation to reactivity to proteins and DNA. In this regard, X-ray photoelectron spectroscopy (XPS) is a key analytical technique to investigate the surface chemistry of ICP particles although this technique is applied to the dried materials only. For this reason, we will briefly discuss its basic principles.

This chapter is divided into the following sections:

Principles and applications of XPS
Sterically stabilized polypyrrole colloids
Conducting polymer-silica nanocomposites
Conducting polymer-coated latex particles

Each section concerning the three types of ICP particles mentioned above will deal with their preparation, properties, and biological applications.

II. BASIC PRINCIPLES OF X-RAY PHOTOELECTRON SPECTROSCOPY

In XPS, solid materials (e.g., plates, thin films, powders, and fibers) irradiated, in high vacuum, by monoenergetic soft X-rays (Al Kα or Mg Kα, $h\nu = 1486.6$ or 1253.6 eV, respectively), emit core electrons the binding energy (BE) of which is characteristic of the target element present at the surface (Fig. 2). The measured kinetic energy (KE) is given by:

$$KE = h\nu - BE - \phi_s$$

where $h\nu$ is the energy of the photon, BE is the binding energy of the photoelectron, and ϕ_s is the spectrometer work function. The binding energy of a core level is characteristic of the emitting element. All elements can be detected by XPS except hydrogen, the 1s electron of which is involved in chemical bonding. Because the emitted photoelectrons have low mean free paths (λ) in the 1- to 4-nm range, it follows that photopeaks arise from the outermost layers only. The analysis depth probed by XPS is given by:

$$d = 3\lambda \cos \theta = 2\text{–}10 \text{ nm}$$

where θ is the analysis angle relative to the surface normal. This small depth analysis makes XPS a very sensitive surface analytical technique.

The most important advantage of XPS is the possibility to detect binding energy shifts that depend on the chemical states of the target elements. The so-

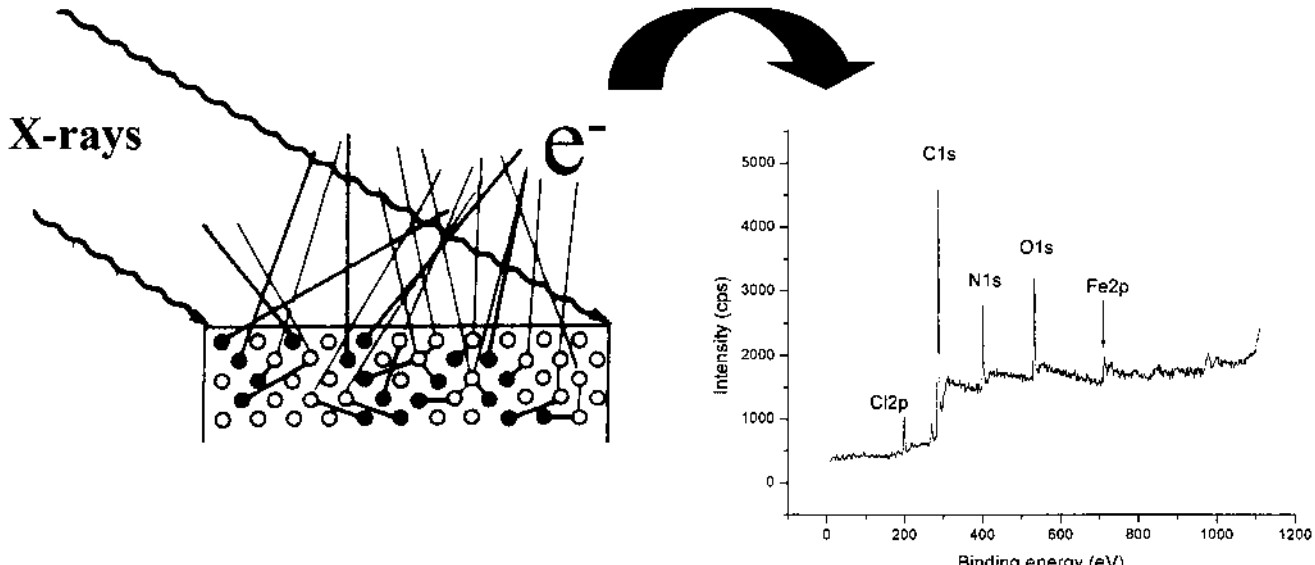

FIG. 2 X-ray-induced photoionization of a surface. The emitted electrons give what is called a photoelectron spectrum. Example is given for a polypyrrole-coated polystyrene latex particle.

called chemical shift is the cornerstone of XPS since, for example, one can distinguish between aliphatic hydrocarbon from carboxylic carbon, sulfides from sulfates, metals from oxides, within a depth on 10 nm maximum only. Table 1 reports some reference BE values for carbon, nitrogen, oxygen, silicon, and sulfur in organic materials.

TABLE 1 Typical Binding Energies for C1s, N1s, O1s, Si2p, and S2p in Selected Functional Groups

Functional group	Chemical structure	Binding energy (eV)
C1s		
Hydrocarbon	C−H, C−C	285.0
Amine	C−N	285.7
Ether, alcohol	C−O−C, C−O−H	286.5
Ketone	C=O	287.8
Amide	N−C=O	288.0
Carboxylic acid, ester	−COOH, −COOR	289
Carbamate	O−C(=O)−N	289.6
Carbonates	−O−C(=O)−O	290.5
Fluorocarbon	C−F	287.8
Difluorocarbon	F−C−F	292
Trifluorocarbon	$-CF_3$	293–294
N1s		
Imine (in PPy)[a]	−N=C	398.5
Aromatic N (in P4VP)[b]	−N=C	399.3
Amide (in nylon 6)	N−C=O	399.8
Carbamate	N−COO−	400.3
Ammonium	$-NH_3^+$	401.5
Nitro	$-NO_2$	405.5
O1s		
Carbonyl	C=*O*, O−C=*O*	532.2
Alcohol, ether	C−O−H, C−O−C	532.8
Ester	−*O*−C=O	533.7
Si2p		
Siloxane (in PDMS)[c]	$-Si(CH_3)_2-$	101.8
Silicon dioxide	Si−O	103.4
S2p		
Thioether (in cysteine)	C−S	164
Sulfonate (in PSS)[d]	$-SO_3^-$	168.2

[a]Deprotonated pyrrole repeat units in PPy.
[b]Poly(4-vinylpyridine).
[c]Poly(dimethylsiloxane).
[d]Poly(styrenesulfonate).

Figure 3 displays a high-resolution C1s spectrum of polyethyleneterephthalate (PET) with the main components due to C−C/C−H, C−O, and O−C=O functional groups centered at 285, 286.5, and 289 eV, respectively. In addition to the chemical shifts that the functionalized carbon atoms in PET undergo, one can also observe a minor feature at high binding energy side (~7 eV higher than the reference C−C/C−H carbon type) termed "shake-up satellite." This satellite is observed with aromatic polymers such as polystyrene (PS) and PET. In Fig. 3, the shake-up satellite is actually located at lower kinetic energy (KE) and accounts for an energy loss that the carbon atoms from the aromatic ring undergo to promote a $\pi \rightarrow \pi^*$ transition. This satellite can be used as a fingerprint of aromatic rings and in particular could be used to trace polystyrene as shown below in the specific examples (see Section III.C).

For a homogeneous sample within the analyzed volume, the peak intensity (I) is related to $[A]$, the surface concentration of element A by:

$$I \propto s[A]$$

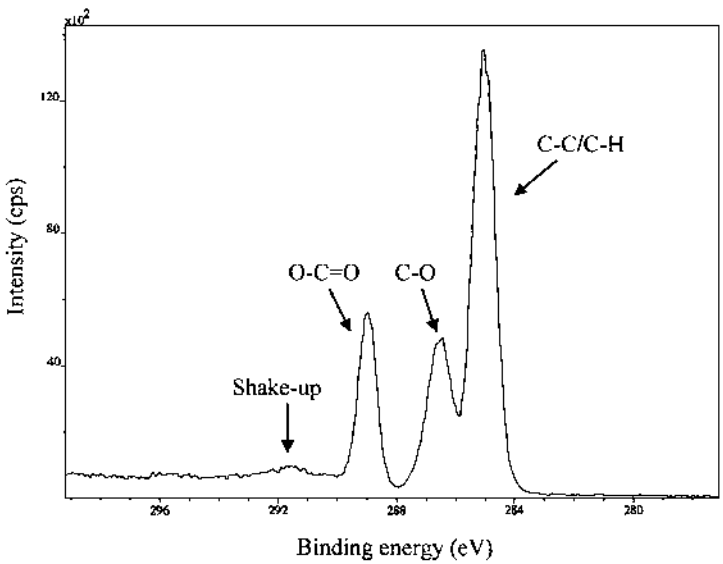

FIG. 3 High-resolution C1s region from polethyleneterephthalate (PET). The fine structure indicates the type of carbon atoms appearing at 285, 286.5, and 289 eV for C-C/C-H, C-O, and O-C=O, respectively. The minor high binding energy feature is a shake-up satellite due to $\pi \rightarrow \pi^*$ transition associated with the phenyl ring. (Courtesy of Kratos Analytical Ltd., Manchester, UK.)

where s is the sensitivity factor. It follows that the general expression for determining the surface composition in atomic percents is given:

$$\%A = \frac{(I_A/s_A)}{\Sigma(I_n/s_n)} \times 100\%$$

where I_n and s_n are the integrated peak areas and the sensitivity factors, respectively.

As far as polymers and colloids are concerned, XPS has exensively been used to characterize these materials for three decades. XPS analyses of conventional polymers resulted in the publication of a handbook [44] and several book chapters [45–47]. Conducting polymers have been studied by several groups especially the team led by Kang [30,48] and also by Sabbatini and coworkers [49–51]. While latex particles was the subject of numerous studies by several groups [52–56], to our knowledge there is no review on XPS analysis of conducting polymer particles but some specific studies related to polypyrrole-silica nanocomposites [57–59], and conducting polymer-coated PS [60–63] and poly(methyl methacrylate) (PMMA) latex [64] particles. It is not the purpose of this chapter to review exhaustively the XPS analysis of conducting polymer particles, but in the following sections we will give examples demonstrating the usefulness of the technique to solve problems related to this class of materials.

II. PREPARATION AND PROPERTIES OF CONDUCTING POLYMER PARTICLES

A. Preparation and Properties of Sterically Stabilized Conducting Polymer Latex Particles

The preparation of conducting polymer dispersions is one of the ways to prepare polypyrrole latex particles. It was also one of the first methods proposed for improving the processibility of this polymer and to obtain electrically conducting composites.

In a typical dispersion polymerization, the monomer is miscible in the reaction medium whereas the resulting polymer is insoluble under the same conditions. When polymerization proceeds in the presence of a steric stabilizer, which is soluble in the reaction medium, macroscopic precipitation of the polymer can be prevented (in contrast to precipitation polymerization) and submicrometer dispersion particles are obtained. The steric stabilizers used to prepare polypyrrole particles range from simple water-soluble polymers such as poly(vinyl alcohol) poly(*N*-vinylpyrrolidone), and poly(vinyl methyl ether), to name but a few stabilizers, to sophisticated tailor-made copolymer architectures [42].

The principle of dispersion polymerization has recently been applied to the preparation of PANI particles. Formation of spherical PANI particles of about

200 nm diameter has been reported by Gospodinova [65] *et al*. who used poly (vinyl alcohol-*co*-vinyl acetate) for stabilization. Also, the presence of poly(vinyl alcohol) provided PANI particles with hydrodynamic diameters in the 200- to 500-nm range. The use of a variety of tailor-made copolymers produced PANI dispersions with rice grain or needle-like morphology. Similar results were described by Armes *et al*. for poly(vinyl alcohol-*co*-vinyl acetate) functionalized with aniline moieties. Banerjee *et al*. [66]., who polymerized aniline in alcohol–water mixtures containing poly(methyl vinyl ether), also obtained rice grain morphologies.

The ICP colloids are believed to be two-component systems consisting of an inner core of the conducting polymer and an outer layer of adsorbed stabilizer (Fig. 4). The colloidal stability of such particles is strongly dependent on the nature of the steric stabilizer. For example, both methylcellulose- and poly (methyl vinyl ether)–stabilised polypyrrole particles can be reversibly flocculated in hot aqueous solution due to the inverse temperature solubility behavior of this stabilizer in aqueous solution. Similary, the reversible pH-induced flocculation of poly(vinylpyridine)-stabilized polypyrrole particles was reported by Armes [42].

1. Immobilization of Proteins onto Polypyrrole Core/ Polyacrolein Shell

Although proteins can be attached to polypyrrole surfaces by hydrophobic interactions [67], this process may not be satisfactory for the long shelf life of protein–microsphere preparations due to protein leaching. This led Miksa and Slomkowski [38] to prepare polypyrrole core/polyacrolein shell (PPy/PA) particles with polyacrolein being the aldehyde group containing polymer for the attachment of proteins by the formation of a Schiff base. This is schematically shown in Fig. 5. The PPy/PA were synthesized in two steps. First, PNVP-stabilized PPy latex particles (124 nm) were obtained according to the method of Armes and Vincent [68], which consists of polymerizing pyrrole using iron chloride III as the oxidizing agent in the presence of PNVP as a steric stabiliser

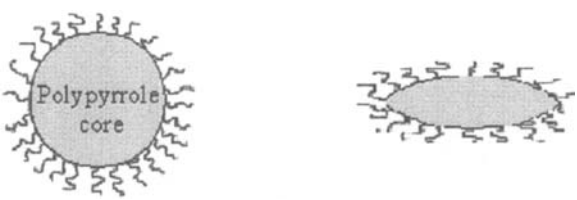

FIG. 4 Shematic representation of sterically stabilized conducting polymer particles showing spherical and rice grain shapes for polypyrrole and polyaniline, respectively.

FIG. 5 Covalent attachment of proteins to polypyrrole particles bearing surface aldehyde groups.

(see above, Section III.A). In the second step, PA was synthesized in water in the presence of PPy/PNVP particles and using $K_2S_2O_8$ to initiate acrolein polymerisation. The resulting particles (154 nm) have a core-shell morphology with polyacrolein as the shell. Two types of PPy/PA were prepared: PPy/PA1 and PPy/PA2, the second being synthesized with two fold higher polyacrolein concentration. PPy particles without surface PA were used as control sample for the attachment of human serum albumin (HSA) and gamma globulin (γG). The values of protein attachment to the various particles are reported in Table 2.

It is interesting to note that HSA does not bind to PPy particles and requires a covalent attachment by the formation of a Schiff base. Although the difference in the behavior of the two proteins was not explained by the authors, it was nevertheless outlined that the PPy/PA particles could accommodate up to 240–270 γG macromolecules per latex particle, which is near the maximum of 285 for particles of similar size.

2. Application of Sterically Stabilized Polypyrrole Particles in Immunodiagnostic Assays

Polyvinyl alcohol–stabilized polypyrrole particles (PPy/PVA) were used as support for the immobilization of proteins in view of developing immunodiagnostic assays [40]. However, the former PPy/PVA particles were functionalized prior to protein attachment and susbsequent immunodiagnostic assays. In this regard, Tarcha *et al*. developed multistep methods for the surface derivatization of polyvinyl alcohol stabilized polypyrrole particles in organic solvents such as *N*-methylpyrrolidone [40]. According to this method, polypyrrole latex was acetylated in *N*-methylpyrrolidone by using bromoacetyl bromide. The bro-

TABLE 2 Adsorption of Human Serum Albumin and Gamma Globulin onto PPy/PA and PPy Particles (mg/g)

	PPy	PPy/PA1	PPy/PA2
HSA	0	10	11
γG	16	33	31

moacetylated latex could be converted to latexes with carboxylic or amino groups in reaction with thioacetic acid and triethylene tetramine (Figs. 6 and 7). Latexes obtained in this way were suitable for covalent immobilization of proteins and for diagnostic assays for the human chorionic gonadotropin (HCG), HIV antibody, and hepatitis B surface antigen. However, the methods mentioned above involved multistep procedures as well as several transfers between aqueous and nonaqueous solvents.

We shall briefly describe the application of these particles to the attachment of the protein HCG, a marker for pregnancy. Figure 8 shows a strip (nitrocellulose) on which dried functionalized PPy/PVA latex particles are deposited in horizontal bar. On a vertical bar that intersects the horizontal bar was deposited antibody against HCG. When patient's sample, which may or may not contain antigen, is added to the dried latex, the particles become hydrated and redispersed and migrate along the strip. If there is no antigen in the sample, the particles that contain antibody bind to the horizontal bar, which contains predeposited antigen, forming a minus sign. If the sample contains antigen, it binds to the antibody on the PPy/PVA particles and the antigen-antibody particle complex is captured by the vertical bar, which contains antibody. The particles are always in excess, hence, those particles that were unsuccessful in competing for the limited antigen are captured by the horizontal bar, completing the plus sign.

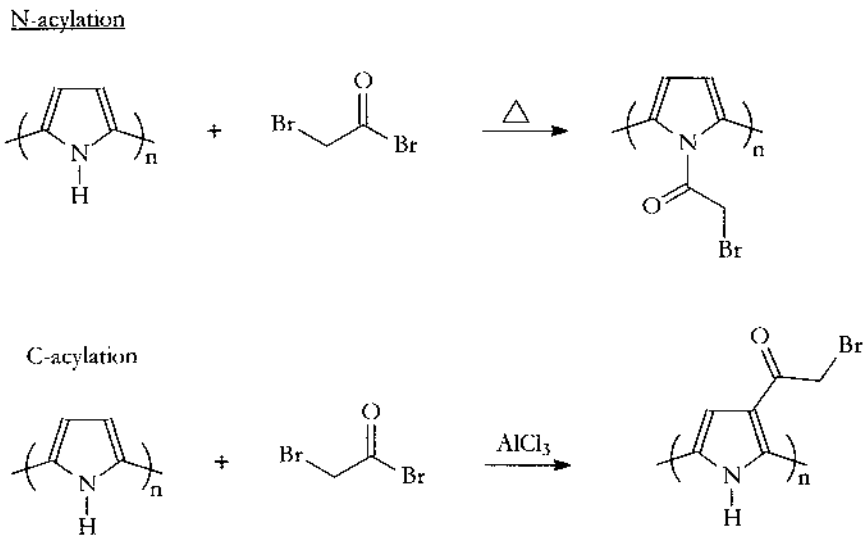

FIG. 6 N-Acylation and C-acylation of polyrrole latex with bromoacetyl bromide.

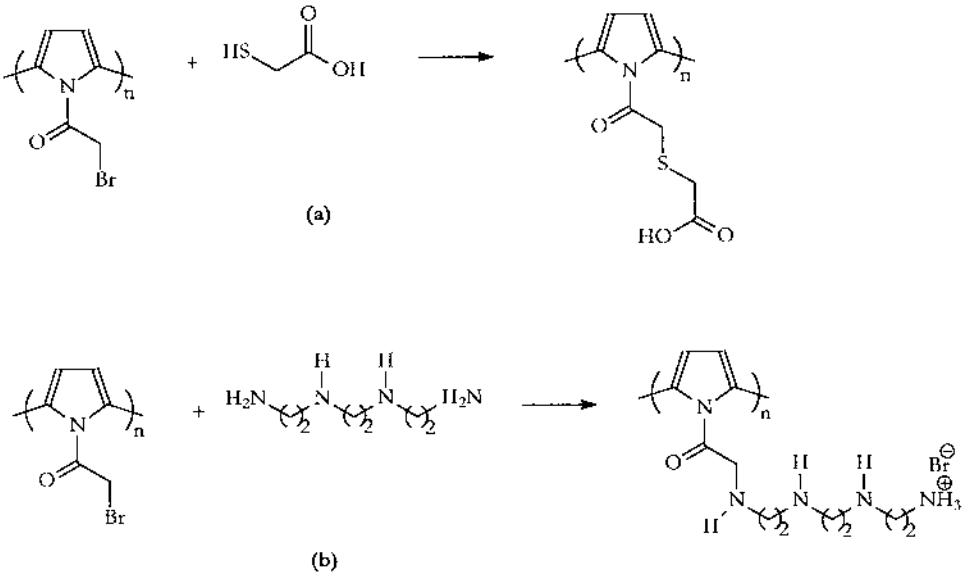

FIG. 7 Conversion of bromoacetylated polyrrole to (a) carboxylated latex and (b) aminated latex.

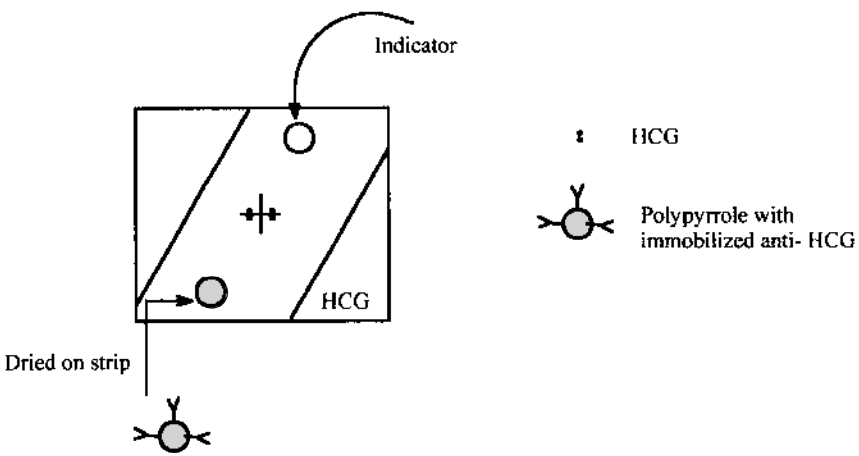

FIG. 8 Schematic representaion of a chromotagraphy-based self-performing assay for the pregnancy marker HCG, employing a dried polypyrrole latex immunoreagent.

B. Conducting Polymer-Silica Nanocomposites

1. Synthetic Routes to Conducting Polymer-Silica Nanocomposites

Colloidal particles can also be obtained by using silica sols for stabilization of the dispersion polymerization of conducting polymers. The deposition of thin polyaniline and polypyrrole coating onto monodisperse silica particles of 1 μm was reported by Armes *et al*. [69]. They reported that the chemical polymerization of aniline or pyrrole in aqueous media in the presence of silica particles led to the formation of stable conducting colloids in the absence of any added polymer or surfactant. In this case, the silica particles act as high surface area colloidal substrate for the precipitating polyaniline or polypyrrole [69]. The resulting composite particles consist of microaggregates of silica particles "glued" together by the conducting polymer component (Fig. 9).

Recently, Stejkal *et al*. [70] prepared polyaniline camphorsulfonate or hydrochloride in the presence of silica gel of 7 and 15 μm diameter. Polyaniline-coated silica gel particles were separated from polyaniline precipitate using a difference in sedimentation rate. In the literature, it has been reported that the colloidal stability of such particles is much better when $(NH4)_2S_2O_8$ is used as the oxidant than when Fe^{3+} is utilized [71].

In the last decade, Armes *et al*. have examined several synthetic routes for the surface functionalization of polypyrrole-silica nanocomposites [69]. Carboxylated polypyrrole-silica nanocomposites have been prepared, as schematically shown in Fig. 10, by copolymerizing a functionalized pyrrrolic comonomer [either 1-(2-carboxyethyl) pyrrole or pyrrole-3-acetic acid] with pyrrole in the presence of the silica sols [58,72]. The raspberry shape of the nanocomposites has been evidenced by TEM [34]. In the case of polyaniline-silica nanocomposites, small-angle X-ray scattering results showed that the raspberry-shaped nano-

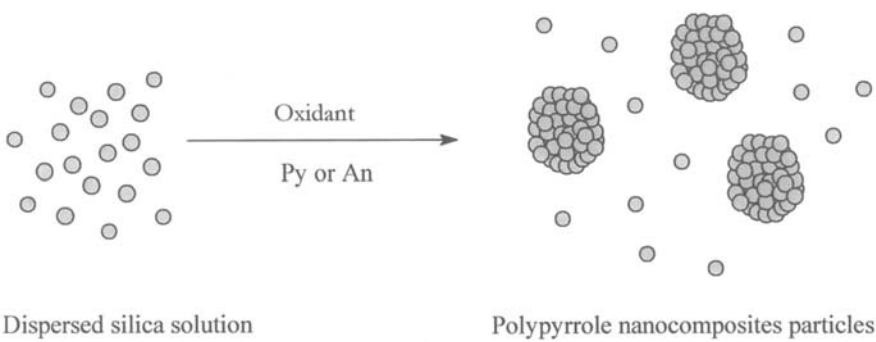

FIG. 9 Schematic representation of the formation of polyrrole-silica particles.

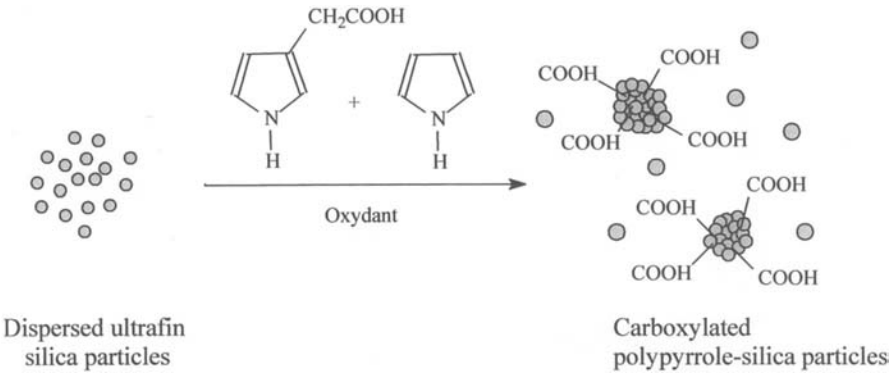

FIG. 10 Schematic representation of carboxylated polypyrrole-silica particles.

composites have a silica-silica separation distance of about 4 nm [73]—an indication that silica and the ICP have nanoscale dimensions. They are thus true nanocomposites. In addition, Maeda *et al.* [57] demonstrated by XPS that the ICP-silica nanocomposites have a silica-rich surface. Actually, the survey spectra are superimposable with those of silica, with an addition of carbon and nitrogen from the polymer backbone. Similar spectra will be shown in Section III.B.5. The surface Si/N ratio was found to be higher than that of the bulk material. This result is in line with electrophoretic measurements, indicating an isoelectric point of polypyrrole-silica nanocomposites of 2, i.e., that of silica sols. Polypyrrole-silica and surface-functionalized polypyrrole-silica nanocomposites were further used for DNA fragments and protein attachment experiments either by hydrophobic interactions or by the formation of covalent bonds at the nanocomposite–protein interface (see Sections III.B.2 to III.B.5).

2. Immobilization of DNA Fragments onto Silica-Polypyrrole Nanocomposites

Calf thymus DNA fragments were adsorbed onto PPy-silica, PPy-COOH-silica, PPy-silica-NH_2, and the reference materials PPyCl powder, the ultrafine silica sol, and the surface-aminated silica sol (silica-NH_2), at pH 7 and 20°C, in the presence of 0.10 M sodium phosphate buffer [74]. Figure 11 shows DNA adsorption isotherms with plateau values in the 1.5–32 mg/g range. No DNA adsorption onto the unmodified silica sol was observed at a salt concentration of 0.10 M (this is only possible at much higher salt concentrations in the 1–6 M range, at pH 8 [75]), whereas aminating this silica sol resulted in substantial DNA adsorption. Surface functionalization with either carboxylic acid or amine groups produced much higher extents of DNA adsorption in the decreasing order: PPy-silica-NH_2 > PPy-COOH-silica > PPy-silica. In particular, the adsorp-

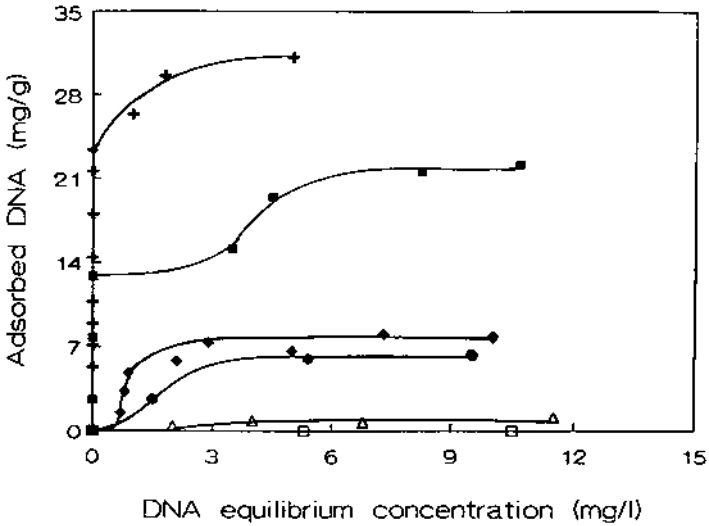

FIG. 11 DNA adsorption isotherms onto PPyCl powder (◆), silica (□), PPy-silica (△), silica-NH_2 (+), PPy-silica-NH_2 (■), and PPy-COOH-silica (●). The conditions were 0.10 M sodium phosphate buffer (pH 7) at 20°C. Adsorbed amounts are expressed in mg/g rather than mg/m^2 to avoid incurring errors due to uncertainties in the effective surface areas of the nanocomposites.

tion capacity (mg/g) of PPy-silica-NH_2 for DNA is about 15 times higher than that of the untreated PPy-silica nanocomposite due to favorable electrostatic interactions between the negatively charged DNA fragments and $-NH_3^+$ species at the surface of polypyrrole-silica-NH_2 particles (although these particles do not bear a net positive charge at pH 7).

Despite the net negative charge of polypyrrole-COOH-silica particles from pH 2 to 11 [76], DNA adsorption occurs on these particles perhaps due to the presence of cationic adsorption sites in the conducting polypyrrole backbone. In addition, hydrogen bonding between the nonionized or ionized surface carboxylic groups and the N-H from, e.g., the guanine and cytosine moieties in DNA may contribute to the overall adsorption interaction.

It is interesting to compare the adsorption isotherms obtained for PPyCl, silica-NH_2, and polypyrrole-silica-NH_2. The isotherm obtained for the latter ("stepped" isotherm) could be viewed as a convolution of the iosotherms for PPyCl (sigmoidal shape) [77] and silica-NH_2 ("all-or-none" type). It was suggested that the aminated surface sites of the PPy-silica-NH_2 particles operate independently from the cationic polypyrrole sites.

3. Adsorption of Human Serum Albumin onto Silica-Polypyrrole Nanocomposites

Human serum albumin (HSA) has been adsorbed onto polypyrrole powders and polypyrrole-silica nanocomposites in 0.1 M PBS at pH 7.4 [78]. Figure 12 displays HSA adsorption isotherms before and after removal of excess physically adsorbed protein macromolecules. Adsorption was found to be as high as 147 mg/g onto polypyrrole-silica nanocomposite, much higher than that obtained on the bulk powder (63 mg/g). This is partly due to the high surface area of the nanocomposite [34]. Favorable electrostatic interactions between negatively charged sites in, for example, HSA and the positively charged PPy chains at the surface of the nanocomposites are likely to play an important role. It is also clear that in PBS conditions, the HSA still has positively charged aminated sites that can interact favorably with the negatively charged sites of the nanocomposite, i.e., $\equiv SiO^-$ bonds. In addition, it has recently been shown that hydrophobic interactions play an important role for the polypyrrole–water–HSA system. Interestingly, PPy-silica is 10 times more adsorptive toward HSA than polypyrrole latex particles bearing surface polyacrolein chains [38]. Adsorption is up to 13 times more favorable for HSA on the polypyrrole-silica nanocomposite than for DNA, which undergoes repulsive interactions with the negatively charged substrate and thus requires surface functionalization of the adsorbent, with $-NH_2$ or −COOH groups yielding a significant adsorption up to 22 mg/g.

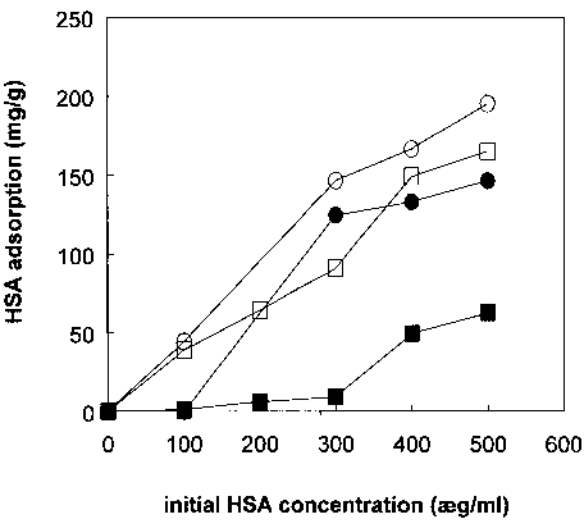

FIG. 12 HSA adsorption isotherms onto $PPySO_4$ bulk powders (□, ■) and the corresponding polypyrrole-silica nanocomposites (○, •) before and after washing.

4. Specific Activity of COOH and Amine-Functionalized Polypyrrole-Silica Nanocomposites

Pope *et al*. [79] have studied the specific activity of a monoclonal antibody to human chorionic gonadotropin (anti-HCG) in solution to that immobilized on aminated and carboxylated polypyrrole-silica colloidal particles. The amine-functionalized particles were subsequently treated with sulfosuccinimidyl 4-(*N*-maleimidomethyl)cyclohexane-1-carboxylate to provide thiol-reactive maleimide groups grafted on the surface of intrinsically highly colored polypyrrole nanoparticles.

Anti-HCG was used as a model antibody, and the Fc region was functionalized for covalent attachment. All forms of polypyrrole retained the equivalence of 12–33 μg of IgG activity/mg of colloidal solids, relative to the end-modified soluble IgG. Comparisons of various particle surface functionalities on both the nanocomposites and the latex revealed no obvious advantage for surface modification and covalent linkage compared to passive adsorption of the antibody. The "passive" adsorption may be more than passive in that nucleophilic groups may bind to polypyrrole and its derivatives by an alternative mechanism. The minimal differences in immunoreactivity among the various surfaces studied, including native polypyrrole, as well as the surface chemical data on fluorinated thiols suggest that nucleophilic groups on the protein may have a predominant interaction with the polypyrrole chains irrespective of the specific coupling chemistry employed.

5. Synthesis and Characterization of Polypyrrole-silica Nanocomposites Bearing *N*-Hydroxysuccinimide Reactive Groups

In Section III.B.4, NH_2- and COOH-functionalized polypyrrole-silica are not reactive in the physiological conditions and require activation to immobilize proteins. This can be achieved by the addition of coupling agents such as *N*-hydroxysuccinimide in the presence of carbodiimide (NHS/EDC) during the incubation of these particles with proteins. However, postactivation may be difficult to control; moreover, the positively charged EDC may adsorb onto silica and hamper protein attachment. Alternatively we suggest to prepare polypyrrole-silica nanocomposites bearing *N*-hydroxysuccinimide functional groups (polypyrrole-silica-NHS) by copolymerizing pyrrole and *N*-functionalized pyrrole with NHS group. The esterification of 1-(2-carboxyethylpyrrole) (Fig. 13) was carried out according to the method described by Patel *et al*. [80] for the modification of carboxylate-terminated self-assembled monolayers (SAM*s*). The resulting SAMs were NHS-functionalized and reacted with protein side-chain lysine residues to form amide bonds. Basically, 0.863 g ($7.5\ 10^{-3}$ mol) of NHS (Acros) and 1.917 g (10^{-2} mol) of EDC (Sigma) were dissolved in 50 mL of distilled water; then 0.7 g ($0.5\ 10^{-3}$ mol) of 1-(2-carboxyethylpyrrole) was added

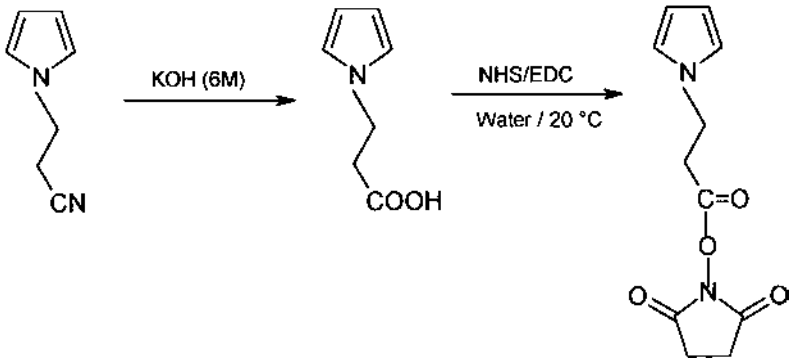

FIG. 13 Esterification of 1-(2-carboxyethylpyrrole).

to the mixture. The reaction took place at ambient temperature and was almost instantaneous. However, it was maintained for 30 min. The white precipitate was collected by filtration on Büchner, washed with distilled water, and dried under vacuum. The structure of the product was confirmed by nuclear magnetic resonance (NMR) (^{1}H, ^{13}C), Fourier transform infrared (FTIR) spectroscopy and melting point (159°C), much higher than that of monomer *1* but close to that of the succinimide, which is 150°C [81].

XPS was also used to characterize the NHS-functionalized pyrrole comonomer. Figure 14 depicts C1s and O1s peaks. C1s (Fig. 2a) exhibits a wide component at 288.1 eV characteristic of the N-C=O (pyrrolidinone) function of the succinimide group, together with a component centred at 289.3 eV and due to

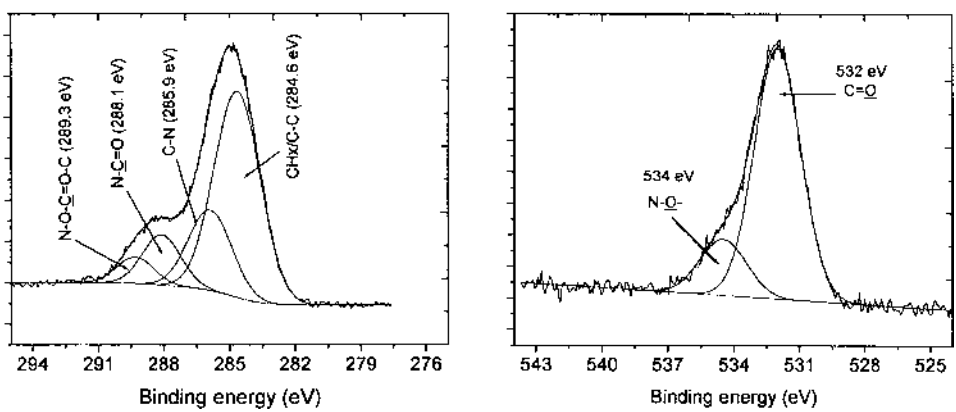

FIG. 14 XPS C1s and O1s high-resolution spectra of the esterified 1-(2-carboxyethylpyrrole).

the ester group. It is worth noting that for carbon in amide and ester groups, the (N-*C*=O)/ (O-*C*=O) ratio is 2, corresponding to the structure of the comonomer. The O1s spectrum was fitted with two components centered at 532 and 534 eV and corresponding to the carbonyl and the succinimide groups, respectively. The (C=*O*)/(N-*O*-) ratio is 3, in line with the reactive group grafted on the pyrrole nitrogen atom.

The polypyrrole-silica-NHS nanocomposite has been prepared by oxydative copolymerization of *N*-ester pyrrole and pyrrole in the presence of silica sols (Fig. 15). The pyrrole and pyrrole-NHS concentrations were in the 50:50 mol % concentrations and $FeCl_3$,$6H_2O$ was the oxidizing agent. The resulting suspension was centrifuged several times to eliminate the excess silica, and the purity of the nanocomposite was checked by the pH measurement of the final washing (pH 5.6, the distilled water pH). The nanocomposite was then redispersed ultrasonically. The final nanocomposite was highly stable in water and did not suffer any flocculation for more than a year.

The size distribution was determined by photon correlation size (PCS) and disc centrifuge photosedimentry (DCP). The nanocomposite had an average size of 200 nm with a polydispersity of 1.12 and density of 1.69 g/cm^3. XPS analysis confirmed the existence of the NHS group at the surface of polypyrrole-silica-NHS since the C1s spectrum is highly comparable to that of the pyrrole-NHS shown in Fig. 14, confirming the existence of the NHS group. It is important to note at this stage that the NHS group is stable and does not suffer any hydrolysis.

FTIR was employed to check the stability of the ester function of the nanocomposite. It showed that the ester group at 1738 cm^{-1} is stable even if the nanocomposite was stored several weeks prior to FTIR analysis. We also ob-

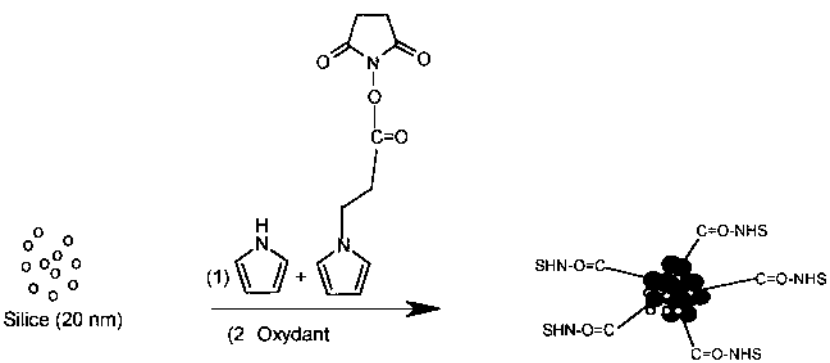

FIG. 15 Schematic synthesis of polypyrrole-silica-NHS nanocomposite.

served a wide band at 1117 cm^{-1}, characteristic of the silica sol in the nanocomposite.

Human serum albumin was immobilized onto polypyrrole-silica nanocomposite in PBS at physiological conditions. UV-visible spectroscopy showed that a massive adsorption up to 400 mg/g of HSA was obtained prior to a washing procedure. Nevertheless, this is much more than in the case of immobilization by hydrophobic interactions (see Section III.B.2). In addition, the nancomposite was tested qualitatively in order to check the antigen/antibody visual agglutination test and was found to flocculate only when it bore HSA and reacted with anti-HSA.

The immobilization of HSA onto polypyrrole-silica-NHS has been monitored by XPS. Figure 16 shows survey spectra of the reactive nanocomposite before and following protein attachment. The spectrum of the untreated nanocomposite is very comparable to that published by Maeda *et al.* [57] for unfunctionalized polypyrrole-silica. It is noteworthy that attachment of HSA leads to an increase of the C1s and N1s relative intensities and decrease in that of the Si2p (Fig. 16).

Sodium insertion at the surface is probably due to the counterbalance of the negative charges of HSA. Indeed, HSA can be counterbalanced by the polypyrrole-positive chains at the nanocomposite–HSA interface; however, at the surface of the nanocomposite–HSA system, adsorption of sodium cations is necessary for the charge balance.

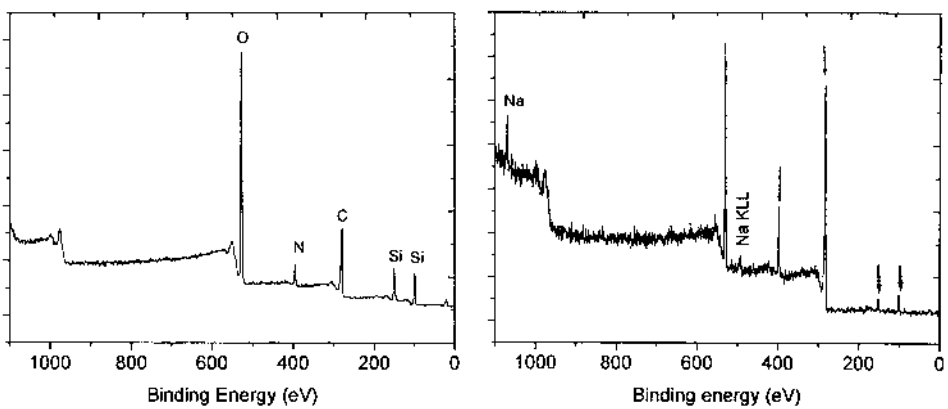

FIG. 16 Survey spectra of polypyrrole-silica-NHS before (a) and after (b) HSA immobilization.

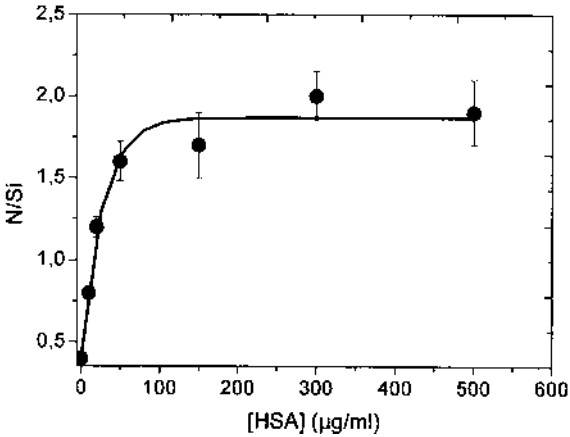

FIG. 17 Adsorption isotherm of HSA onto polypyrrole-silica-NHS as determined by XPS.

The XPS adsorption isotherm was obtained by the plot of (N/Si) ratio *vs.* initial protein concentration (Fig. 17). The surface reached saturation at low protein concentration and the isotherm fit a Langmuir type.

The polypyrrole-silica-NHS nanocomposites were further immobilized onto APS-treated glass plates to serve as assemblies for the immobilization of proteins. These assemblies might play an important role in the recognition of specific analytes of biological importance. Such immobilization of the nanocomposites followed by that of the proteins is schematically presented in Fig. 18. The immobilization of polypyrrole silica nanocomposite onto aminated glass was evidenced by XPS; the decrease of the N-C=O component (NHS leaving group) suggesting the covalent attachment of the particles (Fig. 19). SEM micrographs shown in Fig. 20a confirm that the nanocomposite is monodisperse; but with some degree of aggregation of the nanocomposites. Adsorption of HSA

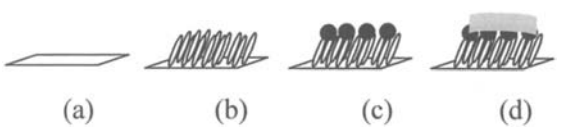

FIG. 18 An "ideal" assembly of polypyrrole-silica-NHS nanocomposites onto silane-treated glass plates with subsequent attachment of proteins. (a) Untreated glass; (b) silane-treated glass; (c) nanocomposite assembly onto silane-treated glass; (d) attachment of proteins to nanocomposites immobilized on silane-treated glass.

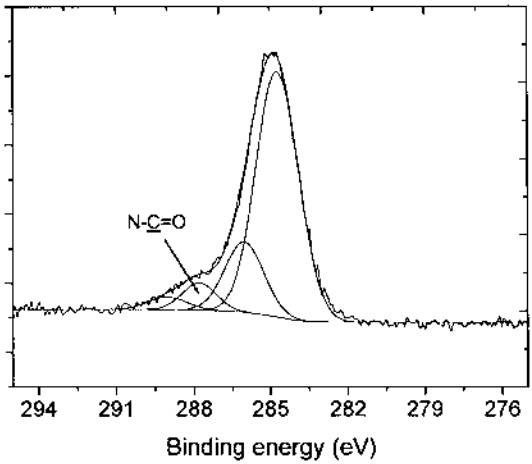

FIG. 19 C1s spectrum of immobilized nanocomposite onto aminated glass.

onto polypyrrole-silica-NHS nanocomposites immobilized onto aminated glass is highly selective as shown by SEM (Fig. 20). This looks like a "cloud" on top of nanocomposite aggregates. No such material appears in the case of uncoated nanocomposite assemblies.

The attachment of proteins to the immobilized nanocomposites was further evidenced by FTIR, which showed that attack of the ester group is proportional

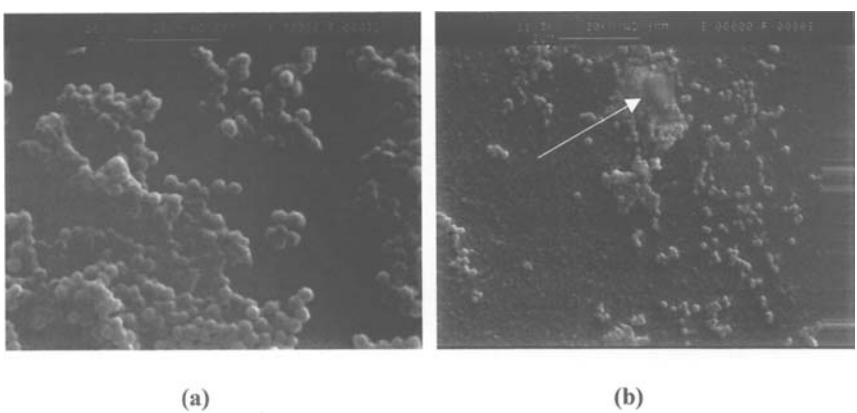

FIG. 20 SEM images of the nanocomposite grafted onto aminated glass (a) before and (b) after HSA immobilization.

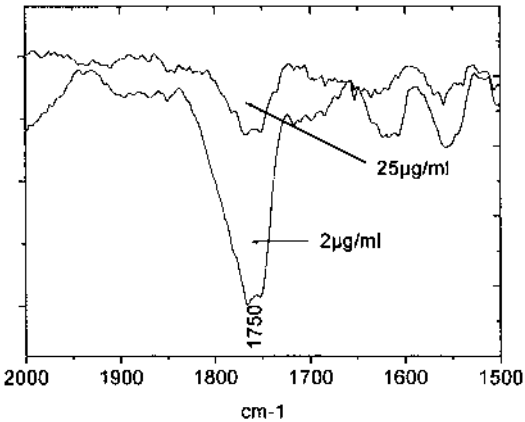

FIG. 21 FTIR spectra of immobilized HSA onto nanocomposite-grafted aminated glass.

to the amount of immobilized protein (Fig. 21). The glass plates decorated with nanocomposites before and after protein attachment were characterized by XPS. Determination of the C/Si and N/Si atomic ratios is depicted in Fig. 22 for the specimens under test. The immobilization of polypyrrole nanoparticles onto aminated glass and adsorption of HSA onto these immobilized particles led to an increase in carbon and nitrogen and a decrease in the silica surface atomic composition. The change in the shape of the high resolution spectra are indicative also of the modification of nanocomposite-decorated glass plates by the adsorbed protein.

C. Conducting Polymer-Coated Latex Particles

1. Synthesis

Since Yassar *et al.* [82] first proposed that conducting core-shell latexes could be prepared by an in situ polymerization of the pyrrole at the surface of polystyrene particles, the technique has attracted significant interest. The authors synthesized polystyrene/polypyrrole composite particles by the polymerization of pyrrole in the presence of 0.1-µm PS particles having sulfonic or carboxylic groups at the surface that can act as dopant for the growing conducting polymer. The conductivity of pressed pellets of the dried latex was found to be 0.25 S/cm.

Several groups have modified the protocol of Yassar *et al.* [82] to prepare ICP coatings on polyurethane [83], polystyrene [29,84–87], polymethyl methacrylate [64], and polybutyl methacrylate [88] latex particles. It is worth noting

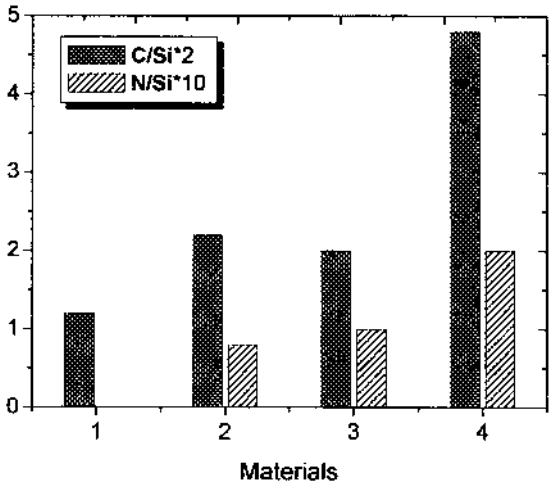

FIG. 22 C/Si and N/Si atomic ratios determined by XPS for several glass plates: (1) untreated glass; (2) glass-APS; (3) glass-APS-nanocomposite 20%; and (4) glass-APS-nanocomposite 20%-HSA 2 μg/mL. Twenty percent was the dilution of the initial nanocomposite suspension in water and 2 μg/mL the initial concentration of HSA.

that recently Kros *et al*. [29] reported on the synthesis of colloidal polypyrrole particles with 202-nm polystyrene core; they showed that no bulk poly(pyrrole) was formed in the voids of the latex layer. The thickness of the uniform poly (pyrrole) layer was estimated to be 30–40 nm. This spherical polypyrrole-coated latex was used as a matrix for the immobilization of glucose oxidase. The so-immobilized enzyme latex can be incorporated in a conducting ink to enhance the handling possibilities of the sensor, making screen printing procedures feasible. This amperometric biosensor can detect glucose in the absence of any oxygen mediators.

Of relevance to this section, polystyrene latex particles were used as organic substrates for the in situ polymerization of aniline [85], pyrrole [84,86], and ethylenedioxythiophene [87]. Lascelles *et al*. [84] reported the coating of stabilized PS latexes in the 1.6- to 1.8-μm range with polypyrrole in aqueous media to form conducting polypyrrole-coated latexes with good colloidal stability. The use of the polymeric stabilizer such as polyvinylpyrrolidone, (polyethylene glycol) is critical for producing stable colloidal dispersion. The conducting shell was formed upon oxidative chemical polymerization of the pyrrole monomer in the presence of the PS latex, which acted as colloidal substrates for deposition of polypyrrole (Fig. 23)

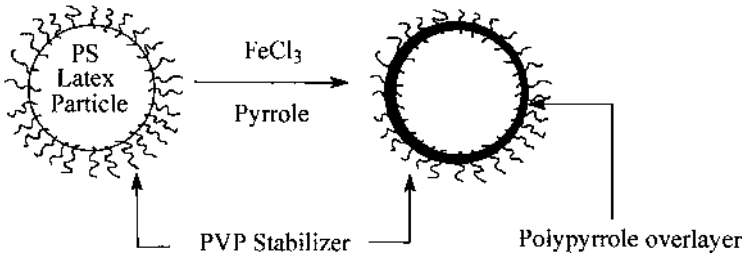

FIG. 23 Schematic representation of the synthesis of a polypyrrole-coated, PVP-stabilized polystyrene latex.

In the case of PANI-coated PS, Armes *et al.* [85] showed that these composites have considerable surface roughness (nonuniform and inhomogeneous morphology), in contrast to the relatively smooth morphologies obtained for the deposition of polypyrrole onto the same micrometer-sized PS latex particles. This differs for the polystyrene-PEDOT latex particles, which have reasonably smooth and uniform PEDOT adlayer morphology and a higher conductivity than that obtained for polypyrrole- and polyaniline-coated latexes [87].

For PPy, PANI, or PEDOT coatings, Armes and coworkers showed that the conducting polymer loading, which could be easily controlled by varying the initial latex concentrations, influences the particle morphology (Fig. 24) [84,86,87]. For example, at low polypyrrole loading, the conducting shell is formed as a smooth and uniform layer on the surface with no direct evidence for the deposited polypyrrole overlayer (Fig. 24c). At intermediate loadings the polystyrene particles are uniformly coated with a globular polypyrrole overlayer (Fig. 24b); and at higher concentrations, separate polypyrrole subphase is clearly apparent in addition of the polypyrrole-coated PS particles (Fig. 24a).

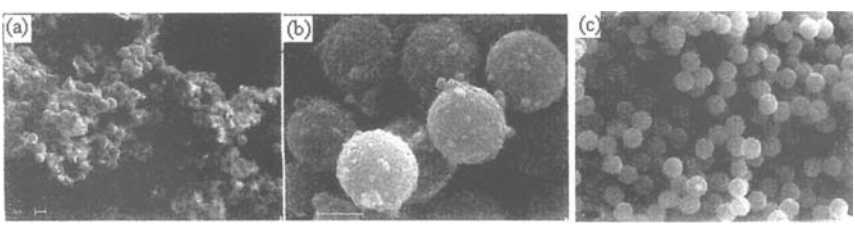

FIG. 24 Scanning electron micrographs of a polypyrrole-coated polystyrene latex with (a) a relatively high polypyrrole loading (51.1%), (b) an intermediate polypyrrole loading (25.1%), and (c) a relatively low polypyrrole loading (6.1%).

Lascelles et al. reported the use of solvent extraction to examine the morphology of polypyrrole-coated polystyrene particles. They treated a dried PPy-coated polystyrene latex (6.5 wt % PPy loading) with THF to remove the non-cross-linked underlying PS core. Examination of the PPy residues by SEM revealed a "broken egg shell" morphology, thus providing irrefutable evidence for the core-shell morphology of the original polypyrrole-coated polystyrene particles (Fig. 25) [89].

2. XPS Characterization of Conducting Polymer-Coated Polystyrene Particles

XPS has been extensively used to characterize the surface composition of ICP-coated polystyrene latex particles in order to determine the surface content of the ICP under test, the steric stabilizer, and the PS core. Such studies required the analysis of reference ICP*s* prepared in powdery form in the absence of PS particles, and also the pure steric stabilizer, pure PS, and the uncoated PS particles. Three types of ICP particles were examined: polypyrrole- [60,62], polyaniline- [61], and PEDOT-coated PS particles [63]. For micrometer-sized PANI-coated polystyrene, PNVP was the steric stabilizer (PS-PNVP-PANI) and the synthesis was performed under various conditions. Examination of the N1s spectra indicated that PANI and PNVP were indeed at the surface of the PS core. Nonuniform PANI coatings were obtained using conventional aniline polymerization conditions (aniline monomer, ammonium persulfate, and 1.2 M HCl at 25°C). In contrast, more homogeneous PANI coatings were obtained when polymerizing aniline hydrochloride at 0°C in water. The relative proportion of PANI at the surface of the PS latex was estimated by comparing the surface nitrogen contents of the coated and the uncoated PS-PNVP latex to that of the PANI bulk powder prepared in the absence of any latex. The C1s spectra of PS-PNVP-PANI synthesized at 0°C with 5.6% mass loading of PANI was comparable to that of the bulk powder PANI in the same conditions. However, the maximal

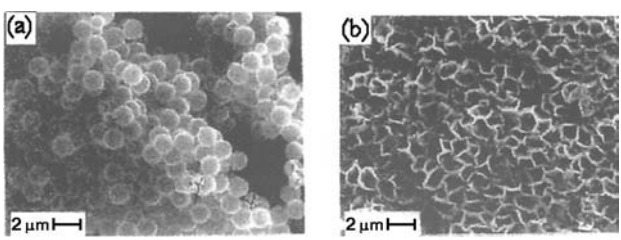

FIG. 25 Scanning electron micrographs of a polypyrrole-coated polystyrene latex with (a) a relatively low polypyrrole loading (6.1%) and (b) the same coated latex after extraction of the polystyrene core with THF.

proportion of PANI (expressed in aniline repeat unit content at the surface) was at best 60%, i.e., lower than the 94% obtained for polypyrrole coatings on micrometer-sized PS core [60]. Similarly, the highest PEDOT surface coverage was about 75% for a mass loading of 38% [63].

Examination of the XPS spectra obtained for polypyrrole-coated polystyrene particles is worth describing in detail as it is related to polypyrrole coatings on polystyrene particles prepared by dispersion and emulsion polymerization of styrene (1.8 μm and 129 nm, respectively). Figure 26 shows the wide scans of bulk powder polypyrrole (a), polyethylene glycol–coated PS (PS-PEG) before (b) and following coating with PPy (c) at mass loading of 28.1% (PS-PEG-PPy28.1), micrometer-sized PS-PNVP before (d) and after coating with PPy (e) at a mass loading of 8.7%. The PS-PEG was obtained by coating emulsion-polymerized PS particles (129 nm) [86]. It is worth noting that PPy is very effective in coating PS-PNVP in contrast to PS-PEG core, and this occurs even for a low mass loading (8.7% *vs*. 28.1%). The massive loading of polypyrrole

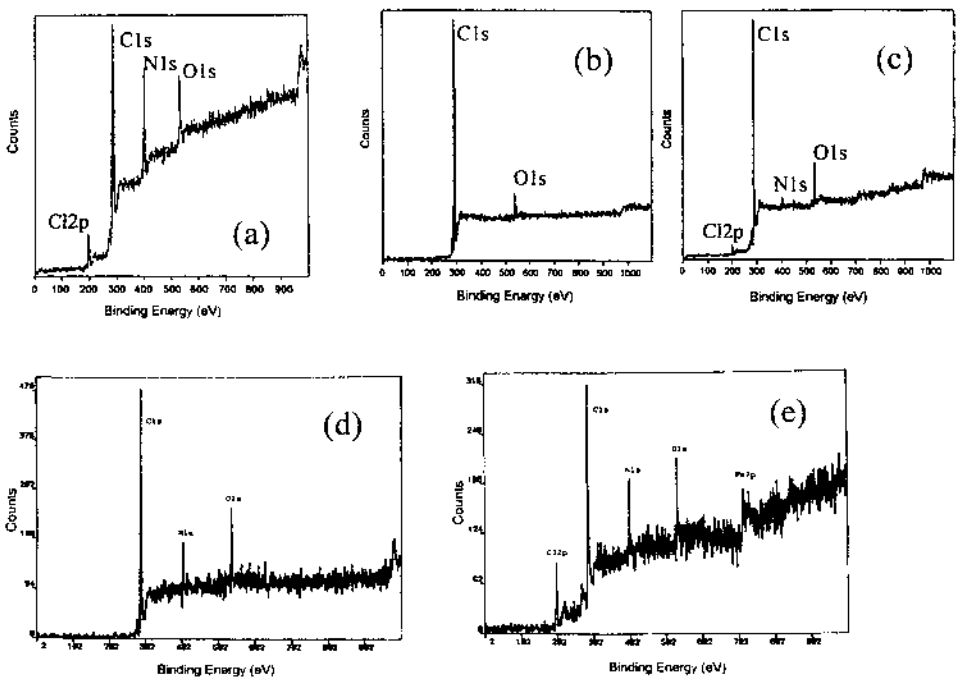

FIG. 26 XPS survey scans of (a) bulk powder polypyrrole, (b) polyethylene glycol-coated PS (PS-PEG), (c) PS-PEG-PPy 28.1%, (d) micrometer-sized PS-PNVP, and (e) PS-PNVP-PPy 8.7%.

at the surface of PS-PNVP is evidenced by the N1s and Cl2p (from chloride dopants). Even for low surface area PS-PEG obtained by coating PEG on micrometer-sized PS particles and for 4.2% mass loading of PPy, the surface proportion of the ICP remained low (24.4%). These XPS results are summarized in Table 3 in terms of relative proportions of repeat units from PS, PEG (or PNVP), and PPy.

Figure 27 displays C1s spectra for PS-PEG, bulk powder PPy, PS-PEG-PPy (28.1%), PS film, PS-PNVP, and PS-PNVP-PPy (8.7%). PS shows a sharp C1s peak at 285 eV with a shake-up satellite at high binding energy characteristic of aromatic rings (d). The same satellite is clearly visible in the case of PS-PEG (a) and PS-PNVP (e), but with a lower relative intensity for the latter particle since the relative proportion of PNVP is higher than that of PEG; hence, an attenuation of characteristic peaks from the PS core. Although the mass loading of PPy levels off at 28.1% at the surface of PS-PEG, the shake-up satellite is clearly visible (c) by contrast to PS-PNVP-PPy (8.7%). This is strong supporting evidence for the thick and continuous coating of PPy at the surface of PS-PNVP but not PS-PEG. The C1s peak from bulk powder PPy (b) has a shape that is very comparable to that of PS-PNVP-PPy, which explains why there is a massive surface coverage of the ICP at the surface of micrometer-sized PNVP-stabilized PS latex particles.

It is interesting to note that whilst PS-PNVP-PPy have a real core/shell structure [60,84], thus with a polypyrrole-rich surface, SEM studies indicated that the PPy component is present as discrete 20–30 nm nanoparticles, rather than a uniform overlayer at the surface of PS-PEG-PPy [86]. Moreover, PS-PNVP-PPy do not exhibit charging effects in XPS due to the continuous conducting overlayer, the PS-PEG-PPy does exhibit such effects and thus behaves as an insulating material.

It is also worth noting the great difference in polypyrrole surface coverage for PS-PEG-PPy (8.7%) and PS-PNVP-PPy (8.7%), 7.7 and 94%, respectively.

TABLE 3 Relative Proportions of Polypyrrole, Stabilizer, and Polystyrene Cores at the Surface Polypyrrole-Coated Polystyrene Latex Particles

Matertials	PS	PEG	PNVP	PPY
PS-PEG	74.9	25.1		
PEG-PPy (4.2%)	71.5	24.0		4.5
PS-PEG-PPy (8.7%)	69.1	23.2		7.7
PS-PEG-PPy (28.1%)	57.2	19.2		23.6
PS-PEG-PPy LSA (4.2%)	56.6	19.0		24.4
PS-PNVP (1.8 μm)	49		51	
PS-PNVP-PPy (8.7%)	0–4		0–2	94–100

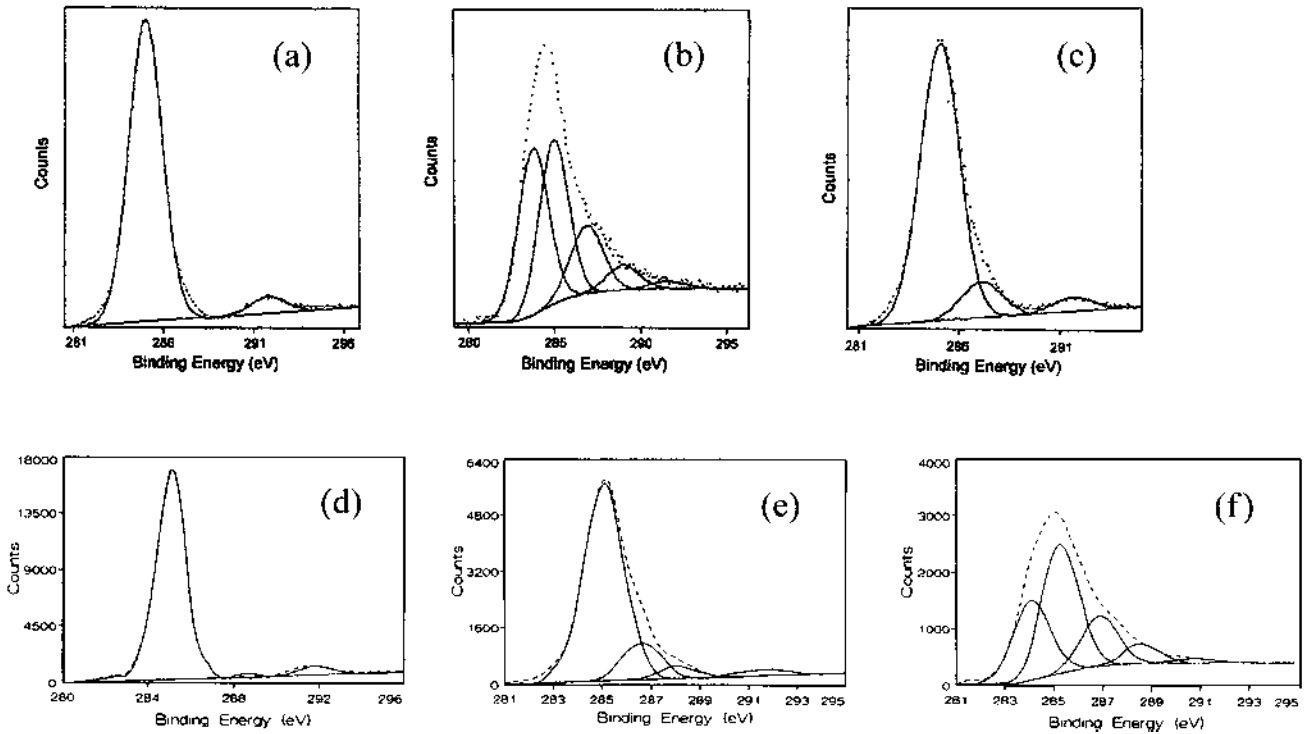

FIG. 27 C1s spectra for (a) PS-PEG, (b) bulk powder PPy, (c) PS-PEG-PPy 28.1%, (d) PS reference spin cast film, (e) PS-PNVP, and (f) PS-PNVP-PPy 8.7%.

Therefore, the surface analysis of polypyrrole-coated PS latex particles shows that the steric stabilizer nature has a major effect on the morphology of polypyrrole adlayers. This could be due to a difference in the specific surface area of the core, which is much higher for emulsion PS particles. However, this material property can certainly be ruled out since low surface area PS-PEG does not lead to a uniform and thick polypyrrole coating. Perhaps the answer lies in the relative hydrophilicity of PEG and PNVP, polypyrrole being known to interact favorably by hydrophobic forces with silane-treated glass [90], proteins [67], and polyaromatic hydrocarbons [18].

4. Reactive Polypyrrole-Coated Polystyrene Particles

Work done by the group of Armes in the late 1990*s* dealt with coating PPy, PANI, and PEDOT on the surface of PS particles. In view of preparing similar ICP-coated PS latex particles bearing reactive groups toward proteins, we have focused on the synthesis of N-substituted pyrrole and its corresponding copolymerization with pyrrole at the surface of PS. The target reactive substituent was NHS esters as it is an easily replaceable leaving group at the end of the alkyl chain. Indeed, it is well known from peptide chemistry that activated esters react with amine under very mild conditions to form the corresponding amides in high yields. NHS ester–fuctionalized polypyrrole should then allow subsequent surface attachments of proteins via their side amine groups, if the active ester groups withstand the polymerization conditions (Fig. 28).

The monomer synthesis has been described in details in Section III.B.5.

Functionalized PPy-PS latexes prepared by two general methods:

1. PPy coating on emulsion PS with differing initial pyrrole to pyrrole-NHS monomer ratios (methods A and B)
2. PPy coating on dispersion PS using a 50:50 initial pyrrole to pyrrole-NHS monomer ratio (methods C)

Anionic polystyrene latex, which provides the core particles, was prepared by the batch polymerization method. For this purpose, 20 g of styrene, 200 g of distilled water, and 0.65 g of KPS was added to a 250 cm^3 container and the

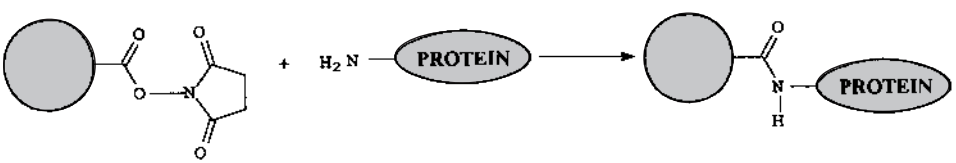

FIG. 28 Schematic illustration of proteins onto NHS-functionalized polypyrrole-coated PS latex particles.

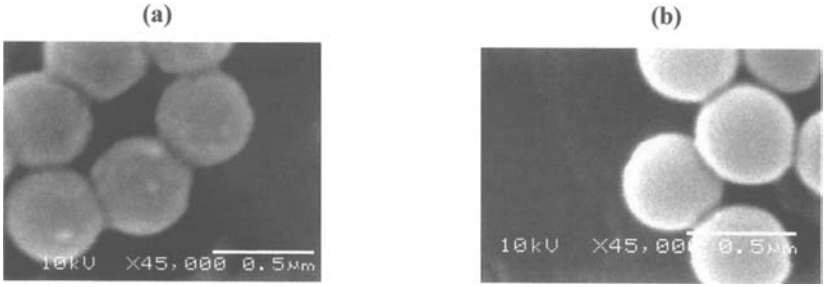

FIG. 29 SEM pictures of (a) poly(styrene [pyrrole/pyrroleNHS]) particles (method A) and (b) polystyrene particles prepared by emulsion polymerization.

mixture purged with nitrogen to eliminate oxygen effects. The solution was stirred at 75°C for 24 h.

The coating procedure consists of the in situ copolymerization of the monomers in the presence of polystyrene latex. Thus, pyrrole and ester functionalized pyrrole were premixed in 50:50 and 25:75 molar ratios. This comonomer mixture was then added to a vigorously stirred solution containing the polystyrene solution (about 1 g of dry weight polystyrene), $FeCl_3$ (1.8 g), and PNVP (0.2 g) to prevent aggregation of the polystyrene particles. The solution was stirred at 25°C for 24 h; the resulting colloidal nanocomposites were isolated by five centrifugation redispersion cycles and redispersed in deionized water.

A typical SEM pictures of the obtained composite colloids are illustrated in Fig. 29. All particles are in spherical shape and have monodisperse size distribution. The number-average particle diameters are nearly the same. The surface concentration of the anions ($[SO^-_4]$ from potasium persulfate used for initiation of the polymerization in the synthesis of latex), values of ζ potential, and values of number-average diameter are given in Table 4.

TABLE 4 Properties of Poly(styrene[pyrrole/pyrrole-NHS] Latexes

Latex	D_n(nm)	$[SO_4^-]$ mol/m$^2 \times 10^5$	ζ (mV)
PS	450	5.25	− 67
PS-PPy 50:50 A	460	—	+ 1.4
PS-PPy 25:75 B	465	—	+ 1.4

D_n, averaged diameter determined from SEM micrographs; PS, uncoated polystyrene particles; PS-PPy 50:50 A, PS synthesized by method A and coated with functionalized [Py]/[PyNHS] 50:50; PS-PPy 25:75 A, PS synthesized by method A and coated with functionalized [Py]/[PyNHS] 25:75.

The correct incorporation of the active ester groups into the latex was proven by FTIR spectra of PSA and PSB. The spectra exhibit strong carbonyl absorptions at $\nu = 1735$ cm^{-1}(ester) and 1810 cm^{-1} (pyrrolidinedione, NHS), showing that the NHS ester fuctions have withstood the chemical oxydation conditions and are intact. In addition, characteristic bands of doped polypyrrole were observed (1560, 1470, 1300, 1200, 1050, and 938 cm^{-1}) besides the typical vibrations of polystyrene.

XPS has been used to characterize the NHS group within the fully functionalized bulk powder polypyrrole (PPyNHS) and estimate the relative proportions of pyrrole and pyrrole-NHS repeat units at the surface of PS-PPyNHS. Figure 30 shows wide scans of PPyNHS (a) and PS-PNVP-PPyNHS (b). For the bulk powder PPyNHS, the main features are C1s, N1s, and O1s together with a minor Cl2p from the dopant. The intense O1s peak is due to oxygen in the ester group grafted on the pyrrole nitrogen atom (four oxygen atoms per pyrrole-NHS monomer). In the case of PS-PPyNHS C, there is an increase of the relative intensity of C1s due to the contribution of the underlying PS core. Figure 31 exhibits C1s spectra from PPyNHS and PS-PNVP-PPyNHS. Superimposition of the spectra clearly indicate the important contribution of the CC/CH bonds from the PS core. Using the surface composition in atomic percent of the PS-PPyNHS C together with the fitted C1s speftrum shown in Fig. 31, we estimated the following relative proportions of the repeat units at the surface of the latex particles: Pyrrole-NHS: 12.2%; pyrrole: 40.7%; styrene: 32.6; and *N*-vinylpyrrolidone: 14.4%.

It is noteworthy that the total pyrrole and pyrrole-NHS repeat units contribute to 52.9%, i.e., lower than that obtained for the same type of particles but with pure PPy [60] but higher than the case of PS-PEG-PPy (up to 23.6%) [62]. Moreover, the Py/Py-NHS ratio is 3.3, much higher than 1, the initial ratio prior to copolymerization. Therefore, pyrrole is much more favorably copolymerized than pyrrole-NHS. Nevertheless, this may not be a drawback when one considers the attachment of proteins to NHS-functionalized PS-PPy latex particles (see below).

The dependence of the surface concentration of attached protein (Γ) on the concentration of protein in solution has been studied in a series of experiments with the constant concentration of latexes (3 mg/mL) and with varied concentration of protein (HSA). The time of incubation was equal to 20 h, the immobilization isotherms for HSA are given in Fig. 32. The dependence of the concentrations of immobilized proteins on the concentrations of protein in solution indicate that initially Γ_{HSA} increases with increasing concentration of protein in solution until the plateau is reached that corresponds to the complete coverage of the surface of latex particles with protein macromolecules. According to the plots given in Fig. 7, for PSA and PSB Γ_{HSA}(max) are equal to 0.02 mg/m^2 and 0.2 mg/m^2. For the same concentrations of protein in solution, the surface

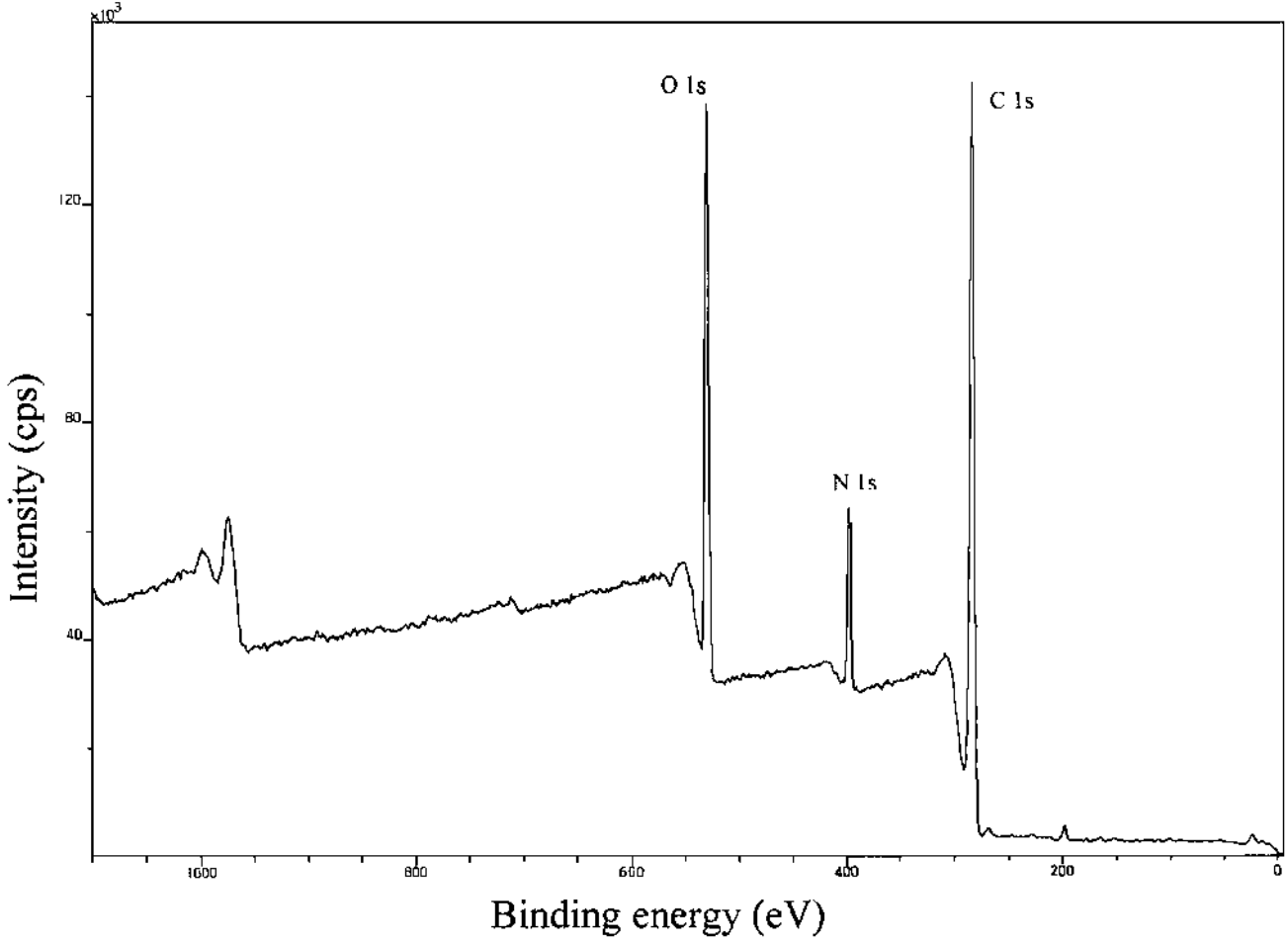

FIG. 30a Survey scans of (a) NHS-functionalized polypyrrole bulk powder and (b) PS-PPyNHS C.

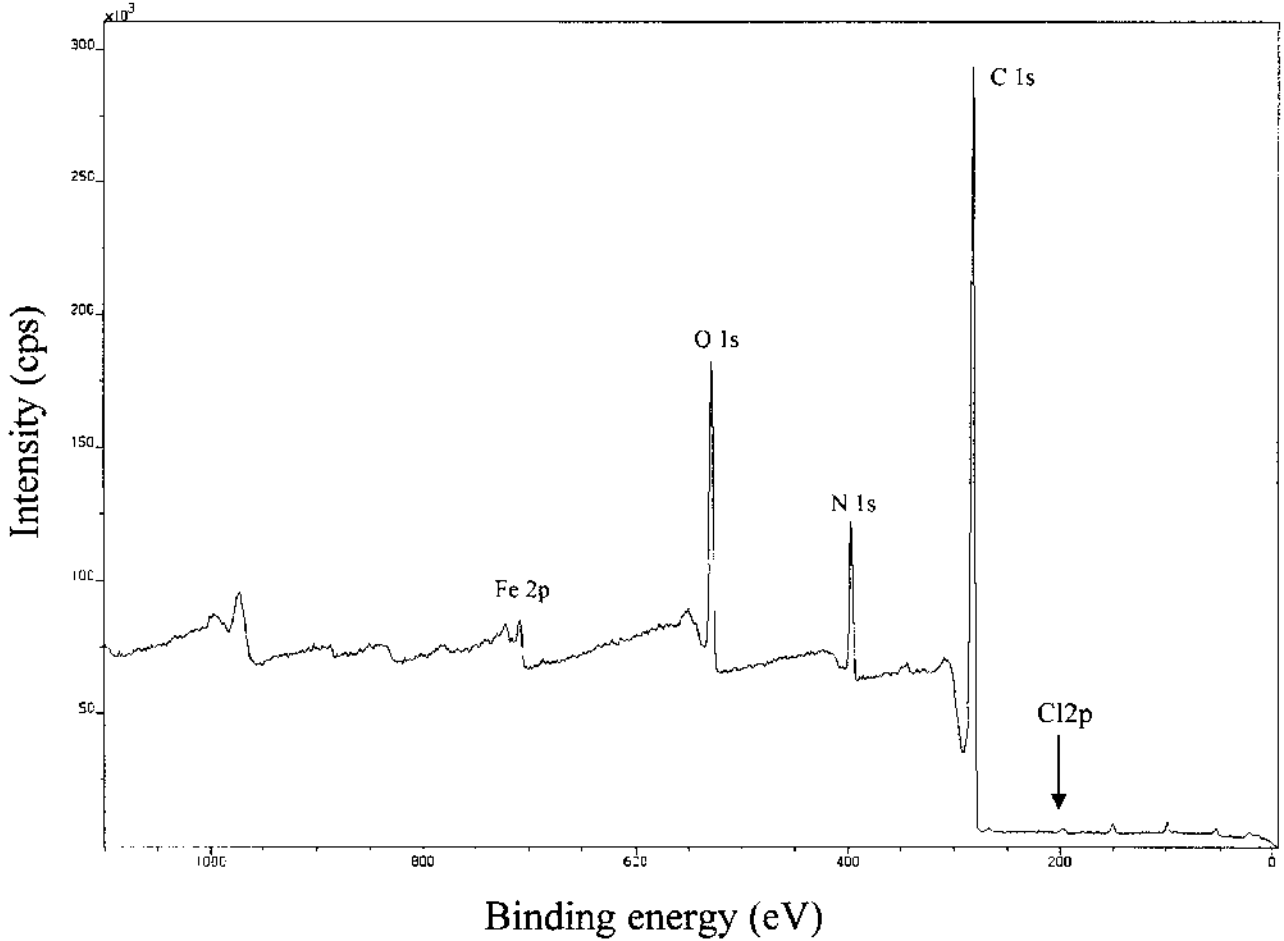

FIG. 30b

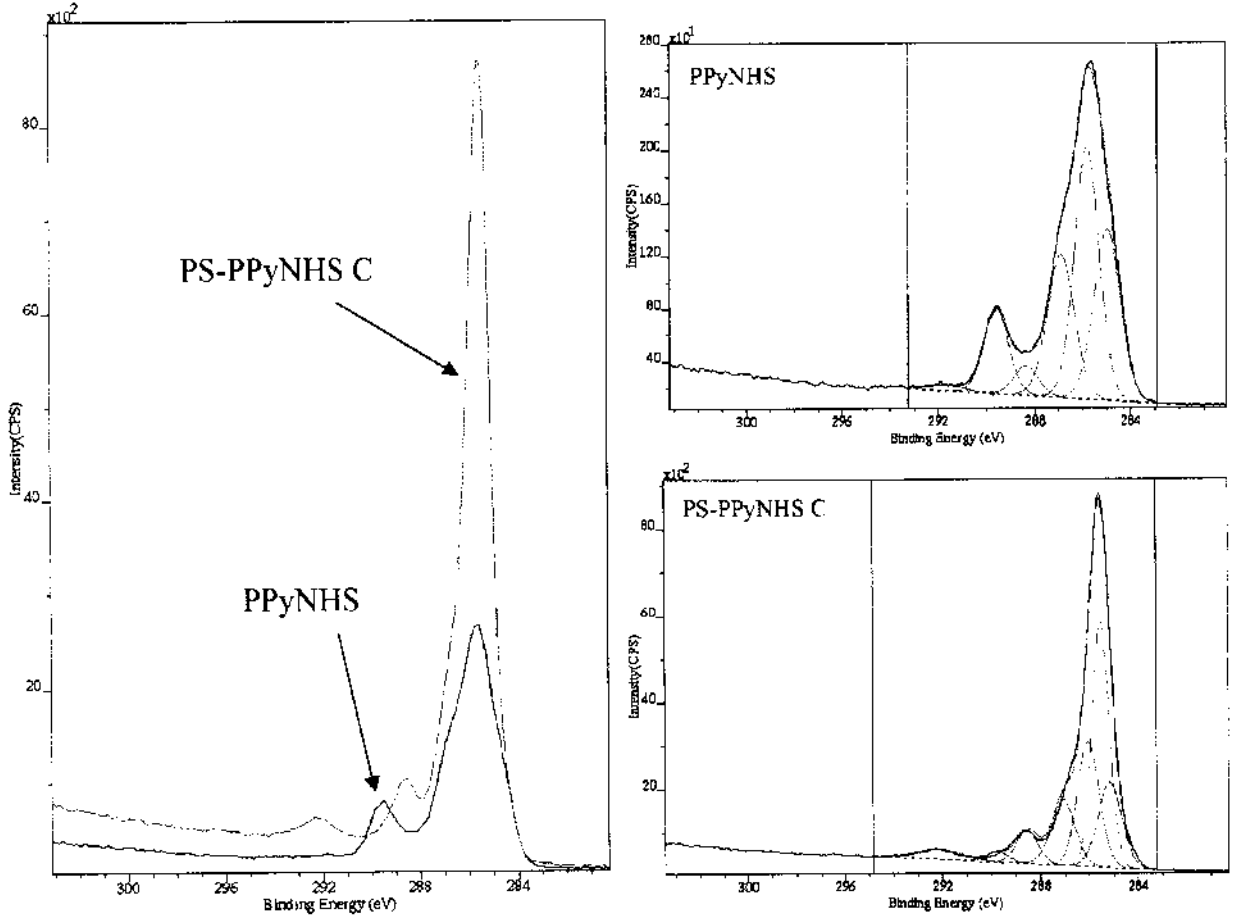

FIG. 31 High-resolution C1s spectra of bulk powder PPyNHS and PS-PPyNHS C latex particles. Note the sharp signal centered at 285 due to the underlying TiS core in PS-PPyNHS C latex.

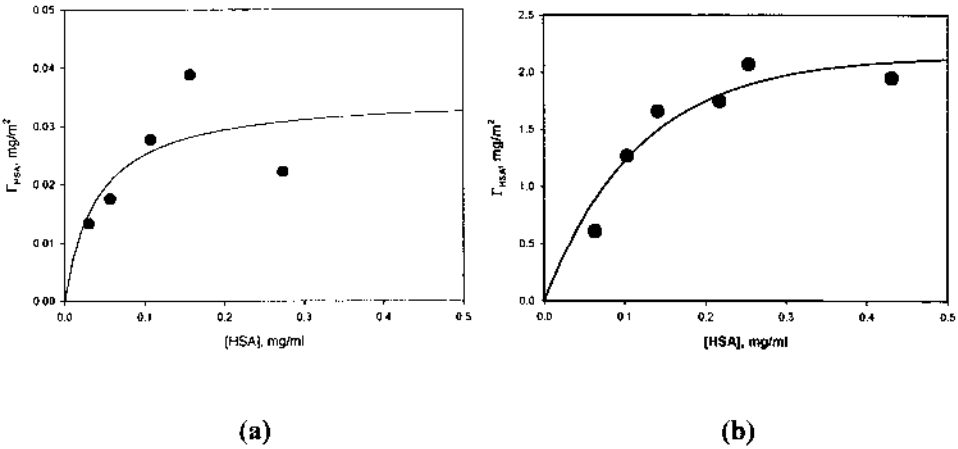

FIG. 32 Concentration of HSA attached to the surfaces of poly(styrene [pyrrole/pyrroleNHS]). (a) [Py]/[PyNHS] = 25:75 (molar ratio); (b) [Py]/[PyNHS] = 50:50 (molar ratio).

concentration of attached proteins is lower for latexes with high fraction of NHS in the surface layer. Presumably, initially the protein macromolecules became attached flatly, maximizing their contact with the polymer surface. The new protein macromolecules could be accommodated only when the already attached ones change their orientation making space for them. Such orientation, rather easy for protein adsorbed due the physical interactions, becomes impossible for macromolecules immobilized covalently. Thus, for latexes with higher fraction of (PPyNHS), providing NHS groups for the covalent immobilization, the lower surface concentration of attached proteins could be expected.

Experiments described previously indicate that the poly(styrene/[pyrrole/pyrroleNHS]) latexes can be used for the attachment of protein with the controlled proportion of protein macromolecules covalently immobilized due to the reaction of NH_2 groups of protein with NHS groups from the underlying latex. These novel latexes with the attached appropriate proteins can be used for preparation of agglutination tests.

IV. CONCLUSION

This chapter discusses a selection of methods for the preparation of inherently ICP particles: sterically stabilised ICP*s*, ICP-silica nanocomposites, and ICP-coated polymer latex particles. In the 1980*s*, the first ICP particles were pro-

posed to improve the processability of conducting polymers, but their interesting physicochemical properties (*e.g.*, deep black color) also made them good candidates for biological applications. ICP particles can be used as bioadsorbents and as protein carriers in the development of visual immunodiagnostic assays.

Examples shown in this chapter, concerned adsorption of DNA fragments and proteins onto polypyrrole powders and nanocomposites, the latter exhibiting a massive adsorption capacity toward proteins. However, DNA may also be immobilized on some ICP particles (polypyrrole-silica nanocomposites) if the latter bear amino (positively charged at pH 7) or carboxy groups.

Several approaches have been suggested for preparing reactive polypyrrole particles (aldehyde, acyl, triethylenetetramine, etc.) for the covalent attachment of proteins. We suggested the preparation of *N*-succinimide ester–functionalised polypyrrole particles. These particles readily react to attach proteins via covalent bonds on the one hand and self-assemble onto amino-treated glass substrates on the other hand.

On several occasions, XPS results have been presented and it is very clear that this technique informs not only on the surface chemistry of the particles but also on the morphology of outermost layers. Indeed, XPS is a very sensitive surface analytical technique that permits detection of the reactive groups (-NH_2, COOH, succinimide, etc.) that exist within 10 nm at the surface of latex particles. Moreover, examples taken from the literature show how this surface analytical technique can be used to verify whether or not ICP particles have core-shell morphology.

It is clear that conducting polymers will continue to attract scientists working in colloid science and technology with a view to biomedical applications.

ACKNOWLEDGMENTS

The authors are indebted to Professor S. Slomkowski (Polish Academy of Science, Lodz, Poland) and his research team for help with the synthesis of functionalized polystyrene-polypyrrole particles. SB thanks the University Paris 7 and the Conseil Régional d'Ile de France for their grant support during a 6-month visit to Poland.

REFERENCES

1. Skotheim, T.A., Ed. *Handbook of Conducting Polymers*, *Vols. 1 and 2;* Marcel Dekker: New York, 1986.
2. Skotheim, T.A.; Elsenbaumer, R.L.; Reynolds, J.R.; Eds. *Handbook of Conducting Polymers*, 2nd Ed.; Marcel Dekker: New York, 1998.
3. Aldissi, M., Ed. *Intrinsically Conducting Polymers*: *An Emerging Technology*; Kluwer Academic: Dordrecht, 1993.

4. Nalwa, H.S., Ed. *Handbook of Organic Conductive Molecules and Polymers*: *Vol. 2. Conductive Polymers*: *Synthesis and Electrical Properties*. John Wiley and Sons: Chichester, 1997.
5. Rodriguez, J.; Grande H.-J.; Otero, T.F. Polymers: from basic researh to technological applications. In *Handbook of Organic Conductive Molecules and Polymers*, *Vol. 2*; Nalwa, H.S., Ed., John Wiley and Sons: Chichester, 1997; 415.
6. Thiéblemont, J.C.; Planche, M.F.; Petrescu, C.; Bouvier, J.M.; Bidan, G. Synth. Met., 1993, *59*, 81.
7. Cheah, K.; Forsyth, M.; Truong, V.-T.; Olsson-Jacques, C. Synth. Met. **1997**, *84*, 829.
8. Lin, H.-K.; Chen, S.-A. Macromolecules **2000**, *33*, 8117.
9. Kobayashi, N.; Uemura, S.; Kusabuka, K.; Nakahira T.; Takahashi, H. J. Mater. Chem. **2001**, *11*, 1766.
10. Oh, E.J.; Jang, K.S. Synth. Met., **2001**, *119*, 109.
11. Oh, E.J.; Jang, K.S.; McDiarmid, A.G. Synth. Met. **2002**, *125*, 267.
12. Wusheng Yin, E.; Ruckenstein, E. J. Appl. Polym. Sci. **2001**, *79*, 86.
13. Schottland, P.; Bouguettaya, M.; Chevrot, C. Synth. Met. **1999**, *102*, 1325.
14. Ahn, S.-H.; Czae, M.-Z.; Kim, E.-R.; Haiwon Lee, S.H.; Han, S.-H.; Jaegeun Noh, M.; Hara, M. Macromolecules, **2001**, *34*, 2522.
15. Wessling, B. In *Handbook of Conducting Polymers*, 2nd edition. Marcel Dekker: New York, 1999; 467.
16. Ferreira, C.A.; Domenech, S.C.; Lacaze, P.C. J. Appl. Electrochem. **2001**, *31*, 49.
17. Reut, J.; Idla, K.; Öpik, A. Proc. Eston. Acad. Sci. Chem. **1996**, *45*, 152.
18. Perruchot, C.; Chehimi, M.M.; Dardoize, F.; Delamar, M. J. Chrom. A, **2002**, *969*, 167.
19. Ge H.; Wallace, G.G. J. Liq. Chromatogr. **1990**, *13*, 326.
20. Teasdale, P.R.; Ge, H.; Gilmore, K.; Wallace, G.G. Polym. Int. **1992**, *29*, 299.
21. Chriswanto, H.; Ge, H.; Wallace, G.G. Chromatographia **1993**, *37*, 423.
22. Chriswanto, H. PhD thesis, Wollongong University, Wollongong, Australia, 1995.
23. Chriswanto, H.; Ge, H; Wallace, G.G. Chromatographia, **1996**, *42*, 191.
24. Friend, R.;Burroughes, J.; Shimoda, T. Physicians World **1999**, *12*, 35.
25. Xuejun, S.A.; Jenekhe, S.A. Macromolecules **2000**, *33*, 2069.
26. Bao, Z. Rogers, J.A.; Katz, H.E. J. Mater. Chem. **1999**, *9*, 1895.
27. Pozo-Gonza lo, C.; Khan, T.; McDouall, J.J.W.; Skabara, P.J.; Roberts, P.M.; Light, M.E.;. Coles, S.J.; Hursthouse, M.B.; Neugebauer, H.; Cravino, A.; Sariciftci, N.S. J. Mater. Chem. **2002**, *12*, 500.
28. Bidan, G. Sensing effects in electroconducting conjugated polymers. In *Polymer Films in Sensor Applications*; Harsányi, G., Ed.; Technomic Publishing: Lancaster, 1995; 206–260.
29. Kros, A.; van Hovel, S.W.F.M.; Nolte., R.J.M.; Sommerdijk, N.A.J.M. Sensors Act. B **2001**, *80*, 229.
30. Kang, E.T.; Neoh, K.G.; Tan, K.L. Adv. Polym. Sci. **1993**, *106*, 135.
31. Ge, H.; Wallace, G.G. React. Polym. **1992**, *18*, 133.
32. Chehimi, M.M.; Abel, M.-L.; Perruchot, C.; Delamar, M.; Lascelles, S.F.; Armes, S.P. Synthetic Metals **1999**, *104*, 51.

33. Chao, T.H.; March, J. J. Polym. Sci. Polym. Chem. Ed. **1988**, *26*, 743.
34. Maeda, S.; Armes, S.P. J. Colloid Interface Sci. **1993**, *159*, 257.
35. Perruchot, C.; Chehimi, M.M.; Delamar, M.; Fievet, F. Surf. Interface Anal. **1998**, *26*, 689.
36. Zinger, B.; Miller, L.L. J. Am. Chem. Soc. **1984**, *106*, 6861.
37. Smith, A.B.; Knowles, C.J. J. Appl. Polym. Sci. **1991**, *43*, 399.
38. Miksa, B.; Slomkowski, S. Colloid Polym. Sci. **1995**, *273*, 47.
39. Minehan, D.S.; Marx, K.A.; Tripathy, S.K. Macromolecules **1994**, *27*, 777.
40. Tarcha, P.J.; Misun, D.; Finley, D.; Wong, M.; Donovan, J.J. Synthesis, analysis and immunodiagnostic applications of polypyrrole latex and its derivatives. In *Polymer Latexes*: *Preparation*, *Characterization and Application*; Daniels, E.S., Sudol, E.D., El-Aassar, M.S., Eds.; ACS Symp. Series 492; American Chemical Society: Washington, DC, 1992; chap. 22.
41. Armes, S.P. Potential applications of conducting polymer colloids. In *Intrinsically Conducting Polymers*: *An Emerging Technology*; Aldissi, M., Ed.; NATO ASI Series E: Applied Sciences, Vol. 246; Kluwer Academic: Dordrecht, 1993; 35–43.
42. Armes, S.P. Colloidal dispersions of conducting polymers. In *Handbook of Conducting Polymers*, 2nd Ed.; Skotheim, T.A., Elsenbaumer, R.L., Reynolds, J.R., Eds.; Marcel Dekker: New York, 1998; 423–435.
43. Gangopadhyay, R.; De, A. Chem. Mater. **2000**, *12*, 608.
44. Beamson, G.; Briggs, D.; Eds. *High Resolution XPS of Organic Polymers*. *The Scienta ESCA300 Database*; John Wiley and Sons: Chichester, 1992.
45. Briggs, D.; Seah, M.P.; Eds. *Practical Surface Analysis*, 2nd Ed., *Vol. 1*, *Auger and X-Ray Photoelectron Spectroscopy*; John Wiley and Sons: Chichester, 1990.
46. Garbassi, F.; Morra, M.; Occhiello, E.; Eds. *Polymer Surfaces*: *from Physics to Technology*; John Wiley and Sons: Chichester, 1994; 92–113.
47. Ratner, B.; Castner, D. Electron spectroscopy analysis of conducting polymers. In *Surface Analysis*: *the Principal Techniques*; Vickerman, J.C., Ed.; John Wiley and Sons: Chichester, 1997; 43–98.
48. Kang, E.T.; Neoh, K.G.; Ong, Y.K.; Tan, K.L.; Tan, B.T.G. Macromolecules **1991**, *24*, 2822.
49. Malitesta, C.; Morea, G.; Sabbatini, L.; Zambonin, P.G. X-ray photoelectron spectroscopy analysis of conducting polymers. In *Surface Characterization of Advanced Polymers*; Sabbatini, L., Zambonin, P.G., Eds.; VCH: Weinheim, 1993, chap. 5.
50. Malitesta, C.; Losito, I.; Sabbatini, L.; Zambonin, P.G. J. Electron Spectrosc. Relat. Phenom. **1998**, *97*, 199.
51. Sabbatini, L.; Malitesta, C.; De Giglio, E.; Losito, I.; Torsi, L.; Zambonin, P.G. J. Electron Spectrosc. Relat. Phenom. **1999**, *100*, 35.
52. Basinska, T.; Slomkowski, S.; Delamar, M. J. Bioactive Compatible Polym., **1993**, *8*, 205.
53. Dobler, F.; Affrossman, S.; Holl, Y. Colloids Surf. A, **1994**, *89*, 23.
54. Davies, M.C.; Lynn, R.A.P.; Hearn, J.; Paul, A.J.;Vickerman, J.C.; Watts, J.F. Langmuir **1996**, *12*, 3866.55. Deslandes, Y.; Mitchell, D.F.; Paine, A.J. Langmuir **1993**, *9*, 1468.
56. Basinska, T.; Slomkowski, S.; Dworak, A.; Panchev, I.; Chehimi, M.M. Colloid Polym. Sci. **2001**, *279*, 916.

57. Maeda, S.; Gill, M.; Armes, S.P.; Fletcher, I.W. Langmuir **1995**, *11*, 1899.
58. Maeda, S.; Corradi, R.; Armes, S.P. Macromolecules **1995**, *28*, 2905.
59. McCarthy, G.P.; Armes, S.P.; Greaves, S.J.; Watts, J.F. Langmuir **1997**, *13*, 3686.
60. Perruchot, C.; Chehimi, M.M.; Delamar, M.; Lascelles, S.F.; Armes, S.P. Langmuir **1996**, *12*, 3245–3251.
61. Barthet, C.; Armes, S.P.; Chehimi, M.M.; Bilem, C.; Omastova, M. Langmuir **1998**, *14*, 5032–5038.
62. Cairns, D.B.; Armes, S.P.; Chehimi, M.M.; Perruchot, C.; Delamar, M. Langmuir **1999**, *15*, 8059–8066.
63. Khan, M.A.; Armes, S.P.; Perruchot, S.P.; Ouamara, H.; Chehimi, M.M.; Greaves, S.J.; Watts, J.F. Langmuir **2000**, *16*, 4171.
64. Omastová, M.; Pavlinec, J.; Pionteck, J.; Simon, F.; Košina, S. Polymer **1998**, *39*, 6559.
65. Gospodinova, N.; Mokreva, P.; Terlemezyan, L. J. Chem. Soc. Chem. Commun. **1992**, 923.
66. Banerjee, P.B.; Digar, M.L.; Bhattacharyya, S.N.; Mandal, B.M. Eur. Polym. J. **1994**, *30*, 499.
67. Azioune, A.; Chehimi, M.M.;. Miksa, B.; Basinska, T.; Slomkowski, S. Langmuir **2002**, *18*, 1150.
68. Armes, S.P.; Vincent, B. J. Chem. Soc. Chem. Commun. **1987**, 288.
69. Armes, S.P.; Gottesfeld, S.; Beery, J.G.; Garzon, F.; Agnew, S.F. Polymer **1991**, *32*, 2325.
70. Stejskal, J.; Quadrat, O.; Sapurina, I.; Zemek, J.; Drelinkiewicz, A.; Hasik, M.; Krivka, I.;Proke, J. Eur. Polym. J. **2002**, *38*, 631.
71. Lascelles, S.F.; McCarthy, G.P.; Butterworth, M.D.; Armes, S.P. Colloid Polym. Sci. **1998**, *276*, 893.
72. McCarthy, G.P.; Armes, S.P.; Greaves, S.J.; Watts, J.F. Langmuir **1997**, *13*, 3686.
73. Terril, N.J.; Crowley, T.; Gill, M.; Armes, S.P. Langmuir **1993**, *9*, 2093.
74. Saoudi, B.; Jammul, N.; Chehimi, M.M.; McCarthy, G.P.; Armes, S.P. J. Colloid Interface Sci. **1997**, *192*, 269.
75. Melzak, K.A.; Sherwood, C.S.; Turner, R.F.B.; Haynes, C.A. J. Colloid Interface Sci. **1996**, *181*, 635.
76. Butterworth, M.D.; Corradi, R.; Johal, J.; Lascelles, S.F.; Maeda, S.; Armes, S.P. J. Colloid Interface Sci. **1995**, *174*, 510.
77. Saoudi, B.; Jammul, N.; Abel, M.L.; Chehimi, M.M.; Dodin, G. Synth. Met. **1997**, *87*, 97.
78. Azioune, A.; Pech, K.; Saoudi, B.; Chehimi, M.M.; McCarthy, G.; Armes, S.P. Synth. Met. **1999**, *102*, 1419.
79. Pope, M.R.; Armes, S.P.; Tarcha, P. Bioconj. Chem. **1996**, *7*, 436.
80. Patel, N.; Davies, M.C.; Hartshorne, M.; Heaton, R.J.; Roberts, C.J.; Tendler, S.J.B.; Williams, P.M. Langmuir **1997**, *13*, 6485.
81. Azioune, A.; Ben Slimane, A.; Chehimi, M.M.; Perruchot, C.; Armes, S.P. Paper presented at Modification, Degradation and Stabilisation of Polymers (MODEST 2002) Conference, Budapest, Hungary, 2002.
82. Yassar, A.; Roncali, J.; Garnier, F. Polym. Commun. **1987**, *28*, 103.

83. Wiersma, A.E.; Steeg, L.M.A.; Jongeling, T.J.M. Synth. Met. **1995**, *71*, 2269.
84. Lascelles, S.F.; Armes, S.P. Adv. Mater. **1995**, *7*, 864.
85. Barthet, C.;Armes, S.P.; Lascelles, S.F.; Shen, Y.L.; Stanly, H.M.E. Langmuir **1988**, *14*, 2032.
86. Cairns, D.B.; Armes, S.P.; Bremer, L.G.B. Langmuir **1999**, *15*, 8052.
87. Khan, M.A.; Armes, S.P. Langmuir **1999**, *15*, 3469.
88. Huijis, F.M. PhD thesis, The Netherlands, **2000**, (http://www.ub.rug.nl/ldoc/dis/science/f.m.huijs).
89. Lascelles, S.F.; Armes, S.P.; Zhadan, P.A.; Greaves, S.J.; Brown, A.M.; Watts, J.F.; Leadly, S.R.; Luk, S.Y. J. Mater. Chem. **1997**, *7*, 1349.
90. Perruchot, C.; Chehimi, M.M.; Delamar, M.; Cabet-Deliry, E.; Miksa, B.; Slomkowski, S.; Khan, A.M.; Armes, S.P. Colloid Polym. Sci. **2000**, *278*, 1139.
91. Perruchot, C.; Chehimi, M.M.; Dardoize, F.; Delamar, M . J. Chromatogr. A, in press.

11

Preparation of Magnetic Latices

ABDELHAMID ELAISSARI, FLORENCE SAUZEDDE, FRANCK MONTAGNE, and CHRISTIAN PICHOT
CNRS-bioMérieux, Lyon, France

I. INTRODUCTION

Magnetic latexes belong to the family of colloids known as composites or hybrid materials. In the colloidal field, this term corresponds to all spherical particles with a mixed structure, i.e., containing organic (i.e., polymers) and inorganic material (i.e., oxides). The latter can be composed of a metal oxide such as iron oxide, silica, gold particles, or quartz powder. Each of the organic and inorganic components plays a specific role for a given application.

The presence of a magnetic material endows the polymer particle with additional properties [1]. For example, iron oxides and ferrites are used to elaborate conducting polymers [2,3], to modify the optical properties of films [4], and also in inks used in magnetic printers [5]. The paper industry also uses magnetic composite particles to eliminate carbon in duplicated copies [6]. Other applications, such as high-density recording media [7] and catalyst carriers [8], use specific magnetic properties of iron oxides.

In the biomedical field, numerous papers describe various applications of magnetic polymers [9–11]. The role of polymers in the preparation of magnetic composite particles is generally to protect the inorganic part and to induce reactive chemical functions capable of immobilizing biological species via chemical reaction. That of magnetic iron oxide is to ensure the migration of composite particles when a magnetic field is applied [12].

A great variety of magnetic composite particles are available. They have diameters from 30 nm to several micrometers, and are in the form of a capsule, a microgel, or a smooth or porous microsphere. In this case, the organic matrix can be composed of a natural polymer, produced, for example, from albumin [13], cellulose [14], or starch [15], eventually forming biodegradable particles. These can also contain a synthetic polymer derived in particular from glutaraldehyde and cyanoacrylate [16]. Hydrophilic magnetic microspheres are synthe-

sized by using acrylamide, acrylic acid [14], and methacrylic acid [10] derivatives. Hydrophobic magnetic polymer particles are generally prepared using styrene [17] and styrene derivatives. Given the variety of synthesis processes, the latexes obtained have a wide range of properties and can be adapted to a large number of biological applications. The purpose of this chapter is to present different elaboration methodologies used to obtain magnetic colloids and principally magnetic latexes.

II. SYNTHESIS OF FERROFLUIDS

A. Introduction

Magnetic fluids (i.e., ferrofluid solution) are stable colloidal dispersions of ferrite or iron oxide nanoparticles (10 nm) dispersed in an aqueous or organic medium. Ferrites are customarily defined as the metallic oxides in which iron is the principal component. The two most commonly encountered types of ferrite are iron oxide magnetite nanoparticles (Fe_3O_4) and maghemite (γ-Fe_2O_3). The strong interactions between magnetic oxide particles and solvent molecules in a high solid content ensure magnetic behavior throughout the fluid. In the presence of a magnetic field, the fluid behaves like a single-phase system [18]. Because of this unique combination of fluid and magnetic properties, ferrofluids have applications in a vast range of domains [19].

There are two principal methods for preparing ferrofluid dispersions. The first involves the prolonged crushing of the specific material in a ball mill until the particles are of nanometric size. A second method yields iron oxide nanoparticles much more rapidly through a well-known chemical process by which an aqueous solution of metal salts is precipitated with a given basic solution. The first chemical synthesis of ferrofluids is credited to Elmore [20] in 1938. This method directly provides nanometric-sized ferrite nanoparticles for subsequent dispersal in an aqueous or organic medium. While this synthesis method is the most frequently reported in the literature, we will see that there are others, some rather original.

The substantial work conducted over the past 20 years has made available a wide range of magnetic fluids that differ both in the type of solvent and in the type of metallic nanoparticles. Mastery of the synthesis processes for ferrofluids and of their physical properties has considerably extended the fields of their applications.

Aqueous ferrofluids are widely used in the biomedical domain [21,22]. For such applications, particular care is required in the synthesis of a ferrofluid that remains stable in the acidity and salinity levels of human serum and is isotonic. In vivo and ex vivo applications further require a magnetic fluid that is nontoxic, biocompatible, and sometimes even biodegradable. To avoid induction of an

acute immune response to the presence of the ferrofluid in the human body, the ferrite nanoparticles are coated with a hydrophilic polymer [21] such as polysaccharides (i.e., dextran) [23].

The functionalized ferrite nanoparticles are used to immobilize various types of biological molecules, including nucleic acids, enzymes [24], antibodies [25], and proteins [26]. Nonetheless, one essential condition is the conservation of most of their biological activity. The great specificity of biological reactions offers enormous potential for cell sorting [25] [27] and for diagnosis [23,28]. The ferrofluid are used as carriers because of their magnetic properties. In this domain, a simple magnet is needed to guide the magnetic particles carrying diverse drug substances to infected cells or organs [11]. For example, a diseased cell is exclusively recognized by sensitive magnetic nanoparticles that can be totally destroyed by the application of an alternative magnetic field; this phenomenon is called magnetocytolysis. The magnetic energy is transformed into thermal energy, and this heating of the particles induces cell lysis. Ferrofluids also have applications as contrast agents in medical imaging (MRI) and as radioactive isotope vectors in the radiation treatment of some tumors [11].

B. Methods of Synthesizing Ferrofluids

1. Synthesis of Surfactant Ferrofluids

Surfacted ferrofluids are characterized as ferrite nanoparticles stabilized by the adsorbed surfactant layer(s). These dispersing agents are polymers or surfactants. The surfactants most often used to stabilize these iron oxide nanoparticles, in both aqueous and organic media, are fatty acids.

A first, rather rudimentary synthesis method consists of crushing the magnetic material for several days so as to obtain nanometric particles. First proposed at the beginning of the 1960s by Papell et al. [29] with the idea of using a magnetic fluid as a fuel additive, this preparation technique was adopted and improved by Rosenweig [30]. After milling into fine grains, the magnetic material is dispersed in an organic solvent containing oleic acid. The surfactant is adsorbed on the particles surface and thus stabilizes the dispersion by introducing sterical stabilization. This technique makes it possible to obtain ferrofluids in various types of organic solvents. While this method, as described by Rosenweig [30], yields a stable, homogeneous magnetic fluid, the synthesis is nonetheless long and tedious. Working at very low temperatures, however, it is possible to significantly reduce not only the duration of the milling but also the particle size and particle size distribution of the magnetic particles [31].

In 1973, Khalafalla et al. [32] proposed a less restrictive method that resulted in stable magnetic particles in organic and aqueous media. In the first stage, addition of an excess of ammonia precipitates a mixture of ferrous and ferric salts. Oleic acid is then added to the aqueous solution; it reacts with the excess

ammonia to form an ammonium oleate soluble in the water adsorbed on the particle surfaces. A hydrophobic coating thus forms around the particles, which aggregate and are subsequently extracted from the aqueous phase and finally redispersed in an organic solvent. Khalafalla et al. [33] showed that it is also possible to stabilize magnetite effectively in an aqueous medium simply by replacing oleic acid (C_{18}) with dodecanoic acid (C_{12}), a more hydrophilic fatty acid. The dispersion medium dictates the type of surfactant. The affinity of a surfactant for a given solvent is adequately described by the concept of the hydrophilic–lipophilic balance (HLB) number: the shorter the carbon chains of the surfactant, the higher its HLB value and the more hydrophilic its character. For this reason, dodecanoic acid durably stabilizes magnetite in aqueous media.

Using a mixture of iron sulfate and a similar process, Jolivet [34] prepared magnetite particles coated with oleic acid and then redispersed the particles in an aqueous solution containing a second surfactant, with a high HLB value. A double surfactant layer forms on the surface of the grains, thereby ensuring the stability of the colloidal system in water. Nonetheless, the stability of this surfactant layer is sensitive to pH variations and to the ionic strength of the medium.

In turn Shinkai [35] described a process by which magnetic nanoparticles could be dispersed in toluene. The synthesis of magnetic particles is substantially different because an iron sulfate solution is first oxidized by a sodium nitrite solution before being precipitated by concentrated ammonia. The magnetite particles thus obtained are redispersed in an aqueous solution containing fatty acid surfactant such as oleic acid; the addition of hydrochloric acid induces the colloidal aggregation of the magnetic particles. The water is finally eliminated, and the nanoparticles coated by the surfactant layer are dispersed in the toluene. Depending on the quantity of sodium nitrite used to oxidize the iron sulfate, particle size varies between 4 and 70 nm. These three processes of chemical synthesis are presented in Fig. 1.

Other more original synthesis methods are also described in the literature. Nanoparticles composed of iron and barium are prepared by a precipitation process in a heterogeneous phase [36]. The particles are obtained by mixing two microemulsions (water-in-oil), one containing barium and iron salts, and the other a basic solution. The homogenization of the system results in precipitation of the oxide, which is stabilized in the organic medium by the surfactant initially present on the microreactor surface. Another original method involves using electrochemical means to synthesize the maghemite nanoparticles [37]. The iron oxide particles are stabilized in dimethylformamide by a quaternary ammonium salt. The intensity of the electrical field circulating between the iron anode and the platinum cathode controls the size of the nanoparticles. The maghemite thus obtained is amorphous but nonetheless exhibits a superparamagnetic property. Another ingenious process is described by Nakatani [38], which consists of

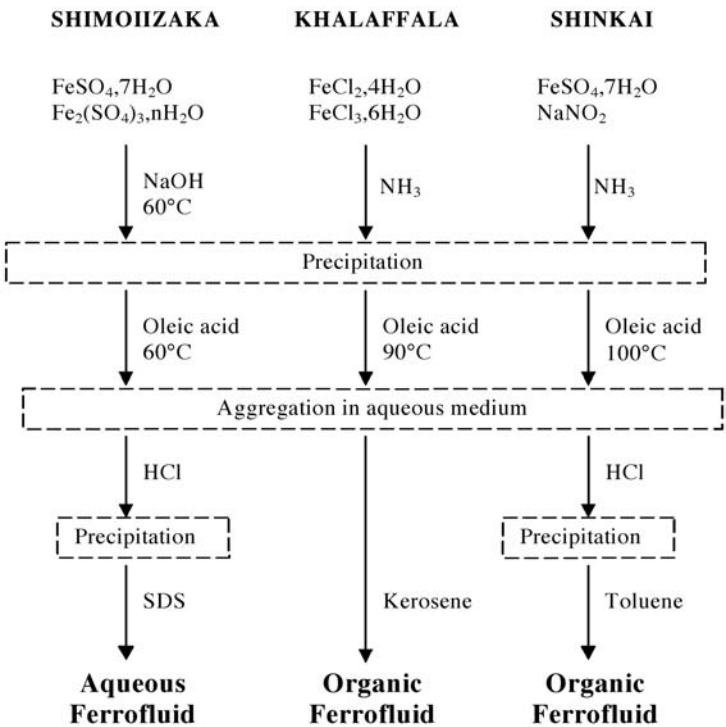

FIG. 1 Methods for synthesizing surfacted ferrofluids [35].

distributing fine particles of metal evaporated in a vacuum with a spherical chamber system onto the surface of an organic solvent (naphthalene) containing a given polymer concentration. The adsorption of polymer onto the metal (Fe, Ni, or Co) particles favors their dispersion in organic phase. Drastic heat treatment with argon causes the particles to agglomerate. They are then separated from the organic medium by centrifugation and redispersed by ultrasound in a mixture of toluene and polymer. With this method, Nakatani et al. [38] obtained superparamagnetic particles of approximately 20 nm.

2. Synthesis of Ionic Ferrofluids

The chemical synthesis method proposed by Massart [39] at the beginning of the 1980s yields stable aqueous surfactant free ferrofluids. In this process, the surface charge density of magnetic particles depends on the pH of the medium (Fig. 2). The iron oxide nanoparticles are usually obtained by using a highly basic solution to induce precipitation of ferrous and ferric chlorides solutions mixture. This stage of metal salt coprecipitation is essential because it deter-

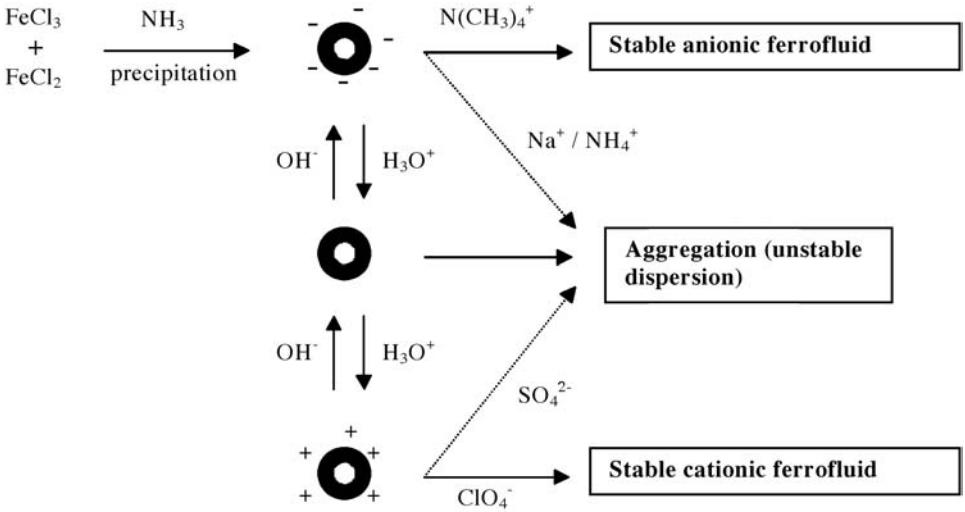

FIG. 2 Synthesis of a ferrofluid in an aqueous medium [40].

mines the subsequent properties of the ferrofluid. The experimental conditions under which this reaction takes place, such as the initial molar ratio between the ferrous and ferric ions, the type of base used, the temperature, the pH, or the type and concentration of cations present, strongly influence the size and yield of magnetic materials [40]. The synthesis of magnetic nanocolloids in an ammonia medium leads to particle aggregation [41] because the strong polarizing power of the NH_4^+ cation prevents interactions between the magnetic grains and water molecules. To solve this problem, Massart [39] proposed substituting ions with weaker polarizing property in order to enhance the colloidal stability of the dispersion. The most commonly used counterions are tetramethylammonium cations $(CH_3)_4N^+$ and perchlorate anions ClO_4^-. Their use makes it possible to obtain stable anionic (alkaline) and cationic (acid) sols. Typically, Massart et al. obtained ferrite particles of unequal size, ranging from 3 to 20 nm. These particles, stable in aqueous media, can also be obtained in an organic medium by modifying the type of interface between the particle and the solvent. Stabilization of the particles in an organic medium requires coating their surfaces with a protective surfactant that has an affinity with the solvent [42]. Binding the surfactant to the surface of particles involves electrostatic interactions or, if the molecule has complexing groups (chelating groups), complexation with metal atoms. Some studies have clearly shown the probable mechanism of complexation of fatty acids such as oleic acid on the surface of iron oxide nanoparticles [43].

The divalent metal associated with the ferric ion is not always a ferrous ion. Depending on the desired final properties of the ferrofluid, it could be strontium [44], barium [45], cobalt [46–48], or manganese [49]. Some oxides are even composed of three different metal atoms ($ZnNiFe_2O_4$) [50]. Of course, the type of metals incorporated during the synthesis affects the final magnetic properties of the particles.

C. Colloidal Stability

Colloidal stability is an essential parameter that must take into account the subsequent applications. Oxides particles do not remain naturally dispersed but tend to sediment under the influence of gravity because their density (approximately 5 g/cm^3) is much greater than that of standard solvents. Nonetheless, if the nanoparticles are small enough (around 10 nm), Brownian motion should maintain the homogeneity of the dispersion with no sedimentation phenomena.

The colloidal stability of the ionic ferrofluids is principally related to the pH of the medium [39] as schematically represented in Fig. 3. In a pH ranging from

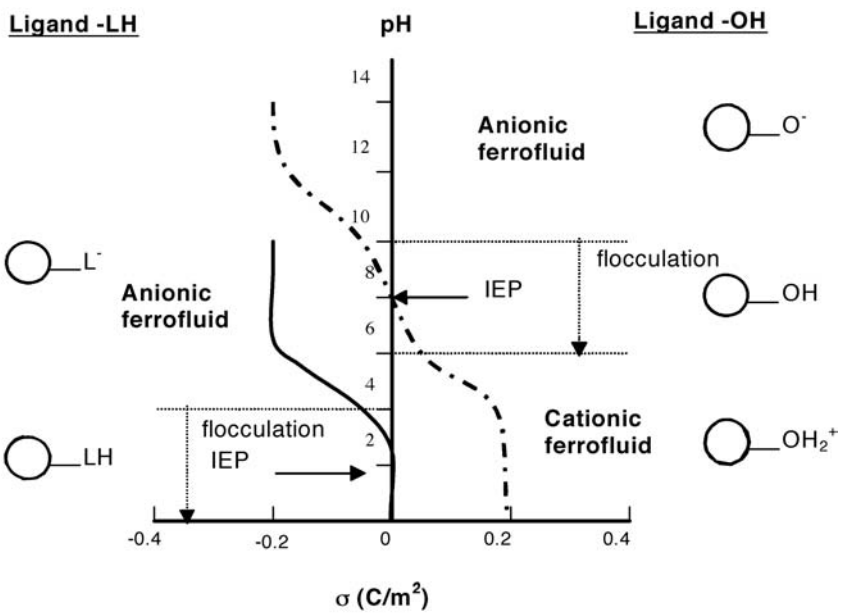

FIG. 3 Colloidal stability of an ionic ferrofluid as a function of pH [51].

6 to 10, the oxygen atoms are not sufficiently charged to ensure the repulsive electrostatic interactions essential to enhance the colloidal stability in aqueous media; thus, the particles flocculate. There is even a pH value at which the global net surface charge of the particles is zero: this is the isoelectric point (IEP).

This instability at a neutral pH is a major disadvantage for biomedical applications. To remedy this problem, the type of surface charge must be modified by replacing the hydroxylate ligand with a citrate ligand [51]. The IEP is accordingly displaced from pH 7 to pH 3 and the ferrofluid is thus stable from pH 4 upward (Fig. 3).

D. Characterization of Ferrofluids

The physicochemical and colloidal properties of the magnetic nanoparticles constituting a ferrofluid dispersion can be achieved using various techniques such as X-ray diffraction, elementary analysis, magnetic measurement, transmission electron microscopy visualization, and colloidal stability, as summarized in Table 1.

III. SYNTHESIS OF MAGNETIC POLYMER PARTICLES

A. Introduction

The development in around 1950 of polymer particles of uniform size by Dow Chemical [16] has permitted the first biomedical applications for latexes. The

TABLE 1 Table Summarizing the Main Techniques for Characterizing Ferrofluids

Analysis techniques	Properties
X-ray spectroscopy	Type of oxide
	Chemical structure
	Nanoparticle sizes
Infrared spectroscopy	Type of oxides
Elementary analysis	Chemical composition
Thermogravimetric analysis	Chemical composition
Mösbouer spectroscopy	Composition
	Type of oxide
Electron microscopy	Particle sizes
	Morphology
Magnetic measurements	Nanoparticle sizes
	Magnetic material concentration
	Magnetic properties
Turbidity analysis	Colloidal stability

synthesis of magnetic composite microspheres was the subject of much research [52]. Avremas et al. [53] played a pioneering role in producing composite particles for biomedical applications. As early as 1975, they reported the synthesis of hydrophilic magnetic particles by the polymerization of acrylamide and agars in the presence of magnetic iron oxide nanoparticles. However, the final particles were polydispersed and the distribution of the magnetite was uneven.

Since then many preparation methods have been developed and, according to the mode of synthesis and the properties of the original material, the final particles have three different structures and morphologies, illustrated in Figure 4. These have, for example, a core-shell structure with a magnetic core (Fig. 4a). Conversely, the magnetic material is distributed throughout the polymer particle (Fig. 4b) or forms a magnetic layer on the surface of the organic core (Fig. 4c).

These different types of particle are obtained according to three different strategies, described in this section:

1. The magnetic pigment and the polymer chains (or matrixes) are synthesized separately.
2. The magnetic material is obtained or prepared on the latex by adsorption or precipitation processes.
3. Polymerization is carried out in the presence of iron oxides nanoparticles.

B. Separated Synthesis of Polymer and Magnetic Components

The magnetic particles and the polymer chains have been obtained by specific and independent processes. Two methods are then used to form the polymer matrix around the inorganic pigment and are illustrated in Fig. 5. Either the magnetic nanoparticles are impregnated in the final particle or the polymer chains are immobilized on the inorganic surface.

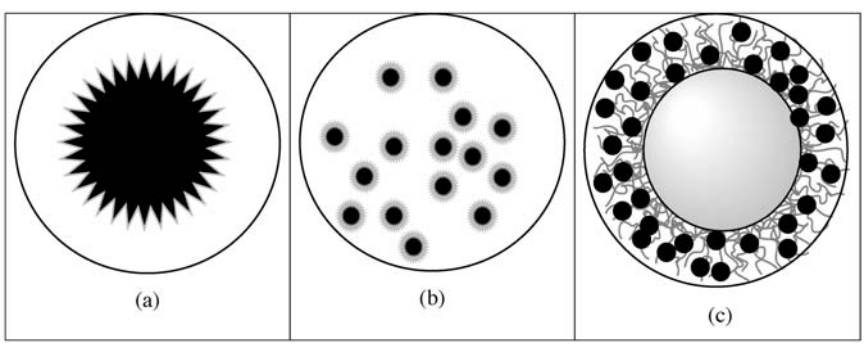

FIG. 4 Different structures of the existent magnetic latex particles.

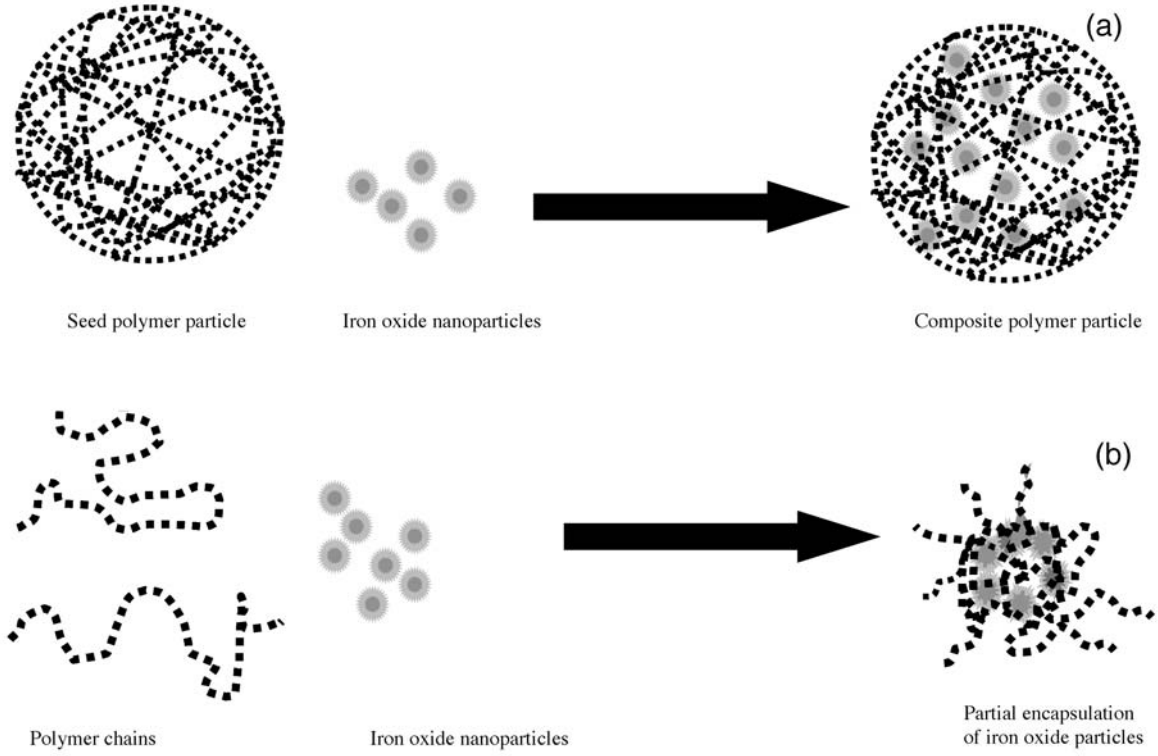

FIG. 5 Composite particles obtained via impregnation process (a) and polymer chains encapsulation of aggregated iron oxide nanoparticles (b).

1. Impregnation of Ferrites in the Polymer Matrix

One of the first types of magnetic particle dispersions used as a carrier in biomedical applications was prepared in a dispersed medium. The aqueous solution containing albumin, the active ingredient, and the iron oxide nanoparticles is emulsified by applying ultrasound in natural oil. In order to harden and cross-link the albumin as a matrix, this emulsion is then introduced drop by drop either into the oil at high temperature (110–165°C) or into the oil at 25°C containing the cross-linking agent [54]. The final magnetic microspheres are conserved in lyophilized form. They contain 20–50 wt % of Fe_3O_4 and have a size distribution of about 1 μm [55]. Such colloidal particles can be considered as biocompatible and biodegradable material, but can also generate the adsorption of other proteins; therefore, the carrier is not very specific [56]. The reactive groups (amine and carboxylic functions) of the protein constituting the matrix can be used for the covalent binding of modified nucleic acids such as oligonucleotides (single-stranded DNA fragments) or antibodies.

It is also possible to obtain smaller magnetic particles (200 to 500 nm) by modifying the previous operating mode with respect to the quantities of solvent, monomer, and agitation by ultrasound. However, their monodispersity remains low (with a standard deviation close to 20%) and they contain only small amount of Fe_3O_4 (from 5% to 9%) [57]. The final polydisperse particles can be fractionated in order to obtain reasonable narrowly size distribution of the dispersion by controlling the centrifugation rate or the sedimentation time and conditions.

To avoid the disadvantages encountered with albumin protein, the latter is replaced with polyvinyl alcohol (PVA). Nonspecific adsorption of proteins and antibodies is reduced and, in addition, the polymer provides hydroxyl functions [56]. The magnetic latex particles are obtained by cross-linking in a water–oil solution. The aqueous phase, containing the PVA and magnetic nanoparticles, is emulsified in vegetable oil by agitation in the presence of surfactant such as a polyethylene oxide–based polymer. The particle formation is achieved by adding glutaraldehyde as cross-linker. This process is easy to implement and takes only 15 min. The final particles, with low monodispersity, have a diameter in the region of several dozen micrometers, which permits relatively rapid separation in spite of a low ferrite content. They have a density of 1.2 g/cm^3, which corresponds to a weight in ferrites less than 5% of overall weight.

Another method consists of the mechanical capture of the magnetic particles in the polymer chains without using a cross-linking agent. The composite microspheres are obtained from polystyrene chains of 50,000 g/mol and iron oxide nanoparticles (having a diameter of 200 nm) mixture by evaporating a solvent. The polymer and magnetic material are contained in methylene chloride, often used as a volatile solvent. It is emulsified in a solution of PVA by mechanical

agitation. After evaporation of methylene chloride, the hard colloids are washed with water and then lyophilized. They have a diameter in the region of several hundredths of a micrometer and can contain up to 50% of Fe_3O_4 in weight. However, they are polydispersed and the beads obtained do not have a spherical, regular shape beyond 30% of magnetic material in volume [58].

In contrast with the previous methods, it is also possible to introduce the magnetic pigments in particles that have already been cross-linked.

Sepharose particles are composed of a gel in which ferrite nanoparticles are incorporated via adsorption or precipitation process. Even after washing several times with a given buffer, the magnetic particles remain inside the microgel. A ligand is fixed to the polymer matrix before incorporating the ferrites. The magnetic polymer particles obtained are used as affinity chromatographic media and have the same affinity properties as the nonmagnetic polymer particles [59]. However, as the small magnetic nanoparticles are not strongly fixed inside the microgels particles, washing by any buffer solutions may lead to the desorption or release of the ferrites, which is a major disadvantage in biomedical applications.

2. Polymer Immobilization onto Inorganic Magnetic Material

Another strategy consists of immobilizing the polymer on the surface of inorganic pigments. Two types of composite particles are obtained from ferrite particles with a diameter in the region of about 10 nm [9], or from 200–400 nm [60,61]. The polymer chains are then fixed onto the iron oxide surface by physical adsorption [60] or chemical grafting [9,61] and form a thin organic polymer layer. The interactions between the two species (polymer chains and inorganic material) are promoted by chemical functions provided by the polymer (OH, COOH, PO_3H_2, NH_2) and magnetic particles. In this case, the active sites correspond to adsorbed water molecules on the surface of the iron oxides or to functional groups such as acid anhydride [9] or mercaptosilanes [61] obtained after activation of the inorganic surface [60]. The polymers used are generally hydrophilic such as an acrylic acid [61], a methyl methacrylate [60], a propylene glycol [9], or a siloxane derivative. It should be noted that the thin layer of immobilized polymer on inorganic magnetic nanoparticles does not modify the superparamagnetic behavior of the bare colloidal suspension. In fact, the magnetic nanoparticles cores are not chemically modified in order to avoid modification of their magnetic properties.

C. Synthesis of Magnetic Material on Polymer Particles

Composite particles can be obtained from polymer microspheres formed beforehand, obtained according to the different polymerization processes in dispersed media. These are generally functionalized in order to promote the incorporation

of the magnetic material onto seed polymer particles. The latexes are dispersed in a solution of metal salts (such as $FeCl_2$ and $FeCl_3$ mixture), often iron and sometimes cobalt or nickel. The magnetic material is then deposited by precipitation process or by oxido-reduction of metallic ions.

1. Incorporation of Iron Oxide by Precipitation

Ugelstad et al. [62] had a pioneering role in synthesizing monosized magnetic latex particles. The process is illustrated in Fig. 6 and is based on four steps: (1) initial synthesis of porous polymer particles (as a seed latex particles) with a large diameter in the region of several micrometers (from 2 to 4 μm) and a very narrow size distribution; (2) diffusion of metal salts into porous latex particles; (3) precipitation of metal salts onto porous latex particles (using basic solution such as ammonia or sodium hydroxide); and (4) encapsulation of immobilized iron oxides onto porous latex particles by polymerization process.

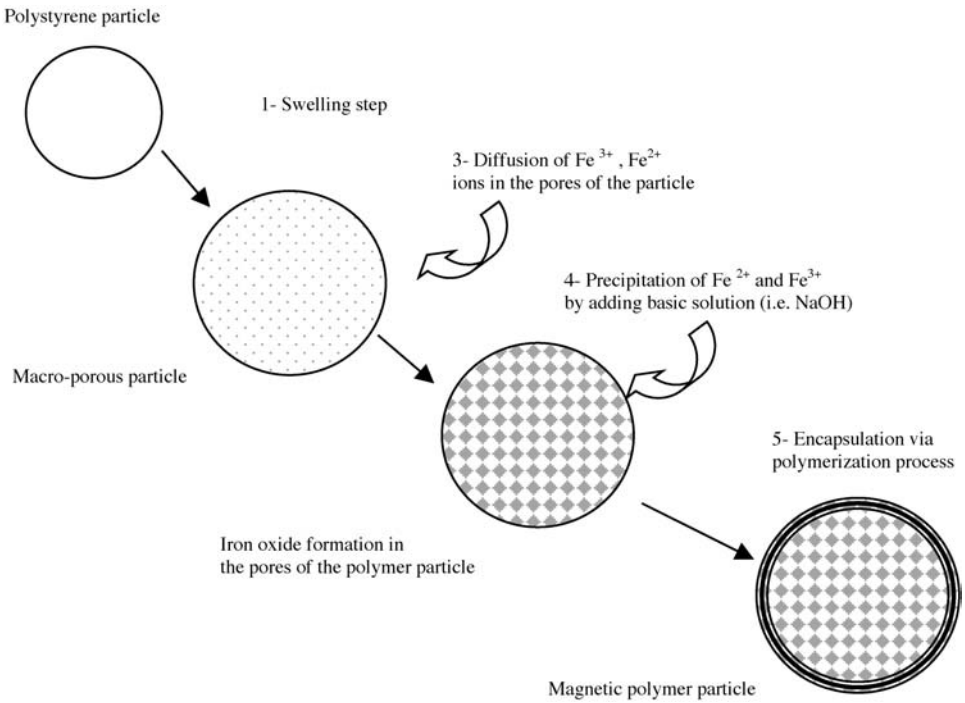

FIG. 6 Schematic illustration of the synthesis of magnetic particles using the process developed by Ugelstad et al. [62].

The porous latex particles (used as a seed) are obtained via a dynamic swelling method followed by an emulsion polymerization process. Monodispersed seed particles in the region of several hundredths of a nanometer (from 800 to 1000 nm) can be swollen from 50 to 1000 times their initial volume by a vinyl monomer solution (Z) possibly containing other reactants such as porogen solvent. All of the reactants are contained in the swollen seed particle before emulsion polymerization starts so as to avoid a secondary nucleation. Then the swollen particles are considered as a small polymerization reactors. This increase in volume is obtained using a two-stage swelling process. The first stage corresponds to the activation of the seed latex particles by introducing a compound Y. Compound Y, with a low molar weight and very insoluble in water, diffuses inside the particles. For example, Y can be hexadecane or dioctanyl peroxide, which also has the role of emulsion polymerization initiator, can be used. The second swelling step corresponds principally to diffusion of the vinyl monomer inside the activated seed latex particles.

The swelling process is based on the thermodynamic equilibrium between the three phases present: the seed latex particles, the monomer droplets (Z), and the continuous phase (water). The equilibrium balance of the system is expressed by the equality of the variation of the Gibbs energy (ΔG) of the three phases. The free energy of each of the phases is directly related to their volume fraction, their superficial tension, and the particle size of the seed latex particles. To obtain porous latex particles, a volatile solvent (inert as regards polymerization) introduced during the swelling step is then evaporated to form pores [63–65] in and on the microspheres.

Porous, monosized polystyrene- and divinylbenzene-based polymer particles of a few micrometers have been obtained using the described swelling process [66]. The chemically modified porous latex particles via oxidation process (to induce NO_2, ONO_2) are then dried and redispersed in an aqueous solution of ferric and ferrous salts (Fe^{2+} and Fe^{3+}). The ferrous and ferric ions concentration corresponds to the desired ratio (Fe^{3+}/Fe^{2+} between 1 and 2) generally chosen to obtain γ-Fe_2O_3 or Fe_3O_4 structures, respectively. The presence of oxidizing functions along with the increase in pH and temperature increase the precipitation yield of iron hydroxides in the form of iron oxides (Fe_3O_4 or γ-Fe_2O_3) at the pores sites of the porous polymer particle used as a seed support.

The final microspheres obtained have a spherical shape and irregular porous surface [10] containing iron oxide nanoparticles. In order to fill the accessible pores and to encapsulate the immobilized iron oxide, a last polymerization step has been performed. The size of the final magnetic latex particles ranges from 1 to 5 μm and contain up to 10% weight of iron oxide.

The second polymer layer induced during the encapsulation step can be chemically modified by inducing reactive groups such as amine, hydroxyl, carboxylic, thiol, and aldehyde compounds [67,68] for the covalent grafting of

TABLE 2 Colloidal Properties of Dynabeads M450 and M280 [64]

Properties	M450	M280
Diameter (μm)	4.5	2.8
Quantity of iron (% mass)	22	12
Density (g/cm^3)	1.5	1.3
Specific surface (m^2/g)	3–5	4–6
Functional group	OH	OH
Application	Cell separation	Diagnosis and DNA technique

biomolecules. The colloidal properties of such magnetic latex particles are given in Table 2 [64], and the TEM image is given in Fig. 7.

By also using precipitation of ferric and ferrous salts impregnated in divinylbenzene-based porous particles, Winnik et al. [69] showed, by comparison with polystyrene-based seed particles having sulfate functions, that the presence of sulfonated groups permits the oxidation of ferrous hydroxides into α-FeO(OH). The final particles demonstrate superparamagnetic behavior at ambient temperature.

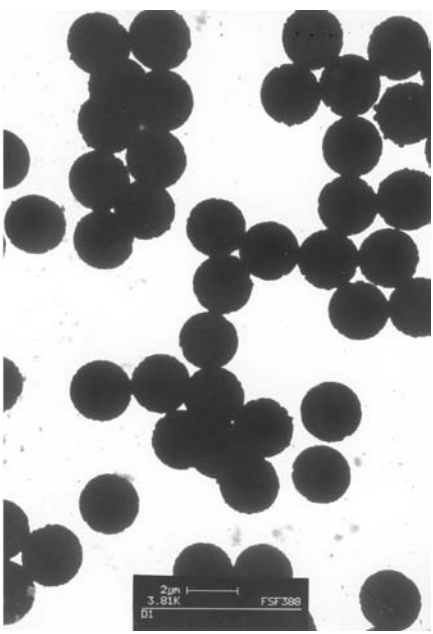

FIG. 7 TEM image of the magnetic latex particles Dynabed M280.

The use of polyacrylamide-based microgel particles swollen with water also permits homogeneous distribution of magnetic material throughout the particle. Dispersed in a solution of ferric and ferrous salts, the quantity of water and consequently of the salt contained in the microgel particles depends on the cross-linking density. By increasing the pH and the temperature of the incubation medium, ferric and ferrous salts are transformed into iron oxide nanoparticles inside the polyacrylamide microgel particle. However, by applying ultrasound for dispersing the formed magnetic microgel particles, the iron oxide nanoparticles can be desorbed or released from the polyacrylamide matrix latex. In addition, the obtained magnetic microspheres have a very porous surface, which can be a major disadvantage if used as a solid phase in immunoassays.

The process proposed by Kawaguchi et al. [70] is similar to the above-described methodology. The particles with acrylamide, methacrylic acid, and bisacrylamide are dispersed in a solution of ferric and ferrous salts which are then precipitated by addition of ammonia solution. Precipitation is limited in the aqueous phase by the presence of dextran. The latter "dextran" can have two actions: (1) improve compatibility between polymer chains and biomolecules, and (2) prevent the aggregation of ferrite particles in the dispersed medium. The composite microspheres are then covered by a layer of glycidyl methacrylate–based polymer in order to prevent the release of the magnetic nanoparticles and to functionalize the particle surface by providing oxirane functions. The final particles have a diameter of approximately 0.4 μm and contain from 20–25 wt % iron oxides, corresponding to half of the initial amount of iron oxide introduced [70] in the preparation process. The prepared magnetic latex particles do not appear to be narrow size distribution, but their use in immobilizing polypeptides gives satisfactory results.

2. Deposition of Magnetic Metals

Iron, cobalt, and nickel atoms have magnetic properties and are also used for magnetic polymer particle preparation. This method, developed by Rhône-Poulenc [71], uses nonporous hydrophobic seed particles with a narrow size distribution. These polystyrene-based microspheres are synthesized by classical emulsion polymerization and have a diameter in the region of 0.35 μm. A second stage of seeded polymerization permits one to obtain larger particles sizes (1.35 μm). A terpolymer is formed around the seed particles by suspension polymerization in toluene of a well-defined mixture of styrene, divinylbenzene, and 4-vinylpyridine. The toluene containing cobalt carbonyl [$Co_2(CO)_8$] swells the latex particles and thus ensures homogeneous distribution of the metal precursor. The thermolysis reaction of cobalt carbonyl is initiated by 4-vinylpyridine, and the release of carbon oxide is the evidence that the metal salt decomposes into cobalt.

The behavior of the final magnetic particles is superparamagnetic. However, the released carbon monoxide (CO) during the reaction leads to surface defor-

mation of the particles. The appearance of blisters increases with the concentration of the cross-linker, but the latter cannot be reduced below a certain value without drastically modifying the properties of the particles. This process has been validated using various cross-linked polymers particles having polar groups capable of forming complexes that are thermally decomposable with a metal salt [71].

Reduction of metal salts is another way to induce magnetic properties on the surface of polymer particles, which are then used as a conducting polymer material or as a solid support of chemical reactions in catalysis domain.

The metal cations associated with chlorides, such as Fe^{2+}, Ni^{2+}, and Co^{2+}, permit depositing or fixing very small metal nanoparticles onto polystyrene latex surface (of particle size close to 300 nm). These are obtained by emulsion copolymerization of styrene and a functional comonomer. The chemical function provided by acrylonitrile ($-CN$), acrylamide ($-CONR_2$), and *N*-vinylimidazole permits the immobilization of metal ions (via complexation process) on the surface of polymer particles which are then reduced by $NaBH_4$ or NH_2NH_2. The amount of metal deposited depends on the nature and the initial concentration in metal salts and the type of polymer used. In the case of iron, it represents several percentage points while in the case of cobalt it can reach up to 50% of the total mass of the composite particle [8].

Using a similar method to that described above, nickel atoms are deposited on the surface of poly[styrene/acrylic acid]-based particles after chemical reaction of NaH_2PO_2 solution on a nickel salt impregnated on the particle. However, in this case the final microspheres have ferromagnetic properties with non-nil remanence and coercive force [72].

D. Polymerization in the Presence of Magnetic Nanoparticles

The different systems of polymerization in dispersed media are used in the presence of magnetic material to produce composite latexes.

A frequently used process to prepare composite colloids is the encapsulation of a mineral pigment (magnetic or nonmagnetic) by emulsion polymerization process, since it permits obtaining spherical particles of uniform size [73]. Generally, seeded polymerization competes with secondary nucleation and the formation of new latex particles. Several emulsion polymerization methods are used to perform the encapsulation of inorganic seed particles.

1. The surface property of inorganic colloids can be modified using radical polymerization. In fact, they can be made hydrophobic (or more hydrophobic) by adsorption of a surfactant [74,75], by chemical modification [76], or by grafting of a coupling agent that has both an alkoxy group capable of reacting with the hydroxide functions of metal oxides and a part capable of

establishing chemical and physical interactions with the polymer (e.g., silanes, titanates, and compounds of the diacid family).

2. The colloidal stability of such small inorganic particles can be controlled before the polymerization process. Such particles can be sterically stabilized by adsorption of surfactants as commonly used in emulsion polymerization and latex stabilization. In addition, the colloidal stability of inorganic particles can be reinforced by ultrasound agitation [77,78].
3. The capture surface developed by these inorganic nanoparticles is very large and depends on the number and diameter of the particles. The minimal number of inorganic seed particles with a given diameter, avoiding any secondary nucleation, can be calculated using the model proposed by Hergeth et al. [79].

To promote encapsulation of a given seed particles, the concentration of surfactant must be lower than the critical micelle concentration (CMC) in order to prevent the formation of micelles and therefore polymerization sites not containing any pigment (i.e., leading to secondary nucleation particles). Likewise during classical emulsion polymerization, the solvent solubility (such as water solubility) of the monomer is preferably as low as possible, with the initiator being nonionic in order to prevent the formation of free polymer chains in continuous phase, such as water-soluble polymer when the encapsulation is performed in aqueous phase.

Concerning the choice of suitable initiator, Haga [80] showed that use of a charged initiator with a sign opposed to those borne by the seed particles increases the efficiency of the oligomer capture efficiency at the onset of the polymerization process. This can be principally applied when the colloidal stability of the seed particles is assured. However, the encapsulation of seed particles remains possible with an initiator with the same charge, since chemical affinity can override electrostatic repulsions.

Magnetic nanoparticles such as ferrite are often prepared in the aqueous phase and stabilized by one or more layers of interfacial surfactant (as illustrated in Fig. 8). In this case, the first layer is strongly adsorbed on the surface of the iron oxide particles while the second is much less so.

The stabilizing agent (dodecylbenzene sodium sulfonate), adsorbed on the surface allow the iron oxide nanoparticles to remain colloidally stable in water (or in appropriate medium). The surface of the ferrites coated by a double layer of surfactants is anionic and the emulsion polymerization of styrene is initiated by an anionic initiator such as potassium persulfate (KPS). This is in contradiction to the results of Haga et al. [80], which show that polymerization is promoted when the oligomers formed and the seed inorganic particles have charges of opposing signs.

However, Yanase et al. [17] studied the influence of several parameters on the encapsulation of iron oxide nanoparticles: the ferrite/styrene weight ratio,

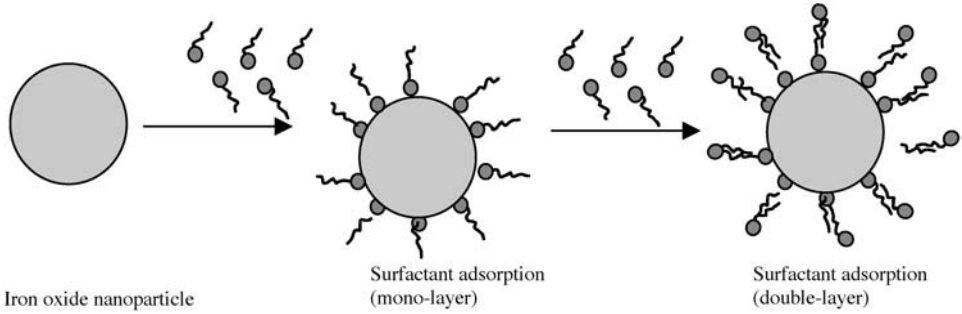

FIG. 8 Stabilization of magnetic nanoparticles (such as iron oxide) by a monolayer and a double layer of charged surfactants.

the KPS initiator concentration and amount of monomer, the salt concentration ($CaCl_2$), and the presence of surfactant. The latter is adsorbed onto ferrites nanoparticles and the excess can be eliminated by classical dialysis process.

A mass ratio (ferrite/styrene) of 0.44 is close to the theoretical values corresponding to the complete encapsulation of the seed nanoparticles by the formed polymer. According to the explored recipe, the diameter of the final particles containing from 12% to 14% in weight of ferrite ranges from 50 to 150 nm. From 60% to 80% of the polymer formed is located around the particles, and the coagulum only represents a few percentage points. However, to obtain particles with a diameter of about 1 μm, the ionic strength is increased and the surfactant is eliminated. The particles are less stable and the polymer is essentially formed of coagulum [74]. Anyway, this encapsulation method will be a very interesting and promising process for preparing small functionalized magnetic core-shell particles with a magnetic core and a polymer in the shell.

By using an inverted emulsion process, Huang et al. [81] obtained hydrophilic composite particles larger than 1 μm in diameter after several stages of synthesis. In the beginning, the seed ferrite particles, the principal monomer (acrylamide), and the cross-linker (*N*-methylenebisacrylamide, MBA) agent are contained in the aqueous phase (Fig. 9).

The water/oil emulsion is then formed by mixing the aqueous phase with the organic phase, o-xylene (Figure 8) in the presence of a polyethylene oxide–polypropylene oxide surfactant. The magnetic particles are encapsulated by reverse emulsion polymerization of acrylamide with an initiator soluble either in the water phase (i.e., KPS) or in the continuous phase (diazo initiators with nitrile functions).

The hydrophilic magnetic latex can be used as a seed composite latex to obtain a core-shell latex by direct emulsion polymerization of styrene, methyl methacrylate, or vinyl acetate initiated by an ionic initiator such as KPS. The

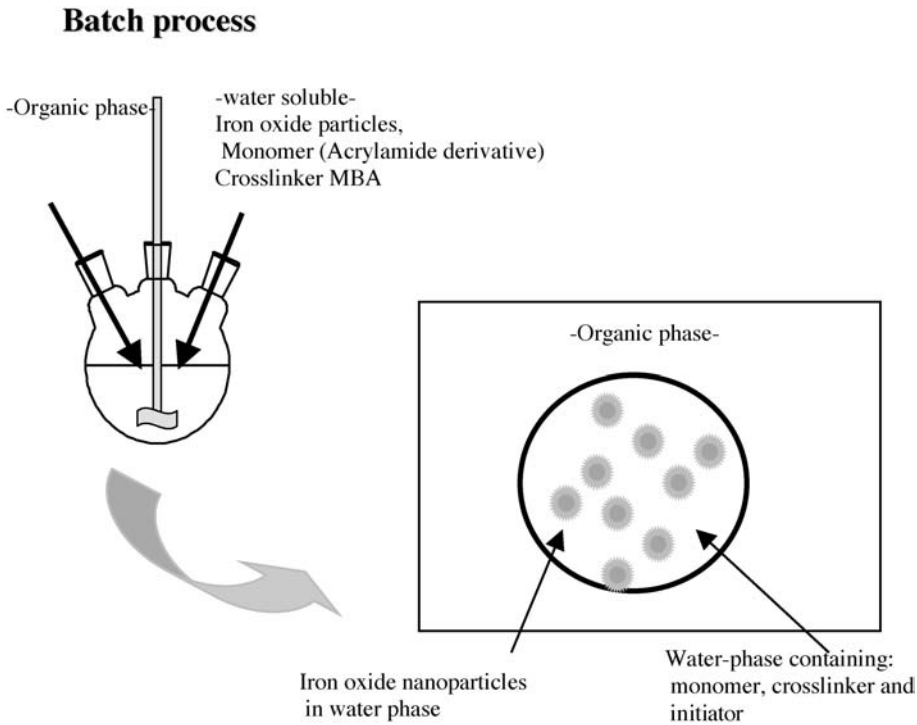

FIG. 9 Emulsion preparation, water-in-oil.

amount of monomer introduced semicontinuously during the polymerization process is limited to form polymer particles without inorganic cores (i.e., starving conditions). The final particles are polydispersed and have a diameter ranging from 1 to 3 μm and contain 13–23 wt % of ferromagnetic material [81].

Hofman-Caris [9] have also described surfactant-free emulsion polymerization process of methyl methacrylate, with an anionic or cationic initiator to form composite particles bearing magnetic material in the core, especially iron oxides. They have highlighted the influence of the nature of the charges of the initiator and the inorganic particles on the percentage and the molar mass of the polymer chains formed.

The polymerization of paraethylphenol in a water/oil microemulsion is catalyzed by an enzyme in the presence of oxygenated water and occurs on the surface of ferrite particles in reverse micelles. The composite particles obtained have a diameter in the region of 0.7 μm with superparamagnetic behavior at

ambient temperature. They contain only 5% in weight of ferrites, distributed evenly in the particle [5].

Encapsulation of particles over 1 μm is more difficult due to the lower surface capture. Other processes have been considered such as suspension [82] and dispersion [83] polymerization, which lead to particles with very large diameters.

1. Suspension Polymerization

The principle of suspension polymerization in the presence of ferrofluid patented by Rhône-Poulenc [84] is as follows:

The magnetic particles dispersed in the organic phase (containing styrene and non-water-soluble initiator) are then mixed with an aqueous solution of surfactant to form magnetic emulsion or magnetic droplets. The size of the final particles ranges from 0.03 to 5 μm and they contain less than 65% in mass of polymer [84]. Suspension polymerization under these conditions results in magnetic latexes with a broad size distribution (i.e., the standard deviation being in the region of 60%).

For certain biomedical applications the standard deviation must be reduced to 3–5% in order to have homogeneous dispersion. Regarding synthesis, the range of particle size distribution depends on the surfactant concentration, which drastically influences the size of the monomer droplets [85]. However, this parameter does not permit sufficient reduction of the size distribution range. To achieve this, the obtained polydispersed magnetic polymer particles are fractionated by using a depletion method. The polydispersed magnetic latex microspheres are first dispersed in aqueous phase; then the surfactant is added until the two phases appear (phases separation). The liquid phase contains the free particles, whereas the more associated particles are found in the solid phase. After separation of the two phases, the operation is repeated on the solid phase until the desired size distribution range is obtained. Using such repetitive fractionation process, a large quantity of particles is lost.

Suspension polymerization of styrene and divinylbenzene has also been investigated in the presence of magnetic powder to synthesize magnetic composite latex particles with large diameters, in the region 100–300 μm. The magnetic particles have a diameter of 20 μm and their powder is dispersed in the organic phase as a result of an ultrasound technique. The mixture is then dispersed in water phase and polymerization, initiated by a peroxide, takes place at a temperature of 80°C. After polymerization, the particles are functionalized by photooxidation using UV radiation. The degradation of the polystyrene shell leads to the appearance of vinyl acetone functions. The presence of carbonyl (C=O) groups, highlighted by infrared spectroscopy, then permits covalent coupling of biomolecules such as enzyme [86]. The amount of iron oxides incorporated in the polymer matrix is very low, representing only 1.25% of the monomer mass with a high polydispersity index.

The acrylamide-based magnetic microspheres are obtained either by crushing of an acrylamide-based magnetic gel at −10°C or by suspension polymerization in carbon tetrachloride in the presence of a surfactant such as Tween 20. The acrylamide-based gel is formed by mass polymerization of a mixture of acrylamide, MBA, and *N*-acryloxysuccinimide (NAS), initiated by the ferrite in the presence of KPS at 0°C. During suspension polymerization, monomer, crosslinker, and initiator (acrylamide, MBA, KPS) are present in the aqueous phase and NAS is solubilized in dimethylsulfoxide solution. Polymerization is initiated by oxide reduction reaction by adding iron oxide particles in the presence of KPS initiator. The magnetic latex particles obtained are then washed by centrifuging to eliminate the solvent and the supernatant containing residual reactants.

The magnetic microspheres obtained by such polymerization in a heterogeneous medium are smaller and more regularly shaped than those produced by crushing. The small ferrite nanoparticles are not released after polymerization, as their diameter is larger than the pores of the acrylamide gel network. However, the amount of ferrite does not appear to be very high. To offset the low content of magnetic material in the microgel particles, separation is carried out by applying a magnetic field in a magnetic column. This system permits intensification of the gradient of the magnetic field inside the column tube (containing macroscopic metal particles) and retains the magnetic gel particles during elution (Fig. 10).

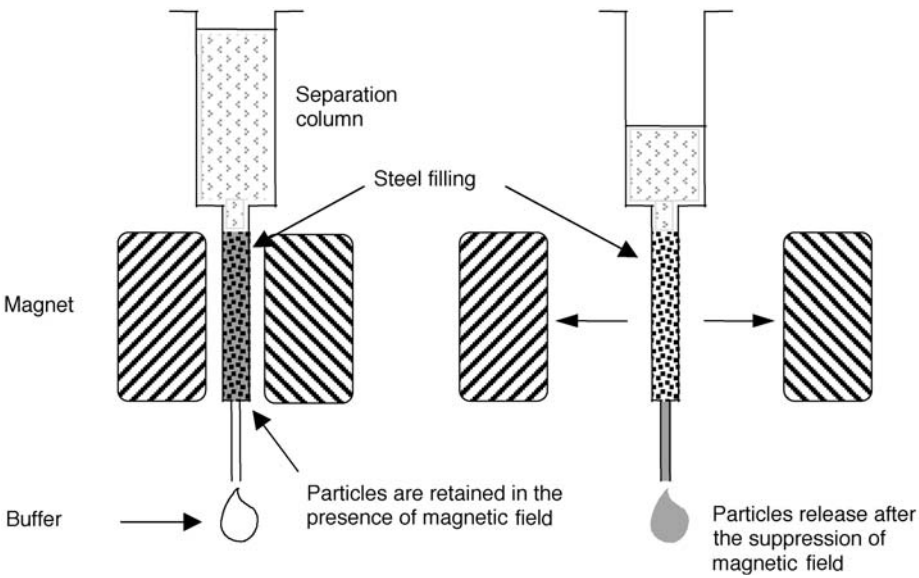

FIG. 10 Magnetic separation using column tube and gradient of the magnetic field.

2. Dispersion Polymerization

Superparamagnetic particles of polystyrene containing 12% of ferrites in volume and with a diameter of 1 μm have been elaborated by dispersion polymerization [87]. The ferrite nanoparticles are obtained in the styrene and dispersed in styrene-alcohol solution containing a surfactant and the initiator. Pigment encapsulation is very high and only a small amount of microspheres amount is formed without ferrite. Encapsulation by a styrene- and hydroxyethyl methacrylate (HEMA)–based copolymer by dispersion polymerization is carried out after modification of the surface of the iron oxide particles [83].

Polyethylene glycol (PEG) chains are first adsorbed on the surface of the ferrite nanoparticles of 0.3–0.4 μm under ultrasound dispersion conditions. The presence of PEG improves the affinity between the ferrites and the monomers. Dispersion polymerization is therefore initiated (using KPS) on the surface of the metal oxides. The final particles have a diameter in the region of 50–60 μm and have hydroxyl functions on the surface capable of fixing the enzyme via chemical reaction [83].

3. Synthesis of Thermally Sensitive Particles

In the case of thermally sensitive particles, a variation of temperature is accompanied by a modification of the particle's colloidal properties. This phenomenon is largely described in various papers [88,89]. The first reported thermally sensitive magnetic particles are used for antibody purification and are obtained by a two-stage process [75].

The first stage is the emulsion polymerization of styrene initiated by KPS in the presence of magnetite particles. During the second stage, the hydrophilic layer is obtained by polymerization of a mixture of *N*-isopropylacrylamide (NIPAM), methacrylic acid, and KPS. The synthesis of hydrophilic, magnetic particles has been studied as a function of the ferrites to total monomers ratio introduced in the polymerization process.

The size of the final particles is affected by the content of magnetite in the medium. The particles are polydispersed, have a diameter ranging from 150 to 300 nm, and contain more than 20% ferrite amount. Consequently, the magnetic separation of the isolated microspheres takes a long time, more than 1 h when using classical magnet. However, this separation time can be reduced by flocculation of the particles. By increasing the ionic strength and the temperature of the medium above the volume phase transition temperature of the thermally sensitive polymer (40°C), the particles lose their electrostatic and steric stability and form aggregates.

Using an original process, Mizutani et al. [90] have synthesized thermally sensitive acrylamide- and NIPAM-based gels in the presence of a ferrofluid and an enzyme. The gel containing the ferrites is heated from the interior to the exterior by application of an alternating magnetic field at a frequency of 2 kHz.

Heating from the interior avoids the formation of a dehydrated layer on the exterior of the gel, which forms when using an external heating method and prevents the enzymatic reaction of sucrose degradation from occurring.

4. Other Polymerization Processes

The use of other polymerization methods makes it possible to vary the nature and the properties of composite particles. Some examples are mentioned in the following paragraphs.

A relatively old polymerization method with ferrite particles is the polymerization of methacrylate derivatives initiated by γ irradiation of cobalt [91] or by an oxidoreduction reaction in the presence of FeS_2O_8 [92]. The final diameter remains smaller than 50 nm, and the ferrite suspension keeps its initial magnetic properties and can be considered as a ferrofluid (i.e., magnetic fluid).

Polymerization of a mixture of a HEMA, *N*,*N*-methylenebisacrylamide, and methacrylic acid is initiated on the surface of nanoparticles of iron oxides by using their oxidizing properties in the presence of KPS. The thinness of the polymer layer explains the high proportion of magnetic material, which composes nearly the whole of the final composite particle. Nonetheless, after grafting of a functionalized spacer arm, these particles permit the rapid separation of target cells, with sensitivity reaching nearly 100% [92].

The surface modification of inorganic pigments determines the chemistry of the encapsulation polymerization process to be used. Surfactants are often used, but this is not the only approach. For example, in the case of a ferrofluid obtained in organic methanol phases, the ferrite particles are covered by a derivative of trimethoxysilane fixed via adsorption or chemical grafting. Polymerization of silane by condensation in an organic medium leads to core-shell formation with a magnetic core and a polysilane shell.

By dehydrating the hydroxyl (OH) groups on the surface of the ferrites, the polysilanes make covalent binding with the mineral particles. In fact, silanization is induced by increasing the temperature to 90°C in acid medium containing an appropriate surfactant. The presence of glycerol in the medium permits, on the one hand, preventing the aggregation of particles and, on the other hand, evaporating the excess water, silane, and organic solvent after polymerization, by increasing the temperature to 160°C. The final particles have a diameter ranging from 0.1 to 1.5 μm and are redispersed by mechanical agitation in water. The microsphere magnetic particles obtained have been explored in vitro and in vivo [93].

The surface of the magnetic particles can also be modified by another mineral compound. Before polymerization, the inorganic pigments are covered by silica particles. Polymerization of pyrrole is then initiated by an oxidizing mixture of $H_2O_2/Fe^{3+}/HCl$ or $H_2O_2/(NH_4)_2S_2O_8/HCl$ on the surface of the silica. The final particles contain from 10% to 17% of magnetite in volume. However, accord-

ing to the oxidizing solution used, the particles tend to flocculate (when H_2O_2/Fe^{3+}/HCl solution is used) or be widely dispersed [when H_2O_2/$(NH_4)_2S_2O_8$ is used] [3].

Furthermore, the biodegradable and magnetic particles are obtained by different methods of polymerization in a heterogeneous medium. Anionic polymerization of isobutylcyanoacrylate takes place in the presence of ferrite particles and the active reactants to be transported. With 28% of ferrite in volume, the final particles with a diameter of 0.22 μm increase the concentration of particles in the left kidney of the mouse (near a magnet) by a factor of 3 in comparison with the right kidney [94].

Finally, polymerization at the ferrofluid–monomer phase interface gives rise to the formation of capsules by gelification or by interfacial precipitation "coarcervation" [95]. The encapsulation of magnetic liquid droplets prepared in the organic phase is described by Neveu-Prin et al. [96]. The first stage consists of forming an emulsion of magnetic liquid in water with a dispersing agent such as a maleic anhydride–based copolymer. The polymer on the interface is precipitated by acidifying the medium and then cross-linked at 90°C. It then forms a rigid capsule around the ferrofluid that keeps its magnetic properties and can be used as a polymer particle.

5. Synthesis of Multilayer Composite Particles

This section describes two processes permitting the production of composite particles with a multilayer structure. They are composed of an organic core, a magnetic envelope (around the core) formed by iron oxide nanoparticles, and, possibly, a final polymer shell.

The first method consists in irreversible fixation of small composite particles onto polystyrene seed particles. Emulsion polymerization of styrene is performed at low temperature in the presence of ferrites and polystyrene particles simultaneously using potassium metabisulfite (as an initiator) and surfactant. The presence of surfactant micelles (i.e., sodium oleate) leads to the formation of new polymer particles during the seeded polymerization [1].

The final microspheres, of approximately 4 μm particle size, have a rough surface and a low ferrite content. The amount of iron oxides must be limited in order to reduce the aggregation of seed particles. Favorable polymerization conditions require that the ratio of ferrite to polymer material (seed + monomers) is 1:12; this limits the final content of magnetic material.

The second method of synthesizing multilayer composite particles was developed by Furusawa et al. [97] and is illustrated in Fig. 11.

The cationic metal oxide particles ($NiO.ZnO.Fe_2O_3$ powder), 20 nm in diameter, are adsorbed on the surface of the negative polystyrene microspheres (sulfate and carboxylic). Electrostatic interactions permit the formation of complexes or heterocoagulates between the two types of particles with opposing

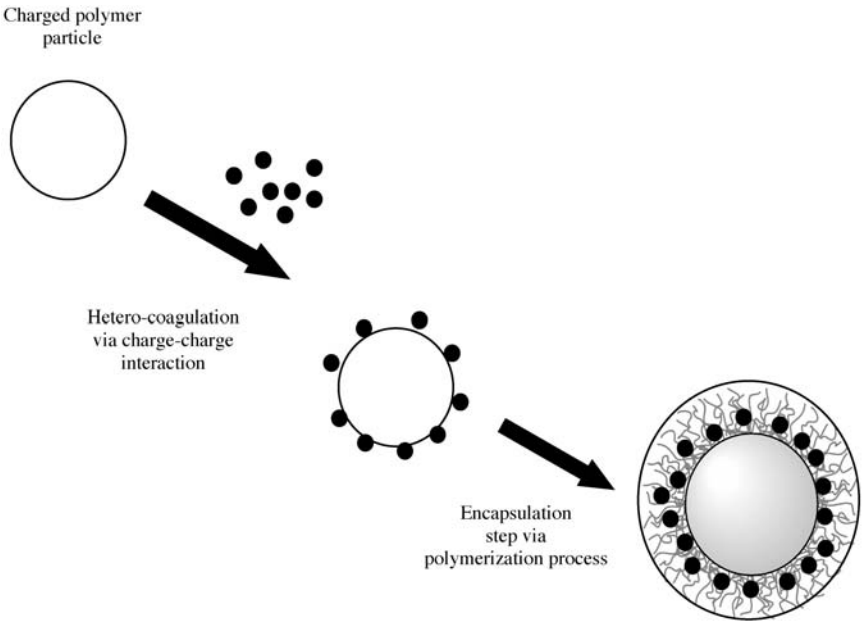

FIG. 11 Different steps of synthesis according to the Ref. 97.

charges. These electrostatic interactions are influenced by the medium's ionic strength, solvent nature, and pH. Above pH 9, the metal oxides have the same charge as the latex and the amount adsorbed of inorganic nanoparticles onto polymer particle surfaces is low according to repulsive electrostatic interactions. The amount of magnetic material adsorbed can represent up to 40% in volume of all the polymer and mineral particles and therefore corresponds to the ferrite multilayers.

In order to prevent releasing of the metal oxides and the contact with the biomolecules, the heterocoagulates (polymer particles coated with inorganic nanoparticles) are coated with a fine layer of polymer (Fig. 11). Seeded polymerization is studied as a function of the concentration of styrene in relation to the amount of seed particles, as well as the nature and concentration of surfactant and initiator.

The presence of charged surfactant (i.e., sodium oleate) appears vital in obtaining coagulum-free composite particles. However, its concentration must be limited to avoid the desorption of the magnetic particles (from the polystyrene latex surface) and the formation of particles without iron oxide [97]. Under

these conditions, the formation of new particles or the flocculation of seed particles is reduced by the presence of an anionic initiator (KPS) rather than a cationic initiator.

This method permits fixing the final diameter of the composites by the choice of seed particles size. However, neither the size distribution nor the content of metal oxides of the final composite particles is reported.

According to the original work reported by Furusawa et al. [97], a new approach has recently been reported by Sauzedde et al. [98,99] by performing the preparation of hydrophilic thermally sensitive magnetic latexes using the heterocoagulation concept as illustrated in Fig. 12. Magnetic latex particles were obtained using the following three-step strategy: (1) seed particles and ferrofluid syntheses; (2) ferrofluid adsorption onto seed latex particles; and (3) encapsulation of iron oxide nanoparticle–seed particle heterocoagulates.

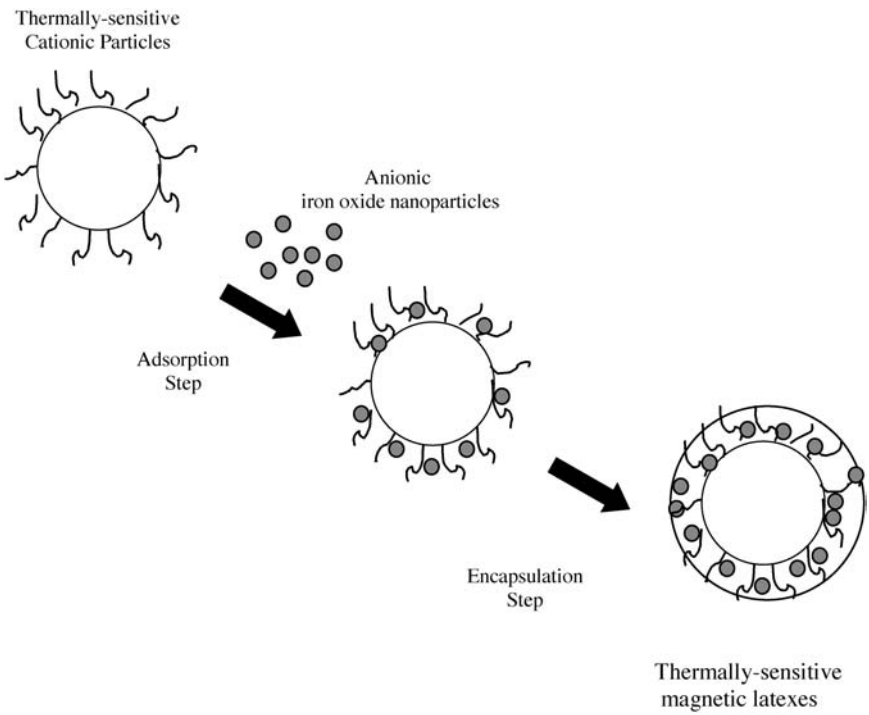

FIG. 12 Schematic illustration of hydrophilic thermally sensitive magnetic latex particles.

Three cationic latexes bearing amine and amidine groups under cationic form were used as seed particles for the immobilization of ferrofluid nanoparticles: polystyrene [100,101], poly(*N*-isopropylacrylamide) [102], and core-shell poly(-styrene/*N*-isopropylacrylamide) [103,104].

These various latexes were synthesized by emulsifier-free emulsion polymerization using 2,2′-azobis(2-amidinopropane) dihydrochloride as initiator, whereas negatively charged iron oxide were obtained by sodium hydroxide–induced precipitation of ferric and ferrous chloride.

The preparation of such magnetic latex particles was performed by immobilization of ultrafine metal oxide nanoparticles (anionic ferrofluid) on latex particles bearing positively charged groups. After the adsorption step, the encapsulation was carried out in the presence of NIPAM, methylenebisacrylamide, and in some cases itaconic acid in order to impart carboxylic groups at the particle surface. The final hydrophilic magnetic latexes (Fig. 13) were characterized with regard to particle-size thermal-sensitivity, electrokinetic behavior, ferric oxide content, and magnetic properties. The prepared hydrophilic thermally sensitive magnetic particles were found monodisperse and bearing carboxylic groups, available for the covalent binding of biomolecules. Finally, the magnetic particles obtained were evaluated and used for covalent immobilization of anti-

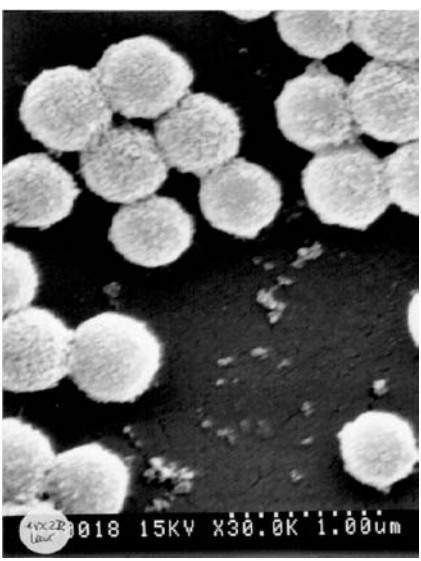

FIG. 13 SEM image of the core-shell magnetic latex particles.

bodies and the resulting conjugates were tested as solid phases in immunoassay to evaluate their application potentiality in biomedical diagnosis [105].

IV. CONCLUSION AND DISCUSSION

Composite microspheres can be obtained by numerous processes but each method has its own limits, in particular the content in inorganic nanoparticles and the polydispersity index of particle size distribution. The properties (diameter and ferrite content) of the magnetic particle support differ according to the targeted biomedical application.

On the biological level, microspheres larger than 10 μm have numerous interaction sites and tend to be unfavorable to the specific recognition of biomolecules. Regarding their physical properties, in spite of a frequently low content of magnetic material, separation can be rapid due to large particle diameters. The large particle size can also induce sedimentation phenomena, leading to a redispersion problem.

On the contrary, various biomedical applications are well adapted and explored in the case of particles with a diameter smaller than 1 μm. However, due to their small size, such particles must contain a large percentage of ferrites to make fast separation possible. In addition, low particle size offers a high specific surface compared to the large particle size.

First, regarding the production of magnetic composites from polymers and ferrites obtained separately, it appears that particles obtained by impregnation generally have a diameter larger than 10 μm with low polydispersity index. Moreover, grafting of polymer chains to the surface of inorganic pigments can constitute a preparation stage in terms of later polymerization of a larger amount of polymer facilitating the production of superparamagnetic particles larger than 100 nm.

The approach consisting of precipitating iron oxides on the surface of isodispersed and porous polymer particles satisfies a large number of criteria, but it remains limited to the use of particles with a diameter larger than 1 μm to allow the formation of pores. Initially hydrophobic microspheres can be made to be more hydrophilic by carrying out an additional functionalization step. According to the chemical process used, the deposition of metal salts can lead to the particle's degradation, but it permits the transport of metals that are nonmagnetic though biocompatible.

Finally, the interactions between inorganic particles and oligomers during their growing step (i.e., formation) are a dramatic problem during polymerization in the presence of a pigment. However, by using an adjusted concentration of surfactant, polymer chain formation can proceed on the surface of inorganic particles without the formation of a second population (secondary nucleation).

The prior modification of the surface of the inorganic pigments also favors interactions during polymerization [106] leading to a good encapsulation process. Nevertheless, it is often difficult to control the size distribution and the quantity of magnetic material encapsulated. Consequently, the separation of magnetic particles by a magnetic field is not homogeneous.

The presence of a polymer core (seeded polymerization) thus appears to be another alternative that permits the fixing of particle diameter and the obtaining of narrow and homogeneous distribution. In the case of multilayer composites, encapsulation of iron oxide particles by a polymer layer permits keeping the magnetic material inside the polymer particles. However, the presence of a polymer core can restrict the final content of ferrites. The use of a porous or hydrogel-based particle is a possible way of avoiding this disadvantage.

Despite the many strategies considered, none has completely satisfied the requirements of biomedical applications. This demonstrates the difficulty of obtaining monosized, functionalized magnetic particles of a given size. However, on the strength of results reported by certain authors, the formulation of composite particles by a multistep process using synthesized polymer seed particles and ferrite particles depends on the following points:

The presence of a magnetic material in the form of nanoparticles of about 10 nm must render the final particles superparamagnetic.

The surface of the ferrite particles must be compatible with the formation of polymer with regard to electrostatic charges and chemical affinity.

The purpose of seed particles is to determine the magnitude of the sizes of the final particles and obtain a homogeneous distribution of magnetic material in the final particle.

In addition, the narrow size distribution of seed microsphere particles can be conserved if the formation of a new population, coalescence, and coagulation of particles are prevented during polymerization.

Nowadays the problem is the elaboration of magnetic latex particles with low particle size (<300 nm), narrow size distribution (i.e., monodisperse), high iron oxide content (above 50% w/w), negligible sedimentation, no iron oxide releases from the particles, and bearing reactive groups for covalent immobilization of biomolecules.

REFERENCES

1. Lee, J.; Senna, M. Colloid Polym. Sci. **1995**, *273*, 76.
2. Jarjayes, O.; Fries, P.H.; Bidan, G. Synthet. Metal. **1995**, *69*, 343.
3. Butterworth, M.D.; Bell, S.A.; Armes, S.P.; Simpson, A.Q. J. Colloid Interface Sci. **1996**, *183*, 91.
4. Sohn, B.H.; Cohen, R.E. Chem. Mater. **1997**, *9*, 264.

5. Kommaredi, N.S.; Tata, M.; Vijay, T.J.; McPherson, G.L.; Herman, M.F. Chem. Mater. **1996**, *8*, 801.
6. Neveu-Prin, S. P. thesis, Pierre and Marie Curie University, **1992**.
7. Kwon, O.; Solc, J. J, Magnet. Magnet. Mater, **1986**, *54–57*, 1699.
8. Tamai, H.; Sakura, H.; Hirota, Y.; Nishiyama F.; Yasuda, H. J. Appl. Polym. Sci. **1995**, *56*, 441.
9. Hofman-Caris, C.H.M. New J. Chem. **1994**, *18*, 1087.
10. Haukanes, B. I.; Kvam, C. Biotechnology **1993**, *11* (Jan), 60.
11. Joubert, J.-C. Anales De Quimica **1997**, *93*, S70–S76.
12. Giaever, I. US Patent 3,970,518, 1976.
13. Widder, K.J.; Senyei, A.E.; Scarpelli, D.G. Proc. Soc. Exp. Biol. Med. **1978**, *58*, 141.
14. Plastoucas, C.D.; El-Aasser, M.S.; Fitch, R.M. *Future Directions in Polymer Colloids*; Martinus Nijhoff: Dordrecht, **1987**, 321.
15. Mosbach, K.; Schröder, U. FEBS Lett. **1979**, *102* (1), 112.
16. Schütt, W.; Grüttner, C.; Häfeli, U.; Zborowski, M.; Teller, J.; Putzar, H.; Schümichen, C. Hybridoma **1997**, *16* (1), 109.
17. Noguchi, H.; Yanase, N.; Uchida, Y.; Suzuta, T. J. Appl. Polym. Sci. **1993**, *48*, 1539.
18. Khalafalla, S.E. Chemtech **1975**, 540.
19. Bacri, J.C.; Perzynski, R.; Salin, D. La Recherche **1987**, *192*. 1150.
20. Elmore, W.C. Phys. Rev. **1938**, *54*, 308.
21. Häfeli, U.; Schütt, W.; Teller, J.; Zborowski, M. Plenum, New York, **1997** .
22. Roath, S. J. Magn. Magn. Mater. **1993**, *122*, 329.
23. Molday, R.S.; Molday, L.L. FEBS Lett. **1984**, *170*(2), 232.
24. Koneracka, M.; Kopcansky, P.; Mehta, R.V. J. Magnet. Magnet. Mater. **1999**, *201*, 427.
25. Hancock, R.D. Analyst **1997**, *122*, 51R.
26. Guerra, J.M.; Srinivasarao, M.; Stein, R. Science **1993**, *262*, 1395.
27. Miltenyi, S.; Müller, W.; Weichel, W.; Radbruch, A. Cytometry **1990**, *11*, 231.
28. Molday, R.S.; Mackenzie, D. J. Immunol. Meth. **1982**, *52*, 353.
29. Papell, S. Low Viscosity Magnetic Fluid Obtained by the Colloidal Suspension of Magnetic Particles, US Patent 3,215,572, 1965.
30. Rosenweig, R.E. Ferrofluid Compositions and Process of Making Same, US Patent 3,917,538, 1975.
31. Pant, R.P.; Rao, N.N.; Mehta, R.V.; Suri, D.K. Indian J. Eng. Mater. Sci. **1998**, *5*, 485.
32. Khalafalla, S.E.; Reimers, G.W. Procede De Preparation De Liquide Magnetique, 73,272,90, 1973.
33. Khalafalla, S.E.; Reimers, G.W. IEEE Trans. Magnet. **1980**, *16* (2), 178.
34. Shimoiizaka, J.; Nakatsuka, K.; Chubachi R.; Sato, Y. **1976** .
35. Shinkai, M.; Honda, H.; Kobayashi, T. Biocatalysis **1991**, *5*, 61.
36. Pillai, V.; Kumar, P.; Multani, M.S.; Shah, D.O. Colloid Surf. A Physicochem. Eng. Asp. **1993**, *80*. 69.
37. Pascal, C.; Pascal, J.L.; Favier, F. Chem. Mater. **1999**, *11*, 141.

38. Nakatani, I.; Furubayashi, T.; Takahashi, T.; Hanaoka, H. J. Magnet. Magnet. Mater. **1987**, *65*, 261.
39. Massart, R. C. R. Acad. **1980**, *291* (1) series C, 1.
40. Massart, R.; Cabuil, V. J. Chim. Phys. **1987**, *84* (7–8), 967.
41. Jolivet, J.P.; Massart, R.; Fruchart, J.M. Nv. J. Chimie **1983**, 7 (5), 325.
42. Bacri, J.C.; Perzynski, R.; Salin, D.; Cabuil, V.; Massart, R. J. Magnet. Magnet. Mater. **1990**, *85*, 27.
43. Rocchiccioli-Deltcheff, C.; Franck, R.; Cabuil V.; Massart, R. J. Chem. Res. S **1987**, 126.
44. Choy, J.-H.; Han, Y.-S.; Song, S.-W. Mater. Lett. **1994**, *19*, 257.
45. Jacobo, S.E.; Domingo-Pascual, C.; Blesa, M.A. J. Mater. Sci. **1997**, *32*, 1025.
46. Weisenhorn, A.L.; Egger, M.; Ohnesorge, F.; Gould, S.A.C.; Heyn, S.P.; Hansma, H.G.; Sinsheimer, R.L.; Gaub, H.E.; Hansma, P.K. Langmuir **1991**, *7*, 8.
47. Jordan, B. M/S **1990**, *10*, 1007.
48. Allen, M.J.; Hud, N.V.; Balloch, M.; Tench, R.; Siekhaus, W.J.; Balhorn, R. Ultramicroscopy **1992**, *42/44*, 1095.
49. Tourinho, F.A.; Franck, R.; Massart R.; Perzynski, R. Progr. Colloid Polym. Sci. **1989**, *79*, 128.
50. Zins, D.; Cabuil, V.; Massart, R. J. Molec. Liq. **1999**, *83*, 317.
51. Massart, R.; Dubois, E.; Cabuil, V.; Hasmonay, E. J. Magnet. Magnet. Mater. **1995**, *149*, 1.
52. Lea, T.; Vartdal, F.; Nustad, K.; Funderud, S.; Berge, A.; Ellingsen, T.; Schmid, R.; Stenstad, P.; Ugelstad, J. J. Molec. Recog. **1988**, *1* (1), 9.
53. Guesdon, J.L.; Avraemas, S. IMM **1977**, *14*, 443.
54. Widder, K.; Flouret, G.; Senyei, A. J. Pharm. Sci. **1979**, *68* (1), 79.
55. Senyei, A.; Widder, K.; Czerlinski, G. J. Appl. Phys. **1978**, *49* (6), 3578.
56. Müller-Schulte, D.; Füss, F.; De Cuyper, M.; Häfeli, U.; Schütt, W.; Teller, J.; Zborowski, M. *Scientific and Applications of Magnetic Carriers*; Plenum: New York, 1997; 93.
57. Kandzia, J.; Scholz, W.; Anderson, M.J.D.; Müller-Ruchholtz, W. J. Immunol. Meth. **1984**, *75*, 31.
58. Hertzog, B.; Mottl, T.; Yim D.; Mathiowitz, E.; In *Scientific and Clinical Applications of Magnetic Carriers*; Plenum: New York, **1997**, 77.
59. Mosbach, K.; Anderson, L. Nature **1977**, *270*, 259.
60. Nakamae, K.; Tanigawa, S.; Tsujiguchi, T.; Okamoto, S.; Yamaguchi, K. Colloid Surf. A **1993**, *80*, 85.
61. Shimomura, M.; Kikuchi, H.; Yamaguchi, T.; Miyauchi, S. Pure Appl. Chem. **1996**, *A33* (11), 1687.
62. Ugelstad, J.; Ellingsen, T.; Berge, A.; Helgee, B. European Patent 0 106,873, 1986.
63. Ugelstad, J.; Berge, A.; Ellingsen, T.; Schmid, R.; Nilsen, T.-N.; Mork, P.C.; Stenstad, P.; Hornes, E.; Olsvik, O. Prog. Polym. Sci. **1982**, *17*, 87.
64. Ugelstad, J.; Mork, P.C.; Schmid, R.; Ellingsen, T.; Berge, A. Polym. Int. **1993**, *30*, 157.
65. Ugelstad, J.; Mork, P.C.; Kaggerud, K.H.; Ellingsen, T.; Berge, A. Adv. Colloid Interface Sci. **1980**, *13*, 101.

66. Gould, S.A.C.; Drake, B.; Prater, C.B.; Weisenhorn, A.L.; Manne, S.; Kelderman, G.L.; Butt, H.J.; Hansma, P.K.; Magonov, S.; Cantow, H.J. Ultramicroscopy **1990**, *33*, 93.
67. Ugelstad, J.; Olsvik, O.; Schmid, R.; Berge, A.; Funderud S.; Nustad, K.; Ngo, T. 1st Ed.; Plenum: New York, **1993**, 229.
68. Ugelstad, J.; Kilaas, L.; Aune, O.; Bjorgum, J.; Herje, R.; Schmid, R.; Stenstad, P.; Berge, A.; Uhlén, M.; Hornes, E.; Olsvik, O. *Advances in Biomagnetic Separation*; Eaton: Stockholm, **1993;** 1.
69. Winnik, F.M.; Morneau, A.; Ziolo, R.F.; Stöver, H.D.H.; Li, W.-H. Langmuir **1995**, *11*, 3660.
70. Kawaguchi, H.; Fujimoto, K.; Nakazawa, Y.; Sakagawa, M.; Ariyoshi, Y.; Shidara, M.; Okazaki H.; Ebisawa, Y. Colloids Surf. A **1996**, *109*, 147.
71. Charmot, D. Prog. Colloid Polym. Sci. **1989**, *76*, 94.
72. Wang, Y.; Feng, L. J. Appl. Polym. Sci. **1997**, *64*, 1843.
73. Richrdson, J.; Hawkins, P.; Luxton, R. **2001**, *16*, 989.
74. Yanase, N.; Noguchi, H.; Asakura, H.; Suzuta, T. J. Appl. Polym. Sci. **1993**, *50*, 765.
75. Kondo, A.; Kamura, H.; Higashitani, K. Appl. Microbiol. Biotechnol. **1994**, *41*, 99.
76. Bourgeat-Lami, E.; Espiard, P.; Guyot, A. Polymer **1995**, *36*, (23), 4385.
77. Caris, C.H.M.; van Elven, L.P.M.; van Herk A.; German, A.L. Br. Polym. J. **1989**, *21*, 133.
78. Templeton-Knight, R. Chem. Ind. **1990**, (August), 512.
79. Hergeth, W.-D.; Starre, P.; Schmutzler, K.; Wartewig, S. Polymer **1988**, *29*, 1323.
80. Haga, Y.; Watanabe, T.; Yosomiya, R. Angew. Makromol. Chem. **1991**, *189*, 23.
81. Huang, T.-C.C. Dissert. Abstr. Int. **1986**, *48* (4), 1127.
82. Tokuoka, K.; Senna, M.; Kuno, H. J. Mater. Sci. **1986**, *21*, 493.
83. Li, X.; Sun, Z. J. Appl. Polym. Sci. **1995**, *58*, 1991.
84. Daniel, J.-C.; Schuppiser, J.L.; Tricot, M. US Patent 4,358,388, 1981.
85. Bibette, J.; Charmot, D.; Schorsch, G. US Patent 5,242,964, 1991.
86. Iman, M.; Celebi, S.S.; Ozdzural, R. React. Polym. **1992**, *17*, 325.
87. Richard, J.; Vaslin, S. French Patent FR 9,507,485, 1995.
88. Pelton, R.H.; Pelton, H.M.; Morphoresis, A.; Rowell, R.L. Langmuir **1989**, *5*, 816.
89. Nabzar, L.; Duracher, D.; Elaissari, A.; Chauveteau, G.; Pichot, C. Langmuir **1998**, *14*, 5062.
90. Takahashi, F.; Sakai, Y.; Mizutani, Y. J. Ferment. Bioeng. **1997**, *83* (2), 152.
91. Molday, R.S.; Yen, S.P.S.; Rembaum, A. Nature **1977**, *268*, 437.
92. Kronick, P.L.; G.L.; Kenneth, J. Science **1978**, *200*, 1074.
93. Chagnon, M.S.; Groman, E.V.; Josephon, L.; Whitehood, R.A. European Patent 0,125,995, 1984.
94. Ibrahim, A.; Couvreur, P.; Roland, M.; Speiser, P. J. Pharm. Pharmacol. **1982**, *35*, 59.
95. Lévy, M.-C.; Poncelet, D. Biofutur **1994**, *132*, 15.
96. Neveu-Prin, S.; Cabuil, V.; Massart, R.; Escaffre, P.; Dussaud, J. J. Magnet. Magnet. Mater. **1993**, *122*, 42.

97. Furusawa, K.; Nagashima, K.; Anzai, C. Colloid Polym. Sci. **1994**, *272*, 1104.
98. Sauzedde, F.; Elaïssari, A.; Pichot, C. Colloid Polym. Sci. **1999**, *277*, 1041.
99. Sauzedde, F.; Elaïssari, A.; Pichot, C. Colloid Polym. Sci. **1999**, *277*, 846.
100. Sauzedde, F.; Ganachaud, F.; Elaïssari, A.; Pichot, C. J. Appl. Polym. Sci. **1997**, *65*, 2331.
101. Ganachaud, F.; Sauzedde, F.; Elaïssari, A.; Pichot, C. J. Appl. Polym. Sci. **1997**, *65*, 2315.
102. Meunier, F.; Elaissari, A.; Pichot, C. Macromol. Symp. **2000**, *150*, 283.
103. Duracher, D.; Sauzedde, F.; Elaïssari, A.; Pichot, C.; Nabzar, L. Colloid Polym. Sci. **1998**, *276*, 920.
104. Duracher, D.; Sauzedde, F.; Elaïssari, A.; Perrin, A.; Pichot, C. Colloid Polym. Sci. **1998**, *276*, 219.
105. Sauzedde, F.; Elaissari, A.; Pichot, C. Macromol. Symp. **2000**, *150*, 617.
106. Hergeth, W.D.; Steinau, U.J.; Bittrich, H.J.; Simon, S.; Schmutzler, K. Polymer **1989**, *30*, 254.

12

Polymer Beads in Biomedical Chromatography

Preparation and Characterization

ALI TUNCEL, ENDER ÜNSAL, and SERAP ŞENEL Hacettepe University, Ankara, Turkey

I. INTRODUCTION

Polymeric microspheres have attracted significant attention in the various applications such as affinity chromatography, high-performance liquid chromatography (HPLC), enzyme immobilization, drug delivery, and cell culturing. The size, polydispersity, porosity properties, and functional groups are important factors affecting the overall performance of the particles in biomedical applications. The polymeric microspheres from nanometer to millimeter scale are obtained by applying different processes including suspension, emulsion, dispersion, and polymerization. The polymerization methods for producing polymer beads with different size and surface properties are reviewed below.

II. SUSPENSION POLYMERIZATION

Suspension polymerization is known as a suitable process for the production of polymeric microspheres usually larger than 50 (μm, with some size distribution. The coefficient of variation indicating the size distribution of the particles usually varies between 15% and 30%. This method has been extensively used in the production of polydisperse microspheres both in the nonporous and macroporous forms. The hydrogel beads manufactured by the suspension polymerization process are particularly suitable as support materials for different chromatographic applications. A suspension polymerization for producing spherical and microporous poly(hydroxyethyl methacrylate) [poly(HEMA)] beads was first proposed by Mueller et al. [1]. HEMA-based hydrogel beads with macroreticular structure were also chemically modified [2]. The macroporous poly(HEMA) gel beads were first produced by Horak et al. [3,4]. The size and porosity prop-

erties of the cross-linked glycidyl methacrylate beads were extensively investigated by the same group [5–7].

In our studies, the spherical gel beads that are particularly suitable for chromatographic applications were obtained by suspension polymerization [8–11]. The hydrophilic monomers carrying different functional groups (i.e., hydroxyl, carboxyl, and amine) were included in the polymerization recipes for obtaining hydrogel beads suitable for the covalent attachment of different ligands. The production and characterization of different types of hydrogel beads are discussed below.

A. Hydrogel Beads in the Swellable Form

Hydrogel beads have usually been produced by the suspension polymerization of acrylic monomers. Hydroxyalkyl acrylate/methacrylate monomers are considered to be the most suitable for the production of these beads because their polymeric materials are nontoxic and for the most part biocompatible. However, these monomers are highly soluble in water. This factor makes the formation of two-phase systems necessary for conducting the suspension polymerization process difficult. One of the basic approaches used to overcome this difficulty is the inclusion of organic diluents immiscible in water in the suspension polymerization recipe [8–11]. For this purpose, organic liquids at which the hydrophilic acrylic monomers are highly soluble are selected as the diluent phase. The higher alcohols such as cyclohexanol (Cyc-OH) and octanol (Oct-OH) or the aromatic liquids such as toluene are the most widely prefered diluents in the suspension polymerization of hydrophilic acrylic monomers [8–11]. The use of diluent together with a cross-linking agent also causes the formation of macroporosity in the forming beads by the phase separation taking place between the cross-linked polymer and the diluent [11].

We have synthesized different types of hydrogel beads in the swellable form by the suspension polymerization of acrylic monomers performed based on the above principles [8–11]. For this purpose, three different monomers—2-hydroxypropyl methacrylate (HPMA), polyethylene glycol methacrylate (PEGMA), and acrylic acid (AAc)—were used as the main monomer in the presence of ethylene glycol dimethacrylate (EGDMA) as the cross-linking agent [8–11]. The components of the suspension polymerization systems are summarized in Table 1. All these systems provided hydrogel beads with excellent spherical shape and gel-type microporosity [8–11]. The representative optical micrographs of cross-linked PEGMA-based gel beads is given in Fig. 1 [10]. These photographs were taken with the gel beads swollen in water. The transparent view of the microspheres in water indicated that the produced gel beads possesed conventional gel-type microporosity in their swollen form [10]. In our studies, the effects of initiator, the feed concentration of cross-linking agent, the monomer/diluent ra-

TABLE 1 Components of Suspension Polymerization Systems Developed for Hydrophilic Acrylic Monomers

Monomer	Cross-linker	Diluent	Initiator	Stabilizer	Medium	Ref.
HEMA	EGDMA	Toluene	BPO	PVA (M_r:96.000)	Water	8
HPMA	EGDMA	Cyc-OH/Oct-OH	BPO	PVP (M_r:360.000)	Water	9
AAc	EGDMA	Toluene	BPO	PVA (M_r:96.000)	Water	10
PEGMA	EGDMA	Cyc-OH	BPO	PVP (M_r:360.000)	Water	11

tio, and the stirring rate on the properties of the gel beads (e.g., the bead yield, the average size and size distribution, the swelling behavior, and the functional group content) were investigated. The important results obtained in these studies are presented below:

The initiator type is effective particularly on the shape of the hydrogel beads. The oil-soluble initiators like benzoyl peroxide (BPO) having no significant water solubility are most suitable. The use of initiators with significant water solubility may lead to the formation of coagulum and the hydrogel beads with irregular shape [10]. For instance, BPO and 2,2′-azobisizobutyronitrile (AIBN) was comparatively tried in the suspension polymerization of PEGMA under identical conditions. BPO provided hydrogel beads with excellent spherical shape, whereas relatively irregular beads were obtained with AIBN [10]. This behavior was explained by the water solubility of AIBN. On the other hand, the

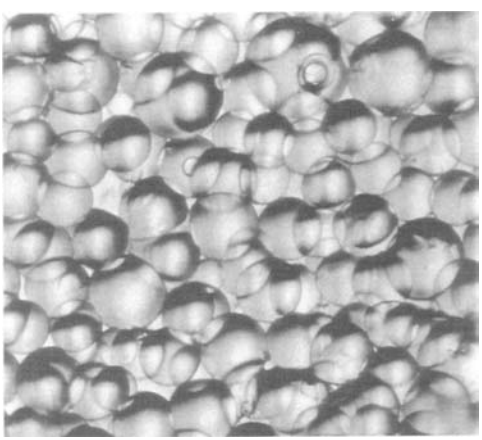

FIG. 1 Optical micrograph of PEGMA-based gel beads in distilled water. Magnification: ×110. (Reprinted from Ref. 10, Copyright © 2000, Springer-Verlag.)

initiator concentration of 1% mol based on the total monomer is usually enough to conduct the polymerization with a satisfactory bead yield [8–11]. Initiator concentrations lower than 0.1% mol based on total monomer may lead to reasonably low bead yields [9]. On the other hand, the initiator concentration is not significantly effective on bead yield, the average bead size and size distribution, and the swelling properties of the resulting hydrogel beads [9].

The diluent/monomer volume ratio should be considered as the another parameter for controlling the properties of resulting beads. The increase in the diluent monomer ratio usually results in an increase in the bead yield and the equilibrium swelling ratio of the hydrogel beads [10–11]. On the other hand, this parameter is not strongly effective on the average particle size in the range 0.5–3.0 mL/mL [10,11]. However, the use of exteremly high diluent/monomer volume ratios (i.e., higher than 3.0 mL/mL) may lead to a broad size distribution in the final product. In the case of suspension copolymerization of hydroxyalkyl methacrylate-type monomers with the reasonably polar functional monomers like AAc, the increase in the diluent monomer ratio causes an increase in the incorporation yield of functional comonomer into the resulting bead structure [9]. The diluent type and its concentration is particularly important for the synthesis of hydrogel beads with permanent macroporosity. The macroporous form of the hydrogel beads can only be obtained when a sufficently high feed concentration of cross-linking agent was used together with a suitable diluent and a sufficiently high diluent/monomer feed ratio [11]. For instance, in the suspension polymerization of AAc performed by using EGDMA as the cross-linking agent and toluene as the diluent, the macroporous form could be achieved when the cross-linker feed concentration and the diluent/monomer ratio were kept higher than 50 vol % and 0.5 mL/mL, respectively [11]. The AAc-EGDMA-based hydrogel beads in the macroporous form is exemplified in Fig. 2. The opaque view of the beads under optical microscope is the most practical indicator for the formation of macroporous structure [10,11]. High cross-linking agent feed concentrations and high diluent/monomer ratios usually makes the formation of phase separation within the forming beads easier. This case involves the generation of macroporous structure in the hydrogel beads. However, excessive increase in the diluent/monomer ratio may lead to the formation of mechanically unstable hydrogel beads in the macroporous form [10].

The stirring rate is the most important factor controlling the average size and the size distribution of resulting hydrogel beads. In our studies, stirring rates between 300 and 600 rpm were used [8–11]. In this range, the studied suspension polymerization systems provided hydrogel beads with an average size in the range 50–150 μm and with the coefficients of variation ranging between about 10% and 30% [8–11]. The increase in the stirring rate usually results in a significant decrease in the average particle size. However, the use of stirring

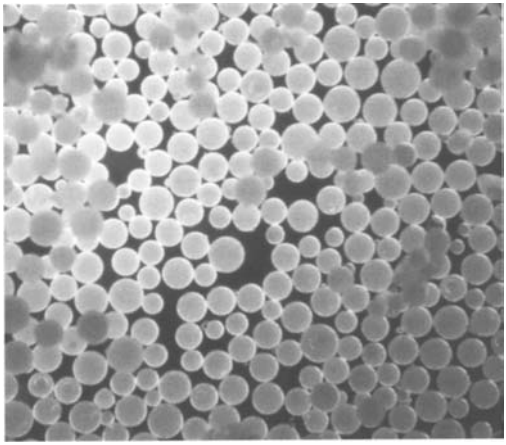

FIG. 2 Optical micrograph of poly(AAc-EGDMA) gel beads in the macroporous form in the dry state. (Reprinted from Ref. 11, Copyright © 1996, John Wiley & Sons, Inc.)

rates higher than 600 rpm may lead to the formation of bimodal size distribution in the product [8–11].

The feed concentration of the cross-linking agent mainly controls the equilibrium swelling behavior of the hydrogel beads [9–11]. For instance, the cross-linked HPMA gel beads produced with different cross-linker feed concentrations ranging between 5 and 50 mol % exhibited equilibrium swelling ratios ranging between 80% to 20% based on the dry weight [9]. A decrease in the feed concentration of cross-linking agent usually results in an increase in the water sorption capacity of the beads [9,10]. The feed concentration of the cross-linking agent is not strongly effective both on the bead yield and the average size of final particles [8–11]. However, for the suspension copolymerization of hydroxyalkyl methacrylates with the reasonably polar acrylic monomers like AAc, the increase in the feed concentration of cross-linking agent (i.e., EGDMA) resulted in a decrease in the AAc incorporation into the final bead structure [9]. The formation of hydrogel beads with conventional gel-type microporosity can be achieved with the cross-linking agent feed concentrations lower than 10 mol % based on the total monomer. However, cross-linking agent feed concentrations higher than 30–40 mol % are usually necessary for the generation of macroporosity within the forming hydrogel beads [11].

The introduction of acrylic comonomers carrying ionizable groups into the suspension polymerization of hydroxyalkyl methacrylate-type monomers usually results in the synthesis of pH-responsive hydrogel beads. AAc or meth-

acrylic acid (MAAc) are the comonomers generally preferred to obtain the hydrogel beads exhibiting appreciable swelling ratios, particularly in slightly alkaline medium. As an example, HPMA-MAAc gel beads produced with the EGDMA feed concentration of 4.6 mol % exhibited equilibrium swelling ratios up to 650% (w/w) in the slightly alkaline pH region (i.e., pH 7.5–9.0) [9]. Alternatively, the hydroxyalkyl methacrylate based hydrogel beads exhibiting high swelling behavior in the slightly acidic region (pH 4–6) can be obtained by including the cationic monomers like 2-aminoethyl methacrylate (AEM), *N*,*N*-dimethylaminoethyl methacrylate (DMAEM), or *N*-3-dimethylaminoethyl methacrylamide (DMAPM) in the suspension polymerization recipe.

In the suspension polymerization of polar acrylic monomers performed in the presence of EGDMA as the cross-linker, a coaxial bead structure comprising an EGDMA-rich core and a shell layer richer in the functional polar monomer was obtained [8,11]. This structure was confirmed by the comparison of Fourier transform infrared (FTIR) and FTIR-DRS spectra of the hydrogel beads possessing gel-type microporosity or permanent macroporosity [8,11]. This comparison indicated that most of the AAc or HEMA was preferentially collected on the surface layer of the hydrogel beads [8,11].

B. Polycationic Gel Beads

Polycationic gels have been extensively investigated by different researchers since these materials attracted attention particularly for biomedical studies on drug release, cell culturing, and DNA isolation/immobilization. The dynamic swelling behavior of 2-hydroxyethyl methacrylate-dimethylaminopropyl methacrylate (HEMA-DMAPM) gels were investigated by Chou et al. [12]. The cationic gels sensitive to both temperature and pH changes were produced by the copolymerization of *N*-isopropylacrylamide (NIPA) and DMAEM. Another polycationic structure sensitive to temperature and glucose concentration was obtained by Aoki et al. [13]. The proposed polymer exhibited a lower critical solution temperature (LCST) behavior depending on the glucose concentration [13]. Although the polycationic gels in the form of soluble polymers or membranes have been extensively studied, studies on the particle form of these materials are limited.

The monomers commonly used for the synthesis of polycationic gel structures (AEM, DMAEM, and DMAPM) are strongly polar monomers due to the primary or tertiary amine groups present in their structures. For this reason, these types of monomers have reasonably high water solubility. This property also makes difficult the formation of two-phase systems needed for the suspension polymerization process in which water usually is used as the continuous medium. In the suspension polymerization of such monomers, a two-phase system composed of a dispersed phase, in the form of stable droplets including

both cationic monomer and the cross-linking agent, and a continuous phase can be obtained by the use of polymeric molds for the stabilization of monomer droplets. Among these stabilizers, a Ca-Na alginate system is one of the most preferred. In the case of this stabilizer system, Na-alginate is usually added to the monomer phase dispersed in the water whereas CaCIZ is dissolved in the continuous medium [14]. By the addition of monomer phase into the continuous medium, a polymeric mold around the monomer phase droplets is immediately formed by the rapid cross-linking of alginate via the exchange of Na-Ca ions. Therefore, the polymerization of cationic monomers progresses in the monomer droplets stabilized by the alginate mold [14]. However, the mold should be semipermeable for achieving satisfactory bead yields. In other words, the polymeric mold should prevent the diffusion of forming polymer into the continuous medium while it allows the diffusion of initiator to the disperse phase. Recently, we proposed a suspension polymerization protocol for the production of uniform polycationic particles exhibiting a drastic response against pH [14]. For this purpose, we selected a relatively new cationic monomer, dimethylaminopropyl methacrylamide (DMAPM).

Uniform gel beads 3 mm in size under production conditions were obtained by the suspension copolymerization of DMAPM and acrylamide (AA) in aqueous medium by using *N*,*N*-methylenebisacrylamide (MBA) as the cross-linking agent [14]. In this method, potassium persulfate/tetramethylethylenediamine (KPS/TEMED) redox couple and Na-alginate/calcium chloride system were selected as the initiator and stabilizer, respectively [14]. The copolymer gel beads were in the swollen form in the acidic pH region and passed to the fully shrunken form at pHs higher than 6.0 [14]. The representative optical micrographs of the swollen beads in the acidic medium and the shrunken beads in the neutral medium are given in Fig. 3. The surface and internal morphologies of the freeze-dried forms of the beads swollen at pH 3 are also shown in the figure. Electron microscopic examination indicated that the gel beads had a macroporous interior surrounded by a skin layer with relatively lower porosity with respect to the internal part [14].

Polycationic gels beads in the cross-linked form are strongly responsive to pH changes. Most of these structures exhibit extremely high swelling ratios, particularly in the pH range 4.0–5.5. The complete ionization of primary or tertiary amine groups in this pH region should be responsible for high water uptake. For the poly(DMAPM) gel beads, approximately 40 folds of volume increase with respect to that in the neutral pH could be achieved in this pH region [14]. The dynamic swelling and shrinking behaviors of poly(DMAPM) gel beads were also determined by applying a step input on the medium pH [14]. For this purpose, pH was changed between 3 and 7 in both directions. In the case of dynamic swelling or shrinking, the process was nearly completed within 4 h [14].

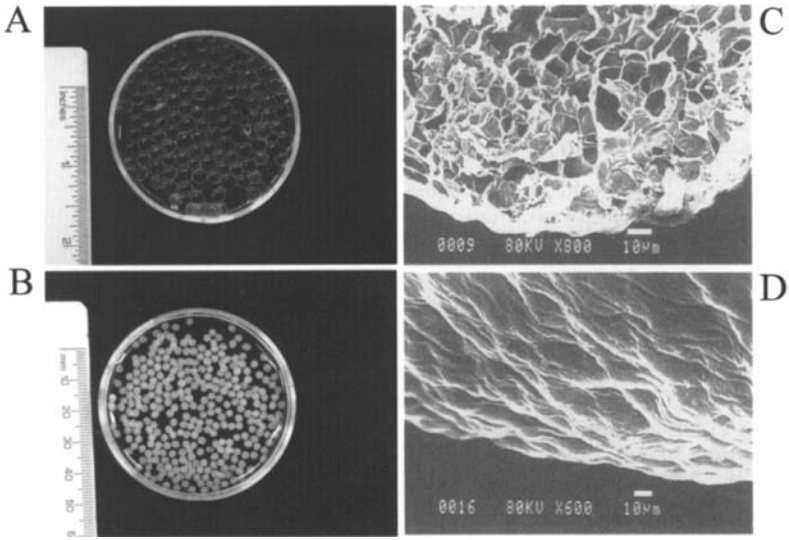

FIG. 3 Representative optical micrographs of (A) swollen beads in the acidic medium, (B) shrunken beads in the neutral medium, and (C) the internal and (B) surface morphologies visualized by SEM. Magnification for (C): × 800, for (D): × 600. (Reprinted from Ref. 14, Copyright © 2000, John Wiley & Sons, Inc.)

III. DISPERSION POLYMERIZATION

Another approach used in the preparation of polymeric microspheres is dispersion polymerization. This method is particularly suitable for the production of uniform polymeric particles in the size range 1–10 μm. In this method, the polymerization starts with a homogeneous medium at which the monomer, the initiator, and the stabilizer are dissolved. The initiator radicals formed in the homogeneous medium react with the monomer molecules to give short-chain initiator-monomer radicals. When the growing oligomer chains reach a certain length, they precipitate and flocculate on the steric stabilizer chains dissolved in the polymerization medium. By this process, termed nucleation, the growing oligomer chains are separated from the continuous medium in the form of smaller primary particles. After the formation of primary particles, polymerization progresses within the particles in the presence of monomer diffusion from the continuous phase to the forming particles. At the end of the polymerization, a two-phase system including monodispersed polymer particles in the micrometer size range and the inertial dispersion medium is obtained. The mechanism and the basic features of the dispersion polymerization were extensively reviewed by Barret [15]. The dispersion polymerization systems providing uni-

form particles in the micrometer size range were developed for the monomers with different polarities. Among them, styrene (S), methyl methacrylate (MMA), chloromethystyrene (CMS), divinylbenzene (DVB), hydroxyethyl methacrylate (HEMA), glycidyl methacrylate (GMA), ethylcyanoacrylate (ECA), *N*-isopropylacrylamide (NIPA), and *N*-isopropyl methacrylamide (NIPMA) were the most widely tried [16–28].

A. Single-Stage Process

The kinetics of the dispersion polymerization of styrene was investigated in alcohol-water media [19,20]. In these studies, AIBN and poly(acrylic acid) (PAAc) were used as the initiator and the stabilizer, respectively. The effects of initiator, stabilizer, monomer, and alcohol concentrations on the polymerization rate, final monomer conversion, average size and size distribution were determined [19,20]. Monodispersed polystyrene particles in the range 1–3 μm were obtained with different experimental conditions [19, 20]. In the dispersion polymerization process, the polymerization rate and the average particle size usually increase with increasing initiator concentration. As described in the literature, higher number of oligomer chains with shorther length are formed by increasing initiator concentration [19,20]. This case involves the formation of lower number of primary particles by the aggregation of these chains. The decrease in the number of primary particles involves an increase in the final particle size at constant monomer conversion [19,20].

On the other hand, an increase in the stabilizer concentration causes an increase in the polymerization rate and a decrease in the average particle size [20]. Similar to conventional emulsion polymerization, the rate of dispersion polymerization is proportional to the number of particles in the polymerization medium [20]. Therefore, for constant monomer conversion, a decrease in the final particle size originates from the formation of higher number of particles in the polymerization medium. This case provides an increase in the polymerization rate [20].

On the other hand, an increase in the water content of the dispersion medium led to a significant decrease in the average particle size and an increase in the polymerization rate. The formation of smaller particles with higher polymerization rate was explained by the formation of higher number of primary particles by the aggregation of shorter polymer chains during the nucleation stage [19, 20]. In most of the dispersion polymerization systems involving the use of alcohol–water mixtures as the dispersion media, the polarity of the dispersion medium is controlled by adjusting the volume ratio of alcohol to water [16,19,20]. The polarity of the dispersion medium is considered the most important factor controlling the polymerization rate, average size, and size distribution of the final particles. In the case of relatively polar dispersion medium, the growing oligomer chains formed by the polymerization of relatively apolar monomers

like styrene (S) or methyl methacrylate (MMA) lead to the nucleation with lower molecular weights. This allows the formation of more primary particles by the aggregation of a higher number of shorter chains, which in turn leads to final particles of lower average size [20]. Therefore, the formation of a higher number of primary particles involves higher polymerization rates. On the other hand, the decrease in the polarity of dispersion medium involves the formation of particle nucleation with the oligomer chains of higher molecular weight. In such a case, lower numbers of primary particles are formed due to the presence of a lower number of longer oligomer chains. This involves the distribution of total monomer mass to a lower number of primary particles, resulting in an increase in the average particle size [20]. In the case of dispersion medium with highly apolar character, the nucleation period becomes longer and successive nucleations occur with the aggregation of oligomer chains of different molecular weights. This usually results in the formation of polydispersed particles [19].

The effects of monomer concentration on the polymerization rate, average size, and size distribution are shown in Fig. 4 [20]. As seen in the figure, the polymerization rate and the final particle size significantly increased with the increasing feed concentration of the monomer. The formation of larger particles by increasing monomer concentration was explained by the lower polarity of the dispersion medium [20].

Reactive microspheres were also obtained by the dispersion polymerization process [21–24]. Horak and Shapoval developed a dispersion polymerization method for glycidyl methacrylate [21]. Polychloromethylstyrene (PCMS) is another reactive structure preferred in the design of microcarriers for various biotechnological applications. Margel et al. developed a dispersion polymerization procedure for the monodisperse PCMS microspheres in the micrometer size range [22]. In their procedure, chloromethylstyrene (CMS) was polymerized in a medium containing dimethylsulfoxide and ethanol by using AIBN and polyvinylpyrrolidone (PVP) as initiator and stabilizer, respectively [22]. Li et al. proposed a two-stage polymerization protocol for the synthesis of core-shell poly(chloromethylstyrene-co-divinylbenzene) microspheres in the macroporous form [23].

In our studies, monodispersed PCMS microspheres in the size range 1.7–3.7 μm were obtained by an alternative dispersion polymerization process conducted in ethanol/methoxyethanol medium using AIBN and PAAc as initiator and stabilizer, respectively [24]. A typical electron micrograph of the monodispersed PCMS microspheres produced by dispersion polymerization is given in Fig. 5 [24]. By the proposed procedure, the monodispersity and the isolation yield of PCMS particles were significantly improved relative to the methods discussed in the literature [24]. In the case of monodispersed particles, the average particle size increased from 1.74 to 3.73 μm and the monomer conversion significantly decreased following an increase in the methoxyethanol/ethanol vol-

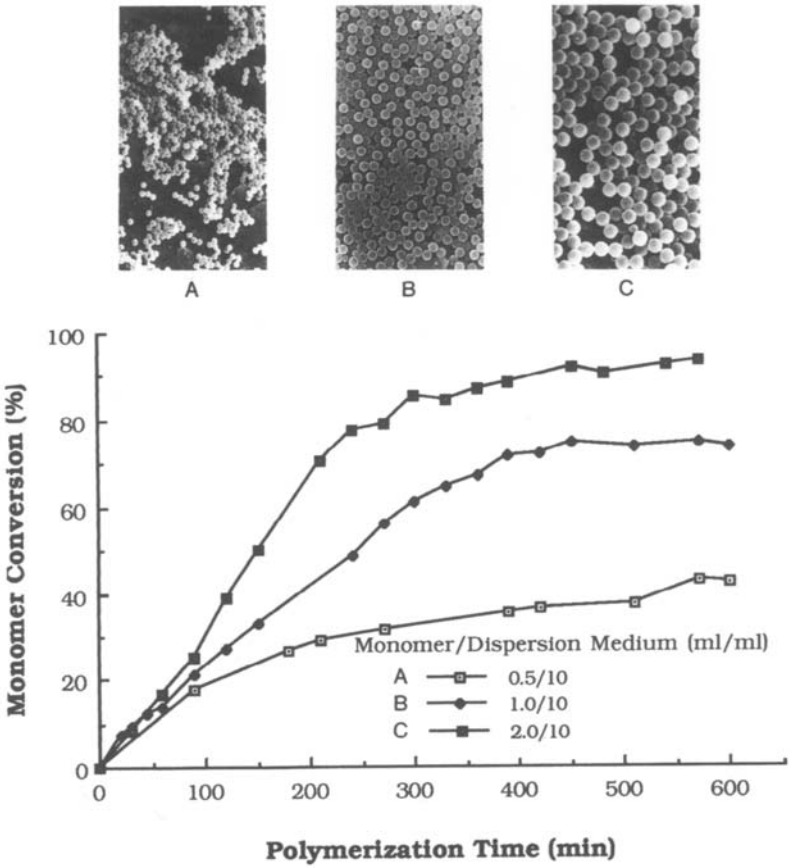

FIG. 4 Effects of monomer concentration on the polymerization rate, the average size and size distribution in the dispersion polymerization of styrene. Monomer/dispersion medium (mL/mL): (A) 5:100, (B) 10:100, (C) 20:100. The original SEM photographs were taken with 2600×, 2000×, and 2600× magnifications for (A), (B) and (C), respectively, and reduced at a proper ratio. (Reprinted from Ref. 20, Copyright © 1994, John Wiley & Sons, Inc.)

ume ratio from 0.077 to 0.75 mL/mL [24]. On the other hand, the stabilizer (i.e., PAAc) concentration is also effective for controlling the average size of PCMS particles particularly in the relatively polar dispersion medium. By keeping the particle monodispersity, the average particle size decreased from 2.08 to 1.67 μm as the PAAc concentration increased from 5.4 to 42.9 mg/mL [24].

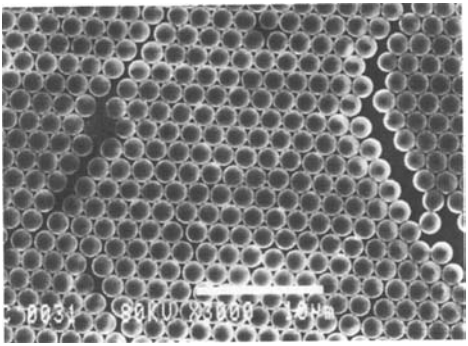

FIG. 5 Typical electron micrograph of the monodisperse PCMS microspheres produced by dispersion polymerization. Magnification: ×3000. (Reprinted from Ref. 24, Copyright © 2000, American Chemical Society.)

B. Multistage Procedures for Functional Latex Particles

The functionalization of monodispersed latex particles usually involves the use of multistage polymerization protocols. Relatively hydrophilic acrylate- or methacrylate-based monomers [AAc/MAAc, acrylamide (AAm), HEMA, AEM, and DMAEM] are usually preferred for the introduction of functional groups into the structure of relatively hydrophobic latex particles made of styrene or MMA. These functional comonomers and their homopolymers are highly soluble in the polar media at which the dispersion polymerization of relatively hydrophobic monomers is conducted. Direct addition of these hydrophilic monomers into the dispersion polymerization of hydrophobic monomers usually results in the formation of unstable latexes (i.e., coagulum). For this reason, in most of the functional latex preparations the seed particles were obtained by the conventional emulsion or dispersion polymerization of the hydrophobic monomers in a relatively polar medium (i.e., water or alcohol–water solution) [20]. In the second stage, the seed particles were swollen by the functional monomer including an oil-soluble initiator in a suitable dispersion medium by keeping the particle monodispersity. In the last stage, the functional monomer was repolymerized within the swollen seed particles in the presence of an oil-soluble initiator [20].

A two-stage polymerization procedure based on the above principles was proposed for the synthesis of polystyrene-based uniform latex particles with different functionalities [20]. In the repolymerization stage, AAc, HEMA, and DMAEM were included as the comonomer together with styrene. The applied procedure provided monodisperse polystyrene based latex particles carrying carboxyl (negatively charged), dimethylamino (positively charged), and hydroxyl

(uncharged) groups without producing new particles in the repolymerization stage [20]. The presence of functional groups on the surface was shown by elemental analysis, FTIR, and XPS (x-ray photoelectron spectroscopy) measurements [20]. The functional latex particles of 2.3 μm size exhibited ζ potentials varying between −37 and −45 at neutral pH [20]. It should be noted that similar latexes produced by multistage emulsion polymerization method had ζ-potential values around −70 [20]. Therefore, lower surface charge of the functional latex particles produced by the proposed polymerization protocol should be considered as an advantage in the surface-related biomedical applications of these materials because it allows a larger parking area for the biological molecules located on the surface of these particles.

IV. MACROPOROUS LATEX PARTICLES

Macroporous particles have been commonly utilized as packing material in HPLC. Currently most of the available HPLC column materials are in the polydisperse form. Beginning in the 1990s, monodispersed particles in the macroporous form were proposed as "new generation column materials" [29]. More regular flow regime in the chromatographic column, lower back pressure, and liquid chromatograms with higher resolutions are the most important advantages of these packings [29–31].

Monodispersed latex particles of larger size were produced in microgravity medium in the early 1980s. Various multistage polymerization techniques were proposed for the production of monodisperse-macroporous particles [29–49]. A two-step microsuspension polymerization was first developed by Ugelstad et al. [29]. This method was established based on the activation of seed particles by a low molecular weight organic agent. The particles with similar structures were also obtained by using a different polymerization protocol termed “seeded emulsion polymerization” [32,33]. In this procedure, the seed particles 7.8 μm in size were synthesized by a series of swelling and repolymerization stages. Then the monomer phase (i.e., styrene and DVB) was polymerized within the seed particles, including toluene or *n*-hexane as the diluent. This method provided monodisperse-macroporous particles 11 μm in size [32,33]. Frechet et al. produced uniform-macroporous poly(styrene-co-divinylbenzene) beads 7.4 μm in size by using linear polystyrene as a component of the porogenic mixture [30,31]. These particles were successfully used as chromatographic packing in size exclusion chromatography (SEC) [30,31]. One of the recent methods proposed for the synthesis of relatively monodisperse-macroporous particles up to 10 μm in size is microporous glass membrane (MPG) emulsification [34–36]. The MPG method was first used for the suspension polymerization of styrene [34]. It was also applied for the production of carboxyl- and glycidyl-carrying macroporous particles [35–36].

The basic principles of the various multistage polymerization protocols developed for the synthesis of monodisperse-macroporous particles may be summarized as follows: In the first stage, the seed particles are synthesized by a polymerization process providing latexes in the monodispersed form. The soapless emulsion polymerization is one the polymerization methods commonly preferred by different researchers [29,30–34]. This method is simple and usually leads to particles with reproducible sizes. In the case of soapless emulsion polymerization, the impurities (particularly primary and secondary emulsifiers) that may generate some undesirable effects (i.e., secondary particle formation originated from the undesired polymerization loci) in the later stages of the multistage polymerization are not found in the seed latex. This method usually provides monodispersed polystyrene latex particles in the size range 1–2 μm [29,30–34]. However, both the particle size in this range and the average molecular weight of the synthesized particles are not suitable for the direct synthesis of macroporous particles by a single repolymerization stage. The monodispersity of seed particles is an important consideration at the initial stage since deviations from monodispersity are magnified by the repeated swelling stages.

For this reason, the seed particles are usually swollen by a low molecular weight organic agent (i.e., activating agent) by keeping the monodispersity in an aqueous emulsion medium obtained by the use of mostly an anionic stabilizer such as lauryl sulfate in water [29,30–34]. The introduction of the low molecular weight organic agent into the structure of seed particles causes relaxation in the polymeric chains. Hence, the monomer absorption capacity of seed particles increases significantly. The low molecular weight organic liquids like dibutylphthalate (DBP), dodecyl chloride (DDC), cyclohexanol (Cyc-OH), cyclohexane, and toluene are the most widely used activating agents for the first-stage swelling of seed particles [29–34,37–49].

In the following stage, the activated seed particles are reswollen by a monomer phase composed of mostly apolar monomers like styrene or MMA and an oil-soluble initiator like BPO in a similar aqueous emulsion medium containing an anionic stabilizer [29–34]. After introducing the monomer phase into the seed particles, the polymerization of monomer within the swollen seed particles allows the formation of second-generation seed latex particles with a larger size. The particle size value reached at this stage should be sufficiently high for the synthesis of macroporous particles with a desired size by applying a single-stage repolymerization process. At this stage, adjustment of the molecular weight of polymer formed within the seed particles is important because this material behaves as the polymeric component of the porogen mixture for the generation of macroporous structure during the repolymerization. For this purpose, the initiator concentration should be kept in a sufficiently high level for the synthesis of polymeric porogen with a sufficiently low molecular weight suitable for the formation of final particles with sponge-like porosity in the following repoly-

merization stage [30,31,45,46]. Oppositely, the formation of high molecular weight porogen usually results in the synthesis of macrporous particles with crater-like pore structure that are not suitable for chromatographic applications [30,31,45,46]. In the multistage microsuspension polymerization method developed in our laboratory, large monodispersed seed particles with a sufficiently low molecular weight were directly obtained by the dispersion polymerization of styrene [45,46]. Hence, the swelling and repolymerization stages for adjusting the size and molecular weight properties of the second-generation seed latex were eliminated [45,46]. Therefore, the dispersion polymerization can be considered as another method for the production of monodispersed seed latexes that can be directly used for the synthesis of macroporous particles in the monodispersed form.

After having the seed latex containing polymeric porogen, the seed particles were reswollen by an organic phase including the monomer (styrene), the cross-linker (DVB), the diluent (e.g., DBP, DDC, Cyc-OH, or toluene) and the oil-soluble initiator (e.g., BPO) in the aqueous emulsion medium containing an anionic emulsifier (e.g., lauryl sulfate, LS) [29–33,37–44]. The repolymerization of monomer phase (i.e., monomer and cross-linking agent) in the swollen seed particles, including the diluent and the polymeric porogen, provides macroporous particles in the monodispersed form. The polymerization by keeping the monodispersity of swollen particles can be achieved by elevating the temperature to a sufficiently high value (i.e., mostly 70°C) [29–33,37–44]. In this stage, the polymeric stabilizers (i.e., PVA or PVP) can be included for protecting the stability of swollen particles during the polymerization [30,31,45,46].

In our procedure, we took a different approach because the seed latex properties were suitable for the synthesis of macroporous product with a single-stage repolymerization [45,46]. In an aqueous emulsion medium, the seed particles were swollen by a low molecular weight organic agent (i.e., DBP) acting as both an activation agent and diluent [45–49]. The next stage was the reswelling of DBP swollen seed particles by a monomer mixture containing an oil-soluble initiator (BPO), a monomer (styrene) and a cross-linking agent (DVB) in the same emulsion medium [45–49]. During these swelling stages, the monodispersity of seed particles was protected by adjusting DBP/seed latex and monomer phase/seed latex ratios to the appropriate values. In the last stage, the monomer phase was polymerized in the swollen seed particles at 70°C, by using PVA as the stabilizer [45–49]. Hence, no additional swelling and repolymerization process were applied for the generation of polymeric porogen within the seed particles. This property allowed the synthesis of highly monodisperse-macroporous particles with a simpler multistage polymerization protocol relative to the methods available in the literature [45–49]. A typical electron micrograph of the monodisperse-macroporous poly(S-DVB) particles produced with the multistage-microsuspension polymerization is given in Fig. 6 [46].

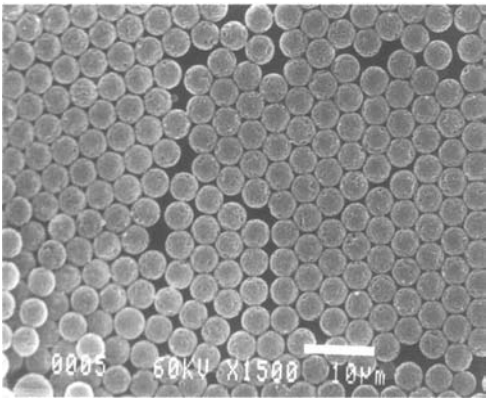

FIG. 6 Typical electron micrograph of the poly(styrene-divinylbenzene) particles in the monodisperse-macroporous form synthesized by multistage-microsuspension polymerization. Magnification: ×1500. (Reprinted from Ref. 46, Copyright © 1999, John Wiley & Sons, Inc.)

To remove the constituents of the porogen mixture (i.e., linear polystyrene and diluent), the monodispersed particles should be extracted by a suitable organic solvent after washing with an alcohol. The most widely used extraction solvents were toluene, methylene chloride, and tetrahydrofuran [30–45,46].

The size and average molecular weight of the seed latex are the most effective factors controlling the size and the porosity properties of final macroporous particles. In the polymerization protocol developed in our laboratory for the synthesis of poly(S-DVB)-based monodisperse-macroporous particles, polystyrene seed latexes with different average diameters and average molecular weights were prepared by dispersion polymerization [45]. The developed process is suitable for the synthesis of monodispersed polystyrene particles in the size range 2–6 μm [45]. To obtain monodispersed polystyrene particles with a prescribed size, the most practical approach is to adjust the polarity of the dispersion medium [45]. In our study, the polystyrene seed latexes with different size and average molecular weights were synthesized using dispersion media including a relatively polar compound (ethanol) and a relatively apolar one (2-methoxyethanol) at different ratios [45]. The seed latexes with higher average molecular weight obtained in the relatively polar dispersion media give monodisperse-macroporous particles with a crater-like pore structure [45,46]. These particles were not suitable as a support material in the chromatographic applications particularly due to their high average pore size and low specific surface area. However, the monodisperse-macroporous particles with a sponge-like porosity (i.e., corresponding to an average pore size range suitable for liquid chro-

matography) can be obtained by starting from the seed latexes with relatively lower molecular weight [45,46]. In the case of a sponge-like porous structure, the pores were homogeneously distributed throughout the cross-section of the particles [45,46]. The surface and internal morphologies of the monodisperse-macroporous particles produced with the seed latexes of different size and average molecular weights are exemplified in Fig. 7 [45].

Although the diluent/seed latex ratio is not effective on the average size, this parameter strongly affects on the the porosity properties of final particles. The increase in the diluent/latex ratio causes a decrease in the average pore size and an increase in the porosity [45–49]. In the case of poly(S-DVB) monodispersed particles, the effect of diluent/seed latex ratio on the pore structure of monodispersed particles is exemplified in Fig. 8 [45]. A similar effect was also observed

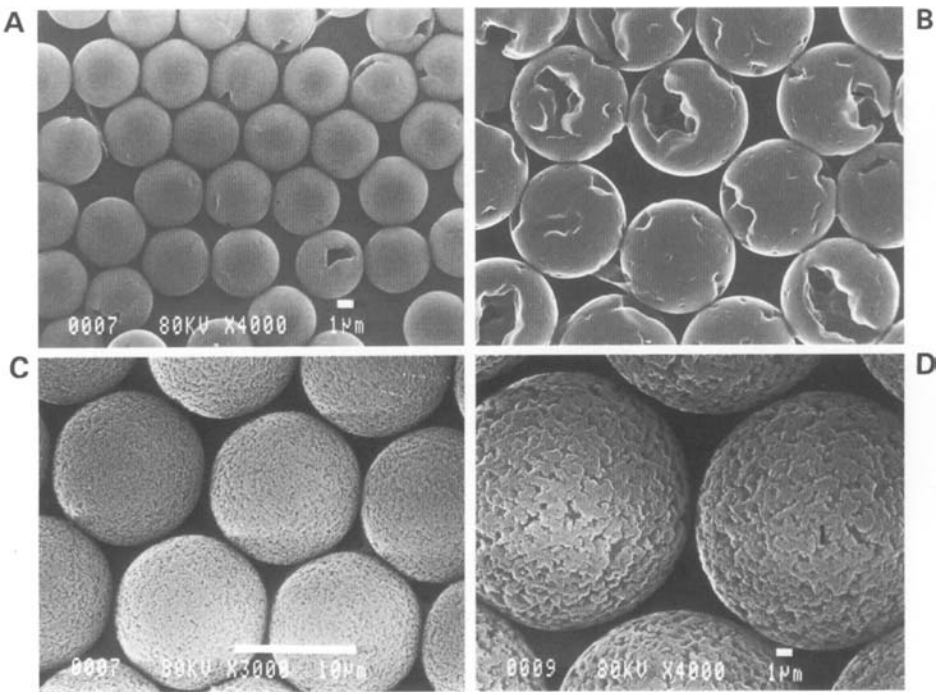

FIG. 7 Surface morphologies of the monodisperse-macroporous particles produced with the seed latexes with different diameters and average molecular weights. Seed latex size (μm), average-weight molecular weight and magnification (A), 1.9, 5.4×10^4, ×4000; (B) 3.6, 4.62×10^4, ×4000; (C) 5.5, 1.99×10^4, ×3000; (D) 7.4, 2.75×10^4, ×4000. (Reprinted from Ref. 45, Copyright © 1999, John Wiley & Sons, Inc.)

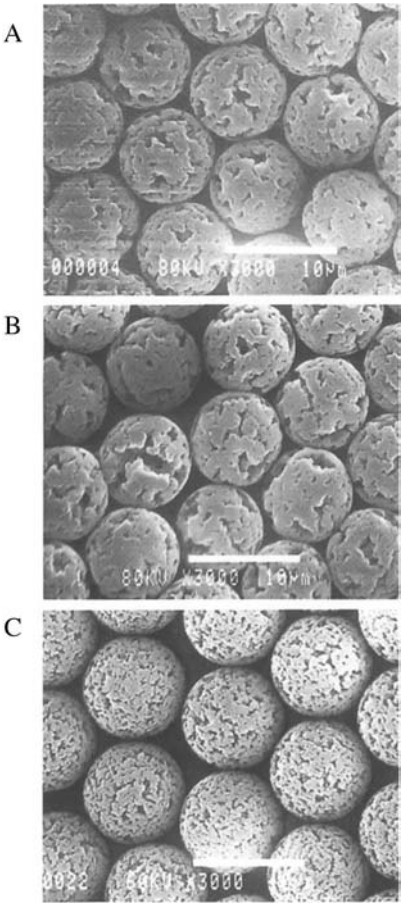

FIG. 8 Effect of DBP/seed latex ratio on the pore structure of monodisperse particles, DBP/seed latex ratio (mL/g): (A) 0.42, (B) 0.83, (C) 1.67. Magnification: ×4000. (Reprinted from Ref. 45, Copyright © 2000, John Wiley & Sons, Inc.)

for the particle interior by TEM photographs taken with the thin cross-sections of the macroporous particles [45].

Another parameter significantly affecting on the porous structure of monodispersed particles is the monomer/seed latex ratio. The average size and the polydispersity index increase significantly with the increasing monomer/seed latex ratio [45,48,49]. In other words, larger particles with broader size distribution were obtained. The monomer/seed latex ratio can be increased by decreasing the amount of seed latex for a constant monomer volume in the polymerization

medium [45,48,49]. In such a case the monomer mass is absorbed by the lower number of seed particles, which in turn leads to an increase in the average size of final macroporous particles [45,48,49]. However, the use of monomer/seed latex ratios higher than 10 mL/g usually results in reasonably wider size distribution in the final product [45]. The average size and the polydispersity index values of monodisperse-macroporous particles obtained with different monomer/seed latex ratios are exemplified in Table 2 [45]. The porous structure of monodispersed particles is also controlled by the monomer/seed latex ratio. Low monomer/seed latex ratios usually provide particles with crater-like pore structure, whereas the sponge-like porosity can be achieved with higher values of this parameter [45,48,49]. In other words, an increase in the monomer/seed latex ratio involves an appreciable decrease in the average pore size both on the particle surface and in the particle interior. The effect of monomer/seed latex ratio on the pore structure of monodisperse-macroporous particles is exemplified in Fig. 9 [45].

The effects of seed latex type as well as the diluent/seed latex and the monomer/seed latex ratios on the macroporous structure of the monodispersed particles can be explained by using the pore formation mechanism proposed by Cheng et al. [33, 45]. According to this mechanism, highly cross-linked gel microspheres were generated in the first stage of the pore formation process in the forming particles [33]. Following this stage, a phase separation between these microspheres and the porogen mixture including the diluent and the linear polystyrene occurred and the separated microspheres were agglomerated. The next stage was the fixation and binding of the agglomerated microspheres in the forming particles. The voids be-

TABLE 2 Variation of Average Size and Size Distribution of Monodisperese Macroporous Particles with the Monomer/Seed Latex Ratio

Seed latex size (μm)	M/SL ratio (mL/g)	Average size (D_n, μm)	Polydispersity index (D_w/D_n)
3.6	5	6.3	1.006
3.6	10	7.6	1.012
3.6	15	7.6	1.011
5.5	4	8.6	1.010
5.5	5	9.3	1.009
5.5	10	12.5	1.015
7.4	4	13.3	1.019
7.4	7	16.5	1.018
7.4	10	16.2	1.022
7.4	15	21.6	1.054

D_n, number-average diameter; D_w, weight-average diameter.
Source: Ref. 45.

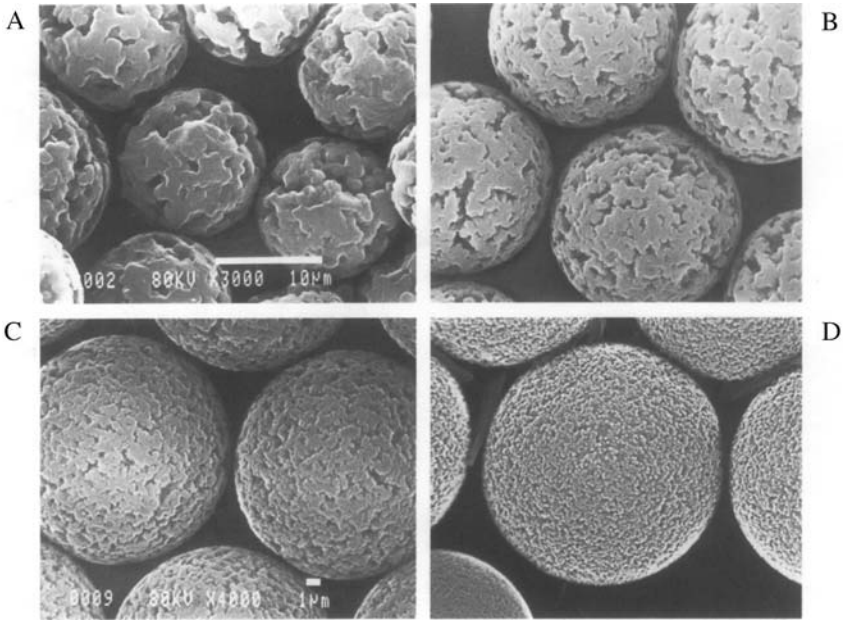

FIG. 9 Effect of monomer/seed latex ratio on the structure of monodisperse-macroporous particles. Monomer/seed latex ratio (mL/g) and magnification: (A) 4, ×3000, (B) 7, ×3000, (C) 10, ×4000, (D) 15, ×3000. (Reprinted from Ref. 45, Copyright © 1999, John Wiley & Sons, Inc.)

tween the fixed microspheres were the macropores filled with the porogen mixture. In the last stage, the porogen mixture was removed from the particles by extraction with organic solvents to obtain the macroporous structure.

Based on this mechanism, the average pore size and the porosity should be strongly related to the average‘ size of the highly cross-linked microspheres formed in the particles; the formation of highly cross-linked microspheres with larger size involves the formation of larger voids (i.e., pores) after the fixation. Our experiments indicated that the viscosity of porogen mixture was strongly effective on the average pore size [45,47–49]. A change in the synthesis conditions providing an increase in the viscosity of porogen solution resulted in the formation of macroporous particles with higher average pore size. The decrease in the diluent/seed latex ratio, the increase in the average molecular weight of the seed latex, and the decrease in the monomer/seed latex ratio should be considered as involving an increase in the viscosity of porogen solution [45]. For this reason, the monodispersed latex particles with a crater-like pore structure, including irregularly distributed and relatively larger pores on the particle cross-section, were obtained with the seed latexes with relatively higher average mo-

lecular weights or with lower monomer/seed latex ratios or with lower diluent/seed latex values [45,46]. However, the use of higher diluent and monomer to seed latex ratios or the seed latex with a low molecular weight led to the synthesis of monodispersed particles with a sponge-like pore structure including homogeneously distributed and reasonably smaller macropores throughout the particle [45,46]. The crater-like and sponge-like porosities are exemplified by the TEM images of the cross-sections of macroporous particles in Fig. 10.

A. Functionalization of Monodisperse-Macroporous Particles

The polarity and the surface chemistry of the stationary phase are particularly important in the HPLC applications aimed at the qualitative or quantitative analysis of biomolecules. These factors predominantly control the interactions be-

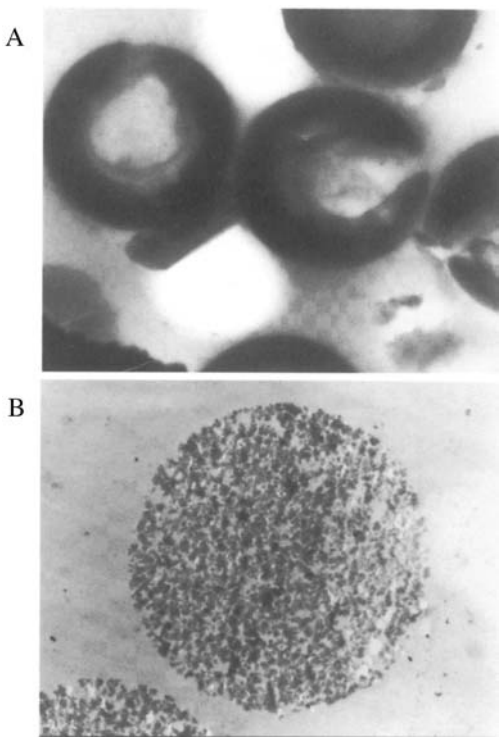

FIG. 10 TEM photographs of the cross-sections of macroporous particles showing crater-like and sponge-like porosity. (A) Crater-like porous structure. (B) sponge-like pore structure. Magnification ×5000. (Reprinted from Ref. 45, Copyright © 1999, John Wiley & Sons, Inc.)

tween the analytes in the mobile phase and the macroporous particles used as the stationary phase. Modification of inertial monodisperse-macroporous particles by the introduction of functional groups onto their surfaces allows either the regulation of surface hydrophobicity or the attachment of ligands for the synthesis of stationary phases with specific recognition abilities against different biomolecules [47]. A series of reactive glycidyl methacrylate-ethyleneglycoldimethacrylate (GMA-EGDMA) beads in the monodispersed and macroporous form, suitable particularly for HPLC applications, were synthesized by a "staged shape template polymerization" [37–41]. In this method, Cyc-OH was mostly included as the diluent for creating macroporosity in the resulting gel beads [37–41]. Pore size–specific functionalization of these beads with both hydrophilic and hydrophobic ligands (e.g., C_8 and C_{18} amines and phenol) was also achieved [40,41]. GMA-EGDMA copolymer beads were hydrolyzed for the synthesis of polar stationary phases for normal-phase HPLC [42]. HEMA-EGDMA-based monodispersed and macroporous beads synthesized by the same group were also used for the synthesis of stationary phases with chiral recognition ability against amino acids [43]. Stöver and Li achieved the synthesis of chloromethyl functionalized DVB–based monodisperse-macroporous particles as column packing material in HPLC [44].

In our laboratory, to produce monodisperse-macroporous S-DVB-based particles with different surface chemistries, a series of acrylic comonomers were introduced into the repolymerized monomer mixture at a concentration of 30% (v/v) [47]. The selected acrylic monomers were butyl methacrylate (BMA), MMA, GMA, HEMA, and MAAc. In order to understand the effect of comonomer on the porosity properties of the particles, the preparation conditions were kept constant in the presence of same seed latex with an average diameter of 6.25 μm [47].

The typical electron micrographs showing the detailed surface and internal morphology of the particles produced in the presence of acrylic monomers with relatively hydrophobic structure (i.e., styrene, MMA, and BMA) are given in Figs. 11 and 12, respectively. As seen here, both the particle surface and the particle interior in the highly porous form could be achieved in the presence of styrene or acrylic monomers with relatively hydrophobic structure [47]. In all cases, the surface or internal structure included homogeneously distributed and smaller pores [47]. The surface and internal morphologies of the monodispersed particles produced in the presence of polar acrylic monomers (i.e., GMA, HEMA, and MAAc) are exemplified in Figs. 13 and 14, respectively. As seen in these figures, a crater-like porosity was obtained for the GMA-functionalized particles [47]. As seen here, the surface porosity gradually decreased in the presence of most polar ones among the tried structures (i.e., HEMA and MAAc). On the other hand, a crater-like pore structure was also observed for the particle interiors [47].

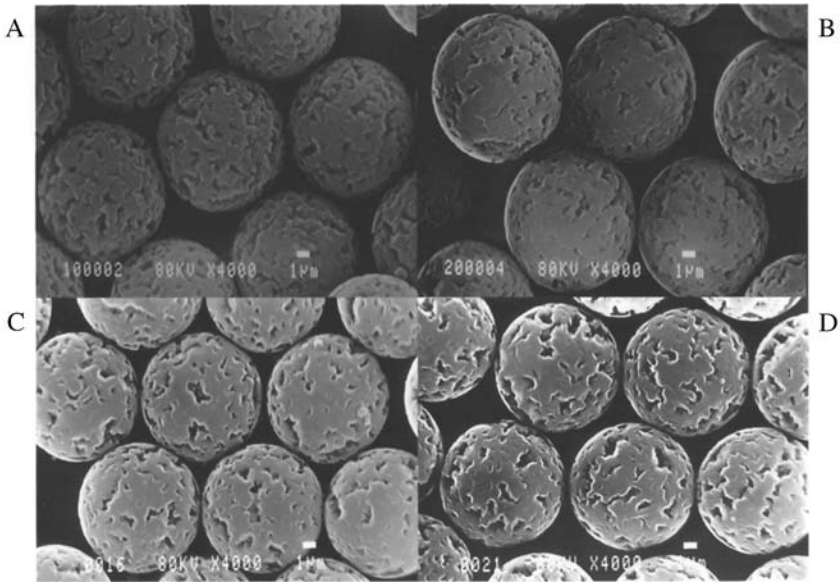

FIG. 11 Typical electron micrographs showing the detailed surface morphology of the particles produced in the presence of acrylic monomers with relatively hydrophobic structure. Magnification: x4000. Particle type (A) poly(S-DVB) in the absence of PVA, (B) poly(S-DVB) in the presence of PVA, (C) poly(S-DVB-MMA), (D) poly(S-DVB-BMA). (Reprinted from Ref. 47, Copyright © 2002, John Wiley & Sons, Inc.)

These results can be explained by considering the -pore formation mechanism proposed for monodisperse-macroporous particles [33,47]. In the presence of relatively apolar monomers, more rigid and stable cross-linked gel microspheres are probably 'generated at the beginning of the pore formation process in the forming particles. In the case of rigid (i.e., probably more hydrophobic) microspheres, the integrity should be protected during the aggregation. This case probably leads to the formation of homogeneously distributed voids (i.e., macropores) during the fixation. In addition, these microspheres should have a low diluent adsorption capacity due to high cross-linking density. This property leads to the preferential location of diluent phase in the voids between the fixed microspheres at the extended period of the pore formation. All of these factors involve the formation of a macroporous structure including relatively small pores homogeneously distributed throughout the each particle. In contrast, the cross-linked microspheres formed in the presence of relatively polar acrylic monomers should be stickier. This property involves higher diluent adsorption capacity for these microspheres. During aggregation, the adhesion and combination of these

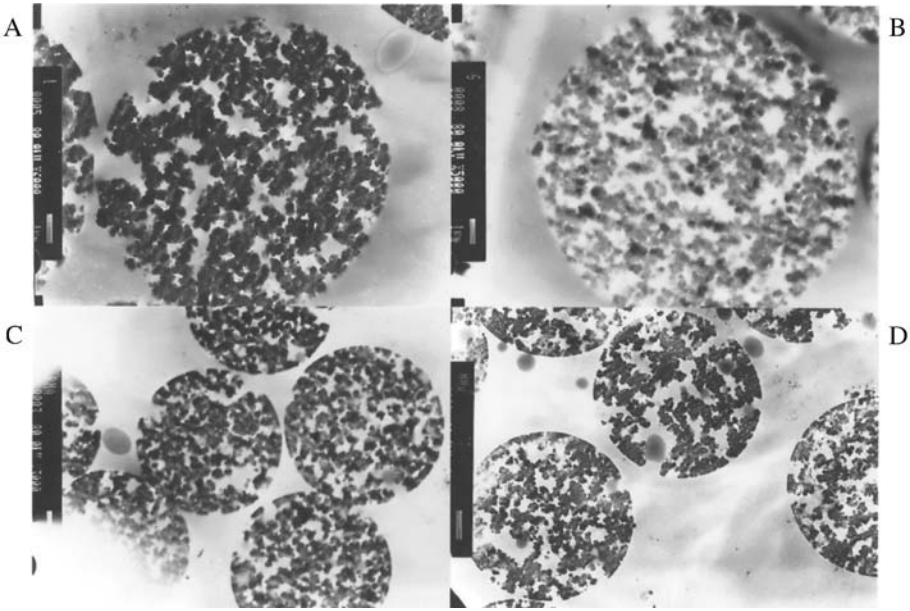

FIG. 12 Typical electron micrographs showing the internal morphology of the particles produced in the presence of acrylic monomers with relatively hydrophobic structure. Magnification: 3000×. Particle type (A) poly(S-DVB) in the absence of PVA, (B) poly(S-DVB) in the presence of PVA, (C) poly(S-DVB-MMA), (D) poly(S-DVB-BMA). Magnification: ×6000 for (A), ×5000 for (B), and ×3000 for (C). (Reprinted from Ref. 47, Copyright © 2002, John Wiley & Sons, Inc.)

microspheres should become easier. Due to the excessive aggregation and adhesion of the stickier gel microspheres with more unstable character, large blocks are probably generated in the forming particles. Then large voids in the form of craters were obtained between these blocks in the presence of relatively polar monomers.

The comparison of FTIR and FTIR-DRS spectra is an appropriate method for understanding the distribution of functional monomer in the particle structure. This comparison indicated that the bulk and surface concentrations were approximately equal for the comonomers with relatively apolar structure (i.e. styrene, BMA, MMA, and GMA) [47]. However, the surface concentration of relatively polar acrylic comonomers (i.e., MAA and HEMA) was found to be higher than that of the particle interior [47]. In other words, a layer dominantly including the polar acrylic comonomer was detected on the surface of the poly(S-DVB-HEMA) and poly(S-DVB-MAAc) particles.

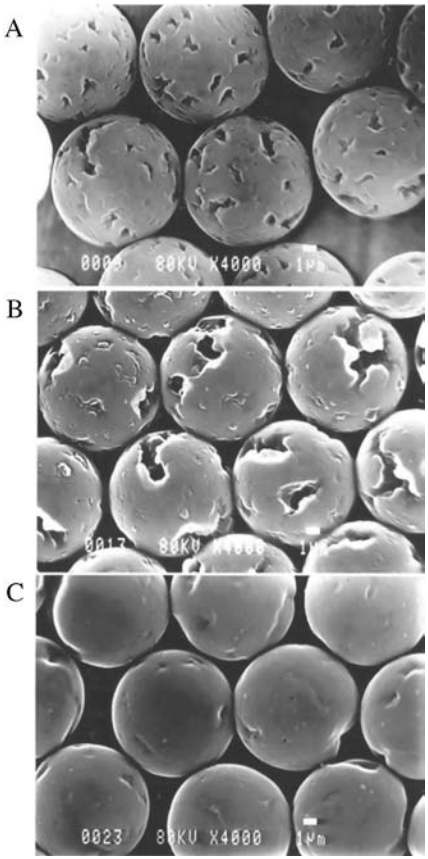

FIG. 13 Typical electron micrographs showing the detailed surface morphology of the particles produced in the presence of acrylic monomers with relatively hydrophilic structure. Magnification: ×4000. Particle type (A) poly(S-DVB-GMA), (B) poly(S-DVB-HEMA), (C) poly(S-DVB-MAAc). (Reprinted from Ref. 47, Copyright © 2002, John Wiley & Sons, Inc.)

It was also possible to modify the multistage-microsuspension polymerization method for the synthesis of functional monodispersed particles with a sponge-like pore structure. Electron micrographs showing the detailed surface morphology of the monodisperse-macroporous particles with a sponge like pore structure and containing polar acrylic units are shown in Fig. 15. As seen here, each structure contained homogeneously distributed, relatively small pores throughout the particle surface. The TEM examination performed by the thin

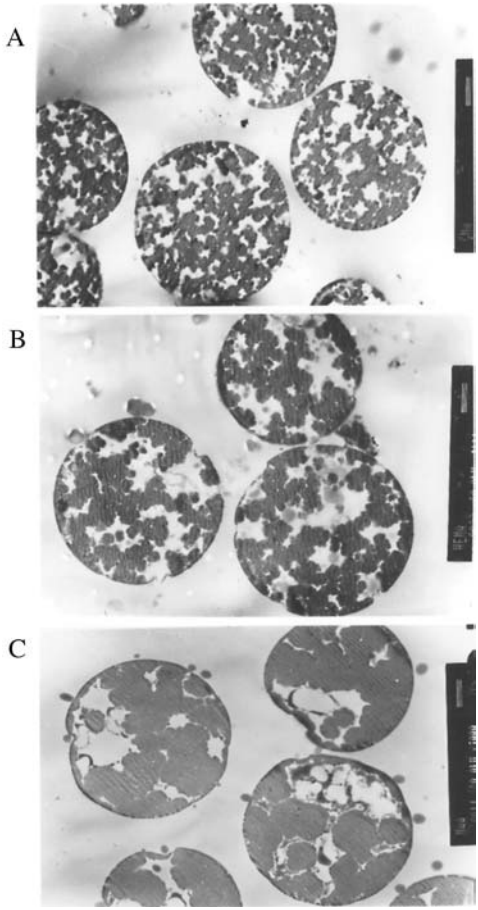

FIG. 14 Typical electron micrographs showing the internal morphology of the particles produced in the presence of acrylic monomers with relatively hydrophilic structure. Magnification: ×3000. Particle type (A) poly(S-DVB-GMA), (B) poly(S-DVB-HEMA), (C) poly(S-DVB-MAA). (Reprinted from Ref. 47, Copyright © 2002, John Wiley & Sons, Inc.)

cross-sections of the same particles also indicated that the surface and bulk morphologies of these particles were very similar [48,49]. For the synthesis of functional macroporous particles with sponge-like pore structure, the most important change in the polymerization conditions was use of a higher monomer/seed latex ratio under conditions similar to those discussed [47]. Hence, the

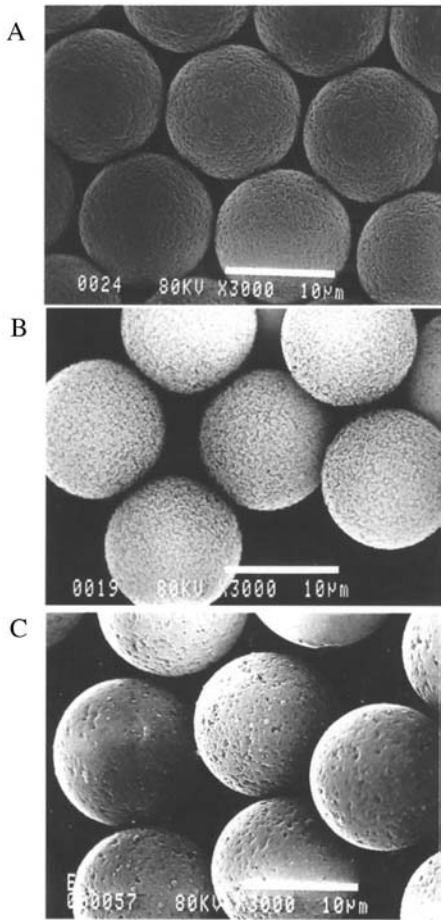

FIG. 15 Electron micrographs showing the detailed surface morphology of the monodisperse-macroporous particles with a sponge-like pore structure and containing polar acrylic units. Magnification: 3000×. Particle type (A) poly(S-DVB-GMA), (B) poly(S-DVB-HEMA), (C) poly(S-DVB-MAAc). (Figure 15B was reprinted from Ref. 48, Copyright © 2001, Society of Chemical Industry. Figure 15C was reprinted from Ref. 49, Copyright © 2002, Elsevier Science.)

viscosity of the porogen mixture was gradually reduced. This case resulted in both the formation of smaller cross-linked gel microspheres in the more rigid form and the prevention of their excessive aggregation in the forming particles. Therefore, the sponge-like pore structure was achieved in the presence of polar acrylic monomers [48,49].

REFERENCES

1. Mueller, K.F.; Heiber, S.J.; Plankl, W.L. Hydrogels as Large Size Spherical Beads. US Patent 4,224,427, 1981.
2. Kahovec, J.; Coupek, J. Chemical modification of macroreticular 2-hydroxyethylmethacrylate copolymers. React. Polym. **1988**, *8*, 105–111.
3. Horak, D.; Lednicky, F.; Rehak, V.; Svec, F. Porous polyHEMA beads prepared bysuspension polymerization in aqueous medium. J. Appl. Polym. Sci. **1993**, *49*, 2041–2050.
4. Horak, D.; Lednicky, F.; Bleha, M. Effect of inert components on the porous structure of 2-hydroxyethylmethacrylate ethylene dimethacrylate copolymers. Polymer **1996**, *37*, 4243–4249.
5. Horak, D.; Svec, F.; Tennikova, T.B.; Nahunek, M. Chromatographic properties of macroporous beads from poly(GMA-co-EDMA). Die Angew. Macromol. Chem. **1992**, *195*, 139–150.
6. Horak, D.; Labsky, J.; Pilar, J.; Bleha, M.; Pelzbauer, Z.; Svec, F. The effect of polymeric porogen on the properties of macroporous poly(glycidyl methacrylate-co-ethyleneglycol dimethacrylate). Polymer **1993**, *34*, 3481–3489.
7. Horak, D.; Straka, J.; Schneider, B.; Lednicky, F.; Pilar, J. Poly(ethylene dimethacrylate) particles with poly(glycidyl methacrylate) functionalities. Polymer **1994**, *35*, 1195–1202.
8. Kesenci, K.; Tuncel, A.; Piskin, E. Swellable ethylene glycol dimethacrylate-hydroxyethylmethacrylate copolymer beads. React. Funct. Polym. **1996**, *31*, 137–147.
9. Tuncel, A.; Çiçek, H. 2-Hydroxypropylmethacrylate based mono and bifunctional gel beads prepared by suspension polymerization. Polym. Int. **2000**, *49*, 485–494.
10. Tuncel, A. Suspension polymerization of polyethyleneglycol methacrylate: a route for spherical swellable gel beads with controlled hydrophilicity and functionality. Colloid Polym. Sci. **2000**, *278*, 1126–1138.
11. Tuncel, A.; Ecevit, K.; Kesenci, K.; Piskin, E. Nonswellable and swellable ethyleneglycoldimethacrylate-acrylic acid copolymer microspheres. J.Polym. Sci. A Polym. Chem. Ed. **1996**, *34*, 45–55.
12. Chou, L.Y.; Blanch, H.W.; Praunitz, J.M. J. Appl. Polym. Sci. **1992**, *45*, 1411–1418.
13. Aoki, T.; Nagao, Y.; Sanui, K.; Ogata, N.; Kikuchi, A.; Sakurai, Y.; Kataoka, K.; Okano, T. Polym. J. **1996**, *28*, 371–375.
14. Tuncel, A.; Unsal, E.; Cicek, H. pH-sensitive uniform gel beads for DNA adsorption. J. Appl. Polym. Sci. **2000**, *77*, 3154–3161.

15. Barret, K.E.J., Ed. *Dispersion Polymerization in Organic Media*. Wiley: London, 1975.
16. Paine, A.J.; Luymes, W.; McNulty, J. Macromolecules **1990**, *23*, 3104–3108.
17. Ober, C.K.; Lok, K.P.; Hair, M.L. J. Polym. Sci. Polym. Lett. Ed. **1985**, *23*, 103–112.
18. Shen, S.; Sudol, E.D.; El-Aasser, M.S. J. Polym. Sci. Polym. Chem. Ed. **1994**, *32*, 1087–1096.
19. Tuncel, A.; Kahraman, R.; Piskin, E. Monosize microbeads by dispersion polymerization of styrene. J. Appl. Polym. Sci. **1993**, *50*, 303–319.
20. Tuncel, A.; Kahraman, R.; Piskin, E. Monosize polystyrene latices carrying functional groups on their surfaces. J. Appl. Polym. Sci. **1994**, *51*, 1485–1498.
21. Horak, D.; Shapoval, P. Reactive poly(glycidyl methacrylate) microspheres prepared by dispersion polymerization. J. Polym. Sci. A Polym. Chem. Ed. **2000**, *38*, 3855–3863.
22. Margel, S.; Nov, E.; Fisher, I. Dispersion polymerization of chloromethylstyrene. J. Polym. Sci. A Polym. Chem. Ed. **1991**, *29*, 347–352.
23. Li, W.H.; Li, K.; Stover, H.D.H. Monodisperse poly(chloromethylstyrene-co-divinylbenzene) microspheres by precipitation polymerization. J. Polym. Sci. A Polym. Chem. Ed. **1999**, *37*, 2295–2303.
24. Bahar, T.; Tuncel, A. Monodisperse poly(p-chloromethylstyrene) microbeads by dispersion polymerization. Polym. Eng. Sci. **1999**, *39*, 1849–1855.
25. Li, W.H.; Stöver, H.D.H. Porous monodisperse poly(divinylbenzene) microspheres by precipitation polymerization. J. Polym. Sci. A Polym. Chem. Ed. **1998**, *36*, 1543–1551.
26. Horak, D.; Krystufek, M.; Spevacek, J. J. Polym. Sci. A Polym. Chem. Ed. **2000**, *38*, 653–663.
27. Horak, D. Effect of reaction parameters on the particle size in the dispersion polymerization of 2-hydroxyethylmethacrylate. J. Polym. Sci. A Polym. Chem. Ed. **1999**, *37*, 3785–3792.
28. Duracher, D.; Elaissari, A.; Pichot, C. J. Polym. Sci. A Polym. Chem. Ed. **1999**, *37*, 1823–1837.
29. Ellingsen, T.; Aune, O.; Ugelstad, J.; Hagen, S. Monosized stationary phases for chromatography. J. Chromatogr. **1990**, *535*, 147–161.
30. Galia, M.; Svec, F.; Frechet, J.M.J. Monodisperse polymer beads as packing material for high performance liquid chromatography: effect of divinylbenzene content on the porous and chromatographic properties of poly(styrene-co-divinylbenzene)-beads prepared in the presence of linear polystyrene as a porogen. J. Polym. Sci. A Polym. Chem. Ed. **1994**, *32*, 2169–2175.
31. Wang, Q.C.; Svec, F.; Frechet, J.M.J. Fine control of the porous structure and chromatographic properties of monodisperse macroporous poly(styrene-co-divinylbenzene) beads prepared by using polymer porogens. J. Polym. Sci. A Polym. Chem. Ed. **1994**, *32*, 2577–2588.
32. Cheng, C.M.; Micale, F.J.; Vanderhoff, J.W.; El-Aasser, M.S. Synthesis and characterization of monodisperse porous polymer particles. J. Polym. Sci. A Polym. Chem. Ed. **1992**, *30*, 235–244.

33. Cheng, C.M.; Vanderhoff, J.W.; El-Aasser, M.S. Monodisperse porous polymer particles: formation of the porous structure. J. Polym. Sci. A Polym. Chem. Ed. **1992**, *30*, 245–256.
34. Omi, S.; Katami, K.; Yamamoto, A.; Iso, M. Synthesis of polymeric microspheres employing SPG emulsification technique. J. Appl. Polym. Sci. **1994**, *51*, 1–11.
35. Omi, S.;Kaneko, K.; Nakayama, A.; Katami, K.; Taguchi, T.; Iso, M.; Ma, G.H. Application of porous microspheres prepared by SPG emulsification as immobilizing carriers of glucoamylase. J. Appl. Polym. Sci. **1997**, *65*, 2655–2664.
36. Omi, S. Preparation of monodisperse microspheres using shirasu porous glass emulsification technique. Colloids Surf. A Physicochem. Eng. Asp. **1996**, *109*, 97–107.
37. Smigol, V.; Svec, F. Preparation and properties of uniform beads based on macroporous glycidylmethacrylate-ethylene dimethacrylate copolymer: use of chain transfer agent for control of the pore size distribution. J. Appl. Polym. Sci. **1993**, *48*, 2033–2039.
38. Horak, D.; Smigol, V.; Labsky, J.; Svec, F.; Pilar, J. An epr study of the effect of suspension polymerization conditions on the properties of glycidylmethacrylate-ethylene dimethacrylate beads. Polymer **1992**, *33*, 2051–2056.
39. Smigol, V.; Svec, F. Synthesis and properties of uniform beads based on macroporous copolymer glycidyl methacrylate-ethylene dimethacrylate: a way to improve separation media for HPLC. J. Appl. Polym. Sci. **1992**, *46*, 1439–1448.
40. Smigol, V.; Svec, F.; Frechet, J.M.J. High performance liquid chromatography of complex mixtures using monodisperse-dual chemistry polymer beads prepared by a pore-size specific functionalization process. Anal. Chem. **1994**, *66*, 2129–2138.
41. Smigol, V.; Svec, F.; Frechet, J.M.J. Two-dimensional high performance liquid chromatography using monodisperse polymer beads containing segregated chemistries prepared by pore size specific functionalization. Single column combinations of size exclusion or ion exchange with reversed phase chromatography. Anal. Chem. **1994**, *66*, 4308–4315.
42. Petro, M.; Svec, F; Frechet, J.M.J. Monodisperse hydrolysed poly(glycidyl methacrylate-co-ethylene dimethacrylate) beads as a stationary phase for normal phase HPLC. Anal. Chem. **1997**, *69*, 3131–3139.
43. Lewandowski, K.; Svec, F.; Frechet, J.M.J. Polar monodisperse, reactive beads from functionalized methacrylate monomers by staged templated suspension polymerization. Chem. Mater. **1998**, *10*, 385–391.
44. Li, W.H.; Stöver, H.D.H. Monodisperse crosslinked core-shell microspheres by precipitation polymerization. Macromolecules **2000**, *33*, 4354–4360.
45. Tuncel, A.; Tuncel, M.; Salih, B. Electron microscopic observation of uniform macroporous particles. I. Effect of seed latex type and diluent. J. Appl. Polym. Sci. **1999**, *71*, 2271–2290.
46. Tuncel, A. Electron microscopic observation of uniform macroporous particles. II. Effect of DVB concentration. J. Appl. Polym. Sci. **1999**, *71*, 2291–2302.
47. Camli, T.; Tuncel, M.; Senel, S.; Tuncel, A. Functional, uniform and macroporous latex particles: preparation, electron microscopic characterization and nonspecific protein adsorption properties. J. Appl. Polym. Sci. **2002**, *84*, 414–429.

48. Tuncel, A.; Tuncel, M.; Çiçek, H.; Fidanboy, O. 2-Hydroxyethylmethacrylate carrying uniform, porous particles: preparation and electron microscopy. Polym. Int. **2001**, *51*, 75–84.
49. Tuncel, A.; Tuncel, M.; Ergun, B.; Alagöz, C.; Bahar, T. Carboxyl carrying large uniform latex particles. Colloids Surf. A Physicochem. Eng. Asp. **2002**, *197*, 79–94.

13

Assembling of Polymer Particles onto Solid Supports for Medical Applications

JEAN-PAUL CHAPEL Claude Bernard–Lyon I University, ISTIL, Villeurbanne, France

TATSUO TANIGUCHI Yamagata University, Yamagata, Japan

I. INTRODUCTION

Development of molecular architectures is one of the final goals of modern chemistry, biology, physics, and electronics. Biological systems are the ultimate molecular devices in which the elaborate systems of molecular recognition, transformation, and translocations are realized by organization of every functional group on the selected position with molecular precision. For a design of artificial intelligent devices, fabrication and control of materials with nanometer scales over chemical and physical attributes has been attracting much attention in recent decades. The emergence of novel materials and processing at the nanoscale that make use of the special properties of substances by controlling their atoms and molecules at the nanolevel has enabled the synthesis of new materials and yielded a breakthrough in a form of technology that had more or less been in limbo. Now that nanotechnology is one of the promising fascinating technologies in both scientific and technological areas in this century. Its applications are foreseen to reach beyond materials and devices to a wide range of fields, including biotechnology, materials science, information technology, and environment, with a better understanding of fundamental phenomena at a nanometer scale.

Accordingly, numerous advanced techniques have been successively developed. They can be generally classified into two approaches for the construction of nanostructured materials. One is "top-down" procedure. Semiconductor microchips are the typical products prepared by photolithography technique for

dwindling size of designed circuit. But technical problems and the costs required for the improvement of nanoscale resolution remain to be solved. On the contrary, "bottom-up" assembly is based on the ordered arrangement of atoms and molecular building blocks into integrated larger levels with the use of self-assembling properties of specific molecules. The well-defined structures are spontaneously fabricated under the right conditions, which are commonly known as "supramolecules." Supramolecular architecture has been tentatively studied as a key role promising nanotechnology directing biomimetic molecular organization systems, i.e., "molecular recognition–directed molecular assembly" phenomena categorized by Lehn [1]. In contrast to molecular chemistry, which is predominantly based on the covalent bonding of atoms, supramolecular chemistry is based on intermolecular interactions, i.e., on the association of two or more building blocks, which are held together by intermolecular bonds. Intermolecular interactions are the ubiquitous and fundamental phenomena for highly specific biological processes, such as the substrate binding with enzymes or receptors, the formation of protein complexes, the intercalation complexes of nucleic acids, the decoding of the genetic code, neurotransmission processes, and cellular recognition (immunology). A better understanding of the energetic and stereochemical characteristics of these non-covalent, multiple intermolecular interactions (electrostatic forces, hydrogen bonding, van der Waals forces, hydrophobic interactions, etc.) within defined structural areas should allow the design of artificial receptor molecules, which bind the substrate strongly and selectively by forming (tailored) supramolecules of defined structure and function.

Recently, a number of attempts have been devoted to construct highly ordered particle assemblies. This is because textured surfaces of strictly controlled periodicity and morphology are to be expected due to their potential use in many areas of science and technology. Random and periodic roughness on a submicrometer scale length can be used to produce a variety of optical elements such as gratings, interferometers, and antireflection coatings. Selective solar absorbers utilize surfaces textured on a micrometer scale, and textured surfaces can also have an important role in photovoltaics. Particle assembling is a particle deposition technique to form a two- or three-dimensionally ordered structure for the development of highly functionalized materials and devices.

In this chapter we first sketch important interactions carried out in the fabrication of particle assemblies. The chapter mainly addresses three aspects of polymer particle assembly from the viewpoint of the establishment of "supraparticles." The first aspect is the basic ideas concerning intermolecular and interparticular interactions that play important roles in the particle assembling process. The second objective is the surface modification procedures applied in the fields of self-assembled monolayers and Langmuir-Blodgett film preparation. Finally, several methods and contemporary topics of the fabrication of supraparticular assemblies will be introduced.

II. FORCES ACTING BETWEEN A SURFACE AND A POLYMER PARTICLE

Four forces govern our everyday life: gravitational, electromagnetic, and strong and weak nuclear forces. Because bodies decay differently with distance, the interaction between two bodies is usually dominated by only one or two of these forces. While the motion of massive bodies is dictated by gravitational forces, interactions within the nucleus are dominated by strong and weak nuclear forces. Between these two extreme of scale, interatomic and intermolecular interactions are dominated by electromagnetic forces. These forces dominate over a range spanning from 0.10 nm to 1 μm; they are not only important between individual molecules and atoms, but also in the short-range interaction between large bodies. The latter are usually known as surface forces. They determine the wetting, adhesion, and lubricant properties of materials and dominate the interaction between objects whose size is close to the range of intermolecular forces. The interaction between a latex particle and a (macroscopic) surface will then be governed by such forces.

When several atoms firmly bind to form a molecule, the forces involved in bond formation are referred to as covalent bonds. Obviously, covalent bonding is of primary importance to the nature of molecules. While covalent bonds are strong and short range in the sense that they act over bond distances of about 0.1–0.2 nm, they are restricted in the range of their actions. They may be considered, as a first approximation, strictly chemical forces. They are, in effect, limited to the interactions between atoms involved in molecular formation and chemical reactions. Most covalent bond energies fall in the range of about 150–900 kJ mol^{-1} ($\approx$100–300 kT), and generally decrease in strength as the bond length increases.

On the other hand, in most systems involving surface and colloidal phenomena, one is not so much concerned with intramolecular forces as with intermolecular (or interatomic) forces acting between discrete, nonbonded atoms or molecules over distances significantly greater than molecular bond dimensions (tens to thousands of nanometers). They are therefore generally unidirectional, nonstochiometric, long-range forces. Interactions due to long-range forces are sometimes referred to as "physical" interactions, implying that no formal chemical reaction is involved. While physical interactions do not, in general, involve electronic transformations analogous to covalent bond formation, they can, under some circumstances, be equally strong.

Intermolecular interactions [2] are of fundamental importance in understanding how atoms and molecules organize in liquids and solids, such as the micelle formation from charged surfactant molecules [3,4]. In contrast to molecular chemistry, which is predominantly based on the covalent bonding of atoms, supramolecular chemistry is constructed on the basis of intermolecular interac-

tions, i.e., on the association of two or more building blocks held together by intermolecular bonds. Intermolecular interactions are the foundation for highly specific biological processes, such as the substrate binding with enzymes or receptors, the formation of protein complexes, the intercalation complexes of nucleic acids, the decoding of the genetic code, neurotransmission processes, and cellular recognition (immunology). The exact understanding of the energetic and stereochemical characteristics of these non-covalent, multiple intermolecular interactions within defined structural areas should allow the design of artificial receptor molecules, which bind the substrate strongly and selectively by forming (tailored) supramolecular structures, "supramolecules," of defined structure and function.

In colloid science, dispersion/aggregation or stabilization/destabilization of charged particles is an important theme. Several theoretical approaches have been carried out to clarify the forces that rule the colloidal stability. It was stated that the fundamental physical forces controlling the nonchemical or physical interactions among atoms and molecules are of two kinds, i.e., coulombic (or electrostatic) interactions and those lumped together under the general term van der Waals forces. The first, coulombic interaction involving at least one formally charged species, will be covered in the following section. Another is commonly termed van der Waals forces, comprising three types of interactions.

Although our aim is to understand interactions at interfaces, it must be remembered that an interface is nothing more than a collection of individual atoms or molecules, and that its macroscopic properties will be a reflection of the interactions of all of the individual atomic or molecular interactions involved. Therefore, we will begin the discussion by addressing the question of the source and nature of the various types of interactions experienced by individual units (atoms or molecules), followed by an integration of those interactions over all of the units in the nature.

A. Coulombic Forces or Electrostatic Interactions

Coulombic interactions are by far the strongest of the physical interactions, equaling and exceeding the magnitude of covalent bonds. The interaction between two oppositely charged atoms or molecules is the strongest form of physical interaction to be considered in colloidal systems. For two point charges Q_1 and Q_2, the free energy of interaction $w(r)$ is given by the following equation.

$$w(r) = \frac{Q_1 Q_2}{4\pi\varepsilon_0\varepsilon_r r} = \frac{z_1 z_2 e^2}{4\pi\varepsilon_0\varepsilon_r r} \tag{1}$$

where ε_0 is the permittivity of a vacuum or free space, ε_r is the relative permittivity or dielectric constant of the medium, and r is the distance between the two charges. The right-hand form of the equation is commonly used, where the two

value of Q can be readily specified in terms of the sign and valency of each ion, z, and the elementary charge, e (= 1.602×10^{-19} C) (coulombs).

The force of the coulombic interaction, F_c, is the differential with respect to r of the free energy.

For the charges of the same sign, both $w(r)$ and F will be positive, which means that the

$$F_c = \frac{dw(r)}{dr} = \frac{Q_1 Q_2}{4\pi\varepsilon_0\varepsilon_r r} = \frac{z_1 z_2 e^2}{4\pi\varepsilon_0\varepsilon_r r} \tag{2}$$

interaction will be repulsive; for unlike charges they will be attractive. In terms of magnitude, the force (where attractive or repulsive) is at maximum when the distance of separation r is a minimum, i.e., when the two ions are in contact and r equals the sum of the two ionic radii. For example, for a sodium and chloride ion in contact, r will be ≈ 0.276 nm, and the binding energy will be

$$w(r) = \frac{(-1)(+1)(1.602 \times 10^{-19})^2}{4\pi(8.854 \times 10^{-12})(0.276 \times 10^{-9})} = -8.4 \times 10^{-19} \text{ J} \tag{3}$$

Throughout the following discussions, reference will be made to a standard unit of the thermal energy, kT, where k is Boltzmann's constant and T is absolute temperature (K). The reference energy at room temperature ($\approx$300 K) will be $kT = (1.38 \times 10^{-23})\ (300) = 4.1 \times 10^{-21}$ J. The energy of the sodium and chloride atom interaction, then, is approximately $200kT$. Obviously, coulombic interactions must be considered to be at least equal in strength to covalent bonds.

B. van der Waals Interactions

Most of interfacial phenomena are influenced to various extents by forces that have their origin in atomic and molecular level interactions caused by induced or permanent polarities associated with the electric fields of neighboring molecules or by instantaneous dipoles resulting from the positions of the electrons around the nuclei. These are known as van der Waals interactions, and they play a major role in determining material properties and behavior important in colloid and surface chemistry. The van der Waals forces contain several contributions. One is the quantum mechanical dispersion interactions (London term). The second term arises from the thermally averaged dipole–dipole interaction (Keeson term) and a third contribution comes from dipole-induced dipole interactions (Debye term). The van der Waals force operates between different apolar and polar molecules and varies rather little between different materials. The London dispersed force is the most fundamental and universal force, and although generally the weakest of the three in absolute terms, it is often the most important contributor to the total van der Waals interaction. Dispersion forces

are of quantum mechanical origin but can be interpreted in more immediate concepts. The electrons in a molecule move quickly compared to the nuclei and the electrical field changes due to the surrounding molecules. However, there are fluctuations in the electron density of molecule regardless of the surroundings, i.e., fluctuations also occur in vacuum. These give rise to momentary dipoles which in turn generate electrical fields. For two argon atoms these two fields can, in analogy with the induction term, interact and give rise to an attraction. It is the correlated movement of electrons that is the source of the dispersion energy. It is always present and is responsible for the attraction between noble gas molecules. The magnitude of the dispersion interaction between two molecules is approximately proportional to the product of their polarizability.

C. DLVO Theory

As seen above, the forces acting between a colloid and a surface are usually classified according to their range. The well-known Derjaguin-Landau-Verwey-Overbeek (DLVO) theory [5,6] (Fig. 1), explains colloidal stability by a simple combination of two interactions; the repulsive electrostatic double-layer force and the attractive van der Waals force. It could predict, for example, why some colloidal systems agglomerate while others do not. Furthermore, phenomena involving deposition of colloidal particles are divided into two distinct regimes:

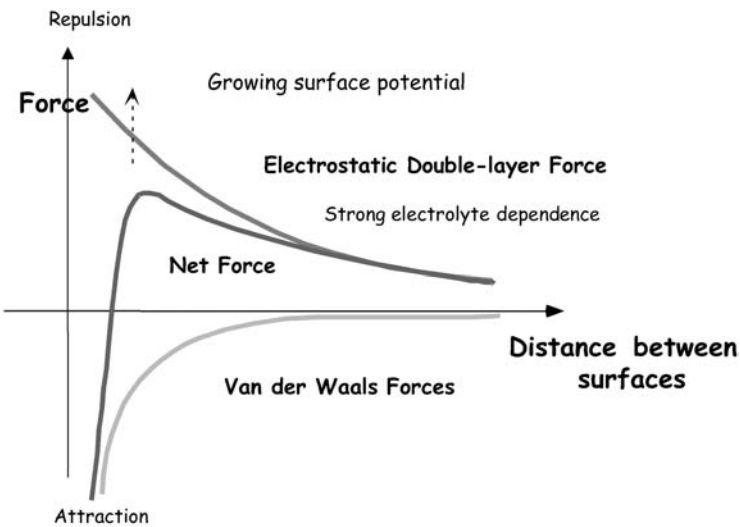

FIG. 1 DLVO principle. The net interaction curve is formed by subtracting the attraction curve from the repulsion curve.

(1) the reasonably well-understood regime of favorable deposition or aggregation, where particle–particle or particle–wall interactions are purely attractive (fast regime), and (2) the unfavorable regime in the presence of a repulsive barrier, which still keeps defying quantitative understanding [7]. DLVO underestimates the initial deposition rates in a wide range of ionic strength by many orders of magnitude. The discrepancies observed between theory and experiments are certainly due to the main assumption of the nondiscreteness of matter (continuum) integrated in the DLVO approach where surfaces are supposed smooth with homogeneous charge distributions [8,9]. An indication of the length scale of such heterogeneity is given in a recent study of the aggregation of weakly charged particles [10]: DLVO theory represents a remarkably accurate description at low ionic strength, as the distance of the repulsive barrier from the surface exceeds a couple of nanometers, but it fails at closer distances. A similar situation occurs when the deposition process is followed beyond early stages. The case of favorable deposition is again reasonably well understood. The deposition is slowed down by blocking of the available surface area by previously adsorbed particles. The quantitative features of this effect, including its dependence on ionic strength, are well described by the random sequential adsorption (RSA) model [11]. An incomparably good picture of the surface coverage in the presence of an energy barrier is lacking, and the most likely reason for this deficiency is again the heterogeneity of the surface.

D. Hydrogen Bonding

A hydrogen atom bound to a strongly electronegative atom, e.g., fluorine (F), nitrogen (N) and oxygen (O) will cause the electron associated with the hydrogen to be displaced toward the electronegative atom. Here the interactions become much more complex and are given the more specific descriptive name "hydrogen bonding" interactions. This results in an enhanced attractive interaction in the condensed state. Molecules undergoing this special hydrogen bonding interaction form a special and very important class of liquids called "associated" liquids. Their nature and the nature of their interactions with other species is of great importance in many practical areas of surface and colloid science, chemistry in general, biology, and so on. For example, water has a considerably higher melting, boiling point, and a latent heat of evaporation in comparison with other low molecular weight molecules, which arise from the characteristics of the hydrogen bonding. Besides, the extraordinary phenomena, such as the maximum density of at 4°C, the lighter in a solid state than in a liquid state is the specific character due to the structured molecular association of water molecules. This oriented interamolecular interaction decreases the entropy of the system, which plays an important role in hydrophobic interactions discussed in the following section.

E. Hydrophobic Interactions

Hydrophobic interactions [12] are perhaps the most important interactions in the organization of the constituent molecules of living matter into complex structural entities such as cell membranes and organelles. It is equally important in the formation of detergent micelles and other phenomena that occur in aqueous solution. The importance of water's unique physical properties and of its unique solvent power, especially for ions, has been frequently cited; however, the equal importance of its unique lack of solvent power for many nonpolar substances has received far less attention. For the interaction between water and methane, the geometrical mean approach predicts a van der Waals constant of 120 whereas experimental values lie more in the range 60–70. That tells us that methane molecules and water molecules greatly prefer to interact with their "own kind." Conventionally, this mutual "dislike" is referred to as the hydrophobic effect.

As mentioned in the above section, the interactions between water molecules are comparably strong due to the hydrogen bonds. Hence, introducing a nonpolar molecule into water strongly disturbs the hydrogen bond network with a loss of interaction energy. The loss of energy can be minimized if the water molecules around the solute adjust themselves, but the price has to be paid in lowered entropy. As a consequence, one usually finds that the free energy of transfer of a nonpolar molecule into water at room temperature contains a large entropy contribution. When nonpolar molecules, are dissolving, they try to minimize the damage to the water hydrogen bond network by aggregating. The hydrophobic interaction can be of considerable strength and is a delicate balance of energetic (enthalpic) and entropic terms.

F. Capillarity

Capillary effects are encountered in many areas of interface and colloidal science, with its importance relative to other processes (e.g., fluid dynamics) depending on the exact situation. For example, the dusts and foams floating on the water make contact to form larger lumps, the extent and duration of flow due to the capillary phenomenon is limited, and fluid dynamics is of little practical importance. A new interest in the capillary interaction between colloidal particles has been arisen by the experimental findings that it can produce formation of two-dimensional arrays from submicrometer particles.

Many works have been devoted to the theoretical description of the capillary forces, but because of the diversity of the approaches and configurations studied an outline is needed. Considering the floating particles on water surface, one can take into account two cases depending on the wettability of particles (Fig. 2). Now, the "capillary charge" of particle, Q, is defined as follows:

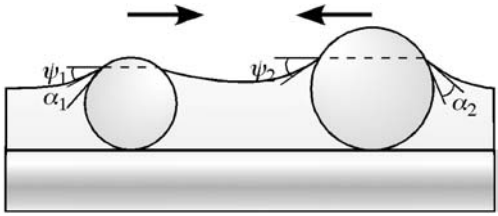

FIG. 2 Meniscus observed in the system composed of two hydrophobic particles and their mutal resulting interaction.

$$Q = rsin\ \phi \tag{4}$$

where Q corresponds to the extent of the transformation of water surface. For the case that two particles of the same hydrophobicity (or hydrophilicity) is floating at the surface of water, asymmetrical transformation of water around particles induce the unbalanced surface tension acting between particles. This situation engenders the attractive and repulsive forces for the same and different particle, respectively. Figure 2 shows the meniscus observed in the system composed from the hydrophobic particles. When r_1, $r_2 << L << q^{-1}$ (q is the capillary constant), the capillary force, F, is given by the following equation:

$$F = \frac{2\pi\gamma Q_1 Q_2}{L} \tag{5}$$

where γ is the surface tension and $q^{-1} = 2.7$ mm for water. This is why Q is called the "capillary charge" of particle. Thus, capillary force is the long-range interaction acting inverse proportionally between particles, which resembles Coulomb's law to some extent.

III. SUBSTRATE MODIFICATIONS

Self-assembled monolayers (SAMs) are defined as molecular assemblies that are formed spontaneously by the immersion of an appropriate substrate into a solution of an active surfactant in an organic solvent [13–15]. Langmuir-Blodgett (LB) films are the first technique to provide the chemist with the practical capability to construct ordered molecular assemblies. Both SAMs and LB films have received much attention because of the potential use in the wide range of fields, such as optoelectronics, molecular electronics, and biotechnology. In this section, the basic concepts for the fabrication of ordered assemblies by SAMs and LB technique will be introduced as an intelligent surface modification.

A. Self-Assembled Monolayers

SAMs are highly ordered molecular assemblies that form spontaneously by chemisorptions and self-organization of functionalized long-chain molecules on the surfaces of appropriate substrates. They are robust, relatively stable, and capable of providing the flexibility, at both the individual molecular and materials levels, required to tailor the properties of surfaces. There are several types of SAMs constructed from alkanethiolates on gold, alkylsilane compounds with glass substrates, and so on. The first report on SAMs is the oriented monolayers of dialkyldisulfides on gold surfaces by Nuzzo and Allara [16]. As gold is not easily oxidized under ordinary conditions, most of the works has been carried out on gold substrate [17–21]. SAMs of alkanethiols on gold can be easily fabricated by spontaneous adsorption of alkanethiols onto gold. Even though the fate of the hydrogen atom and the exact nature of resulting species on gold are not completely understood, the following reaction scheme is generally accepted.

$$RS - H + Au_n^0 \rightarrow RS^- - Au^+ \bullet Au_{n-1}^0 + \frac{1}{2}H_2 \tag{6}$$

Detailed works by Bain's group revealed that the thiol group forms the strongest interaction with the gold surface over all the head groups. Kinetic analysis of formation of alkanethiol monolayers on gold surface estimated from contact angle measurement showed that alkanethiols with longer alkyl chains tend to form stable SAMs due to the strong van der Waals interactions between alkyl chains. In the same manner, it is possible to create a monolayer with controlled chemistry using alkylsilane molecules that could self-assemble on glass substrates following the process described in FIG. 3.

The structures of alkanethiol or alkylsilane SAMs have been well characterized by means of grazing angle Fourier transform infrared (FTIR) spectroscopy and ellipsometry. Grazing angle FTIR is a powerful tool for estimating the orientation of alkyl chain in SAMs on reflecting metallic surfaces due to the strong

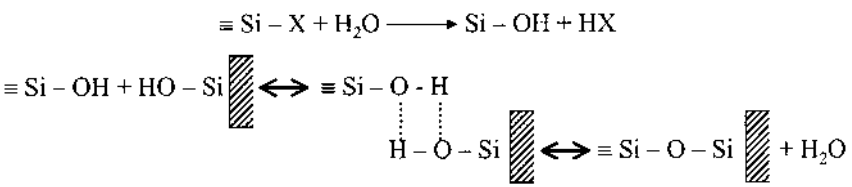

FIG. 3 Chemisorption of alkylsilane on silica surfaces. In the first step, the organosilane is hydrolyzed by water, which is either preadsorbed on the surface or present in the solvent. In the second step, the hydrolyzed silane is adsorbed via hydrogen bonds and can react with the surface silanol groups at the surface to form a silozane Si-O-Si bond.

polarization normal to the metal surface. Nuzzo's group clarified that the tilt angle of the chain axis from the normal in thiol monolayers on gold was estimated to be on the order of about 20–35°. Increase in film thickness per methylene group ($-CH_2$) measured by ellipsometry is 1.3 Å, which is in good agreement with the theoretical data by taking into account of tilt angle (about 20–30°).

Recently, practical application of SAMs has been tentatively developed in interface engineering and microfabrication. Microcontact printing (μCP) is one of the excellent examples to transfer a pattern of alkanethiol molecules to the gold substrate. The alkanethiol assembles rapidly into an ordered monolayer on the surface. Contact printing with alkanethiols on gold can generate patterned SAMs with lateral dimensions as small as 100 nm. Although various attempts have been made for preparation of defect-free SAMs on gold, they utilize the highly localized regions of disorder in SAMs at the edge of steps in topographically patterned evaporated metal films. This topographically directed etching "TODE" methodology makes it possible to generate patterned SAMs with 50 nm of lateral dimensions on curved silver surfaces as well as the planar surfaces (Fig. 4).

B. Langmuir-Blodgett Films

Langmuir-Blodgett films have received much attention from the viewpoint of functional ultrathin films. The LB technique provides uniform films with controlled thickness and well-defined molecular orientation. So far, LB films have been prepared with amphiphilic compounds, such as long-chain fatty acids and dyestuff with long hydrocarbon chains. Water-insoluble amphiphiles dissolved in a volatile solvent are spread at the water surface, following a compression of monolayer to form a stable condensed monolayer at the air–water interface. The solvent that evaporates leaves a monolayer of the molecules in what is called a

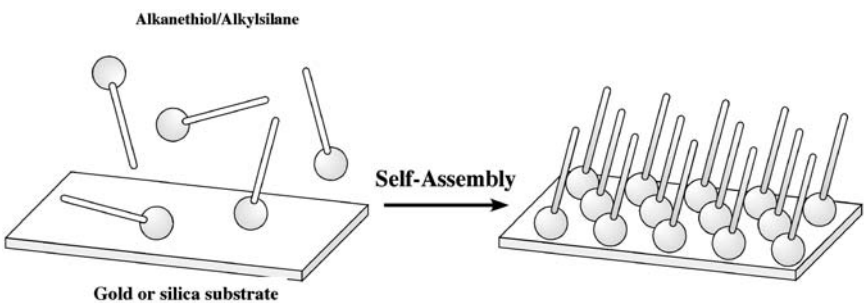

FIG. 4 Schematic view of the self-assembling process.

two dimensional gas phase due to the relatively large distances between the molecules. Monolayer at the air–water interface can exist in different physical states, analogous to the gaseous, liquid, and solid states of matter in bulk. Information regarding these states and the transitions between them can be obtained by measuring the surface pressure (π) of monolayer as a function of surface concentration. The surface pressure is defined as the lateral pressure that must be applied to prevent the film from spreading. However, even when a surface pressure approaches zero, surfactant molecules have a natural tendency to aggregate. Surface concentration may be measured directly on the basis of how much amphiphilic molecule has been deposited on the surface. Measurements are made on a large planar surface, and are often reported in terms of plots of π vs. the available area per molecule (A), which is the reciprocal of the surface concentration. As the barrier moves the molecules are compressed, the intermolecular distance decrease, the surface pressure increases, and, in the case of stearic acid, a phase transition can be observed in the isotherm. This first phase transition is assigned to a transition from the gaseous to the liquid state. When the barrier compressed the film further, a second phase transition can be observed from the liquid to the solid phase. Limiting surface area for one molecules of amphiphile can be determined by extrapolating the steep rise in the π-A isotherm to zero surface pressure. In the condensed solid state, the molecules are closely packed and uniformly oriented. If additional pressure is applied on the monolayer, it collapses due to the mechanical instability, and a sharp decrease in the pressure is observed. This collapse pressure is a function of temperature, pH of the subphase, and the speed with which the barrier is moved (Fig. 5).

Langmuir-Blodgett films are prepared by deposition of monolayers at the air–water interface onto solid substrates under a certain surface pressure. There are several methods to transfer a monolayer from the air–water interface onto a

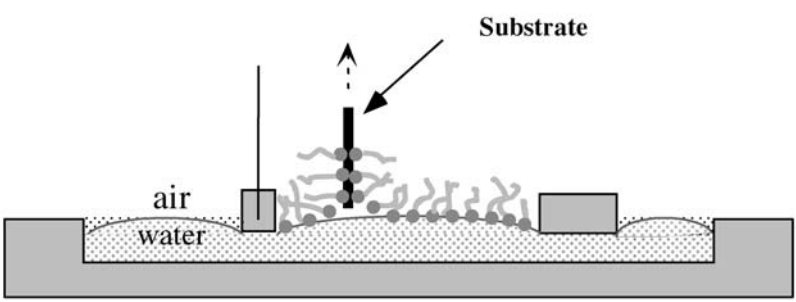

FIG. 5 Lateral view of a Langmuir-Blodgett trough.

solid substrate. The conventional method developed by Blodgett and Langmuir is the *vertical deposition*.

They demonstrated that a monolayer of amphiphiles at the air–water interface could be deposited onto a solid support by the vertical displacement of the substrate. The second method is known as *horizontal lifting*, developed by Schaefer and Langmuir, which is useful for the fabrication of monolayer of protein.

When a substrate is moved through the monolayer at the air–water interface, the monolayer can be transferred onto solid supports during emersion or immersion. Three types of LB film structure can be obtained by the vertical dipping method. A monolayer usually will be transferred during retraction when the substrate surface is hydrophilic, and the hydrophilic head groups interact with the surface. On the other hand, if the substrate surface is hydrophobic, the monolayer will be transferred in the immersion, and the hydrophobic alkyl chains interact with the surface. If the deposition process starts with a hydrophilic substrate, it becomes hydrophobic after the first monolayer transfer, and thus the second monolayer will be transferred in the immersion. This is the usual mode of multilayer formation for amphiphilic molecules in which the head group is very hydrophilic and the tail is an alkyl chain (Fig. 6).

This mode is called the Y-type deposition. However, it was reported, in the early papers of Langmuir and Blodgett that films also can be formed only in

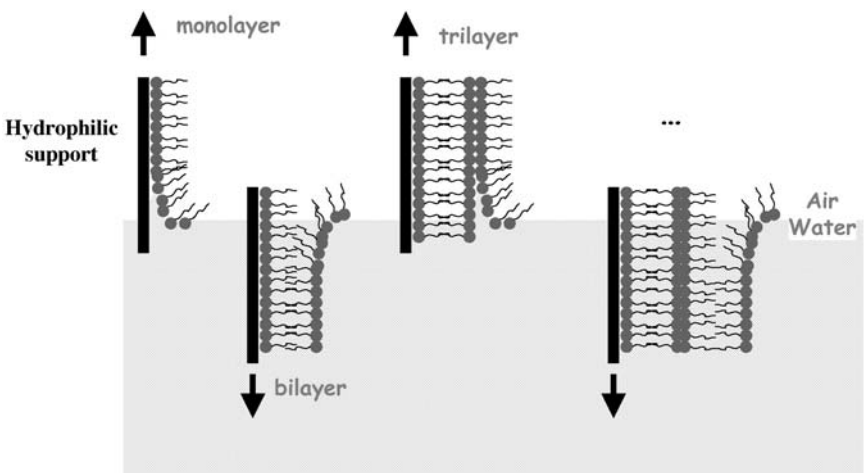

FIG. 6 Creation of multilayers onto a hydrophilic substrate using the LB trough vertical deposition approach (see text). For hydrophobic surfaces, the processes are similar with the hydrophilic heads replaced by the hydrophobic tails.

downstroke (X type), and that deposition speed may affect the deposition mode. A third possible deposition is when films are formed in upstroke only (Z type). These are cases where the head group is not so hydrophilic or where the alkyl chain is terminated in a weak polar group.

Since Kuhn's group investigated the mechanisms of energy migration and photoinduced electron transfer by incorporation of cyanine derivatives with long alkyl chains into LB films, several attempts have been carried out to develop photoelectrochemical devices based on LB technique in these decades [22–26]. However, these LB films composed of monomeric compounds have poor stability to mechanical and thermal treatment, as well as poor resistance to dissolution by organic solvents. In order to overcome these disadvantages, efforts to prepare polymer LB films have been made. Miyashita *et al*. found that poly(*N*-alkylacrylamides) with long hydrocarbon chains have superior film forming properties [27]. They investigated practical applications of polymer LB films by copolymerization with photoeclctrochemical functional monomers [28–34]. Because hydrogen bonds are formed between neighboring amide groups in poly(*N*-alkylacrylamide) LB films, in contrast with conventional amphiphile LB films stabilized by hydrophobic effect and van der Waals interaction between hydrocarbon chains, it has been assumed that crystallization of alkyl chains and dyes is effectively suppressed.

IV. PARTICLE ASSEMBLY PROCESSES

Textured surfaces of strictly controlled periodicity and morphology are useful as a consequence of their potential use in many areas of science and technology. Random and periodic roughness on a submicrometer scale length can be used to produce a variety of optical elements such as gratings, interferometers, and antireflection coatings. Selective solar absorbers utilize surface textured on a micrometer scale length and textured surfaces can also play an important role in photovoltaics. Particle assembling is a particle deposition technique to form a two- or three-dimensionally ordered structure for the development of highly functionalized materials and devices. While the simplest way to fabricate particle arrays is to spread a thin layer of a particle dispersion onto a substrate or air–water interface, following the drying process of a spread particle dispersion, it is the uncontrolled procedure to assemble particles into the two- or three-dimensionally packed arrays. Recently, a number of investigations have been tentatively devoted to organization of randomly dispersed particles.

A. Electrostatic Adsorption

Before discussing electrostatic particle deposition onto the substrate, it is worth mentioning the electrostatic deposition of polymer films carried out by Decher

and Kunitake's group, in which they demonstrated that multilayer film could be prepared from the alternate adsorption of polyanion and polycation onto the substrate by electrostatic interactions [35–43]. The principle of multilayerd assembling is as follows: a solid substrate with negatively charged surface is immersed in a solution containing cationic polyelectrolyte, and a layer of polycation is adsorbed via electrostatic attraction. Since adsorption is carried out at relatively high concentrations of polyelectrolyte, a number of cationic groups remain exposed to the solution; thus, the surface charge is effectively reversed. After being rinsed in water, the substrate is immersed in a solution containing anionic polyelectrolyte. A new polymer layer is adsorbed, but now the original surface charge is restored. By repeating these steps, alternating multilayer assembly is obtained. Kunitake's groups measured the assembling process by UV absorption spectroscopy and quartz crystal microbalance (QCM) technique (Fig. 7). QCM is expected as powerful tool for a sensitive mass detection of deposited monolayers onto the QCM electrode. Frequency of oscillating piezoelectric quartz crystal linearly decreases the mass of the immobilized elements onto the QCM plate surface. The QCM is connected to an oscillator circuit, and the frequency changes are followed by a universal counter attached to a microcomputer system. Increment of transferred mass Δm can be calculated from frequency shift ΔF according to Sauerbrey's equation, which has been well established on AT-cut shear mode QCM.

$$\Delta F = -\frac{2NF_0^2}{A_E\sqrt{\rho_q \mu_q}}\Delta m \tag{7}$$

where F_0 is the parent frequency of QCM, A_e is the electrode area, N is the overtone number, ρ_q is the density of quartz, and μ_q is the shear modulus of quartz.

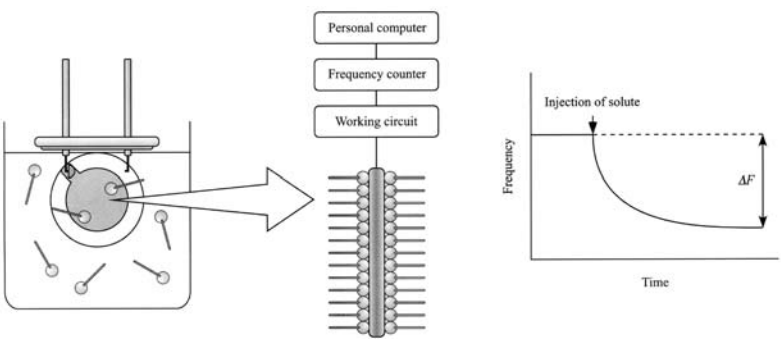

FIG. 7 Schematic view of the quartz crystal microbalance (QCM) system.

The controlled assembly and coagulation of colloidal particles into patterned structures through electrophoresis deposition offers a simple method for the construction of materials with designed microscopic architectures. Akashi's group investigated electrostatic adsorption of polystyrene nanospheres onto the surface of an ultrathin polymer film prepared by using alternate adsorption technique [44,45]. Quantitative and kinetic analysis of particle adsorption processes was carried out by using QCM and scanning electron microscopy (SEM). They demonstrated that anionic polystyrene nanospheres could be adsorbed onto the outermost film surface, which was deposited by using the alternate adsorption technique by electrostatic interaction without three-dimensional aggregation. It was clarified that the dependence of particle deposition amounts against NaCl concentration in polymer precursor film preparation was a sigmoid curve, indicating that there is a critical charge on/in the film for their adsorption.

B. Fluid-Mediated Dynamic Process

As mentioned in the above section, fluid dynamics is one of the key factors for assembly of smaller particles up to micrometer size, where gravity has slight effect except for keeping the film surface planar. Actually, particle assembly onto a substrate through dynamic process has been achieved by several groups. It is worth mentioning that liquid films with water as solvent are commonly employed in these methods, in which thickness of the liquid film is prominently controlled by the balance between the film separation pressure and the wettability of the particle wall.

Burmeister's group presented a novel parallel method for producing nanometer structures on arbitrary surfaces that leaves a surface almost free of contaminants and is easy to apply, according to Micheletto's procedure. Firstly, a drop of diluted colloidal suspension was applied to the slightly tilted substrate, followed by the evaporation of the excess water that took place in a closed chamber. The evaporation process stopped several hours later, leaving a close-packed polycrystalline monolayer on the surface. The obtained hexagonally ordered monolayers of colloid particles were floated off on a water surface from the glass substrate under the constant dipping velocity. Water penetrated the gap between the colloidal monolayer and the glass substrate to strip off and remain in the monolayer at the water surface. After this step, the colloidal monolayer was transferred to the substrate by touching it with the horizontally held substrate. The lithographic masks produced in this manner could be applied to hydrophobic WSe_2 surface and the copper-made TEM grid. Burmeister attempts to utilize this nano-structured material for quantum dots [58].

Nagayama reported the mechanism of formation of two-dimensional crystals from latex particles on substrates [46–51]. The dynamics of two-dimensional ordering of micrometer-sized polystyrene latex spheres on a horizontal glass substrate has been directly observed by means of optical microscopy. It has

been demonstrated that the particles located in the meniscus region begins to move toward the ordered zone and upon reaching the boundary of the array are incorporated into the hexagonal closed-packed structured phase through the microscopic observation of dynamics of the particle ordering process. They pointed out that the main factor governing the particle ordering is the attractive capillary force due to the menisci formed around particles during water evaporation. Theoretical equations of lateral capillary forces acting between colloidal particles have been derived from the viewpoint of flotation and immersion lateral capillary forces according to the thickness of the liquid film.

They quantitatively analyze the continuous formation of two-dimensional particle arrays to clarify the factors. From their pioneering works, it was elucidated that the growth process depends on three parameters shown in the following equation:

$$\eta = 1 - \varepsilon = \beta \frac{j_e}{V_c h} \frac{\phi}{1 - \phi} = \frac{K}{h} \qquad K = \frac{\beta j_e \phi}{V_c (1 - \phi)} \tag{8}$$

where η ($= 1 - \epsilon$) is the porosity of the arrays, j_e is the evaporation flux from a pure water surface, V_c is the array growth rate, and ϕ is the particle volume fraction in the suspension. Under the assumption that h (average thickness of the arrays) is equal to the distance from the substrate to the tops of the particles, this equation is the most important connection determining the relationship between ϵ, η, and h. Hence, K can be calculated by these three parameters; η is in inverse proportion to h with K value as a coefficient. This equation indicates that the array density cannot be indiscriminately determined when h is taken as a variable. In other words, the particle array has an irregular thickness as far as either the thickness or the density is placed in a restriction condition. For the case of the suspension particles in a liquid layer on a substrate, the lateral capillary force gives the restriction to the system.

Picard's groups developed the novel procedure for continuous production of layered protein or particle assemblies, called dynamic thin laminar flow [52–54] (DTLF). The glass-made cylinder, which is covered by a 5-μm thin liquid film and a particle suspension, rotates at 300 μm above a hemicylindrical PTFE trough filled with buffers injected through channels. The transferred particle monolayer is successfully laid down onto a solid surface at a relatively rapid rate (2 cm/s) while traveling over it. While the size of the particle two-dimensional crystal did not reach spectacular limits, this method has advantages for the quality of the monolayer uniformity as important criteria.

C. Langmuir-Blodgett Technique

Fujimoto's group applied LB technique to deposition of polystyrene particle onto the glass substrate [55,56]. Their unique feature is that unsymmetrical mod-

ification of particle could be performed under the rotational limitation of particles at the air–water or the liquid–solid interface. In the case of the air–liquid interface method, first a monolayer of anionic cross-linked polymer particles was prepared on a water surface; then positively charged polymer particles were introduced into the subphase. Through these steps, unsymmetrical binding of cationic particles to the hemisphere of the anionic particles was achieved. On the other hand, in the case of the liquid–solid interface method, the transferred anionic particle monolayer on the glass substrate was immersed in the cationic particle dispersion to allow the unsymmetrical modification. SEM observation revealed that the cationic particles could be successfully imprinted onto the limited region of the oppositely charged polymer particle. They expected that the asymmetrically modified conjugated particles possess the large dipole moment, which will be useful for design and synthesis of two- or three-dimensional structured devices in a wide variety of fields. Hazot et *al.* [57] have shown that is possible to deposit and highly organize hydrophilic latex particles (see Section V below) on hydrophilic substrates using the LB approach. Indeed, they have changed the hydrophilic nature of the water surface by predepositing one monolayer of amphiphilic stearic acid molecules to get a sort of *hydrophobic water surface* able to *support* and *organize* the latex particles. They were then transferred onto the plane support to obtain a two-dimensional hexagonal compact array of latex with a very high specific area (Fig. 8).

D. Electrophoresis

It has long been recognized that both electrostatic repulsive force and steric (or enthalpic) stabilization contribute to colloidal stabilization mechanism. In gen-

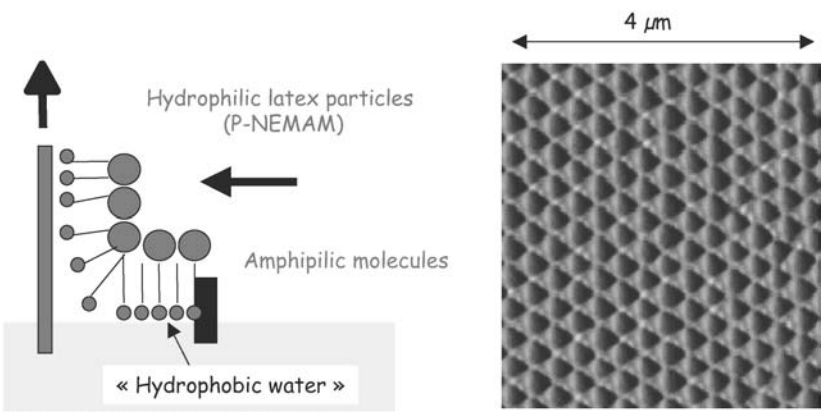

FIG. 8 Heganonal compact array of microgel particles obtained using the LB deposition approach via a "hydrophobic" water layer.

eral, dispersed particles carry a surface electrical charge, so that the repulsive interaction of their respective double layers provides the necessary energy barrier for kinetic stability. In general, a high amount of charged or polar groups can be effectively introduced at the particle surface to gain the stability of dispersion, especially for the case of polymer particles synthesized by emulsion polymerization process. It is the matter of course that electrophoresis is an excellent method for organizing colloidal particles into two-dimensional assemblies [58–62]. As electrophoresis is the phenomenon in which a charged particle migrates in an electric field; the technique is applied for the measurement of ζ-potential of particle. Recently, an electrohydrodynamic methodology has been developed that makes possible the precise assembly of two- and three-dimensional colloidal assays on electrode surface. In this section, some of the electrophoretic particle deposition procedures will be introduced.

Mulvaney's group reported the electrophoretic deposition of citrate- and alkanethiol-stabilized gold colloids onto carbon-coated copper [63,64] grids. They demonstrated that the monolayer of gold colloid is built up of a large number of smaller crystalline domains, each containing 50–200 particles in the form of hexagonally close packed colloid particles and that the monolayer is consisted from these individual domains to form a large crystalline monolayer at an applied positive voltage of 50 mV. On the other hand, the gold colloids desorbed when a cathodic bias of −50 mV was applied. The mechanism of growth of the lattices was investigated by varying the time of polarization in the solution. Microscopy observation showed the existence of the particle clustering from the beginning of the polarization, flowed by the convergence and coalescence of the individual domains. While it is not clear that what kind of attractive force exist between adsorbed gold particles, they suggest that the diffuse layer of repulsion between the negatively charged gold colloid particles is reduced upon adsorption due to shielding of the surface charge by the positive charge on the carbon electrode, thereby facilitating coalescence. It has been also confirmed that the equilibrium antiparticle spacing depends on the thickness of the stabilizer chain length.

Aksay's group has investigated the field-induced layering of colloidal crystals. Silica ($d = 900$ nm) and polystyrene (2 μm) particles are electrophoretically deposited onto a transparent indium tin oxide (ITO) anode electrode coupled to an optical microscope from a dilute suspension. In neither case, the particles adhere to the electrode surface and continue to move in two dimensions through Brownian agitation at relatively weak electric field (~0.5 V). On the contrary, the particle move toward one another across the electrode surface with a sufficiently strong applied voltage (0.5 ~ 1.5 V) in the same manner observed by Richetti *et al*. As is clarified that the strength of the lateral attraction between particles can be adjusted by changing the magnitude of the current, they demonstrated the mono- and multilayers of colloidal particles are successively assembled under the control of dc and low-frequency ac fields. With the dc-field

assembly, the rate of arrival of particles through electrophoretic deposition, R_E, was slow relative to the lateral motion of particles toward other particles on the surface, R_L, due to the lateral attraction force. It has been also revealed that R_E depends mainly on the particle charge and the magnitude of the electric field in the bulk solution and that R_L depends mostly on the current density passing through the particle layer. Their detailed investigation indicates that manipulation of the R_E/R_L ratio control the size of the domains, thereby allowing formation of variety of packing geometries from amorphous to highly crystalline. Particles, however, are compressed in the direction of the filed when the strong dc voltage is applied, particles coagulate with little or no adhesion to the electrode, which indicate the possibility to remove a coagulated sheet of colloidal material by reversing the polarity of the electrode. The procedure, "field-induced annealing", has the effect of sequentially melting ("shaking") and freezing the crystallized colloidal layer until all of the particles are present in the required packing arrangement.

E. Self-Assembly

Since the discovery that alkanethiols will displace practically and impurity on a gold surface and will spontaneously create an ordered monolayer of high quality, interest in these systems has been extensive [65–68]. While extending self-assembly to larger components, such as colloids, and micrometer-scale objects, is a comparatively new research field, a number of attempts have been devoted to extend SAMs beyond the prototype of gold/thiol systems in these days. Pioneering works have been tentatively carried out by Whitesides *et al.* [69–77]. They reported several types of the assembly of objects into ordered arrays or units, namely mesoscopic self-assembly (MESA). As an example of MESA using micron-scale objects is the electrostatic assembly of gold cylinders onto a gold surface patterned with two different alkanethiols terminated in $-COO^-$ and $-NMe_3^+$. The cylindrical gold units are covered with a SAM terminated in $-PO_3H_2$. The cylinders selectively assembled onto regions terminated in $-NMe_3^+$.

It was found that latex polymer particles containing sulfonium groups were successively assembled into highly ordered two-dimensional monolayers by Taniguchi's group. Figure 9 shows the SEM photograph of latex polymer particles assembled onto the gold substrate. Oppositely to the case observed in fluid-mediated particle assembling technique, cationic polymer particles were spontaneously assembled into the tetragonal packed monolayer, due to the strong electrostatic repulsive forces between particles. These particles are also assembled onto the curved hydrophobic surfaces.

Figure 10 is a SEM photograph of the hetero coagulated polystyrene core particles with shell latex particles, which shows that core polystyrene particles are uniformly covered with shell particles. The control of various interactions,

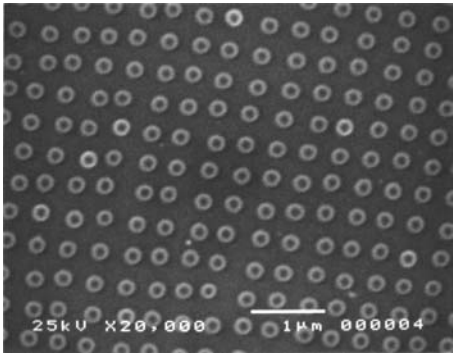

FIG. 9 SEM image of latex polymer particles assembled onto the gold substrate.

such as electrostatic interactions, van der Waals forces, and hydrophobic interactions, between particles and substrates will no doubt be the essential for the fabrication of particle assemblies based on self-assembling technique.

F. Manipulation

There are few techniques of manipulation for small objects, such as cell operation, under optical observation until 1990. Since it was demonstrated that each atom could be individually deposited by using scanning tunneling microscopy (STM) or atomic force microscopy (AFM), which have been originally developed for high-resolution microscopic observation, STM and AFM have been expected as powerful tools for contacting manipulation technique in this decade.

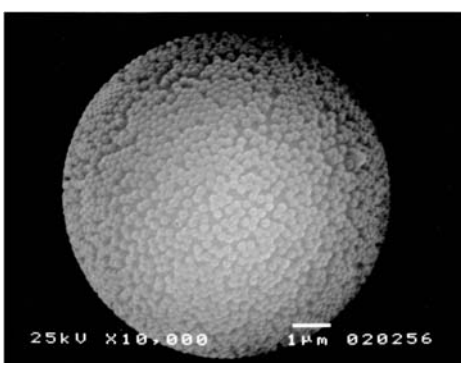

FIG. 10 SEM image of the hetero-coagulated polystyrene core particles with shell latex particles.

The extent of the particle size which can be manipulated is ranging from the atomic and molecular level (1 Å) to over millimeter size. Particle assembling through the manipulation process is the plainest way to organize particle arrays, even though there are disadvantages for large-scale production. As the general ideas and procedures for each objective particles have been established, it seems that each manipulation will spread as a common technique for the development of particular devices. Miyazaki and co-workers have succeeded in deposition of 2 μm sized polymer particles to organize two-dimensional arrays under SEM [78] observation. Because of the highly ordered structure with regular periodicity as wavelength, these arrays have photonic crystal characters. AFM is also used for manipulation of smaller particles with 10 ~ 100 nm diameter. Junnno demonstrated that Semi-conductive GaAs particles are selectively arrayed on the substrate two dimensionally to construct alphabetic [79] characters. It is expected that nanometer sized particle arrays will bring the quantum effect in near future. On the other hand, non-contact laser manipulation technique was applied for particle deposition in fluid systems. It should be noted that a number of particles are effectively captured and assembled at one time by laser manipulation technique, which is impossible by contact manipulation technique (APM or AFM) in current [80].

V. BIOMEDICAL APPLICATIONS

Two dimensional latex particle assemblies can be efficiently used in the biomedical area, from simple diagnostic tools to more complex biosensor devices. The large assortment of latex particles suitable for the immobilization of various proteins in their active form, currently available in the academic and industrial world, offers the possibility to form 2 dimensional constructions appropriate for the controlled immobilization of specific antibodies or antigens.

The best example known as an excellent bio-medical device constructed from assembled particle is the biosensor for a sensitive detection of biomolecules, where the specific bond between the antibody and the antigen is popularly utilized. Fore example the modification of the several wells or channels present on the surface of an ELISA diagnostic test (ensyme-linked immunosorbent assay) in which immuno- and enzymatic reactions take place (Fig. 11).

The 2D latex assemblies tethered onto the side wall of the wells increase notably the sensitivity of the test either via an increase of the number of conformation available to the immobilized proteins leading to a better accessibility of the reactive sites or directly through an increase of the effective surface area of the wells.

Hazot et *al*. [81–84] have shown that is possible to prepare a two-dimensional array of hydrophilic thermosensitive latex particles with very high specific area bearing functional group able to interact with the support (silica) or

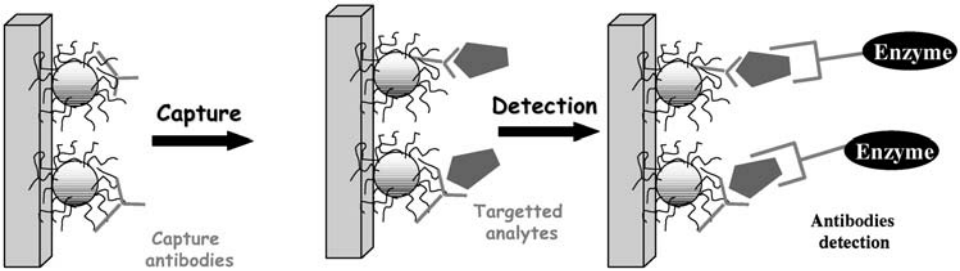

FIG. 11 Schematic principle of the ELISA test based on functionalized microgel particles.

with the surrounding biomolecules. The microgel particles were made from *N*-ethylmethacrylamide (NEMAM) monomer by radical precipitation polymerization with ethyleneglycoldimethacrylate (EGDMA) as hydrophobic cross-linker (Fig. 12). The particle surfaces were functionalized with phenylboronic acid methacrylamide groups known to form stable cyclic ester complex with the *cis*-diol groups of saccharidic molecules but also able to covalently react with the hydroxyl groups present on the silica surfaces. In that case, the degree of coverage, $\theta_c = 65\%$, exceeds greatly the random adsorption limit ("jamming limit" [85]), $\theta_J = 54\%$, due to the possibility of lateral movement or desorption of the particles before the irreversible chemisorption [86]. Furthermore, the nonhexagonal noncompact structure of the particle assembly leads to a 50% increase of the specific area with regard to the case of bare latex particles. Such an organiza-

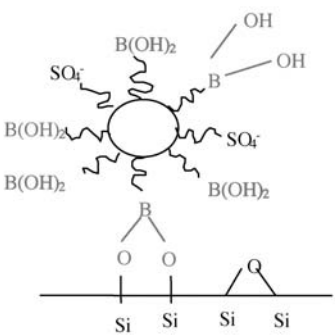

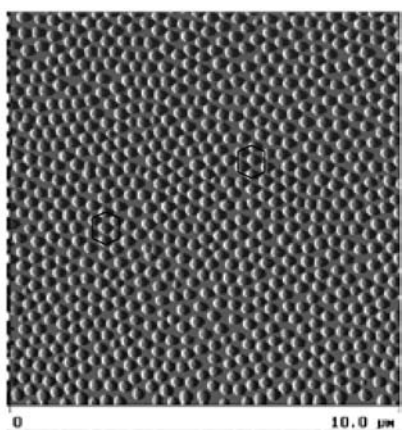

FIG. 12 Functionalized P-NEMAM particles chemisorbed on silicon substrates.

tion should greatly increase the sensitivity of an ELISA test. It should be noted that the dimension between the particles is commensurate with UV-visible wavelength and such a system could have optical applications as well.

As optical measurements, such as the ELISA and fluorescence microscopy observations, are necessary for detection of the specific reaction in general, more convenient devices are now under investigation. Velev's group proposed the following method [87]: IgG and anti-IgG molecules are labeled on latex particles and gold colloids, respectively. Immunoactive latex particles are collected via dielectrophoresis between planar electrodes. If IgG molecules immobilized on colloidal gold bind with anti-IgG on latex particles, the latex particles assembled between electrodes will be covered with an electron-conductive gold layer, resulting in the difference of resistance. For the practical use of this conjugated array, a metastable solution of silver salts is introduced to deposit a silver layer on top of the gold by nucleation with the intention of improving the coverage between gold spheres. The resistance of the electrode bridge is constantly low with decreasing IgG concentration, and the resistance diverges up to 10^3 Ω for an IgG amount of about 2×10^{-4} M or less, which indicates that the limit of detection of the sensor is in the range 2×10^{-13} to 2×10^{-14} M under unoptimized conditions.

VI. CONCLUSIONS

The above-mentioned examples for the application of particle assembling technologies involve the construction and characteristics of the highly ordered particle arrays for medical applications. Although large gaps remain between the present organization and ideal intelligent devices resembling biological systems, the fundamental techniques have reached the advanced stage for assembling the various types of functional particles for well-defined assemblies. We will refer to the following subjects to organize the biomedical materials from the individual particles as future prospects. First, particles should be designed as assembling parts. Because each biomolecule has different chemical and physical properties, the proper functional groups must be introduced into a particle according to the interaction between the particle and the targeting position of biomolecules. In addition, the smaller the particle, the more important the surface properties and the character that atoms and molecules have by themselves, which are never seen in bulk. Although it goes without saying that a technique for controlling size and size distribution must be established, the previous material concepts, divided into organic, inorganic, and biochemical materials, should be united from the viewpoint of particle design. Second, the simpler industrial production techniques should be explored for practical use of assemblies. In most cases, there is considerable room for improvement of the size and the reproducibility in particle assembling process. A mechanical engineering approach seems to be more important for effective mass production of a particle assay. Third

and last, we must find a way to control the spatial arrangement of each functional particle in the assembly. The biomembrane is the crucial model whereby each protein exhibits complicated functions by the ingenious spatial arrangement in a thinner bilayered structure. The extraction of the intelligent mechanism hindered in biosystems will be utilized for the application of particle assemblies via chemical, biological, optical, and electric technologies. The development of the selective deposition based on lithography is just beginning.We are convinced that particle assembly composite will open the doors to the future nanoworld [88].

REFERENCES

1. Lehn, J.-M. Toward self-organization and complex matter. Science **2002**, *295* (5564), 2400–2403.
2. Israelachvili, J.N. *Intermolecular and Surface Forces*: *With Applications to Colloidal and Biological Systems*; Academic Press: San Diego, 1985.
3. Fitch, R.M. *Polymer Colloids*: *A Comprehensive Introduction*; Academic Press: San Diego, 1997.
4. Myers, D. *Surfaces*, *Interfaces*, *and Colloids*; Wiley: New York, 1999.
5. Derjaguin, B.V.; Landau, L.D. Theory of the stability of strongly charged lyophobic sols and of the adhesion of strongly charged particles in solutions of electrolytes. Acta Physicochim. URSS, **1941**, *14*, 633–652.
6. Verwey, E.J.; Overbeek, J.T.G. *Theory of the Stability of Lyophobic Colloids*; Elsevier: Amsterdam, 1948.
7. Grant, M.L.; Saville, D.A. Electrostatic interactions between a nonuniformly charged sphere and a charged surface. J. Colloid Interface Sci. **1995**, *171* (1), 35–45.
8. Thun, C.; van de Ven, T.G.M. Deposition of hairy latex particles onto a glass surface. Colloids Surf. A Physicochem. Eng. Asp. **1998**, *145* (1–3), 205–212.
9. Chapel, J.-P. Electrolyte species dependent hydration forces between silica surfaces. Langmuir **1994**, *10* (11), 4237–4243.
10. Ehrens, S.H.; Borkovec, M.; Schurtenberger, P. Aggregation in charge-stabilized colloidal suspensions revisited. Langmuir **1998**, *14* (8), 1951–1954.
11. Adamczyk, Z.; Warszynski, P. Role of electrostatic interactions in particle adsorption. Adv. Colloid Interface Sci. **1996**, *63*, 41–149.
12. Tanford, C. *The Hydrophobic Effect*: *Formation of Micelles and Biological Membranes*, 2nd Ed.; Krieger, 1980.
13. Ulman, A. *An Introduction of Ultrathin Organic Films*: *From Langmuir-Blodgett to Self-Assembly*; Academic Press: San Diego, 1991.
14. Issacs, L.; Chin, D.N.; Bowden, N.; Xia, Y.X.; Whitesides, G.M. Self-assembling systems on scales from nanometers to millimeters: design and discovery. In *Supramolecular Materials and Technologies*; Reinhoudt, D.N., Ed.; Wiley: New York, 1999: 1–46.
15. Vögtle, F. *Supramolecular Chemistry*; Wiley: New York, 1993.
16. Nuzzo, R.G.; Allara, D.L. Adsorption of bifunctional organic disulfides on gold surfaces. J. Am. Chem. Soc. **1983**, *105*, 4481–4483.

17. Ulman, A.; Tillman, N. Self-assembling double layers on gold surfaces: the merging of two chemistries. Langmuir **1989**, *5*, 1418–1420.
18. Ulman, A.; Eilers, J.E.; Tillman, N. Packing and molecular orientation of alkanethiol monolayers on gold surfaces. Langmuir **1989**, *5*, 1147–1152.
19. Nuzzo, R.G.; Fusso, F.A.; Allara, D.L. Spontaneously organized molecular assemblies. 3. Preparation and properties of solution adsorbed monolayers of organic disulfides on gold surfaces. J. Am. Chem. Soc. **1987**, *109*, 2358–2368.
20. Porter, M.D.; Bright, T.B.; Allara, D.L.; Chidsey, C.E.D. Spontaneously organized molecular assemblies. 4. Structual characterization of *n*-alkyl thiol monolayers on gold by optical ellipsometry, infrared spectroscopy, and electrochemistry. J. Am. Chem. Soc. **1987**, *109*, 3559–3568.
21. Bain, C.D.; Evall, J.; Whitesides, G.M. Formation of monolayers by the coadsorption of thiols on glod: variation in the head group, tail group, and solvent. J. Am. Chem. Soc. **1989**, *111*, 7155–7164.
22. Möbius, D. Designed monolayer assemblies. Ber. Bunsenges Phys. Chem. **1978**, *82*, 848–858.
23. Kuhn, H. Synthetic molecular organizates. J. Photochem. **1979**, *10*, 111–132.
24. Kuhn, H. Electron transfer in monolayer assemblies. Pure Appl. Chem. **1979**, *51*, 341–352.
25. Kuhn, H. Information, electron and energy transfer in surface layers. Pure Appl. Chem. **1981**, *53*, 2105–2122.
26. Yamazaki, I.; Tamai, N.; Yamazaki, T. Electronic excitation transfer in organized molecular assemblies. J. Phys. Chem. **1990**, *94*, 516–525.
27. Miyashita, T.; Mizuta, Y.; Matsuda, M. Studies on Langmuir-Blodgett multilayer formation from preformed poly(*N*-alkylacrylamides). Br. Polym. J. **1990**, *22*, 327–331.
28. Yatsue, T.; Miyashita, T. Elecrtron-transfer quenching accompanied by highly efficient energy migration in polymer Langmuir-Blodgett films. J. Phys. Chem. **1995**, *99*, 16047–16051.
29. Miyashita, T.; Suwa, T. Highly ordered structure in polymerizable *N*-alkylacrylamide LB films. Thin Solid Films **1996**, *284/285*, 330–333.
30. Li, X.; Aoki, A.; Miyashita, T. Spreading behavior of poly(*N*-(polyfluoroaklyl)-acrylamide) monolayers and Langmuir-Blodgett film formation. Langmuir **1996**, *12*, 5444–5447.
31. Aoki, A.; Miyashita, T. Electrochemical characterization of redox polymer Langmuir-Blodgett films containing ferrocene derivatives. Macromolecules **1996**, *29*, 4662–4667.
32. Taniguchi, T.; Yokoyama, Y.; Miyashita, T. Spreading behavior of short-branched *N*-alkylacrylamide polymers and the formation of Langmuir-Blodgett films. Macromolecules **1997**, *30*, 3646–3649.
33. Taniguchi, T.; Fukasawa, T.; Miyashita, T. Photoelectrochemical response of polymer Langmuir-Blodgett films containing tris(2,2′-bipyridine)ruthenium complex. J. Phys. Chem. **1999**, *103*, 1920–1924.
34. Aoki, A.; Abe, Y.; Miyashita, T. Effective photoinduced electron transfer in heterodeposited redox polymer LB films. Langmuir **1999**, *15*, 1463–1469.
35. Decher, G.; Hong, J.D. Buildup of ultrathin multilayer films by a self-assembly

process: I. Consecutive adsorption of anionic and cationic bipolar amphiphiles. Makromol. Chem. Macromol. Symp. **1991**, *46*, 321–327.
36. Decher, G.; Hong, J.D. Buildup of ultrathin multilayer films by a self-assembly process: II. Consecutive adsorption of anionic and cationic bipolar amphiphiles and polyelectrolytes on charged surfaces. Ber. Bunsen-Ges. Phys. Chem. **1991**, *95*, 1430–1434.
37. Decher, G.; Hong, J.D.; Schmitt, J. Buildup of ultrathin multilayer films by a self-assembly process: III. Consecutively alternating adsorption of anionic and cationic polyelectrolytes on charged surfaces. Thin Solid Films **1992**, *210/211*, 831–835.
38. Lvov, Y.; Decher, G.; Möhwald, H. Assembly, structual characterization and thermal behavior of layer-by-layer deposited ultrathin films of poly(vinylsulfate) and poly(allylamine). Langmuir **1993**, *9*, 481–486.
39. Lvov, Y.; Hass, H.; Decher, G.; Möhwald, H.; Mikhailov, A.; Mtchedlishvily, B.; Morgunova, E.; Vainshtein, B. Successive deposition of alternate layers of polyelectrolytes and charged virus. Langmuir **1994**, *10*, 4232–4236.
40. (33) Lvov, Y.; Ariga, K.; Ichinose, I.; Kunitake, T. Assembly of multicomponent protein films by means of electrostatic layer-by-layer adsorption. J. Am. Chem. Soc. **1995**, *117*, 6117–6123.
41. (34) Ariga, K.; Lvov, Y.; Kunitake, T. Assembling alternate dye-polyion molecular films by electrostatic layer-by-layer adsorption. J. Am. Chem. Soc. **1997**, *119*, 2224–2231.
42. (35) Lvov, Y.; Ariga, K.; Kunitake, T. A careful examination of the adsorption steps in the alternate layer-by-layer assembly of linear polyanion and polycation. Colloid Surf. A **1999**, *146*, 337–344.
43. (31) Lvov, Y.; Essler, F.; Decher, G. Combination of polycation/polyanion self-assembly and Langmuir-Blodgett transfer for the construction of superlattice films. J. Phys. Chem. **1993**, *97*, 13773–13777.
44. Serizawa, T.; Akashi, M. Accumulation of cationic-polymer grafted poly(styrene) nanospheres onto an anionic-polymer surface. Chem Lett. **1997**, 809–810.
45. Serizawa, T.; Takeshita, H.; Akashi, M. Electrostatic adsorption of polystyrene nanospheres onto the surface of an ultrathin polymer film prepared by using an alternate adsorption technique. Langmuir **1998**, *14*, 4088–4094.
46. Denkov, N.D.; Delev, O.D.; Kralchevsky, P.A.; Ivanov, I.B.; Yoshimura, H.; Nagayama, K. Two-dimensional crystallization. Nature **1992**, *361*, 26.
47. Denkov, N.D.; Delev, O.D.; Krakchevsky, P.A.; Ivanov, I.B.; Yoshimura, H.; Nagayama, K. Mechanism of formation of two-dimensional crystals from latex particles on substrates. Langmuir **1992**, *8*, 3183–3190.
48. Kralchevsky, P.A.; Nagayama, K. Capillary forces between colloidal particles. Langmuir **1994**, *10*, 23–36.
49. Nagayama, K. Two-dimensional self-assembly of colloids in thin liquid films. Colloid Surf. A **1996**, *109*, 363–374.
50. Dimitrov, A.S.; Nagayama, K. Continuous convective assembling of fine particles into two-dimensional arrays on solid surfaces. Langmuir **1996**, *12*, 1303–1311.
51. Dushkin, C.D.; Kralchevsky, P.A.; Paunov, V.N.; Yoshimura, H.; Nagayama, K. Torsion balance for measurement of capillary immersion forces. Langmuir **1996**, *12*, 641–651.

52. Picard, G.; Nevernov, I.; Alliata, D.; Pazdernik, L. Dynamic thin laminar flow method for making protein monolayers. Langmuir **1997**, *13*, 264–276.
53. Picard, G. Fine particle 2D crystals prepared by the dynamic thin laminar flow method. Langmuir **1997**, *13*, 3226–3234.
54. Picard, G. Fine particle monolayers made by a mobile dynamic thin laminar flow (DTLF) device. Langmuir **1998**, *14*, 3710–3715.
55. Fujimoto, K.; Nakahama, K.; Shidara, M.; Kawaguchi, H. Preparation of unsymmetrical microspheres at the interfaces. Langmuir **1999**, *15*, 4630–4635.
56. Nakahama, K.; Kawaguchi, H.; Fujimoto, K. A novel preparation of nonsymmetrical microspheres using the Langmuir-Blodgett technique. Langmuir **2000**, *16*, 7882–7886.
57. Hazot, P. Synthesis of poly(N-ethylmethacrylamide) thermosensitive particles functionalized with phenyl boronic acid and their immobilization on plane surfaces for biological and optical applications. PhD dissertation, Lyon 1 University, Lyon, France, 2001.
58. Burmeister, F.; Schäfle, C.; Matthes, T.; Böhmisch, M.; Boneberg, J.; Leiderer, P. Colloid monolayers as versatile lithographic masks. Langmuir **1997**, *13*, 2983–2987.
59. Giersig, M.; Mulvaney, P. Preparation of ordered colloidal monolayers by electrophoretic deposition. Langmuir **1993**, *9*, 3408–3413.
60. (51) Ghezzi, F.; Earnshaw, J.C.; Finnis, M.; McCluney, M. Pattern formation in colloidal monolayers at the air-water interface. J. Colloid Interface Sci. **2001**, *238*, 433–446.
61. (52) Hayward, R.C.; Saville, D.A.; Aksay, I.A. Electrophoretic assembly of colloidal crystals with optically tunable micropatterns. Nature **2000**, *404*, 56–59.
62. Trau, M.; Saville, D.A.; Aksay, I.A. Field-induced layering of colloidal crystals. Science **1996**, *272*, 706–709.
63. Giersig, M.; Mulvaney, P. Formation of ordered two-dimensional gold colloid lattices by electrophoretic deposition. J. Phys. Chem. **1993**, *97*, 6334–6336.
64. Giersig, M.; Mulvaney, P. Preparation of ordered colloidal monolayers by electrophoretic deposition. Langmuir **1993**, *9*, 3408–3413.
65. Deckman, H.W.; Dunsmuir, J.H. Natural lithography. Appl. Phys. Lett. **1982**, *41*, 377–379.
66. Micheletto, R.; Fukuda, H.; Ohtsu, M. A simple method for the production of a two-dimensional, ordered array of small latex particles. Langmuir **1995**, *11*, 3333–3336.
67. (58) Burmeister, F.; Schäfle, C.; Matthes, T.; Böhmisch, M.; Boneberg, J.; Leiderer, P. Colloid monolayers as versatile lithographic masks. Langmuir **1997**, *13*, 2983–2987.
68. (59) Boneberg, J.; Burmeister, F.; Schäfle, C.; Leiderer, P. The formation of nanodot and nano-ring structures in colloidal monolayer lithography. Langmuir **1997**, *13*, 7080–7084.
69. Whitesides, G.M.; Mathias, J.P.; Seto, C.T. Molecular self-assembly and nanochemistry: a chemical strategy for the synthesis of nanostructures. Science **1991**, *254*, 1312–1319.
70. Kim, E.; Xia, Y.; Whitesides, G.M. Polymer microstructures formed by moulding in capillaries. Nature **1995**, *376*, 581–584.

71. Xia, Y.; Whitesides, G.M. Soft lithography. Angew. Chem. Int. Ed. Engl. **1998**, *37*, 550–575.
72. Xia, Y.; Whitesides, G.M. Soft lithography. Annu. Rev. Mater. Sci. **1998**, *28*, 153–184.
73. Terfort, A.; Bowden, N.; Whitesides, G.M. Three-dimensional self-assembly of millimetre-scale components. Nature **1997**, *386*, 162–164.
74. Bowden, N.; Terfort, A.; Carbeck, J.; Whitesides, G.M. Self-assembly of mesoscale objects into ordered two-dimensional arrays. Science **1997**, *276*, 233–235.
75. Tien, J.; Terfort, A.; Whitesides, G.M. Microfabrication through electrostatic self-assembly. Langmuir **1997**, *13*, 5349–5355.
76. Black, A.J.; Paul, K.E.; Aizenberg, J.; Whitesides, G.M. Patterning disorder in monolayer resist for the fabrication of sub-100-nm structures in silver, gold, silicon, and aluminum. J. Am. Chem. Soc. **1999**, *121*, 8356–8365.
77. Clark, T.D.; Tien, J.T.; Duffy, D.C.; Paul, K.E.; Whitesides, G.M. Self-assembly of 10-μm-sized objects into ordered three-dimensional arrays. J. Am. Chem. **2001**, *123*, 7677–7682.
78. Miyazaki, H.T.; Tomizawa, Y.; Saito, S.; Sato, T.; Shinya, N. Adhesion of micrometer-sized polymer particles under a scanning electron microscope. J. Appl. Phys. **2000**, *88*, 3330–3340.
79. Junnno, T.; Deppert, K.; Montelius, L.; Samuelson, L. Controlled manipulation of nanoparticles with an atomic force microscope. Appl. Phys. Lett. **1995**, *66*, 3627–3629.
80. Won, J.; Inaba, T.; Masuhara, H.; Fujiwara, H.; Sasaki, K.; Miyawaki, S.; Sato, S. Photothermal fixation of laser-trapped polymer microparticles on polymer substrates. Appl. Phys. Lett. **1999**, *75*, 1506–1508.
81. Hazot, P.; Delair, T.; Elaissari, A.; Pichot, C.; Chapel, J.P.; Davenas, J. Synthesis and characterization of poly(N-ethylmethacrylamide) thermosensitive latex particles. Macromol. Symp. **2000**, *150*, 291–296.
82. Hazot, P.; Chapel, J.P.; Pichot, C.; Elaissari, A.; Delair, T. Preparation of poly(N-ethyl methacrylamide) particles via an emulsion/precipitation process: role of the cross-linker. J. Polym. Sci. A Polym. Chem. **2002**, *40*, 1808–1817.
83. Hazot, P.; Delair, T.; Elaissari, A.; Pichot, C.; Chapel, J.P. Functionalization of poly[N-ethylmethacrylamide] thermosensitive particles by phenylboronic acid. Colloid Polym. Sci. DOI 2002, 10.1007/s00396–002-0664–5.
84. Hazot, P.; Delair, T.; Elaissari, A.; Pichot, C.; Chapel, J.P. Chemisorbed thermosensitive hydrophilic latex organized on plane silica surfaces for biomedical applications, Langmuir submitted (2003).
85. Ugelstad, J.; Berge, A.; Ellingsen, T.; Schmid, R.; Nilsen, T.N.; Moerk, P.C.; Stenstad, P.; Hornes, E.; Olsvik, O. Preparation and application of new monosized polymer particles. Prog. Polym. Sci. **1992**, 17 (1), 87–161.
86. Slomkowski, S.; Kowalczyk, D.; Traznadel, M. Two-dimensional latex assemblies and their potential application in diagnostics. Trends Polym. Sci. **1995**, *3* (9), 297–304.
87. Delve, O.D.; Kaler, E.W. In situ assembly of colloidal particles into miniaturized biosensors. Langmuir **1999**, *15*, 3693–3698.

14

Polymer Colloids

Widespread and Novel Techniques of Characterization

M. LANSALOT and ABDELHAMID ELAISSARI CNRS-bioMérieux, Lyon, France

O. MONDAIN-MONVAL Centre de Recherche Paul Pascal, CNRS, Pessac, France

I. INTRODUCTION

Over the last few years, colloid polymer particles have received an increasing attention in various domains, especially in biomedical fields such as diagnosis or therapy. For instance, such particles can be used as efficient carriers for biomolecules like proteins, enzymes, or nucleic acids. The preparation of polymer particles, hydrogels, composite materials, or stimuli-responsive latexes (smart particles) such as colloidal particles containing thermally sensitive polymers have been reported in many papers, reviews, and books.

The characterization of any prepared dispersion is of great importance whatever the application envisioned, but especially in the biomedical field where reproducibility and control of dispersion properties are strong requirements. Characterization of the particles not only gives information on the main features of the dispersion (particle size and particle size distribution, colloidal stability, surface charge density, morphology, electrokinetic properties), but also opens the way to a better understanding of the mechanisms involved in formation of the particles. Consequently, macroscopic and microscopic analysis of the elaborated particles is a key point.

The aim of this chapter is to give the readers, principally those working at the frontiers of biomedical and chemical fields, the required tools and the basic knowledge in physicochemical and colloidal characterization to be able to check the colloidal properties of their dispersion and predict the interaction between the biomolecules and the particle surface. To help the readers in their process, various techniques are presented and discussed in this chapter.

II. CLEANING PROCESSES

Before the utilization of a colloidal dispersion in any biomedical applications, the composition of its continuous phase has to be well determined. This is referred to as the cleaning process, and it consists of replacing the medium originally suspending the particles by a medium of controlled composition. Indeed, the continuous phase first used as a synthesizing medium may contain the residual reactants introduced before or during the elaboration of the particles. It may also include some impurities due to the degradation of the particles during storage. These can be residual amounts of the initiator and its decomposition products, various electrolytes, surfactants, residual monomer(s), oligomers, etc. When present in the continuous phase, all of these compounds may adsorb at the surface of the particles and hide the functions that are of interest for the chemical grafting of the biomolecules. They may also be responsible for a destabilization of the dispersion. A thorough cleaning using various phase separation techniques is therefore important. There is a whole set of separation techniques available, but the ones the most commonly used in the field are centrifugation, filtration, and ultrafiltration.

A. Centrifugation

In the centrifugation process, which is the most commonly used, phase separation is induced by the difference of density between colloidal particles and their surrounding medium. The sedimentation speed V of a particle of radius r dispersed in a continuous phase of density ρ_0 and viscosity η_0 is well described by the Stokes equation:

$$V = \frac{2r^2(\rho_0 - \rho)g}{9\eta_0} \tag{1}$$

where g is the standard acceleration of the gravity and ρ is the density of the dispersed phase. From this equation it appears that the process is obviously more efficient when dealing with large particles and/or systems exhibiting a large difference of density between the particles and the continuous phase. This technique may be difficult to apply to delicate systems in which the pressure endured during the sedimentation process can lead to coalescence or irreversible aggregation of the particles. Once separated from the continuous phase, the particles can be redispersed in any continuous medium of controlled composition. Such a cycle of sedimentation–redispersion can be repeated as many times as required to lead to a complete replacement of the initial continuous phase. The gravity that induces the phase separation can be increased when working with magnetically sensitive particles (as in the case of magnetic latexes which are widely used in biomedical diagnostic applications). In that case, the sedi-

mentation process can be strongly accelerated by the presence of a small magnet at the bottom of the tube containing the dispersion. The high magnetic field region induced by the magnet attracts the particles. Therefore, suspensions of magnetic particles are much easier to separate than regular suspensions involving no magnetic materials.

B. Filtration and Ultrafiltration

This method is widely used in the field of colloidal purification since it can be applied to any type of suspension, even when the particles and the continuous phase exhibit the same density. Two filtration systems are reported and manufactured. The first relies on the use of a filtering membrane, i.e., a membrane with pores of a precise size, placed at the bottom of a cell containing the crude colloidal dispersion (Fig. 1). In order to avoid any damage of the filtration

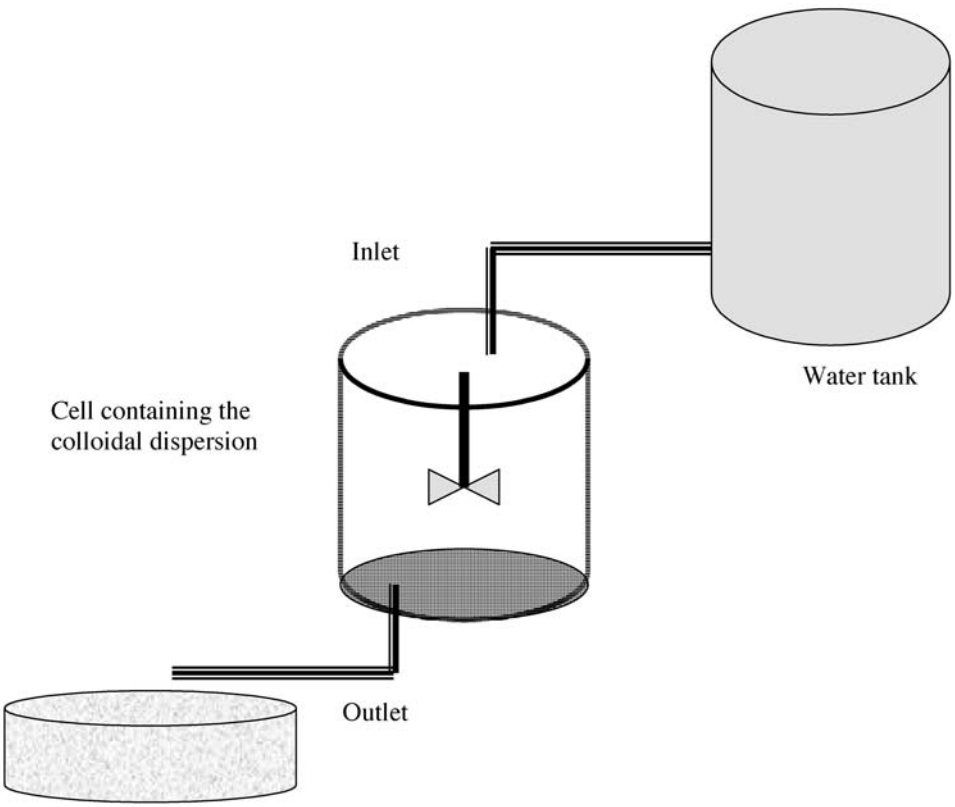

FIG. 1 Schematic representation of the filtration device.

membrane and an overpressure in the cell, the flux of the water (distilled or deionized) from the reservoir to the cell is well controlled. The efficiency of this system is principally related to the solid content of the colloidal dispersion. In addition, the progress of the cleaning process can be easily followed by measuring the conductivity of the collected filtrate as a function of time. After a given filtration period, the washed colloidal particles are directly removed from the cell. This cleaning method is well known as the serum replacement technique.

The second method is based on blood dialysis technology and is termed ultrafiltration process. Colloidal dispersion is injected in a fiber cartridge using a special pump and a well-controlled flux. The fiber cartridge is selected according to the nature of the solvent, the particle size, and the nature of the particle surface. Thanks to the pressure induced by the pump, the serum containing the impurities is expulsed from the cartridge leading to a cleaned dispersion. This cleaning system using washing cycles also induces the concentration of the colloidal particles. As for the first cleaning system, the degree of cleanliness of the colloidal dispersion can be easily followed by measuring the conductivity of the eluted filtrate as a function of washing time. When the conductivity of the eluted filtrate is close to the conductivity of the deionized water used, the cleaning process is completed. This process should be conducted slowly and carefully to prevent any aggregation of the colloidal particles.

III. PARTICLE SIZE AND PARTICLE SIZE DISTRIBUTION

A. Static Light Scattering

This technique consists of measuring the time integrated scattered intensity of a sample as a function of the scattering angle. The description is restricted here to the case of simple scattering and does not discuss the case of multiple scattering that occurs in strongly scattering systems. The scattered intensity is due to a refractive index contrast and reads:

$$I(q) = I_0 \cdot P(q) \cdot S(q) \tag{2}$$

where I_0 is the incident intensity and q the wave vector:

$$q = \frac{4\pi n}{\lambda_0} \sin\left(\frac{\theta}{2}\right) \tag{3}$$

where n is the refractive index of the continuous phase, θ the diffusion angle, and λ_0 the wavelength of the laser beam used.

$P(q)$ and $S(q)$ are called the form factor and the structure factor, respectively.

As can be expected, $P(q)$ is a function of q, which mainly depends on the shape of the scattering objects. Such function has been calculated for different shapes such as spheres, rods, or platelets. In the case of a sphere of radius R, this function reads:

$$P(q) = \left[\frac{3[\sin(qR) - qR\cos(qR)]}{(qR)^3}\right]^2 \tag{4}$$

$S(q)$ is a function that depends on the interactions between the scattering centers. If there is no spatial correlation between the different scattering elements, as for a collection of noninteracting particles (i.e., in a highly diluted suspension), this structure factor is equal to one. In such a case, the particle radius R is obtained by fitting the experimental $I(q)$ curve to Eq. (4). This principle is used in laser granulometers analyzing the particle size distribution of any dispersion. In such apparatus, the experimental $I(q)$ curve is determined and compared to the convolution of pondered form factors calculated with Eq. (4). The ponderation coefficients are here the relative contribution of the different particles to the total scattering signal. Thus, the relative number (or volume, or surface) of particles as a function of their diameter can be determined.

B. Dynamic Light Scattering

The average particle radius R_H of a collection of particles having a narrow size distribution can be easily deduced from dynamic light scattering (DLS) measurement. In a DLS experiment, one measures the time correlation function of the photoelectric current $i(t)$ detected by a photomultiplier. Such a correlation function reads:

$$\langle i(t) \cdot i(\tau)\rangle = I_0^2 \cdot [1 + \exp(-2Dq^2\tau)] \tag{5}$$

where I_0 is the scattered intensity, D the particle diffusion coefficient, and τ the time delay between the first measurement and the following ones. Such a single exponential behavior of the measured signal is observed if the particle size distribution is rather narrow. When the polydispersity exceeds a certain level, the signal is no longer a single exponential but an exponential of higher order (double, triple, etc.), and the analysis gets tricky. Let us focus here on the simplest case.

In a first-order approximation (at low particles concentration), the diffusion coefficient D can be written as:

$$D = D_0(1 + A \cdot \phi) \tag{6}$$

where ϕ is the particle volume fraction. In the high dilution limit ($\phi \to 0$), when the collection of particles can be approximated by an ideal gas of noninteracting

hard spheres, the diffusion coefficient is equal to its extrapolated value D_0 at zero sphere volume fraction (Stokes-Einstein equation):

$$D_0 = \frac{k_B T}{6\pi\eta_S R_H} \tag{7}$$

where $k_B T$ is the thermal energy and η_S the continuous phase viscosity. In Fig. 2, this technique was used to measure the hydrodynamic radius of cationic latex particles made of a polystyrene core and a cross-linked poly(*N*-isopropylacrylamide) (PNIPAM) shell as a function of temperature [1]. The decrease in the hydrodynamic diameter ($D_H = 2R_H$) is due to the gradually poorer solubility of PNIPAM as the temperature is raised. This results in a collapse of the shell, which explains the change in diameter. To compare the capacity of different latex particles to swell, referred to as the "swelling" capacity, the swelling ratio S_W is introduced:

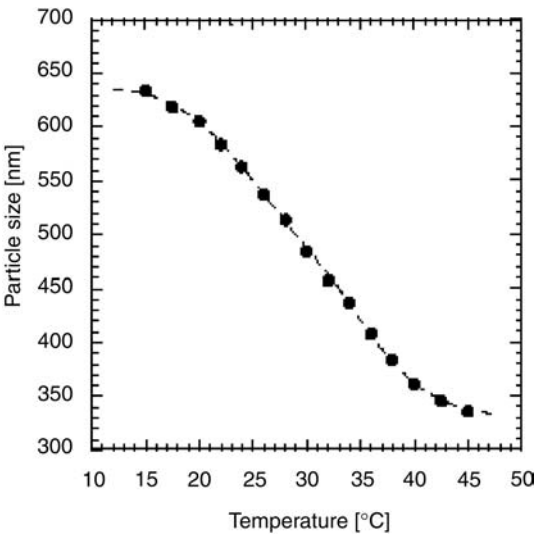

FIG. 2 Evolution of the hydrodynamic radius R_H of latex particles covered by polyNIPAM, as obtained from dynamic light scattering measurements, as a function of temperature. The observed decrease in the radius vs. the incubation temperature is due to a decrease in the solvent quality of water toward polyNIPAM, which leads to a collapse of the interfacial polymer layer.

$$S_w = \left(\frac{R_H}{R_{H,C}}\right)^3 \tag{8}$$

where $R_{H,C}$ is the hydrodynamic radius of the "collapsed" particle, i.e., the value measured at high temperature.

C. Transmission Electron Microscopy

The particle size and the particle size distribution can be analyzed using transmission electron microscopy (TEM). A small amount of a highly diluted dispersion is basically dried on the TEM grid. After the TEM visualization and the micrograph analysis using appropriate software, the number and the weight average diameters ($\bar{D}_n$ and $\bar{D}_w$, respectively) can be deduced using the following mathematical equations:

$$\overline{D_n} = \frac{\Sigma(n_i \cdot D_i)}{\Sigma n_i} \tag{9}$$

$$\overline{D_W} = \frac{\Sigma(n_i \cdot D_i^4)}{\Sigma(n_i \cdot D_i^3)} \tag{10}$$

where n_i is the number of species i with diameter D_i. The polydispersity index (PI) of the dispersion is defined by the uniformity ratio $PI = \bar{D}_w/\bar{D}_n$. Examples of TEM images are displayed in Fig. 3.

The limits of this technique are as follows: (1) it is not very well adapted for small polymer particles (typically smaller than 10 nm); (2) it can be hard to estimate the particle size in the case of microgel and core-shell particles bearing a soft polymer layer, due to the so-called "flatness effect"; (3) an accurate particle size can be determined for spherical colloids only; (4) in some cases, it is hard to get isolated particles in order to determine the particle size. In such a case, appropriate software is required.

IV. SURFACE CHARGE DENSITY

The most frequently used method to quantify the density of charges at the surface of the particles is the conductimetric titration. This method leads to both quantification and identification of the charged groups (weak or strong acid groups, for example). By contrast, this method is not suited for the determination of the amount of functions (hydroxyl, aldehyde, amide, thiol, etc.).

Before performing any measurements, colloidal particles should be carefully "cleaned" using the previously described process. In a typical experiment, a

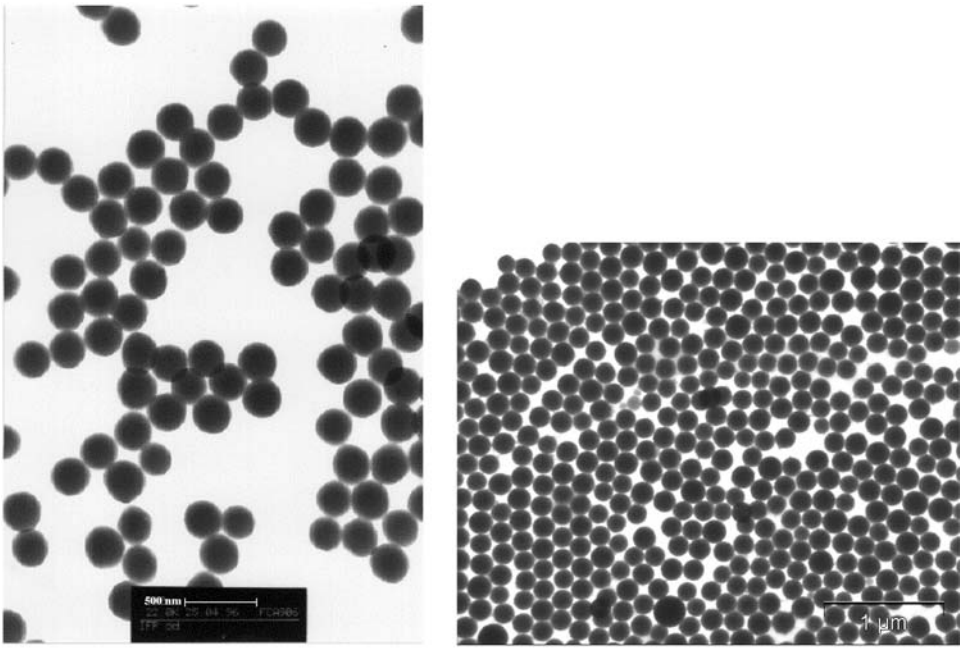

FIG. 3 TEM images of (a) a dispersion of polystyrene latex particles and (b) a magnetic emulsion containing a large amount of iron oxide.

cleaned suspension with a well-defined concentration is placed in a special glass or Teflon reservoir equipped with a magnetic stirrer. The titration is first investigated by measuring the conductivity as a function of the amount of added sodium hydroxide. For back titration, the conductivity of the dispersion is measured as a function of the volume of hydrochloric acid solution continuously added to the colloidal dispersion (Fig. 4). During the titration process, the electrodes and nitrogen inlet are immersed in the colloidal dispersion. From the conductivity vs. NaOH or HCl volume curve, the total amount of carboxylic and/or sulfate groups can be determined.

The surface charge density can also be quantified by other physicochemical methods such as nuclear magnetic resonance (NMR) or electron spectroscopy for chemical analysis (ESCA). However, these approaches imply the use of a solvent that is known to solubilize or swell the superficial polymer layer of the latex particles only (and not the particles themselves). Furthermore, these titration methods are only valid for particles having a large density of functions on

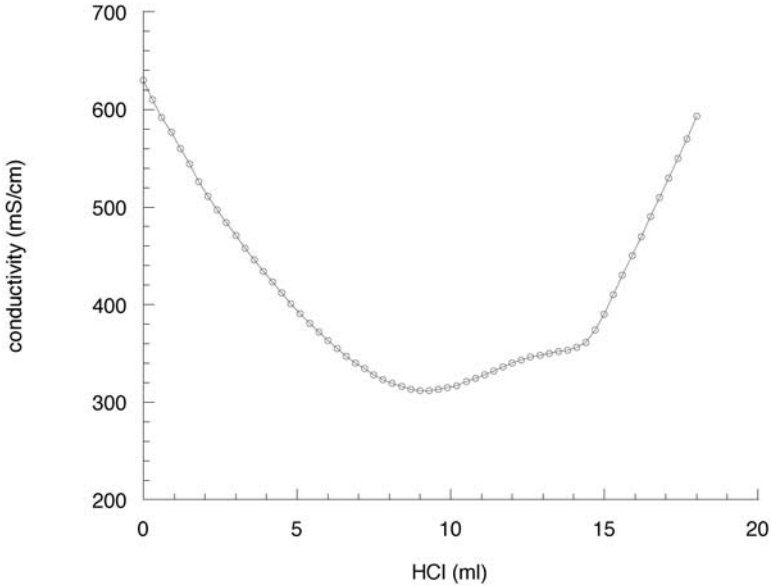

FIG. 4 Evolution of the conductivity of a suspension of composite colloidal particles bearing carboxylic groups as a function of added hydrochloric acid (back titration).

their surface or for particles composed of a large number of detectable atoms (e.g., fluorine or hydrogen for NMR).

The last method mentioned here consists in using compounds giving typical signals by UV, fluorescence, or radiolabel technique (or radioactivity) to react with reactive groups present on the particle surface. In this case, only the accessible reactive groups react with the labeled compounds. However, each new function requires setup of a new operating procedure.

Analysis of the functional groups makes use of both classical and modern physical chemistry methods. Conductimetric and potentiometric titrations remain simple and reliable quantitative methods, mostly for analyzing strong and weak acid groups. New methods have been proposed for other chemical groups, and some examples are given in Table 1.

To some extent, it is also possible to obtain direct information on the charge density of latex particles by methods based on electrophoretic mobility. Numerous instruments currently permit rapid measurement of the electrophoretic mobility (generally converted to ζ potential as discussed below) as a function of various physical parameters such as pH, ionic strength, and so forth. The surface charge density (σ) can be estimated from the relationship between the surface

TABLE 1 Surface Groups and Appropriate Analysis Methods

Surface function	Methods
SO_4^-, SO_3^-	Conductimetry and potentiometry
-COOH	Conductimetry and Potentiometry
-OH	Chemical derivatization
$-NH_2$,-SH, -CHO	Chemical reaction
Epoxy	Chemical derivatization or reaction

potential ψ_0 and the surface charge density, which is based on the Helmholtz and Gouy-Chapman equation for symmetrical electrolytes [2]:

$$\sigma = \left(\frac{\varepsilon_0 \varepsilon_r nkT}{Ze} \right) \left[2 \cdot \sin h \left(\frac{Ze\psi_0}{2kT} \right) \right] \tag{11}$$

where ε_0 is the vacuum permittivity, ε_r the dielectric constant of the bulk fluid, n the electrolyte concentration expressed in ion/m^3, Z the valency of the ion, T the absolute temperature, k Boltzmann's constant, e the electron charge, κ the inverse of the Debye length, and R the particle radius.

This approach has been largely explored in the case of model colloidal particles [3]. However, difficulties remain in establishing the true relationship between the estimated surface charge density obtained from electrokinetic measurements and the directly measured one deduced from conductimetry. In addition, the surface roughness and the morphology ("hairy"-like particles, "soft" morphologies, etc.) have to be taken into account when deducing the surface charge density.

Very recently, Fitch [4] proposed a promising method based on dielectric spectroscopy (10^{-3} to 10^6 Hz) that leads to more accurate determination of particle size, surface charge density, and level of ionization of these charges (by substituting the protons by Na^+ ions via ionic exchange). This rapid technique is applicable to a wide range of latexes and provides very interesting data on surface phenomena, especially in the case of functionalized latex particles.

An example of titration of latex particles bearing surface amine groups is depicted in the reaction scheme presented in Fig. 5. After the reaction between the amine group and the activated ester of 3-(2 pyridyldithio)propionic acid (SPDP), the excess of reagent is removed by particles separation via centrifugation. Then, after particles elimination, the reduction of the disulfide bond of the pyridine-2-thione that is released in the bulk phase can be quantified using UV light at a wavelength of 343 nm. However, the possible adsorption of SPDP or of the released pyridine-2-thione onto the surface of the particles as well as the

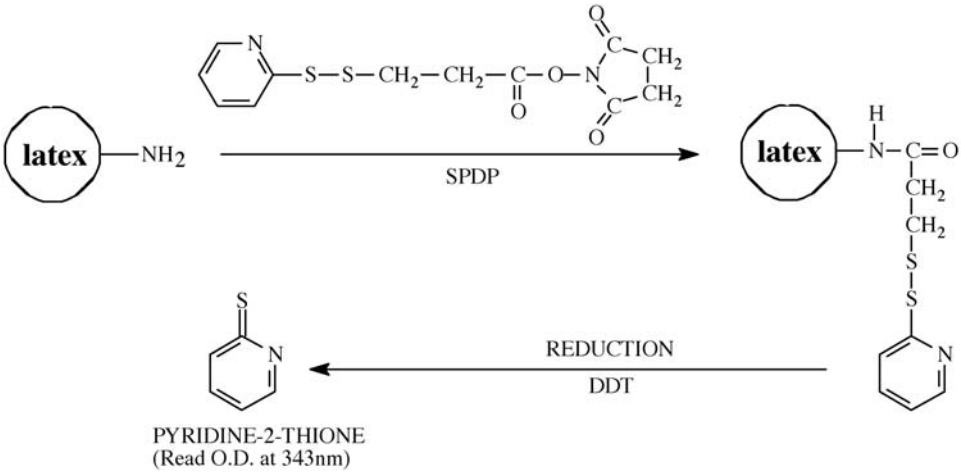

FIG. 5 Surface reaction involved for the determination of the surface charge density of amine groups at the surface of latex particles.

chemical yield of the reaction (even when performed with an excess of reactant SPDP) should be carefully controlled.

An interesting fluorescence method introduced by Locascio-Brown [5] was recently applied to obtain a direct titration of the amine groups present on the latex surface. This method is based on the chemical coupling of the amine function present at the surface of the particles with nonfluorescent molecules such as fluorescamine (Fig. 6). The resultant conjugate becomes fluorescent and can

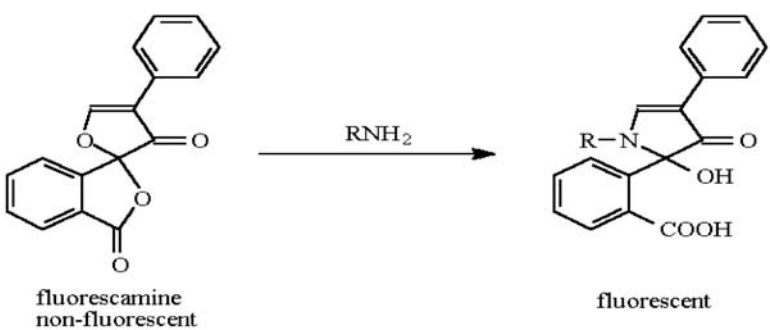

FIG. 6 Reaction involved for the surface charge density determination of the amine function. Here *R* is the colloidal particle bearing amine groups.

be easily quantified using any classical fluorimeter at an excitation wavelength of 393 nm and an emission wavelength of 477 nm.

For more details on these two complementary chemical titration methods of amine groups, the reader should consult Ref. 6.

V. MORPHOLOGY STUDY

Nowadays it is possible to elaborate or to obtain latex particles having various morphologies (Figs. 7 and 8), including relatively simple homogeneous spherical particles, core-shell type, or much more complex morphologies ("raspberry"-like, "moon"-like, etc.). Numerous extensive reviews and detailed works on the subject have been reported in discussions of experimental results [7] and morphologies predicted on the basis of various thermodynamic theories [8]. Here particular emphasis is placed on the use of microscopic techniques for morphology determination.

TEM is widely used for particle size and particle size distribution analysis, as mentioned above. In addition, this powerful technique enables one to analyze the surface morphology via shape identification, as illustrated in Fig. 7, and the particle structure. This is achieved by labeling the appropriate polymer matrix using suitable labels such as OsO_4, RuO_4, and phosphotungstenic acid (PTA).

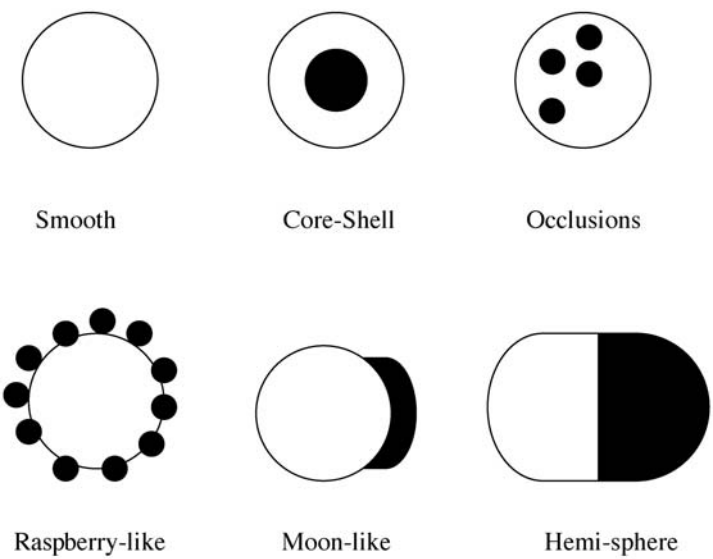

FIG. 7 Schematic representation of the different kinds of particles' morphology.

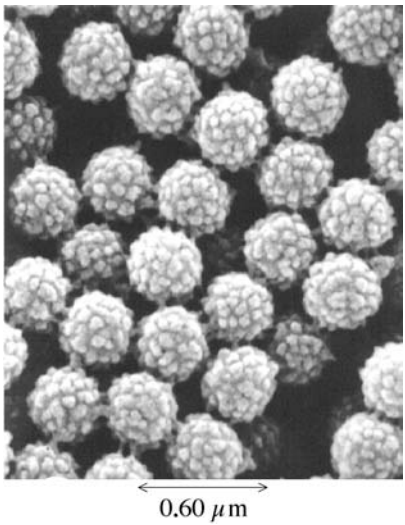

FIG. 8 SEM images of polystyrene (core)-cross-linked poly(NIPAM) (shell) microspheres. The morphology is of the "raspberry" type.

The labeling process not only leads to the exaltation of the considered polymer domain but also to the frontier identification of two polymer matrixes [7].

Scanning electron microscopy (SEM) is generally used for two main purposes: particle size analysis and surface morphology analysis. Moreover, this technique can also help the understanding of the mechanism involved in the particle formation. In the polymer colloids field, progress has been achieved by combining SEM with other techniques. For instance, the mechanism of batch radical polymerization of styrene/NIPAM in the presence of water-soluble initiator (i.e., KPS or V50) was discussed on the basis of SEM images (Fig. 8). The raspberry-like surface morphology of polystyrene (core)/poly(NIPAM) (shell) particles was attributed to the presence of poly(NIPAM) nodules originating from chains precipitation [9]. The individual conversion kinetics of each monomer combined with the observed morphology and particle number as a function of polymerization time allow the proposal of a mechanism for such emulsion–precipitation polymerization process.

In addition to TEM and SEM, atomic force microscopy (AFM) was also found to be a powerful tool for flat solid surface and colloidal dispersion analysis. In polymer colloids, AFM is widely used to investigate latex film formation and polymer particle flatness, as well as for particle morphology studies. The

surface morphology of submicrometer-sized particles can be easily determined or viewed after establishment of appropriate analysis conditions. One of the pioneering works in this area has been recently reported by Duracher et al. [9] and deals with the analysis of polystyrene latexes and polystyrene-poly(NIPAM) core-shell particles as illustrated on Fig. 9.

VI. COLLOIDAL STABILITY

A. Colloidal Forces

The problem of colloidal stability is one of the most attractive subjects from both the industrial and the academic point of view. Much research has been performed in this area, and it is not the purpose of this paper to summarize the research here. However, the interactions between colloidal particles are one of the key parameters for the stability of a colloidal suspension. If the net force acting between particles is attractive, the particles will no longer remain suspended in the continuous phase and will flocculate. By contrast, if a net repulsion takes place between colloids, they will remain as individual objects in the medium. Indeed, the net force acting between the spheres, which usually is the sum of several contributions of different nature, is essential. Besides, each of these forces is defined by a different function of the distance separating two spheres. The different forces liable to act at the colloidal level are as follows:

1. The van der Waals forces which are dispersive in origin and attractive when acting between two identical objects interacting in a continuous medium. Between two spheres of radius R separated by a distance h much smaller than R, the attractive potential reads (in a first order approximation):

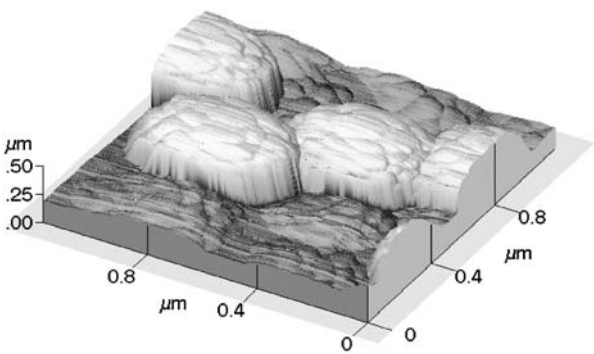

FIG. 9 Atomic force microscopy image of polystyrene and polystyrene (core)-cross-linked poly(NIPAM) (shell) microspheres.

$$U_{VdW} = -(A/12)\ (R/h) \tag{12}$$

where A is the Hamaker constant. Some values of the Hamaker constant are given in Ref. 10.

2. The repulsive electrostatic double layer forces, which are entropic in nature and take place between two charged objects immersed in a continuous medium. The expression of the force acting between two spheres can be approximated using a linear version of the Poisson-Boltzman equation and is given in the next paragraph. The expression of the repulsive force is of the type:

$$F(h) = A\ \exp(-h/\kappa^{-1}) \tag{13}$$

where A is a constant homogeneous to a force depending on the square of the surface potential, and κ^{-1} the inverse of the Debye length that is the characteristic size of the diffuse double layer. This length is a decreasing function of the electrolyte concentration in the bulk.

3. The steric forces, which are also entropic in nature and due to the presence of adsorbed or grafted molecules on the surface of the particles. Such forces are repulsive when the continuous phase is a good solvent of the adsorbed species. In such a case, the range of the repulsion and the expression of the force depend on the type of molecules present at the interface. When these are polymer chains, the range depends on the architecture of the molecules, as will be discussed below. When the continuous phase is a bad solvent of the surface molecules, the force becomes attractive.
4. The hydration forces, which are also steric in nature and due to the presence of water solvating the layer of molecules adsorbed onto the interface. These are repulsive forces that are oscillating and with ranges on the order of the size of a water molecule.
5. The attractive depletion forces that occur when a high density of objects having a much smaller size than the colloidal particles (like polymer coils or surfactant micelles, for example) are present in the continuous phase. This force is attractive and its range is on the order of the effective diameter of the small objects.
6. The attractive bridging forces that occur when polymer chains are present at the interface and when their number density is low enough to allow some of the chains to be simultaneously adsorbed onto two particles.

Of course, some of these forces can act together at the same time in a suspension, and the net force will then be the sum of these different contributions. In the next paragraph, we describe a method that allows the net repulsive force between colloidal particles to be measured as well as some results that were obtained in polymer-stabilized emulsions. Of course, the colloidal stability does not only depend on the interaction between the particles, and the reader may

find some interesting considerations about other relevant phenomena (two-dimensional rheology of the interface, surface tension, curvature effects, etc.) in other books dealing with the very complicated and much discussed matter of colloidal stability.

B. Force Measurement Between Particles

A few years ago, a new technique was set up allowing determination of the repulsive forces between magnetic emulsion droplets or magnetic latex particles. This technique exploits the anisotropy of the forces between magnetic dipoles that causes particles to form linear chains. The technique thus requires the use of monodisperse oil-in-water ferrofluid emulsions [11,12]. The resultant droplets are paramagnetic, so that the applied field induces a magnetic dipole in each drop, causing the drops to form chains. At low particle volume fraction, these one-droplet-thick chains are well separated and oriented in the field direction (Fig. 10). Due to the presence of this one-dimensional ordered structure, intense Bragg scattering is observed, enabling a precise measurement of the interdroplet distance. Moreover, because the dipolar magnetic interaction can be calculated, the repulsive forces between droplet interfaces can be measured. By varying the intensity of the applied field, the full force–distance profile can be determined.

Stable magnetic droplets can be obtained from the use of a ferrofluid. Small paramagnetic iron oxide grains (Fe_2O_3, of size around 10 nm) are dispersed and chemically stabilized in an organic or an aqueous solvent. In the first case, the ferrofluid is used to produce a direct emulsion, whereas an inverted one is obtained by mixing the aqueous ferrofluid with an organic solvent. In each case, the ferrofluid is introduced in the solvent–surfactant mixture under shear. Using

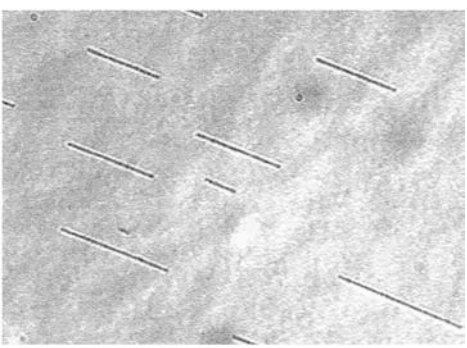

FIG. 10 Light microscopy picture of a monodisperse magnetic emulsion enduring a magnetic field. The droplets chains align in the direction of the applied field (width of the pictures 100 μm).

the analog of a fractionated crystallization technique [13], a monodisperse population of oil droplets of radius $R \approx 100$ nm can be obtained from the initially crude emulsion.

Because of their magnetic properties, the droplets align along the applied magnetic field direction. With the oil droplets' volume fraction being kept at a value lower than 0.1%, each chain can be considered as one droplet stick and the characteristic length is the core–core distance between two droplets (Fig. 11). The spacing between droplets is directly deduced from the determination of the spectral distribution of scattered light at a constant angle. For perfectly aligned particles with a separation distance d, illuminated by incident white light parallel to the chains, the first Bragg condition reduces to:

$$2d = \lambda_0/n \tag{14}$$

where n is the refractive index of the suspending medium ($n = 1.33$ for water), and λ_0 is the wavelength of the scattered light at an angle of 180°. Some representative data of the normalized scattered intensity are shown in Fig. 12. The pronounced first-order diffraction peaks are clearly observed as expected from visual observation. The droplets' surface separation h can be deduced from:

$$h = d - 2R \tag{15}$$

From that relation, it is clear that an accurate determination of R is of prime importance to get the reference state where the droplet surfaces are in contact ($h = 0$). Two methods are used to measure R: the first consists of fitting the form factor obtained from static light scattering of a very dilute emulsion. A second way is to measure the Bragg peak wavelength in a nonionic emulsion that can be considered as a hard-sphere system. In such a case, the droplets are in contact and the center-to-center distance is equal to the droplet diameter

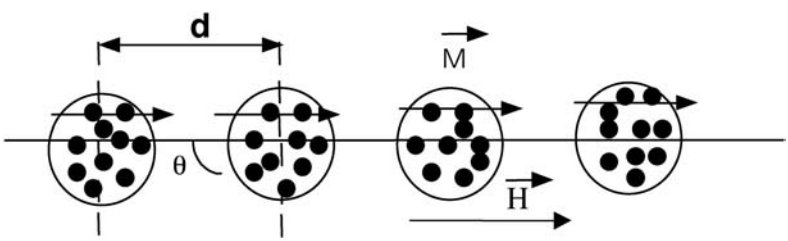

FIG. 11 Schematic of a chain of magnetic droplets in the magnetic field. Because of the magnetic field and the presence of Fe_2O_3 grains contained in each droplet, a magnetic dipole appears at the level of each droplet. A regular (d or h) spacing takes place as a consequence of the local equilibrium between attractive magnetic forces and repulsive forces due to the species adsorbed at the interfaces.

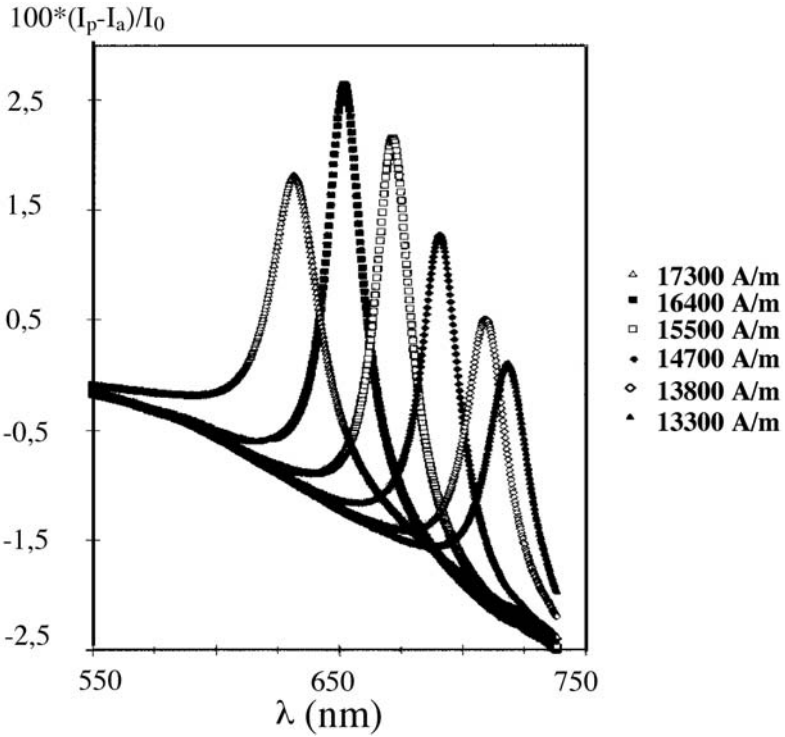

FIG. 12 Bragg scattered peaks reflecting the preferential diffusion of one particular wavelength whose value depends on the applied magnetic field intensity.

($d = 2R$). As we shall see in the next section, the two methods are in good agreement and lead, within the experimental uncertainty, to the same radius value.

The repulsive force between droplets exactly balances the magnetically induced attractive force between dipoles. Since these dipoles are aligned parallel to the field, this force can be calculated exactly and is given by:

$$F(d) = (1{,}202/2\mu_0\pi)\ (3m^3/d^4) \tag{16}$$

where μ_0 is the vacuum magnetic permeability and m the induced magnetic moment of each droplet. The induced magnetic moment can be determined from the intrinsic ferrofluid susceptibility, the spherical shape of the drops, and the presence of neighboring drops. Thus:

$$m = \mu_0\ 4/3\ \pi R^3\ \chi_s\ H_t \tag{17}$$

where H_t is the total magnetic field acting on each drop and χ_s is the susceptibility of a spherical droplet. Taking into account the demagnetization effect due to polarization, one obtains:

$$\chi_s = \chi/(1 + \chi/3) \tag{18}$$

where χ is the intrinsic susceptibility of the ferrofluid that has been measured with a SQUID susceptometer and follows Langevin's law:

$$\chi = (\alpha/H_{ext}) \; [\coth(\beta H_{ext}) - 1/(\beta H_{ext})] \tag{19}$$

where H_{ext} is the applied external field and $\alpha = 465$ A/m and $\beta = 1.8\ 10^{-4}$ m/A. The total applied field H_t is given by the sum of the external applied field and the field from the induced magnetic moments of all the neighboring droplets in the chain. This can be calculated for an infinite chain, assuming point-like dipoles:

$$H_t = H_{ext} + 2.404m/(4\pi\mu_0 d^3) \tag{20}$$

The magnitude of the second term makes at most a 20% correction to the externally applied field. Expressions (16) to (20) constitute a self-consistent set of equations. Multipole terms that should normally contribute to the expression of the force but that are found to be smaller than 10^{-3} F_m are neglected here.

From a more technical point of view, a few more experimental details should be given. First, the time scale of one experiment ranges from 30 to 60 min depending on the continuous-phase viscosity (that can be quite high in, for example, polymer solutions). The experiment requires the use of very small amounts (typically 10^{-2} cm^3) of dilute ferrofluid emulsions (less than 0.1%). Special isolation from vibrations or particular care of the temperature control is not needed. However, the emulsion polydispersity must be reduced to its minimal level. This is the main difficulty of that technique.

1. Electrostatic Stabilization of Colloidal Particles

The measurements of electrostatic repulsive forces were performed in a direct octane ferrofluid emulsion stabilized by an ionic surfactant that gives birth to a charged interface. The measurements are presented in Fig. 13.

These experimental exponentially decaying profiles can be compared with a theoretical expression of the double-layer repulsion that is derived from Poisson-Boltzmann theory. Between two charged spheres (of radius R) of low surface charge densities immersed in a continuous phase of ionic concentration C_s, the repulsive force F_r reads [11]:

- when $\kappa R < 5$

$$F_r(h) = 4\pi\varepsilon\psi_0^2 R^2 \; [\kappa/(h + 2R) + 1/(h + 2R)^2] \; \exp(-\kappa h) \tag{21}$$

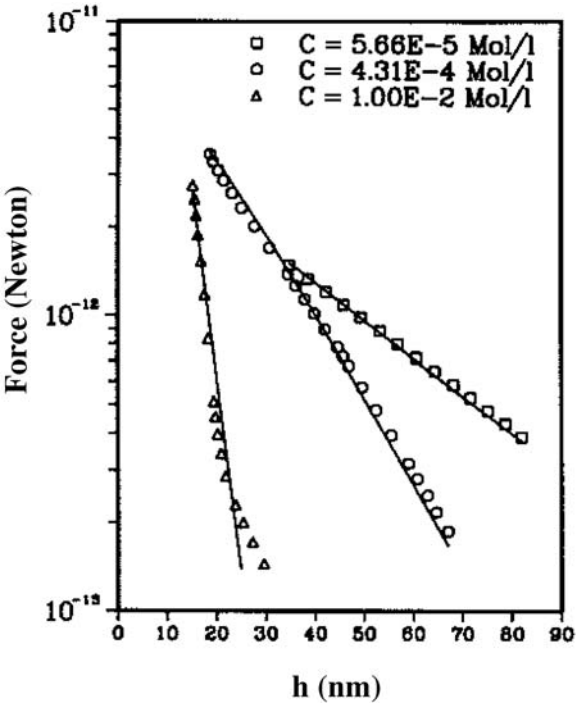

FIG. 13 Force–distance profiles measured between magnetic emulsion droplets in the presence of various concentrations of the ionic surfactant sodium dodecyl sulfate (SDS). As its concentration increases, the range of the force decreases due to an increasing amount of ions in the continuous phase. The continuous lines are the best fits to Eqs. (21) and (22) in the text with just the surface potential ψ_0 as unique free parameter in the fit, κ^{-1} being determined with Eq. (23) where C_s is taken to be equal to the bulk SDS concentration indicated on the figure. The scale is semilogarithmic. (From Ref. 11.)

- when $\kappa R > 5$

$$F_r(h) = 2\pi\varepsilon\psi_0^2 R\kappa \exp(-\kappa h)/[1 + \exp(-\kappa h)] \tag{22}$$

where ε is the water dielectric permittivity, ψ_0 the droplet surface potential, and κ^{-1} the Debye length that is connected to the electrolyte concentration C_s. In the case of symmetrical 1:1 electrolytes, κ^{-1} reads:

$$\kappa^{-1} = [(4\pi q^2/\varepsilon kT)\ 2C_s]^{-1/2} \tag{23}$$

where q is the ion charge and kT the thermal energy. From Eqs. (21) and (22), it is clear that the intensity of the electrostatic force is mostly fixed by the

surface potential while its range is determined by κ^{-1}. The data are compatible with Eqs. (21) and (22) (see Fig. 13) since the screening lengths κ^{-1} [computed through Eq. (23)] that determine the slopes of the semilogarithmic plots are in all cases in good agreement with the experimental slopes. In these fits, the Debye lengths are never treated as adjustable parameters and the only free parameter is the droplet surface potential. This agreement between the measured and the theoretical slope is the main proof for the accuracy of that experimental technique. Moreover, such experiment allows the droplet surface potential to be determined.

2. Steric Stabilization by Adsorbed Macromolecules

(*a*) *Diblock Copolymers*. Another feature of that technique is to show the adsorption at the surface of the droplets of diblock copolymers based on polybutadiene and poly(ethylene oxide) [14]. The diblock copolymers, synthesized by P. Hoerner and G. Riess, display the characteristics listed in Table 2. In such copolymers, the hydrophobic polybutadiene block is larger than the hydrophilic poly(ethylene oxide) one. Consequently, such polymers will be used to stabilize inverted water-in-oil emulsions. In that case, an aqueous ferrofluid was emulsified in an organic phase made of methylcyclohexane.

In Fig. 14, repulsive force–distance profiles between water-in-oil emulsion droplets measured at various polymer concentrations are plotted. An increase in the range of the forces that is due to the adsorption of a copolymer layer is clearly observed. Also plotted for comparison's sake is the force–distance profile obtained in the presence of sorbitan monooleate only (a short-chain surfactant of low hydrophilic–lipophilic balance hereafter referred to as Span 80). In all the force profiles of Fig. 14, the Span 80 concentration is kept at a constant value of 0.5%. It clearly comes out that the presence of the polymer generates repulsive forces with characteristic ranges larger than the ones obtained with the surfactant only. According to Fig. 14, different regimes can be distinguished. For the lowest polymer concentrations ($C_p < 0.1\%$) and in the presence of Span

TABLE 2 Characteristics of the Diblock Copolymers Studied

Copolymer PBut-PEO	M(PBut) (g/mol)	M(PEO) (g/mol)	Polydispersity index	Weight fraction of PEO
7.7–8 K	7700	8000	1.06	0.51
21–9.3 K	21000	9300	1.10	0.30
58–20 K	58000	20000	1.12	0.26
98–13.5 K	98000	13500	1.19	0.13
150–30 K	150000	30000	1.22	0.17

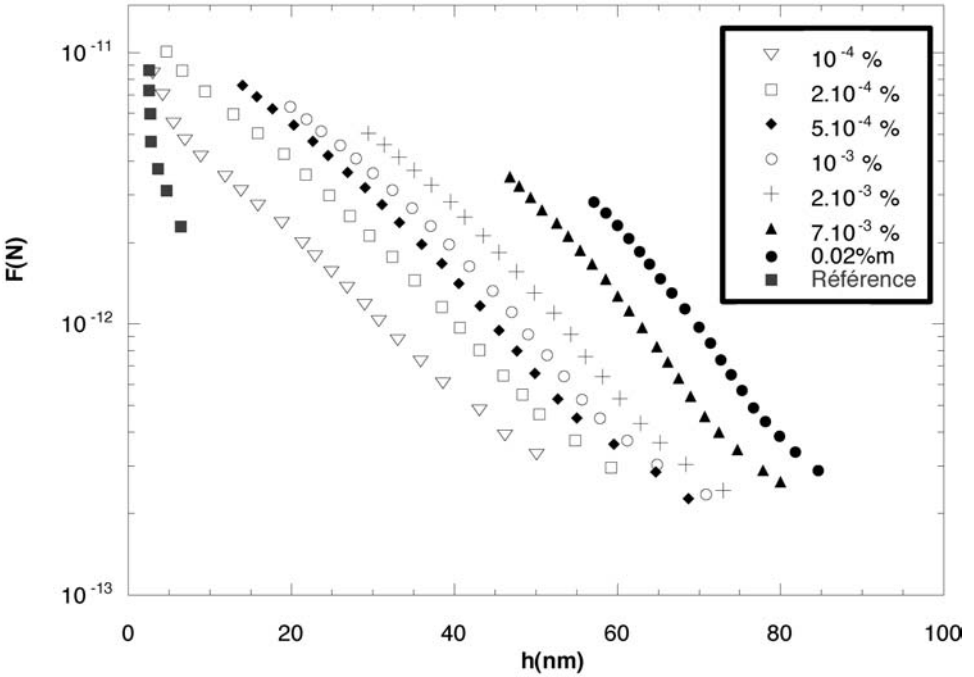

FIG. 14 Evolution of the force–distance profile between aqueous ferrofluid emulsion droplets in methylcyclohexane as a function of the polymer concentration and at a constant Span 80 concentration (0.5%). The used polymer is the 98–13.5 K of Table 2. The concentrations are given in weight percents. The "reference" profile is the one found in the absence of any polymer when the droplets are stabilized by the "short-tail" surfactant Span 80 (sorbitan monooleate, from Aldrich) only. The scale is semilogarithmic. (From Ref. 14.)

80, the force range increases with the polymer concentration to reach a plateau value. However, by decreasing the Span 80 concentration, it is possible to measure force–distance profiles having a longer range, as shown in Fig. 15. This is compatible with a competitive adsorption of the two species (see Fig. 15 where the surfactant concentration varies at constant C_p). According to Fig. 15, the force range gradually decreases as C_{S80} increases. This behavior is also observed with the other copolymers, indicating an increase in the surface coverage followed by a saturation of the interface as C_p increases and C_{S80} decreases. In Fig. 16a and b is plotted the evolution of the force–distance profiles as a function of the polybutadiene block molecular weight in two limited concentration ranges. One respectively refers to as "low" (Fig. 16a: $0.002\% < C_p < 0.08\%$ and

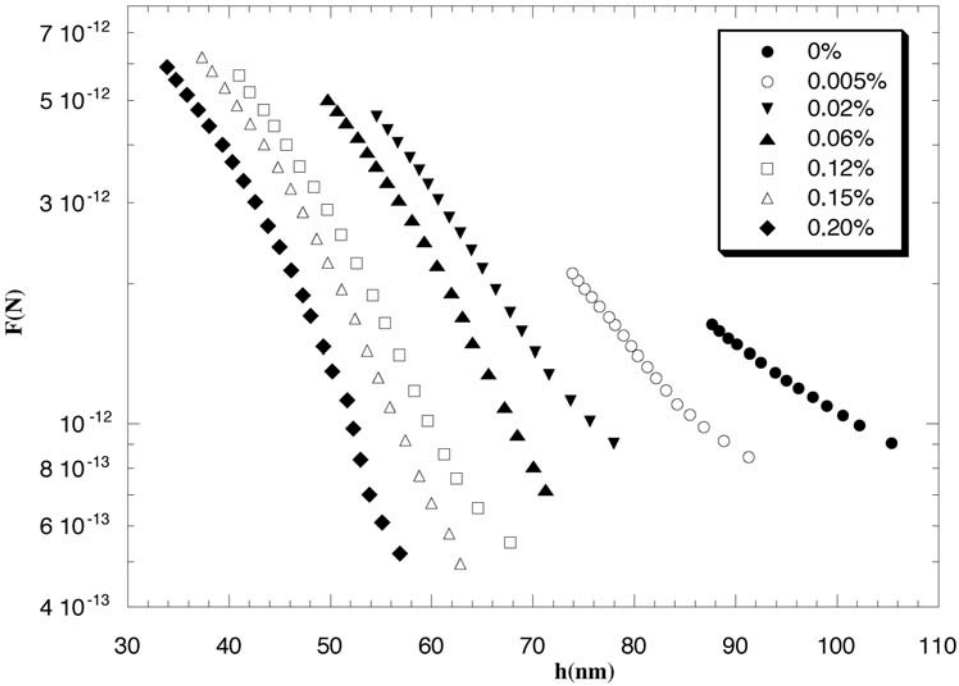

FIG. 15 Evolution of the force–distance profile as a function of the Span 80 concentration at a constant 98–13.5 K polymer concentration of 0.3 wt % in methylcyclohexane. The scale is semilogarithmic. (From Ref. 14.)

$C_{S80} = 0.1\%$) and the other one as "large" (Fig. 16b: $C_p = 0.5\%$ and $C_{S80} = 0\%$) polymer concentration regimes. In both cases, the force range clearly increases with the polybutadiene block length.

These results suggest that the adsorbed chain conformations change from a Gaussian shape to a more extended conformation as polymer concentration is increased (see Fig. 17a and b). If so, the force profiles should reflect the compression of polymer "mushrooms" at low concentration (17a) and polymer "brushes" at high concentration (17b). The data are fully consistent with this hypothesis as confirmed by the excellent agreement between the experimental results and applications of the theoretical models adapted to each situation [15]. They are also in full agreement with previous results obtained between solid surfaces [16]. In that case, and as shown in Fig. 18, the characteristic layer length deduced from the fits of our data to the theoretical models and representative of the polymer conformation in the layer, is proportional to the polybutadiene block gyration radius (which is itself proportional to $M_{W,PBut}{}^{0.6}$) at low

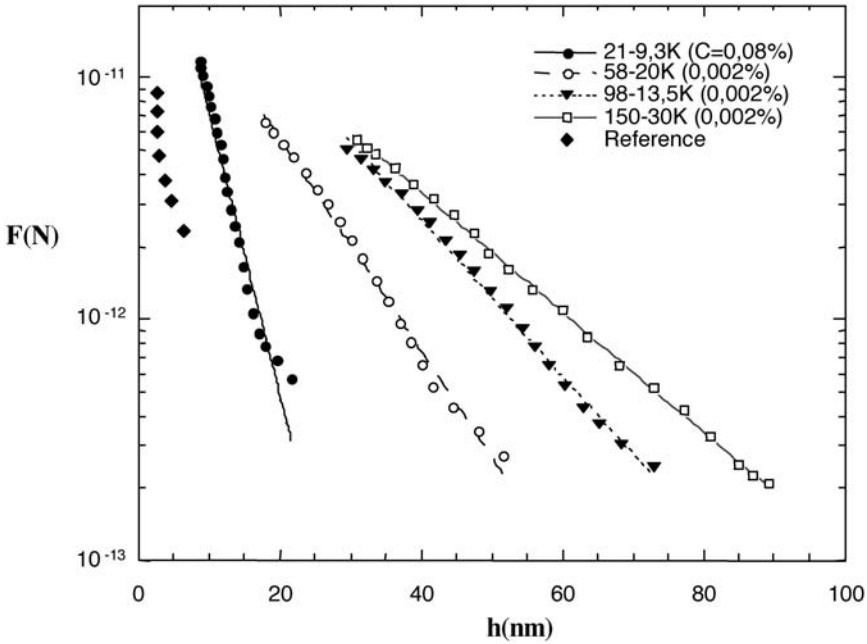

FIG. 16a Evolution of the force–distance profiles as a function of the polybutadiene block molecular weight in the low concentration regime. The solid lines are the best fits of our data to the Dolan-Edwards model described in Ref. 15, which treats the cases of the compression of polymer "mushroom" layers [17a]. The scale is semilogarithmic. (From Ref. 14.)

concentration and to the polybutadiene block extended length at high concentration (about $M_{W,PBut}$).

(*b*) *Statistical Copolymers*. Emulsions can also be stabilized by adsorbing polymers that do not have the diblock chemical structure. Here a statistical copolymer [polyvinyl alcohol (88%)-*co*-polyvinyl acetate (12%), PVA-VAc, of average molecular weights M_w = 10,000, 55,000, and 155,000 g/mol] was used to stabilize a direct emulsion [17]. According to Fig. 19, the presence of the polymer clearly ensures a long-range repulsion between the droplets. As the profile is insensitive to any changes in the ionic strength of the solution, it comes out that the forces are steric and due to the adsorption of a polymer layer. Exponentially decaying forces with ranges that increase with the polymer molecular weight are observed here. Following the most recent theories [18] on polymer adsorbed layers, the profiles can be fitted by the following expression:

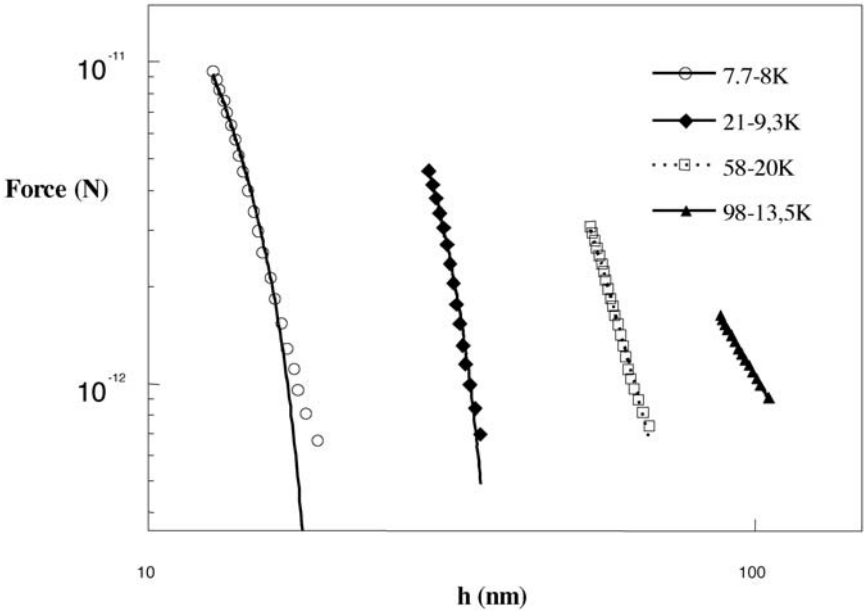

FIG. 16b Evolution of the force–distance profiles as a function of the polybutadiene block molecular weight in the high concentration regime. The solid lines are the best fits of our data to the Alexander-de Gennes model described in Ref. 15, which treats the cases of the compression of polymer "brushes" layers [17b]. The scale is in log-log. (From Ref 14.)

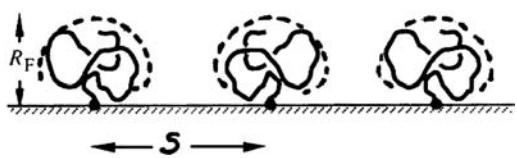

FIG. 17a "Mushroom" polymer layer. Schematic of a diblock adsorbed layer at low concentration. Since the surface concentration is low, the polybutadiene block can adopt a coil conformation and the adsorbed chains do not interact with each other (the average spacing between neighboring coils is larger than $2R_{g,PBut}$). (From Ref. 14.)

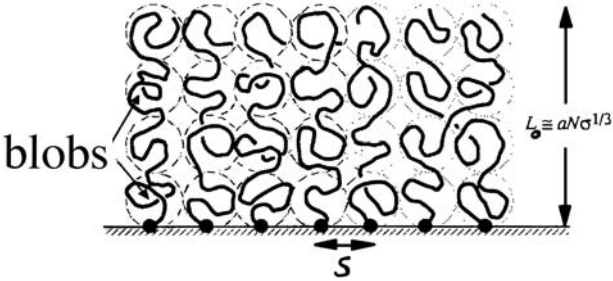

FIG. 17b "Brush" polymer layer. Schematic of a diblock adsorbed layer at high concentration. Since the surface concentration is large, the polybutadiene block can no longer adopt a coil conformation, and the adsorbed chains interact with each other and extend in the continuous phase (the average spacing between neighboring coils is smaller than $2R_{g,PBut}$). (From Ref. 14.)

$$F(h) = A\ h\ \exp(-h/\lambda) \tag{24}$$

where A is a constant and λ a distance characteristic of the adsorbed polymer layer that can be, in a first approximation, considered as proportional to the layer thickness. These force profiles are sensitive to an increase in the temperature value (Fig. 20). This can be explained by the decrease of the solvent quality toward the used polymer as the temperature increases, leading to a partial collapse of the adsorbed polymer layer. Interestingly, it can be shown that the polymer layer characteristic distance is proportional to the polymer coil gyration radius R_g:

$$\lambda \sim R_g \tag{25}$$

as evidenced in Fig. 21. This proportionality is in agreement with the earliest [19] as well as the most recent theories [18] on polymers at interfaces. In a recent paper [20], it was also shown that these findings are independent of the nature of the involved interfaces (solid–liquid, liquid–liquid, or liquid–gas).

Force measurements can be used to gain insights into an estimate of the potential colloidal stability of one system. Indeed, the range of the repulsive force, together with the force intensity, partially determines the stability of colloidal dispersions. From the presented work, which is not an exhaustive presentation of all the force measurement studies at the colloidal scale but a summary that is focused on the use of the technique described in Section VI.B, the following conclusions can be drawn:

1. The range of the repulsive force is one of the key parameter in the emulsion stability.

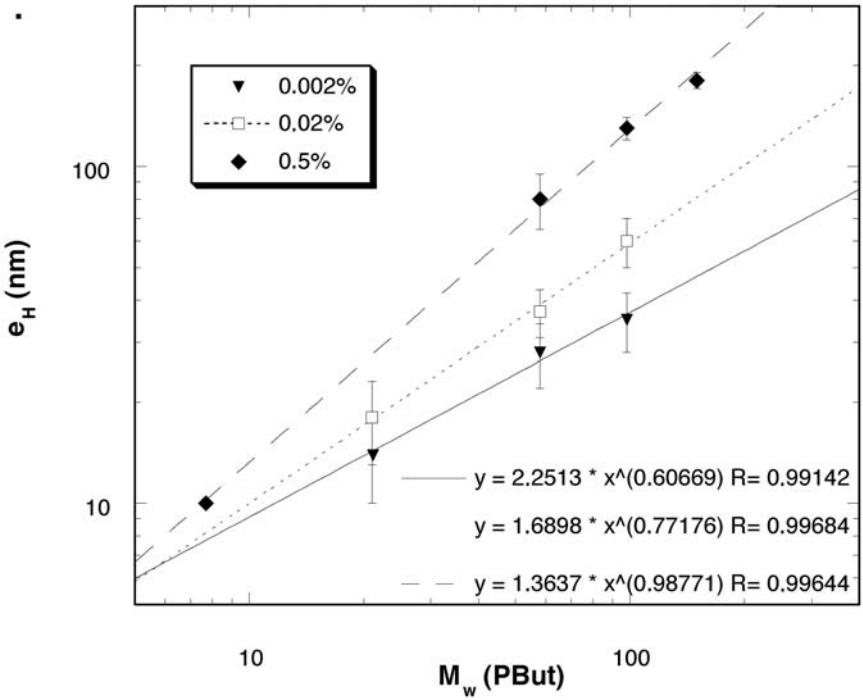

FIG. 18 Log-log evolution of the characteristic layer length as a function of the polybutadiene block length (in kg/mol) and at various polymer bulk concentration. At low concentrations, the length follows a power law with an exponent of about 0.6 for $M_{W,Pbut}$, as predicted when the polymer layer adopts a coillike conformation in good solvent. At large concentration, the linear behavior (with an exponent around 1) reflects an extended conformation of the adsorbed chain, as schematized on Fig. 17b.

2. This range can be estimated by just considering the type of species used to stabilize the emulsion:
   a. Ionic species: electrostatic forces having values in the order of the Debye length
   b. Macromolecular species:
      (i) Diblock copolymers: at low concentration, the range is proportional to the gyration radius of the chain part that is soluble in the continuous phase. At high concentration, the range extends to attain a size proportional to the continuous phase extended conformation of the soluble chain.

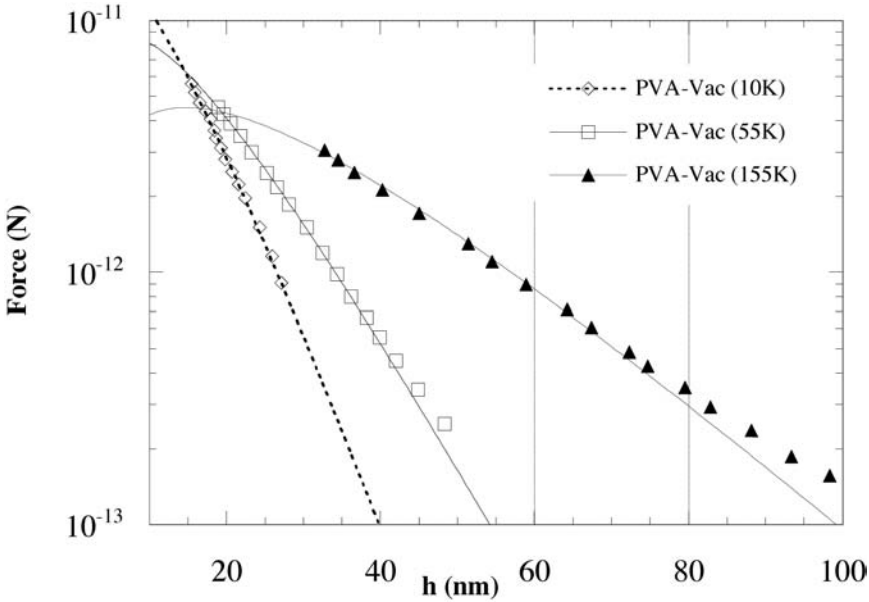

FIG. 19 Evolution of the force–distance profiles between oil-in-water emulsion droplets stabilized by the statistical copolymer PVA-Vac of different molecular weights (10,000, 55,000, and 155,000 g/mol). The profiles are exponentially decaying with ranges that depend on the polymer molecular weight. The solid lines are the best fits of our data to Eq. (24) in the text. The extracted value of λ are plotted vs. the polymer gyration radius on Fig. 21. The scale is semilogarithmic. (From Ref. 17.)

(ii) Statistical copolymers: in that case, the force range is proportional to the polymer coil gyration radius.

One must also point out the different important experimental parameters that obviously play a role in fixing the value of the range force. First, as known for a long time and reflected by Eq. (23), the ionic strength of the continuous phase determines the range of the force in electrostatically stabilized colloidal systems. This is not the case for systems stabilized by adsorbed neutral polymer layers in which the layer thickness is no longer a matter of ionic strength but which should preferentially be discussed in terms of solvent quality of the polymer in the used solvent phase. Of course, these parameters can be determining at the same time when colloidal dispersions come to be stabilized by polyelectrolytes that present the characteristics of both macromolecules and ionic species.

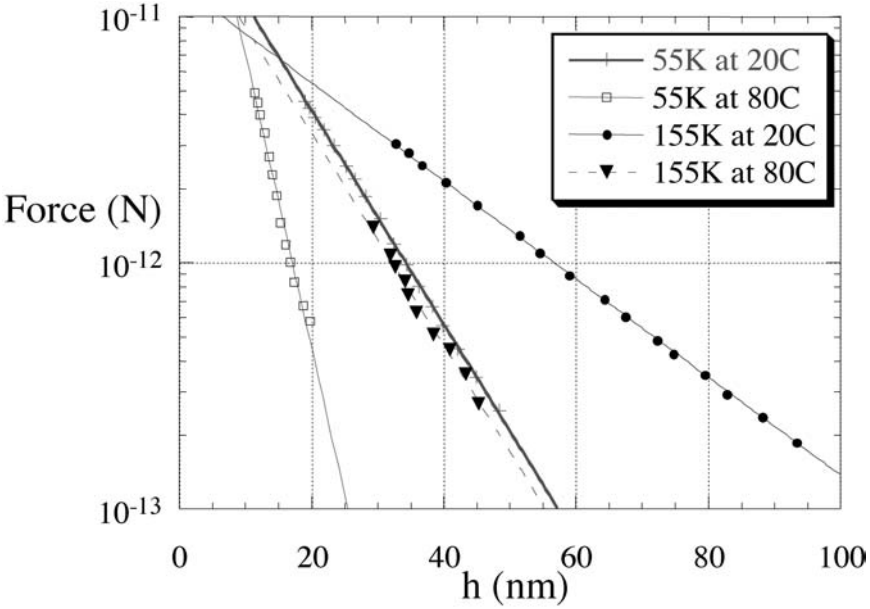

FIG. 20 Evolution of the force–distance profiles between oil-in-water emulsion droplets stabilized by PVA-Vac at different temperatures. As the temperature increases, the force range decreases due to a decrease in the solvent quality and to a consecutive collapse of the adsorbed polymer layer. The solid lines are the best fits of our data to Eq. (24) in the text. The scale is semilogarithmic. (From Ref. 17.)

VII. ELECTROKINETIC PROPERTIES

A. Relationship Between Electrophoretic Mobility and Zeta Potential

When a charged spherical particle of radius R is immersed in an aqueous medium under an electrical field E, the displacement velocity V and the electrophoretic mobility μ_e of the particles are related via the following equation:

$$\mu_e = \frac{V}{E} \tag{26}$$

The electrophoretic mobility values are related to the shearing plan position in the vicinity of the particle surface at which the ζ potential is defined. The relationship between the measured electrophoretic mobility and the ζ potential

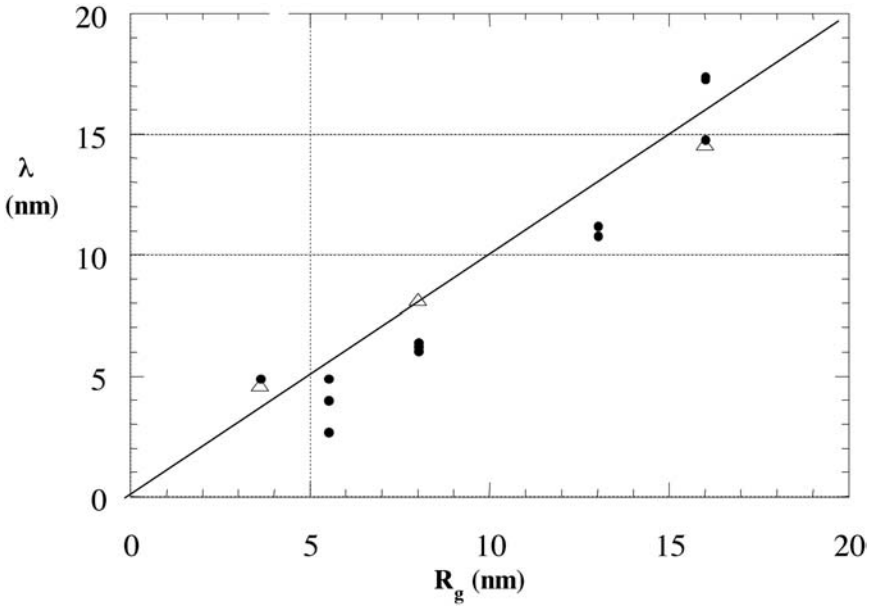

FIG. 21 Evolution of the characteristic length λ deduced from the best fits of the data from Figs. 19 and 20 to Eq. (24) in the text, as a function of the polymer coils gyration radii (which were deduced independently from viscometric measurements). The different symbols correspond to different sets of emulsions. (From Ref. 17.)

is dependent on the value of the product $R\kappa$ where κ is the inverse of the Debye length.

i) $\kappa R >> 1$

In this case, the electrical double layer (EDL) is much thinner than the particle size and the electrical field lines are tangent to the EDL of the particle. Then, the integration of the Navier-Stokes equation between the shearing plan and the infinite position far from the surface leads to the Smoluchowski's equation:

$$\mu_e = \varepsilon \cdot \frac{\zeta}{\eta} \tag{27}$$

where ε is the permittivity constant of the liquid, η the viscosity of the liquid, μ_e the electrophoretic mobility, and ζ the ζ potential. This basic equation is used in the case of $e\zeta << k_B T$, where e is the electron charge, k_B is the Boltzmann's constant, and T is the absolute temperature. In addition, this equation is only

valid for nonconducting particles with the same permittivity and viscosity in the electrical double layer and in the continuous phase.

ii) $\kappa R << 1$

In this case of extended EDL, the electrophoretic mobility is related to the ζ potential using the following equation:

$$\mu_e = \frac{2}{3}\frac{\varepsilon\zeta}{\eta} \tag{28}$$

A more complete equation has been developed and is known as the Henry's equation:

$$\mu_e = \frac{2}{3}\frac{\varepsilon\zeta}{\eta} f(\kappa R) \tag{29}$$

in which $f(\kappa R)$ is a function of the product κR [21].

The above given relationships between the electrophoretic mobility and the ζ potential are far from being well adapted for all colloidal dispersions and in a large κR domain. Then, O'Brien and White proposed a new approach in which the electrophoretic mobility may be related to the ζ potential values through the following equation:

$$\overline{\mu_e} = \frac{3}{2}\bar{\zeta} - \left[\frac{3\bar{\zeta} - 6\ln 2\left(1 - e^{-\frac{\bar{\zeta}}{2}}\right)}{2 + \dfrac{\kappa a e^{-\bar{\zeta}/2}}{1 + 3m}}\right] \tag{30}$$

where $\bar{\mu}_e$ and $\bar{\zeta}$ are the reduced electrophoretic mobility and ζ potential, respectively. They read:

$$\bar{\mu}_e = \frac{3\eta e}{2\varepsilon kT}\mu \tag{31}$$

$$\bar{\zeta} = \frac{e}{kT}\zeta \tag{32}$$

m is the mobility of ions:

$$m = \frac{2\varepsilon}{3\eta D}\left(\frac{kT}{e}\right)^2 \tag{33}$$

In this case, the influence of the mobility of ions ($m \sim 0.184$) that was neglected in basic theories is now considered.

B. Influence of pH on the Electrophoretic Mobility

The electrophoretic mobility of colloidal particles is generally investigated as a function of pH in order to point out the cationic or the anionic character of the particle surfaces. The measurements are investigated for highly diluted dispersion and at constant temperature and salt concentration. As an example, the evolution of the electrophoretic mobility of three types of colloidal particles as a function of pH is given in Fig. 22.

The first curve exhibits the behavior that is observed in the case of colloidal particles bearing primary amine groups. The measurements reveal the cationic character of the particle surface at pH value below 9. The isoelectric point is found to be around pH 9.5, which corresponds to the pK_a of primary amine functions. The second curve corresponds to the sulfate-containing particles. In this case, the negative electrophoretic mobility is constant irrespective of the pH, due to the strong acidic character of such compound. The last curve is typical of the behavior of particles bearing carboxylic groups. The change in the electrophoretic mobility from positive to negative values is attributed to the

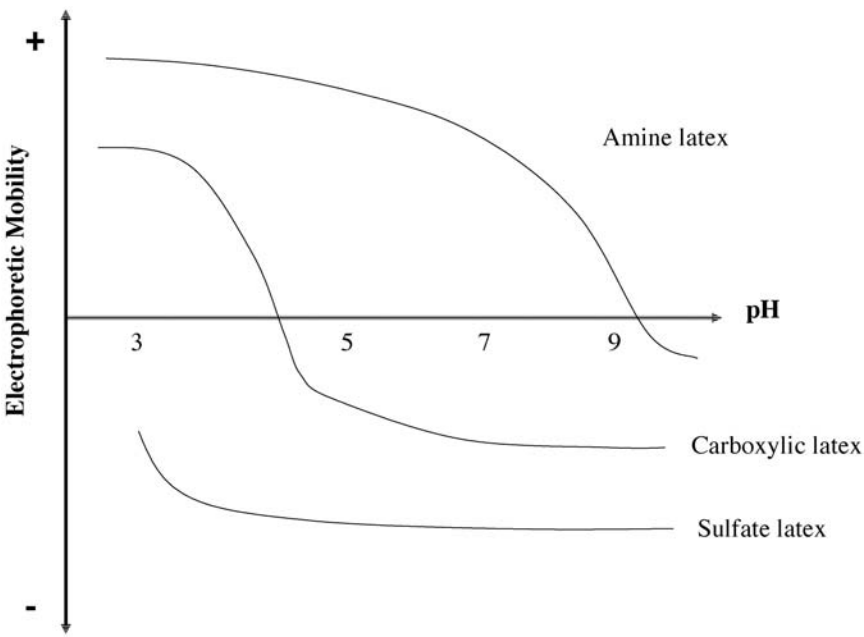

FIG. 22 Illustration of the electrophoretic mobility of amine, carboxylic, and sulfate latexes as a function of pH.

dissociation of the surface carboxylic groups, with an isoelectric point close to pH 4.5.

C. Influence of the Ionic Strength on the Electrophoretic Mobility

The influence of ionic strength on the electrophoretic mobility is investigated for two main reasons. These measurements can give some insights into characteristic properties such as the surface conductance, roughness, amount of adsorbed ions, and type of morphology of the particle surface ("hairy"-like particles). An example of latex particles made of a polystyrene core and a poly(NIPAM) shell is displayed in Fig. 23. The curve obtained for the DD4 latex (shot-growth polymerization and cross-linked shell) is characteristic of particles stabilized by short-chain surfactant or by point surface charges. By contrast, DD1 (batch soap-free and cross-linker-free recipe) reveals a different kind of surface morphology. The observed maximum can be explained by the presence of charged polymer chains that form a fluffy layer at the interface and is interpreted using a hairy layer model attributed to the interfacial polymer chains. However, let us point out that the full understanding of this type of behavior is still the object of debate and controversy.

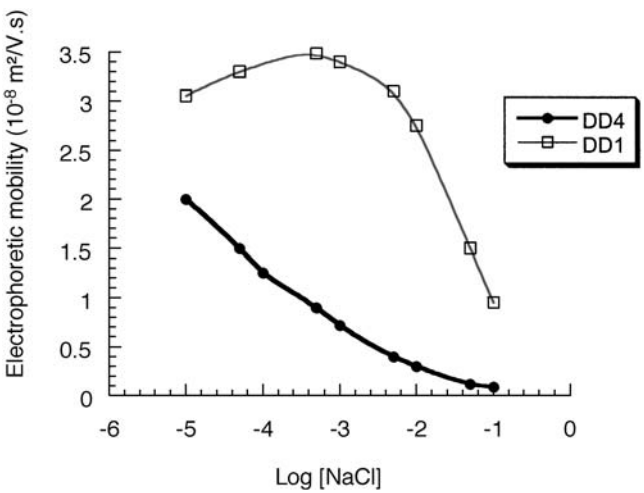

FIG. 23 Electrophoretic mobility of latex particles made of a polystyrene core and a polyNIPAM shell (which is cross-linked, DD4, or not, DD1) as a function of ionic strength at pH 6.0 and at 20°C. See the text for detailed experimental conditions.

These measurements can also provide a rough estimate of the surface potential (ψ_0) and the shearing plan position (Δ). First, from the electrophoretic mobility, one can deduce the ζ potential using Eq. (28). Then, the values of Δ and ψ_0 can be deduced by using the evolution of the ζ potential as a function of κ (in the case of a symmetrical electrolyte as NaCl, expression (23) of the Debye-Huckel length can be used) and using the following Eversole-Boardman equation:

$$\tan h\left(\frac{e\zeta}{4kT}\right) = \tan h\left(\frac{e\psi_0}{4kT}\right)\exp(-\kappa\Delta) \tag{34}$$

The plot of $-\ln[\tan h(e\zeta/4kT)]$ as a function of κ leads to a straight line with ψ_0 at the ordinate intercept and Δ as the slope, as shown in Fig. 24 in the case of negatively charged colloidal particles at two pH values.

VIII. HYDROPHILIC–HYDROPHOBIC CHARACTER OF LATEX SURFACES

The investigation of the hydrophilic or hydrophobic character of a colloidal dispersion is of great importance for the application envisioned. In painting domain, the filmification process clearly depends on the affinity between the latex and the surface on which it is deposited. In the biomedical field, the graft-

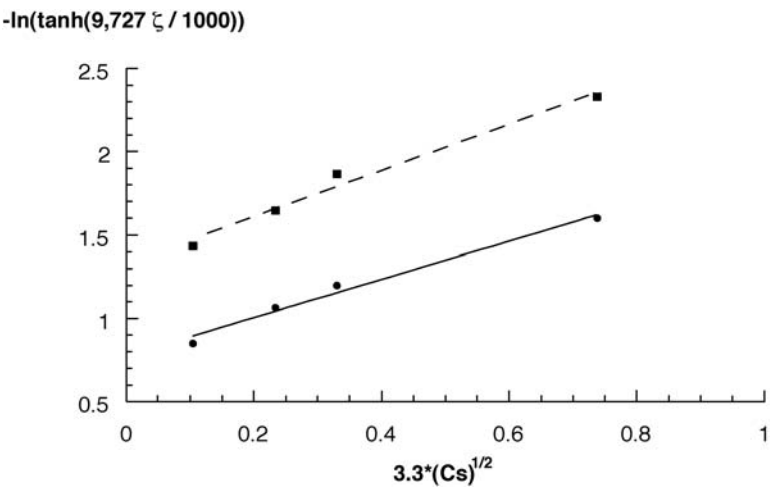

FIG. 24 Variation of $-\text{Ln}(\tan h(e\zeta/4kT))$ as a function of κ ($\kappa = 3.3C_s^{1/2}$) at 25°C and at pH 5 (■) and pH 9 (●).

ing or trapping step of biomolecules, as well as their conformation at the latex surface, requires the knowledge of the colloidal surface in terms of its hydrophilic or hydrophobic nature. Here are presented a few techniques that lead to a good determination of the surface polarity of the colloidal particles.

A. Contact Angle Measurement

Contact angle measurements can be performed on films made by the drying of a latex suspension. It is a powerful technique to investigate the surface polarity (hydrophilic–hydrophobic property) and a very promising method for determining the effect of incorporating functional groups on the surface polarity of latex particles. From the angle measurement, which is illustrated in Fig. 25, and the following Young's equation [22], it is possible to deduce the surface tension between the liquid and the solid phase:

$$\gamma_{lv}.\cos(\theta) = \gamma_{sv} - \gamma_{sl} \tag{35}$$

where θ is the contact angle and γ_{lv}, γ_{sv}, and γ_{sl} are, respectively, the liquid–vapor, solid–vapor, and solid–liquid surface tensions. Of course, determination of γ_{sl} requires the previous measurement of the liquid–vapor (γ_{lv}) and the solid–vapor (γ_{sv}) surface tensions.

Various approximations have been used in the past but the main accepted one is to consider that the surface tension (γ) is the sum of two contributions: a dispersive one and a polar one. The surface tension of a given solid support (γ_s) [or liquid (γ_l)] is then the sum of two components γ^d_s and γ^p_s (respectively the dispersive and the polar ones): $\gamma_s = \gamma^d_s + \gamma^p_s$. The dispersive component includes the van der Waals interactions, whereas the polar component includes all other types of interactions, such as electrostatic and hydrogen binding. The contact angle (θ) can be related to these two contributions through the following equation:

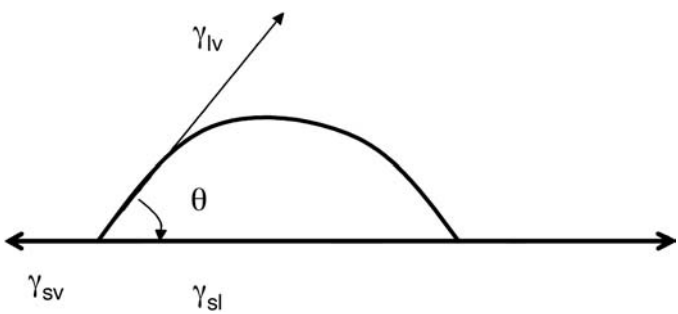

FIG. 25 Schematic presentation of the contact angle measurement.

$$[1 + \cos(\theta)] \cdot \gamma_l = 4\frac{\gamma_s^d \gamma_l^d}{\gamma_s^d + \gamma_l^d} + 4\frac{\gamma_s^p \gamma_l^p}{\gamma_s^p + \gamma_l^p} \tag{36}$$

The polar factor X_p is defined by [24]:

$$X_p = \frac{\gamma_s^p}{\gamma_s^d + \gamma_s^p} \tag{37}$$

The polar factor is therefore a direct measurement of the surface polarity. The knowledge of this quantity is important in terms of adsorption or grafting of the different functions carried by molecules, such as surfactant, polymers, or biomolecules, on the surfaces of the colloidal particles.

B. Surfactant Adsorption

The surface polarity of colloidal particles can be estimated by determining the surfactant adsorption energy using Maron's technique [23]. This technique consists of measuring the molecular area of the surfactant molecule at the colloidal particle interface. This method has already been used to show the hydrophobic character of various latex particles. A theoretical approach relating the adsorption of a surfactant and the polarity of a polymer surface has been proposed by Vijayendran [24]. The author considers a Langmuir-like adsorption process, and the adsorption free energy is controlled by the interfacial tension at the solid–liquid (in this case, the polymer–water) interface. The molecular area (A_s) of the adsorbed molecule is directly related to the polarity of the interfacial material (X_p) by the following equation:

$$\log A_s = k + (X_p) \tag{38}$$

where k is a constant. This relation can be applied quite well to latex particles or encapsulated colloids of various polarities. However, precautions have to be taken when applying this method (choice of the surfactant molecule and of the adsorption measurement technique, influence of the size and density of the particle charges, temperature effects, latex purity, etc.).

IX. CONCLUSION

The techniques available for the purpose of colloidal characterization are numerous. However, it is generally necessary to use many of them before gaining good insight into the system studied. These characterizations are also a prerequisite before any use of latex particles in a given application. It is particularly the case in the biomedical field in which the targeted biomolecules are present in such small concentrations that any perturbation from the added colloidal suspen-

sion has dramatic effects on the sensitivity and specificity measurements. Thus, the colloidal characterization is a compulsory step in the setup of new processes in diagnosis.

ACKNOWLEDGEMENTS

O.M.M. thanks everyone who contributed to the work on force measurements, especially P. Omarjee-Rivière and J. Philip. Part of this work was performed with the financial support of IFCPAR (Indo-French Centre for the Promotion of Advanced Research) directed by PG Mony.

REFERENCES

1. Elaissari A. In *Handbook of Surface and Colloid Chemistry*, 2nd ed.; Birdi, K.S., Ed.; CRC Press: Boca Raton, FL, 2002, Chapter 12, pp 581–609.
2. Hunter, R.J. In *Zeta Potential in Colloid Science Principles and Applications*; Academic Press: London, 1981, Chapter 6, p 335.
3. Fennell Evans, D.; Wennerström, H. In *The Colloidal Domain*, *Where Physics*, *Chemistry*, *and Biology Meet*, 2nd ed.; Wiley-VCH: Weinheim, 1999, Chapter 3, p 135.
4. Fitch, R.M. In *Polymer Colloids*; Academic Press: San Diego, 1997, Chapter 5, pp 120–128.
5. Locascio-Brown, L.; Plant, A.L.; Durst, R.A.; Brizgys, M. Anal. Chim. Acta **1990**, *228*, 107.
6. Ganachaud, F. PhD dissertation no. 265–97, Claude Bernard University, Lyon, France, 1997.
7. Lee, S.; Rudin, A. In *Polymer Latexes*: *Preparation*, *Characterization*, *and Applications*, Daniels, E.S.,Sudol, E.D., El-Aasser, M.S., Eds.; ACS Symposium Series 492, 1992, Chapter 15, pp 234–254.
8. Sundberg, D.C.; Durant, Y.G. Thermodynamic and kinetic aspects for particle morphology control. In *Polymeric Dispersions Principles and Applications*, Asua, J.M., Ed.; NATO ASI Series E, Vol. 335, Kluwer Academic: Dordrecht, 1996, pp 177–188.
9. Duracher, D.; Sauzedde, F.; Elaïssari, A.; Perrin, A.; Pichot, C. Colloid Polym. Sci. **1998**, *276*, 219–231.
10. Israelachvili, J.N. In *Intermolecular and Surface Forces*; Academic Press: San Diego, 1992, Chapter 11, p 186.
11. Leal Calderon, F.; Stora, T.; Mondain-Monval, O.; Poulin, P.; Bibette, J. Phys. Rev Lett. **1994**, *72*, 2959.
12. Mondain-Monval, O.; Leal Calderon, F.; Bibette, J. J. Physique **1996**, *II* (6), 1313.
13. Bibette, J. J. Colloid Interface Sci. **1991**, *147*, 474; Bibette, J. J. Magnet. Magnet. Mater. **1993**, *122*, 37.
14. Omarjee, P.; Hoerner, P.; Riess, G.; Cabuil, V.; Mondain-Monval, O. Eur. Phys. J. **2001**, *E 4*, 45.

15. “Mushrooms”: Dolan, A.K.; Edwards, S.F. Proc. R. Soc. **1974**; *335*, 509; “Brushes”: Alexander, S. J. Phys. (Paris) **1977**, *38*, 983; de Gennes, P.G. Macromolecules **1980**, *13*, 1069.
16. Taunton, H.J.; Toprakcioglu, C.; Fetters, L.J.; Klein, J. Macromolecules **1990**, *23*, 571; Kuhl, T.L.; Leckband, D.E.; Lasic, D.D.; Israelachvili, J.N. Biophys. J. **1994**, *66*, 1479.
17. Mondain-Monval, O.; Espert, A.; Omarjee, P.; Bibette, J.; Leal Calderon, F.; Philip, J.; Joanny, J.-F. Phys. Rev. Lett. **1998**, *80*, 1778; Espert, A.; Omarjee, P.; Bibette, J.; Leah Calderon, L.; Mondain-Monval, O. Macromolecules **1998**, *31*, 7023.
18. Semenov, A.N.; Bonet-Avalos, J.; Johner, A.; Joanny, J.-F. Macromolecules **1996**, *29*, 2179; Semenov, A.N.; Joanny, J.-F.; Johner, A.; Bonet-Avalos, J. Macromolecules **1997**, *30*, 1479.
19. de Gennes, P.G. Macromolecules **1981**, *14*, 1637; de Gennes, P.G. Macromolecules **1982**, *15*, 492; de Gennes, P.G. In *Scaling Concepts in Polymer Physics*; Cornell University Press: London, 1979. Chapter 1, p 29, and Chapter 3, p 69.
20. Omarjee, P.; Espert, A.; Mondain-Monval, O.; Klein, J. Langmuir **2001**, *17*, 5693.
21. Kralchevsky, P.A.; Danov, K.D.; Denkov, N.D. In *Handbook of Surface and Colloid Chemistry* K.S. Birdi, Ed.; CRC Press: Boca Raton, FL, 1997. Chapter 11, p 435.
22. Young, T. Trans. R. Soc. London **1805**, *95*, 65.
23. Maron, S.H.; Elder, M.E.; Ulevitch I.N. J. Colloid Interface Sci. **1954**, *9*, 89.
24. Vijayendran, B.R. J. Appl. Polym. Sci. **1979**, *23*, 733.

15

Electrokinetic and Small-Angle Neutron Scattering Studies of Thermally Sensitive Polymer Colloids

BRIAN R. SAUNDERS University of Manchester and UMIST, Manchester, United Kingdom

I. INTRODUCTION

A. General Introduction

In this chapter an overview of thermally sensitive water-swellable polymer colloids will be given with particular emphasis on structure–property relationships. Consideration will be given to their use (current and future) in biomedical applications. It will be shown that complementary structural information on polymer colloids can be obtained using a combination of electrokinetic and small-angle scattering techniques. The value in understanding the structure of these polymer colloids lies in the opportunity to engineer the particles to suit specific applications (e.g., controlled release of drug molecules).

Thermally responsive polymer colloids exhibit a property change in response to temperature. We have been particularly interested in water-swellable microgel particles [1]. A microgel particle is a cross-linked latex particle that is swollen by a good solvent. The particularly interesting aspect of these particles is that the polymer exhibits a temperature-induced conformational change upon heating that is reversible. There are strong analogies between the ability of thermally responsive microgel particles to change conformation on heating and protein denaturation.

The microgels of interest here are based on poly(NIPAM) (NIPAM = *N*-isopropylacrylamide). The structure of poly(NIPAM) appears in Fig. 1. The amide group hydrogen bonds with water at room temperature; water is a good solvent. At higher temperatures the hydrogen bonding is disrupted and a coil-to-globule transition occurs [2]. The thermodynamics of the transition originate from the behavior of water:

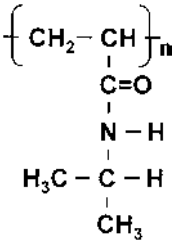

FIG. 1 The structure of the monomer unit of poly(NIPAM).

$$dG = dH - T\,dS \tag{1}$$

where dG, dH, and dS are the free energy, enthalpy, and entropy changes of the water molecules due to the coil-to-globule transition; T is temperature. Because the water molecules effectively condense onto swollen coils dH is positive. The water molecules that hydrate the swollen chain have a lower entropy than bulk water; thus, dS is also positive. Therefore, the lower critical solution temperature (LCST) corresponds to the point where $dG = 0$. At temperatures higher than the LCST the entropy term dominates and the coil-to-globule transition is spontaneous. The situation is depicted in Fig. 2.

The ability of thermally sensitive polymers to exhibit a temperature-induced collapse presents an opportunity to use them as excipients for controlled release

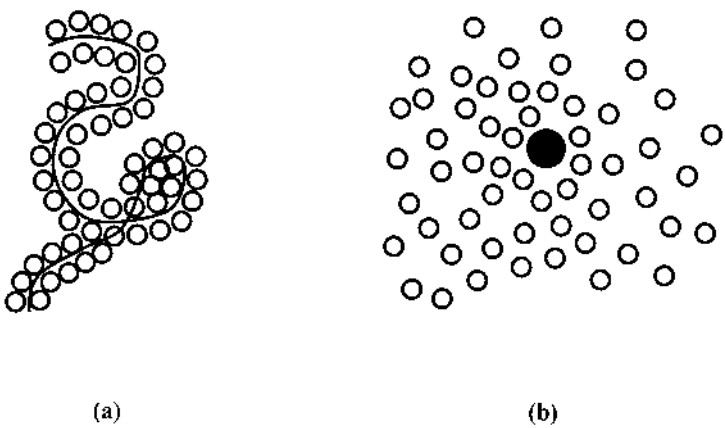

FIG. 2 A depiction of the coil-to-globule transition for poly(NIPAM) in water. The line and open spheres represent the polymer chain and some of the hydrating water molecules, respectively. In (a) water is a good solvent, whereas in (b) water has become a poor solvent and the polymer chain has collapsed into a globule (closed sphere).

of drug molecules. Of course, poly(NIPAM) microgels may present some problems for such an application because the monomer is known to be toxic. However, it is an excellent system for proof of concept studies. Considerable work has been directed to understanding the properties of temperature-sensitive microgel particles because of this type of application. Poly(NIPAM) microgels were first synthesized by Pelton and Chibante [3] 16 years ago. Their ability to take up model drug molecules has been studied by a number of authors [4]. To act as a good excipient for drug delivery the microgel particles must meet the four established design criteria for excipients. The host vehicle for drug transfer must allow it to be retained and evade the body's neutralizing strategies as well as facilitating targeting of the active site (tumors, etc.) and finally permit release of the drug molecules. This is made more achievable by the ability to synthesize particles with a diameter less than the value known to trigger immune responses (about 100 nm). The use of temperature to cause microgel particle collapse and expulsion of the drug is attractive in principle because localized heating of imbibed particles can be achieved. The LCST of poly(NIPAM) is 32–34°C for the pristine polymer in water, but can be modified by copolymerization or substitution within the amide [5]. In order to design better thermally sensitive microgel particles for excipients an improved understanding of microgel structure and hence structure–property relationships is required.

B. Microgel Synthesis: Structure–Property Relationship

Poly(NIPAM) microgel dispersions are synthesized using emulsion polymerization. Surfactant-free emulsion polymerization (SFEP) is preferred for academic studies because the particle distribution is narrow and no residual added surfactant is present. The method is based on that originally developed by Ottewill et al. for polystyrene [6]. An ionic initiator (often ammonium persulfate) is added to a heated, well-stirred solution containing NIPAM and a cross-linking monomer. The latter is usually methylenebisacrylamide but other alternatives are possible. This results in nucleation of poly(NIPAM) particles which are electrostatically stabilized. Upon cooling the particles expand to give an electrosterically stabilized dispersion. The final particle size can be decreased by adding surfactant prior to synthesis or increased (in the absence of added surfactant) by adding salt. Specific details of conditions used to prepare poly(NIPAM) microgel dispersions can be found elsewhere [5].

Swollen microgel particles contain low segment concentrations. Poly(NIPAM) microgel particles often have a particle size in the range 150–1000 nm (depending on synthetic method) and polymer volume fractions (ϕ_p) in the swollen state of less than 0.10. The upper portion of this size range is comparable to the values reported for *Escherichia coli*. The low values for ϕ_p mean that the particles have a low effective Hamaker constant. This renders the attractive van der

Waals force weak. In addition, peripheral chains are believed to extend outward from the particle surface that confer steric stabilization. Poly(NIPAM) microgel dispersions have excellent stability in the swollen state due to a combination of electrosteric stabilization (electrostatic plus steric stabilization) and low effective Hamaker constants. Although the equations for the effective Hamaker constant for microgels has been derived by Vincent et al. [7], the electrostatic component has not been properly accounted for in the context of classical two-particle interaction curves often used in colloid science (DLVO theory). This is discussed further below.

The act of heating a microgel dispersion to above the LCST causes the particles to collapse. (An interesting alternative to this was provided by Bouillot et al. [8] who recently prepared microgel particles that swelled upon heating.) An example of temperature-induced collapse is shown in Fig. 3 for poly(NIPAM) microgel particles. The particles collapse abruptly when the temperature exceeds 33°C. Note that these particles were dispersed in D_2O for comparison to small-angle neutron scattering (SANS) studies (below). The abrupt change in particle size causes strong rheological changes for concentrated microgel dispersions. If the concentration of particles is sufficiently high then the dispersion will change from an entangled gel to a free-flowing fluid upon heating to above the LCST. We have investigated the effect of cross-link density on the volume-phase transition and have found that the sharpest transitions are caused by the lowest concentration of added cross-linking monomer. The internal structure of the particle controls the sharpness and this becomes inhomogeneous upon incorpo-

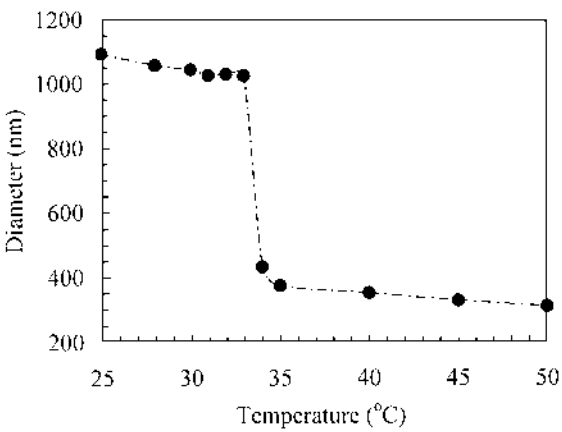

FIG. 3 Variation of particle diameter with temperature for poly(NIPAM) microgel particles. The particles were prepared according to the method given by Daly and Saunders [16].

ration of the cross-links, leading to a distribution of local segment concentrations and LCSTs.

The key to understanding the behavior of thermally sensitive particles and therefore modifying them for biomedical use (e.g., excipients) is to obtain a clear picture of the internal structure. This is not possible using conventional techniques (e.g, X-ray crystallography due to the amorphous nature of the swollen state). A combination of techniques that probe structure in the mesoscopic scale in a complementary manner is required. In the following it will be shown that the use of electrophoretic mobility measurements and SANS studies (with reference to light scattering data) provides considerable insight into the particle structure and the changes in particle structure during temperature-induced collapse.

II. ELECTROKINETIC STUDIES

A. The Electrical Double Layer and ζ Potential

Particles dispersed in aqueous media are normally charged by virtue of adsorption of ions from solution, repulsion of one particular charge type from the surface, or the presence of ionic groups. The latter give rise to the charge on poly(NIPAM) microgel particles and proteins. Charged initiator fragments (often of a strong acid) are incorporated during polymerization that give a net charge for the microgel particles. Of course, the situation for proteins is more complex due to the presence of weak acid and basic groups yielding a pH-dependent charge (and sign) for the particle. Neyret and Vincent have shown that it is possible to prepare ampholytic microgel particles that have opposite charges [9].

Electrokinetic phenomena result from the relative motion of charge at the surface–solution interface. In this discussion we are concerned only with electrophoretic mobility. One of the oldest (and most trusted) methods used to measure absolute electrophoretic mobility is microelectrophoresis. A Rank Brothers instrument was the key instrument for such measurements for many years. The principle of operation utilised an applied DC voltage and ultramicroscopy to measure the drift velocity of the particles. The mobility is simply the gradient of a velocity vs. electric field graph. In modern laboratories instruments based on laser Doppler velocimetry, phase analysis light scattering, and electrosonic amplitude measurements are used to measure electrophoretic mobility to a much greater degree of sensitivity and precision. A discussion of these techniques can be found elsewhere [10,11].

Figure 4 shows a simplified depiction of the charge separation and potential decay for a charged surface of a hard-sphere particle in aqueous solution containing electrolyte. The surface has a net negative charge (which is often, but

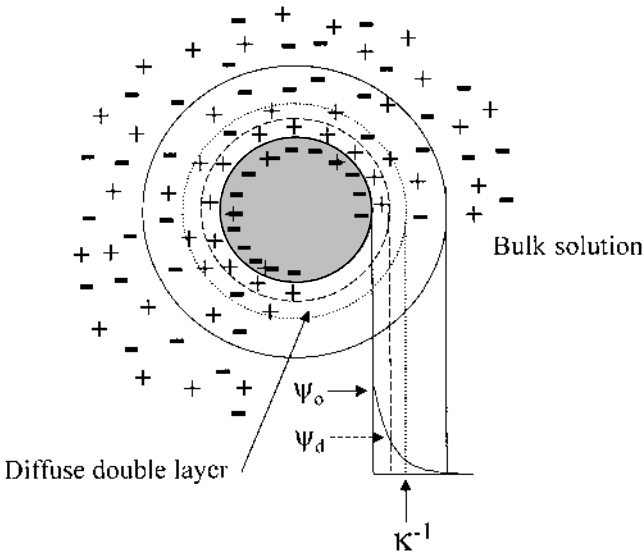

FIG. 4 Depiction of an electrical double layer surrounding a negatively charged particle in water. The surface potential (ψ_o), diffuse layer potential (ψ_d), and double layer thickness (κ^{-1}) are shown.

not always, the case). A layer of specifically adsorbed counterions is depicted. At a distance greater than that corresponding to a hydrated counterion diameter the ions are not specifically adsorbed. This is the position of the Stern plane and has a potential, ψ_d. This point corresponds to the surface of shear, which can be thought of as the point where the viscosity abruptly decreases from a very high value to that for the bulk fluid. The potential at the surface of shear is lower than the surface potential (ψ_0) due to the specifically adsorbed ions; however, this is not always the case. The electric potential at the surface of shear is the ζ potential (ζ) which is the measurable quantity. At distances from the particle greater than the surface of shear the counterions (and associated coions) experience the opposing effects of electrostatic attraction for the surface and thermal (randomizing) energy. These give rise to the diffuse double layer. The thickness of the double layer ($1/\kappa$) is a measure of the screening length of the solution and corresponds roughly to the point where the potential reaches 37% of ψ_d and gives a measure of the length scale over which the ions strongly experience the diffuse layer potential. In cases where the particle does not contain an adsorbed layer of polymer it is often assumed that $\psi_d \sim \zeta$, but this is a gross assumption. It should be noted that the value for $1/\kappa$ is easily calculated [12] using $1/\kappa = 3.3 \times 10^9 c^{0.5}$ for a monovalent electrolyte in water at 20°C

where c is the concentration in mol dm^{-3}. The relationship between the surface potential and distance is one of an exponential decrease (provided the surface potential is low) [12]:

$$\psi = \psi_d \exp[-\kappa x] \tag{2}$$

where x is the distance from the Stern plane. This is shown in Fig. 4.

The electrophoretic mobility (u) and ζ are related by the Henry equation:

$$u = \frac{2}{3}\frac{\varepsilon_r \varepsilon_0}{\eta}\zeta[1 + f(\kappa a)] \tag{3}$$

where ε_o and ε_r are the permittivity of a vacuum and relative permittivity, respectively. The viscosity of the medium is η and $f(\kappa a)$ is a factor that depends on the relationship between the double-layer thickness and particle radius (a). If $1/\kappa$ is much less than a then the surface can be considered flat and the Smoluchowski equation applies, i.e., $f(\kappa a) = \frac{1}{2}$. If $1/\kappa$ is much greater than a then the particle can be considered as a point charge and the Huckel equation applies, i.e., $f(\kappa a) = 0$. There is a rather significant region where $1/\kappa$ is comparable to a and neither the Huckel nor the Smoluchowski equation applies. It is for this region that a computer program of O'Brien and White was invaluable [13]. An attractive option has been provided by Ohshima who published a semiemperical equation that allows $f(\kappa a)$ to be easily calculated with a relative error of less than 1% over the entire range [14] for κa. The expression for the geometrical factor is:

$$f(\kappa a) = \left(\frac{1}{2[1 + (\delta/\kappa a)]^3}\right) \tag{4}$$

where

$$\delta = \frac{2.5}{1 + 2\exp(-\kappa a)} \tag{5}$$

B. Electrophoretic Mobility of Soft Particles

The discussion given above applied to hard-sphere particles and is relevant to collapsed microgel particles. However, the surface of swollen microgel particles most likely is similar to that of the periphery of polymer coils in a good solvent. Under such conditions the concept of a surface potential is not appropriate. The concept of a ζ potential is tenuous for such systems. Certain proteins can be considered to have expanded macromolecular peripheries. These types of geometries require specific theoretical treatment in order to extract structural information from elecrokinetic data.

Ohshima et al. have derived equations for hard-sphere latex particles covered by an expanded polyelectrolyte layer that is ion penetrable [15] with a thickness of δ. The number density of fixed charges in the layer is N. It is assumed that δ must be greater than $1/\kappa$ (otherwise the charged groups of the core would contribute to the mobility). Ohshima derived a set of six equations that describe the mobility of the polymer-coated latex. The central equation is given below:

$$u = \frac{\varepsilon_r \varepsilon_0}{\eta} \frac{\psi_0/\kappa_m + \psi_{DON}/\lambda}{1/\kappa_m + 1/\lambda} + \frac{zeN}{\eta\lambda^2} \tag{6}$$

where ψ_{DON} and ψ_o are the Donnan potential of the layer and the potential between the surface layer and the surrounding solution, respectively. $1/\kappa_m$ is the double-layer thickness within the surface charge layer, and λ is the degree of friction experienced by the liquid flowing through the surface layer. The reciprocal of λ is the softness factor.

To apply Eq. (6) the mobility is measured as a function of electrolyte concentration. At high electrolyte concentration only the last term on the right of Eq. (6) remains significant and u is equal to the *limiting* mobility (u_L). The latter, which is a measurable quantity, can be reinserted into the other equations (as a function of λ) and the data fitted with only one adjustable parameter (N). This approach was used in our work on poly(NIPAM) microgel particles [16]. Mobility vs. electrolyte concentration data are shown in Fig. 5 at different temperatures. The fits are reasonable and support the view that a core-shell type structure is present. The values for $1/\lambda$ and were calculated from the fits. The fact that $1/\lambda$ remained finite at 46°C implied that the outer layer of the particles did not completely collapse. This interesting result shows that the periphery of these particles behaves in manner different to that expected for uncharged poly(NIPAM)—which exhibits complete collapse at around 32°C in water. This is a key piece of evidence suggesting an inhomogeneous structure. Garcia-Salinas et al. [17] performed experiments on a related system and also found that Ohshima's model provided a good fit to the temperature-dependent mobility data. An alternative model [18] that assumed the charges to be located on a hydrodynamic equivalent hard sphere was tested without success [19]. Rasmusson et al. [20] undertook a comprehensive investigation of the applicability of the porous-sphere, soft-plate, and soft-sphere models for describing the mobility of poly(NIPAM) particles. They noted that the "soft" models neglected the relaxation effect.

A method for comparing the bulk vs. surface structure of the particles is to conduct light scattering (photon correlation spectroscopy) and electrophoretic mobility measurements on the particles as a function of temperature using identical conditions. We conducted experiments using several electrolyte concentra-

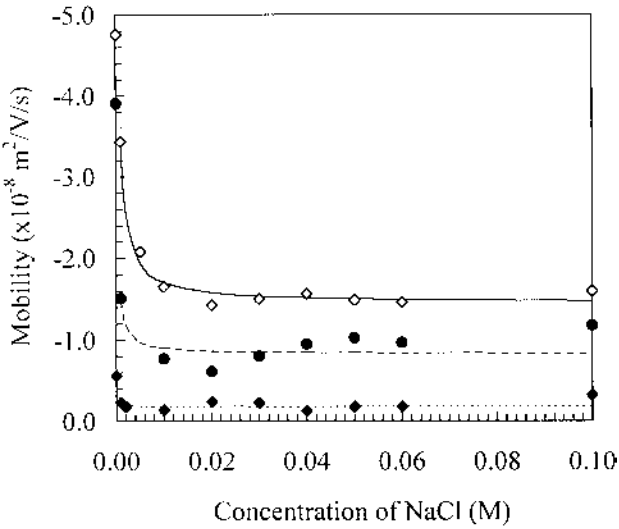

FIG. 5 Variation of the electrophoretic mobility of poly(NIPAM) microgel particles as a function of NaCl concentration. The dispersion temperature was 25°C (◆), 38°C (•), and 46°C (open diamond). (Reproduced by permission of The Royal Society of Chemistry on behalf of the PCCP Owner Societies.)

tions [19]. Data obtained in the presence of 0.001 M NaCl appear in Fig. 6. The data clearly show a difference between the temperatures at which mobility and diameter change. As the sample is heated, the mobility increases in magnitude at a slow rate under conditions where major deswelling occurs. The mobility increase is due to an increase in N as a consequence of network collapse at the periphery. The apparent decoupling of electrokinetic and hydrodynamic behavior is particularly interesting. The behavior is consistent with a model where the periphery of the particles contains polymer chains rich in ionic groups (cf, core) which have a relatively high [19] LCST. This outer region collapses at a higher temperature than the core. This contrasts to a homogeneous particle, which would be expected to have closely aligned mobility and hydrodynamic diameter changes.

In summary, the electrophoretic mobility measurements on poly(NIPAM) microgel particles have provided a consistent picture of the particle structure. There is a strong indication that the outer layer is a polyelectrolyte with a higher LCST than that of the interior of the particle.

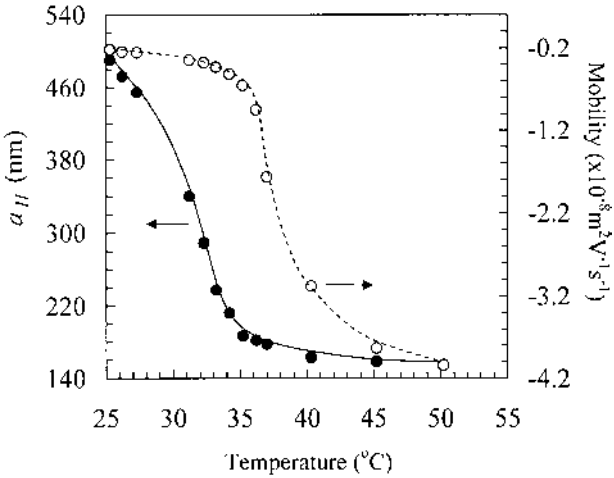

FIG. 6 Variation of the electrophoretic mobility (○) and hydrodynamic radius (•) as a function of temperature for poly(NIPAM) microgel dispersions in aqueous 10^{-3} M NaCl. (Reproduced by permission of The Royal Society of Chemistry on behalf of the PCCP Owner Societies.)

III. SMALL-ANGLE NEUTRON SCATTERING STUDIES

A. Introduction to SANS

Small-angle neutron scattering is a powerful diffraction technique for studying structural detail of polymers on the scale 10–1000 Å. Neutrons are deeply penetrating because they are uncharged and have relatively low energy (cf. X-rays of the same wavelength). The neutrons used in SANS experiments [21] normally have wavelengths in the range 0.15–2.5 nm. A particularly useful aspect of neutron scattering is that the ability of nuclei to scatter neutrons varies irregularly with atomic mass. The difference in the scattering length (or phase of scattered neutrons) between hydrogen and deuterium is large, which is reasonable because hydrogen does not contain a neutron (cf. deuterium). It is the ability to selectively deuterate parts of complex polymer mixtures without appreciably changing the structure and properties that has made SANS such an invaluable technique for structural investigation of polymer colloids [22]. The contrast in an X-ray scattering experiment results from differences in electron density, and this varies in a regular manner with increasing atomic number. Consequently, it is more difficult to use contrast variation to selectively screen out scattering within an X-ray scattering experiment.

In a SANS experiment the sample is subjected to an incident stream of neutrons. The scattered intensity is measured at small angles and converted to the scattering vector ($\boldsymbol{q}$). If the angle between the incident beam and scattered beams is θ, then q is the resultant of the incident and scattered vectors and is given by:

$$q = \frac{4\pi}{\lambda} \sin\left(\frac{\theta}{2}\right) \tag{7}$$

(Here the neutron refractive index is taken to be unity.) The scattering geometry is depicted in Fig. 7. The scattering of interest is elastic and therefore the magnitude of the incident ($\boldsymbol{k_0}$) and scattered ($\boldsymbol{k_s}$) radiation vectors are identical (equal to $2\pi/\lambda$). Simple geometry allows Eq. (7) to be derived. The dimension for q is reciprocal distance and it is related to the distance scale probed (d) by $d = 2\pi/q$. The SANS experiment provides a scattering profile consisting of the scattered intensity, $I(q)$ vs. q. This can be thought of as the Fourier transform of the radial distribution profile for the system.

SANS experiments require instruments capable of supplying a high flux of collimated neutrons. This is only possible from reactor or spallation sources. There are a number of SANS facilities available around the world, although beam time is expensive and competitive. There are a number of circumstances in which SANS can provide unique information. However, the experiments must always be well thought out, and it is advisable for new users to discuss the experiment with the local instrument scientist prior applying for beam time.

There is one general equation that governs the dependence of $I(q)$ with q for any material:

$$I(q) = b_v^2 N V^2 P(q) S(q) \tag{8}$$

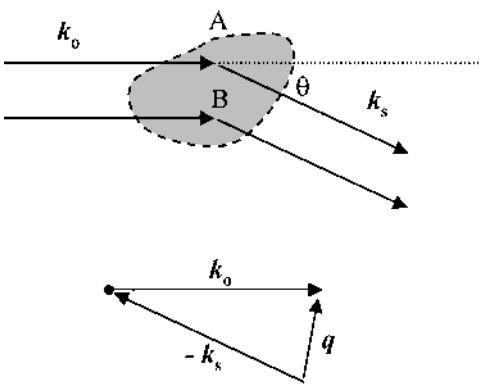

FIG. 7 Scattering geometry and vector diagram for a SANS experiment.

where b_v, N, and V are the contrast factor per unit volume, number of scattering centers per unit volume, and volume of the scattering centers, respectively. $P(q)$ and $S(q)$ are the form factor and structure factor, respectively. The form factor arises from interference of scattered neutrons from within the same macromolecule (or particle) (intramolecular interference term). It is sensitive to the size and shape of the scattering entity. The structure factor arises from interference from different scattering entities (intermolecular interference). It only becomes significant when concentrated solutions (dispersions) are used. The use of deuterated polymers and solvents allows the contrast term to be set to zero experimentally. The use of deuterated solvents or H/D solvent mixtures is a particularly powerful method for selectively enhancing and reducing the scattering for complex systems. The calculation of b_v is straightforward and relies on knowledge of the empirical formula [21]. A detailed and comprehensive discussion of SANS for polymers can be found elsewhere [22].

The form factor is of considerable interest for scattering experiments on polymer colloids. This is because it contains all the important geometrical information about particle structure. This can be extracted using a suitable mathematical model. For monodispersed hard-spherical particles (with a radius, R) the form factor is given by:

$$P(q) = \frac{9}{\nu^6} (\sin \nu - \nu \cos \nu)^2 \tag{9}$$

where $\nu = qR$. This expression is an oscillating function that can be simplified according to the geometry of the system concerned. There are several approximations for the form factor that are applicable for microgel particles and these are considered below.

After reducing the SANS data (to remove scattering from solvent and the incoherent background), the next stage is to determine the scattering exponent(s) present. A log $I(q)$ vs. log(q) plot is a useful first step as this will show regions of linearity clearly and permit an initial estimate of the scattering exponents for those regions [from $d \log I(q)/d \log(q)$]. A more accurate check for the exponent is to use a Kratky plot, i.e., a plot of $I(q)q^n$ vs. q where n is the scattering exponent. Regions of zero gradient for such a plot indicate that the exponent is operative for that particular q range. Based on the experimental exponent and a conceptual model for the system of interest, specific solutions to the form factor can be considered in order to extract structural information for the system.

The discussion given below considers simple geometries for which simplifications of Eq. (9) can be given. We consider (1) a small particle, (2) a large particle (cf. $1/q$), and (3) a polymer chain in a good solvent. More complicated geometries are considered in detail by Higgins and Benoit [22].

In the first case a particle with a radius, R, is considered such that R is much smaller than the dimension probed (thus $qR << 1$). A series expansion of Eq. (9) and substitution into Eq. (8) leads to the Guinier equation:

$$I(q) = b_v^2 NV^2 \exp\left(-\frac{(qR)^2}{5}\right) \tag{10}$$

A plot of the logarithm of the scattered intensity vs. q provides R from the gradient at low q values provided linearity exists. This is usually not applicable for microgel particles because the size of the particles is often large compared to the dimension probed (greater than 50 nm).

In the case of larger particles where R is much larger than the dimension probed ($qR >> 1$), one may use the average values of the trigonometric functions given in Eq. (9). This leads to the simple formula:

$$I(q) = \frac{2\pi b_v^2 S_t}{q^4} \tag{11}$$

where S_t is the total surface area of the dispersion (given by NS, where S is the surface area of each particle). This equation allows the total surface area of the dispersion to be determined from an appropriate plot; e.g., from the intercept for the y axis of an $I(q)g^4$ vs. q plot. In the case of particles with a diffuse interface (region of rapidly diminishing volume fraction profile), an extra term is introduced into the Porod equation and is given by:

$$I(q) = \frac{2\pi b_v^2 S_t}{q^4} \exp(-\sigma^2 q^2) \tag{12}$$

where σ is the width of the diffuse interface. This model was introduced by Thomas et al. to describe scattering from proteins deposited on pore walls [23].

In the case of solution polymer chains obeying Gaussian statistics (a Gaussian chain), the form factor is derived using the Gaussian approximation [22]:

$$I(q) = \frac{2}{x^2} b_v^2 NV^2 [x - 1 + \exp(-x)] \tag{13}$$

where $x = (gR_g)^2$. Thus, the data would need to exhibit a gradient of -2 at high q values for Eq. (13) to be considered. Note that R_g is the radius of gyration for the coils.

For microgel particles there are more than one contribution to the scattering curve, i.e., the scattering profile contains contributions from two or more scattering environments with their own form factors. This makes interpretation challenging. In such circumstances investigators either combine existing form fac-

tors or derive their own based on the structural model that is most physically reasonable for the system studied. A difficulty in the use of many-parameter models is that identification of a unique solution becomes difficult. It is advisable to start from simple expressions whereever possible and build in complexity only as needed. In the following we will illustrate how useful structural information can be obtained from such an approach for poly(NIPAM) microgel particles as a function of temperature.

B. SANS Studies of Soft Particles

SANS experiments were conducted on poly(NIPAM) microgel particles in D_2O at LOQ (ISIS Rutherford Appleton Laboratory, Didcot, UK) as a function of temperature in the presence and absence of added salt (NaCl). The internal structure of these particles has been a somewhat controversial topic in the past. Figure 8 shows plots of the scattering intensity as a function of q on a log-log scale. [Note that the $I(q)$ values for the data obtained at 34°C and 50°C were multiplied 10 and 100, respectively, for clarity.] The data were corrected for the solvent as well as incoherent background. The latter is not a trivial exercise and considerable care must be taken to ensure that an appropriate level is removed as the high-q data are particularly sensitive to the level of incoherent removed.

The data measured at 32°C and 50°C exhibit either a q^{-2} or q^{-4} dependence, respectively. Interestingly, the data obtained at the volume phase transition temperature (VPTT, which is about 34°C in D_2O) exhibit contributions from both

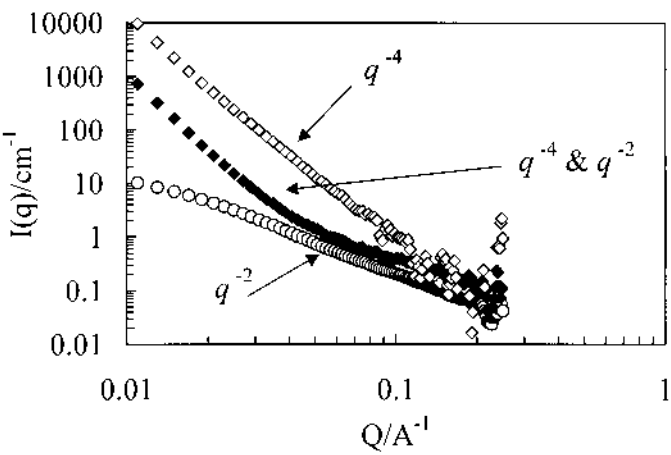

FIG. 8 Scattering profiles for poly(NIPAM) microgel dispersions in D_2O measured at 32°C (O), 34°C (closed diamond), and 50°C (open diamond). The scattering exponents that apply are identified in the figure.

types of behavior. (VPTT is used for gels instead of LCST due to the presence of cross-links.) Figure 9 shows Kratky plots for an exponent of 2. This representation shows how the q^{-2} dependence is lost when the temperature exceeds the VPTT. The scattering profiles can be summarized as follows:

$$\text{At } T < \text{VPTT} \qquad I(q) = A_2 q^{-2} \tag{14a}$$

$$\text{At } T \sim \text{VPTT} \qquad I(q) = A_2 q^{-2} + A_4 q^{-4} \tag{14b}$$

$$\text{At } T >> \text{VPTT} \qquad I(q) = A_4 q^{-4} \tag{14c}$$

where A_2 and A_4 are constants. The first expression (14a) is consistent with Gaussian chains and arises from polymer chains in a good solvent. At near the VPTT the particles have partially collapsed and q^{-4} behavior is evident at low q (large dimensions). This indicates coexistence of an interface (Porod scattering) as well as Gaussian chains. An intermediate phase is indicated. At higher temperatures only the Porod-type dependence is evident, which is suggestive of conversion of the Gaussian chains into spherical poly(NIPAM) hard spheres.

Figure 10 shows a scattering profile for poly(NIPAM) at 50°C. For this figure the data have been corrected for solvent and cell scattering, but not incoherent scattering. The data were fitted with Eq. (12). The incoherent background was 0.050 cm^{-1} and σ was 1.7 nm. Equation (12) provides a better fit than the case of a sharp interface (i.e., $\sigma = 0$) and is consistent with the electrophoretic

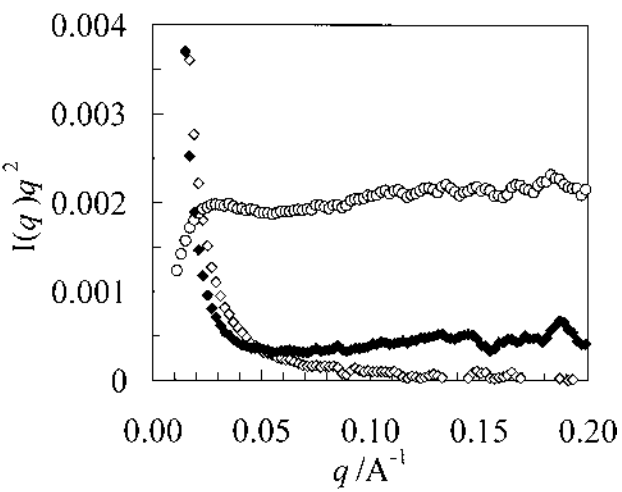

FIG. 9 Kratky plots for poly(NIPAM) microgel dispersions in D_2O measured at 32°C (O), 34°C (closed diamond), and 50°C (open diamond).

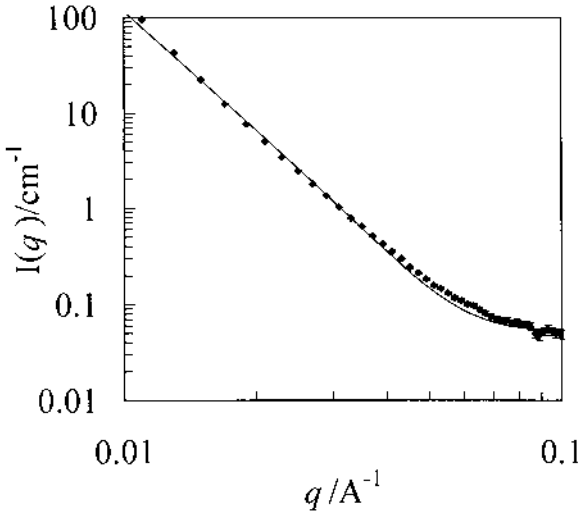

FIG. 10 Scattering profiles for poly(NIPAM) microgels at 50°C in D_2O. The data shown were fitted using Eq. (12) with a flat background for incoherent background. The data were fitted using the program FISH, written by Dr. Heenan of ISIS, RAL.

mobility data. A swollen outer layer, which is rich in polyelectrolyte, exists for these particles at higher temperatures than the VPTT.

The final data to be considered were obtained when measurements were made in the presence of high concentrations of NaCl. However, the measurements were conducted at 25°C. The data are shown in Fig. 11. [Note that the $I(q)$ values for the data obtained in the presence of 0.70 and 0.71 M NaCl were multiplied 10 and 100, respectively, for clarity.] We have previously shown that particle collapse and flocculation can occur under related conditions [16]. The data shown in Fig. 11 are interesting because they show that particle structural collapse is caused by the presence of salt concentrations of 0.70 M or greater at room temperature. This is evidenced by the increased gradient at low q values indicating evolution of a precipitated phase. However, the process in not completed, even at 0.71 M, since Porod scattering [$I(q) \sim q^{-4}$] is not evident across the entire q range. Indeed, the scattering profile is strongly similar to the data obtained in the presence of 0.70 M NaCl. A critical coagulation concentration of about 0.72 M was found using light scattering data for this system. The SANS data shows that the particles have not collapsed fully at the point corresponding to flocculation. It is not surprising that flocculation occurs since a loss of electrostatic stabilization (due to screening) and an increase in the Hamaker constant (discussed above) occurs under these salt conditions. Our data show

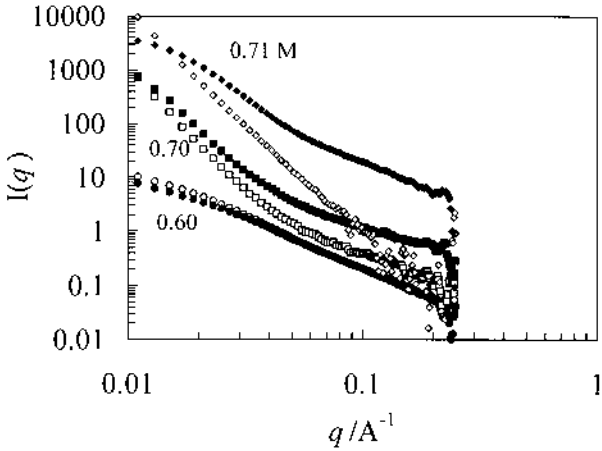

FIG. 11 Scattering profiles for poly(NIPAM) in D_2O/NaCl solutions (closed symbols). The numbers refer to the concentration of NaCl present. For comparison data obtained in the absence of NaCl at various temperatures are shown (open symbols). Reproduced from Fig. 8. All data have been corrected for background and incoherent scattering.

clearly that particle–particle interactions become attractive before complete collapse of the microgel particles occurs.

IV. CONCLUSIONS

The combination of electrophoretic mobility and SANS data has provided a complementary picture of the structure of the microgel particles and the transformations that occur during thermally induced collapse in the absence (and presence) of salt. There is considerable evidence for the existence of peripheral chains that remain strongly hydrated at temperatures exceeding the VPTT. These chains probably contain a high concentration of ionic groups (cf. bulk particle) and are essentially a polyelectrolyte layer. The interionic repulsion causes an increase in the local LCST. The interior of the particle has a lower VPTT and exhibits collapse prior to the sheath. The interior is believed to have a higher cross-link density.

The effect of salt on the microgel dispersion behavior is interesting. It is clear that salt-induced collapse occurs at room temperature and the structural rearrangements are similar to those observed by heating the dispersion to the VPTT in the absence of salt. However, incomplete collapse occurs prior to flocculation. This may explain why the process is reversible (upon cooling or dialysis against pure water) as the hydrated regions provide a ready channel system

(and driving force) for ingress of solvent once the driving force for (partial) collapse has been removed. The advantage of SANS is that the internal structure is probed in aggregated conditions where photon correlation spectroscopy (PCS) becomes uninformative.

The discussions here have shown that a combination of electrophoretic mobility and SANS (in combination with PCS measurements) provide useful structural information about complex colloidal materials. This information provides a useful starting point for excipient design. For instance, the presence of anionic polyelectrolyte barrier at the particle surface would need to be considered since this could interfere with drug migration or adsorption onto cells. This could be altered to be cationic to facilitate adsorption onto anionic surfaces if required. The microgels would be expected to exude an organic soluble phase from the interior outward based on the swelling mechanism discussed above. The presence of high salt concentrations would also trigger partial collapse (and flocculation) of the particles. This could be advantageous if an electrolyte-based triggering effect was sought. Future research will need to consider preparation of responsive microgels based on nontoxic polymers. There are a number of candidates that are capable of providing temperature responsive behavior and have been approved by the FDA.

REFERENCES

1. Saunders, B.R.; Vincent, B. Microgel particles as model colloids: theory, properties and applications. Adv. Colloid Interface Sci. **1999**, *80*, 1.
2. Schild, H.G.; Tirrell, D.A. Microcalorimetric detection of lower critical solution temperature in aqueous polymer solutions. J. Phys. Chem. **1990**, *94*, 4352.
3. Pelton, R.H.; Chibante, P. Preparation of aqueous latices with N-isopropylacrylamide. Colloids Surf A **1986**, *20*, 247.
4. Kawaguchi, H.; Fujimoto, K.; Mizuhara, Y. Hydrogel microspheres. III. Temperature dependent adsorption of proteins on poly(NIPAM) hydrogel microspheres. Colloid Polym. Sci. **1992**, *270*, 53.
5. Saunders, B.R.; Vincent, B. Responsive microgel dispersions. In *Encyclopedia of Surface and Colloid Science*; Hubbard, A., Ed.; 2002, p 4544–4559.
6. Goodwin, J.W.; Hearn, J.; Ho, C.C.; Ottewill, R.H. The preparation and characterisation of polymer latices formed in the absence of surface active agents. Br. Polymer Journal **1973**, *5*, 347.
7. Snowden, M.J.; Marston, N.J.; Vincent, B. The effect of surface modification on the stability characteristics of poly(NIPAM) latices under brownian and flow conditions. Colloid Polym. Sci. **1994**, *272*, 1273.
8. Bouillot, P.; Vincent, B. A comparison of the swelling behaviour of copolymer and interpenetrating network microgel particles. Colloid Polym. Sci. **2000**, *278*, 74.
9. Neyret, S.; Vincent, B. The properties of polyampholyte microgel particles prepared by microemulsion polymerization. Polymer **1997**, *38*, 6129.

10. Hunter, R.J. *Introduction to Modern Colloid Science*; Oxford University Press: Oxford, UK, 1994.
11. O'Brien, R.W.; Cannon, D.W.; Rowlands, W.N. Electroacoustic determination of particle size and zeta potential. J. Colloid Interface Sci. **1995**, *173*, 406.
12. Shaw, D.J. *Introduction to Colloid and Surface Chemistry*, 4th Ed.; Butterworth: Oxford, 1992.
13. O'Brien, R.W.; White, L.R. Electrophoretic mobility of a spherical colloidal particle. J. Chem. Soc. Faraday Trans. **1978**, *274*, 1607.
14. Ohshima, H. A simple expression for Henry's function for the retardation effect in electrophoresis of spherical colloidal particles. J. Colloid Interface Sci. **1994**, *168*, 269.
15. Ohshima, H.; Makino, K.; Kato, T.; Fujimoto, K.; Kondo, T.; Kawaguchi, H. Electrophoretic mobility of latex particles covered with temperature-sensitive hydrogel layers. J. Colloid Interface Sci. **1993**, *159*, 512.
16. Daly, E.D.; Saunders, B.R. A study of the effect of electrolyte on the swelling and stability of poly(N-isopropylacrylamide) microgel dispersions. Langmuir **2000**, *16*, 5546.
17. Garcia-Salinas, M.J.; Romero-Cano, M.S.; de las Nieves, F.J. Electrokinetic characterisation of poly(NIPAM) microgel particles: effect of electrolyte concentration and temperature. J. Colloid Interface Sci. **2001**, *241*, 280.
18. Pelton, R.H.; Pelton, H.M.; Morphesis, A.; Rowell, R.L. Particle sizes and electrophoretic mobilities of poly(NIPAM) latex. Langmuir **1989**, *5*, 816.
19. Daly. E.D.; Saunders, B.R. Temperature-dependent electrophoretic mobility and hydrodynamic radius measurements of poly(NIPAM) microgel particles: structural insights. PCCP **2000**, *2*, 3187.
20. Rasmusson, M.; Vincent, B.; Marston, N. The electrophoresis of poly(NIPAM) microgel particles. Colloid Polym. Sci. **2000**, *278*, 253.
21. King, S.M. In *Experimental Methods in Polymer Characterization*; Pethrick, R.A.D.J.V., Ed.; Wiley: New York, 1999.
22. Higgins, J.S.; Benoit, H.C. *Polymers and Neutron Scattering*; Clarendon Press: Oxford, UK, 1996.
23. Su, T.J.; Lu, J.R.; Cui, Z.F.; Thomas, R.K.; Heenan, R.K. Application of small angle neutron scattering to the in situ study of protein fouling on ceramic membranes. Langmuir **1998**, *14*, 5517.